VOL. 652 NO. 2 OCTOBER 22, 1993
THIS ISSUE COMPLETES VOL. 652

5th Int. Symp. on High Performance Capillary Electrophoresis Orlando, FL, January 25–28, 1993 Part II

JOURNAL OF
CHROMATOGRAPHY A
INCLUDING ELECTROPHORESIS AND OTHER SEPARATION METHODS

SYMPOSIUM VOLUMES

ELSEVIER

JOURNAL OF CHROMATOGRAPHY A

INCLUDING ELECTROPHORESIS AND OTHER SEPARATION METHODS

Scope. The *Journal of Chromatography A* publishes papers on all aspects of **chromatography, electrophoresis** and related methods. Contributions consist mainly of research papers dealing with chromatographic theory, instrumental developments and their applications. In the *Symposium volumes*, which are under separate editorship, proceedings of symposia on chromatography, electrophoresis and related methods are published. *Journal of Chromatography B: Biomedical Applications* —This journal, which is under separate editorship, deals with the following aspects: developments in and applications of chromatographic and electrophoretic techniques related to clinical diagnosis or alterations during medical treatment; screening and profiling of body fluids or tissues related to the analysis of active substances and to metabolic disorders; drug level monitoring and pharmacokinetic studies; clinical toxicology; forensic medicine; veterinary medicine; occupational medicine; results from basic medical research with direct consequences in clinical practice.

Submission of Papers. The preferred medium of submission is on disk with accompanying manuscript (see *Electronic manuscripts* in the Instructions to Authors, which can be obtained from the publisher, Elsevier Science Publishers B.V., P.O. Box 330, 1000 AH Amsterdam, Netherlands). Manuscripts (in English; *four* copies are required) should be submitted to: Editorial Office of *Journal of Chromatography A*, P.O. Box 681, 1000 AR Amsterdam, Netherlands, Telefax (+31-20) 5862 304, or to: The Editor of *Journal of Chromatography B: Biomedical Applications*, P.O. Box 681, 1000 AR Amsterdam, Netherlands. Review articles are invited or proposed in writing to the Editors who welcome suggestions for subjects. An outline of the proposed review should first be forwarded to the Editors for preliminary discussion prior to preparation. Submission of an article is understood to imply that the article is original and unpublished and is not being considered for publication elsewhere. For copyright regulations, see below.

Publication information. *Journal of Chromatography A* (ISSN 0021-9673): for 1994 Vols 652–682 are scheduled for publication. *Journal of Chromatography B: Biomedical Applications* (ISSN 0378-4347): for 1994 Vols. 652–662 are scheduled for publication. Subscription prices for *Journal of Chromatography A*, *Journal of Chromatography B: Biomedical Applications* or a combined subscription are available upon request from the publisher. Subscriptions are accepted on a prepaid basis only and are entered on a calendar year basis. Issues are sent by surface mail except to the following countries where air delivery via SAL is ensured: Argentina, Australia, Brazil, Canada, China, Hong Kong, India, Israel, Japan, Malaysia, Mexico, New Zealand, Pakistan, Singapore, South Africa, South Korea, Taiwan, Thailand, USA. For all other countries airmail rates are available upon request. Claims for missing issues must be made within six months of our publication (mailing) date. Please address all your requests regarding orders and subscription queries to: Elsevier Science Publishers, Journal Department, P.O. Box 211, 1000 AE Amsterdam, Netherlands. Tel.: (+31-20) 5803 642; Fax: (+31-20) 5803 598. Customers in the USA and Canada wishing information on this and other Elsevier journals, please contact Journal Information Center, Elsevier Science Publishing Co. Inc., 655 Avenue of the Americas, New York, NY 10010, USA, Tel. (+1-212) 633 3750, Telefax (+1-212) 633 3764.

Abstracts/Contents Lists published in Analytical Abstracts, Biochemical Abstracts, Biological Abstracts, Chemical Abstracts, Chemical Titles, Chromatography Abstracts, Current Awareness in Biological Sciences (CABS), Current Contents/Life Sciences, Current Contents/Physical, Chemical & Earth Sciences, Deep-Sea Research/Part B: Oceanographic Literature Review, Excerpta Medica, Index Medicus, Mass Spectrometry Bulletin, PASCAL-CNRS, Referativnyi Zhurnal, Research Alert and Science Citation Index.

US Mailing Notice. *Journal of Chromatography A* (ISSN 0021-9673) is published weekly (total 52 issues) by Elsevier Science Publishers (Sara Burgerhartstraat 25, P.O. Box 211, 1000 AE Amsterdam, Netherlands). Annual subscription price in the USA US$ 5132.25 (US$ price valid in North, Central and South America only) including air speed delivery. Second class postage paid at Jamaica, NY 11431. **USA POSTMASTERS**: Send address changes to *Journal of Chromatography A*, Publications Expediting, Inc., 200 Meacham Avenue, Elmont, NY 11003. Airfreight and mailing in the USA by Publications Expediting.

See inside back cover for Publication Schedule, Information for Authors and information on Advertisements.

0021-9673/93/$06.00

This issue is printed on acid-free paper.

Printed in the Netherlands

For Contents see p. I.

VOL. 652, NO. 2 JOURNAL OF CHROMATOGRAPHY A OCTOBER 22, 1993

CONTENTS

5TH INTERNATIONAL SYMPOSIUM ON HIGH PERFORMANCE CAPILLARY ELECTROPHORESIS, ORLANDO, FL, JANUARY 25–28, 1993, PART II

Journal of Chromatography A, 652 (1993) 301–308
Elsevier Science Publishers B.V., Amsterdam

CHROM. 25 081

Automated pK_a determination at low solute concentrations by capillary electrophoresis

J.A. Cleveland, Jr. and M.H. Benko

Discovery Research, DowElanco, 9410 Zionsville Road, Indianapolis, IN 46268-1053 (USA)

S.J. Gluck* and Y.M. Walbroehl

Analytical Sciences, 1897B Building, Dow Chemical Co., Midland, MI 48667 (USA)

ABSTRACT

Capillary electrophoresis is investigated for the determination of thermodynamic pK_a measurements at low solute concentrations, a current limitation of potentiometric titrations. It is not necessary to accurately know the concentration of a titrant or solute. The method relies on measuring the ionic mobility of the solute as a function of pH. Mobility and pH data are fitted to an equilibrium expression with a non-linear regression. The detection limit for benzoic acid is 2 μM. Equations are introduced to remove the need to measure buffer pH outside of the capillary and to handle potential discontinuities in solute mobility between different buffer solutions caused by changes in the shape of the solute molecule and the buffer viscosity.

INTRODUCTION

Knowledge of dissociation constants (*i.e.*, pK_a) is fundamental for understanding and quantifying chemical phenomenon, biological activity and environmental fate [1–3]. The determination of dissociation constants of weakly acidic or basic compounds is routine using established techniques if the compound has amenable physical properties [4–7]. However, the low solubility of many pharmaceutical and agricultural compounds in water precludes convenient pK_a determinations. Recently [8,9] capillary electrophoresis (CE) has been introduced as a method for convenient and precise aqueous pK_a determination. Our principal reason for investigating this approach lies in the high sensitivity and selectivity of CE relative to potentiometry. In this paper we, therefore, explore the benefits of CE for pK_a measurements.

CE offers several advantages over the two most commonly used methods for pK_a determination: potentiometric titration and ultraviolet spectroscopy [4–6]. Precise potentiometric titration at low concentrations requires time-consuming solvent preparation for carbonate-free solutions and the availability of fully automated, commercial instrumentation for multiple sample determinations is limited. Furthermore, compounds must be soluble at a concentration ≥ 1 mM, although indirect determination of pK_a below this limit is possible using computer-assisted techniques [10]. Solubility limitations may also be circumvented by working in mixed solvents. The obtained pK_a values may provide information for ranking compounds within a family; however, extrapolation of the data to an aqueous state is dubious because of different solvation mechanisms and uncertainty in defining the standard state [4–6]. Another common alternative for determining the pK_a of low solubility compounds is UV–Vis spectrophotometric titration [4–6,11]. Determination of pK_a values by

* Corresponding author.

UV–Vis spectrometry hinges on the neutral and ionic species having different spectra. When this criterion is met, excellent precision is obtained; however, these measurements are time-consuming and no automated instrumentation is available commercially. Other, less common but not all inclusive, methods include conductivity [5], calorimetry [12] and isotachophoresis (ITP) [13–15] for determining pK_a values. Conductivity was largely replaced by potentiometry, calorimetry remains a rather specialized approach and, as outlined by Beckers *et al.* [8], the calculation of mobilities and pK_a values in ITP can be laborious as compared to the CE methodology.

The advantages of using CE to determine accurate thermodynamic pK_a values of compounds with diverse solubilities are numerous. CE requires small amounts of sample at low solute concentrations. Indeed, the procedure does not require measurement of solute or titrant concentrations, only migration times. Commercial CE instruments are automated and as a result, ionic species distribution curves of the solute can be generated in a timely manner, thereby minimizing potential solute decomposition. Furthermore, calculations are straightforward and independent of solute purity. This procedure has the potential to become a universal technique for determining aqueous pK_a values in the 1 to 12 pH range.

THEORETICAL

Definition of pK_a^{th}

The thermodynamic equilibrium constant associated with the dissociation of a weak acid, *e.g.*,

$$HZ \rightleftharpoons H^+ + Z^- \quad (1)$$

is defined as

$$K_a^{th} = \gamma_{Z^-}\gamma_{H^+} \cdot \frac{[H^+][Z^-]}{[HZ]} \quad (2)$$

where γ_{HZ}, the activity coefficient of the undissociated acid, is assumed to be 1. Eqn. 2 can be rewritten in the form

$$pK_a^{th} = pH - \log \gamma_{Z^-} - \log \frac{[Z^-]}{[HZ]};$$

$$pH = -\log [H^+] \quad (3)$$

Activities can be calculated from Debye–Hückel theory at 25°C according to the relationship

$$-\log \gamma = \frac{0.5085 z^2 \sqrt{\mu}}{1 + 0.3281 a \sqrt{\mu}}; \quad \mu = \frac{1}{2} \sum_{i=1} C_i z_i^2 \quad (4)$$

where a is the hydrated diameter of an ion in Å, C is the molarity of the ion, z is the valency of the ion, and μ is the ionic strength of the solution. In general the exact value of the parameter a, which can range from 1–11 Å, will not be known. Throughout this study, the value 5 Å was assumed.

Substituting eqn. 4 into eqn. 3 gives

$$pK_a^{th} = pH - \log \frac{[Z^-]}{[HZ]} \pm \frac{0.5085 z^2 \sqrt{\mu}}{1 + 0.3281 a \sqrt{\mu}} \quad (5)$$

where the activity correction is positive for acids and negative for bases.

Mobility and pK_a^{th}

In CE, a voltage, V, is applied across a capillary of length, L_c, resulting in an electric field strength E given by

$$E = V/L_c \text{ (kV/cm)} \quad (6)$$

The electrophoretic mobility of an ion is generally expressed as

$$m_e = v_e/E \quad (7)$$

where v_e is the local electrophoretic velocity and E is the local electric field strength. If the distance from the injection point to the detector is L_d, and the migration time of an analyte is t_{app}, the apparent mobility, m_{app}, is given by

$$m_{app} = \frac{v_{app}}{E} = \frac{L_c L_d}{t_{app} V} \quad (8)$$

In general, m_{app} does not equal m_e because the observed velocity is the sum of electrophoretic and electroosmotic flow (EOF)

$$m_{app} = (v_e + v_{EOF})/E \quad (9)$$

Hydrated cations in the vicinity of the capillary wall result in electroosmotic flow of the bulk liquid through the detector towards the cathode (ground). EOF is calculated by spiking the analyte solution with a marker which remains neutral throughout the entire sequence of buffers

used in a determination. Hence, electrophoretic mobility is determined according to the relation

$$m_e = (m_{app} - m_{EOF}) = \frac{L_c L_d}{V}\left(\frac{1}{t_{app}} - \frac{1}{t_{EOF}}\right) \quad (10)$$

When an acid, HZ, is deprotonated, the net electrophoretic mobility, m_e, in a given buffer of a given concentration is given by $m_e = \alpha m_a$, where m_a is the electrophoretic mobility of the fully deprotonated species Z^- and α is the fraction of analyte ionized. Using this relation, it is possible to rewrite $[Z^-]/[HZ]$ in terms of mobility:

$$\frac{[Z^-]}{[HZ]} = \frac{\alpha}{1-\alpha} = \frac{m_e}{m_a - m_e} \quad (11)$$

For acids, this relation can be substituted into eqn. 5 to give

$$pK_a^{th} = pH - \log\left(\frac{m_e}{m_a - m_e}\right) + \frac{0.5085 z^2 \sqrt{\mu}}{1 + 0.3281 a \sqrt{\mu}} \quad \text{(acids)} \quad (12)$$

It is also possible to derive an analogous expression for bases, B:

$$pK_a^{th} = pH + \log\left(\frac{m_e}{m_b - m_e}\right) - \frac{0.5085 z^2 \sqrt{\mu}}{1 + 0.3281 a \sqrt{\mu}} \quad \text{(bases)} \quad (13)$$

where m_b is the electrophoretic mobility of the fully protonated species, BH^+.

EXPERIMENTAL

Buffer considerations

A number of factors must be considered in forming a standard buffer series for automated pK_a determination. Electroosmotic flow can be expressed as

$$m_{EOF} = \epsilon\zeta / 4\pi\eta \quad (14)$$

where ϵ is the dielectric constant of the solution, η is the viscosity, and ζ is the zeta potential measured at the shear plane close to the liquid–solid interface. The zeta potential is inversely proportional to the charge per unit surface area, the valency, and the square root of the buffer concentration. Hence, the run time is directly proportional to the square root of the buffer concentration. In cases of very low EOF such that $m_{EOF} < m_e$, anions will not be detected.

While dilute buffers are desirable from considerations of the run time, Joule heating and activity, concentrated buffers also offer certain advantages, such as buffering capacity. Concentrated buffers are less likely to exhibit pH shifts due to CO_2 dissolution. Sample stacking, which can lead to sensitivity enhancements of 10–100×, also increases as the ionic strength of the run buffer is increased relative to the sample.

The buffer series given in Table I represents a reasonable compromise of the considerations given above and is by no means the only possible series.

TABLE I

STANDARD BUFFER SERIES

Component	pH	[HZ]	$[Z^-]$	μ	$\log \gamma^a$
(1) citrate	2.64	0.009	0.002	0.002	0.020
(2) citrate	3.14	0.002	0.002	0.002	0.020
(3) acetate	3.75	0.020	0.002	0.002	0.020
(4) acetate	4.25	0.006	0.002	0.002	0.020
(5) acetate	4.75	0.002	0.002	0.002	0.020
(6) acetate	5.25	0.001	0.005	0.005	0.028
(7) acetate	5.75	0.001	0.014	0.014	0.045

[a] Sign of correction is (+) for acids and (−) for bases.

Instrument parameters

A SpectraPHORESIS 1000 (Spectra-Physics Analytical, Fremont, CA, USA) was used for all experiments. A 2-s hydrodynamic injection was performed. Since the hydrodynamic injection rate is 6 nl/s for a 70 cm × 75 μm untreated fused-silica capillary (Polymicro Technology, Phoenix, AZ, USA), 12 nl was loaded onto the column. The separation distance, L_d, was 68 cm. The temperature was set at 25°C. Absorption was monitored at 220 nm. With the instrument operating at 25 kV, currents of <20 μA were observed.

In order to equilibrate the column and thereby minimize hysteresis effects, the following wash cycle was performed prior to each run in a sequence: (1) 2.5 min with 0.1 *M* NaOH, (2) 2.5 min with water, and (3) 5.0 min with running buffer.

Because the SpectraPHORESIS 1000 is equipped with a single reservoir for the buffer near the detector, it is not possible to match running and trailing buffers in a sequence. This feature can lead to significant back-migration through the column if the reservoir is filled with an alkaline (highly mobile) buffer while the running buffer is acidic (weakly mobile). No back-migration was observed when the reservoir was filled with the pH 4.25 acetate buffer in Table I.

Method

All solutions were prepared using distilled, deionized, and filtered water (ASTM type I specification). Stock citrate buffers were prepared by titrating citric acid solutions with 0.1 *M* NaOH until the desired pH was reached. Stock acetate buffers were prepared by combining appropriate amounts of sodium acetate and glacial acetic acid to achieve the proper pH and concentration. Prior to an experiment, stock solutions were diluted by a factor of 10.

Equal volumes of the neutral marker (200 μ*M* mesityl oxide) in water and analyte solutions were combined and filtered into a 2-ml sample vial. Mesityl oxide was preferred as a marker over toluene and benzyl alcohol because of its larger absorption coefficient; peak shapes for the three molecules were nearly identical when compared on normalized amplitude and time scales.

Because the buffers are relatively dilute, CO_2 dissolution or absorption can change pH significantly over time. Prior to each analysis, an Orion pH meter was calibrated using NIST (National Institutes of Standards and Technologies)-traceable buffers having pH 2.00 ± 0.02, 4.00 ± 0.01 and 6.00 ± 0.01. The autosampler in the CE apparatus was purged with nitrogen during runs as an added precaution against CO_2 absorption.

Unless otherwise noted, the seven buffers given in Table I were used in order from high to low pH. Since each mobility determination was 20 min in length, the total analysis time per sample (including wash cycles) was 3.5 h. No attempt was made to optimize total analysis time which could probably be cut in half by optimizing the column length, field strength, run time and wash cycle time.

Mobilities were calculated according to eqn. 10. Data pairs of pH and m_e were imported into MathCad (MathSoft, Cambridge, MA, USA) where m_a and pK_a were determined by performing a non-linear fit to eqns. 12 and 13.

RESULTS

It has been observed that at low pH silica capillaries can exhibit hysteresis over many days [16]. Table II shows calculated m_{app}, m_{EOF} and m_e values for benzoic acid in ascending and descending pH sequence modes. In ascending mode, m_{EOF} is significantly lower in every instance due to hysteresis; however, m_e is remarkably reproducible. As a result, the order in which the buffers are run does not appreciably affect the outcome of the pK_a determination.

Plots of m_e *vs.* pH are given in Fig. 1 for acids and in Fig. 2 for bases. Simulated curves using the parameters obtained from the non-linear fit are superimposed on the data. In Table III, CE-determined pK_a values are compared with literature values ($\mu = 0$) [12]. Agreement is to within 0.07 pH units in all cases. The largest discrepancy exists for pyridine, which because of its weak UV chromophore, necessitated preparation at the 1 m*M* level. Because buffer concentrations range from 4–22 m*M*, an analyte at the 1 m*M* level changes the pH. As a result, the pH of the local environment of the analyte will not be

TABLE II

STABILITY OF EFFECTIVE MOBILITY

Buffer pH	Sequence direction	m_{app} ($\times 10^5$ cm^2/V s)	m_{EOF} ($\times 10^5$ cm^2/V s)	m_e ($\times 10^5$ cm^2/V s)
6.59	Descending	53.905	90.741	−36.836
	Ascending	42.813	79.870	−37.057
6.06	Descending	48.756	85.515	−36.759
	Ascending	38.477	75.269	−36.792
5.71	Descending	50.725	87.578	−36.853
	Ascending	39.692	75.969	−36.277
4.68	Descending	36.870	65.203	−28.333
	Ascending	24.691	52.688	−27.997
4.01	Descending	36.995	51.770	−14.775
	Ascending	41.142	44.384	−14.456
3.19	Descending	41.142	44.384	−3.242
	Ascending	36.787	40.033	−3.246

TABLE III

CE-DETERMINED pK_a VALUES *VS.* LITERATURE VALUES AT 25°C [12]

Molecule	Acid/Base	pK_a (lit.)	pK_a (CE)	Solute concentration (CE)
Pyridine	Base	5.19	5.26	1 m*M*
Aniline	Base	4.60	4.66	150 μM
Cinnamic acid	Acid	4.40	4.40	50 μM
Benzoic acid	Acid	4.20	4.18	50 μM
p-Bromoaniline	Base	3.88	3.85	50 μM
Salicylic acid	Acid	2.98	2.96	50 μM
o-Bromoaniline	Base	2.53	2.55	50 μM

equivalent to that measured for the buffer alone which is a reasonable explanation for the error in the pyridine measurement. For the buffer series used here, accuracy to within 0.03 pH units is possible for analyte concentrations of <100 μM.

Very few data are required to attain an accurate pK_a by this technique. In fact, it is not even necessary to bracket the pK_a. For example, only

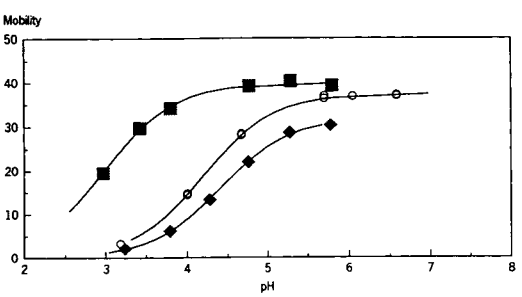

Fig. 1. Plots of mobility ($m_e \times 10^5$ cm^2/V s) *vs.* pH for acids with superimposed curve fits. ■ = Salicylic acid; ○ = benzoic acid; ◆ = cinnamic acid.

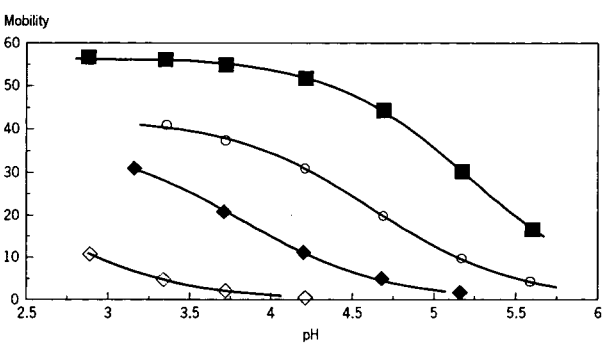

Fig. 2. Plots of mobility ($m_e \times 10^5$ cm^2/V s) *vs.* pH for bases with superimposed curve fits. ■ = Pyridine; ○ = aniline; ◆ = *p*-bromoaniline; ◇ = *o*-bromoaniline.

four points were used for *o*-bromoaniline, all of which were above the pK_a. Similarly, six points were used for salicylic acid, all above the pK_a of the acid.

DISCUSSION

Limitations/factors impacting precision

The practical range for buffer pH in CE is between 2 and 12. For pH values greater than 12, the concentration of highly mobile OH^- results in excessive conductivity. For pH values less than 2, the same effect can be attributed to the presence of H^+. It is reasonable, then, that the pK_a range for this technique is between 1 and 12 since it is not necessary to cross the pK_a in the experiment.

The upper sample concentration limit depends on the accuracy required for the measurement and the concentrations of the running buffers. For the buffers used in this study, sample concentrations of $<100\ \mu M$ were necessary in order to obtain pK_a values to within 0.03 of the reported values.

Detection limit in CE is a function of a number of parameters, the most significant for this application being the optical absorption coefficient. Using increasingly dilute solutions of benzoic acid, $S/N = 2$ was observed at a concentration of 2 μM. Therefore, the detection limit under the conditions of this study can be expressed as $\varepsilon^{220}bc = 1 \cdot 10^{-4}$, where ε^{220} is the molar extinction coefficient at 220 nm, b is the path length and c is the solute concentration. Alternate detection schemes must be sought for those cases where the analyte is a very weak UV chromophore and/or has sparingly low solubility in water.

Sample stacking is a means of increasing sensitivity by a factor of 10–100 by preconcentrating the analyte [17]. While some sample stacking does occur, as manifest by the narrow widths of analyte peaks relative to marker peaks, the effect is not as great as it might be because of the low ionic strengths ($0.002 < \mu < 0.014$) of the running buffers. Another limitation to sample stacking is the inability to further preconcentrate at the solubility limit of the solute. If the sample is injected from a saturated solution, stacking is limited according to the solubility relations

$$S = S_0 + \frac{S_0}{\gamma_{\pm}^2}\,\text{antilog}\,(\text{pH} - pK_a) \quad \text{(acids)} \qquad (15a)$$

$$S = S_0 + \frac{S_0}{\gamma_{\pm}^2}\,\text{antilog}\,(pK_a - \text{pH}) \quad \text{(bases)} \qquad (15b)$$

where S_0 is the molecular or intrinsic solubility.

A potential source of error is solute adsorption to the capillary wall. Though not observed in our work, it is most likely to occur for bases and larger molecules. Even if the analyte were not totally bound to the capillary wall, severely skewed peak shapes could lead to errors in the mobility measurement.

For the mobility calculations, it was assumed that the electric field strength was carried entirely by the running buffer. Because of the small injection size, coupled with the diluteness of the buffers, this assumption is reasonably valid. The 12-nl injection volume corresponds to 2.7 mm, or <0.5% of the total column length. In this study, because of the inherent resolution of CE and the ideal behavior of the solutes studied, the largest factor impacting precision appears to be measurement of buffer pH.

Potential improvements

Electrophoretic mobility is usually expressed by the following equation

$$m_e = q/6\pi a\eta \qquad (16)$$

where q is the charge of the species' ionic cloud, a is its Stokes radius and η is the buffer viscosity. However, a more accurate treatment would include a numerical factor, f, accounting for the shape of the ion [18]. Since the parameters η, q and a are all sensitive to the buffer used, m_a will also be sensitive to these parameters. Discontinuities are most likely to occur when buffer composition is changed, such as when making the transition from acetate to citrate.

While η, a property of the buffer, can easily be measured experimentally, the parameters q, a, and f cannot . It is possible to calculate m_a from the ionic equivalent conductance, λ_c, and Faraday's constant, F [8]. However, an empirical

approach might prove more practical for routine analysis. The samples could be spiked with both neutral and ionized markers; the ionized marker being a species which is totally ionized for every buffer in the series. The mobility of the ionized marker, m_+, could then be used as an additional parameter and included in modified versions of eqns. 12 and 14:

$$pK_a^{th} = pH - \log\left[\frac{m_e}{(m_a m_+/m_{max}) - m_e}\right] + \frac{0.5085 z^2\sqrt{\mu}}{1 + 0.3281 a\sqrt{\mu}} \quad (17)$$

$$pK_a^{th} = pH + \log\left[\frac{m_e}{(m_b m_+/m_{max}) - m_e}\right] - \frac{0.5085 z^2\sqrt{\mu}}{1 + 0.3281 a\sqrt{\mu}} \quad (18)$$

where m_{max} is a normalization constant corresponding to the maximum absolute value of m_+ measured.

A second potential improvement lies in the measurement of buffer pH which is the largest source of error in these measurements and also one of the most labor intensive operations. A solute with a well established pK_a (pK'_a) is added to the sample injection mixture to serve as an internal pH and activity correction reference. Eqn. 17 becomes

$$pK_a^{th} = pK'_a + \log\left[\frac{m'_e}{(m'_a m_+/m_{max}) - m'_e}\right] - \log\left[\frac{m_e}{(m_a m_+/m_{max}) - m_e}\right] \quad (19)$$

where the reference compound is an acid and the unknown is an acid and

$$pK_a^{th} = pK'_a - \log\left[\frac{m'_e}{(m'_a m_+/m_{max}) - m'_e}\right] - \log\left[\frac{m_e}{(m_a m_+/m_{max}) - m_e}\right] + \frac{1.017 z^2\sqrt{\mu}}{1 + 0.3281 a\sqrt{\mu}} \quad (20)$$

where the reference compound is a base and the unknown is and acid. Eqn. 18 becomes

$$pK_a^{th} = pK'_a - \log\left[\frac{m'_e}{(m'_a m_+/m_{max}) - m'_e}\right] + \log\left[\frac{m_e}{(m_b m_+/m_{max}) - m_e}\right] \quad (21)$$

where the reference compound is a base and the unknown is a base, and

$$pK_a^{th} = pK'_a + \log\left[\frac{m'_e}{(m'_b m_+/m_{max}) - m'_e}\right] + \log\left[\frac{m_e}{(m_a m_+/m_{max}) - m_e}\right] - \frac{1.017 z^2\sqrt{\mu}}{1 + 0.3281 a\sqrt{\mu}} \quad (22)$$

where the reference compound is an acid and the unknown is a base.

CONCLUSIONS

An automated method for obtaining pK_a values for acids and bases using CE was described and investigated. The method has several advantages for determining the pK_a values of compounds with low water solubility. For example, compounds of limited water solubility need not be prepared in a co-solvent and it is not necessary to accurately know the concentration of a titrant or solute. There is no time-consuming preparation of carbonate-free buffers. The detection limit using the parameters, instrumentation and electrolytes of this study was $\varepsilon^{220} bc = 1 \cdot 10^{-4}$ which, for benzoic acid, was 2 μM, 500 times lower than a typical detection limit via potentiometric titration. The accuracy was within 0.03 pH units for sample concentrations below 100 μM. The potential pK_a range which may be achieved is between 2 and 12. The analysis time was 3.5 h/sample, which could be reduced by a factor of two by optimizing experimental parameters.

Equations were introduced for handling potential discontinuities between buffer solutions in a, η and f. These equations were expanded remove the need to measure pH values of the running buffers by using an *in situ* probe of known pK_a to determine the pH in the CE column. Implement-

ing both of these procedures would be expected to improve the accuracy and decrease the labor for a determination.

ACKNOWLEDGEMENTS

The authors are thankful for early stage discussions with Eric Martin and the careful review and comments of Robert Reim.

REFERENCES

1 L.Z. Benet and J.E. Goyan, *J. Pharm. Sci.*, 56 (1967) 665.
2 A. Roda, A. Minutello and A. Fini, *J. Lipid Res.*, 31 (1990) 1433.
3 W.J. Lyman, W.F. Reehl and D.H. Rosenblatt, *Handbook of Chemical Property Estimation Methods*, American Chemical Society, Washington, DC, 1990.
4 R.F. Cookson, *Chem. Rev.*, 74 (1974) 1.
5 A. Albert and E.P. Serjeant, *The Determination of Ionization Constants: A Laboratory Manual*, Chapman & Hall, New York, 3rd ed., 1984.
6 E.J. King, *Acid-Base Equilibria*, Pergamon Press, Oxford, 1965.
7 J.B. Hansen and O. Hafliger, *J. Pharm. Sci.*, 72 (1983) 429.
8 J.L. Beckers, F.M. Everaerts and M.T. Ackermans, *J. Chromatogr.*, 537 (1991) 407.
9 J. Cai, J.T. Smith and Z. El Rassi, *J. High Resolut. Chromatogr.*, 15 (1992) 30.
10 A.P. Ijzerman, *Pharm. Res.*, 5 (1988) 772.
11. H. Yamazaki, R.P. Sperline and H. Freiser, *Anal Chem.*, 64 (1992) 2720.
12 J.J. Christensen, L.D. Hansen and R.M. Izatt, *Handbook on Ionization Heats*, Wiley-Interscience, New York, 1976.
13 J. Pospipchal, P. Gebauer and P. Boček, *Chem. Rev.*, 89 (1989) 419.
14 M. Polasek, B. Gas, T. Hirokawa and J. Vacik, *J. Chromatogr.*, 598 (1992) 265.
15 J. Beckers, *J. Chromatogr.*, 320 (1985) 147.
16 W.J. Lambert and D.L. Middleton, *Anal Chem.*, 62 (1990) 1585.
17 R.L. Chien and D.S. Burgi, *Anal Chem.*, 64 (1992) 489A.
18 J.T.G. Overbeek and B.H. Bijsterbosch, in P.G. Righetti, C.J. van Oss and J.W. Vanderhoff (Editors), *Electrokinetic Separation Methods*, Elsevier, Amsterdam, 1979, p. 15.

Journal of Chromatography A, 652 (1993) 309–316
Elsevier Science Publishers B.V., Amsterdam

CHROM. 25 180

Characterization of quartz capillaries for capillary electrophoresis

Jörg Kohr and Heinz Engelhardt*

Angewandte Physikalische Chemie, Universität des Saarlandes, 6600 Saarbrücken (Germany)

ABSTRACT

Different brands of commercially available quartz capillaries were investigated with respect to their optical and surface properties. Differences in inner diameter influence the detection sensitivity. Surface properties influence the electroosmotic flow (EOF). It is recommended to control the inner diameter and determine the EOF as a function of pH if new batches of capillaries are used. GC measurements and the dependence of retention on temperature permit one to characterize the coating procedure for non-polar coatings and to differentiate between polar and non-polar interactions. These values are in good agreement with measurements of the EOF and its dependence on pH.

INTRODUCTION

Although capillary electrophoresis (CE) has received wide application in recent years, so far no satisfactory method to characterize the surface of the capillaries has been described. Both systems, with the most widely used uncoated capillaries and also the coated capillaries, which are of growing importance [1–20], can only be characterized by the measurement of the electroosmotic flow (EOF) itself or its dependence on the pH of the applied buffer [4,21].

Stationary phases for HPLC or the coating of capillaries for GC are usually characterized by standard test procedures [22–24]. For the characterization of LC stationary phases, additionally a range of independent spectroscopic methods are available. The surface concentration of silanol groups can be determined easily [25]. Via the carbon content, the surface concentration of bonded groups can be calculated with good reliability.

The inner surface area of capillaries for CE with a usual length of less than 100 cm and an I.D. between 50 and 100 μm is of the order of a few square centimetres, hence the established methods cannot be used.

In addition to the magnitude of the EOF, mainly indirect methods for surface characterization are applied to the resulting effect, *e.g.*, the suppression of interactions of proteins with the surface wall [8,10–17]. To determine the layer thickness of a positively charged polyethylenimine coating, the adsorption of picric acid has been measured photometrically [17]. Non-polar and hydrophobic coatings have been characterized by GC measurements [19], and the layer thickness could be derived from the retention behaviour of *n*-nonane as a standard. In this paper, means for the characterization of uncoated and coated capillaries for CE are described by interpretation of the results of EOF measurements with quartz capillaries from different suppliers, and the combination of EOF and GC measurements to demonstrate the effectiveness of various coating procedures.

Correlation of EOF measurements with surface charges

In CE, the EOF is superimposed on the electrophoretic migration of charged species.

* Corresponding author.

0021-9673/93/$06.00

The magnitude of the EOF depends, as an interfacial phenomenon, on the applied electric field E and on the distribution of charges in the interfacial layer. The latter is usually described as the zeta potential (ζ) [26]. The Helmholtz–Smoluchowski equation is

$$v_{eo} = -\frac{E\varepsilon_r\varepsilon_0}{\eta_0} \cdot \zeta \quad (1)$$

where v_{eo} is the electroosmotic velocity (mm/s), ε_r the relative dielectric constant, ε_0 the dielectric constant in vacuum and η_0 the viscosity of the buffer solution. From this equation the zeta potential can be calculated. In Table I some typical values for CE are summarized. EOF values up to 4 mm/s are typical in CE. As can be seen, the calculated zeta potentials are in the range 1–100 mV. These values are in good agreement with published data [27] for electrolytes in contact with glass surfaces.

A mathematical correlation has been given [28] between the zeta potential and the specific surface charges at the boundary of the immobile double layer. These specific surface charges are a function of the charges on the quartz surface. The specific surface charge σ (in $\mu C/cm^2$) correlates with the zeta potential according to the equation [28]

$$\sigma = (8kT\varepsilon_r\varepsilon_0\eta_0)^{1/2} \sinh\left(\frac{ze\zeta}{2kT}\right) \quad (2)$$

By inserting all the constants at 298 K, this equation becomes

TABLE I

CALCULATED ZETA POTENTIALS FOR DIFFERENT LINEAR VELOCITIES OF THE ELECTROOSMOTIC FLOW (ACCORDING TO EQN. 1)

Constants: $E = 40$ kV/m; $\eta = 10^{-4}$ Pa s (water at 25°C); $\varepsilon_0 = 8.854 \cdot 10^{-12}$ C^2 N^{-1} m^{-2}; $\varepsilon_r = 80$.

v_{eo} (mm/s)	ζ (mV)
0.1	3.1
1	31.7
2	63.5
3	95.2
4	127.0

$$\sigma = 11.7\sqrt{c^*}\sinh(19.5z\zeta) \quad (3)$$

where z is the charge number, c^* the total concentration of the solution (mol/l) and the zeta potential is in volts. The electroosmotic mobility μ_{eo} ($cm^2/V \cdot s$) is correlated with the specific surface charge by

$$\sigma = 11.7\sqrt{c^*}\sinh(2477.7z\mu_{eo}) \quad (4)$$

(the numerical values given in Table I are used in this reduced equation).

In Fig. 1, the surface charge concentration, given in the usual measure of $\mu mol/m^2$, is plotted for the usual range of mobilities in CE in the range of $1 \cdot 10^{-4}$–$12 \cdot 10^{-4}$ cm^2 $N \cdot s$.

The discussion of this curve is of great importance for the surface characterization of both uncoated and coated capillaries. Mobilities above $10 \cdot 10^{-4}$ $cm^2/N \cdot s$ are approached with quartz capillaries at pH values above 9. Here a surface charge concentration of 0.8 $\mu mol/m^2$ is calculated. If one assumes that all charges arise from dissociated surface silanols, the total concentration of silanol groups is almost an order of magnitude smaller than commonly accepted for silanol concentrations on crystalline quartz surfaces, for which values around 8 $\mu mol/m^2$ are calculated [25]. Two reasons for these differences can be discussed. The quartz capillaries are not totally hydrated owing to their production procedure. It is known from GC that the surfaces of quartz capillaries have to be "activated" prior to coating or bonding procedures by "leaching" and "etching" with sodium hydroxide, hydrofluoric acid, etc., to produce a sufficient number of active binding sites, *i.e.*, silanol

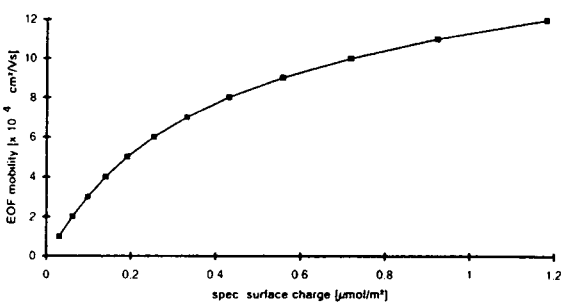

Fig. 1. Relationship between the specific surface charge and electroosmotic mobility calculated for a 10 mM buffer according to eqn. 4.

groups. Capillaries from various suppliers showing differences in surface concentrations might explain this assumption. On the other hand, the surface charges calculated with this equation are those at the boundary of the double layer. These charges are only proportional to those at the solid surface and the smaller number might be caused by the decrease in the electrical potential in the stagnant double layer. (The zeta potential is the electrical potential at the boundary between the stagnant and diffuse double layer [27].)

Fig. 1 also demonstrates that extremely high surface charges are required to accelerate further an already high EOF. As can be seen on doubling the surface charges from 0.6 to 1.2 μmol/m^2, the electroosmotic mobility increases only from $9.5 \cdot 10^{-4}$ to $10 \cdot 10^{-4}$ cm^2/N·s. This is usually achieved with uncoated capillaries if the pH of the buffer is increased from 7 to 9.5 (compare Fig. 6).

More important for surface characterization, especially for modified capillary surfaces, is the opposite end of this curve at low surface charges. Even an extremely low concentration of surface charges (30 nmol/m^2) results in a relatively high electroosmotic mobility of 10^{-4} cm^2/V·s. This means that to suppress the EOF totally, very good coverage of the quartz surface or high electroneutrality at the surface has to be achieved.

The possibilities of this approach for capillary surface characterization is discussed in the following.

EXPERIMENTAL

Reagents and materials

Fused-silica capillary tubes were purchased from Microquarz (a subsidiary of Siemens, Munich, Germany), Chrompack (Frankfurt, Germany), Polymicro (Laser 2000, Munich, Germany) and SGE (Weiterstadt, Germany).

Trichlorovinylsilane and trimethoxyvinylsilane were purchased from Chemische Werke Hüls (Marl, Germany) and *n*-butylamine, trimethylamine (gas), benzyl alcohol and all buffer substances from Fluka (Neu Ulm, Germany).

Methods

The real inner diameter was determined by weighing (Sartorius 4503 MP) an empty and a water-filled section (*ca.* 5 cm) of the corresponding type of capillary and calculating the difference.

Before use, all capillaries were rinsed with 1 *M* KOH solution (10 min), water (5 min), 1 *M* HCl (10 min) and water (5 min). Before silanization the capillaries were additionally rinsed with methanol (5 min) and subsequently dried overnight at 120°C under a gentle stream of argon.

Preparation of vinyl-modified capillaries

For all wall modifications only pretreated capillaries were used (see above).

Capillary V1. The capillary was filled with an emulsion of 3% (w/w) trimethoxyvinylsilane in water, containing 100 ppm of *n*-butylamine as a catalyst. After standing overnight at room temperature, the capillary was finally washed with methanol and water (20–30 min).

Capillary V2. The capillary was filled with a solution of 10% (w/w) trichlorovinylsilane in toluene and both ends were sealed. For reaction the capillary was kept in an oven at 120°C for 18 h. The solution was then driven out by a gentle stream of trimethylamine gas during 20 min at 120°C. After reaction the capillary was successively rinsed with toluene, dichloromethane, methanol and water.

Capillary V3. The capillary was filled with pure trichlorovinylsilane and both ends were sealed. For reaction the capillary was kept in an oven at 120°C for 18 h. After reaction the capillary was rinsed as for V2.

Apparatus

For EOF measurements a Beckman P/ACE system 2050 was used. Data acquisition was accomplished with Beckman Gold software (V 6.0) and an IBM PS 65 personal computer.

Benzyl alcohol was used as a neutral marker. Between the individual runs the capillary was washed for several minutes with methanol, water, 10 m*M* phosphate buffer (pH 9), water and the corresponding running buffer.

GC experiments were carried out with a Carlo Erba GC 6000 Vega Series instrument with flame

ionization detection. The length of the capillaries used for GC characterization was 1.5 m. The temperatures of the injection and detection system were set to 180°C. Nitrogen was used as the carrier gas with a linear velocity of 3.5 cm/s and the splitting ratio was higher than 1:20. To avoid overloading effects, very small amounts were injected (if possible the syringe was filled with the vapour of the sample).

RESULTS AND DISCUSSION

Comparison of uncoated quartz capillaries

General properties. So far quartz capillaries have not been produced exclusively for application in CE. Therefore, it is not surprising that materials from different suppliers vary in wall thickness, type and thickness of the protective polymeric coating, etc. In Table II the properties of four quartz capillaries available in Germany are summarized.

The greatest differences were found in the wall thickness of the capillaries, which varied between 49 and 129 μm. The optimum wall thickness is difficult to define. A thick wall is a good reservoir for generated Joule heat, and can serve for heat dissipation while working without additional cooling [29]. In this case the Polymicro capillary with a thickness of 130 μm certainly has some advantages. For thermostated systems this thick wall, on the other hand, prevents speedy heat exchange. In this case thin-walled capillaries would be more advantageous. The smallest wall diameter we found was 50 μm with the SGE capillary. This capillary also had the thinnest polymeric coating, with a 10-μm film thickness. The thickest coating we found was 30 μm. The frequency of breakages did not correlate with the wall and protecting film thicknesses.

The effective inner diameter did not always correspond to the manufacturer's statement; in most instances the differences were within a range of 5% and only in one instance did the stated diameter of 75 μm differ widely from that measured. Because the inner diameter is identical with the optical path length, the detection sensitivity varies with the type of capillary used. From this point of view differences of 30% are intolerable. It is therefore recommended that the inner diameter of capillaries be determined experimentally by weighing the capillary empty and filled with water. The accuracy of these simple measurements is better than 1%. This procedure is recommended if longer pieces of capillaries are purchased, because we found that over a 10-m quartz capillary the inner diameter can vary by more than 5%.

Also important for detection sensitivity is the spectral transparency of the capillaries at low wavelengths. Fig. 2 demonstrates that at wavelengths below 220 nm the absorption of the quartz increases. Only the SGE material has a better transparency down to 210 nm, because of the smaller wall thickness. With the Polymicro capillary, which has the thickest wall, the absorbance of the wall increases continuously with decreasing wavelength, especially below 230 nm.

The influence of wall absorption on the detec-

TABLE II

MEASURED AND CALCULATED DIMENSIONS OF DIFFERENT TYPES OF FUSED-SILICA CAPILLARIES

Parameter	Supplier			
	Microquarz	SGE	Chrompack	Polymicro
I.D. (quoted) (μm)	75	75	75	75
I.D. (actual) (μm)	71	74	53	74
O.D. (μm)	260	190	232	366
O.D. (no coating) (μm)	205	172	200	322
Coating thickness (μm)	28	9	16	17
Wall thickness (μm)	67	49	74	129

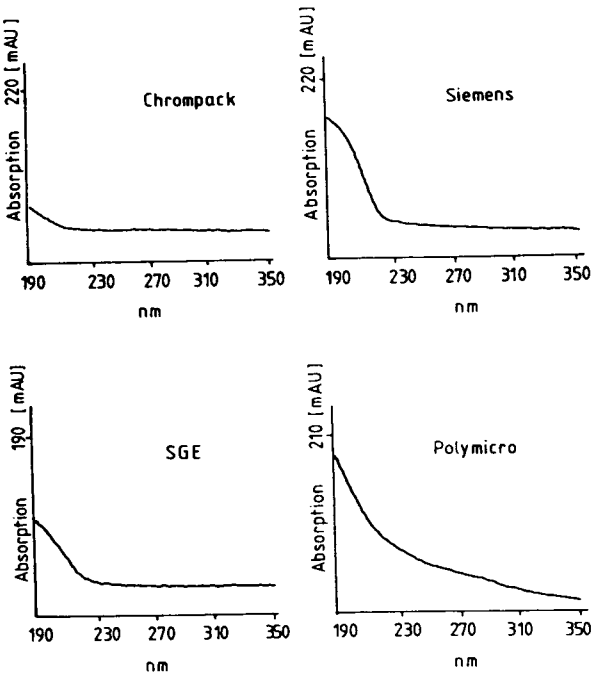

Fig. 2. UV spectra of different capillaries in the range 190–350 nm. Detector, GAT LDC 502 with CE cell (analogue of the Linear cell). All capillaries were filled with water.

tion sensitivity at 200 nm determined with sodium benzoate solution is negligible, however. The detection sensitivity is much more influenced by the inner diameter of the capillary and its position in the light beam and by focusing the beam through the liquid.

Electroosmotic flow and surface properties. The magnitude of the EOF is one of the most important factors in the optimization of CE separations. Therefore, the EOF was studied with the four different capillaries in the pH range 3–9. The resulting mobility measurements are shown in Fig. 3. Each capillary was treated identically by washing with sodium hydroxide and hydrochloric acid to achieve a reproducible and clean surface. In each instance the expected sigmoid shape could be observed [21]. At pH 3 the mobilities with all four capillaries are very similar. Only one (SGE) showed slightly higher mobilities than the others. The general shapes of the curves are identical, with an inflection point at pH 5–6. However, the differences in mobilities become significant at pH >5. With the

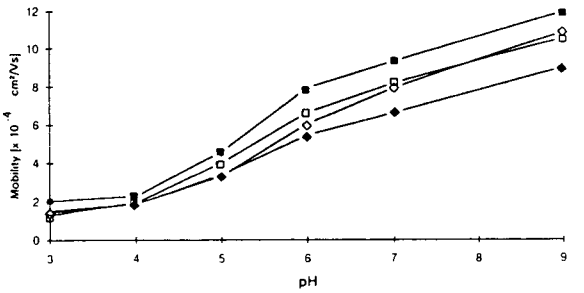

Fig. 3. EOF *versus* pH curves for four different fused-silica capillaries. Conditions: $L = 40/47$ cm; buffer, 10 m*M* phosphate; neutral marker, benzyl alcohol; field, 425 V/m. ■ = SGE; □ = Microquarz; ◆ = Chrompack; ◇ = Polymicro.

SGE capillary at pH 9 the highest mobility of $12 \cdot 10^{-4}$ cm/V·s was measured, compared with $8 \cdot 10^{-4}$ cm^2/V·s with the Chrompack capillary. The other two capillaries showed very similar mobility values of $1 \cdot 10^{-3}$ cm^2/V·s. This demonstrates that it is very problematic to transfer a separation from one type of capillary to another, because the mobilities may vary by more than 30% at higher pH values. In the standard CE mode (detection at the cathode) a high EOF is desirable to transport anions to the detector. The smaller the EOF at high pH, the longer the analysis time can become; it might even happen that fast anions are not transported to the detector and are lost for analysis.

As discussed in the Introduction, it is possible to determine the specific surface charges on the capillary wall from EOF measurement. In a first approximation one can assume that the inflection point around pH 5.5 of the curves shown in Fig. 3 corresponds to the pK_s values of the different types of quartz. Therefore, at pH 9 the surface silanols on the capillary wall should be totally dissociated. Consequently, it should be possible to determine from the magnitude of the EOF the concentration of surface silanols. As discussed already, the EOF is caused by differences in the zeta potential, which is active at the boundary of the stagnant and diffuse double layer. However, the charge density at this layer is a function of the surface silanols. The differences between this surface silanol concentration from EOF measurements and those calculated from crys-

talline quartz surfaces have already been discussed.

In Table III, the calculated surface concentrations of silanol groups are summarized. Because there is no linear correlation between mobility and surface charge density, the differences in silanol surface concentrations are higher than the differences in mobilities. The smallest value of 0.5 μmol/m^2 was calculated for the Chrompack capillary, whereas for the SGE capillary a value more than twice as high was calculated.

High silanol concentrations are certainly advantageous when chemical surface modification has to be achieved. The stability and the effectiveness of the binding increase with increasing number of bonds of the coating to the surface. On the other hand, the silanol groups are active sites for cation exchange. Positively charged solutes, especially proteins, interact with these sites. This may cause a decrease in efficiency or a total loss of samples. Capillaries with a lower concentration of surface silanols may have advantages for these separations.

Characterization of coated capillaries

The effectiveness of coating procedures can only be measured in CE via the variation of the EOF or the efficiency variations of solutes which may interact with the silanols as a function of coating procedure. Non-polar coatings can be additionally characterized by GC measurements [19] via retention parameters. From the temperature dependence of retention parameters, Van 't Hoff plots can be generated, the slopes of the curves being proportional to the heat of sorption of the solutes on the surface.

Coatings with linear acrylamide prepared by transferring a method developed for the preparation of LC stationary phases [30] to CE capillaries have some advantages with respect of stability and efficiency in protein separation [13]. The crucial step in the preparation of this type of stationary phase is the reaction of surface silanols with trichlorovinylsilane. In a second step the introduced bonded vinyl groups are copolymerized with acrylamide and other acrylic acid derivatives. In LC it has been found that the better the first reaction shields the silanols, the better the stability of the stationary phase becomes, and the less important is the contribution of silanols to solute retention. Therefore, a method was developed to characterize via GC measurements the CE capillaries modified with vinylsilane in different ways. This step is of paramount importance because with capillaries modified with polar groups, such as linear acrylamide, it is hardly possible to differentiate between the influence of unshielded silanols and that of the polar bonded groups.

The properties of capillaries reacted with vinylsilanes in different modes were compared with those of the untreated capillary. Capillary V1 was prepared with trimethoxyvinylsilane and *n*-butylamine in aqueous suspension. Capillary V2 was obtained after treating the capillary with trichlorovinylsilane in toluene and an additional trimethylamine treatment. Capillary V3 was prepared in the same way as capillary V2, but without the introduction of a catalyst (for details, see Experimental).

TABLE III

SPECIFIC SURFACE CHARGES FOR DIFFERENT FUSED-SILICA CAPILLARIES (CALCULATED FROM EOF AT pH 9) (ACCORDING TO EQN. 4)

Supplier	μ_{eo} (cm^2/V·s × 10^{-4})	ζ (mV)	σ (μC/cm^2)	σ/F [a] (μmol/m^2)
Microquartz	10.59	134	7.93	0.82
SGE	12.00	152	11.90	1.17
Chrompack	9.02	114	5.33	0.55
Polymicro	10.91	138	8.58	0.91

[a] F = 96 500 C/mol.

The gas chromatographic characterization was done with two different aspects. First, to measure the hydrophobic properties, the retention of *n*-heptane was studied. This molecule should show only the contribution of the bonded vinyl groups. Second, diethyl ether as a probe should demonstrate the polar interaction with the residual silanols.

In Fig. 4, the Van 't Hoff plot for heptane with the three different stationary phases is shown. The retention of heptane with the plain quartz capillary is very low, as it is with the vinyl-coated capillary prepared without a catalyst. The slope and hence the heat of sorption are identical and very small ($\Delta H = -13.5$ kJ/mol) in this case. The reaction of the silanes with silanols improves in the presence of a catalyst. As can be seen, for the other two capillaries not only are higher retention values obtained, but also the heat of sorption is much higher and relatively similar (V1, $\Delta H = -49.1$ kJ/mol; V2, $\Delta H = -55.9$ kJ/mol). If one assumes that with *n*-heptane only dispersive forces contribute to retention, it can be concluded that without a catalyst a silanization reaction hardly takes place. With the two other capillaries almost identical coatings must have been obtained with slightly higher coverage for V2.

The retention behaviour of diethyl ether and its temperature dependence, shown in Fig. 5, are much more difficult to explain. Diethyl ether interacts with silanol groups, and consequently the absolute retention on the uncoated capillary is high, as is the heat of sorption ($\Delta H = -53$ kJ/mol). Surprisingly low retention values were measured with capillary V3 prepared without a

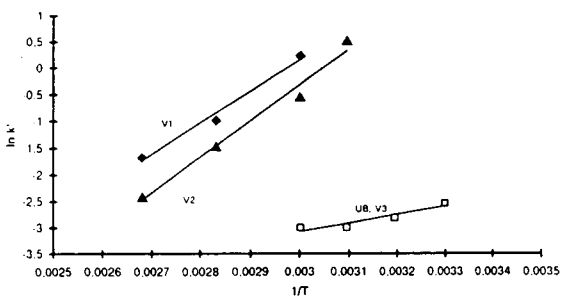

Fig. 4. Ln *k' versus* $1/T$ (Van 't Hoff plot) for heptane with different modified and unmodified capillaries.

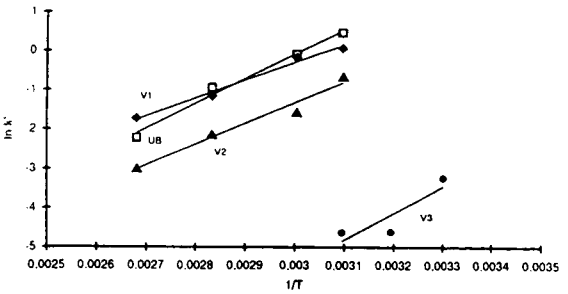

Fig. 5. Ln *k' versus* $1/T$ (Van 't Hoff plot) for diethyl ether with different modified and unmodified capillaries.

catalyst. However, the heat of sorption (slope) for diethyl ether is of the same order of magnitude ($\Delta H = -56$ kJ/mol) as with the untreated capillary. This indicates that the main contribution to retention is the interaction of diethyl ether with the silanol groups. Because of the small number of bonded groups, the dispersive interaction of diethyl ether is negligible. With the two other capillaries, where a higher coating was achieved, two mechanisms contribute to the retention of diethyl ether with the surface: dispersive forces and silanophilic interactions. Again, the heats of sorption determined for both capillaries are very similar, making it impossible to differentiate between the two mechanisms. The slightly higher value determined with capillary V2 ($\Delta H = -44.2$ kJ/mol) makes it feasible that dispersive interactions are the main contribution to retention of diethyl ether, and that here a slightly larger number of vinyl groups has been bonded to the surface.

In good correspondence with these findings are the conclusions that can be drawn from the EOF measurements as a function of pH shown in Fig. 6. By chemical modification the number of surface silanols and, consequently, the EOF are reduced. As can be seen in Fig. 6, the EOF with capillary V3 (slightly coated) shows a sigmodial shape identical with that for the uncoated capillary. At pH 9 the EOF is still 65% of that with the uncoated capillary. With the two other capillaries at pH 9 the EOF is only 30% of the initial value. Also, the shape of the curve is slightly different. Up to pH 6 the EOF is almost unaffected by pH. This can be explained by the finding from silica modification that mainly the

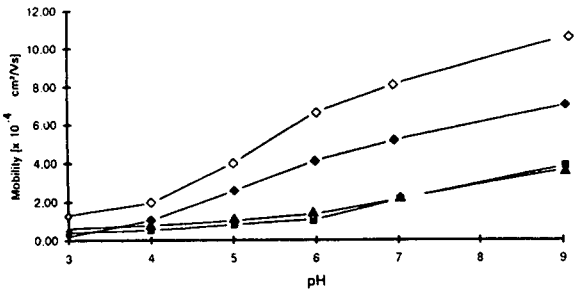

Fig. 6. EOF *versus* pH curves for modified and unmodified capillaries. Conditions as in Fig. 3. ▲ = V1; □ = V2; ◆ = V3; ◇ = uncoated.

highly acidic surface silanols react during silanization whereas the less acidic vicinal groups remain unreacted on the surface [31]. These groups are deprotonated at higher pH and only then contribute to the EOF.

There is a good correlation between the GC measurements and the dependence of EOF on pH. Consequently, it is possible to characterize at least non-polar coated capillaries. GC retention is dependent on the number of bonded groups. Further work is required in order to be able to obtain at least some insight into the total number of bonded groups. EOF measurements are correlated with the charge density at the double layer, which at least in part is influenced by the number of bonded groups on the surface. Both methods can therefore be used to obtain information on the surface properties of capillaries for CE.

ACKNOWLEDGEMENT

Financial support of this work by the Deutsche Forschungsgemeinschaft, Bonn-Bad Godesberg, and the Fonds der Chemischen Industrie is deeply appreciated.

REFERENCES

1 J. Jorgenson and K. Lukacs, *Science*, 222 (1983) 266–272.
2 S.A. Swedberg, *Anal. Biochem.*, 185 (1990) 51.
3 A. Balchumas and M. Sepaniak, *Anal. Chem.*, 59 (1987) 1466–1470.
4 A. Dougherty, C. Woolley, D. Williams, D. Swaile, R. Cole and M. Sepaniak, *J. Liq. Chromatogr.*, 14 (1991) 907–921.
5 M. Sepaniak, D. Swaile, A. Powell and R. Cole, *J. High Resolut. Chromatogr.*, 13 (1990) 679.
6 G. Bruin, J. Chang, R. Kuhlman, K. Zegers, J. Kraak and H. Poppe, *J. Chromatogr.*, 471 (1989) 429–436.
7 G. Bruin, R. Huisden, J. Kraak and H. Poppe, *J. Chromatogr.*, 480 (1989) 339–349.
8 R. McCormick, *Anal. Chem.*, 60 (1988) 2322–2328.
9 Y.-F. Maa, K. Hyver and S. Swedberg, *J. High Resolut. Chromatogr.*, 14 (1991) 65.
10 S. Hjerten, *J. Chromatogr.*, 347 (1985) 191–197.
11 S. Hjerten, K. Ellenbring, F. Kilar and J. Kiao, *J. Chromatogr.*, 403 (1987) 47–61.
12 K. Cobb, V. Dolnik and M. Novotny, *Anal. Chem.*, 62 (1990) 2478–2483.
13 J. Kohr and H. Engelhardt, *J. Microcol. Sep.*, 3 (1991) 491–495.
14 D. Bentrop, J. Kohr and H. Engelhardt, *Chromatographia*, 32 (1991) 171–178.
15 M. Strege and A. Lagu, *Anal. Chem.*, 63 (1991) 1233–1236.
16 C. Bolger, M. Zhu, R. Rdiguez and T. Wehr, *J. Liq. Chromatogr.*, 14 (1991) 895–906.
17 F. Regnier and J. Towns, *J. Chromatogr.*, 516 (1990) 69–78.
18 S. Terabe, H. Utsumi, K. Otsuka, T. Ando, T. Inonata, S. Kuze and Y. Hanaoka, *J. High Resolut. Chromatogr. Chromatogr. Commun.*, 9 (1986) 666.
19 J. Lux, H. Yin and G. Schomburg, *J. High Resolut. Chromatogr.*, 13 (1990) 145.
20 S. Mayer and V. Schurig, *J. High Resolut. Chromatogr.*, 15 (1992) 129–131.
21 K.D. Lukacs and J.W. Jorgenson, *J. High Resolut. Chromatogr. Chromatogr. Commun.*, 8 (1985) 407.
22 H. Engelhardt and M. Jungheim, *Chromatographia*, 29 (1990) 59–69.
23 H. Engelhardt, H. Löw and W. Götzinger, *J. Chromatogr.*, 544 (1991) 371–379.
24 K. Grob, *Making and Manipulating Capillary Columns for Gas Chromatography*, Hüthig, Heidelberg, 1986.
25 R.K. Iler, *The Chemistry of Silica*, Wiley, New York, 1979.
26 A.W. Adamson, *Physical Chemistry of Surfaces*, Wiley, New York, 4th ed., 1982.
27 J.T. Davies and E.K. Rideal, *Interfacial Phenomena*, Academic Press, New York, 1961.
28 A. Bard and L. Faulkner, *Electrochemical Melthods: Fundamentals and Aplications*, Wiley, New York, 1980.
29 R.J. Nelson, A. Paulus, A.S. Cohen, A. Guttman and B.L. Karger, *J. Chromatogr.*, 480 (1989) 111–127.
30 H. Engelhardt, H. Löw, W. Eberhardt and M. Mauss, *Chromatographia*, 27 (1989) 535–543.
31 M. Mauss and H. Engelhardt, *J. Chromatogr.*, 371 (1986) 235–242.

Journal of Chromatography A, 652 (1993) 317–327
Elsevier Science Publishers B.V., Amsterdam

CHROM. 25 151

Thermally induced fluctuations of the electric current and baseline in capillary electrophoresis

Michael S. Bello[☆], Patrizia de Besi and Pier Giorgio Righetti*

Faculty of Pharmacy and Department of Biomedical Sciences and Technologies, University of Milan, Via Celoria 2, Milan 20133 (Italy)

ABSTRACT

Fluctuations of the electric current and baseline that appear in air-cooled capillaries when a high voltage is applied were studied both theoretically and experimentally. The theoretical part relates the amplitudes of the baseline and electric current fluctuations with the fluctuations of the buffer temperature originating from the thermal fluctuations at the outer surface of the capillary. It is shown theoretically that an increase in the outer diameter of the capillary decreases the amplitudes of the electric current and the baseline fluctuations and does not lead to a substantial elevation of the buffer temperature. Experiments confirmed the mutual correlation of the baseline and current fluctuations as predicted by the theory. Jacketing of the outer surface of the capillary with a polymer tubing is shown to be useful for reducing the fluctuations in capillary electrophoresis units lacking liquid cooling.

INTRODUCTION

It is observed, we believe, by almost every user of a capillary electrophoresis (CE) unit lacking liquid cooling that, when a relatively high voltage is used for an analysis, substantial fluctuations of the electric current and UV detector baseline occur.

The electric current stability in CE having cooling provided by natural air convection, forced air convection and solid thermostat cooling has been studied by Nelson *et al.* [1], who showed that the highest current fluctuations occur for a capillary cooled by natural air convection, which is the least effective means of cooling. When a capillary was subjected to forced air cooling or to solid-state thermoelectric cooling, the amplitude of the fluctuations decreased significantly for the case of forced air cooling and vanished for thermoelectric cooling. It is clear that the amplitude of the electric current fluctuations depends on the effectiveness of the heat removal from the capillary. However, the origin of the fluctuations has not been investigated.

As many of the commercially available and laboratory-made CE units lack liquid or solid thermostat cooling (which appear to be the best means of avoiding difficulties with internal overheating and current fluctuations), the problem of suppressing the electric current and baseline fluctuations remains important. Our preliminary experiments and the results presented by Nelson *et al.* [1] show that the relative amplitude of the electric current fluctuations increases with the applied voltage much faster than the square root of the relative absolute buffer temperature as one might expect according to general thermodynamic reasoning.

This paper investigates the nature and mechanism of the current and baseline fluctuations in capillary electrophoresis. The paper consists of theoretical and experimental parts. The theoretical part relates the amplitudes of the electric

* Corresponding author.
☆ Permanent address: Institute of Macromolecular Compounds, Bolshoi 31, 199004 St. Petersburg, Russian Federation.

0021-9673/93/$06.00

current and baseline fluctuations with the parameters of the capillary, cooling system and operating conditions. The theory predicts that an increase in the capillary outer diameter (O.D.) reduces the fluctuations whereas the buffer temperature in the capillary lumen does not increase significantly. The experimental part confirms the main results of the theory and gives examples of the reduced current and baseline fluctuations in the air-cooled capillary. A decrease in the fluctuations is obtained by jacketing the capillary with a polymer tubing.

THEORY

The thermal theory of capillary electrophoresis [2–8] deals with steady-state [2–6] and unsteady, *i.e.*, varying with time [7,8], distributions of the buffer temperature within the capillary. In the following section we present the basic theory necessary for further considerations.

General

Let us assume the buffer temperature within the capillary to be uniform along the capillary axis and the capillary to be air-cooled. The first condition together with the suggestion that the electric conductivity is linearly dependent on the buffer temperature gives for the electric current

$$I = I_0[1 + \alpha(T - T_0)] \tag{1}$$

$$I_0 = V/r_0 \tag{2}$$

where T_0 denotes a reference temperature, T is the buffer temperature averaged over the cross-section of the capillary, I is the electric current in the capillary, α is the thermal coefficient of the electric conductivity, I_0 is the value of the current that would be in the capillary if the temperature of the buffer is equal to the reference temperature, V is the applied voltage and r_0 is the capillary electrical resistance at reference temperature. Eqn. 1 represents the linear dependence of the electric current on the buffer temperature and eqn. 2 is Ohm's law.

The second condition implies that the temperature profile within the capillary lumen is flat and the inside wall temperature is approximately equal to the buffer average temperature [7,8]. The average buffer temperature at steady state may be expressed as

$$T_S = T_C + \frac{\Delta T_{ref}[1 + \alpha(T_C - T_0)]}{2Bi_{OA} - \alpha\,\Delta T_{ref}} \tag{3}$$

$$\Delta T_{ref} = \frac{VI_0}{\pi L \chi_L} \equiv \frac{V^2}{\pi L \chi_L r_0} \equiv \frac{E^2 \sigma_0 D_L^2}{4\chi_L} \tag{4}$$

where T_S is the steady-state average temperature of the buffer, Bi_{OA} is the overall Biot number representing an integral relative thermal conductivity of the capillary and the cooling system, ΔT_{ref} is the characteristic temperature of the Joule heating, T_C is the temperature of the coolant, V is the applied voltage, χ_L is the buffer thermal conductivity, E is the intensity of the electric field, σ_0 is the buffer conductivity at the reference temperature, D_L is the capillary inner diameter (I.D.) and L is the capillary length. The equation for the overall Biot number is given in the Appendix.

Eqn. 3 is derived by rearranging terms in eqn. 17a in ref. 7 and is valid (as the original equation is) for relatively small values of Bi_{OA}, when terms having the order of Bi_{OA} are negligible in comparison with unity. This is usually the case with the air-cooled capillaries being considered here. Eqn. 3 agrees with the approximate eqn. 12 of Gobie and Ivory [6] for $Bi_{OA} \ll 1$ and if T_C is set equal to T_0 in eqn. 3. When comparing these two equations, note that Bi_{OA} as defined in ref. 6 is twice as large as ours. Eqn. 4 gives three equivalent equations for the reference temperature.

It is useful to introduce a dimensionless function which would show the influence of the Joule heating on the electric current:

$$f = \left(\frac{2Bi_{OA}}{\alpha\,\Delta T_{ref}} - 1\right)^{-1} \tag{5}$$

The dimensionless function f will be called below the "function of the electric current non-linearity". It can be expressed as follows:

$$f = \frac{I}{I_C} - 1$$
$$I_C = I_0[1 + \alpha(T_C - T_0)] \tag{6}$$

where I_C is the value of the electric current that

would flow through the capillary in the absence of the Joule heating at a temperature equal to that of the coolant.

Eqn. 3 for the buffer steady-state temperature may be rewritten as

$$T_S = T_C + f\left(\frac{1}{\alpha} + T_C - T_0\right) \quad (7)$$

For low applied voltages and good cooling conditions, f is negligibly small whereas if $\alpha\,\Delta T_{ref}$ approaches $2Bi_{OA}$, values of f and, thus, the buffer temperature, electric current and transient time grow infinitely [6,8]. This effect has been called "autothermal runaway" [6].

In order to analyse the influence of variations of the coolant temperature on the buffer temperature and the electric current, we consider first relatively slow variations of the coolant temperature. A fluctuation of the coolant temperature is regarded as either fast or slow by comparing its characteristic time (the time it takes the fluctuation to occur) with the characteristic transient time of the capillary (the time that is necessary to reach steady-state current and temperature after application of a voltage) [7,8]. The latter depends on the outer and inner capillary diameters, applied voltage and cooling conditions. If the fluctuation time is much longer than the characteristic transient time we call the fluctuation "slow" and, *vice versa*, if it is shorter we call it "fast".

Slow fluctuations of the coolant temperature

A characteristic transient time τ for the commonly used air-cooled capillary of *ca.* 360–385 μm O.D. is about 1 s [8]. If a fluctuation of coolant temperature occurs within 10 s or longer it may be considered as quasi-static. This means that the buffer temperature and electric current fluctuations follow in time the coolant temperature. Thus, the buffer temperature and the electric current are given by eqns. 1 and 2.

Assume that the coolant temperature fluctuates during a relatively long time (in the sense discussed above) from a certain value T_C to $T_C + |\delta T_C|$. By differentiating eqns. 1 and 7 and taking into account eqns. 5 and 6, one obtains the following expressions:

$$|\delta T| = (f+1)|\delta T_C| \quad (8a)$$

$$\frac{|\delta I|}{I_0} = \alpha(f+1)|\delta T_C| \quad (8b)$$

where $|\delta T_C|$ is the amplitude of the fluctuation of the coolant temperature, $|\delta T|$ and $|\delta I|$ are the amplitudes of the fluctuations of the buffer temperature and the electric current, respectively, and $f+1$ is the derivative of the buffer temperature with respect to the coolant temperature.

It is seen from eqn. 8a that $(f+1)$ is a magnification factor for the buffer temperature which is never less than unity. For example, for an air-cooled (forced) capillary Bi_{OA} is approximately equal to 0.05. Assume that a buffer solution has $\alpha \approx 0.02$ (K^{-1}), $\chi_L \approx 0.6$ (W/mK) and $\sigma_0 = 6$ (mS/cm). A capillary of 75 μm I.D. and 50 cm long filled with this buffer has at 25°C a resistance $r_0 = 1.89 \cdot 10^8\ \Omega$. For $V = 20$ kV, eqn. 4 gives $\Delta T_{ref} = 2.21$°C and for f from eqn. 5 it follows $f \approx 0.8$. Then eqn. 8a shows that an increase of the coolant temperature of 1°C leads to an increase of 1.8°C in the buffer temperature and eqn. 8b gives 3.6% for the relative amplitude of the electric current fluctuation. This effect is relevant in the vicinity to the critical point of the autothermal runaway. If 10 kV are applied, the magnification factor $(f+1)$ is only 1.01. For large Bi_{OA} corresponding to very good cooling conditions or low applied voltages, f approaches zero and $f+1$ approaches unity.

Fast fluctuations of the coolant temperature

The case of fast fluctuations is not so straightforward as that of slow fluctuations, as the steady-state eqns. 1 and 2 are no longer applicable. According to our previous results [7], time evolution of the average buffer temperature is approximately governed by an ordinary differential equation:

$$\frac{dT}{dt} = -\frac{1}{\tau_1}(T - T_S) \quad (9a)$$

with the initial condition

$$T(0) = T_C^0 \quad (9b)$$

where t is the time, T_C^0 is the value of the coolant

temperature at the moment when the voltage has been applied and τ_1 is the characteristic transient time. In ref. 8 the transient time τ_{tr} was also introduced as the time necessary to reach the steady state and is equal to the characteristic transient time τ_1 multiplied by a factor of 4. The characteristic time τ_1 may be calculated by a procedure described in ref. 7. Additionally, an approximate equation for a capillary having a thick polymer coating will be derived below. The temperature T_S in eqn. 9a now depends on time as it includes the time-dependent coolant temperature.

Assume the coolant temperature to be the sum of the constant value T_C^0 and a relatively small fluctuation δT_C:

$$T_C = T_C^0 + \delta T_C \tag{10}$$

In order to estimate the influence of the coolant temperature fluctuations on the buffer temperature, we represent the temperature fluctuation of the coolant as a harmonically oscillating function:

$$\delta T_C = |\delta T_C| \cos \omega t \tag{11}$$

where ω is the circular frequency of the fluctuation.

The solution to eqns. 9a and 9b with T_C given by eqns. 10 and 11 is

$$T = T_C^0 \exp(-t/\tau_1) + T_S^0[1 - \exp(-t/\tau_1)] - \frac{|\delta T_C|(f+1)\exp(-t/\tau_1)}{1+\omega^2\tau_1^2} + \frac{|\delta T_C|(f+1)\cos(\omega t - \varphi)}{\sqrt{1+\omega^2\tau_1^2}} \tag{12}$$

where $\varphi = \arctan(\omega\tau_1)$.

It is seen from eqn. 12 that an oscillating part of the buffer temperature representing the fluctuation is given by

$$\delta T = |\delta T| \cos(\omega t - \varphi) \tag{13a}$$

$$|\delta T| = \frac{(f+1)|\delta T_C|}{\sqrt{1+\omega^2\tau_1^2}} \tag{13b}$$

Obviously, eqn 13b reduces to eqn. 8a for a limiting case of slow fluctuation ($\omega\tau_1 \ll 1$).

An important result can be drawn from an analysis of eqn. 13b: one concludes that the amplitude of fluctuations decreases with increasing characteristic transient time τ_1 and/or increasing fluctuation frequency. In other words, high-frequency fluctuations are filtered if the characteristic time τ_1 is large.

A reader familiar with electronics has probably found an analogy between the reaction of the buffer temperature to the external temperature fluctuations with the reaction of an RC integrating circuit to the electric current oscillations.

Fluctuations of the coolant temperature

Above we considered the coolant temperature fluctuations to originate from an external source. Most probably, these fluctuations originate from the temperature pulsations in the turbulent air boundary layer flowing around the capillary. The air flow produced by a fan is turbulent, which means that the air velocity pulsates in time. There are also vortices of different scale depending on the fan power and geometry of the box containing the capillary. We believe that these vortices and pulsations produce temperature fluctuations near the external surface of the capillary which has a temperature higher than that of cooling air. If so, then the amplitude of the temperature fluctuations must be proportional to the temperature difference between the temperature of the air far from the capillary and the temperature of the external surface of the capillary:

$$|\delta T_C| = \gamma(T_{EX} - T_C) \tag{14}$$

where T_{EX} is the temperature of the external surface of the capillary and γ is the coefficient of proportionality reflecting aerodynamic properties of the system.

In order to find T_{EX} we use eqns. A1.3–A1.5a from ref. 7 and substitute the exact solution involving Bessel functions by the approximate eqn. 3 and after some algebra (see the Appendix for the definitions of R_P and h) finally derive the following expression:

$$T_{EX} - T_C = (T_S - T_C)\frac{\chi_L Bi_{OA}}{hR_P} \tag{15}$$

and by using eqn. 14 we find for the amplitude of coolant temperature fluctuations

$$|\delta T_C| = \gamma(T_S - T_C)\frac{\chi_L Bi_{OA}}{hR_P} \quad (16)$$

It is seen from this equation that the higher the buffer temperature the higher is the amplitude of fluctuations of the coolant temperature at the external surface of the capillary.

Baseline and electric current fluctuations

It is reasonable to suppose that fluctuations of the buffer temperature are responsible for both the electric current and the baseline fluctuations. The latter is the consequence of the temperature dependence of the refractive index of water. Therefore, when reducing the amplitude of the fluctuations of the buffer temperature, one reduces the amplitude of the baseline and electric current fluctuations.

By substituting eqn. 14 into eqn. 13b, the following expression for the amplitude of the buffer temperature fluctuations is derived:

$$|\delta T| = \frac{(f+1)\gamma(T_{EX} - T_C)}{\sqrt{1+\omega^2\tau_1^2}} \quad (17)$$

where the temperature of the capillary external surface is given by eqn. 15.

As a result of eqn. 16, the following equation for the relative amplitude of the electric current fluctuations can be derived from eqns. 5, 18b, 15 and 17:

$$\frac{|\delta I|}{I} = f\gamma \cdot \frac{\chi_L Bi_{OA}}{hR_p\sqrt{1+\omega^2\tau_1^2}} \quad (18)$$

Eqn. 18 predicts direct proportionality of the relative amplitude of the current fluctuations to the function of electric current non-linearity f. The latter, as is seen from eqn. 5, can be measured experimentally. Therefore, if the validity of eqn. 18 is proved experimentally, it justifies the theory developed above.

It follows directly from eqn. 17 that the amplitude of the buffer temperature fluctuations may be decreased by decreasing the difference between the surface temperature of the capillary and that of the coolant and by increasing the characteristic transient time. The next section shows that these goals may be reached simply by increasing the thickness of the capillary polymer coating.

Increasing the polymer coating thickness

At first glance, increasing of the coating thickness (*i.e.*, the capillary O.D.) seems to cause a significant elevation of the buffer temperature owing to some prevention of the heat removal. However, a variation of the radius of the polymer coating affects simultaneously the overall Biot number, the heat transfer coefficient and the characteristic transient time. The first two parameters determine the increase in the buffer temperature provided that other parameters are fixed. Fig. 1 shows the dependences of the buffer temperature and the temperature of the external surface of the capillary on the radius of the polyimide coating. The buffer temperature was calculated by using eqn. 3. Eqn. 15 was used for the temperature of the external surface.

The capillary and buffer parameters were the same as those which were used in the example following eqn. 8b. Additionally, we specified the radius of the fused-silica wall $R_W = 170$ μm,

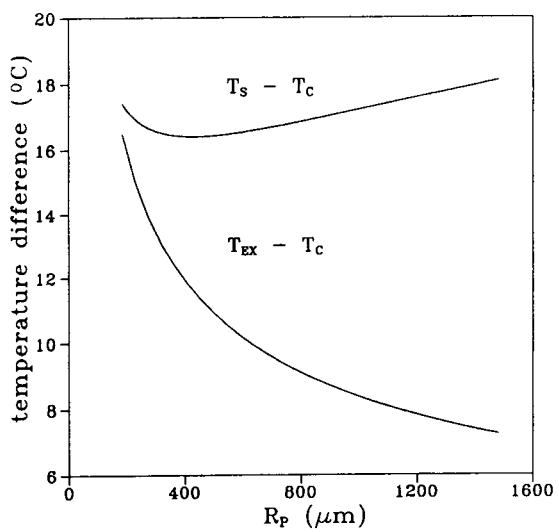

Fig. 1. Dependences of the buffer temperature (upper curve) and the temperature of the external surface (lower curve) on the radius of the polyimide coating (simulation). The temperature difference scale on the ordinate represents the temperature above that of the coolant. The capillary and the buffer parameters are given in the text.

thermal conductivity of the wall $\chi_W = 1.5$ W/mK, thermal conductivity of the polyimide coating $\chi_P = 0.15$ W/mK and heat transfer coefficient $h = 170$ W/m^{2}K, $V = 15$ kV, O.D. = 370 μm and $Bi_{OA} = 0.05$. The value of the heat transfer coefficient h is in agreement with that found in ref. 1. The constant A in eqn. A.2 (see Appendix) is approximately equal to unity if R_P is measured in metres. It is seen from Fig. 1 that an increase in the polyimide coating thickness leads to a significant decrease in the external surface temperature whereas the buffer temperature has a shallow minimum and then increases slightly. Therefore, we expect a decrease in the amplitude of the coolant temperature fluctuations (eqn. 14), lowering the buffer temperature fluctuations (eqns. 8a and 13b) and, hence, a decrease in the electric current and the baseline fluctuations when the thickness of the polyimide coating increases. The decrease in the external surface temperature with increase in the capillary O.D. follows from the facts that the area of the capillary external surface increases proportionally to the capillary O.D. whereas the heat transfer coefficient decreases more slowly (see eqn. A.2), and that the heat flux remains approximately the same.

Another effect of the large O.D. is an increase in the characteristic transient time. In order to derive an estimate for the characteristic transient time for the capillaries having a thick coating and a low coefficient of heat transfer, we assume the electric conductivity to be independent of temperature and the capillary to be uniform and to have thermal properties equal to those of polyimide. The characteristic transient time for this system is determined as [7,9]

$$\tau_1 = \frac{R_P^2}{\kappa_P} \cdot \lambda_1^{-2} \tag{19}$$

where κ_P is the thermal diffusivity of the polyimide and λ_1 is the first root of the following equation:

$$J_0(\lambda) - \left(\frac{\chi_P}{hR_P}\right)\lambda J_1(\lambda) = 0 \tag{20}$$

where J_0 and J_1 are Bessel functions of the first kind. The first root of eqn. 20 can be found in ref. 9.

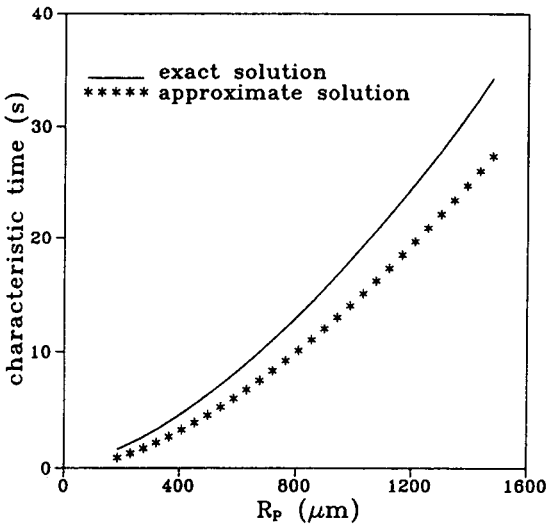

Fig. 2. Characteristic transient time as a function of the radius of the polyimide coating (simulation). Parameters of the buffer, capillary and applied voltage are the same as in Fig. 1. The solid line is the exact solution [7] and the asterisks are the estimates given by eqns. 19 and 20.

The characteristic transient time τ_1 as a function of the polyimide radius is shown in Fig. 2. The solid line is the exact solution obtained by the procedure described in detail in ref. 7 and the asterisks represent the estimated values according to eqns. 19 and 20. Fig. 2 illustrates the growth of transient time with increase in polyimide thickness for the same parameters as in Fig. 1. It is also seen that the approximate eqns. 19 and 20 may be used as an estimate of the characteristic transient time.

The large values of the characteristic transient time shown in Fig. 2 have the positive effect of filtering and smoothing fluctuations of the coolant temperature at the external surface of the capillary, according to eqn. 17. Hence, the theory predicts that an increase in polyimide thickness reduces the amplitude of the fluctuations of the buffer temperature because of the decrease in the temperature of the external surface of the capillary and the increase in the characteristic transient time.

EXPERIMENTAL

This section presents experimental proof of the basic assumptions and results derived in the theoretical section. It also gives an example of

separations with a decreased amplitude of the baseline noise.

The main assumptions and results to be checked experimentally are the following: (1) the baseline signal depends on the buffer temperature and the baseline noise at high voltages is thermally induced; (2) fluctuations of the electric current are also caused by the fluctuations of the buffer temperature; (3) the amplitude of fluctuations of the coolant temperature at the external surface is proportional to the temperature difference between the surface and the coolant (eqn. 14); and (4) an increase in thickness of the polyimide coating decreases the surface temperature of the capillary and the characteristic transient time and thus decreases the amplitude of the baseline and electric current fluctuations.

Materials and methods

The following experimental procedure was utilized. During a run, progressively increasing voltages $V_1, V_2, \ldots, V_j, \ldots, V_n$ were applied, for certain time intervals Δt, to the capillary filled with the buffer solution. The electric current and UV detector signal were monitored simultaneously at a rate of four points per second and stored on the hard disk of a computer. Mean values of the electric current and the baseline were calculated for the time intervals $\overline{\Delta t} = \Delta t - \tau_{tr}$, where τ_{tr} is the transient time necessary to obtain a steady-state buffer temperature [8]. In order to eliminate the influence of slow baseline and current drifts, regression lines were calculated for each of the time intervals $\overline{\Delta t}$ and the amplitudes of the fluctuations were obtained as square roots of the mean squares about the regression.

Mean values of the electric current I_j corresponding to applied voltages V_j were used to find the I.D. of the capillary and calculate its overall Biot number and the temperature of the buffer, T_j [10,11]. In order to simulate a capillary with a very thick polyimide coating an ordinary capillary was covered with polymer tubing.

A Waters (Millipore, Milford, MA, USA) Quanta 4000 unit having fan cooling and a UV detector set at 254 nm was used. The unit was connected to a NEC APC 4 computer and the data were stored by using BASELINE 810 software. The voltages were turned on and off manually during the run. The data were translated into ASCII files and statistically processed by laboratory-written software. Calculation of the buffer temperature and of the I.D. were performed by using the CZEA software package developed in our laboratory [11]. A fused-silica capillary of 75 μm I.D., total length 50 cm, obtained from Polymicro Technologies (Phoenix, AZ, USA) was used. The buffer solution was 50 m*M* Na_2HPO_4 titrated to pH 6 with orthophosphoric acid. The specific conductivity of the solutions at 25°C was $\sigma_0 = 6.59 \pm 0.02$ mS/cm and its thermal coefficient was $\alpha = 0.0221 \pm 0.0003$ K^{-1}. (It was found that both the specific conductivity and thermal coefficient of the buffer solution depend on the degree of degassing. Thus, the specific conductivity and thermal coefficient of the same buffer stirred for 30 min without degassing were $\sigma_0 = 6.43 \pm 0.04$ mS/cm and $\alpha = 0.0233 \pm 0.0003$ K^{-1}, respectively. These values are different from those of the degassed buffer given above.) Deionized, distilled water was utilized. Before the experiments the buffers were degassed for 30 min with water pumps, under stirring. The tubings used for covering the capillaries were made of polyethylene (PE) with I.D. 1 mm and O.D. 2 mm, obtained from LKB, and PVC with I.D. 0.8 mm and O.D. 2.4 mm (Isoflex Kartell). Immobilines were obtained from Pharmacia-LKB (Bromma, Sweden). The length of the covered part of the capillary was 33 cm.

RESULTS AND DISCUSSION

Synchronized time behaviours of the electric current and the baseline UV signal obtained as described in the previous section are shown in Fig. 3a and b. The time intervals Δt during which a constant voltage was applied were 1.2 min, the idle time intervals were 0.6 min each and the time intervals used for data processing were $\overline{\Delta t}$ = 0.7 min. The progression of the applied voltages was from 2 to 18 kV in steps of 2 kV. Voltages are shown by the italic numbers in Fig. 3. The capillary was an ordinary one, without a cover. The actual I.D. (A.I.D.) and the overall

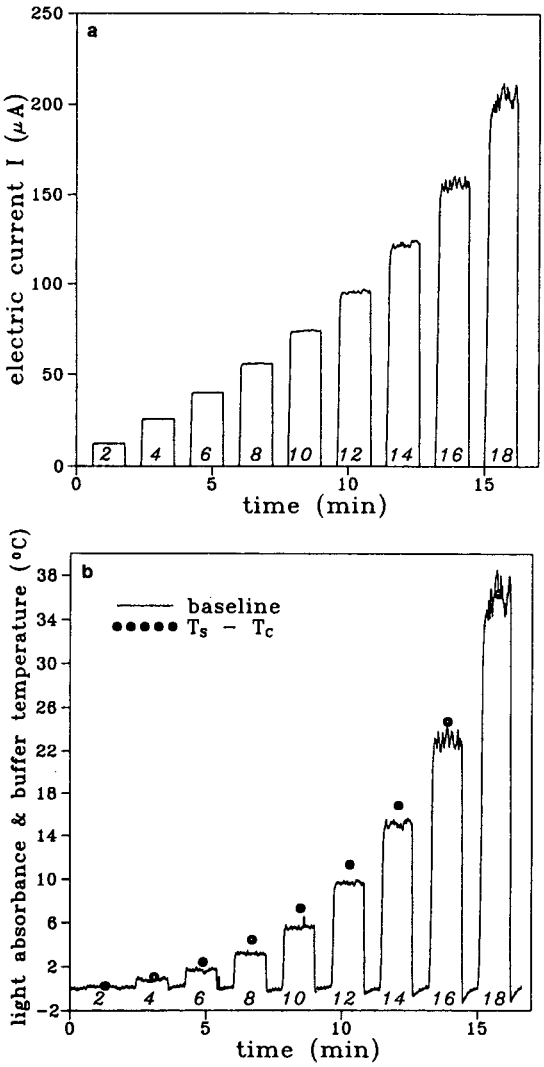

Fig. 3. (a) Electric current in the capillary for progressively increasing voltages in steps of 2 kV from 2 kV to 18 kV (italic numbers). $T_C = 27°C$. Parameters of the capillary and the buffer are given in the text. (b) Baseline for progressively increasing voltages (italic numbers, kV). The baseline is plotted in arbitrary units. Solid circles represent the elevation of the buffer temperature above that of the coolant. All parameters as in (a).

Biot number were found by statistical processing of the mean values of the electric current [11]: A.I.D. $= 77 \pm 1$ μm, $Bi_{OA} = 0.053 \pm 0.002$. The electrical resistance of the capillary at 25°C was $r_0 = (0.163 \pm 0.001) \times 10^9$ Ω.

It can be seen from Fig. 3a and b that starting from 12 kV both the electric current and baseline show fluctuations with an amplitude increasing with increments of the applied voltage. An analysis of the time dependences of the electric current and the baseline showed that the fluctuations of both values are correlated if voltage is applied. The highest correlation coefficient ρ between the baseline and electric current is $\rho = 0.88$ in the last time interval when a voltage of 18 kV is applied. (It is worth remembering that the correlation coefficient of two variables is equal to unity if these variables are linearly dependent and approaches zero for two stochastic independent variables. The correlation coefficient should not be confused with the regression coefficient, which is the slope of the regression line and can have any value for linearly dependent variables.) For lower voltages (*i.e.*, lower heat dissipation) the correlation coefficient becomes smaller and for 2 kV applied it is 0.07. These results show unambiguously that fluctuations of the baseline and the electric current occurring at high voltage originate from the same source.

Elevations of the buffer temperature for each time interval are shown as solid circles in Fig. 3b. We stress that these temperatures were calculated by using only mean values of the electric current. It can be seen that the baseline level

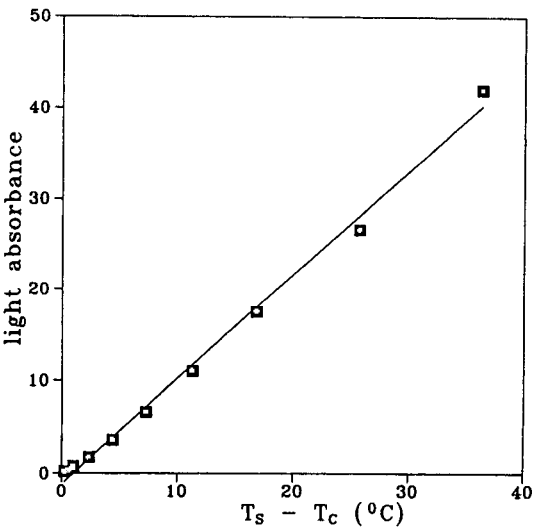

Fig. 4. Time-average values of the baseline (in arbitrary units) *versus* elevation of the buffer temperature. The solid squares are experimental points and the straight line is the regression line. Correlation coefficient $\rho = 0.997$.

follows the buffer temperature. Fig. 4 shows the mean values of the baseline signal *versus* the buffer temperature. The correlation coefficient between the buffer temperature and the mean baseline is $\rho = 0.996$. This value is very close to 1 and it justifies our assumption that the baseline signal is directly proportional to the temperature of the buffer.

Fig. 5 shows the relative amplitude of the fluctuations of the electric current *versus* the function of the current non-linearity. It can be seen that these variables are directly proportional to each other, as it is predicted by eqn. 18 (the correlation coefficient is 0.997). This result proves that fluctuations of the electric current are thermally induced. The same is valid for the baseline fluctuations, as they are correlated with the fluctuations of the electric current, as has been shown above. Additionally, this result proves our assumption in eqn. 16 and, therefore, the theoretical conclusions that an efficient means of suppressing fluctuations is to increase the thickness of the polymer coating.

An example of the time behaviour of the electric current in an ordinary capillary and in a capillary covered with polyethylene tubing is shown in Fig. 6. It can be seen that the amplitude of the current fluctuations for the jacketed capillary is significantly smaller than that for the ordinary capillary. The mean values of the electric current are higher for the covered capillary. This indicates that the buffer temperature in the covered capillary is higher than that in the ordinary capillary. The buffer temperature differences between the covered and the ordinary capillaries were found to be 1.1, 2, 4.2 and 10.2°C for 4, 8, 12 and 16 kV, respectively. The difference of 1.1°C for 4 kV is equal to the difference between the temperatures of the coolant corresponding to the two runs. The increase in buffer temperature for high voltages in the jacketed capillary relative to the ordinary capillary is due to additional thermal insulation caused by a layer of air between the capillary and the tubing covering the capillary. This effect was not taken into account by the theory and appears to be not very significant. Fig. 6 demonstrates also an increase in the transient time for a covered capillary in comparison with that of the ordinary capillary. Experiments with the capillary covered with PVC tubing showed that the buffer temperature remains approximately the same as in the capillary covered with the PE tubing whereas the transient time grows.

Fig. 7 compares the separation of a mixture of

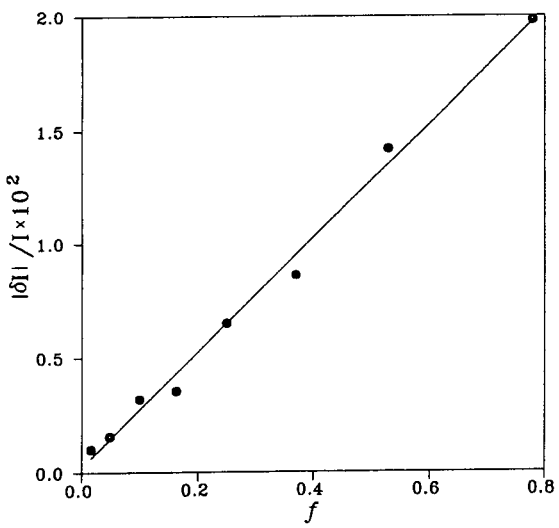

Fig. 5. Relative amplitude of the electric current fluctuations *versus* function of the current non-linearity. The circles are experimental points and the solid line is the regression line. Correlation coefficient $\rho = 0.996$.

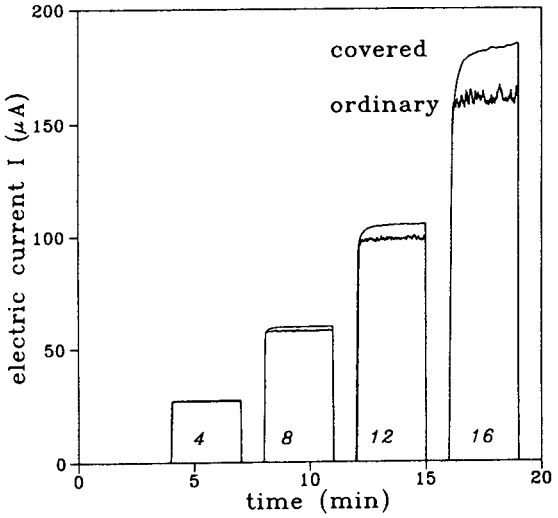

Fig. 6. Electric current in ordinary and covered capillaries for progressively increasing voltages. $T_C = 28.5$°C for the ordinary capillary and 29.4°C for the covered one.

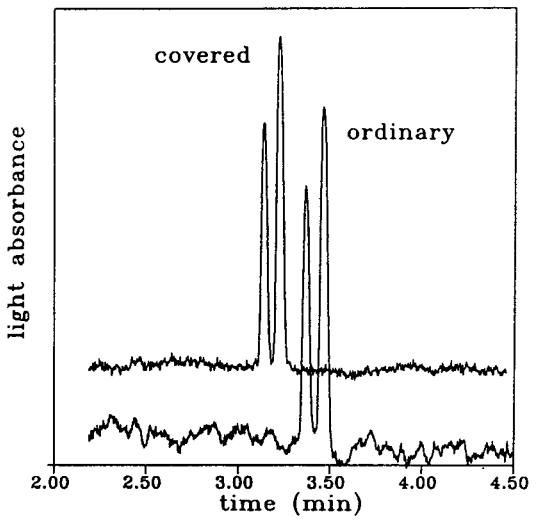

Fig. 7. Separation of a mixture of two Immobilines, pK = 8.5 and 9.3, in ordinary and covered capillaries. V = 14 kV.

two Immobilines of 0.4 mM concentration in the ordinary capillary and in that covered with PE tubing. It illustrates a large decrease in the baseline noise with the covered capillary. The migration time of the Immobilines in the covered capillary is less than that in the ordinary capillary because of an increase in buffer temperature by *ca.* 4°C.

CONCLUSIONS

The baseline and electric current fluctuations have been shown to originate from one source, namely fluctuations of the buffer temperature. The latter fluctuations are produced by the temperature fluctuations at the outer surface of the capillary, which increase with elevation of the buffer temperature. Theoretical solutions for the amplitudes of the baseline and electric current fluctuations predict a large increase near the point of autothermal runaway. It follows from the theory presented here that an increase in the capillary O.D. decreases the amplitudes of both the baseline and current fluctuations and does not lead to a substantial increase in the buffer temperature.

Experiments have shown that the elevation of the baseline that occurs when the applied voltage increases is directly proportional to the increase in buffer temperature. Theoretically predicted proportionality of the relative amplitude of the electric current fluctuations to the function of the current non-linearity has been confirmed experimentally. Jacketing of the capillary with polymer tubing is useful for decreasing baseline and electric current fluctuations.

SYMBOLS

Bi_{OA}	overall Biot number
E	electric field strength
f	function of electric current non-linearity
h	heat transfer coefficient
I	electric current
L	length of the capillary
R	radius
r	electric resistance of the capillary
T	temperature
t	time
V	voltage

Greek letters

α	temperature coefficient of electric conductivity of the buffer
χ	thermal conductivity
κ	thermal diffusivity
σ	specific conductivity
τ	transient time
ρ	correlation coefficient
ω	circular frequency of the temperature fluctuation

Subscripts

L, W, P	lumen, capillary wall and polyimide coating, respectively
0, C	at reference temperature and at the temperature of the coolant, respectively

ACKNOWLEDGEMENTS

This work was supported in part by grants from the Agenzia Spaziale Italiana (ASI, Rome) and the Consiglio Nazionale delle Ricerche (CNR), Progetto Finalizzato Chimica Fine II. M.S.B. thanks ASI for a fellowship at the University of Milan; P.D.B. is the winner of

the F. Marinotti fellowship from SNIA–BPD (Milan).

APPENDIX

For a capillary consisting of a fused-silica wall and coated with a layer of a polymer (polyimide), the reciprocal value of the Biot number is given by [1,4,6,7]

$$Bi_{OA}^{-1} = \chi_L[\ln(R_W/R_L)/\chi_W + \ln(R_P/R_W)/\chi_P + (R_P h)^{-1}] \quad (A.1)$$

where χ_W and χ_P are the thermal conductivities of the capillary wall and polymer coating, R_L, R_W and R_P are the radii of the capillary lumen, wall and the coating, respectively, and h is the heat transfer coefficient. R_P is equal to the capillary O.D.

For a forced air-cooled capillary the heat transfer coefficient is given by (see ref. 8 and references cited therein)

$$h = AR_P^{-0.6} \quad (A.2)$$

where A is a constant for a given coolant and fan rate.

REFERENCES

1 R.J. Nelson, A. Paulus, A.S. Cohen, A. Guttman and B.L. Karger, *J. Chromatogr.*, 480 (1989) 111–127.
2 M. Coxon and M.J. Binder, *J. Chromatogr.*, 101 (1974) 1–16.
3 J.F. Brown and J.O. Hinckley, *J. Chromatogr.*, 109 (1975) 218–224.
4 E. Grushka, R.M. McCormik and J.J. Kirkland, *Anal. Chem.*, 61 (1989) 241–246.
5 A.E. Jones and E. Grushka, *J. Chromatogr.*, 466 (1989) 219–225.
6 W.A. Gobie and C.F. Ivory, *J. Chromatogr.*, 516 (1990) 191–210.
7 M.S. Bello and P.G. Righetti, *J. Chromatogr.*, 606 (1992) 95–102.
8 M.S. Bello and P.G. Righetti, *J. Chromatogr.*, 606 (1992) 103–111.
9 H.S. Carslow and J.C. Jaeger, *Conduction of Heat in Solids*, Clarendon Press, Oxford, 2nd ed., 1959.
10 M.S. Bello, M. Chiari, M. Nesi, P.G. Righetti and M. Saracchi, *J. Chromatogr.*, 625 (1992) 323–330.
11 M.S. Bello, E.I. Levin and P.G. Righetti, *J. Chromatogr. A*, 652 (1993) 329.

Journal of Chromatography A, 652 (1993) 329–336
Elsevier Science Publishers B.V., Amsterdam

CHROM. 25 054

Computer-assisted determination of the inner temperature and peak correction for capillary electrophoresis

Michael S. Bello[☆], Eugene I. Levin[☆☆] and Pier Giorgio Righetti*

Faculty of Pharmacy and Department of Biomedical Sciences and Technologies, University of Milan, Via Celoria 2, Milan 20133 (Italy)

ABSTRACT

A statistical algorithm, software package and experimental validation are presented for the buffer temperature and electric current predictions and recalculations of peak migration times. The statistical procedure allows the calculation of the confidence intervals for the buffer temperature and electric current and shows the necessity for an accurate determination of the thermal coefficient of the buffer electric conductivity. The software package implements predictions of the buffer temperature, electric current and migration times for any given voltage and coolant temperature.

INTRODUCTION

The temperature dependence of the analyte migration velocity in capillary electrophoresis (CE) weakens the reproducibility of this powerful technique because the buffer temperature varies with the variations of the coolant temperature and with dissipation of the Joule heat. Even when thermostating a capillary within a CE unit, one can guarantee only a constant coolant temperature, whereas the inner temperature of the buffer may vary from run to run owing to the Joule heating if the buffer conductivity and/or voltage changes. In principle, direct measurements of the buffer temperature are possible [1] and, provided that the temperature dependence of migration velocities is known, the correct migration times can be derived. However, direct measurements need special equipment and can hardly be recommended as a tool for routine analysis. Temperature measurements by means of thermochromic solutions [2] are useful for obtaining the buffer temperature without a sample inside but the possibility of using them during an analytical run is not clear.

Another way to obtain the buffer temperature has been proposed recently [3]. The procedure of capillary calibration presented there consists of two steps: (1) at low voltage, when thermal effects are negligible, one determines the capillary resistance by measuring the electric current at this voltage; (2) then, also by measuring the electric current at a certain voltage, which must be high enough to produce thermal effects, one finds the overall Biot number, which is a thermal characteristic of a given capillary in a given cooling system.

These data are sufficient to predict the temperature and electric current within the capillary for any given voltage, provided that the buffer electric conductivity and its thermal coefficient are known. The usefulness of this procedure is that, after some algebraic transformations, it gives the buffer temperature and electric current not only for the calibrated capillary–buffer pair

* Corresponding author.
☆ Permanent address: Institute of Macromolecular Compounds, Bolshoi 31, St. Petersburg 199004, Russian Federation.
☆☆ Permanent address: A.F. Ioffe Physico-Technical Institute, St. Petersburg 194021, Russian Federation.

0021-9673/93/$06.00

but also for a capillary once calibrated and filled with another buffer of known properties. A shortcoming of the calibration procedure [3] is that it relies on intuitive definitions such as "low voltage" and "high voltage" and does not give a quantitative criterion for the accuracy of the predicted values.

It was verified by Hjertén [4] that the migration velocity of a species at constant current is almost independent of temperature. Later, many workers showed that migration velocities are directly proportional to the electric current even when the temperature elevation is significant (see references cited in ref. 5). These results had been summarized and extended by Lee and Yeung [5], who introduced a migration index as a quantity proportional to the integral of electric current over time. Therefore, an ability to predict buffer temperature, which is important in itself, allows the prediction of electric current and migration time for a given voltage on condition that a migration time for a certain voltage is known.

The first aim of this paper is to report a method for the calculation of confidence intervals for the temperature and electric current predicted on the basis of the calibration measurements. Confidence intervals reflect the accuracy of predictions and indicate if the calibration has been made properly, *i.e.*, the electric current has been measured at both low and high voltage.

We present here a software package for an IBM-compatible PC implementing the calibration procedure, statistical algorithm, temperature and current prediction and peak correction due to the temperature changes. The package works under Microsoft Windows version 3.0 or later and does not require any preliminary knowledge of the thermal theory of CE.

A typical example of calibration, temperature and electric current predictions and comparison of the calculated peaks with the experimental peaks is given.

THEORY

Statistical algorithm

The purpose of this statistical algorithm is to process the data obtained as a result of a calibration procedure and to give estimates of the electric current and buffer temperature and their confidence intervals. This paper calls "calibration" a series of measurements of electric current I and the coolant temperature T_C corresponding to the applied voltage V.

We shall base the following treatment on the relationships from ref. 6:

$$I\left(r_0 - \frac{\alpha V^2}{2Bi_{OA}\pi\chi L}\right) = [1 + \alpha(T_C - T_0)]V \quad (1)$$

$$T = T_C + \frac{V^2[1 + \alpha(T_C - T_0)]}{2Bi_{OA}\pi\chi L\left(r_0 - \frac{\alpha V^2}{2Bi_{OA}\pi\chi L}\right)} \quad (2)$$

$$r_0 = \frac{4L}{\kappa_0\pi d_L^2} \quad (3)$$

where I is the electric current, V the voltage, T the buffer temperature, κ_0 the specific conductivity of the buffer at the reference temperature T_0, α the temperature coefficient of electric conductivity, χ the thermal conductivity of the buffer, T_C the temperature of the coolant, r_0 the capillary resistance at reference temperature and in the absence of the Joule heating, d_L the capillary inner diameter, L the capillary length and Bi_{OA} is the overall Biot number.

For the ith measurement eqn. 1 can be rewritten in the following form:

$$r_i = a_i r_0 + b_i x, \quad i = 1, n \quad (4)$$

where $r_i = V_i/I_i$, $x = \alpha/Bi_{OA}\chi$, $a_i = 1/[1 + \alpha(T_{Ci} - T_0)]$, $b_i = -a_i(V_i^2/2\pi L)$, n is the number of measurements, r_i is the resistance of the capillary at the voltage V_i and coolant temperature T_{Ci} and a_i and b_i are coefficients. We are interested in estimates of unknown parameters r_0 and x and their covariation matrix. These values are necessary for finding the estimates and confidence intervals for the temperature and/or electric current.

In order to find estimate values of r_0 and x, which we denote by $\bar{r}_0$ and $\bar{x}$, the least-squares (LS) method is applied [7]. Normal LS equations are to be solved [7]:

$$S\begin{pmatrix}\bar{r}_0\\ \bar{x}\end{pmatrix} = Q \quad (5)$$

where S is the matrix of the range two with elements given by

$$s_{11} = \sum_{i=1}^{n} \frac{a_i a_i}{\sigma_i^2}, \quad s_{12} = s_{21} = \sum_{i=1}^{n} \frac{a_i b_i}{\sigma_i^2},$$

$$s_{22} = \sum_{i=1}^{n} \frac{b_i b_i}{\sigma_i^2}$$

Q is a vector with two components:

$$q_1 = \sum_{i=1}^{n} \frac{a_i r_i}{\sigma_i^2}, \quad q_2 = \sum_{i=1}^{n} \frac{b_i r_i}{\sigma_i^2}$$

and σ_i^2 are the variances for each measurement.

Absolute values of σ_i are not important for solving eqn. 5, but rather their ratios to each other. Assuming that the variance of r_i in eqn. 5 is determined by the variance of the electric current I_i, and that the experimental error in the current measurements is the same for all measured currents, we assume $\sigma_i \approx 1/I_i$ in our software and in this paper.

The covariation matrix C for estimates of r_0 and x is given by

$$C = \frac{1}{n-2} \sum_{i=1}^{n} \sigma_i^{-2} (r_i - a_i \bar{r}_0 - b_i \bar{x})^2 S^{-1} \quad (6)$$

where S^{-1} is the inverse matrix to the matrix S.

Variances for r_0 and x are the diagonal elements of the matrix C:

$$\sigma_r^2 = c_{11}, \quad \sigma_x^2 = c_{22} \quad (7)$$

When estimate values $\bar{r}_0$ and $\bar{x}$ are obtained, one can find an estimate of the electric current in the mutually calibrated capillary–buffer pair for any voltage by substituting $\bar{r}_0$ and $\bar{x}$ into eqn. 1:

$$\bar{I} = \frac{[1 + \alpha(T_C - T_0)]V}{\bar{r}_0 - \frac{\bar{x}V^2}{2\pi L}} \quad (8)$$

The electric current variance is found by the equation [7]

$$\sigma_I^2 = \left(\frac{\partial \bar{I}}{\partial \bar{x}}\right)^2 c_{22} + \left(\frac{\partial \bar{I}}{\partial \bar{r}}\right)^2 c_{11} + 2 \cdot \frac{\partial \bar{I}}{\partial \bar{r}} \cdot \frac{\partial \bar{I}}{\partial \bar{x}} \cdot c_{12} + \left(\frac{\partial \bar{I}}{\partial \alpha}\right)^2 \sigma^2(\alpha) \quad (9)$$

which gives, after substituting eqn. 8 into eqn. 9,

$$\sigma_I^2 = \left(\frac{\bar{I}}{\bar{r}_0 - \frac{\bar{x}V^2}{2\pi L}}\right)^2 \left[\sigma_r^2 + \frac{V^2}{\pi L} \cdot c_{12} + \left(\frac{V^2}{2\pi L}\right)^2 \sigma_x^2\right] + \left[\frac{\bar{I}(T_C - T_0)}{1 + \alpha(T_C - T_0)}\right]^2 \sigma_\alpha^2 \quad (10)$$

The relative standard deviation of the electric current caused by the uncertainty in the thermal coefficient is

$$\left(\frac{\sigma_I}{\bar{I}}\right)_\alpha = \frac{\sigma_\alpha (T_C - T_0)}{1 + \alpha(T_C - T_0)} \quad (11)$$

if we assume $\alpha = 0.021\ \mathrm{K}^{-1}$, $\sigma_\alpha = 0.002\ \mathrm{K}^{-1}$ and $T_C - T_0 = 5$ K, then we have a relative standard deviation of only 1%.

Therefore, the only information needed for eqn. 8, apart from the calibration points, is the capillary length. Having this and, say, ten calibration points, one is able to predict the electric current and, thus, the shift in migration time with reasonable accuracy. To obtain higher accuracy a more precise value for α is necessary.

For acquiring the estimate of the actual inner diameter of the capillary one needs the value of the electric conductivity at a reference temperature T_0 [3] and eqn. 3 is used. The corresponding variance is given by

$$\sigma_d^2 = \frac{d_L^2}{4} \left(\frac{\sigma_r^2}{r_0^2} + \frac{\sigma_\kappa^2}{\kappa_0^2}\right) \quad (12)$$

where σ_κ^2 is the variance of the electric conductivity at the reference temperature. Our experiments usually give $\sigma_d \approx 0.5$ μm for the standard deviation of the capillary diameter.

For the temperature estimate one obtains from eqns. 2 and 4

$$\bar{T} = T_C + \frac{V^2 [1 + \alpha(T_C - T_0)]\bar{x}}{2\pi L \alpha \left(\bar{r}_0 - \frac{\bar{x}V^2}{2\pi L}\right)} \quad (13)$$

The temperature variance can be found by using eqn. 9 in analogy with that of the electric current. The important difference is that the part of the relative standard deviation associated with the error in the determination of α is

$$\left(\frac{\sigma_T}{\bar{T}-T_C}\right)_\alpha \approx \frac{\sigma_\alpha}{\alpha} \tag{14}$$

If σ_α and α have the same values as given in an example following eqn. 9, the temperature relative standard deviation is about 10%. In order to obtain better accuracy one is expected to find α with higher accuracy.

Now let us consider the case when the capillary has been calibrated with some buffer and then filled with another buffer with different electric conductivity κ_{02} and thermal coefficient of electric conductivity α_2 but the same heat conductivity. It was shown previously [3] that even in this instance one can expect a reasonable accuracy of the electric current prediction.

For a calibrated capillary its inner diameter estimate and corresponding standard deviation are $\bar{d}_L$ and σ_d, where $\bar{d}_L$ is obtained from eqn. 3 (r_0 is replaced by its estimate $\bar{r}_0$) and σ_d is given by eqn. 12. The Biot number variance, as follows from eqn. 4, is given by

$$\sigma_{Bi}^2 = Bi_{OA}^2\left[\left(\frac{\sigma_x}{\bar{x}}\right)^2 + \left(\frac{\sigma_\alpha}{\alpha}\right)^2\right] \tag{15}$$

Thus, new values of $\bar{x}_2$ and $\bar{r}_{02}$ and their variances are given by

$$\bar{x}_2 = \frac{\alpha_2}{Bi_{OA}\chi}, \quad \bar{r}_{02} = \frac{4L}{\kappa_{02}\pi\bar{d}_L^2} \tag{16}$$

$$\sigma_{x2}^2 = \bar{x}_2^2\left(\frac{\sigma_x^2}{\bar{x}^2} + \frac{\sigma_\alpha^2}{\alpha^2} + \frac{\sigma_{\alpha 2}^2}{\alpha_2^2}\right),$$

$$\sigma_{r2}^2 = \bar{r}_{02}^2\left(4\cdot\frac{\sigma_d^2}{\bar{d}_L^2} + \frac{\sigma_{\kappa 2}^2}{\kappa_{02}^2}\right) \tag{17}$$

It is seen from eqn. 15 that σ_{x2}^2 and, hence, the accuracy of the electric current and temperature predictions depends strongly on the precision of the thermal coefficient α. Nevertheless, if the precision is high enough, the predictions come out in good agreement with experimental measurements.

When one is able to calculate and predict electric current and buffer temperature for a given voltage, one has a possibility of predicting the transformation of the migration time and the dispersion of the experimentally obtained peak.

Peak transformations

We assume, according to previous findings [4,5] that the migration velocity of the analyte varies according to the following expression for migration time:

$$t_m = t_m^* \cdot \frac{I^*}{I} \tag{18}$$

where t_m^* is the experimentally observed migration time and I^* is the experimental electric current, both corresponding to the applied voltage V^* and coolant temperature T_C^*, t_m is the predicted migration time and I is the predicted current, both corresponding to voltage V and coolant temperature T_C.

Transformation of the peak dispersion is much more complex. Diverse origins of the peak broadening in CZE have been extensively discussed in a number of papers [8–16]. They include initial zone broadening, diffusion, convection, Joule heat, electroosmosis, adsorption, conductivity and pH differences between the analyte zone and the buffer and broadening due to the size of the detection zone. All broadening mechanisms are divided by us into two classes: those leading to symmetrical peaks and those causing skewed peaks. This division is correct only if the compositions of the analyte and the buffer are kept the same from run to run. For instance adsorption can lead to either symmetrical or skewed peaks depending on the concentrations of the analyte and adsorbing sites.

For the first class of symmetrical peaks an efficient diffusion coefficient D_{eff} can be introduced as has been done in chromatography. The peak shape is assumed to be Gaussian:

$$p_G(t) = \frac{A(t_m)^{1/2}}{\sigma_G(2\pi t)^{1/2}} \cdot \exp\left[-\frac{(t-t_m)^2 t_m}{2\sigma_G^2 t}\right] \tag{19}$$

$$\sigma_G = (2D_{eff}t_m)^{1/2}/v_m \tag{20}$$

$$A = \int_0^\infty p_G\,dt \tag{21}$$

where p_G is the peak indicated by a detector, t is the time, σ_G is the standard deviation, A is the peak area found by peak integration over time and v_m is the migration velocity.

At this stage we assume the efficient diffusion coefficient to be independent of the buffer temperature:

$$D_{eff} = D^*_{eff} \quad (22)$$

where D^*_{eff} is the experimentally found efficient diffusion coefficient, corresponding to the applied voltage V^* and the coolant temperature T^*_C. This assumption appears to be restrictive; however, experimental results presented by Huang *et al.* [16] show that the efficient diffusion coefficients may be twenty times higher than the molecular diffusion coefficients. Our experiments confirmed these observations. These high values cannot be explained either by a viscosity decrease due to the temperature rise or by additional broadening caused by the buffer temperature profile. Therefore, additional efforts should be applied to understanding peak broadening in CZE and our assumption is not worse than any other previously presented.

The transformation rule for the peak standard deviation follows from eqns. 18 and 20:

$$\sigma_G = \sigma^*_G \left(\frac{I^*}{I}\right)^{3/2} \quad (23)$$

where σ^*_G is the experimentally obtained standard deviation.

The peak area transforms as follows [16,17]:

$$A = A^* v^*_m / v_m = A^* t_m / t^*_m = A^* I^* / I \quad (24)$$

where A^* is the experimentally obtained peak area.

It is worth noting that the product Av_m is proportional to the analyte mass divided by the capillary cross-sectional area and is, therefore, a constant provided that the same amount of analyte is loaded for every run.

For the second class of skewed peaks we assume the shape of the peak to be exponential:

$$p_S(t) = \begin{cases} h \exp[(t_m - t)/\sigma_S], & t_m > t \\ 0, & t < t_m \end{cases} \quad (25)$$

where h is the peak height and σ_S is a parameter responsible for the peak width.

It is assumed for the skewed peaks that the height of the peak remains independent of the buffer temperature: $h = h^*$. This assumption, together with eqn. 24, gives for σ_S

$$\sigma_S = \sigma^*_S I^* / I \quad (26)$$

Software package

All algorithms and ideas described above have been implemented in a software package called "Capillary Zone Electrophoresis Assistant" (CZEA). We shall describe its main features briefly. The package runs under Microsoft Windows and does not require any preliminary knowledge of the CE thermal theory. The following input information should be provided: the capillary length, its name and the inner diameter given by a manufacturer (this value is assumed to be corrected by CZEA), the specific conductivity of the buffer at 25°C and the thermal coefficient of conductivity. To perform calibration and to predict buffer temperature, CZEA needs experimental points of electric current for incremented voltage. The coolant temperature should be also given for every point.

A user can choose one of the two models for the peak shape, either "GAUSSIAN" or "SKEWED". Depending on this choice, the peak is modelled either by eqn. 19 or by eqn. 25. Additional characteristics of the peak are required: the migration time, the peak area and the peak height. Two peaks can be displayed simultaneously and their transformation caused by the voltage and/or coolant temperature can be performed according to eqns. 18–26.

EXPERIMENTAL

A fused-silica capillary of 75 μm I.D., total length 50 cm and distance from the injection to detection point 42.5 cm was obtained from Polymicro Technologies (Phoenix, AZ, USA). The temperature of the air surrounding the capillary was measured by a thermosensor positioned 10 cm from the capillary. The thermosensor was a Digiterm Quartz 1505 (Hanhart, Schwenningen, Germany). The electric current and voltage were read from the Waters (Milford, MA, USA) Quanta 4000 displays. Immobilines of pK 8.5 and 9.3 were obtained from Pharmacia–LKB (Uppsala, Sweden).

RESULTS AND DISCUSSION

An example of CZEA calibration is presented below. It consists of twelve readings of the electric current and the ambient temperature for incremented voltage. Two series of readings each of six points were made with a time interval of 3 days. The capillary was of 75 μm nominal I.D. and length 50 cm. The buffer used for calibration was 100 mM phosphate buffer, pH = 7.0, κ_0 = 9.64 mS/cm (at T_0 = 25°C), σ_κ = 0.1 mS/cm, α = 0.021 K^{-1} and σ_α = 0.0003 K^{-1}. Results of the calibration given by CZEA are that the actual I.D. is 79.3 ± 1.4 μm and the overall Biot number Bi_{0A} = 0.0544 ± 0.006. Fig. 1, which is the image of the computer screen, shows two graphs, one for the electric current and the other for the buffer temperature dependences on the applied voltage. Solid lines represent predicted values and dashed lines show confidence intervals. Both graphs were computed for T_C = 27.3°C. This value is displayed in the upper box and may be changed by the user (Fig. 1), in which event new graphs for the electric current and buffer temperature will be drawn. Values for the electric current and buffer temperature corresponding to the particular voltage of 12 kV are shown with their confidence intervals. It is seen that the buffer temperature is 19°C higher than the coolant temperature and is 46°C.

In order to check the ability of CZEA to predict migration times, electric current and temperature if the voltage or coolant temperature change, we used the capillary calibration reported above and filled it with another buffer, namely 50 mM phosphate buffer, pH = 7.7, κ_0 = 5.88 mS/cm. A 2.5 mM model mixture of two Immobilines of pK 8.5 and 9.3 diluted in the buffer was separated at V = 12 kV. The temperature of the cooling air during the run was T_C = 27.3°C. The electric current fluctuated within the range 87.6–88 μA. Fig. 2 shows two peaks, both skewed. The migration times are t_{m1} = 3.68 min and t_{m2} = 3.83 min. The ratio of the peak heights is 1:0.64. In order to simulate transformations of the peaks when the voltage changes one has to classify the peak shapes. The shape and transformation model for the first peak was chosen with certainty as "SKEWED". The second peak (Fig. 2) appears to be subject to diffusional broadening and we tentatively classified it as "GAUSSIAN". This means that eqns. 19–24 are used for the peak transformations and quantitative prediction for the peak broadening is not expected. All these data were entered into CZEA. The predicted electric current and temperature were I = 87.6 μA and T = 37.4°C, respectively. The first value is in excellent agreement with the experimental value. Note that the

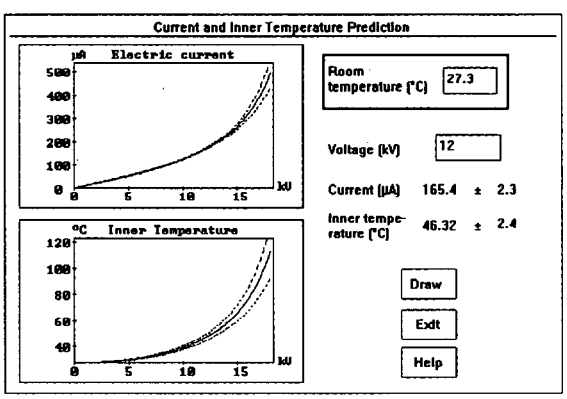

Fig. 1. Computer screen image of electric current and temperature as functions of applied voltage. The solid curves are the mean values and the dashed lines represent 97% confidence intervals.

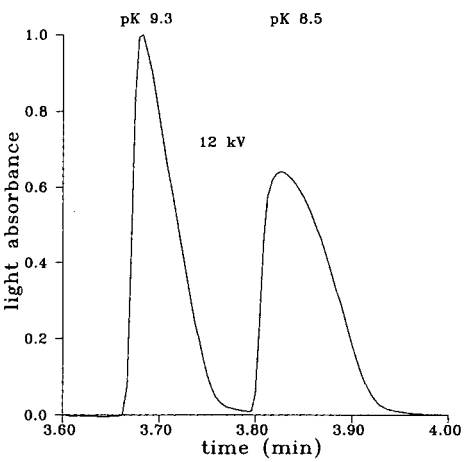

Fig. 2. Experimental electropherogram of a 2.5 mM mixture of two Immobilines having pK values of 8.5 and 9.3 and diluted in 50 mM, pH = 7.7, κ_0 = 5.88 mS/cm phosphate buffer. The sample was loaded hydrostatically for 10 s with a height difference of 9.8 cm. The applied voltage was V = 12 kV. The temperature of the cooling air during the run was T_C = 27.3°C.

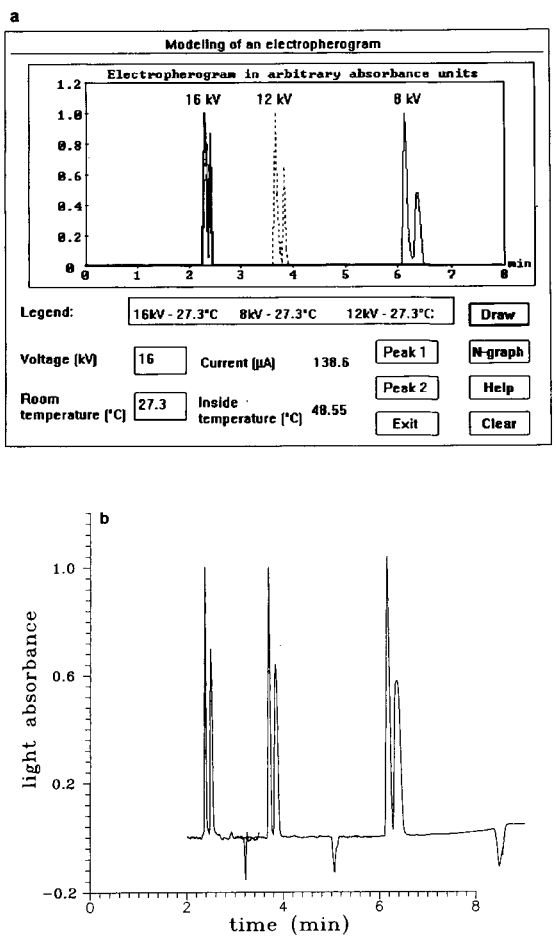

Fig. 3. Separation of the model mixture at $V = 8$, 12 and 16 kV. (a) image of the computer screen; (b) experimental. Peaks obtained at $V = 12$ kV were used as a template for the prediction of peaks at 16 and 8 kV. All experimental conditions except voltages as in Fig. 2.

capillary had been calibrated with a buffer different to that used for the separation.

Fig. 3 shows predicted and experimentally obtained results for the separation of the same mixture at 12, 16 and 8 kV. The pair of peaks corresponding to $V = 12$ kV was used as a template for CZEA. The two other pairs corresponding to $V = 16$ and 8 kV in Fig. 3a are the results of a calculation performed by CZEA. The buffer temperatures calculated by CZEA were 48.6 and 33.3°C at 16 and 8 kV, respectively. Comparison of Fig. 3a and b shows very good agreement between predicted and experimental peaks, especially for the skewed peaks. The peak classified as "GAUSSIAN" is predicted to be broader than it is experimentally. That means that the dispersion of the second peak is not fully diffusional but is determined also by electrochemical and wall interactions.

Experimental and predicted values of the electric current and migration times for two positive and one negative peaks are shown in Table I. The agreement between the predicted and experimental values is within 2%. The best agreement is obtained for the capillary filled with the same buffer as was used for its calibration. It was observed also that the discrepancy between the predicted and experimental retention times was a minimum for negative peaks (less than 1%) which represent the initial zone moving without interactions with the capillary walls. On the other hand, when a sample was diluted in water, the relative difference between the predicted and experimental migration times was maximum (up to 6%). Therefore, a significant

TABLE I

COMPARISON OF EXPERIMENTAL AND PREDICTED MIGRATION TIMES FOR TWO POSITIVE (t_{m1} AND t_{m2}) AND ONE NEGATIVE (t_{m3}) PEAKS OBTAINED AT $V = 16$ AND 8 kV

Parameter	$V = 16$ kV				$V = 8$ kV			
	I (μA)	t_{m1} (min)	t_{m2} (min)	t_{m3} (min)	I (μA)	t_{m1} (min)	t_{m2} (min)	t_{m3} (min)
Experimental	140	2.36	2.39	3.22	51.8	6.13	6.344	8.48
Predicted	139	2.33	2.42	3.20	52.5	6.14	6.39	8.45
Error	0.7%	1.3%	1.3%	0.6%	1.3%	0.2%	0.73%	0.35%

difference between predicted and experimental values indicates that effects additional to the temperature dependence of viscosity are involved in the migration of the analyte.

CONCLUSIONS

The statistical procedure described in this paper allows one to calculate the buffer temperature and the electric current in the capillary and confidence intervals for both values. The latter make it possible to separate the shift in migration times caused by the temperature dependence of the buffer viscosity from other temperature-sensitive phenomena such as changes in the buffer pH, pK values of the analyte and degree of ionization of the silanol groups. The accuracy of predicted values for the buffer temperature, electric current and migration times depends strongly on the accuracy of the thermal coefficient of electric conductivity.

The CZE software package allows easy calibration of the capillary and prediction of the temperature and electric current in the capillary, and also recalculation of the experimental electropherograms to different voltages and different temperatures of the ambient air.

The best agreement between the predicted and experimental migration times was obtained for the capillary filled with the same buffer as was used for its calibration. It was observed that the discrepancy between predicted and experimental migration times was a minimum for negative peaks (less than 1%) representing the initial zone moving without interactions with the capillary walls.

ACKNOWLEDGEMENTS

This work was supported in part by the Agenzia Spaziale Italiana (ASI, Rome) and by Progetto Finalizzato Chimica Fine II (CNR, Rome).

REFERENCES

1 T.L. Rapp, W.K. Kowalchyk, K.L. Davis, E.A. Todd, K.L. Liu and M.D. Morris, *Anal. Chem.*, 64 (1992) 2434–2437.
2 H. Wätzig, *Chromatographia*, 33 (1992) 445–448.
3 M.S. Bello, M. Chiari, M. Nesi, P.G. Righetti and M. Saracchi, *J. Chromatogr.*, 625 (1992) 323–330.
4 S. Hjertén, *Chromatogr. Rev.*, 9 (1967) 122–219.
5 T.T. Lee and E.S. Yeung, *Anal. Chem.*, 63 (1991) 2842–2848.
6 M.S. Bello and P.G. Righetti, *J. Chromatogr.*, 606 (1992) 95–102.
7 R. Rao, *Linear Statistical Inference and its Applications*, Wiley, New York, 1965.
8 R. Virtanen, *Acta Polytech. Scand., Chem.* 123 (1974) 1–67.
9 J.H. Knox and I.H. Grant, *Chromatographia*, 24 (1987) 135–143.
10 F. Foret, M. Deml and P. Bocek, *J. Chromatogr.*, 452 (1988) 601–603.
11 J.H. Knox, *Chromatographia*, 26 (1988) 329–337.
12 E. Grushka, R.M. McCormick and J.J. Kirkland, *Anal. Chem.*, 61 (1989) 241–246.
13 W.A. Gobie and C.F. Ivory, *J. Chromatogr.*, 516 (1990) 191–210.
14 S. Hjertén, *Electrophoresis*, 11 (1990) 665–690.
15 G.O. Roberts, P.H. Rhodes and R.S. Snyder, *J. Chromatogr.*, 480 (1989) 35–67.
16 X.H. Huang, W.F. Coleman and R.N. Zare, *J. Chromatogr.*, 480 (1989) 97–110.
17 S. Hjertén, K. Elenbring, F. Kilár, J.L. Liao, A.J.C. Chen, C.J. Siebert and M.D. Zhu, *J. Chromatogr.*, 403 (1987) 47–61.

Journal of Chromatography A, 652 (1993) 337–345
Elsevier Science Publishers B.V., Amsterdam

CHROM. 25 064

Computer-assisted pH optimization for the separation of geometric isomers in capillary zone electrophoresis

J.C. Jacquier, C. Rony and P.L. Desbene*

Laboratoire d'Analyse des Systèmes Organiques Complexes, Université de Rouen, IUT, 43 Rue Saint Germain, 27000 Evreux (France); and Institut Européen des Peptides, Université de Rouen, 76134 Mont Saint Aignan Cedex (France)

ABSTRACT

With the rapid development of capillary electrophoresis, several workers have considered the theoretical pH optimization for the separation of geometric isomers. However, for samples composed of more than two isomers, these mathematical treatments lead only to an optimum pH range. In this work, the application of software based on the iterative computation of the resolution as a function of pH was studied, in order to have direct access to the optimum pH value for complex mixtures of isomers. The values deduced were compared with the experimental values for acids and bases.

INTRODUCTION

Capillary electrophoresis is becoming an increasingly used analytical tool for the resolution of complex mixtures of ionic or ionizable compounds. Nevertheless, capillary zone electrophoresis (CZE), even though more efficient, is often supplanted by micellar electrokinetic chromatography (MEKC) in studies of complex mixtures of ionizable molecules [1–4]. This is sometimes disadvantageous and is often due to a lack of evaluation of the two methods for particular applications. It is considered important to predict, as far as possible, the potential of CZE before resorting to MEKC.

In this context, we present here a computer program for the calculation of the evolution of the resolution in CZE of a complex mixture of ionizable molecules as a function of the predominant parameter of this technique, pH. Although previous workers have undertaken the optimization of the pH in CZE for one pair of compounds [5–7], for three compounds their predictions lead only to an optimum pH range. Moreover, those studies concerned the optimization of the pH with regard to the maximum charge difference between the two compounds involved (i.e., the maximum selectivity), disregarding the evolution of the electroosmotic mobility with pH depending on the ionization state of the silica. The determination of pK_a values and absolute mobilities using CZE has also been reported [8], but optimization of the analytical conditions was not achieved.

THEORETICAL

The program developed allows the prior calculation of the resolution of each compound pair (i, j) at a fixed pH according to the classical equation

$$R_{s(i,j)} = 2\left(\frac{t_j - t_i}{w_i + w_j}\right) \quad (1)$$

and then, by extraction, to retain the limiting pair of compounds for which the resolution is minimum at this pH value. By successive iteration as a function of pH, the step being fixed at 0.05 pH unit, the program calculates the pH

* Corresponding author.

0021-9673/93/$06.00

value for which the resolution of the limiting pair(s) is maximum. This pH value corresponds to the optimum conditions.

In order to perform this evaluation, a limited number of experimental applications are required, depending on two cases: if the pK_a values of the different compounds are known under the analytical temperature conditions, only one experiment is required; and if the pK_a values are not known, two electropherogams are required. This procedure is shown schematically in Fig. 1.

Taking into account the nature of the most commonly employed capillaries, *i.e.*, fused silica, the evolution of the electroosmotic flow as a function of pH cannot be neglected. Indeed, as demonstrated by Lukacs and Jorgenson [9], this evolution depends on the ionization of the silanol groups at the capillary surface and is similar to a bilogarithmic function with an approximate pK of 6 pH units. This fit is reliable if one takes account of the hysteresis effect [10] and the need for a constant ionic strength [11].

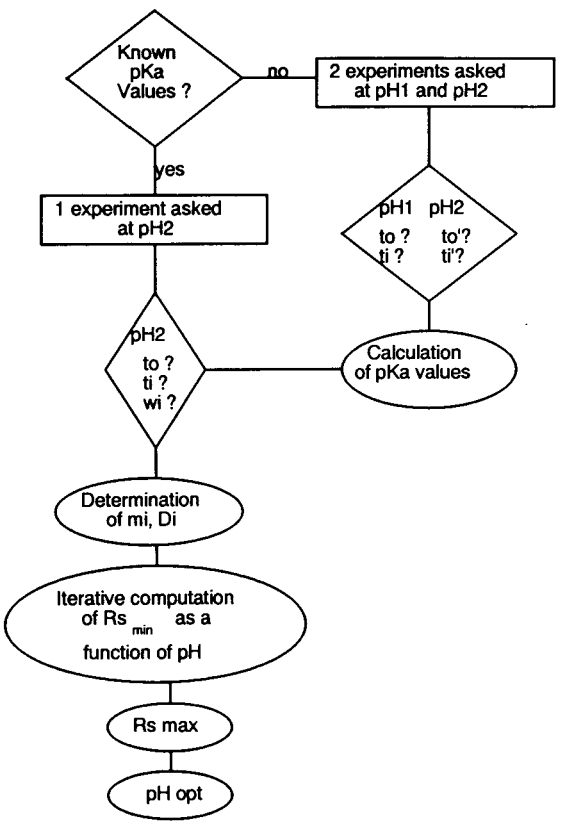

Fig. 1. Schematic diagram of the computation treatment.

Therefore, we modelled the evolution of the electroosmotic flow according to the following equations:

$$\underset{(1-x_s)}{\text{–Si–O–H}} \rightleftharpoons \underset{(x_s)}{\text{Si–O}^-} + \text{H}^+ \quad (2)$$

where x_s is the silanol fraction in its ionized form:

$$\log\left(\frac{x_s}{1-x_s}\right) = \text{pH} - pK_s \quad (3)$$

with $pK_s = 6$, where pK_s is the silanol pK_a:

$$\mu_{e0} = x\mu_0 \quad (4)$$

where μ_{e0} is the effective electroosmotic mobility and μ_0 the absolute electroosmotic mobility when the silica surface is fully ionized. As shown in Fig. 2, the fit between the experimental and the theoretical pK_s values is satisfactory, although the fit between the two curves is less satisfactory in particular for pH values between 3 and 5.

This important point have been established, it is then possible to undertake the evolution of the resolution of a mixture of ionizable compounds as a function of pH. As noted above, two cases must be considered: (i) the pK_a values of the

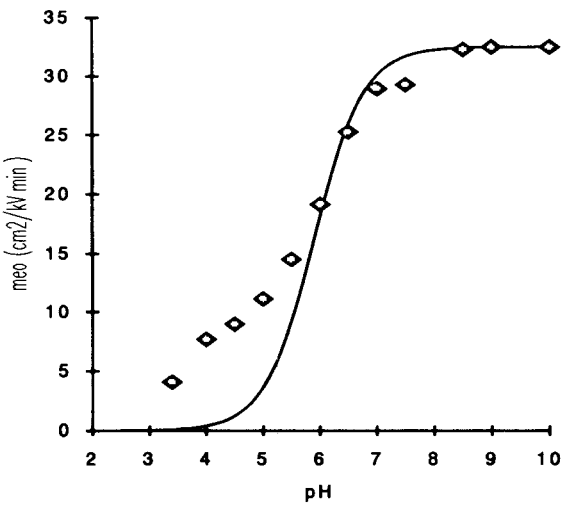

Fig. 2. Evolution of the electroosmotic mobility as a function of pH.

different compounds are known at the experimental temperature or (ii) the pK_a values of the studied compounds are not known or have not been reported in the literature under the required analytical conditions.

In the case of ionizable molecules of known pK_a values, a single experiment is necessary for the determination of the electrophoretic mobilities and the molecular diffusion coefficients of the different compounds. This unique manipulation of the sample has to be done at a pH value for which the compounds are ionized, *i.e.*, pH_1. The calculation of the migration times and the peak widths at different pH values is done through the following equations.

Acids

$$\underset{(1-x_i)}{A-H} \rightleftharpoons \underset{(x_i)}{A^-} + H^+ \tag{5}$$

$$pH = pK_a + \log\left(\frac{x_i}{1-x_i}\right) \tag{6}$$

where x_i is the fraction of the compound i in its ionized form and can be calculated at any pH value with

$$x_i = \frac{10}{1+10^{pH-pK_{ai}}} \tag{7}$$

We then have access to the apparent mobility (μapp_i) of compound i, knowing its electrophoretic mobility (μ_i) and its molecular diffusion coefficient (D_i) through the experiment at pH_1:

$$\mu_{app_i} = x_s\mu_0 - x_i\mu_i \tag{8}$$

$$t_i = \frac{lL}{V\mu_{app_i}} \tag{9}$$

$$w_i = \left(\frac{32D_it_i^3}{l^2}\right)^{1/2} \tag{10}$$

where L is the total capillary length and l the capillary length from the inlet to the detection window. Therefore, it is possible to calculate the resolution $R_{s(i,j)}$ for each pair of compounds using eqn. 1.

Bases

The determination of the electrophoretic mobilities and the molecular diffusion coefficients of basic compounds of known pK_a values is done using the same approach. The calculation is based again on one electropherogram, this time performed at a low pH value in order to visualize the compounds in their ionic form but not too low in order to visualize the electroosmotic flow also:

$$\underset{x_i}{B-H^+} \rightleftharpoons \underset{(1-x_i)}{B} + H^+ \tag{11}$$

$$pH = pK_a + \log\left(\frac{1-x_i}{x_i}\right) \tag{12}$$

$$x_i = \frac{1}{1+10^{pH-pK_{ai}}} \tag{13}$$

$$\mu_{app_i} = x_s\mu_0 + x_i\mu_i \tag{14}$$

In the case of ionizable molecules for which the pK_a values are unknown or have not been reported in the literature at the temperature of the analysis, one more electropherogram is needed at a different pH value in order to elucidate the variation of the ionized fraction of the compound as a function of pH. Hence for acidic molecules, the pK_a is deduced from the equation

$$pK_a = -\log\left(\frac{\mu_{eff_2}\cdot 10^{-pH_2} - \mu_{eff_1}\cdot 10^{-pH_1}}{\mu_{eff_1} - \mu_{eff_2}}\right) \tag{15}$$

In a similar way, the pK_a of basic molecules is deduced from the equation

$$pK_a = -\log\left[\frac{(\mu_{eff_2} - \mu_{eff_1})\cdot 10^{-pH_2-pH_1}}{\mu_{eff_1}\cdot 10^{-pH_2} - \mu_{eff_2}\cdot 10^{-pH_1}}\right] \tag{16}$$

where μ_{eff_i} is the effective mobility of the compound at pH_i and calculated with the following equation, for either acidic or basic molecules:

$$\mu_{eff_i} = \mu_{app_i} - \mu_{e0} \tag{17}$$

The choice of the pH_1 and pH_2 values in the case of basic molecules is restricted by the fact that it is necessary to visualize both the electroosmotic flow and the partially ionized compounds. Too low pH values, corresponding to high ionization of the basic molecules, induce too low electroosmotic flows which are difficult to access in reasonable times.

EXPERIMENTAL

Reagents

Buffer and sample solutions were prepared with water purified by reverse osmosis and filtered using a Milli-Ro + Milli-Q system (Millipore, Molsheim, France). The reagents used for the electrolytes, *i.e.*, borax, boric acid, phosphoric acid, dibasic sodium phosphate, sodium acetate, sodium hydroxide and sodium chloride, were of analytical-reagent grade from Aldrich (La Verpillère, France). Compounds used for the validation of the program, *i.e.*, nitrophenols, chlorophenols and chloroanilines, were of 99% purity from Aldrich. For the determination of the electroosmotic flow, mesityl oxide of analytical-reagent grade from Aldrich was used.

Apparatus

All experiments were carried out on a P/ACE 2100 system (Beckman, Fullerton, CA, USA) monitored by a PS/2 computer (IBM, Greenock, UK) using P/ACE software (Beckman), Data collection was performed with the same software. Samples were loaded by a 1-s pressure injection into a fused-silica capillary (50 cm × 50 μm I.D.). UV detection was performed at 214 nm through the capillary at 50 cm from the inlet.

The pH values of the electrolytes were measured using a Beckman Model Φ pH meter at the temperature of the analyses. The separations were performed three to five times for each pH value studied, in order to ensure good reproducibility of the measurements.

Buffer preparation

Stock solutions of borax (12.5 m*M*), boric acid (50 m*M*), dibasic sodium phosphate (50 m*M*), phosphoric acid (50 m*M*), sodium acetate (50 m*M*) and sodium hydroxide (50 m*M*) were prepared daily prior to their dilution with sodium chloride (50 m*M*) in order to prepare electrolytes with good pH buffer characteristics and a quasi-constant ionic strength.

Software

The calculation software was developed using BASIC, pre-installed on IBM DOS machines. This choice, which deliberately excluded a complex and more powerful language, appeared to be fast enough to compute the results in a satisfactory time (less than 1 min).

RESULTS AND DISCUSSION

In order to validate the treatment and establish its generality, we undertook the separation of various mixtures and compared the evolution of the minimum resolution as a function of pH with the calculated values. Three mixtures, two composed of acids and one of bases were analysed by CZE at different pH values over a wide range, *i.e.*, 2.2–10.

For weak acid compounds, we undertook the separation of the geometric isomers of the chlorophenols and the nitrophenols. The pK_a values, taken from the literature [12,13], are 8.48, 9.02 and 9.38 for *o*-, *m*- and *p*-chlorophenol, respectively, and 7.23, 8.40 and 7.15 for *o*-, *m*- and *p*-nitrophenol, respectively. The separation of the nitrophenols presents much more difficulty owing to the close pK_a values for the *ortho* and *para* isomers.

Study of the influence of pH on the resolution of the chlorophenol geometric isomers

The separation of the three monochlorophenols was performed experimentally over the pH range 7–10, the minimum resolution for this mixture being measured every 0.5 pH unit. The temperature was kept constant at 25°C, a value at which the pK_a values have been reported in the literature [12].

The values obtained were compared with the theoretical curve based on the analysis performed at pH 10. As shown in Fig. 3, a very satisfactory fit is found for the whole studied pH range. The minimum resolution of this mixture is maximum at pH 9.3, as predicted by the calculation.

Moreover, the pK_a values calculated from the electropherograms obtained at pH 9 and 10 were in excellent agreement with those reported in the literature. The fit between the experimental values and the calculation treatment using the so-deduced pK_a values is also very satisfactory (Fig. 4).

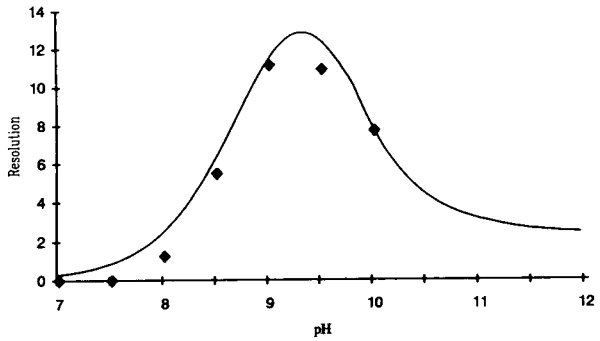

Fig. 3. Evolution of the minimum resolution as a function of pH for the geometric isomers of chlorophenol. Solid line, computed curve calculated from an electropherogram obtained at pH 10 and based on the literature pK_a values, *i.e.*, 8.48, 9.02 and 9.38 for the *ortho*, *meta* and *para* isomers, respectively.

Study of the influence of pH on the resolution of the nitrophenol geometric isomers

The validation of the program having been successfully accomplished, we undertook the separation of the three nitrophenol isomers, where the pK_a values of the *ortho* and *para* isomers are much closer and therefore present a major difficulty for the pH optimization.

We first computed the resolution of the nitrophenol geometric isomers as a function of pH using an electropherogram obtained at pH 10 and the pK_a values from the literature [12] (Fig. 5).

The computed curve shows a complete loss of resolution at pH 8.45 and two maxima of resolution at pH 7 and 10. This indicates inversion of migration for two compounds. In order to confirm this effect, and therefore to validate the treatment, we undertook, as with the chlorophenol isomers, a series of analyses at different pH values over a wide range, *i.e.*, 6–10. The corresponding electropherograms allowed us to calculate the experimental minimum resolution for each pH value considered. These values are also reported in Fig. 5.

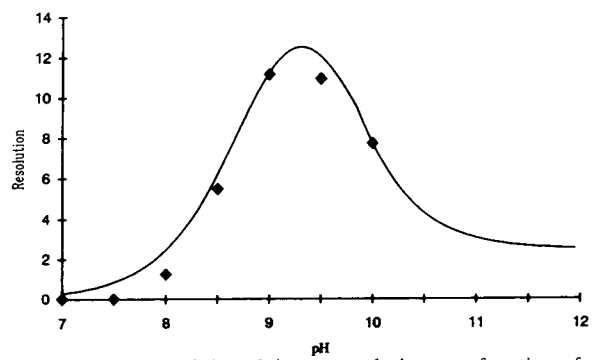

Fig. 4. Evolution of the minimum resolution as a function of pH for the geometric isomers of chlorophenol. Solid line, computed curve calculated from an electropherogram obtained at pH 10 and based on the computed pK_a values, *i.e.*, 8.472, 9.022 and 9.366 for the *ortho*, *meta* and *para* isomers, respectively.

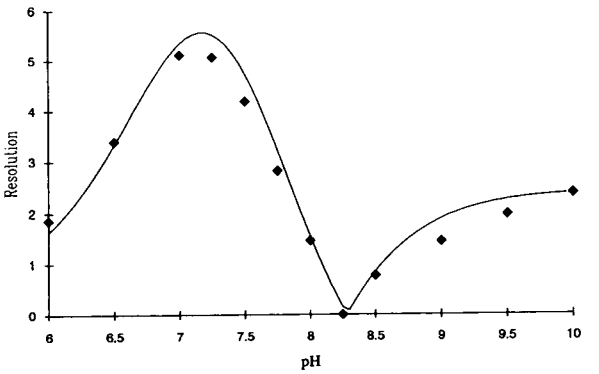

Fig. 5. Evolution of the minimum resolution as a function of pH for the geometric isomers of nitrophenol. Solid line, computed curve calculated from an electropherogram obtained at pH 10 and based on the literature pK_a values, *i.e.*, 7.23, 8.40 and 7.15 for the *ortho*, *meta* and *para* isomers, respectively.

As for the chlorophenol isomers, a good fit between the experimental and computed values is observed throughout the pH range. Furthermore, the comparison of the electropherograms obtained at the pH values for which the resolution of the mixture is a maximum, *i.e.*, pH 7 (Fig. 6) and pH 10 (Fig. 7) reveals, as predicted, an inversion in the order of migration of two peaks. Co-elution analyses confirmed the peak inversion and assigned it to the *ortho* and *para* isomers, as reported in Figs. 6 and 7.

Finally, when substituting the pK_a values from the literature for the values calculated from the electropherograms obtained at pH 10 and 9, the fit between the computed curve and the experimental resolutions appears to be less satisfactory (Figs. 5 and 8). This indicates that our method for the determination of pK_a values using CZE is less precise than that used in the literature. Nevertheless, this imprecision does

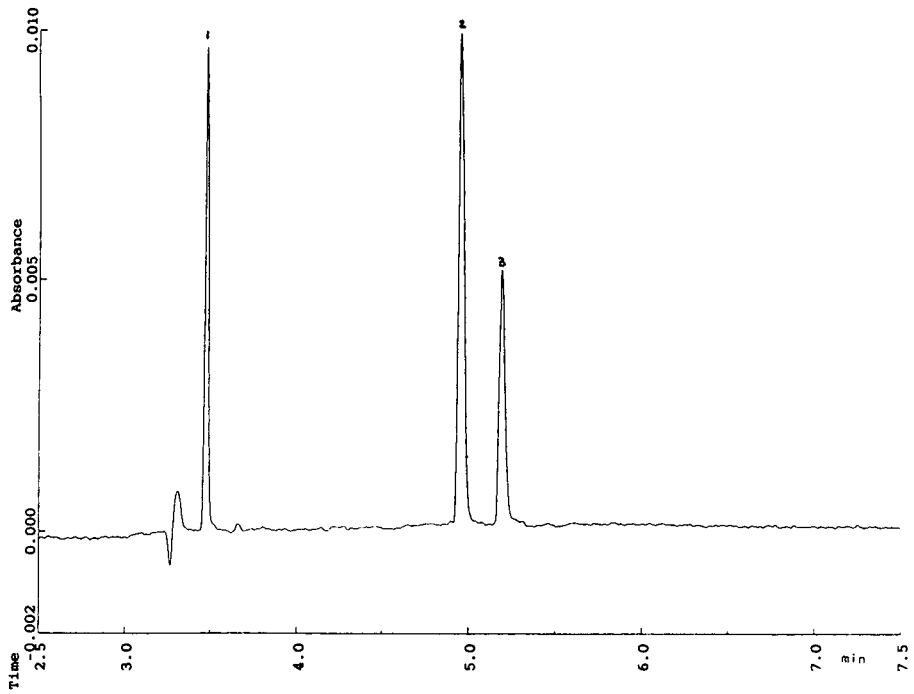

Fig. 6. Electropherogram of the geometric isomers of nitrophenol obtained by CZE at pH 7. Capillary tube, 57 cm × 50 μm I.D.; temperature, 25°C; applied voltage, 30 kV. Peaks: 1 = *m*-; 2 = *o*-; 3 = *p*-nitrophenol.

not alter the validity of the essential predictions deduced from the treatment, *i.e.*, the optimum pH values corresponding to the maximum resolution for this mixture and the inversion of migration order between the *ortho* and *para* isomers at pH 8.45.

Study of the influence of pH on the resolution of the chloroaniline geometric isomers

As the theoretical approach for the prediction of the behaviour of acidic compounds in CZE thus appeared to be very satisfactory, we completed the study by investigating the electrophoretic behaviour of basic geometric isomers. The compounds chosen were the geometric isomers of the chloroaniline, for which the pK_a values at 25°C have been reported in the literature [13] as 2.64, 3.52 and 3.98 for the *ortho*, *meta* and *para* isomers, respectively. Their electrophoretic behaviour was studied experimentally in the pH range 2.2–6.

As the computation of the resolution as a function of pH needs a complete electropherogram, the choice of the pH value at which the reference electropherogram will be measured is important. As described above, the pH value must be as low as possible in order that the fraction of the compounds in their ionic form is the maximum. Nevertheless, as the chlorophenols have very low pK_a values, this choice is limited by the ionization state of the capillary wall. Therefore, a compromise was found at pH 3.75, at which the electroosmotic flow was not too slow and the geometric isomers were partially ionized. Under such conditions, the comparison of the computed curve and the experimental results is less satisfactory than with acid solutes (Fig. 9). Moreover, the substitution of the pK_a values from the literature by those deduced from the electropherograms obtained at pH 3.75 and 4.25 does not lead to a better fit between the computed curve and the experimental results.

To explain such an observation, two considerations can be invoked: (i) a very slow equilibrium of the ionization state of the capillary wall in this pH range, as evidenced by Lambert and

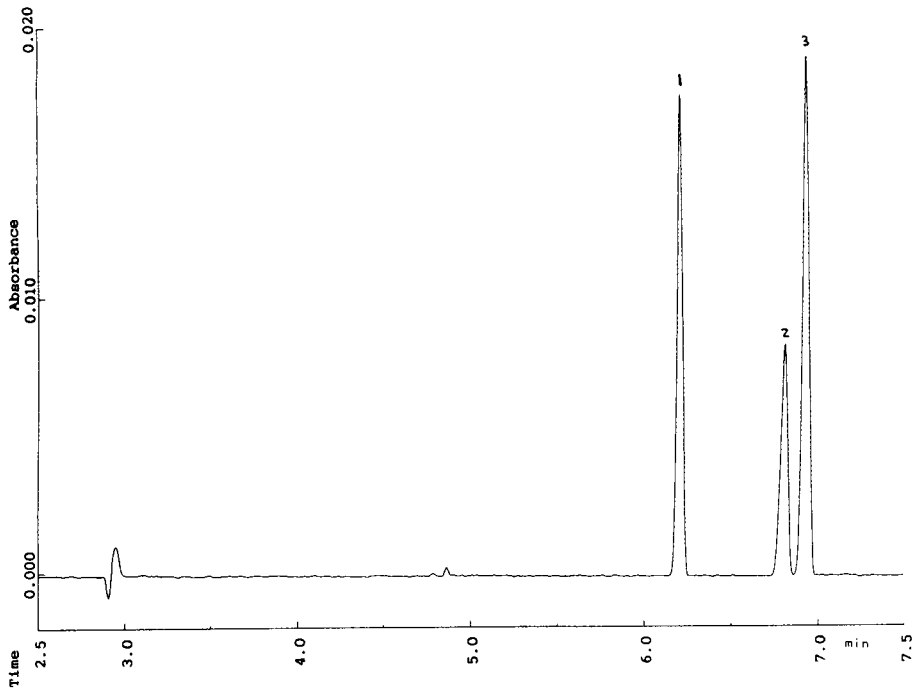

Fig. 7. Electropherogram of the geometric isomers of nitrophenol obtained by CZE at pH 10. Conditions as in Fig. 6. Peaks: 1 = *m*-; 2 = *p*-; 3 = *o*-nitrophenol.

Middleton [10]; and (ii) tailing peaks, leading to a decrease of resolution not taken into account in the computed treatment owing to the adsorption phenomena that occur between basic compounds and the capillary wall, especially as our experiments were performed on capillaries of small I.D. (50 μm).

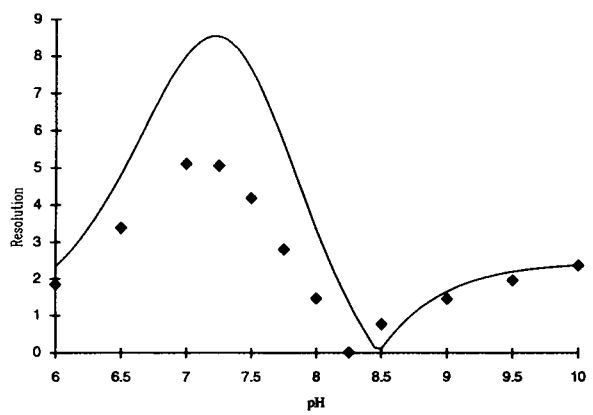

Fig. 8. Evolution of the minimum resolution as a function of pH for the geometric isomers of nitrophenol. Solid line, computed curve calculated from an electropherogram obtained at pH 10 and based on the computed pK_a values, *i.e.*, 7.272, 8.289 and 7.155 for the *ortho*, *meta* and *para* isomers, respectively.

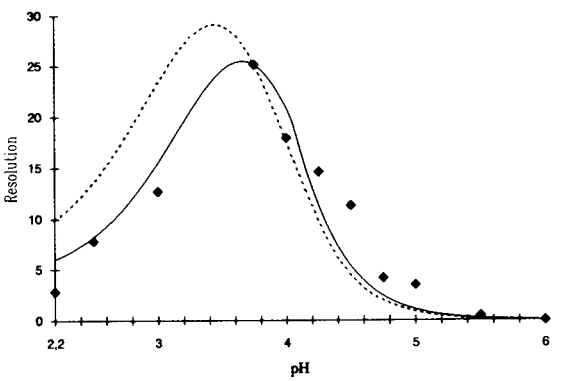

Fig. 9. Evolution of the minimum resolution as a function of pH for the geometric isomers of chloroaniline. Solid line, computed curve calculated from an electropherogram obtained at pH 3.75 and based on the literature pK_a values, *i.e.*, 2.64, 3.52 and 3.98 for the *ortho*, *meta* and *para* isomers, respectively; dashed line, computed curve calculated from an electropherogram obtained at pH 3.75 and based on the computed pK_a values, *i.e.*, 3.046, 3.244 and 3.574 for the *ortho*, *meta* and *para* isomers, respectively.

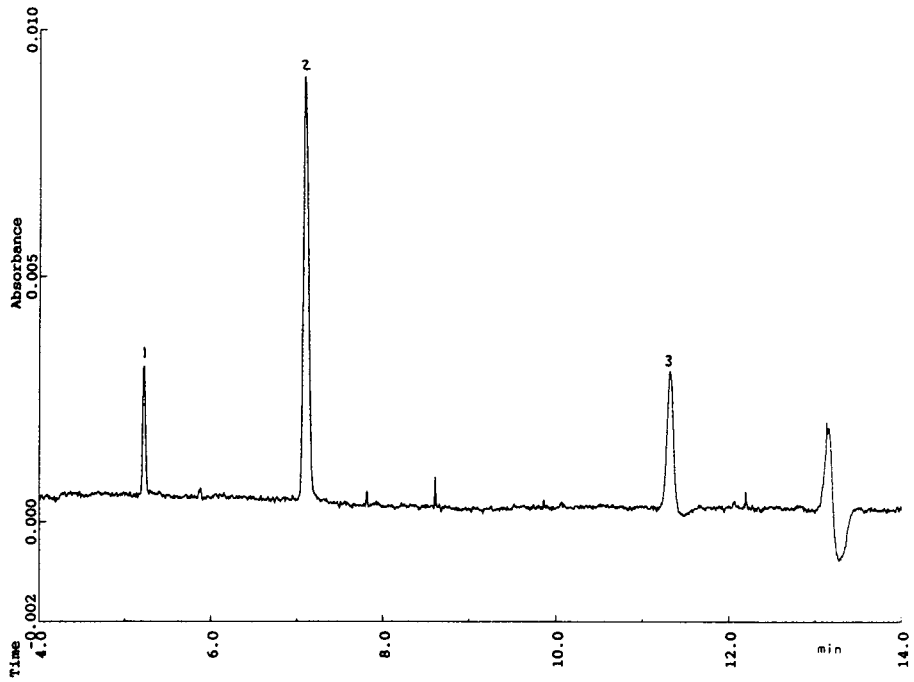

Fig. 10. Electropherogram of the geometric isomers of chloroaniline obtained by CZE at pH 3.75. Capillary tube, 57 cm × 50 μm I.D.; temperature, 25°C; applied voltage, 30 kV. Peaks: 1 = *p*-; 2 = *m*-; 3 = *o*-chloroaniline.

Nevertheless, as shown in Fig. 9, the predicted optimum pH value at which the resolution is maximum for this mixture is in good agreement with the experimental results. The corresponding electropherogram obtained at this pH value (3.75) is shown in Fig. 10.

Finally as predicted by the computation, no inversion of the migration order of the geometric isomers of chloroaniline was observed.

CONCLUSIONS

This series of experiments concerning the resolution of mixtures containing either acid or basic compounds showed a satisfactory fit between the experimental results and the computed values of the resolution as a function of pH. This good agreement leads to a precise determination of the optimum pH value *a priori*, for compounds for which the pK_a values are either tabulated or not. In addition, a good idea of the electrophoretic behaviour of the different constituents of the mixture can be predicted, allowing one to detect, *a priori*, an inversion in the migration order of the solutes. This possibility of the computation treatment appears to be very useful for the optimization of analyses of mixtures containing some compounds at low concentration levels, allowing a better detection.

Considering these very encouraging results, the extension of this treatment to amphoteric molecules is in progress.

REFERENCES

1 K. Otsuka, S. Terabe and T. Ando, *J. Chromatogr.*, 348 (1985) 39.
2 M.G. Khadeli, S.C. Smith and J.K. Strasters, *Anal. Chem.*, 63 (1991) 1820.
3 J.K. Strasters and M.G. Khadeli, *Anal. Chem.*, 63 (1991) 2503.
4 J. Vindevogel and P. Sandra, *J. High Resolut. Chromatogr.*, 14 (1991) 795.
5 S. Terabe, T. Yashima, N. Tanaka and M. Araki, *Anal. Chem.*, 60 (1988) 1673.
6 M.W.F. Nielen, *J. Chromatogr.*, 542 (1991) 173.
7 S. Wern, *J. Microcol. Sep.*, 3 (1991) 147.

8 J.L. Beckers, F.M. Everaerts and M.T. Ackermans, *J. Chromatogr.*, 537 (1991) 407.
9 K.D. Lukacs and J.W. Jorgenson, *J. High Resolut. Chromatogr. Chromatogr. Commun.*, 8 (1985) 407.
10 W.J. Lambert and D.L. Middleton, *Anal. Chem.*, 62 (1990) 1585.
11 J. Vindevogel and P. Sandra, *J. Chromatogr.*, 541 (1991) 483.
12 A. Albert, *Ionization Constants of Acids and Bases*, Wiley, New York, 1962.
13 D.D. Perrin, *Dissociation Constants of Organic Bases in Aqueous Solutions*, Butterworths, London, 1965.

Journal of Chromatography A, 652 (1993) 347–353
Elsevier Science Publishers B.V., Amsterdam

CHROM. 25 055

High-efficiency filter fluorometer for capillary electrophoresis and its application to fluorescein thiocarbamyl amino acids

Edgar Arriaga, Da Yong Chen, Xiao Li Cheng and Norman J. Dovichi*

Department of Chemistry, University of Alberta, Edmonton, Alberta T6G 2G2 (Canada)

ABSTRACT

Fluorescence detection has produced excellent detection limits in capillary electrophoresis. Laser excitation produces the highest sensitivity detection. The perceived difficulties associated with the use of the laser has discouraged applications of fluorescence to capillary electrophoresis. In particular, difficulties in wavelength selection limit the choice of chemistry available in capillary electrophoresis. We report the design of a filter fluorometer based on a compact 75 W xenon arc lamp for capillary electrophoresis; the instrument produces detection limits (3σ) of 20 zeptomol (1 zeptomol = 10^{-21} mol) for fluorescein and 200 zeptomol for fluorescein labeled amino acids.

INTRODUCTION

Laser-based fluorescence detection has produced spectacular results for capillary electrophoresis [1–25], with state-of-the-art detection limits in the yoctomol ($=10^{-24}$ mol) range [22,24]. While lasers produce spectacular detection performance in fluorescence instrumentation, they suffer from a number of perceived limitations, including high cost and limited lifetime. In reality, the limited choice of excitation wavelengths may be the most important limitation of lasers [26].

The performance of fluorometers built with incoherent excitation sources tends to be many orders of magnitude poorer than the laser-based systems [27–32]. The best results for non-laser-based fluorescence detection came from Jorgenson's group, who reported detection limits of 83 amol (1 attomol = 10^{-18} mol) for *o*-phthalaldehyde–glycine excited with a mercury–xenon arc lamp in a post-column detector [29]. Wallingford and Ewing [30] used a 200-W mercury lamp for fluorescence excitation, but they did not report detection limits. Commercial instruments have used a pulsed xenon flash lamp, focused directly onto the capillary, for fluorescence detection [31]. Workers from Applied Biosystems compared xenon, deuterium and tungsten lamps for fluorescence excitation [32]. That system employed a monochromator to select excitation wavelength, an aperture to control the size of the illuminated region in the capillary, fiber optics to collect fluorescence, and an emission filter placed before a photomultiplier tube detector. A xenon lamp produced the best detection limits, 500 attomoles of 9-fluorenylmethyl chloroformate–glycine.

At first glance, use of an incoherent arc lamp fluorometer appears difficult in capillary electrophoresis. The very small excitation volumes required in capillary separations (less than 1 nl) and the stringent requirements on light scatter are challenging constraints. However, recent work in this laboratory has provided evidence that lamp-based excitation should be possible with high sensitivity. In particular, we have found that low-power coherent excitation

* Corresponding author.

0021-9673/93/$06.00

sources can produce yoctomole detection limits in fluorescence instrumentation; an instrument based on a 0.75 mW helium neon laser (λ = 543.5 nm) produces detection limits of 500 tetramethylrhodamine molecules [24]. Theory suggests that a xenon arc lamp in a filter fluorometer will produce 0.75 mW of optical power at the sample.

In this paper, we report a filter fluorometer based on a xenon arc lamp. This instrument produces excitation from the near ultraviolet at 250 nm through the infrared; an appropriate bandpass interference filter isolates the desired wavelength. The system is designed to excite fluorescence efficiently. A 75-W xenon arc lamp, with an integral parabolic reflector, efficiently couples light to the experiment. An aspheric lens efficiently illuminates a limiting aperture; this aperture blocks stray light from the lamp and defines the excitation volume. A high-quality microscope objective images the aperture onto a sheath flow cuvette. The sheath flow cuvette has excellent optical properties, resulting in background scatter that is lower than would be produced with on-column detection. A high-quality microscope objective collects fluorescence from the sample and images it onto an adjustable aperture. This aperture blocks stray light in the instrument, decreasing the background signal.

We chose to use an interference filter to isolate fluorescence rather than a monochromator. In our experience, it is much easier to achieve much higher transmission through a filter compared with the monochromator. We use an aperture to define the illumination volume rather than imaging the entire source onto the sample; light scatter is reduced with this aperture. We use a sheath flow cuvette rather than direct illumination of the capillary; light scatter is minimized. We use a high-efficiency microscope objective to collect fluorescence rather than fiber optics. The objective generates an excellent image of the excited sample; stray light is easily blocked with an aperture placed in the image plane of the objective.

THEORY

Consider a 75-W xenon arc lamp that acts as black-body radiator at 5600 K. Plank's black-body radiation equation may be written as

$$E_T(\lambda)\,d\lambda = \frac{2C^2h}{\lambda^5}\frac{d\lambda}{e^{hc/\lambda kT}-1} = \frac{1.19\cdot 10^{-16}\ \mathrm{W\,m^{-2}\,steradian^{-1}}}{\lambda^5} \cdot \frac{d\lambda}{e^{1.44\cdot 10^{-2}(Km)/\lambda T}-1} \quad (1)$$

where E_T is the spectral radiance of a surface in units of W m^{-2} steradian^{-1} over the spectral region $d\lambda$, λ is wavelength in m, C is the speed of light, h is Planck's constant, k is Boltzmann's constant and T is absolute temperature [33]. Table I lists the spectral radiance, integrated across a 10-nm spectral band-width for 5600 K black body.

Light from the lamp must be imaged onto the sample stream with an optical system. If the arc is imaged directly into the cuvette, a large amount of stray light will be generated. To reduce this stray light, the arc is first imaged onto an aperture; this limiting aperture is then imaged onto the cuvette.

From the second law of thermodynamics, the radiance at the image of the lamp will be less than or equal to the radiance of the lamp itself. In a filter fluorometer for capillary electrophoresis, the lamp is assumed to illuminate a 50-μm radius region in a fluorescence detection chamber. The optical power, P, that is available to illuminate the detection chamber is then given by

TABLE I

SPECTRAL RADIANCE OF A 5600-K BLACK BODY IN A 10-nm SPECTRAL BAND

λ (nm)	250	300	400	500	600	700
E (W m^2 steradian^{-1})	42 200	93 900	190 000	225 000	215 000	185 000

TABLE II

POWER DELIVERED TO SAMPLE THROUGH OPTICAL SYSTEM

λ (nm)	250	300	400	500	600	700
P (μW)	40	90	190	225	210	175

$$P = E_T A \Phi_{\text{illumination}} T_{\text{illumination}} \quad (2)$$

where A is the illuminated area of the pinhole, $\Phi_{\text{illumination}}$ is the collection efficiency for the illuminating optics and $T_{\text{illumination}}$ is the transmission of the illumination filter. For a system with illuminated area of $8 \cdot 10^{-9}$ m^2 (50-μm radius pinhole), collection efficiency of π steradians (25%), and average filter transmission of 50%, then the optical power delivered to the sample is given in Table II. That is, with a reasonable optical system, it appears possible to use a lamp to *deliver* microwatts of optical power (in a 10-nm spectral bandwidth) to a highly miniaturized fluroescence detector.

Use of a higher-power lamp is neither desirable nor useful in capillary electrophoresis. Xenon arc lamps tend to operate at constant temperature, independent of power; increased optical power is produced by increasing the size of the arc. After imaging the arc onto an appropriate size limiting aperture, the power delivered to the sample is independent of the lamp power, as long as the arc is larger than the limiting aperture. The increased power from a higher power lamp is lost on the limiting aperture.

EXPERIMENTAL

Illumination system

Fig. 1 shows a block diagram of the optical system. We use a 75-W xenon arc lamp (ILC Technology, Sunnyvale, CA, USA) for excitation. A Model 03 MHG 009 cold mirror (Melles Griot, Nepean, Canada) eliminates infrared radiation by reflection at 45° from the optical axis. This filter transmits visible light of wavelength shorter than 650 nm. An aspheric lens (Melles Griot Model 01 LAG 019) images the arc onto a 400 μm diameter pinhole placed at the focal point of the aspheric lens. In front of

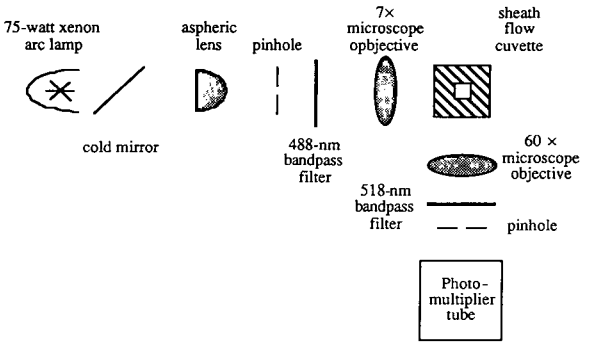

Fig. 1. Filter fluorometer. Light from a 75-W xenon arc lamp is filtered with a cold mirror, which reflects infrared radiation from the optical path. An aspheric lens is used to image the arc onto a 400-μm diameter pinhole. The transmitted radiation is spectrally filtered with a 10-nm bandpass interference filter centered at 488 nm. A 7× microscope objective images the pinhole into a sheath flow cuvette. Fluorescence is collected with a 60× microscope objective, filtered with a 518-nm bandpass filter, imaged onto an adjustable pinhole, and detected with a photomultiplier tube.

the pinhole, we use a 488-nm, 10-nm FWHM bandpass filter (Model 488 DF10; Omega Scientific, Burlington, VT, USA) to select the excitation wavelength. The pinhole is imaged onto the fluroescence detection chamber with a 7 × [N.A. (numerical aperture) 0.20] microscope objective (Melles Griot Model 04O AS 013), which produces a spot about 180 μm in diameter. This objective is 5.0 cm in front of the aspheric lens, mounted on a mirror holder that provides vertical adjustment and a Model 421-1S two-axis translation stage (Newport Instruments, Mississauga, Canada) to provide horizontal adjustment. An aluminum cover encloses the illumination system to minimize stray light. Additional baffles provide an effective blockage of all light not going through the microscope objective.

Post-column fluorescence detector

The quartz sheath flow cuvette is mounted onto a three-axis translation stage (constructed from three Newport Model 421-1S). The sheath flow chamber (NSG-Precision Cells, Farmingdale, NY, USA) has a square cross section of 0.04 mm^2 with 1-mm thick windows; the stainless-steel holder for the flow chamber is constructed locally. The illuminated volume is *ca.* $8 \cdot 10^{-3}$ mm^3. Adjustment of the height differ-

ence between the buffer reservoir and waste reservoir (3 cm approximately) allows control of the sheath flow. The fused-silica separation capillary is placed within the flow chamber; the excitation region is *ca.* 200 μm down stream from the capillary tip. The polyimide coating at the tip of the capillary inside the sheath flow cuvette has been previously eliminated using a gentle flame.

Collection optics and detection

Fluorescence is collected at right angles to the excitation source with a Model 60X-LWD 60× (N.A. 0.70) microscope objective (Universe Kogaku, Japan). To select fluorescence, we use a 518-nm, 25-nm FWHM bandpass filter (Omega Model 520 DF 25). The field of view is set by adjusting an iris located at the image plane of the objective. We align the components by observing visually the fluorescence from a 10^{-6} *M* fluorescein solution injected continuously at +20 000 V with an eyepiece (10×) instead of a detector. When alignment is optimized, the eyepiece is replaced by a water-cooled photomultiplier tube (Model R1477; Hamamatsu Photonics, NJ, USA) operated at −1200 V. We do a final alignment of the optical components by monitoring the photomultiplier tube output while injecting continuously 10^{-8} *M* fluorescein solution at +20 kV.

Capillary electrophoresis

The injection end of the capillary is less than 1 mm apart from the high voltage electrode (up to +29 000 V) inside a Plexiglas safety box. The other end of the capillary is inside the grounded sheath flow cuvette. The high-voltage power supply for electropherogram development and electrokinetic injection is controlled from a Macintosh IIsi computer with a multipurpose I/O board (National Instruments model MIO16XH).

Signal processing

The photomultiplier tube output is filtered (bandwidth 10 Hz) before it is processed by a Macintosh IIsi. The rate of data acquisition is 10 Hz. Data are displayed in real time using a Lab View 2.2 program and stored in binary files. The data are convoluted with a Gaussian filter characterized by a 0.5-s standard deviation.

Reagents

Stock $8.0 \cdot 10^{-3}$ *M* fluorescein (Molecular Probes, OR, USA) solution was prepared in 98% ethanol. Dilutions were prepared in pH 9.2, 5 m*M* borate buffer. $5.0 \cdot 10^{-3}$ *M* amino acid stock solutions were prepared in 0.2 *M* borate buffer. Fluorescein isothiocyanate (FITC; Sigma, MO, USA) derivatives were produced by mixing $1.55 \cdot 10^{-2}$ *M* FITC stock solution in 98% ethanol with amino acid stock solution in a 1:5 mol ratio and allowing to stand overnight. Dilutions and mixtures of different amino acids were prepared in pH 9.2, 5 m*M* borate + 10 m*M* sodium dodecyl sulfate buffer.

RESULTS AND DISCUSSION

We employ a sheath flow cuvette for post-column detection in our fluorescence detector. The excellent optical properties of the cuvette minimize light scatter, producing low background signals. In previous applications of the cuvette to fluorescence detection in capillary electrophoresis, only laser-based detection has been used [17–25]. Incoherent light sources have been used to excite fluorescence in flow cytometry, a technique which also used the sheath flow cuvette. Van Dilla *et al.* [34] reported the use of a mercury arc source to excite fluorescence in the sheath flow cuvette. Block Engineering used an incoherent light source to excite fluorescence in a flow cytometer based on a sheath flow cuvette [35]. In that instrument, a number of optical beams were used to illuminate the sample. Both a high pressure xenon arc lamp and a mercury arc lamp were used to generate fluorescence in an epilumination configuration.

Our fluorescence system was evaluated with both a 50-μm and 10-μm inner diameter capillary. Because of the large dimension of the sample stream produced by the 50-μm capillary, a rather large aperture was used to collect fluorescence. This large aperture also transmitted fluorescence from the polyimide coating of the capillary, producing unacceptably large background signals. By removing the capillary coat-

TABLE III

LIMITS OF DETECTION (LOD) FOR FLUORESCEIN

	10 μm I.D. capillary	50 μm I.D. capillary
Volume injected (l)	$6.8 \cdot 10^{-11}$	$1.8 \cdot 10^{-9}$
Fluorescein concentration (M)	$8.0 \cdot 10^{-10}$	$8.0 \cdot 10^{-11}$
LOD (M)	$2.0 \cdot 10^{-10}$	$1.5 \cdot 10^{-11}$
LOD (mol)	$1.4 \cdot 10^{-20}$	$2.8 \cdot 10^{-20}$

ing from the last few millimeters with a gentle flame, this background fluorescence was eliminated.

Detection limits were estimated by injecting known amounts of dilute fluorescein solutions. Table III presents the detection limits (3σ), estimated by the method of Knoll [36]. The mass detection limits are similar for the two capillaries; the 50-μm capillary produced superior concentration detection limits because of the use of a larger injection volume. These mass detection limits are roughly an order of magnitude inferior to those produced with an argon ion laser and a sheath flow cuvette [19]. The low excitation power produced by the filter fluorometer, along with the relatively large amount of stray light generated by the system, degrade the system performance compared with laser excitation. On the other hand, these fluorescence detection limits would have been the state-of-the-art in 1988. Improvements in stray light rejection and in illumination efficiency will certainly improve the performance of the filter fluorometer.

The detection limits produced by this filter fluorometer are more than two orders of magnitude superior to previous reports of lamp-based fluorescence detection. The improvement in performance results both from improved excitation efficiency and by use of the sheath flow cuvette to reduce scattered light from the capillary.

The linear dynamic range was estimated by injection of a series of fluorescein solutions. The response is linear ($r > 0.999$, $n = 5$) from the detection limit up to the saturation of the photomultiplier. The dynamic range extends from $8 \cdot 10^{-10}$ to $8 \cdot 10^{-7}$ M when the 10 μm I.D. capillary is used and from $2 \cdot 10^{-11}$ to $8 \cdot 10^{-7}$ M when the 50 μm I.D. capillary is used.

The rather large illumination volume produced by the filter fluorometer degraded the separation efficiency compared with that observed in laser-based detection. For $8 \cdot 10^{-10}$ M fluorescein, plate counts of 10^5 were observed for both the 10-μm and 50-μm inner diameter capillaries.

The post-column detector was applied to the separation of a nine FITC labeled acid mixture. Table IV lists the concentration and mass injected for the electropherogram in Fig. 3. The retention time for these derivatives is roughly three times greater than for fluorescein in Fig. 2, which presumably reflects differences in the ionization state of the molecules. The theoretical plate counts range from 150 000 to 200 000, and are typical for electrophoretic separation of these compounds.

Detection limits (3σ) for the glycine-fluorescein thiocarbamyl derivative are $2 \cdot 10^{-19}$ mol injected onto the capillary. These detection

TABLE IV

CONCENTRATION AND MASS INJECTED FOR FIG. 3

	Concentration (mol/l)	Mass injected (mol) $\times 10^{17}$
Alanine	$1.5 \cdot 10^{-5}$	27
Aspartate	$9.6 \cdot 10^{-6}$	35
Lysine	$2.2 \cdot 10^{-6}$	3.1
Glycine	$2.0 \cdot 10^{-6}$	3.8
Isoleucine	$4.9 \cdot 10^{-6}$	8.6
Methionine	$1.6 \cdot 10^{-6}$	2.9
Phenylalanine	$9.0 \cdot 10^{-7}$	1.6
Threonine	$1.6 \cdot 10^{-6}$	3.0
Tryptophan	$4.4 \cdot 10^{-6}$	8.0

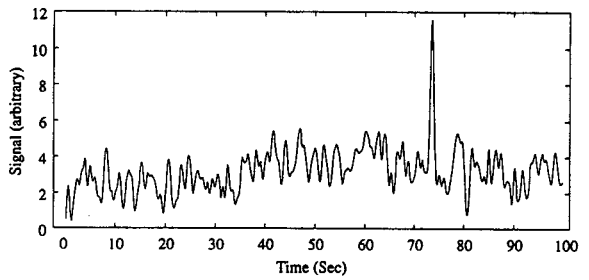

Fig. 2. Injection of $8 \cdot 10^{-10}$ *M* fluorescein. The separation was performed in a 37 cm × 10 μm I.D. capillary. Injection was for 5 s at 1 kV. Electrophoresis proceeded at 29 kV.

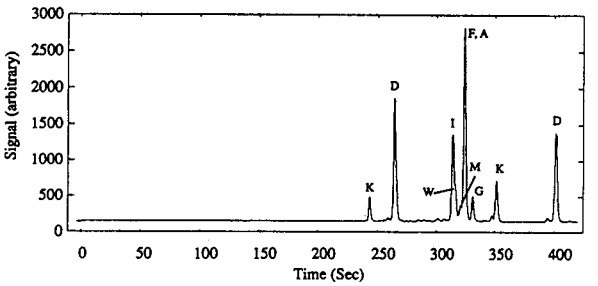

Fig. 3. Electropherogram of 9 fluorescein thiocarbamyl-amino acids. The separation was performed in a 37 cm × 10 μm I.D. capillary. Injection was for 2.5 s at 250 V. Electrophoresis proceeded at 20 kV in a pH 9.2, 5 m*M* borate and 10 m*M* sodium dodecyl sulfate buffer. The concentration and one-letter abbreviation of the derivatives are alanine (A) $1.5 \cdot 10^{-5}$ *M*, aspartate (D) $9.6 \cdot 10^{-6}$ *M*, lysine (K) $2.2 \cdot 10^{-6}$ *M*, glycine (G) $2.0 \cdot 10^{-6}$ *M*, isoleucine (I) $4.9 \cdot 10^{-6}$ *M*, methionine (M) $1.6 \cdot 10^{-6}$ *M*, phenylalanine (F) $9.0 \cdot 10^{-7}$ *M*, tryptophan (W) $4.4 \cdot 10^{-6}$ *M*.

limits are an order of magnitude poorer than those observed for fluorescein. The difference in performance is associated with the longer retention time for the derivative, a factor of two poorer quantum efficiency for FITC derivatives compared with native fluorescein [37], incomplete reaction between fluorescein and glycine, and degradation of the derivatizing reagent.

CONCLUSIONS

High-sensitivity fluorescence detection in capillary electrophoresis is possible without use of a laser. A low power arc lamp can deliver sufficient power to the small detection volume to produce detection limits in the mid-zeptomol range. By appropriate choice of excitation and emission filters, it should be possible to study a wide range of fluorescent materials with a single instrument.

The instrument performance results from several design choices. Excitation with a 75-W xenon arc lamp, with an integral parabolic reflector, efficiently couples light to the experiment. An aspheric lens efficiently illuminates the limiting aperture. A high-quality microscope objective images the aperture onto the cuvette. The sheath flow cuvette has excellent optical properties, resulting in background scatter that is lower than would be produced with on-column detection. A high quality microscope objective collects fluorescence from the sample. When combined with an aperture located at the image plane of the objective, light scatter is reduced dramatically. Further improvements in energy transfer from the lamp to the cuvette would result in gains in sensitivity, with ultimate performance near 1 zeptomol.

ACKNOWLEDGEMENTS

Dionex and the National Sciences and Engineering Research Council (NSERC) of Canada funded this work. N.J.D. acknowledges a Steacie fellowship from NSERC.

REFERENCES

1 E. Gassmann, J.E. Kuo and R.N. Zare, *Science*, 230 (1985) 813–814.
2 M.J. Gordon, X. Huang, S.L. Pentoney and R.N. Zare, *Science*, 242 (1988) 224–228.
3 W.G. Kuhr and E.S. Yeung, *Anal. Chem.*, 60 (1988) 1832–1834.
4 W.G. Kuhr and E.S. Yeung, *Anal. Chem.*, 60 (1988) 2642–2646.
5 B. Nickerson and J.W. Jorgenson, *J. High Resolut. Chromatogr. Chromatogr. Commun.*, 11 (1988) 878–881.
6 Y.F. Cheng, R.D. Piccard and T. Vo-Dinh, *Appl. Spectrosc.*, 44 (1990) 755–765.
7 H. Swerdlow and R. Gesteland, *Nucleic Acids Res.*, 18 (1990) 1415–1419.
8 H. Drossman, J.A. Luckey, A.J. Kostichka, J. D'Cunha and L.M. Smith, *Anal. Chem.*, 62 (1990) 900–903.
9 J.A. Luckey, H. Drossman, A.J. Kostichka, D.A. Mead, J. D'Cunha, T.B. Norris and L.M. Smith, *Nucleic Acids Res.*, 18 (1990) 4417–4421.

10 A.S. Cohen, D.R. Najarian and B.L. Karger, *J. Chromatogr.*, 516 (1990) 49–60.
11 J. Liu, Y.Z. Hsieh, D. Wiesler and M. Novotny, *Anal. Chem.*, 63 (1991) 408–412.
12 J. Liu, O. Shirota and M. Novotny, *Anal. Chem.*, 63 (1991) 413–417.
13 J.V. Sweedler, J.B. Shear, H.A. Fishman, R.N. Zare and R.H. Scheller, *Anal. Chem.*, 63 (1991) 496–502.
14 L. Hernandez, J. Escalona, N. Joshi and N. Guzman, *J. Chromatogr.*, 559 (1991) 183–196.
15 X.C. Huang, M.A. Quesada and R.A. Mathies, *Anal. Chem.*, 64 (1992) 967–972.
16 T. Higashijima, T. Fuchigami, T. Imasaka and N. Ishibashi, *Anal. Chem.*, 64 (1992) 711–714.
17 S. Wu and N. Dovichi, *Talanta*, 39 (1992) 173–178.
18 Y.F. Cheng and N.J. Dovichi, *Science*, 242 (1988) 562–564.
19 S. Wu and N.J. Dovichi, *J. Chromatogr.*, 480 (1989) 141–155.
20 Y.F. Cheng, S. Wu, D.Y. Chen and N.J. Dovichi, *Anal. Chem.*, 62 (1990) 496–503.
21 H. Swerdlow, S. Wu, H. Harke and N.J. Dovichi, *J. Chromatogr.*, 516 (1990) 61–67.
22 D.Y. Chen, H.P. Swerdlow, H.R. Harke, J.Z. Zhang and N.J. Dovichi, *J. Chromatogr.*, 559 (1991) 237–246.
23 J.Z. Zhang, D.Y. Chen, S. Wu, H.R. Harke and N.J. Dovichi, *Clin. Chem.*, 37 (1991) 1492–1496.
24 H. Swerdlow, J.Z. Zhang, D.Y. Chen, H.R. Harke, R. Grey, S. Wu, C. Fuller and N.J. Dovichi, *Anal. Chem.*, 63 (1991) 2835–2841.
25 J.Y. Zhao, D.Y. Chen and N.J. Dovichi, *J. Chromatogr.*, 608 (1992) 117–120.
26 J.D. Olechno, J.M.Y. Tso and J. Thayer, *Am. Lab.*, March (1991) 59–62.
27 J.W. Jorgenson and K.D. Lukacs, *Anal. Chem.*, 53 (1981) 1298–1302.
28 J.W. Jorgenson and K.O. Lukacs, *Science*, 222 (1983) 266–272.
29 D.J. Rose and J.W. Jorgenson, *J. Chromatogr.*, 447 (1988) 117–131.
30 R.A. Wallingford and A.G. Ewing, *Anal. Chem.*, 59 (1987) 681–684.
31 R.G. Brownlee and S.W. Compton, *Am. Biotechnol. Lab.*, October (1988) 10–17.
32 M. Albin, R. Weinberger, E. Sapp and S. Moring, *Anal. Chem.*, 63 (1991) 417–422.
33 R. Stair, R.G. Johnston and E.W. Halbach, *J. Res. Natl. Bur. Stand.*, 64A (1960) 291–296.
34 M.A. Van Dilla, P.F. Mullaney and J.R. Coulter, in *Annual Report, Biological and Medical Research Group (H-4) of the Health Division Report Number LA-3848-MS*, Los Alamos Scientific Laboratory, p. 100.
35 R. Curbelo, R. Schildkraut, T. Hirschfeld, R.H. Webb, M.J. Block and H.M. Shapiro, *J. Histochem. Cytochem.*, 24 (1976) 388–395.
36 J.E. Knoll, *J. Chromatogr. Sci.*, 23 (1985) 422–425.
37 S. Wu and N.J. Dovichi, *J. Appl. Phys.*, 67 (1990) 1170–1182.

Journal of Chromatography A, 652 (1993) 355–360
Elsevier Science Publishers B.V., Amsterdam

CHROM. 25 256

Semiconductor laser-induced fluorescence detection in capillary electrophoresis using a cyanine dye

Fu-Tai A. Chen*, Anton Tusak, Stephen Pentoney, Jr., Ken Konrad, Clarence Lew, Ed Koh and James Sternberg

Beckman Instruments Inc., 2500 Harbor Boulevard, Fullerton, CA 92634 (USA)

ABSTRACT

Cy5, an activated carboxyl cyanine fluorophore, was characterized by capillary electrophoresis (CE) using a semiconductor laser at 652 nm to induce fluorescence. Hydrolysis of the activated Cy5 in the presence of ammonia results in the formation of a mono- and diamide and a dicarboxylic acid. A Cy5-labeled oligonucleotide M_{13} primer for DNA sequencing (M13mp18 template) was synthesized with a purity of better than 95%. The labeled primer was analyzed by liquid chromatography, using UV–visible detection, and by CE, monitored by laser-induced fluorescence (LIF) detection. Analysis of the Cy5-labeled oligonucleotide primer by CE–LIF in a 9% polyacrylamide gel-filled capillary indicated the purity of the major Cy5–oligonucleotide primer was greater than 90%. The detection sensitivity for Cy5-based CE–LIF detection system with a 2.5-mW red semiconductor laser is about 10^{-10} *M*.

INTRODUCTION

Cy5 (Biological Detection Systems, Pittsburgh, PA, USA) is an activated cyanine dye that can be readily coupled with oligonucleotides, peptides and proteins [1,2]. It contains two broad absorption maxima, at 630 and 655 nm ($\epsilon = 150\,000$ and $215\,000$ cm^{-1} M^{-1}, respectively). The high extinction coefficient and fluorescence quantum yield of the Cy5, with its absorption maximum at 655 nm, appeared to make the dye suitable for laser-induced fluorescence (LIF) detection using a semiconductor laser source emitting at 652 nm. The following report deals with the characterization of Cy5 and its derivatives by means of the capillary electrophoresis (CE) technique using a red semiconductor laser and LIF detection. The synthesis of the Cy5-labeled oligonucleotide, a 20-mer M_{13} primer, will also be described. The Cy5-labeled oligonucleotide may potentially be used as a DNA hybridization probe and for sequencing.

* Corresponding author.

EXPERIMENTAL

Capillary electrophoresis procedures

A P/ACE 2100 equipped with a LIF detection system by Beckman Instruments (Fullerton, CA, USA) was used with P/ACE system software controlled by an IBM PS/2 Model 55 SX. Post-run data analysis was performed on System Gold software by Beckman Instruments. An open capillary column, typically of 27 cm length (20 cm to detector window) × 75 μm I.D. (Polymicro Technologies, Phoenix, AZ, USA) was assembled in the P/ACE cartridge format (100 × 200 μm aperture). The buffer used in the open capillary column was 80 m*M* borate, pH 10.0 [3]. The gel-filled capillary was prepared according to the procedure of Heiger *et al.* [4], and modified by Pentoney *et al.* [5]. A 2.5-mW diode laser

emitting at 652 nm and a 10-mW red helium–neon laser emitting at 632.8 nm were purchased from Melles Griot, Irvine, CA, USA. Both the laser headcoupler and the standard SMA-905 fiber connectors were purchased from the OZ optics, Ontario, Canada.

Cy5-labeled oligonucleotide primer

Cy5 was a product of Biological Detection Systems (BDS). M13 primer, ACGTTGT-AAAACGACGGCCA, (80 nmole of 20-mer) with a hexylamino terminus at its 5′-end, was obtained from Genosys, Houston, TX. The 5′-amino-M13 primer was dissolved in 200 μl of water. A 50-μl (20 nmole) aliquot was added to an acetonitrile solution containing Cy5 (80 nmol/100 μl acetonitrile) and allowed to stand at room temperature for 60 min. The resulting products were purified on a C_{18} reversed-phase column (25 cm × 4.1 mm) using a combination of methanol and 20 m*M* phosphate buffer at pH 6.0, on a Beckman System Gold LC with a Model 168 diode array detector. Peaks containing both nucleotide bases (260 nm) and Cy5 (655 nm) at a ratio of approximately 1 to 1.4 were collected. Purity was assessed by LC, CE and UV–visible spectra, as shown in the text.

RESULTS AND CONCLUSIONS

Cy5 is an activated dicarboxyl derivative of a cyanine compound that fluoresces in the near infrared region; its structure is shown in Fig. 1. The fluorescence emission maximum of Cy5 in aqueous solution is at 670 nm with a quantum efficiency of 0.13 [1,2]. Hydrolysis of Cy5 in the presence of 0.1 *M* hydrogencarbonate buffer at pH 9.0 yields Cy5–dicarboxylic acid. Using a red helium–neon laser (632.8 nm), the electropherogram of the Cy5–dicarboxylic acid, shown in Fig. 2A, appears to be fairly homogeneous. The addition of concentrated ammonia to the activated Cy5 results in the formation of Cy5-mono- and diamide along with Cy5–dicarboxylic acid (Fig. 2B), consistent with the structure suggested by Southwick *et al.* [1].

A red semiconductor laser that emits at 652 nm was coupled with the CE system for the LIF detection of the Cy5 and its derivatives. The emission spectrum of the red semiconductor

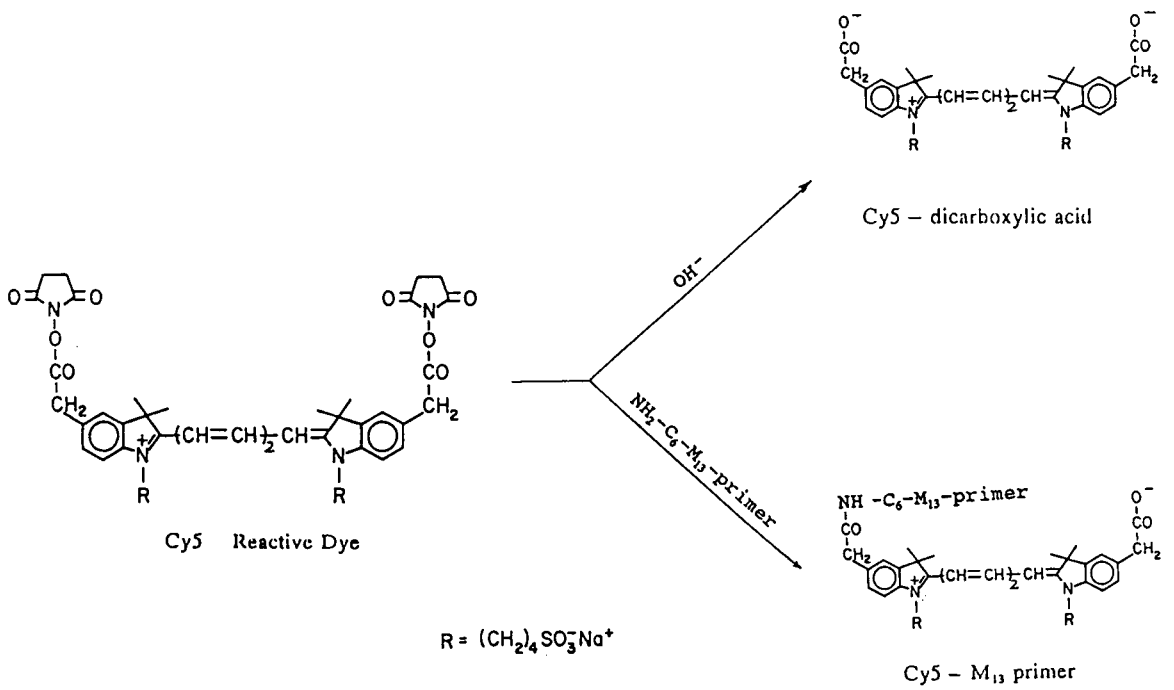

Fig. 1. Structure of the activated Cy5.

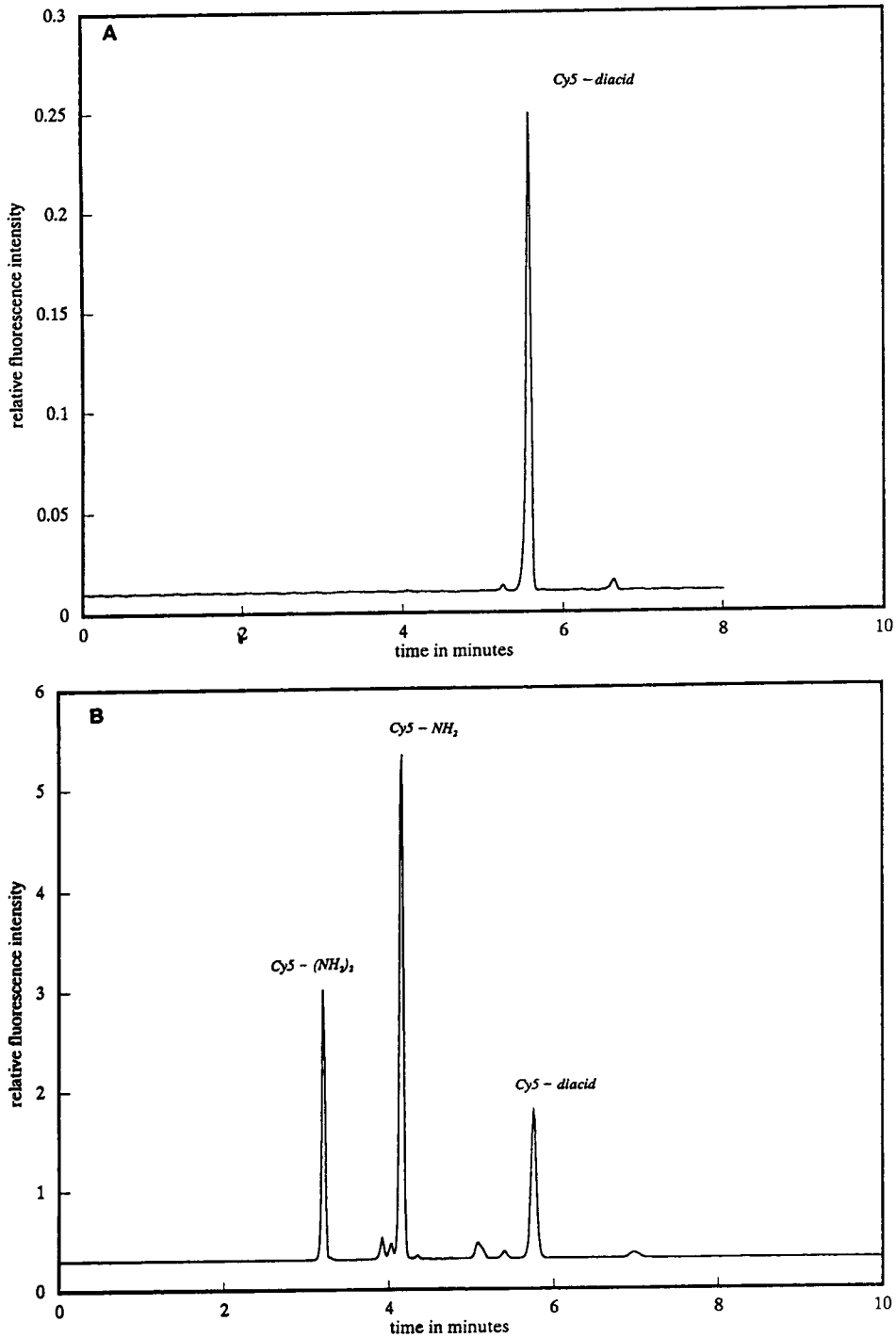

Fig. 2. (A) Electropherogram of hydrolyzed Cy5 at 1.0 n*M*. Conditions: Untreated fused-silica capillary, 25 cm × 75 μm I.D.; light source: 10-mW red helium–neon laser; emission filter: 670 nm ± 10 nm (Oriel, Stratford, CT, USA) and a notch filter at 633 nm (Barr Associates, Westford, MA, USA); applied potential/current: 7 kV/75 μA; buffer: 80 m*M* borate at pH 10.0. (B) Electropherogram of ammonia-treated Cy5 at 20 n*M*. Conditions as in (A).

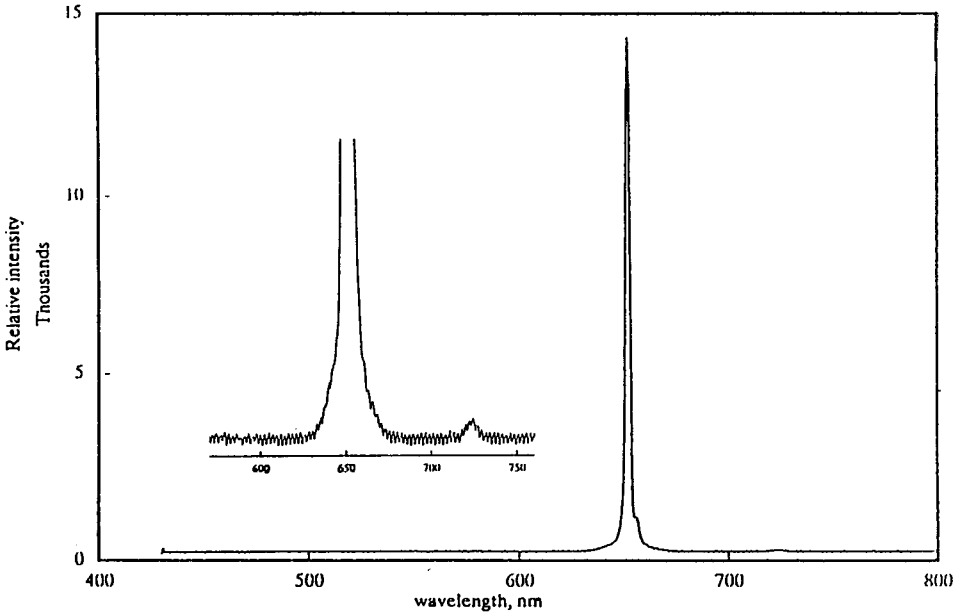

Fig. 3. Spectrum of the red semiconductor laser.

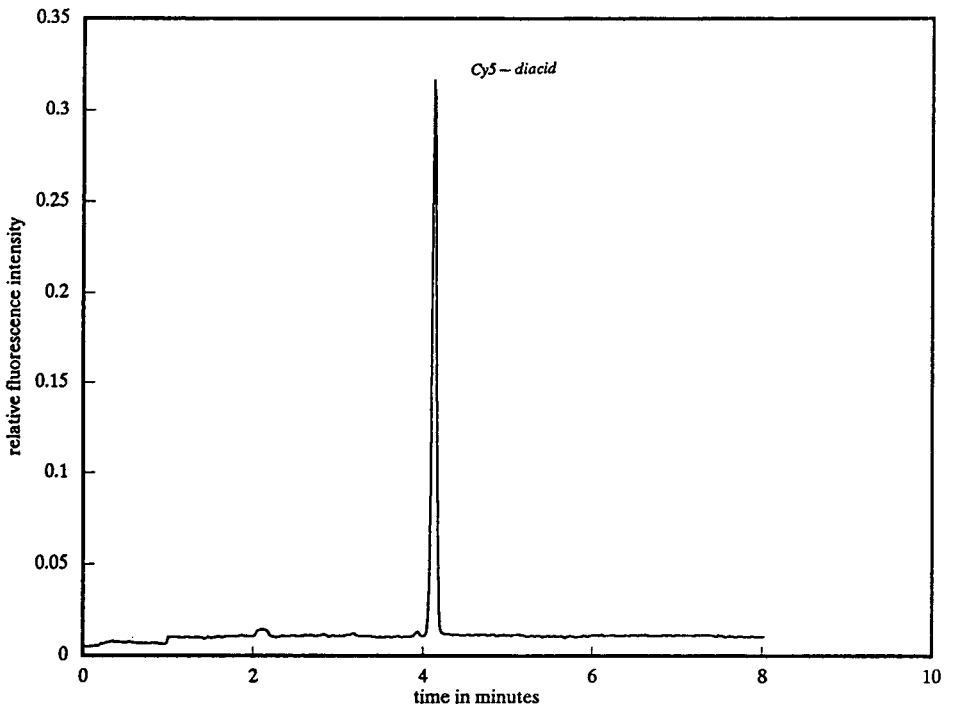

Fig. 4. Electropherogram of hydrolyzed Cy5 at 10 n*M*. Conditions: Untreated fused-silica capillary, 21 cm × 75 μm I.D.; light source: 2.5-mW red diode laser; emission filters: one narrow band filter at 670 nm ± 10 nm (No. 53965) and one long pass filter (No. 51340) (Oriel, Stratford, CT, USA); applied potential/current: 7 kV/82 μA; buffer: 80 m*M* borate at pH 10.0.

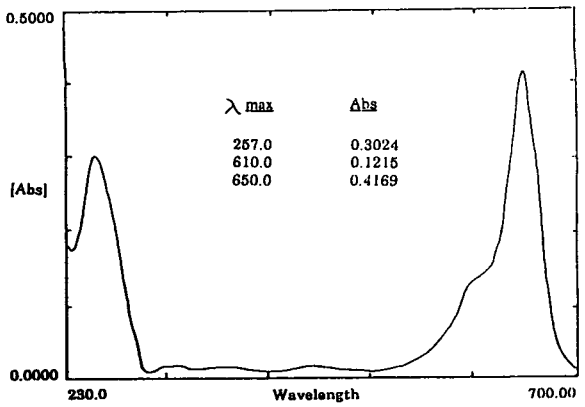

Fig. 5. UV–Vis spectrum of Cy5–M_{13} primer.

laser shown in Fig. 3 was analyzed at room temperature (22–24°C). The emission maximum occurs at 652 nm. A minor emission band at 722 nm was evident upon increasing the detection sensitivity, as shown in the insert in Fig. 3. To detect a fluorescence signal from Cy5 and its derivatives induced by the red diode laser, we have attempted to use the combination of a narrow band filter at 670 ± 10 nm and a long pass filter (cut-off at 660 nm). The electropherogram of a 10 n*M* solution of Cy5–dicarboxylic is shown in Fig. 4.

The synthesis of the Cy5-labeled 5′-amino-oligonucleotide primer was achieved by mixing a four-fold excess molar ratio of the activated Cy5 with 5′-aminohexyl-derivatized oligonucleotide primer, as shown in Fig. 1. The resulting mixture was purified on a reversed-phase column. The fraction showing absorbances at both 260 and 650 nm was collected. The total isolated yield from LC is approximately 70%, based on using 20 nmol of starting material, and obtaining 14 nmol of the final labeled primer.

The UV–Vis spectrum of Cy5-labeled primer is shown in Fig. 5 and the ratio of A_{257nm} *vs.* A_{650nm} is 0.725. Using an average molar extinction coefficient of 9000 for each nucleotide, the A_{257nm} of the 20-mer would be 180 000. The calculated ratio of A_{257nm} *vs.* A_{650nm} for the Cy5-labeled primer is 0.84. Thus, the UV–Vis spectrum observed for the Cy5-labeled primer is consistent with the expected values. Furthermore, analysis of the isolated Cy5-labeled primer

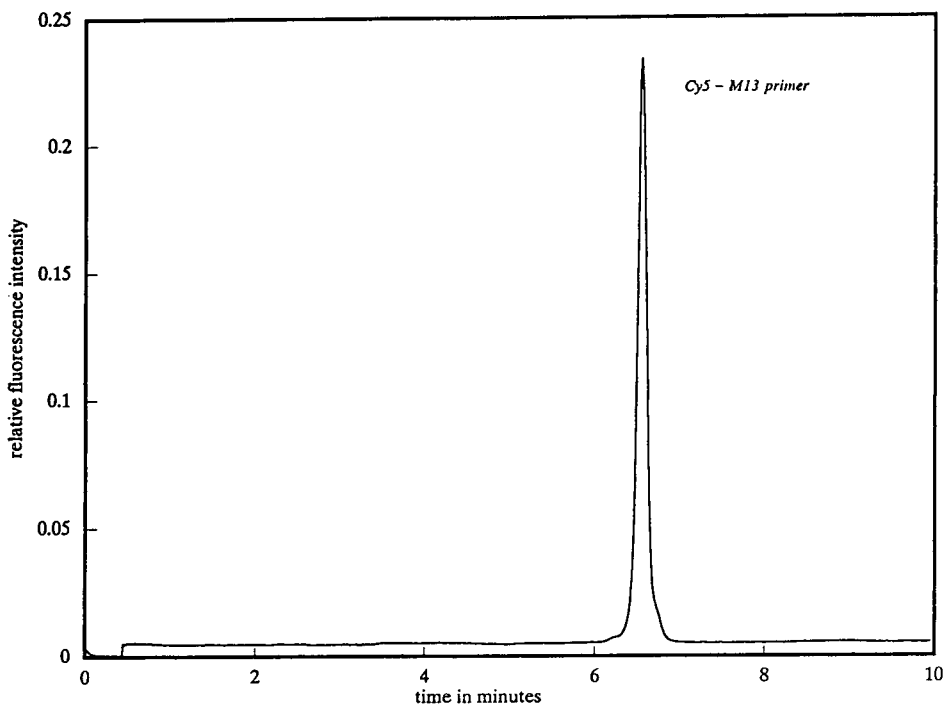

Fig. 6. Electropherogram of Cy5–M_{13} primer at 10 n*M*. Conditions as in Fig. 4.

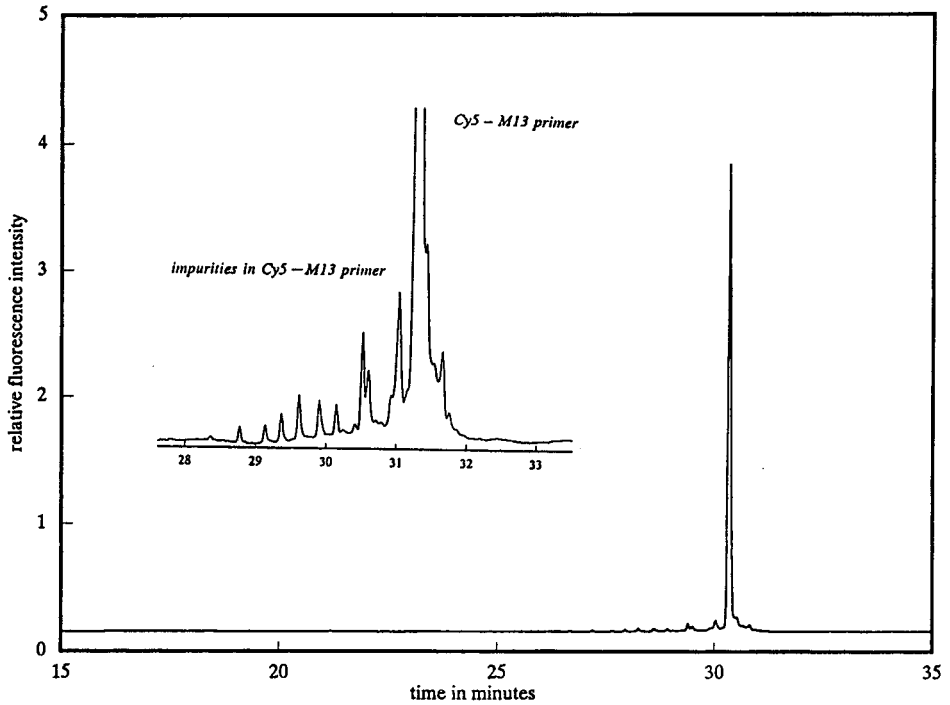

Fig. 7. Electropherogram of Cy5–M_{13} primer at 10 n*M*. Conditions: polyacrylamide gel-filled capillary, 47 cm × 100 μm I.D.; light source: 2.5-mW red diode laser; emission filters: same as those in Fig. 3; applied potential/current: 15 kV/14 μA; buffer: 100 m*M* Tris–borate buffer with 7 *M* urea, pH 8.3.

by CE–LIF in an open tube indicates its purity to be greater than 95% (Fig. 6).

The electropherogram of the labeled primer, obtained using a gel-filled capillary, is shown in Fig. 7. Clearly the isolated labeled primer is about 90% pure, and many small impurity peaks appear to be related to the original amino primer. The impurity peaks are not likely to be associated with the impurities of Cy5 or its hydrolyzed products, since their migration is substantially different from that of the labeled primers and did not exhibit a pattern similar to that shown in Fig. 7.

The detection limit of LIF detection using the red semiconductor laser for Cy5 and its derivatives is about 10^{-10} *M*. A further improvement in the optics may yield a sensitivity of 10^{-11} *M* with Cy5 as the fluorophore.

The functional utility of the Cy5-labeled primer was evaluated in DNA sequencing reactions. Preliminary results indicate that this labeled primer can be used for DNA sequencing by capillary gel electrophoresis using LIF with a red semiconductor laser.[a] Use of the semiconductor laser with Cy5 and its derivatives simplified the instrumentation design, providing a less expensive and more durable light source.

REFERENCES

1 P.L. Southwick, L.A. Ernst, E.W. Tauriello, S.R. Parker, R.B. Mujumdar, S.R. Mujumdar, H.A. Clever and A.S. Waggoner, *Cytometry*, 11 (1990) 418–430.
2 R.B. Mujumdar, L.A. Ernst, S.R. Mujumdar, C.J. Lewis and A.S. Waggoner, *Bioconj. Chem.*, 4 (1993) 105–111.
3 F.-T.A. Chen, *J. Chromatogr.*, 559 (1991) 445–453.
4 D.N. Heiger, A.S. Cohen and B.L. Karger, *J. Chromatogr.*, 516 (1990) 33–48.
5 S.P. Pentoney Jr., D.K. Konrad and W.I. Kaye, *Electrophoresis*, 13 (1992) 467–474.

[a] The results obtained using a 652-nm semiconductor laser for DNA sequencing using a Cy5-labeled primer will be published elsewhere.

Journal of Chromatography A, 652 (1993) 361–367
Elsevier Science Publishers B.V., Amsterdam

CHROM. 25 083

On-line chemiluminescence detection of proteins separated by capillary zone electrophoresis

Tadashi Hara*, Junichi Yokogi, Shinobu Okamura, Shigeru Kato and Riichiro Nakajima

Department of Chemical Engineering, Faculty of Engineering, Doshisha University, Karasuma Imadegawa, Kamikyo-ku, Kyoto 602 (Japan)

ABSTRACT

In a capillary zone electrophoretic (CZE) experiment in phosphate buffer (pH 3.5), Eosin Y was found to migrate together with protein in a capillary tube as a supramolecular complex. This finding gave the possibilities not only of overcoming the problem of protein determination but also of measuring the Eosin Y comigrating with protein by a chemiluminescence (CL) method with high sensitivity. Labelling of protein with dyestuff was achieved simply by mixing the protein and a dyestuff. On-line CL detection of the protein separated by CZE was feasible by measuring the CL intensity of a bis(2,4,6-trichlorophenyl) oxalate (TCPO)–H_2O_2–dyestuff system by means of an interface between CZE and CL detection. Several xanthene dyestuffs including Eosin Y were examined and Rose Bengal was found to be more sensitive than Eosin Y used in previous work. Using the present method, $5 \cdot 10^{-7}$–$1 \cdot 10^{-4}$ mol dm^{-3} of bovine serum albumin (BSA) could be determined using Rose Bengal in about 20 min with a detection limit of $2 \cdot 10^{-7}$ mol dm^{-3} (signal-to-noise ratio = 3), corresponding to 4 fmol of BSA. The results for fifteen kinds of proteins including BSA are reported.

INTRODUCTION

The separation and detection of a protein as a supramolecular complex using capillary electrophoresis were reported in a previous paper [1]. The method was based on the fact that Eosin Y migrated together with protein through a capillary tube as a supramolecular complex, where the protein was detected by measuring Eosin Y. Eosin Y accompanied by protein could be determined by measuring the chemiluminescence intensity of a bis(2,4,6-trichlorophenyl) oxalate (TCPO)–H_2O_2–Eosin Y system by means of an interface between capillary zone electrophoresis (CZE) and chemiluminescence (CL) detection. This was the first report of on-line CL detection of proteins separated by CZE. However, the method was not very sensitive for the detection of proteins, and several problems remained unresolved. So far, two successful studies involving luminol CL detection [2] and acridinium CL detection [3] have been reported on the application of CL detection to CZE. Wide-bore CZE with CL detection [4] has also been reported for the determination of dansylated compounds.

As Eosin Y is a xanthene dyestuffs, other xanthene dyestuffs such as Rose Bengal, Erythrosin B and Phloxin B were examined in this study, and Rose Bengal was found to be more sensitive than Eosin Y. The present system of coupling CZE and CL detection was successfully applied to the separation and detection of various proteins, including albumin and globulin. The interaction between a protein and a dyestuff and the behaviour of the supramolecular com-

* Corresponding author.

0021-9673/93/$06.00

plex formed were examined by spectrophotometry and CZE. The present system should be also applicable to other experiments involving CL detection.

EXPERIMENTAL

Apparatus

The apparatus shown in Fig. 1 was used. A high-voltage supply delivering 0–30 kV (Model HepLL-30PO, 08-L1; Matsusada Precision Device, Shiga, Japan) was used for the application of high voltages. Separation was performed in a fused-silica capillary tube (50 mm I.D.) (Polymicro Technologies, Phoenix, AZ, USA). CL detection was carried out by means of the CL detector shown in Fig. 1b. The CL reagent solution, obtained by dissolving TCPO and H_2O_2 in acetonitrile, and the buffer solution were fed into a four-way joint by use of two pumps [LC-9A (Shimadzu, Kyoto, Japan) and CCPD (Tosoh, Tokyo, Japan)], where the protein–dyestuff complex that passed through a capillary tube from the upper part to the lower part was mixed with the above-mentioned feed solution consisting of the CL reagent solution and the buffer solution. All the Teflon tubes were of 500 μm I.D. The resulting CL was detected by a photomultiplier (R-464; Hamamatu Photonics, Shizuoka, Japan) and measured by a photon counter (C1230; Hamamatu Photonics). A Shimadzu SPD-6AV UV–Vis spectrophotometric detector was used for the measurement of absorption in the UV–Vis region in CZE. A Shimadzu UV-1200 spectrophotometer was used for examining the optical properties of proteins, dyestuffs and their complexes.

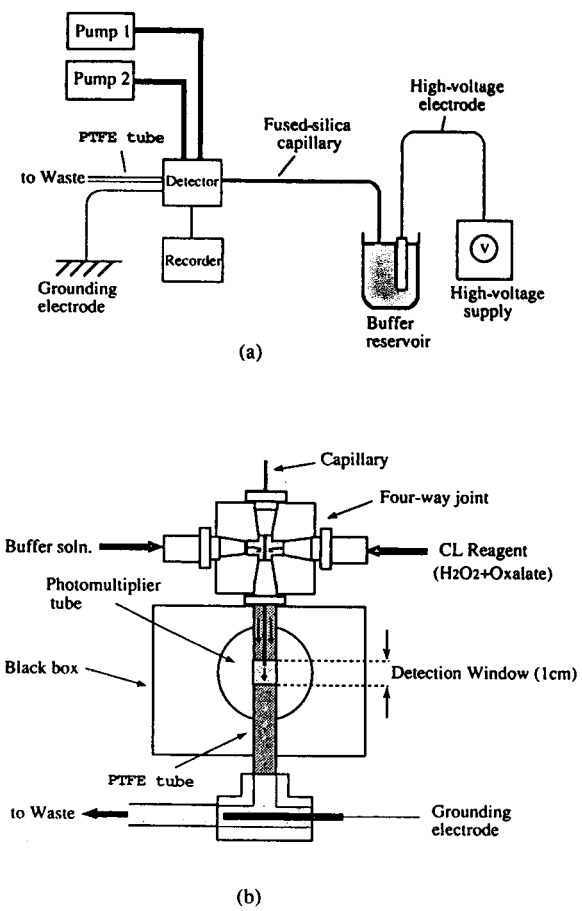

Fig. 1. Schematic diagrams of (a) the apparatus and (b) the CL detector.

Reagents

All of the reagents used were of commercially available special grade. Ion-exchanged water was distilled prior to use. A 0.01 *M* aqueous solution prepared by dissolving a definite amount of a dyestuff, *i.e.*, Eosin Y, Rose Bengal, Erythrosin B, Uranine (special grade from Nacalai Tesque, Kyoto, Japan), Phloxin B (special grade from Tokyo Kasei Kogyo, Tokyo, Japan), 3,4,5,6-tetrachlorofluorescein (TCFl), 2′,7′-dichlorofluorescein (2′,7′-DCFl) or 4′,5′-dichlorofluorescein (4′,5′-DCFl) (donated by Professor Y. Nishikawa, Kinki University, Osaka, Japan), in water was diluted with buffer solution prior to use. Bovine serum albumin (BSA), human serum albumin (HSA), rabbit serum albumin (RSA), bovine serum γ-globulin (BγG), human serum γ-globulin (HγG), ovalbumin (Ova) (from chicken egg, grade V), conalbumin (Cona) (from chicken egg), α-lactalbumin (α-lacta) (from bovine milk), β-lactglobulin (β-lact) (from bovine milk), haemoglobin (from bovine blood), myoglobin (from horse skeletal muscle, type I), avidin (from chicken egg), α-chymotrypsinogen (bovine), ribonuclease A (bovine) and β-casein (from bovine milk) were all pur-

chased from Sigma (St. Louis, MO, USA) and were used after dissolution in buffer solution (pH 3.5) consisting of 50 m*M* phosphoric acid and sodium hydroxide solutions. Commercially available hydrogen peroxide (30%) and TCPO from Nacalai Tesque were used as CL reagents, and actonitrile was used to dissolve these reagents. Surfactant FC-135 (provided by Sumitomo–3M, Tokyo, Japan) was also used to improve CZE separations.

Procedure

A fused-silica capillary tube was filled with phosphate buffer solution by using a 100-μl microsyringe. CL reagent solution (H_2O_2 + oxalate) was fed at a rate of 15 μl min^{-1} from pump 1 and buffer solution was fed at a rate of 5 μl min^{-1} from pump 2. The introduction of sample solution into the capillary tube was achieved by siphoning (injection time = 15 s) under the operation of pumps 1 and 2. CZE separation was carried out by applying a voltage of up to 20 kV between a high-voltage electrode and a ground electrode. The protein–dyestuff complex leaving the end of the capillary tube was immediately mixed with a mixture of CL reagent solution and buffer solution, followed by measurement of the CL intensity.

RESULTS AND DISCUSSION

The absorption spectra of xanthene dyestuffs and their complexes with BSA are shown in Fig. 2. As can be seen the bathochromic shift, in which the wavelength of maximum absorption of the xanthene dyestuffs Eosin Y, Phloxin B, Rose Bengal and Erythrosin B shifted to higher values, was observed in the presence of BDA. In a previous study [5] the authors examined the interaction between Eosin Y and BSA in phosphate buffer (pH 3.1) and the following data were obtained by the Klotz's method [6]: Eosin Y:BSA = 10.1:1 (mole ratio in combination), and association constant = $3.97 \cdot 10^5$ mol^{-1} dm^3 [5]. These values seemed to be reasonable, but they did not guarantee that Eosin Y would migrate with proteins in a capillary. Eosin Y showed its λ_{max} at 522 nm in phosphate buffer (pH 3.5), and

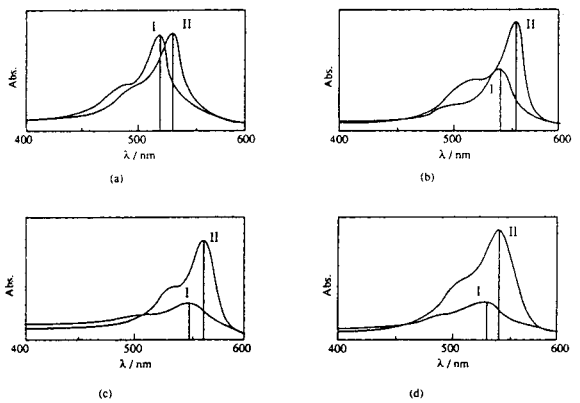

Fig. 2. Absorption spectra of xanthene dyestuffs and their complexes with BSA. Peaks: I = BSA absent and II = BSA present. (a) Eosin Y; (b) Phloxin B; (c) Rose Bengal; (d) Erythrosin B.

λ_{max} shifted to 535 nm in the presence of BSA. These bathochromic shifts are shown in Table I together with the migration times in CZE. As can be seen, no dyestuff gave a migration peak in the visible region except Uranine, showing that the dyestuff itself did not migrate at all under the experimental conditions. The migration time of BSA alone in CZE was obtained by detection at 210 nm and it was shown in Table I to agree with those of the dye–BSA complexes except for Uranine.

Electropherograms of the Eosin Y–BSA system are shown in Fig. 3. The peak in Fig. 3B is attributed to the Eosin Y–BSA complex as Eosin Y alone did not give any peak in the visible region, as mentioned above.

It was concluded from these results that the xanthene dyestuffs such as Eosin Y, Phloxin B, Rose Bengal and Erythrosin B and TCFl, 2′,7′-DCFl and 4′,5′-DCFl migrated together with BSA as their complexes.

The optimization of the interface between CZE separation and CL detection was carried out with regard to the following: (1) relationship between the pH of buffer solution and CL intensity; (2) relationship between TCPO concentration and CL intensity or signal-to-noise ratio; and (3) relationship between H_2O_2 concentration and CL intensity or signal-to-noise ratio. From a CL intensity–pH plot in the pH range 4–7, the optimum pH of the buffer solu-

TABLE I

COMPARISON OF DIFFERENT FLUORESCENT DYES

Sample	λ_{max} (nm)		Migration time in CZE (min)[a]	
	BSA absent	BSA present	BSA absent	BSA present[b]
Eosin Y	519	531	No peak	3.5
Rose Bengal	551	562	No peak	3.5
Erythrosin B	529	541	No peak	3.5
Phloxin B	540	553	No peak	3.5
TCFl	–	470	No peak	3.5
2′,7′-DCFl	–	503	No peak	3.5
4′,5′-DCFl	–	495	No peak	3.5
Uranine	–	430[c]	20.4	20.4[c]
BSA	–	–	–	3.5[d]

[a] Conditions as in Fig. 3.
[b] Detected at λ_{max} in the presence of BSA.
[c] No interaction with BSA was observed.
[d] Detected at 210 nm.

tion was adjusted at 6.0, where the CL intensity of the TCPO–H_2O_2 system was maximum. Although the CL intensity or signal-to-noise ratio of the TCPO–H_2O_2 system increased linearly with increase in TCPO concentration up to $1.0 \cdot 10^{-3}$ mol dm^{-3}, a $1.0 \cdot 10^{-3}$ mol dm^{-3} TCPO concentration was selected because the TCPO solubility under the experimental conditions was limited. The CL intensity of the TCPO–H_2O_2 system increased with increase in H_2O_2 concentration up to 0.12 mol dm^{-3}, but the signal-to-noise ratio gave a maximum value against H_2O_2 concentration, and 0.10 mol dm^{-3} H_2O_2 was chosen.

As the surfactant FC-135 had been reported to prevent the adsorption of proteins on the inner wall of a capillary and to give reproducible results [7], it was also used in the present study. The effects of FC-135 concentration on the peak sharpness (Fig. 4) and the CL intensity (Fig. 5) of the Eosin Y–BSA system were examined in

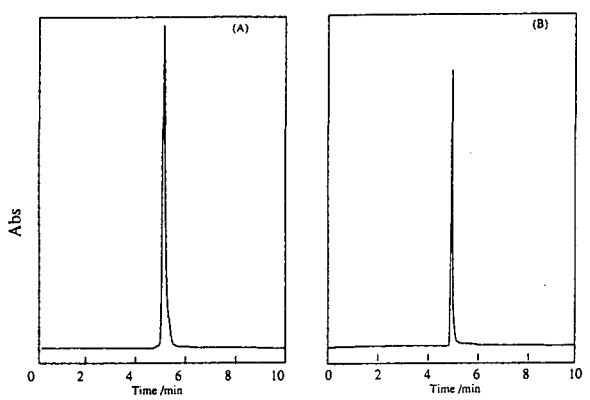

Fig. 3. Electropherograms of Eosin Y–BSA systems. Capillary, 59 cm of 50 μm I.D. fused-silica tube; applied voltage, 15 kV; buffer, 25 m*M* phosphate solution (pH 3.5) containing FC-135; sample, 5.0 g l^{-1} BSA solution containing $3 \cdot 10^{-4}$ *M* Eosin Y. Detection at (A) 210 and (B) 532 nm.

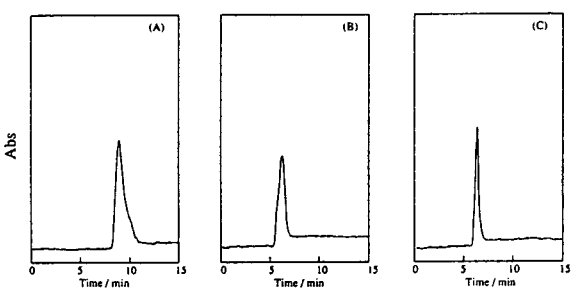

Fig. 4. Effect of FC-135 concentration on the peak shape of Eosin Y–BSA in phosphate buffer (pH 3.5). Capillary, 59 cm of 50 μm I.D. fused-silica tube; applied voltage, 15 kV; sample, 6.6 g l^{-1} BSA solution containing $3 \cdot 10^{-4}$ *M* Eosin Y; detection, 532 nm (corresponding to Eosin Y–BSA). Concentration of FC-135: (A) 25; (B) 50; (C) 100 mg dm^{-3}.

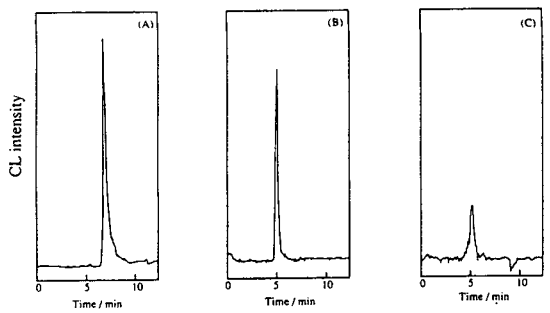

Fig. 5. Effect of FC-135 concentration on the CL intensity of Eosin Y–BSA in phosphate buffer (pH 3.5). Capillary, 85 cm of 50 μm I.D. fused-silica tube; applied voltage, 20 kV; sample, 1.0 g l^{-1} HSA solution containing $5 \cdot 10^{-5}$ *M* Eosin Y. Concentration of FC-135: (A) 25; (B) 50; (C) 100 mg dm^{-3}.

phosphate buffer (pH 3.5). The peak of Eosin Y–BSA became sharper with increase in FC-135 concentration (Fig. 4), but the CL intensity decreased (Fig. 5). The final concentration of FC-135 in the buffer solution used in the capillary tube was adjusted to 50 μg dm^{-3} in subsequent experiments.

Various samples containing 1 g l^{-1} of BSA and $3 \cdot 10^{-5}$ mol dm^{-3} each of Eosin Y, Rose Bengal, Erythrosin B, Phloxin B, TCFl, 2′,7′-DCFl and 4′,5′-DCFl were subjected to CZE separation and CL detection. The results obtained are given in Table II, where the CL intensity in the batch reaction, the peak height at each λ_{max} and the Cl intensity in CZE separation are shown relative to those of Eosin Y (= 100). The values for Rose Bengal were higher and the values for the other dyestuffs were lower than those for Eosin Y.

In the presence of Rose Bengal, the calibration graph for BSA was linear in the concentration range $5 \cdot 10^{-7}$–$1 \cdot 10^{-4}$ mol dm^{-3} with a detection limit of $2 \cdot 10^{-7}$ mol dm^{-3} (signal-to-noise ratio = 3) and a correlation coefficient of 0.998. In the presence of Eosin Y, the calibration graph was linear in the concentration range $1 \cdot 10^{-6}$–$1 \cdot 10^{-4}$ mol dm^{-3} BSA with detection limit 5×10^{-7} mol dm^{-3} (signal-to-noise ratio = 3) and a correlation coefficient of 0.998. According to the present method, BSA in the above-mentioned concentration range could be determined with a relative standard deviation of 4.9% and its detection limit was satisfactory in comparison with the usual detection limits (*ca.* 10^{-5} mol dm^{-3}) with UV detection in CZE.

The relative CL intensities for various proteins with respect to the BSA–Eosin Y complex (= 100) are given in Table III. For all the proteins tested, the Rose Bengal complexes gave larger relative CL intensities than those for Eosin Y complexes. CL was observed for all protein–Rose Bengal complexes. The relative CL intensities for the complexes between Rose Bengal and BSA, HSA, RSA, BγG, HγG, Ova and Cona were relatively large whereas those for the complexes between Rose Bengal and the other proteins were much smaller. Similar results were obtained for various protein–Eosin Y complexes, but no CL was observed for Eosin Y

TABLE II

RELATIVE SIGNAL INTENSITIES[a]

Sample[b]	Batch reaction: CL intensity	CZE	
		Peak height at λ_{max}	CL intensity
Eosin Y	100	100	100
Rose Bengal	102	112	138
Erythrosin B	84.0	90.8	78.1
Phloxin B	97.4	80.8	90.6
TCFl	95.0	30.5	–
2′,7′-DCFl	102	29.9	–
4′,5′-DCFl	88.4	28.0	–

[a] Relative signal intensity with respect to the value for Eosin Y (= 100).
[b] Sample containing 1 g l^{-1} of BSA and $3 \cdot 10^{-5}$ *M* of each dyestuff.

TABLE III

RELATIVE CL INTENSITIES FOR VARIOUS PROTEINS

Proteins ($1 \cdot 10^{-4}$ *M*)	Relative CL intensity[a]	
	Eosin Y	Rose Bengal
Serum albumin (bovine)	100	138
Serum albumin (human)	93.9	123
Serum albumin (rabbit)	114	130
γ-Globulin (bovine)	89.4	136
γ-Globulin (human)	94.5	130
Ovalbumin (chicken egg)	42.2	66.1
Conalbumin (chicken egg)	26.1	86.1
α-Lactalbumin (bovine milk)	20.0	28.3
β-Lactglobulin (bovine milk)	–	12.2
Haemoglobin (bovine)	12.0	16.6
Myoglobin (horse)	10.0	14.4
Avidin (chicken egg)	7.88	10.6
α-Chymotrypsinogen (bovine)	3.33	7.07
Ribonuclease A (bovine)	–	1.63
β-Casein (bovine milk)	–	1.01

[a] Relative CL intensity with respect to that of the BSA–Eosin Y complex (= 100).

complexes of β-lact, ribonuclease A and β-casein.

Electropherograms of (A) protein–Eosin Y complexes and (B) protein–Rose Bengal complexes with CL detection are shown in Fig. 6. In Fig. 6A HSA and RSA were selected whereas in Fig. 6B HγG, HSA and α-lacta were selected as model proteins. As can be seen, each protein in the protein–dyestuff complexes produced a sharp CL peak. The theoretical plate number for peak (b) in Fig. 6B is 42 000 according to the equation of Karger *et al.* [8].

Further efforts are being made to improve the sensitivity of the method.

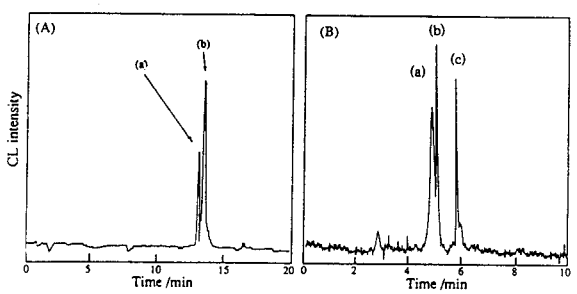

Fig. 6. Electropherograms of (A) protein–Eosin Y and (B) protein–Rose Bengal complexes with CL detection. Capillary, 85 cm fused-silica tube; applied voltage, 20 kV; buffer, 25 m*M* phosphate (pH 3.5) containing 50 mg/l of CFC-135. (A) Sample solution containing 3.3 g l^{-1} of protein and $3 \cdot 10^{-4}$ *M* Eosin Y; (B) sample solution containing 0.5 g l^{-1} of protein and $3 \cdot 10^{-4}$ *M* Rose Bengal. TCPO–CL reaction conditions were as follows: (1) 1 m*M* TCPO and 100 m*M* hydrogen peroxide in acetonitrile (15 μl min^{-1}); (2) 25 m*M* phosphate buffer (pH 6.0) (5 μl min^{-1}). (A) (a) = HSA, (b) = RSA; (B) (a) = HγG, (b) = HSA and (c) = α-lacta.

CONCLUSIONS

On the basis of the above results, the following conclusions were drawn: (1) some kinds of dyestuffs, especially xanthene dyestuffs, migrated together with certain proteins in a capillary tube as their complexes; (2) the dyestuff in a protein–dyestuff complex separated by CZE could be detected in place of protein by measuring its CL intensity; (3) of the dyestuffs tested, Rose Bengal was most sensitive and gave the highest CL intensity; (4) some protein–dyestuff complexes were obtained simply by mixing them and then labelling of the protein was easily carried out; (5) on-line CL detection of the proteins separated by CZE was feasible by measuring the CL intensity of the TCPO–H_2O_2–dyestuff system by means of an interface between CZE and CL detection; (6) with the present method, $5 \cdot 10^{-7}$–10^{-4} mol dm^{-3} of BSA was determined using Rose Bengal in about 20 min with a detection limit of $2 \cdot 10^{-7}$ mol dm^{-3} of BSA (signal-to-noise ratio = 3); (7) BSA, HSA, RSA, BγG, HγG, Ova and Cona, among fifteen proteins tested, could be sensitively determined by the present method.

ACKNOWLEDGEMENT

The authors acknowledge the assistance of Professor Y. Nishikawa, Kinki University, for kindly providing some of the reagents.

REFERENCES

1 T. Hara, S. Okamura, S. Katou, J. Yokogi and R. Nakajima, *Anal. Sci. (Suppl.)*, 7 (1991) 261.

2 R. Dadoo, L.A. Colon and R.N. Zare, *J. High Resolut. Chromatogr.*, 15 (1992) 133.
3 M.A. Ruberto and M.L. Grayeski, *Anal. Chem.*, 64 (1992) 2758.
4 A. Zhu and Q. Zhao, presented at the *1st International Symposium on High Performance Capillary Electrophoresis, Boston, MA, April 10–12, 1989,* poster T-P-127.
5 T. Hara and T. Imai, unpublished work.
6 I.M. Klotz, *J. Am. Chem. Soc.*, 68 (1946) 2299.
7 Å. Emmer, M. Jansson and J. Roeraade, *J. Chromatogr.*, 547 (1991) 544.
8 B.L. Karger, K.R. Snyder and C. Horvath, *An Introduction to Separation Science*, Wiley, New York, 1973.

Journal of Chromatography A, 652 (1993) 369–376
Elsevier Science Publishers B.V., Amsterdam

CHROM. 25 207

Cetyltrimethylammonium chloride as a surfactant buffer additive for reversed-polarity capillary electrophoresis–electrospray mass spectrometry

Johnson Varghese and Richard B. Cole*

Department of Chemistry, University of New Orleans, New Orleans, LA 70148 (USA)

ABSTRACT

The rapid analysis of picomole quantities of various cationic molecules (laser dyes, tripeptides and larger bioactive peptides) has been achieved by on-line capillary electrophoresis–electrospray mass spectrometry (CE–ES-MS). Use of the cationic surfactant, cetyltrimethylammonium chloride (CTAC) in the CE buffer greatly facilitated the analyses. Under reversed-polarity conditions (negative potential at the source vial), CTAC induces electroosmotic flow towards the mass spectrometer, presumably due to the creation of a cationic layer on the inner surface of the fused-silica capillaries. CTAC diminishes analyte–capillary wall interactions, allowing efficient separations and symmetrical peak shapes. It may be used over a wide range of pH values without loss of electroosmotic flow. Added selectivity, provided by the surfactant properties of CTAC, played a critical role in resolving closely related tripeptides as well as larger (five to thirteen amino acid units) peptides. Above the critical micelle concentration of CTAC, interactions with the pseudostationary micellar phase increased selectivity even for ionic analytes.

INTRODUCTION

When dealing with cationic species, either singly or multiply charged, the diminution of analyte–silica wall interactions is imperative to achieving high-efficiency separations in capillary electrophoresis (CE). An effective approach in this regard is to reverse the charge on the silica surface from negative to positive by chemical derivatization procedures, or by modification of the CE buffer system. These approaches require reversed-polarity operation in order to direct electroosmotic flow towards the detector.

Recently, aminopropyl-silylated (APS) fused-silica capillaries have been used by Moseley *et al.* [1] for on-line capillary zone electrophoresis–electrospray mass spectrometry (CZE–ES-MS) analysis of peptides. The capillary modification process involves the chemical bonding of (3-aminopropyl)trimethoxysilane to surface silanol sites. This afforded a positively charged column at pH 3.4 and below, corresponding to the pK_a value for APS. The number of derivatized sites was increased by pretreating the fused-silica with strong acid [2]. The use of APS columns not only reversed the direction of electroosmotic flow relative to standard fused-silica columns (corrected by reversing the polarity), but also increased the flow-rate relative to the latter.

The rate of electroosmotic flow in standard fused-silica capillaries can also be altered by varying the composition of employed buffer systems. Moreover, this represents an alternative approach to reversing the direction of electroosmotic flow. Cationic surfactants belonging to the alkyltrimethylammonium class of compounds have proven to be particularly effective in this regard. Terabe *et al.* [3] first reported the use of cetyltrimethylammonium bromide (CTAB) which formed a positively charged layer on the inner wall of the capillary and induced the

* Corresponding author.

0021-9673/93/$06.00

reversal of flow. In addition, under otherwise equivalent conditions, Altria and Simpson [4] showed that the rate of this reversed flow was one order of magnitude greater for capillaries filled with CTAB (2 m*M*), as compared to bare silica capillaries containing phosphate buffers (2 m*M*). Interestingly, a ten-fold dilution of the CTAB concentration only diminished the flow-rate by 36%. Addition of acetonitrile (1:1, v/v) to a solution of the surfactant changed the direction of flow once again, allowing normal-polarity operations at low flow-rates.

When employing surfactants in CE systems, the mechanism of separation may involve contributions from several components. Above the critical micelle concentration (CMC) of the surfactant, partitioning into the micellar pseudo-phase contributes significantly to overall selectivity, as practiced in micellar electrokinetic capillary chromatography (MECC) [5]. Below the CMC, analyte–surfactant interactions are more poorly defined.

The analytical utility of performing CE separations utilizing cationic surfactants has been well documented. Separation of anionic polystyrene "nanospheres" has been demonstrated utilizing the CTAB surfactant [6]. In that study, particle–capillary wall interactions were postulated to retain larger particles to a higher degree. Kasper *et al.* [7] also exploited properties afforded by CTAB (20 m*M*), including ion-pairing interactions, to efficiently separate linear DNA fragments. Selectivity was found to improve in the presence of urea (4 *M*). Liu *et al.* [8] demonstrated the separation of a series of angiotensin peptides consisting of seven to ten amino acid units in a buffer system containing dodecyltrimethylammonium bromide (DTAB). Selectivity was clearly shown to be superior when the concentration of DTAB was above its CMC value (14 m*M*), indicating that micellar interactions can play an important role in separations of charged components. Tetradecyltrimethylammonium bromide (TTAB) was used by Huang *et al.* [9] for the rapid separation of a series of low-molecular-mass carboxylic acids. Since electrophoresis and electroosmotic flow occurred in the same direction, analysis times were very short (<3.5 min).

We report the utilization of cetyltrimethylammonium chloride (CTAC) as a primary buffer system for on-line CE–ES-MS. The surfactant additive has been used to aid in the analysis of a laser dye (Rhodamine 6G), tripeptides, and larger bioactive peptides (five to thirteen amino acid units). The CMC value for CTAC has been reported to be 1.3 m*M* using the equivalent conductance method [10].

EXPERIMENTAL

Chemicals

All peptides and proteins were purchased from Sigma (St. Louis, MO, USA). Rhodamine 6G (99% purity) was purchased from Eastman Kodak (Rochester, NY, USA). Cetyltrimethylammonium chloride (CTAC) was purchased from Aldrich (St. Louis, MO, USA).

Capillary electrophoresis

Both CE–UV and on-line CE–ES-MS were performed using the Dionex CE System I (Dionex, Sunnyvale, CA, USA). For all applications reported, a constant negative voltage (reversed-polarity) was employed. Vitreous silica capillaries were used in all analyses; 100 μm I.D., 235 μm O.D. were purchased from Polymicro Technologies (Phoenix, AZ, USA).

Electrospray mass spectrometry

A Vestec 201 electrospray mass spectrometer (Houston, TX, USA) was employed for all mass spectral analyses. Collisionally induced dissociations were minimized in all experiments by maintaining a low skimmer-collimator voltage difference.

CE–ES-MS interface

The in-house construction and optimization of the interface has been detailed elsewhere [11]. The interface allows for the delivery of a "make-up" fluid and an electrical contact at the capillary exit, in an analogous fashion to the sheath flow set-up described by Smith *et al.* [12]. For the analysis of the tripeptides and the larger peptides, the silica tip was maintained 0.1 to 0.2 mm outside the stainless-steel needle in order to

achieve maximum sensitivity [11]. However, in the case of the laser dye (strong cation) ES-MS sensitivity was not an issue, hence, the silica capillary was maintained within the stainless-steel needle to afford greater stability [11] and to improve mixing of the CE eluent and sheath flow liquid.

Prior to each CE–ES-MS analysis, the interface was optimized by electroosmotically infusing the analyte mixture and tuning the mass spectrometer on a particular analyte ion. This exercise not only maximized the signal intensity, but also allowed operating parameters (chamber temperatures, liquid flow-rates, and applied potentials) to equilibrate. In order to maintain the optimum probe position and operating conditions, the pressure inject facility on the CE instrument was utilized to clean and fill the capillary with fresh buffer while maintaining the probe inside the mass spectrometer. All reconstructed ion electropherograms contained in this report display raw data with no post-acquisition processing.

RESULTS AND DISCUSSION

Analysis of Rhodamine 6G

Initial normal-polarity CE–ES-MS attempts to evaluate the purity of Rhodamine 6G, a widely used laser dye, were thwarted by high silica wall–analyte interactions which proved detrimental to achieving high-efficiency separations [11]. The incorporation of CTAC (0.5 m*M*)–NaCl (5 m*M*) into the buffer system was effective in generating greater efficiencies, and excellent ES-MS signals were observed for the parent ion (*m*/*z* 443) at picomole levels (6.4 pmol). The presence of isomeric compounds was also evident, although signal-to-noise ratios were poor for these low level impurities. When the same analysis was performed with greater loading (64 pmol on column) the data displayed in Fig. 1 were obtained. Even though the selected ion electropherogram of *m*/*z* 443 indicates overloading of the main component, the desired effect of increasing the ES-MS response for isomeric components as well as for analogues (*m*/*z* 415) was achieved. Clearly, three isomeric *m*/*z* 443

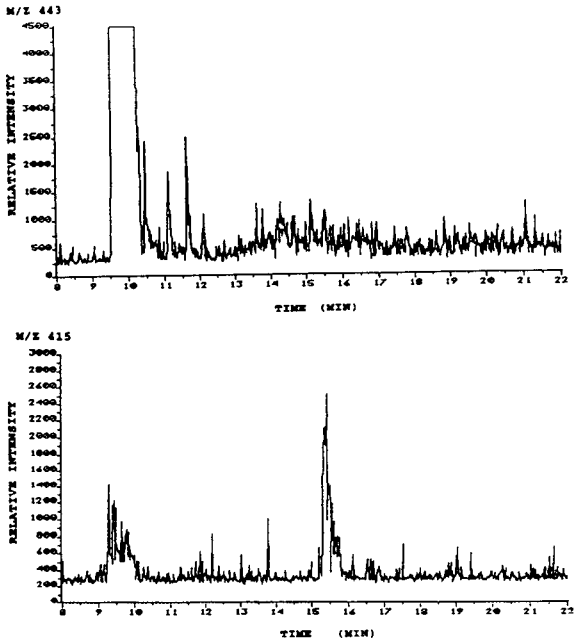

Fig. 1. Selected-ion electropherograms of *m*/*z* 443 (top) and *m*/*z* 415 (bottom) from the CE–ES-MS analysis of Rhodamine 6G (1000 ng/μl solution/64 pmol on column). Buffer: CTAC (0.5 m*M*) and NaCl (5 m*M*), pH 6.2; capillary: 100 μm I.D., 235 μm O.D., 100 cm in length; sample injection: 100 mm/10 s; CE voltage: 20 kV; ES voltage: 2.8 kV; MS scan rate: 1.21 s/scan (*m*/*z* 300 to 600).

peaks (Fig. 1, top) eluting between 10.5 and 12.5 minutes are present in the mixture.

The appearance of two *m*/*z* 415 components (Fig. 1, bottom) having vastly different retention times was also observed. The early eluting compound is likely to correspond to a hydrolyzed form of Rhodamine 6G where the ethyl ester has been converted to the carboxylic acid form, thus reducing its positive character at the operating pH of 6.2. The zwitterionic nature of this species could be responsible for early elution. The later eluting peak (Fig. 1, bottom) may correspond to the replacement of an ethyl group with a hydrogen atom at either nitrogen.

The identity of the early eluting *m*/*z* 415 peak was further clarified by performing mild alkaline hydrolysis (NaOH, pH 8.5) of Rhodamine 6G (100 ng/μl, structure shown in Fig. 2). At given time intervals, aliquots were removed for analysis and diluted ten-fold with the operating buffer (CTAC 0.5 m*M*, NaCl 5 m*M*, pH 6.2). The

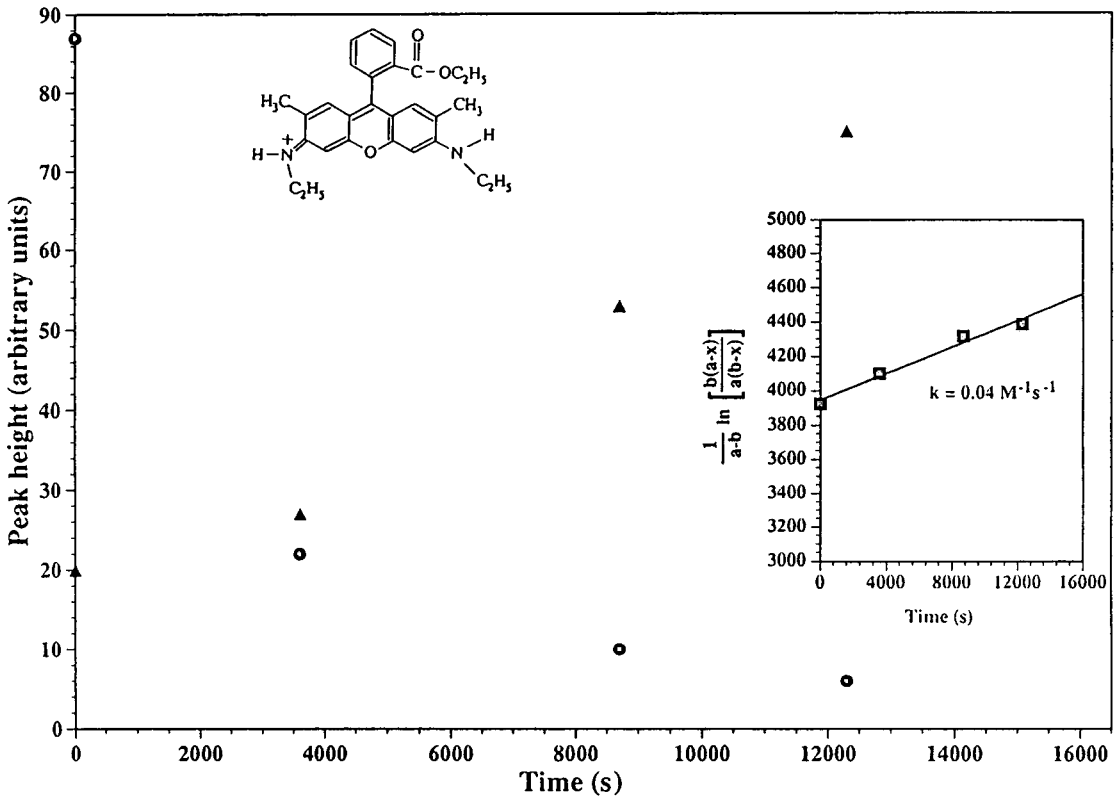

Fig. 2. Plot indicating the change in concentration of (●) the ethyl ester (structure at top) and (▲) the carboxylic acid forms of Rhodamine 6G (100 ng/μl) as functions of time under mild alkaline hydrolysis conditions (NaOH, pH 8.5). At given time intervals, aliquots were removed for analysis and diluted ten-fold with the operating buffer (CTAC 0.5 m*M*, NaCl 5 m*M*, pH 6.2). The reaction was monitored by CE–fluorescence detection (λ_{Ex}: 515 nm, λ_{Em}: 550 nm). Inset: second-order kinetics plot to determine '*k*', the rate constant for alkaline hydrolysis of Rhodamine 6G: a = initial [Rhodamine 6G]; b = initial [OH^-]; x = [product].

reaction was monitored by CE–fluorescence detection (λ_{Ex}: 515 nm, λ_{Em}: 550 nm). The hydrolysis product was observed to elute just before Rhodamine 6G. Depletion of the main component (ethyl ester form) with rapid growth of the hydrolysis product (carboxylic acid form) was evident, as shown in Fig. 2. The plot of second-order kinetics expected for alkaline hydrolysis (inset, Fig. 2) yields the rate constant, $k = 0.04\ M^{-1}s^{-1}$ for the reaction. This experiment adds proof that the early eluting *m/z* 415 peak in Fig. 1 does represent the carboxylic acid (hydrolyzed) form of Rhodamine 6G.

Analysis of tripeptides

The ability to separate component peptides in a mixture using capillary electrophoresis with CTAC-based buffers is aided significantly by analyte interactions with the cationic surfactant. Overall selectivity can be augmented by varying the operating pH quite independently from the CTAC concentration, in order to invoke net

TABLE I

TRIPEPTIDES SUBJECTED TO CE–ES-MS USING THE CTAC BUFFER ADDITIVE

Peptide	M_r	Quantity injected (pmol)
Gly-DL-Leu-DL-Ala	259.3	64
Glu-L-Cys-L-Gly (Glutathione)	307.3	54
Gly-L-Phe-L-Leu	335.4	50
Gly-L-Phe-L-Phe	369.4	45

charge differences between peptides. Two tripeptides (listed third and fourth in Table I) were separated utilizing the CTAC (1 mM) buffer at pH 2.9. As the buffer concentration was below the CMC, no micelles were expected to be present. The peptides (both at 250 ng/μl) were dissolved in the same CTAC buffer (pH 2.9), ensuring both protonation of these molecules and cationic coating of the capillary wall. Single-ion monitoring electropherograms (Fig. 3) display the signals for the protonated species.

The larger tripeptide (M_r 369) was found to elute approximately 1 min before the smaller one (M_r 335). Under the employed operating conditions, both tripeptides appear to exhibit similar behavior toward acquiring charge (protonation). The smaller peptide is retained longer, indicating a higher electrophoretic mobility against the strong electroosmotic flow.

Within these CTAC systems, pH may be varied readily without losing electroosmotic flow. A CTAC buffer system (2.5 mM, above the CMC) was utilized at pH 4.3 to separate the four tripeptides listed in Table I, including the two referred to earlier. Displayed in Fig. 4 are the selected-ion electropherograms, representing protonated forms of peptides having molecular masses ranging from 259 to 369. Baseline resolution of all components was achieved within 8 min. Glutathione (M_r 307) was found to elute first, while the order of elution for the three remaining tripeptides was according to increasing molecular mass. The elution order for the two larger peptides is opposite to the situation illustrated in Fig. 3. Moreover, retention times are lower by approximately a factor of two, indicating changes in their net charge.

The elution of glutathione prior to the other components suggests that the molecule possesses more negative character than the others, most likely originating from dissociation of its glutamic acid residue. As the concentration of CTAC was maintained above the CMC, interaction with micelles now becomes a factor in the

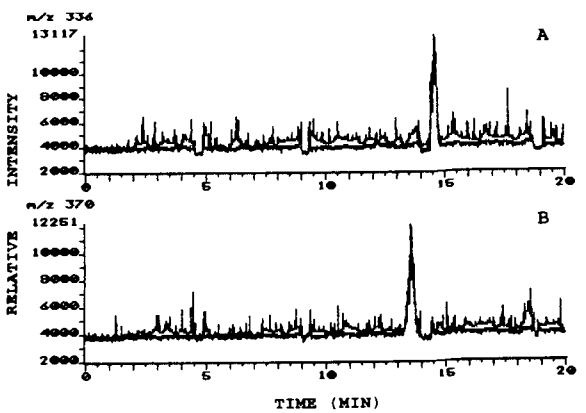

Fig. 3. Single-ion monitoring electropherograms from the CE–ES-MS of (A) Gly-L-Phe-L-Leu (MH^+, m/z 336) and (B) Gly-L-Phe-L-Phe (MH^+, m/z 370). Sample concentration: 250 ng/μl each/25 pmol and 23 pmol injected on column, respectively. Buffer: CTAC (1 mM) and glacial acetic acid (1%, v/v), pH 2.9; capillary: 100 μm I.D., 235 μm O.D., 85 cm in length; sample injection: 100 mm/10 s, CE voltage: 18 kV; ES voltage: 2.84 kV; MS scan rate: 0.63 s/scan.

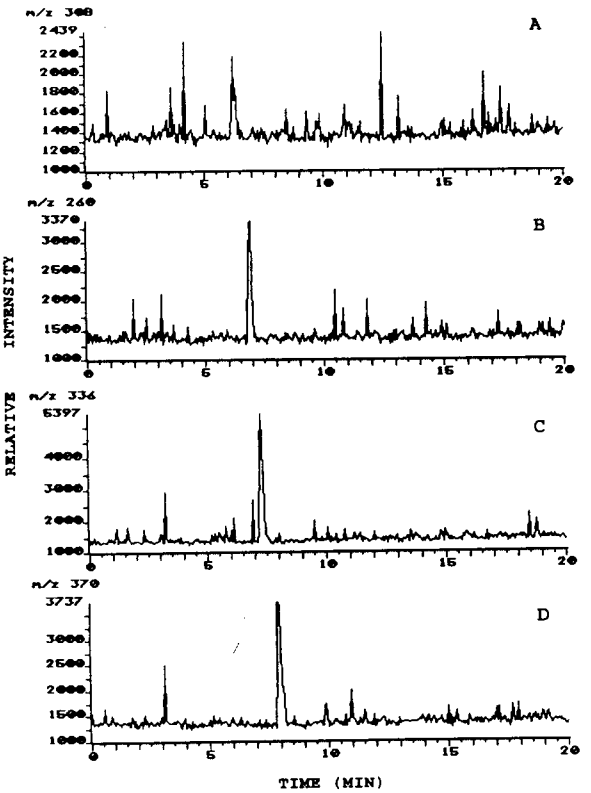

Fig. 4. Selected-ion electropherograms from the CE–ES-MS analysis of tripeptides: (A) Glu-L-Cys-L-Gly (MH^+, m/z 308), (B) Gly-DL-Leu-DL-Ala (MH^+, m/z 260), (C) Gly-L-Phe-L-Leu (MH^+, m/z 336), (D) Gly-L-Phe-L-Phe (MH^+, m/z 370). Buffer: CTAC (2.5 mM), pH 4.3; capillary: 100 μm I.D., 235 μm O.D., 85 cm in length; sample injection: 100 mm/10 s; CE voltage: 18 kV; ES voltage: 2.71 kV; MS scan rate: 3.1 s/scan.

overall separation scheme. If the remaining three peptides exhibit overall negative character (highly unlikely at pH 4.3), then elution with increasing molecular mass could be rationalized on the basis of electrophoretic mobility. It is more plausible that the three remaining tripeptides have positive character, and that micellar interactions play the dominant role in affording selectivity. For this series, the degree of hydrophobicity of the amino acid side chains increases with increasing molecular mass, hence, interaction with the pseudostationary micellar phase is expected to increase, causing the larger molecules to be retained longer.

Off-line ES of certain peptides indicated that in the presence of CTAC, sensitivity fell by a factor of three to four relative to optimium conditions in the absence of CTAC. The CTAC buffer is being continuously infused into the ES ion source during CE–ES-MS operation, hence, the absolute sensitivity for the separated peptide zones is lower than it would have been, if the separation had been conducted in volatile buffers. A major portion of the total electrospray ion current is carried by the cationic surfactant, thus suppressing the protonated peptide signal. As depicted in Fig. 4, the signal-to-noise ratios for all peaks were satisfactory despite the presence of CTAC, which allowed the generation of mass spectrometer scan data (m/z 250 to 280 and m/z 290 to 400). The quadrupole was not scanned over the CTAC cation (m/z 284) in order to avoid "saturation" of the electron multiplier detector.

Analysis of larger peptides

A mixture of larger peptides (five to thirteen amino acid units, see Table II) were prepared in CTAC (2.5 mM, pH 4.3) and subjected to analytical conditions similar to those employed for the tripeptides. The utilization of an acidic sheath flow liquid (methanol-water-glacial acetic acid 80:10:10, pH 2.8) proved particularly favorable in increasing the analyte ion currents in comparison to the use of pure methanol. Nevertheless, it became apparent that ES-MS sensitivities for these larger peptides were not as high as those observed for the tripeptides. For this reason, the mass spectrometer was operated

TABLE II

LARGER PEPTIDES ANALYZED BY CE–ES-MS USING THE CTAC BUFFER ADDITIVE

Peptide	M_r	Quantity injected (pmol)
Leucine enkephalin	555.6	10
β-casomorphin	789.9	7
Ile-Ser-bradykinin	1260.5	5
Angiotensinogen	1644.9	4

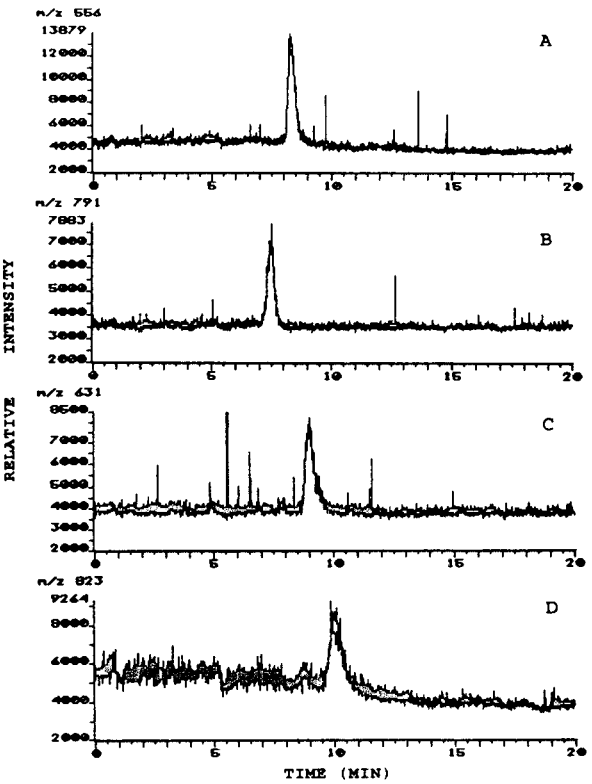

Fig. 5. Single-ion monitoring electropherograms from the CE–ES-MS analysis of larger peptides (five to thirteen amino acid units): (A) leucine enkephalin (MH^+, 556), (B) β-casomorphin (MH^+, m/z 791), (C) Ile-Ser-bradykinin [$(M+2H)^{2+}$, m/z 631] and (D) angiotensinogen [$(M+2H)^{2+}$, m/z 823]. Buffer: CTAC (2.5 mM), pH 4.3; capillary: 100 μm I.D., 235 μm O.D., 85 cm in length; sample injection: 50 mm/4 s, CE voltage: 18 kV; ES voltage: 2.84 kV; MS scan rate: 0.66 s/scan.

in the single ion monitoring (SIM) mode during on-line CE–ES-MS. Off-line ES data for the largest peptides in the series: Ile-Ser-bradykinin and angiotensinogen in the presence of CTAC (pH 4.3), afforded primarily the doubly-charged species $(M+2H)^{2+}$ at m/z 631 and m/z 823, respectively; hence, these ions were chosen to be monitored. The ion currents for leucine enkephalin and β-casomorphin were mainly in the form of the singly charged (protonated) species (m/z 556 and m/z 791, respectively).

The SIM electropherograms are displayed in Fig. 5. From a theoretical standpoint, the CE separation efficiencies are non-ideal; nevertheless, the buffer system has afforded sufficient selectivity to allow baseline resolution of all components. As with the tripeptides, the buffer pH (4.3) and CTAC concentration (2.5 mM) play a critical role in achieving this selectivity. The elution profile is influenced by the basicity of the component amino acids which dictate the charge state at the operating pH. The hydrophobicity of the peptide side chains also plays a role in determining selectivity via micellar interactions [8].

Since leucine enkephalin (M_r 555) elutes after β-casomorphin (M_r 790), interaction with the pseudostationary phase does not appear to be the dominant mechanism for determining selectivity (β-casomorphin has more hydrophobic substituents). The elution order is more consistent with charge-to-size considerations governing electrophoretic mobilities of similarly charged (positive) species. Ile-Ser-bradykinin and angiotensinogen (M_r 1261 and 1645, respectively) were found to elute after the smaller peptides. At the buffer pH of 4.3, these larger peptides carry more protons than the smaller species, which can result in longer retention in the column. The contribution of diffusion processes to band broadening was amplified by the long (100 cm) column length. Reducing the sample loading to improve the efficiency was not feasible due to sensitivity limitations. Increasing the ionic strength of the buffer would also have improved efficiencies, but instability caused by increased conductance down the capillary precluded this possibility.

CONCLUSIONS

The presence of the quarternary ammonium surfactant CTAC in the CE buffer effectively reduces adsorption of cationic species onto the interior of the fused-silica wall while also providing a strong electroosmotic flow. The latter is particularly important for on-line CE–MS where the use of unusually long capillaries may be required, thus increasing analysis times. The non-bonded cationic surfactant layer is constantly regenerated by the buffer system, thus diminishing the problem of fouling of the interior of the capillary, and enabling excellent reproducibility of electropherograms. The strong cationic nature of the surfactant enables operation over a wide pH range without losing electroosmotic flow, and without degradation of any phase. This feature enables rapid sequential analyses which can be exploited for real-time monitoring of fast reactions. No time was spent preparing bonded-phase columns which may have limited operational pH ranges (*e.g.*, pH 3.4 and below for APS columns). Slow degradation of these types of bonded-phase columns limit column lifetime and analytical reproducibility. The main drawback of the surfactant additive approach for on-line CE–MS is the sensitivity limitation caused by the bulk flow of charged reagent into the mass spectrometer ion source. Adsorption of surfactant onto the counterelectrode (nozzle) diminishes sensitivity over time, necessitating cleaning after each full day of use.

ACKNOWLEDGEMENTS

Financial support for this project was provided through NIH grant No. P01-DC00379. The authors thank Dionex Corporation for providing CE instrumentation.

REFERENCES

1 M.A. Moseley, J.W. Jorgenson, J. Shabanowitz, D.F. Hunt and K.B. Tomer, *J. Am. Soc. Mass Spectrom.*, 3 (1992) 289.
2 M.A. Moseley and E.D. Pellizzari, *J. High Resolut. Chromatogr. Chromatogr. Commun.*, 5 (1982) 488.

3 S. Terabe, K. Ishikawa, K. Utsuka, A. Tsuchiya and T. Ando, *Proceedings of the 26th International Liquid Chromatography Symposium, Kyoto, Jan. 25–26, 1983.*
4 K.D. Altria and C.F. Simpson, *Anal. Proc.*, 23 (1986) 453.
5 S. Terabe, K. Otsuka and T. Ando, *Anal. Chem.*, 57 (1985) 834.
6 B.B. VanOrman and G.L. McIntire, *J. Microcolumn Sep.*, 1 (1989) 289.
7 T.J. Kasper, M. Melera, P. Gozel and R.G. Brownlee, *J. Chromatogr.*, 458 (1988) 303.
8 J. Liu, K.A. Cobb and M. Novotny, *J. Chromatogr.*, 519 (1990) 189.
9 X. Huang, J.A. Luckey, M.J. Gordon and R.N. Zare, *Anal. Chem.*, 61 (1989) 766.
10 P. Mukerjee and K. Mysels, *Nat. Stand. Ref. Data Ser. (US Nat. Bur. Stand.)*, 36 (1971).
11 J. Varghese and R. B. Cole, *J. Chromatogr.* 639 (1993) 303.
12 R.D. Smith, C.J. Barinaga and H.R. Udseth, *Anal. Chem.*, 60 (1988) 1948.

Journal of Chromatography A, 652 (1993) 377–383
Elsevier Science Publishers B.V., Amsterdam

CHROM. 25 143

Determination of peptides by capillary electrophoresis–electrochemical detection using on-column Cu(II) complexation

Marian Deacon, Thomas J. O'Shea and Susan M. Lunte*

Center for Bioanalytical Research, University of Kansas, Lawrence, KS 66047 (USA)

Malcolm R. Smyth

School of Chemical Sciences, Dublin City University, Dublin 9 (Ireland)

ABSTRACT

A Cu(II)-coated capillary has been developed for the determination of peptides by capillary electrophoresis with electrochemical detection. Capillaries were prepared by forcing a solution 48 μM in $CuSO_4$, 120 μM in tartaric acid, 2.4 mM in NaOH and 120 μM in KI through them for 25 min; the resulting capillaries are stable for at least 12 h. Under alkaline conditions, peptides complex with Cu(II) present on the walls of the capillary to form Cu(II)–peptide complexes which can be detected oxidatively at a carbon fiber electrode. Di-, tri-, tetra- and pentaglycine were determined with a detection limit of $7 \cdot 10^{-7}$ M for triglycine. N-Terminal-blocked peptides can also be determined via this method. This system is more sensitive than direct detection of peptides by UV at 210 nm and exhibits higher selectivity than commonly employed derivatization procedures based on reactions with a primary amine functionality.

INTRODUCTION

High-performance liquid chromatography (HPLC) determination of peptides complexed with Cu(II) has been accomplished previously by two methods: postcolumn addition of Cu(II) with electrochemical detection (ED) at a glassy carbon electrode [1–5], or detection of eluting peptides at a solid copper electrode [6,7]. Detection at a copper electrode is best suited for determination of dipeptides since the sensitivity has been shown to decrease with increasing peptide length [6]. In 1989, Warner and Weber [1] reported using postcolumn addition of biuret for the selective detection of peptides by liquid chromatography–ED. The resulting Cu(II)–peptide complexes could be detected oxidatively at +0.70–0.90 V *vs.* Ag/AgCl. For many peptides, the oxidation was chemically reversible, and added selectivity could be obtained using dual electrode detection. Detection limits using this method were two orders of magnitude lower than those obtained with a copper electrode.

In this paper, the use of the biuret chemistry in the detection of peptides by capillary electrophoresis (CE)–ED is investigated. CE has been shown to be a powerful technique for the separation of charged compounds, in particular, peptides and amino acids. Because CE can be used for analysis of nanoliter sample volumes, it has been found to be useful in the fields of biotechnology and microanalysis of biological systems [8–10]. The fused-silica capillary used in CE, unlike bonded-phase HPLC columns, is

* Corresponding author.

0021-9673/93/$06.00

stable at high pH, which means that postcolumn derivatization is no longer a necessity.

To date, UV, fluorescence and radiometric detection have been used for the detection of peptides by CE. Due to the pathlengths encountered in CE (25–100 μm), UV detection is very insensitive. In addition, the low wavelength commonly employed for the detection of peptides (210 nm) is not very selective. Fluorescence detection, while sensitive, is limited to naturally fluorescent molecules or fluorescently derivatized compounds. More derivatization reagents react only with peptides possessing a primary amine functionality; therefore, N-terminal-blocked peptides cannot be detected. There is also very little selectivity for peptides over amino acids. Radiometric detection necessitates the use of radioactively labeled species.

ED, unlike UV detection, does not suffer from a loss of sensitivity when the cell volume is decreased. The development of the porous glass coupler [11], the Nafion joint [12], and end-column detection [13] has enabled the use of ED for CE. To date, the investigation of the ED of peptides separated by CE has been limited to the use of a copper electrode for the detection of dipeptides [14] or selective determination of thiol-containing peptides such as glutathione [15]. In this paper, the on-column complexation of peptides with copper and subsequent determination by CE–ED is described.

EXPERIMENTAL

Reagents

All solutions were prepared in deionized water and filtered with a 0.2 μm Acrodisc filter (Gelman Sciences, Ann Arbor, MI, USA). Biuret reagent (0.6 mol/l NaOH, 12 mmol/l $CuSO_4$, 32 mmol/l $C_4H_4KNaO_6 \cdot 4H_2O$, 30 mmol/l KI) was obtained from Sigma (St. Louis, MO, USA). Cupric sulfate, sodium hydroxide and sodium borate were supplied by Fisher Scientific (Pittsburgh, PA, USA). Potassium iodide and sodium potassium tartrate were obtained from Sigma. Di-, tri and tetraglycine, Arg–Gly–Asp–Ser, Arg–Gly–Glu–Ser and Pro–Leu–Gly–amide were obtained from Sigma; di-, tri- and tetraalanine and Ala–Gly–Gly were from Research Plus (Bayonne, NJ, USA). Ultrapure sodium hydroxide was obtained from Aldrich (Milwaukee, WI, USA). 3-(Cyclohexylamino)-1-propanesulfonic acid (CAPS), 2-amino-2-methyl-1-propanol and glycine were obtained from Sigma and were used to prepare buffer solutions. All chemicals were reagent grade and were used as received.

Capillary electrophoresis system

The CE-ED system used was described previously [12]. The detector cell was operated in a three-electrode configuration with a 33-μm carbon fiber working electrode (AVCO Specialty Products, Lowell, MA, USA), a platinum wire auxiliary and a Ag/AgCl reference electrode (Bioanalytical Systems, West Lafayette, IN, USA). The detection cell contained 0.1 *M* NaCl as the electrolyte. An ISCO CV^4 absorbance detector (ISCO, Lincoln, NE, USA) was used for UV detection. Separations were performed on a fused-silica capillary, 1.2 m × 50 μm I.D. × 375 μm O.D. (Polymicro Technologies, Phoenix AZ, USA). Unless otherwise indicated, the separation voltage was 25 kV and the detector potential was +0.900 V *vs.* a Ag/AgCl reference electrode. All washings were accomplished using positive pressure.

Cyclic voltammetry

A solution of $1 \cdot 10^{-2}$ *M* Gly–Gly–Gly was prepared in 50 m*M* NaOH, 1 m*M* $CuSO_4$, 2.6 m*M* tartaric acid and 2.5 m*M* KI and allowed to react for 10 min. This solution was then diluted 1:10 in 10 m*M* NaOH, pH 9.5. Cyclic voltammetry experiments were conducted in a three-electrode configuration using a Model CySy-1 computerized electrochemical analyzer (Cypress Systems, Lawrence, KS, USA). The scan rate was 10 mV/s. A carbon fiber working electrode, a Ag/AgCl reference and a platinum auxiliary electrode were used in all studies.

Electrochemical pretreatment

Two different electrochemical pretreatments of the carbon fiber microelectrode were investigated.

(a) Application of a 50-Hz square-wave waveform of 2 V amplitude for 1 min. This pretreat-

ment was performed while the microelectrode was inserted in the capillary column and operating buffer was flowing past its surface.

(b) Anodization of the microelectrode in an electrochemical cell at +900 mV in a solution of 1 *M* NaOH. This pretreatment was carried out for 15 min.

Precolumn derivatization

Precolumn derivatization was first evaluated for the detection of peptides. In this case, the sample was dissolved in 10 m*M* borate buffer, pH 10.3. To 900 μl of sample was added 100 μl of a solution consisting of 120 μM $CuSO_4$, 319 μM $C_4H_4KNaO_6$, 301 μM KI and 6 m*M* NaOH. The reaction was allowed to proceed for a minimum of 10 min and injected by pressure injection. The run buffer consisted of 10 m*M* borate, pH 10.3.

On-column derivatization

In this case, the Cu(II) was added to the buffer system so that the complexation would occur during the separation. The run buffer consisted of 10 m*M* borate, pH 9.5, 1 m*M* $CuSO_4$ and 3 m*M* tartaric acid. Samples were injected by pressure injection and the separation voltage was then applied.

Derivatization using a Cu(II)-saturated capillary

The capillary was precoated with Cu(II) prior to the separation in this procedure. A solution of 1 *M* NaOH was flushed through the capillary for 5 min, 0.1 *M* NaOH for 5 min and then a solution of 2.4 m*M* NaOH, 48 μM $CuSO_4$, 120 μM potassium tartrate and 120 μM KI was flushed through the capillary for 10 min. Lastly, a 2.5 m*M* NaOH solution was pushed through for 15 min. Separations were performed in the 2.5 m*M* NaOH run buffer.

RESULTS AND DISCUSSION

Electrochemistry

Electrochemical pretreatment is well known to have a pronounced effect on the electron transfer properties of many solution species, in particular, enhancement of the electrochemical response [16,17]. In this study, two pretreatment regimes were investigated. The first was the application of a high-frequency 2 V potential window to the electrode; this was considered a severe pretreatment. A second, milder pretreatment was also investigated, which involved preanodization of the microelectrode in 1 *M* NaOH for 15 min at +900 mV. This second approach was utilized in subsequent studies as it was found to provide activation of the microelectrode comparable to that of the harsher pretreatment, but was simpler to apply. The pretreatment was found to be necessary only for new or unused microelectrodes. Once pretreated, the microelectrodes did not require further pretreatment for reactivation, *i.e.*, oxidation of the Cu(II)–peptide complexes did not foul the surface of the electrodes. It is most probable that the pretreatment removed an initial polymeric layer which inhibited electron transfer on the surface of the carbon fiber. Shown in Fig. 1 is the background response at an unpretreated microelectrode (A) and at a pretreated microelectrode (B). The response of Cu(II)–Gly–Gly–Gly at a pretreated microelectrode is illustrated in Fig. 1C.

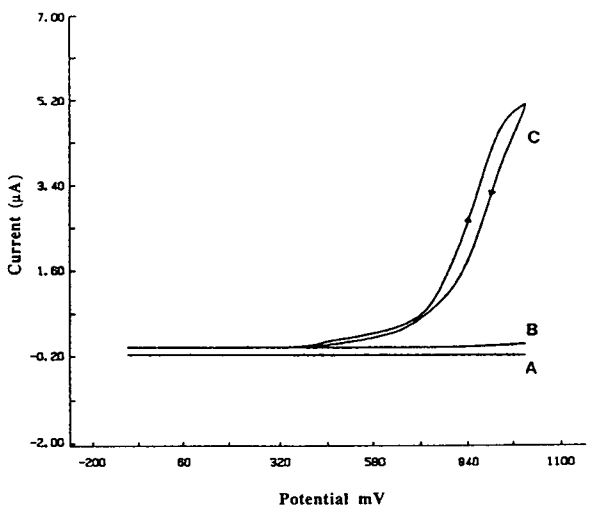

Fig. 1. Cyclic voltammetric behavior of 1 m*M* Cu(II)–Gly–Gly–Gly in 10 m*M* NaOH at a carbon fiber microelectrode. A = Initial response to complex; B = background electrolyte response after pretreatment of the electrode for 15 min in 1 *M* NaOH with stirring; C = response to complex following electrochemical pretreatment. Scan rate 10 mV/s.

Precolumn complexation of peptides with copper

Initial studies focused on precolumn complexation of compounds with the biuret reagent. Samples were derivatized with diluted biuret, allowed to react 10 min, and then injected into the CE system. Using this method, a detection limit of $4 \cdot 10^{-5}$ *M* was achieved (signal-to-noise ratio = 3) for the peptide Ala–Gly–Gly. The high ionic strength of the standard biuret reagent caused band-broadening, so it was diluted prior to derivatization. The run buffer consisted of the same solution. In an attempt to reduce the amount of current generated in the separation capillary, the use of several zwitterionic buffers, including CAPS and 2-amino-2-methyl-1-propanol, was investigated. However, it was found that when a buffer consisting of 10 m*M* CAPS (pH 10.3) was employed, the response for Cu(II)–Ala–Gly–Gly was reduced by 70%. 2-Amino-2-methyl-1-propanol buffers produced high background after electrode pretreatment, which took >30 min to decay to baseline.

On-column complexation of peptides with copper

Derivatization on-column by employing a buffer containing the biuret reagent was investigated. Initially, a buffer consisting of 10 m*M* borate, 1 m*M* $CuSO_4$ and 3 m*M* potassium tartrate was employed, but this resulted in a noisy baseline. It was then found that if the Cu(II) concentration were reduced by a factor of 42, the noise was substantially decreased. Detection limits of $1 \cdot 10^{-4}$ *M* for Ala–Gly–Gly (signal-to-noise ratio = 3) were obtained using a buffer consisting of 1 m*M* borate buffer, pH 10, 24 μM $CuSO_4$, 64 μM $C_4H_4KNaO_6 \cdot 4H_2O$, 60 μM KI, and 1.2 m*M* NaOH. However, even with this buffer system there was a gradual increase in noise over time that was not eliminated by replacing the electrode with a new carbon fiber. Based on this observation, it was concluded that the large amounts of Cu(II) present were interfering with the functioning of the Nafion joint. The high negative potential at the anode caused the Cu(II) to accumulate at the Nafion joint, hindering the flow of ions across the joint and causing a gradual increase in noise at the electrode.

Derivatization using a Cu(II)-saturated capillary

The formation of a "Cu(II)-coated" capillary was investigated. Above pH 2, fused-silica capillaries contain negatively caused silanol groups that can retain metal cations [18]. If a Cu(II)-coated capillary could be produced, Cu(II) would be available for complexation with peptides without the need for it in the running buffer. This would also eliminate the need for prederivatization. Coating the capillary was achieved using a pressure injection system to push a solution containing copper through the column. While copper still comes into contact with the Nafion joint, in this case it is for a minimal period of time, without the presence of the applied voltage. Copper is thus available for complexation with the peptides, but does not accumulate at the Nafion joint.

The coating procedure described in the Experimental section produced a capillary which could be run in 2.5 m*M* NaOH and was stable for >12 h of continuous analysis. The column was coated on a daily basis and the electrode was left in the column during the coating procedure. Increasing the concentration of the Cu(II) solution used for washing did not result in an increase in response for the peptides tested. No response was obtained if the capillaries were not initially coated with Cu(II).

The exact mechanism by which Cu(II) is associated with silica is not known. However, the interaction of metal cations such as Cu(II) with silica is well documented. It is believed that this interaction is not just due to ionic attraction forces but may also involve the formation of covalent bonds between the metal ion and the silanol group. The silica surface may be viewed as a polydentate ligand if one considers the close spacing of the SiOH groups on the surface [19]. In this application, the use of high pH and the presence of an additional complexing agent (tartaric acid) make the exact prediction of the mechanism difficult. However, it has been shown that the SiO^- ion can penetrate and displace a ligand from the coordination sphere of the metal atom, thus forming a covalent bond between the complex and the silica surface [20]. Whether the Cu(II) is bound to the silica is association with tartaric acid is not known. However, it is clear that Cu(II) does become associated with the

capillary wall and is available for peptide complexation.

Increasing the concentration of NaOH used to run the system to 10 m*M* decreased the migration time for the peptides, but also decreased the signal by 66%. However, NaOH was necessary to obtain the best signal. The use of other more conventional buffer systems such as borate, 2-amino-2-methyl-1-propanol, CAPS and glycine caused a decrease in response. Addition of 2.5% methanol or acetonitrile caused a reduction in sensitivity.

Separation of peptides

The separation of di-, tri-, tetra- and pentaglycine is seen in Fig. 2. A detection potential of +900 mV was chosen based on previous reports [1–4] and cyclic voltammograms obtained in our laboratory. The best response was obtained for triglycine with a detection limit of $7 \cdot 10^{-7}$ *M*. The response decreased with increasing size of the peptide. Detection limits for di-, tetra- and pentaglycine were $9.5 \cdot 10^{-7}$ *M*, $1.6 \cdot 10^{-6}$ *M*, and $5.5 \cdot 10^{-6}$ *M*, respectively. For Gly–Gly–Gly, response with linear from $1 \cdot 10^{-4}$ to $5 \cdot 10^{-6}$ *M* with a correlation coefficient of 0.998. The slope was 9 nA/m*M*. The responses for homogeneous peptides of alanine were less than those for glycine. When a 50 μM solution of di-, tri-, and tetraalanine was injected, only the trialanine was detectable. This system can be employed for the detection of heterogeneous peptides as well. Fig. 3 shows a separation of two peptides differing by a single amino acid, Arg–Gly–Asp–Ser (which supports fibroblast attachment and inhibits fibronectin binding to platelets) and Arg–Gly–Glu–Ser (an inhibitor of platelet aggregation).

Most methods for peptide analysis by HPLC or CE rely on the presence of a nucleophilic primary amine for derivative formation [21–23]. The biuret reaction has an advantage over this method, since it is selective for the peptide bond. Thus, the determination of the amide-protected Pro–Leu–Gly–amide was investigated. The detection limit for this compound was $2 \cdot 10^{-6}$ *M* (signal-to-noise ratio = 3). The relative standard deviations for the reproducibility of the detector response and migration time for Pro–Leu–Gly-amide were 6.8 and 3.6%, respectively ($n = 9$). A comparison of electrochemical and UV detection for the determination of Pro–Leu–Gly is shown in Fig. 4. It can be seen that the sensitivity of the Cu(II) complexation method is much

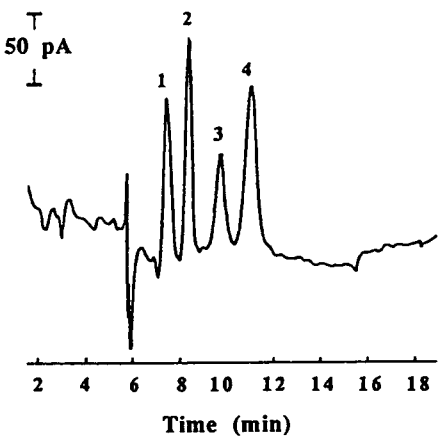

Fig. 2. Separation of $9 \cdot 10^{-6}$ *M* (1) di-, (2) tri-, (3) tetra- and (4) $5 \cdot 10^{-5}$ *M* pentaglycine in 2.5 m*M* NaOH. Capillary 1.2 m, coated at 10 p.s.i. (1 p.s.i. = 6894.76 Pa) for 5 min in 1 *M* NaOH, 5 min in 0.1 *M* NaOH, 10 min in a solution 2.4 m*M* in NaOH, 48 μM in $CuSO_4$, 120 μM in tartaric acid, 120 μM in KI, and finally 15 min in 2.5 m*M* NaOH. Applied potential 25 kV. Detection potential +900 mV.

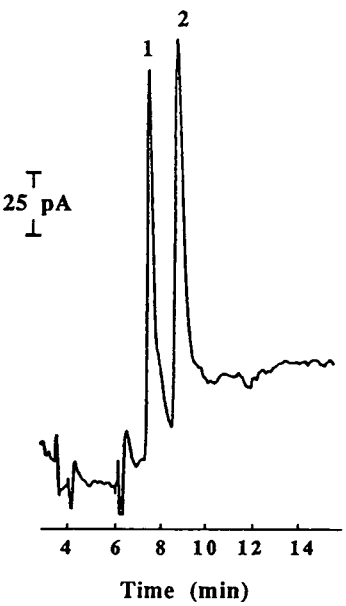

Fig. 3. Separation of $1 \cdot 10^{-5}$ *M* (1) Arg–Gly–Asp–Ser and (2) Arg–Gly–Glu–Ser in 2.5 m*M* NaOH. Run conditions as in Fig. 2.

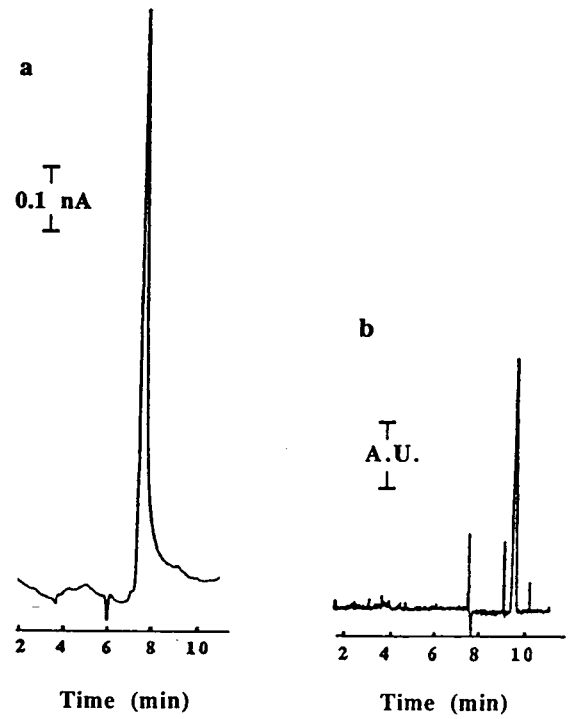

Fig. 4. A comparison of UV detection and ED: $5 \cdot 10^{-5}$ *M* Pro–Leu–Gly–amide. (a) ED, +900 mV; (b) UV detection, 210 nm.

better than with UV detection at 210 nm. In addition, this method affords greater selectivity than other commonly employed derivatization methods where there can be interference from amino acids. Warner and Weber [1] have shown than the selectivity for tripeptides using this method is on the order of 1000 times better than for amino acids.

The use of this method with capillary electrophoresis rather than liquid chromatography makes possible the analysis of submicroliter sample quantities. Since the Cu(II) complexation is accomplished on-column, there is no dilution of sample prior to injection as there is with other commonly employed derivatization reagents. At this time the analysis system is limited to the use of NaOH as the run buffer; however, a search for other compatible buffers is underway.

CONCLUSIONS

A very simple procedure for the determination of peptides has been developed, which allows direct injection of the peptide onto the column without the need for pre- or postcolumn derivatization. Investigations showed that the method can be used for the determination of selected peptides, including N-terminal-blocked peptides. The greater sensitivity and selectivity which can be achieved by the use of electrochemical rather than UV detection has been demonstrated. Future work will investigate the applicability of this method to the detection of larger peptides and the analysis of biological samples.

ACKNOWLEDGEMENTS

The authors gratefully acknowledge the Kansas Technology Enterprise Corporation for financial support of this work and Bioanalytical Systems for the donation of detectors used. We also thank Nancy Harmony for help in the preparation of this manuscript.

REFERENCES

1 A.M. Warner and S.G. Weber, *Anal. Chem.*, 61 (1989) 2664.
2 H. Tsai and S.G. Weber, *J. Chromatogr.*, 515 (1990) 415.
3 H. Tsai and S.G. Weber, *J. Chromatogr.*, 542 (1991) 345.
4 H. Tsai and S.G. Weber, *Anal. Chem.*, 64 (1992) 2897.
5 T.D. Schlabach, *Anal. Biochem.*, 139 (1984) 309.
6 K. Stulik, V. Pacakova and G. Jokuszies, *J. Chromatogr.*, 436 (1988) 334.
7 H. Wang, V. Pacakova and K. Stulik, *J. Chromatogr.*, 509 (1990) 245.
8 R.T. Kennedy, M. Oates, B.R. Cooper, B. Nickerson and J.W. Jorgenson, *Science*, 246 (1989) 57.
9 T.M. Olefirowicz and A.G. Ewing, *Anal. Chem.*, 62 (1990) 1872.
10 T.J. O'Shea, P.L. Weber, B.P. Bammell, C.E. Lunte, S.M. Lunte and M.R. Smyth, *J. Chromatogr.*, 608 (1992) 189.
11 R.A. Wallingford and A.G. Ewing, *Anal. Chem.*, 59 (1987) 1762.
12 T.J. O'Shea, R.D. Greenhagen, S.M. Lunte, C.E. Lunte, M.R. Smyth, D.M. Radzik and N. Watanabe, *J. Chromatogr.*, 593 (1992) 305.
13 X. Huang, R.N. Zare, S. Sloss and A.G. Ewing, *Anal. Chem.*, 62 (1991) 189.
14 C.E. Engstrom-Silverman and A.E. Ewing, *J. Microcolumn Sep.*, 3 (1991) 141.
15 T.J. O'Shea and S.M. Lunte, *Anal. Chem.*, 65 (1993) 247.
16 F.G. Gonon, C.M. Fombarlet, M.J. Buda and J.-F. Pujol, *Anal. Chem.*, 53 (1981) 1386.

17 T.J. O'Shea, A. Costa Garcia, P. Tunon Blanco and M.R. Smyth, *J. Electroanal. Chem.*, 307 (1991) 63.
18 M. Deacon, M.R. Smyth and R.G. Leonard, *Analyst*, 116 (1991) 897.
19 R.K. Iler, *The Chemistry of Silica*, Wiley, New York, 1978.
20 R.L. Burwell, Jr., R.G. Pearson, G.L. Haller, P.B. Tjok and S.P. Chock, *Inorg. Chem.*, 4 (1965) 1123.
21 I. Molnár and C. Horváth, *J. Chromatogr.*, 142 (1977) 623.
22 A.F. Spatola and D.E. Benovitz, *J. Chromatogr.*, 327 (1985) 165.
23 S.M. Lunte and O. Wong, *Current Sep.*, 10 (1990) 19.

Journal of Chromatography A, 652 (1993) 385–392
Elsevier Science Publishers B.V., Amsterdam

CHROM. 25 208

Capillary electrophoresis of inorganic cations and low-molecular-mass amines using a copper-based electrolyte with indirect UV detection

John M. Riviello* and Michael P. Harrold

Dionex Corporation, 1228 Titan Way, Sunnyvale, CA 94088 (USA)

ABSTRACT

An electrolyte system for the separation and detection of common inorganic cations and low-molecular-mass amines using capillary electrophoresis was developed. The electrolyte system is based on copper(II) as the primary electrolyte constituent. The method permits the determination of alkali metals, alkaline-earth metals, and ammonium in less than 5 min. Utility of the method for the separation of low-molecular-mass amines has also been demonstrated. Factors affecting separations using this electrolyte system have been investigated and include pH, buffering, and the addition of selective mobility modifiers. The analytical performance of the electrolyte system is discussed in terms of detection limits, linearity of response, migration time precision and matrix effects.

INTRODUCTION

Alkali and alkaline-earth metals are monitored routinely in a variety of industries. The most common analysis methods used are spectroscopic techniques such as atomic absorption (AA) and atomic emission spectroscopy [1]. Ion chromatography has been used extensively for rapid determination of alkali and alkaline-earth metals [2–4], particularly when the metals must be separated to eliminate inter-element interferences or when ammonium ion must also be determined.

Capillary electrophoresis (CE) has recently received a great deal of attention as a tool for the separation and detection of low-molecular-mass inorganic ions. With the exception of recent research into conductivity detection for CE [5–7], most workers have used indirect methods for the detection of alkali and alkaline-earth metals. The principles of indirect UV and indirect fluorescence methods for CE are well documented [8–13]. The separation of inorganic anions and low-molecular-mass organic acids using CE with indirect UV detection has been the subject of several recent publications [14–20]. Early work on the separation of metal ions by Hjertén [21] and Tsuda *et al.* [22] demonstrated the technique's potential for metal ion determination. Foret *et al.* [23] described the separation of lanthanide metals using indirect UV detection with a creatinine electrolyte. They used α-hydroxyisobutyric acid (HIBA) in the electrolyte to create weak complexes that enhance the small differences in electrophoretic mobility of the lanthanide metals. More recently, metal separations based on a benzylamine and HIBA electrolyte were reported by Chen and Cassidy [24]. Most work on CE of cations has used an organic amine as the primary electrolyte component and used indirect UV or indirect fluorescence detection. Several reports [25–27] describe the separation of inorganic metal ions using a proprietary compound. Inorganic-based electrolytes for the separation of metal ions have been described by Bachmann *et al.* [28] using a cerium(III)-based

* Corresponding author.

0021-9673/93/$06.00

electrolyte with indirect fluorescence detection. Timerbaev *et al.* [29] separated metal ions as anionic complexes with 8-hydroxyquinoline-5-sulfonic acid and used direct UV detection. Swaile and Sepaniak [30] also used 8-hydroxyquinoline-5-sulfonic acid, but detected the fluorescent complexes of the metals.

Metal ions of a given valency in the same row of the periodic table are often difficult to separate because of very small differences in electrophoretic mobility. In many cases, the electrophoretic mobility of an ion can be changed by choosing appropriate electrolyte conditions which modify its charge, mass or charge density. Adding modifiers that complex with analyte cations to control electrophoretic mobility has been described by several workers [23,24,27]. The addition of 18-crown-6 to electrolytes in isotachophoresis has been shown to resolve ammonium and potassium ions, two species that normally co-migrate [31]. Recently, the use of 18-crown-6 in CE for the resolution of ammonium and potassium has also been described [32]. The application of CE for determining non-chromophoric amines has not been extensively investigated, although, recently, the separation of low-molecular-mass amines was reported using indirect UV detection with a quinine-based electrolyte [33].

In this paper, we report on the first CE method using an inorganic chromophore with indirect UV detection. An electrolyte system based on copper(II) has been developed for the determination of alkali and alkaline-earth metals including barium and strontium. The electrolyte system has also been used successfully for the separation and detection of low-molecular-mass amines. Optimization parameters for the method and performance characteristics are presented.

EXPERIMENTAL

Reagents and standards

All reagents were of analytical-reagent or ACS grade unless specified, and prepared in 18 MΩ deionized water. Copper(II) sulfate (pentahydrate) was obtained from MCB (Norwood, OH, USA). Formic acid was obtained from Fluka (Ronkonkoma, NY, USA) and 18-crown-6 was from Aldrich (Milwaukee, WI, USA). Concentrated sulfuric acid was obtained from Fisher Scientific (Pittsburgh, PA, USA).

Standards for magnesium and calcium were obtained as 1000 mg/l ion standard solutions from Fluka. Standards for lithium, sodium, ammonium, potassium, strontium, and barium were prepared from chloride salts obtained from Fisher Scientific.

Amine standards were prepared from the free bases. Monomethylamine, dimethylamine, trimethylamine, monoethylamine, diethlyamine and triethylamine were obtained from Fluka.

Equipment

All electropherograms were generated using a a Dionex CES I system (Dionex, Sunnyvale, CA, USA). Fused-silica capillaries (Polymicro Technologies, Phoenix, AZ, USA) of 50-μm inner diameter, 375-μm outer diameter and various lengths were used. The detection window was located 5 centimeters from the end of the capillary. Data were collected at 10 points/s using a Dionex AI-450 data acquisition system. Unless otherwise specified, injections were performed hydrostatically by raising the sample vial 100 mm above the level of the destination vial for 30 s. To obtain positive peaks when using indirect photometric detection, the polarity of the UV–visible detector was reversed. Wavelength setting was 215 nm unless otherwise noted.

RESULTS AND DISCUSSION

Copper(II) was used as the primary component in the electrolyte because it has an electrophoretic mobility similar to that of the analytes, and also has spectral characteristics required for indirect UV detection. Cupric ion, at pH 3, has an electrophoretic mobility well matched to many inorganic cations and low-molecular-mass amines (Table I). The electrophoretic mobility of copper(II) is well matched to that of the analytes only if copper is present as a free divalent cation. Copper(II) will hydrolyze at pH greater than 5, and this hydrolysis can change its electrophoretic mobility. In order to prevent hydrolysis, the pH of the copper-based elec-

TABLE I

EQUIVALENT IONIC CONDUCTANCE (Λ) OF SELECTED INORGANIC CATIONS

From ref. 34.

Metal ion	Λ (10^{-4} m^2 S mol^{-1})
Ammonium	73.50
Potassium	73.48
Sodium	50.08
1/2 Calcium	59.47
1/2 Magnesium	53.00
1/2 Strontium	59.40
Lithium	38.66
1/2 Barium	63.66
1/2 Copper	55.00
Hydronium	349.82

trolyte is kept below 5. The electroosmotic flow rate will change as a function of electrolyte pH, and a decrease in electroosmotic flow is observed as the pH is lowered. Maintenance of a constant pH is essential for assuring reproducible migration times and minimizing the impact of injected sample pH. Formic acid, with a pK_a of 3.1, was used to adjust the pH of the electrolyte to prevent hydrolysis of copper and to provide buffering capacity to the electrolyte.

The separation of ammonium and potassium using CE is difficult due to their identical electrophoretic mobilities [34]. The use of 18-crown-6 to solve this problem has been documented by other workers [31,32]. Stability constants for 18-crown-6 with selected metals are shown in Table II. Potassium ion has a stability constant with 18-crown-6 approximately six times that of ammonium. The higher stability constant for potassium results in a migration velocity that is slightly retarded relative to ammonium, and the two ions can be separated. We have examined the utility of 18-crown-6 in the copper(II)-based electrolyte system and found it to be useful for the resolution of ammonium and potassium in the copper electrolyte. Fig. 1 shows changes in migration times with the addition of 18-crown-6 to a copper(II)-based electrolyte system. While the effect on the resolution of ammonium and potassium is visible, other changes in selectivity are also noted. Most dramatic is the large change in migration time for barium with the addition of 18-crown-6. A reversal of migration order for strontium and magnesium is also observed, although the magnitude of the change is not as great. The copper(II) electrolyte system we have investigated gave the maximum resolution of these analytes at an 18-crown-6 concentration of 3–5 mM.

The analytes of interest in this work are detected using indirect UV photometry. The use of an indirect method is required since alkali and alkaline earth metals have little or no intrinsic absorbance in the UV or visible region. An electrolyte ion used for indirect UV detection must be of the same charge as the analyte ion, possess a chromophore at a wavelength different than the analytes, and be of a low valency to enhance response. In addition to having a well-suited electrophoretic mobility for the analysis of low-molecular-mass cations, copper(II) ion fulfills the requirements for use with indirect UV detection. The wavelength at which the copper electrolyte gives the greatest signal-to-noise ratio (S/N) was determined by measuring the S/N for lithium ion at several wavelengths. The results of this experiment are shown in Fig. 2. Based on this work, all subsequent electropherograms were run at 215 nm. Using indirect UV for this application has the benefit of universal response to positively charged species. However, the method of indirect UV also has drawbacks, including a noisy, high background, relatively

TABLE II

STABILITY CONSTANTS OF METAL IONS WITH 18-CROWN-6

From ref. 35.

Metal ion	log K at 25°C
Sodium	0.80
Potassium	2.03
Ammonium	1.23
Rubidium	1.56
Cesium	0.99
Strontium	2.72
Barium	3.87

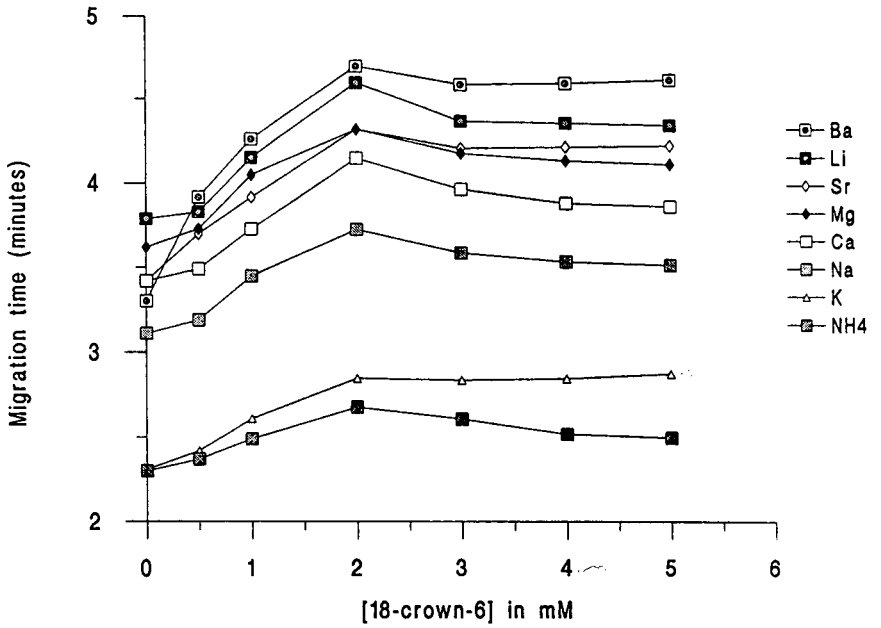

Fig. 1. Effect of 18-crown-6 on migration times of inorganic cations. Electrolyte consists of 4.0 m*M* cupric sulfate, 4.0 m*M* formic acid and varying amounts of 18-crown-6. Separation performed in 50 cm × 50 μm I.D. fused-silica capillary at 20 000 V, detector cathodic.

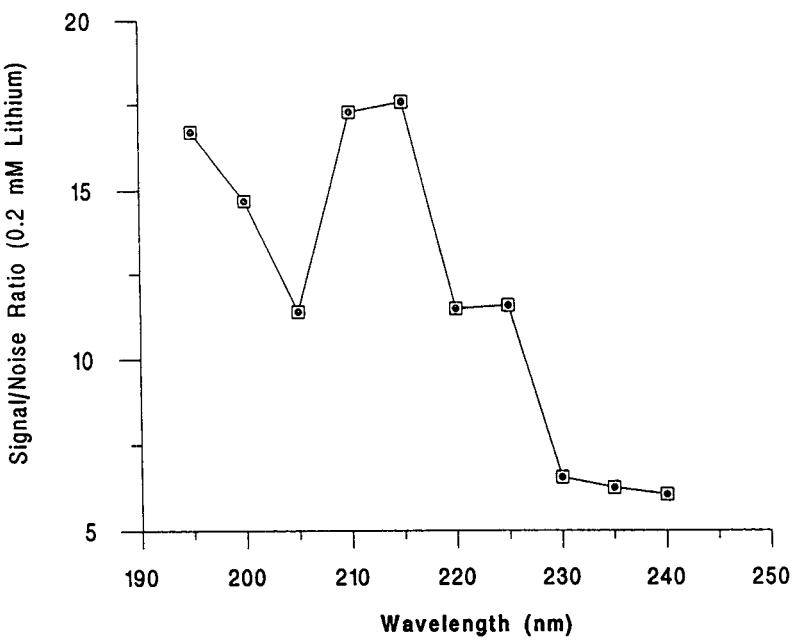

Fig. 2. Signal-to-noise ratio *vs.* detection wavelength for 0.2 m*M* lithium injected. Electrolyte consists of 4.0 m*M* cupric sulfate, 4.0 m*M* formic acid and 4.0 m*M* 18-crown-6 at pH 3.0.

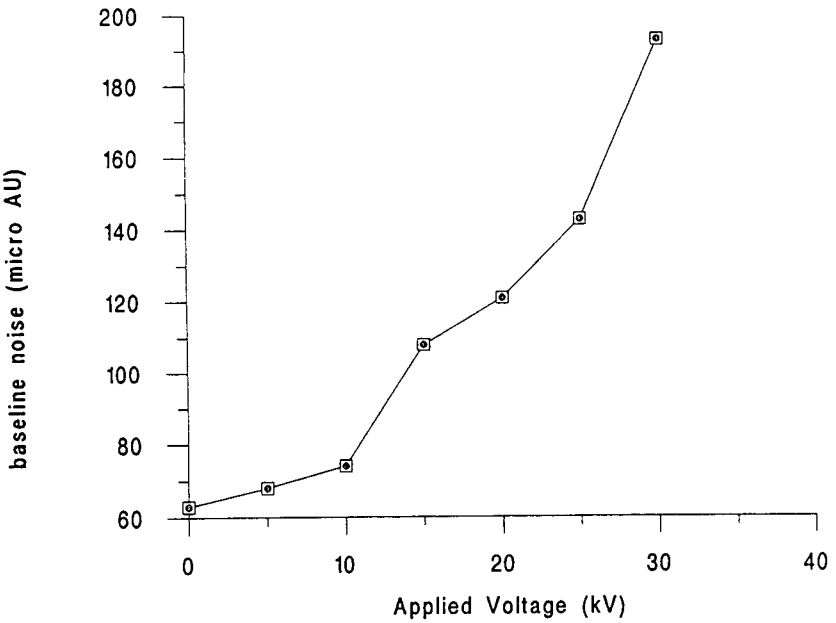

Fig. 3. Baseline noise (absorbance units $\times 10^{-6}$) as a function of applied voltage for cupric sulfate electrolyte.

high detection limits and a limited dynamic range.

Electroosmotic flow rate and analyte migration velocity are proportional to the applied voltage used for separation. The baseline noise in CE is also proportional to applied voltage. The increase in baseline noise as a function of applied voltage is particularly exacerbated when using strongly absorbing electrolytes for indirect UV detection. In optimizing the separation of cations using the copper(II) electrolyte, we have sought to minimize run time and baseline noise. Fig. 3 shows the relationship between baseline noise and applied voltage for a copper(II)-based electrolyte system. Based on these results, we have concluded that 20 000 V minimizes the time of analysis while maintaining acceptably low noise.

Performance of method

A separation using an optimized electrolyte system containing 4.0 m*M* copper(II) sulfate, 4.0 m*M* formic acid and 4.0 m*M* 18-crown-6 is shown in Fig. 4. Detection limits and migration time reproducibility for common inorganic cations are shown in Table III. The stated detection limits are based on a hydrostatic injection at 100 mm for 30 s. Lower detection limits may be obtained by injecting greater volumes, but often at the expense of peak efficiency and resolution.

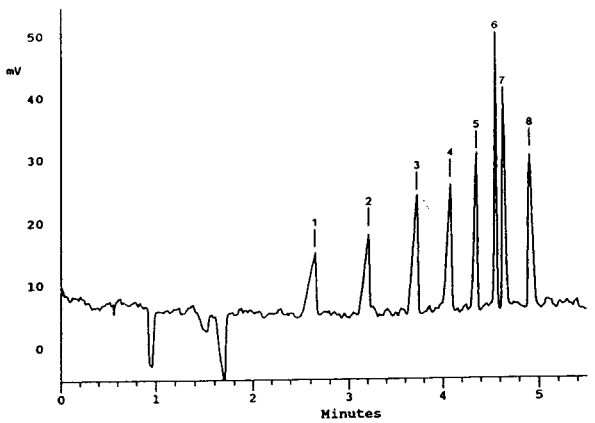

Fig. 4. Separation of alkali metals, alkaline-earth metals and ammonium. Fused silica capillary, 50 cm × 50 μm I.D. Electrolyte consists of 4.0 m*M* cupric sulfate, 4.0 m*M* formic acid and 4.0 m*M* 18-crown-6 at pH 3.0. Separation performed at 20 000 V, detector cathodic. Indirect UV detection at 215 nm, 1000 mV = 0.05 AU. Peaks: 1 = ammonium (3.6 mg/l); 2 = potassium (7.8 mg/l); 3 = sodium (4.6 mg/l); 4 = calcium (4.0 mg/l); 5 = magnesium (2.4 mg/l); 6 = strontium (15 mg/l); 7 = lithium (0.69 mg/l); 8 = barium (27 mg/l).

TABLE III

DETECTION LIMITS AND MIGRATION TIME REPRODUCIBILITY FOR CUPRIC SULFATE ELECTROLYTE

Electrolyte consists of 4.0 m*M* cupric sulfate, 4.0 m*M* formic acid and 4.0 m*M* 18-crown-6, pH 3.0. Separation performed in 50 cm × 50 μm I.D. fused-silica capillary at 20 000 V, detector cathodic. Indirect UV detection at 215 nm.

Analyte	Detection limit (mg/l)[a]	R.S.D. (%) migration time[b]
Ammonium	1.6	0.26
Potassium	1.0	0.28
Sodium	0.40	0.25
Calcium	0.33	0.26
Magnesium	0.32	0.25
Strontium	0.45	0.24
Lithium	0.060	0.25
Barium	0.80	0.28

[a] Detection limit calculated as 3× noise using peak height.
[b] R.S.D.s calculated from $n = 18$ measurements.

The linear dynamic range, measured as r^2, for inorganic cations exceeded 0.995 from the detection limit to 50 mg/l. Loss of resolution between peaks at concentrations above 50 mg/l limited the dynamic range of each analyte. The determination of cations in drinking water using this method is shown in Fig. 5.

The separation of a series of alkyl amines is shown in Fig. 6. All the amines in this separation

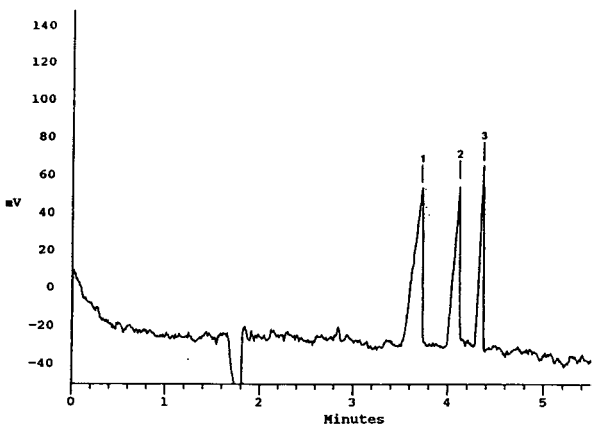

Fig. 5. Determination of cations in drinking water. Conditions as in Fig. 4. Peaks: 1 = sodium (4.9 mg/l); 2 = calcium (4.1 mg/l); 3 = magnesium (2.3 mg/l).

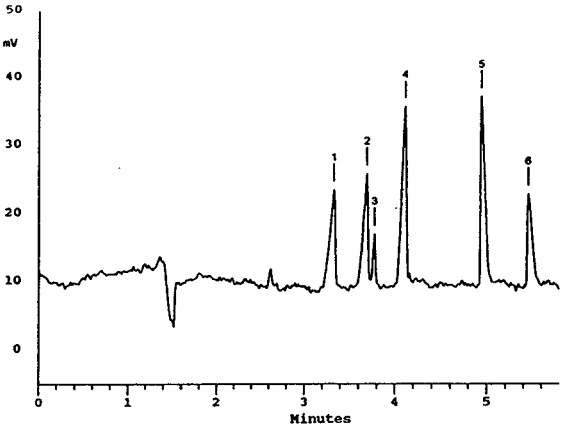

Fig. 6. Separation of amines. Conditions as in Fig. 4. Peaks (all 20 mg/l): 1 = monomethylamine; 2 = dimethylamine; 3 = trimethylamine; 4 = monoethylamine; 5 = diethylamine; 6 = triethylamine.

carry a +1 charge, and their migration from the capillary follows their electrophoretic mobilities.

The sample matrix can often cause considerable problems in separations using CE. For example, alkali and alkaline-earth metals are most stable in acidic conditions, and are often analyzed in an acidic aqueous solution. Fig. 7 shows the effect of a sulfuric acid matrix on cation migration times using a copper(II)-based electrolyte. Small amounts of acid in the sample have the effect of decreasing the migration time for all analytes. Migration times of all analytes begin to plateau as the acid concentration approaches 25 m*M*, but both potassium and ammonium begin to display increasing migration times above 25 m*M* acid. The effect is most pronounced for faster migrating species. Although changes in migration times are observed for all analytes, acid concentration as high as 25 m*M* in the sample will not significantly degrade the separation.

CONCLUSIONS

An electrolyte system based on copper(II) has been developed for the determination of alkali metals, alkaline-earth metals, and low-molecular-mass amines. Separation is carried out using free zone electrophoresis with indirect UV detection. Copper(II) is well suited for this application as its electrophoretic mobility is closely

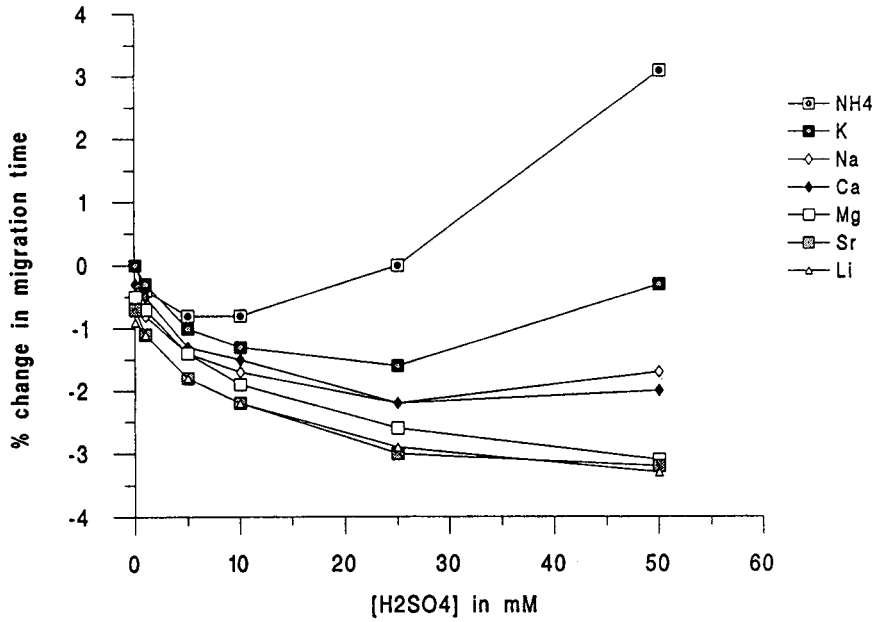

Fig. 7. Effect of sample acid concentration on migration times of inorganic cations. Electrolyte consists of 4.0 m*M* cupric sulfate, 4.0 mM formic acid and 4.0 m*M* 18-crown-6, pH 3.0. Separation performed in 50 cm × 50 μm I.D. fused-silica capillary at 20 000 V, detector cathodic.

matched to the analytes of interest and cupric ion has the required spectral characteristics for indirect UV detection. Resolution of otherwise co-migrating species is accomplished with the selective complexation of some species with 18-crown-6. Detection limits, linearity, and reproducibility of the method are acceptable for a variety of analytes in the 100 μg/l to 50 mg/l range. The electrolyte system is buffered, and matrices as high as 25 m*M* acid may be analyzed without degrading the separation.

REFERENCES

1 L.S. Clesceri, A.E. Greenberg, R.R. Trussell and M.A.H Franson (Editors), *Standard Methods for the Examination of Water and Wastewater*, American Public Health Association, Washington, DC, 1981.
2 D.L. Campbell, J.R. Stillian, S. Carson, R. Joyce and S. Heberling, *J. Chromatogr.*, 546 (1991) 229.
3 R.D. Rocklin, M.A. Rey, J.R. Stillian and D.L. Campbell, *J. Chromatogr. Sci.*, 27 (1989) 474.
4 P. Kolla, J. Kohler and G. Schomberg, *Chromatographia*, 23 (1987) 465.
5 X. Huang, T.K.J. Pang, M.J. Gordon and R.N. Zare, *Anal. Chem.*, 59 (1987) 2747.
6 N. Avdalovic, R.D. Rocklin, J.R. Stillian and C. Pohl, *Anal. Chem.*, 65 (1993) 1470.
7 P.K. Dasgupta and L. Bao, *Anal. Chem.*, 65 (1993) 1003.
8 L. Gross and E.S. Yeung, *J. Chromatogr.*, 480 (1989) 169.
9 E.S. Yeung, *Acc. Chem. Res.*, 22 (1989) 125.
10 E.S. Yeung and W.G. Kuhr, *Anal Chem.*, 63 (1991) 275A.
11 L. Gross and E.S. Yeung, *Anal. Chem.*, 62 (1990) 427.
12 F. Foret, S. Fanali, L. Ossicini and P. Boček, *J. Chromatogr.*, 470 (1989) 299.
13 T. Wang and R.A. Hartwick, *J. Chromatogr.*, 607 (1992) 119.
14 F. Foret, S. Fanali, L. Ossicini and P. Boček, *J. Chromatogr.*, 470 (1989) 299.
15 B.J. Wildman, P.E. Jackson, W.R. Jones and P.G. Alden, *J. Chromatogr.*, 546 (1991) 459.
16 B. Kenney, *J. Chromatogr.*, 546 (1991) 423.
17 A. Nardi, M. Cristalli, C. Desiderio, L. Ossicini, S.K. Shukla and S. Fanali, *J. Microcol. Sep.*, 4 (1992) 9.
18 P. Jandik and W.R. Jones, *J. Chromatogr.*, 546 (1991) 431.
19 W.R. Jones and P. Jandik, *J. Chromatogr.*, 546 (1991) 445.
20 M.P. Harrold, M.J. Wojtusik, J. Riviello and P. Henson, *J. Chromatogr.*, 640 (1993) 463.
21 S. Hjertén, *Chromatogr. Rev.*, 9 (1967) 122.
22 T. Tsuda, K. Nomura and G. Nakagawa, *J. Chromatogr.*, 264 (1983) 385.

23 F. Foret, S. Fanali, A. Nardi and P. Boček, *Electrophoresis*, 11 (1990) 780.
24 M. Chen and R. M. Cassidy, *J. Chromatogr.*, 602 (1992) 227.
25 A. Weston, P.R. Brown, A.L. Heckenberg, P. Jandik and W.R. Jones, *J. Chromatogr.*, 602 (1992) 249.
26 P. Jandik, W.R. Jones, A. Weston and P.R. Brown, *LC · GC*, 9 (1991) 634.
27 A. Weston, P.R. Brown, P. Jandik, W.R. Jones and A.L. Heckenberg, *J. Chromatogr.*, 593 (1992) 289.
28 K. Bachmann, J. Boden and I. Haumann, *J. Chromatogr.*, 626 (1992) 259.
29 A.R. Timerbaev, W. Buchberger, O.P. Semenova and G.K. Bonn, presented at *the International Ion Chromatography Symposium, Linz, September 21–24, 1992*, Poster No. 66.
30 D.F. Swaile and M.J. Sepaniak, *Anal. Chem.*, 63 (1991) 179.
31 F.S. Stover, *J. Chromatogr.*, 298 (1984) 203.
32 P.R. Brown, A. Weston, P. Jandik, W.R. Jones and A.L. Heckenberg, presented at the *16th International Symposium on Column Liquid Chromatography, Baltimore, MD, June 14–19, 1992*, paper No. 480.
33 Y. Ma, R. Zhang and C.L. Cooper, *J. Chromatogr.*, 608 (1992) 93.
34 J.A. Dean (Editor), *Lange's Handbook of Chemistry*, McGraw-Hill, New York, 13th ed., 1985, pp. 5–28.
35 R.M. Smith and A.E. Martell, *Critical Stability Constants*, Plenum Press, New York, 1975.

Journal of Chromatography A, 652 (1993) 393–398
Elsevier Science Publishers B.V., Amsterdam

CHROM. 25 250

In vivo monitoring of glutamate in the brain by microdialysis and capillary electrophoresis with laser-induced fluorescence detection

Luis Hernandez*, Sonia Tucci, Norberto Guzman and Ximena Paez

Laboratory of Behavioral Physiology, Medical School, Los Andes University, Merida (Venezuela)

ABSTRACT

Glutamic acid, an excitatory neurotransmitter, was monitored *in vivo* in the corpus striatum of freely moving rats by brain microdialysis and capillary electrophoresis with laser-induced fluorescence detection. A procedure to derivatize glutamate in complex matrices was developed. Capillary electrophoresis in 12 μm I.D. capillaries was performed to determine glutamate with a migration time of 195 s. Laser-induced fluorescence detection with 488-nm radiation from an argon ion laser and with collinear geometry was used. An injection of haloperidol decreased the concentration of glutamic acid in the dialysates. These experiments support the hypothesis that dopamine receptor blockade decreases glutamate release. The potential of these techniques for the study of chemicals in biomedical experiments is discussed.

INTRODUCTION

In vivo monitoring techniques such as brain microdialysis have been developed for collecting samples of extracellular fluid from different tissues in freely moving animals [1–5]. In this technique a semipermeable hollow fibre is inserted in an organ or a blood vessel. The wall of the fibre allows diffusion of chemicals from the extracellular fluid into the fibre. A concentric tube injects artificial cerebral spinal fluid into the hollow fibre and this current of liquid drags the chemicals from the living tissues into a vial. Once extracted, the chemicals have to be analysed.

An analytical technique suited to microdialysis has to deal with small volumes. In general, microdialysate volumes range from 5 to 30 μl. These volumes are appropriate for high-performance liquid chromatography (HPLC). This technique currently works with 10–50-μl loops in most applications to brain microdialysis.

Because of these volumes, perfusion flow-rates of 1–5 μl/min are most often used in microdialysis with collection times between 5 and 30 min. These perfusion flow-rates are far from the ideal for microdialysis. They produce 80–95% depletion of the chemicals in the extracellular space around the microdialysis probe [6,7]. Such depletion perturbs the extracellular environment and affects the function of the cells around the microdialysis probe. Perfusion flow-rates from microdialysis should be less than 100 nl/min [7]. However, if a conventional analytical technique such as HPLC is used together with a perfusion flow-rate of 100 nl/min, the perfusion time must be increased from 50 to 300 min to collect 5–30 μl. These collection times are generally unacceptable. The question is how to perfuse the probe at a low flow-rate, *i.e.*, 100 nl/min or less, and to maintain a perfusion time of 20 min or less.

* Corresponding author. Address for correspondence: Apartado de Correos 109, Merida 5101A, Venezuela.

0021-9673/93/$06.00

Interestingly, a flow-rate of 100 nl/min gives enough sample volume for capillary electrophoresis (CE). Indeed, 50 pl–10 nl are the sample volume requirements for CE. These volumes can be collected in 0.003–8 s. Therefore, from the sample volume point of view, CE is one of the best analytical techniques for microdialysis. We have already coupled microdialysis and capillary electrophoresis with UV detection [8]. With these techniques, transfer of phenobarbital from blood to brain was studied. However, endogenous compounds, such as neurotransmitters, cannot be studied with CE–UV because of the low concentration sensitivity of UV detection, the limit of concentration detection of CE–UV being about 10^{-6} *M*. The concentrations of many biologically active substances are often less than the micromolar level.

The most sensitive detection method for CE is laser-induced fluorescence detection (LIF), but it requires previous derivatization of the analytes. Most of the biologically interesting compounds exhibit poor native fluorescence at visible excitation wavelengths and some of them do not exhibit native fluorescence at all. Monoamines and amino acids with aromatic rings fluoresce at 260 nm but do not fluoresce at higher wavelengths. Therefore, most of the biologically active compounds have to be derivatized, *i.e.*, tagged with fluorescent molecules, and then analysed. With this procedure several molecules have been analysed by CE–LIF. However, it is technically difficult to derivatize nanolitre volumes. For this reason, some researchers have tried to develop nano-scale techniques for carrying out precolumn derivatization [9].

Another technical drawback of derivatization is that derivatizing agents do not react with their target compounds when the latter are not well concentrated. For instance, when the concentration of a compound is lower than 10^{-6} *M*, the derivatizing reagent does not react with the compound on a mole to mole ratio basis. In order to overcome this problem, excess of reagent can be used. In general, 100 mol in excess with respect to the estimated concentration of the compound will label at concentrations as low as 10^{-9} *M*. However, the excess of reagent will be detected by the detection system and can mask the labelled compound. This last problem can be addressed in different ways. One is to improve the separation efficiency of the technique and another is to measure compounds that migrate before or after the spurious peaks due to the excess of fluorescent agent. We chose the latter strategy to measure glutamic acid. At alkaline pH this compound is negatively charged and migrates later than the reagent peaks, as we have shown in earlier analyses [10].

In a previous study, we showed that it is possible to label glutamate at low concentrations with naphthalene dicarboxaldehyde [10]. In this work, glutamate from brain dialysates was labelled with fluorescein isothiocyanate (FITC), which has a higher quantum efficiency than naphthalenedicarboxaldehyde, and fluorescein thiocarbamyl amino acid (FTC)–glutamate was detected by CE–LIF. With this method the effect of haloperidol injections on glutamic acid levels in the striatum was studied. We describe here the linearity and reproducibility of the technique and then show that a single haloperidol injection lowers glutamic acid levels.

EXPERIMENTAL

Reagents

Fluorescein isothiocyanate isomer I, sodium chloride, potassium chloride and calcium chloride were obtained from Sigma (St. Louis, MO, USA), acetone and sodium hydroxide of HPLC grade from J.T. Baker (Phillipsburg, NJ, USA) and sodium carbonate and sodium hydrogencarbonate from Merck (Darmstadt, Germany). Water was doubly distilled and deionized in a Milli-Q system (Millipore, Bedford, MA, USA) until its conductivity reached 18 MΩ. Haloperidol (Haldol) (Janssen Pharmaceutica, Beerse, Belgium) was obtained from a pharmacy. The buffer for the derivatization and the separation was 20 m*M* carbonate (pH 9.5). Ringer's solution for microdialysis perfusion was 146 m*M* NaCl–3.7 m*M* $CaCl_2$–1.2 m*M* KCl (pH 6.0).

Instrumentation

The laser-induced fluorescence detector and the CE system are described elsewhere [11,12]. Briefly, the samples and standards were injected in a 30 cm × 12 μm I.D. × 150 μm O.D. fused-

silica capillary (Polymicro Technologies, Phoenix, AZ, USA). At 20 cm from the anodic end, a 2-mm wide window was opened by removing the polyimide cover of the capillary with a scalpel under a dissecting microscope. This method is less prone to leave fluorescent residues of charred polyimide, which are common with the conventional burning procedure to make the detection window. The anodic end of the buffer-filled capillary was placed in a buffer reservoir made of a 200-μl Eppendorf pipette tip. This is a very convenient disposable reservoir that prevents contamination with fluorescent material from one sample to another. The cathodic end of the capillary was immersed in a laboratory-made T-shaped buffer reservoir that allowed flushing of the cathode compartment with fresh buffer. This reservoir also allowed a vacuum to be applied at the cathodic end of the capillary for hydrodynamic injection of the sample. The capillary was set on the *xyz* displacer of a microscope (Zeiss, Oberkochen, Germany). An epillumination condenser conducted 488-nm radiation from an argon ion laser (Ion Laser Technology, Salt Lake City, UT, USA) through a 40 × 0.85 NA objective on to the capillary. For this purpose the excitation radiation was reflected by an FT 510 dichroic mirror than reflected radiation of wavelength shorter than 510 nm (Zeiss) and focused through the objective. The fluorescence (usually emitted at 532 nm) was filtered by a high-pass filter centred at 520 nm (LP520; Zeiss). Stray light was attenuated by a notch filter centred at 488 nm (Andover, Salem, NH, USA). The fluorescence was detected by a Model 928 multi-alkali photomultiplier (Hamamatsu, Bridgewater, NJ, USA) operated at 700 V by a Model 2203 high-voltage power supply (Bertan, Hicksville, NY, USA). The signal from the photomultiplier tube was passed through a laboratory-made current-to-voltage converter equipped with a precision potentiometer to offset the background current (due to dark current plus stray radiation) and registered on a strip-chart recorder (Linseis, Princeton, NJ, USA).

Surgical procedure

Thirteen Wistar male rats weighing between 300 and 350 g were anaesthetized with Ketalar (100 mg/kg) and placed on a stereotaxic instrument. The surgical procedure is described elsewhere [2]. Briefly, a guide shaft 10 mm long, made of 21-gauge stainless-steel tubing, was inserted into the brain at the coordinates lateral to the midsaggital suture 3 mm, posterior to bregma 1.2 mm and ventral to the surface of the skull 4 mm. The guide shaft was attached to the skull by jewellers' screws and cemented with acrylic. After 7 days of recovery the rats were ready for microdialysis.

Microdialysis procedure

A microdialysis probe was made of a stainless-steel tube with a cellulose hollow fibre attached to its end and a 10 cm × 76 μm I.D. × 150 μm O.D. fused-silica capillary inserted into the stainless-steel and cellulose tube [13]. The inlet of the probe was connected to a syringe pump loaded with Ringer's solution set at a flow-rate of 100 nl/min. The outlet tube was inserted in a 400-μl microcentrifugue tube. The probe was inserted in the brain of an awake rate. Each sample of dialysate was collected throughout the course of 20 min (final collection volume 2 μl). After two baseline samples had been collected, six rats received an intraperitoneal injection of haloperidol (5 mg/kg) and seven rats received saline, then ten more samples were collected.

Derivatization procedure

The samples were mixed with 5 μl of buffer and 1 μl of $6 \cdot 10^{-4}$ *M* FITC in acetone solution. A blank solution of 2 μl of Ringer's solution or 2 μl of standard solutions of $5 \cdot 10^{-4}$, $5 \cdot 10^{-5}$ and $5 \cdot 10^{-6}$ *M* glutamate were derivatized with the same protocol. These mixtures were allowed to react in the dark for 18 h, then 192 μl of buffer were added to each vial.

Fluorescence measurements

The samples, blank and standard were hydrodynamically injected [a negative pressure of 19 p.s.i. (1 p.s.i. = 6894.76 Pa) applied during 2 s], then 21 kV were applied between the two ends of the capillary. This voltage generated a 4-μA current. After each run the capillary was flushed with 0.1 *M* NaOH followed by water. The peaks for the sample were identified by the migration

times and measured by comparing their heights with those of peaks given by standard solutions.

Three experiments were conducted. In the first a $1 \cdot 10^{-8}$ *M* solution of derivatized glutamate was injected eight times to determine the reproducibility of the migration time and the peak height. In the second experiment four glutamate solutions of $1 \cdot 10^{-5}$, $1 \cdot 10^{-6}$, $1 \cdot 10^{-7}$ and $1 \cdot 10^{-8}$ *M* concentrations were derivatized to yield $1 \cdot 10^{-7}$, $1 \cdot 10^{-8}$, $1 \cdot 10^{-9}$ and $1 \cdot 10^{-10}$ *M* FTC–glutamate solutions. They were then injected to determine the linearity of the derivatization procedure. In the third experiment, the actual concentrations of glutamate in brain dialysates before and after haloperidol or saline injections were measured.

Either regression analysis or one-factor analysis of variance (ANOVA) with repeated samples were used for statistical analysis.

RESULTS

The electropherograms of the blank and $5 \cdot 10^{-9}$, $5 \cdot 10^{-8}$ and $5 \cdot 10^{-7}$ *M* standard solutions are shown in Fig. 1. The blank shows several peaks due to decomposition of FITC and reaction with the aqueous solvent and its impurities. The same peaks are observed for the standard solutions. However, a new peak is observed towards the end of the electropherogram. This peak corresponded to FTC–glutamate. Note that it is absent in the blank. The migration time of this peak was 3 min 15 s.

The results of the reproducibility tests were as follows: mean migration time 187 s (mean standard error ±1.3 s) and mean peak height 102 mm (mean standard error ±2.0 mm).

The migration time was reproducible with an error of ±0.69% and the peak height with an error of ±2%. The points of the log–log plot of concentration *vs.* peak height fitted a straight line with the equation $y = 9.1 + 0.9x$ and the goodness of fit was highly significant [$r = 0.99$, $F(1/2) = 1425$, $p < 0.001$].

Analysis of the dialysate showed a peak that corresponded to glutamate. In addition, several other peaks different to the glutamate peak and to the ghost peaks of the dye were seen (see Fig. 2). These peaks probably corresponded to other substances present in the dialysate and taken up from the brain. The average concentration of glutamate was $3.5 \cdot 10^{-5}$ *M*. This concentration was kept very similar for each rat. For instance, the electropherograms in Fig. 2 correspond to one rat. In six consecutive measurements the height of the glutamate peak remained very constant.

When the data were plotted it was found that haloperidol decreased the glutamate concentration significantly by the second and third samples after haloperidol injection [$F(1/11) = 6.0$, $p <$

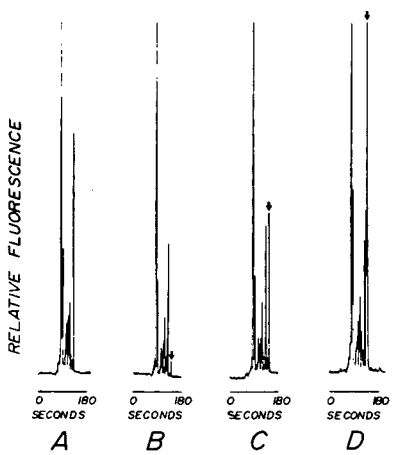

Fig. 1. Electropherograms of (A) a blank and (B) $5 \cdot 10^{-9}$, (C) $5 \cdot 10^{-8}$ and (D) $5 \cdot 10^{-7}$ *M* standard solutions of glutamate. Numerous peaks of FITC products are observed. The glutamate peak is indicated by an arrow.

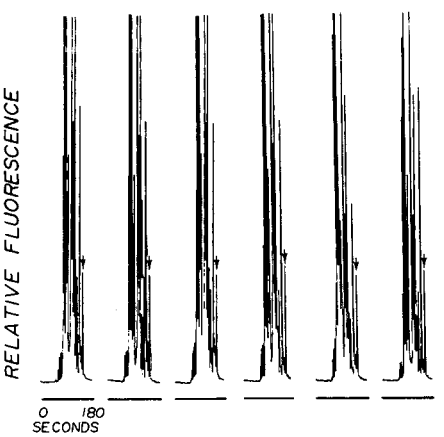

Fig. 2. Six electropherograms of dialysates showing FTC–glutamate signals (indicated by arrows) of consistent amplitude. The horizontal bars represent 180 s.

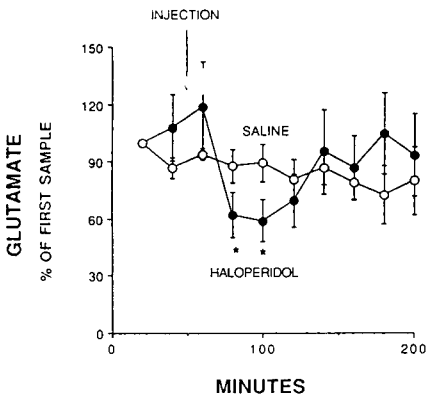

Fig. 3. Decrease of glutamate level in striatal dialysates in the presence of halopendol. Asterisks indicate statistically significant differences.

0.03]. This decrease lasted for about 60 min and then the glutamate level increased towards the base level (see Fig. 3).

DISCUSSION

The results show that it is possible to label nanomolar solutions of glutamate with FITC and detect, by laser-induced fluorescence, FTC–glutamate when a 100-fold molar excess of FITC is used. The linearity of the method is excellent in the range 10^{-7}–10^{-10} *M*, *i.e.*, three orders of magnitude. The reproducibility of the technique is reasonably good. This suggests that the technique might be very useful for the precise determination of glutamate in biological fluids.

The analysis takes 3 min or less, which is acceptable when compared with techniques such as HPLC. It is possible to shorten this time by using potassium-based buffers.

It is possible to measure glutamate in complex matrices such as brain dialysates, because glutamate migrates later than the peaks of FITC owing to the negative charge of FTC–glutamate. In such matrices several peaks corresponding to primary amines are observed. As primary amines are present in monoamines, amino acids and peptides, these unidentified peaks could be biologically interesting compounds.

The measurement of glutamate in brain dialysates requires very small volumes. In the present experiments we used a total sample volume of 2 μl for the measurements. This volume came from a perfusion flow-rate of 100 nl/min, which is very low when compared with the flow-rates currently used in brain microdialysis, which are between 1 and 5 μl/min, *i.e.*, from ten to fifty times greater.

The concentration of glutamate was between one and two orders of magnitude larger than that reported in previous experiments by other workers [3,4,14] using perfusion flow-rates greater than 1 μl/min. This discrepancy might be due to depletion of glutamate caused by the high-flow rates. In some experiments microdialysis probes have been inserted in the brain and microelectrodes for *in vivo* voltammetry have been placed in the neighbourhood of the microdialysis probe [6,7]. With this approach it is possible to determine the concentrations of the biological compounds at different distances from the microdialysis probe. It has been shown that at high flow-rates (2 μl/min or more) the concentration of Ca^{2+}, DOPAC or dopamine in the extracellular compartments is 80% lower than the normal concentration. This is particularly important because the depletion reaches 100 μm away from the microdialysis probe. However, when flow-rates of 100 nl/min or less are used, then the concentration of biological compounds is about normal around the probe.

An acute injection of haloperidol decreased glutamate in the striatum. There is considerable evidence that dopamine and glutamate interact in the striatum. Glutamate increases dopamine release and dopamine increases glutamate release. In this work we found that the blockade of dopamine receptors by haloperidol decreases the glutamate level. This finding supports the proposal that glutamic acid and dopamine regulate each other's release.

The final volume of the derivatized sample was 200 μl and 120 pl were injected for analysis. This means that the analysis of each sample can be repeated many times.

ACKNOWLEDGEMENTS

These experiments were financed by grants BTS37 from BID-CONICIT and M413-03-A from the CDCHT.

REFERENCES

1 L. Hernández, X. Páez and C. Hamlin, *Pharmacol. Biochem. Behav.*, 18 (1983) 159.
2 L. Hernández, B.G. Stanley and B.G. Hoebel, *Life Sci.*, 39 (1986) 2629.
3 H. Benveniste, J. Dryer, A. Schousbou and N.H. Diemer, *J. Neurochem.*, 43 (1984) 369.
4 B.A. Donzanti and B.K. Yamamoto, *Life Sci.*, 43 (1988) 913.
5 P.V. Rada, M.A. Parada and L. Hernandez, *J. Appl. Physiol.*, 74 (1993) 466.
6 C.D. Blaha, in H. Rollema, B. Westerink and W.J. Drijfhout (Editors), *Monitoring Molecules in Neuroscience*, University Centre for Pharmacy, Groningen, 1991, p. 56.
7 J.L. Gonzalez-Mora, T. Guadalupe, B. Fumero and M. Mas, in H. Rollema, B. Westerink and W.J. Drijfhout (Editors), *Monitoring Molecules in Neuroscience*, University Centre for Pharmacy, Groningen, 1991, p. 66.
8 S. Tellez, N. Forges, A. Roussin and L. Hernandez, *J. Chromatogr.*, 581 (1992) 257.
9 R.T. Kennedy, M.D. Oates, B.R. Cooper, B. Nickerson and J.W. Jorgenson, *Science*, 246 (1989) 57.
10 L. Hernandez, J. Escalona, P. Verdeguer and N. Guzman, *J. Liq. Chromatogr.*, 16 (1993) 2149.
11 L. Hernandez, R. Marquina, J. Escalona and N. Guzman, *J. Chromatogr.*, 502 (1990) 247.
12 L. Hernández, J. Escalona, N. Joshi and N. Guzman, *J. Chromatogr.*, 559 (1991) 183.
13 L. Hernandez, to Europhor, *Fr. Pat.*, 2 648 353 (1989); *Eur. Pat.*, 0 403 394 (1990); *US Pat.*, 5 106 365 (1992).
14 S. Dijk, H.C. Klein, W. Krop, T.P. Obrenovitch and J. Korf, in H. Rollema, B. Westerink and W.J. Drijfhout (Editors), *Monitoring Molecules in Neuroscience*, University Centre for Pharmacy, Groningen, 1991, p. 455.

Journal of Chromatography A, 652 (1993) 399–405
Elsevier Science Publishers B.V., Amsterdam

CHROM. 24 974

Collinear laser-induced fluorescence detector for capillary electrophoresis

Analysis of glutamic acid in brain dialysates☆

Luis Hernandez*

Los Andes University, Apartado 109, Merida 5101A (Venezuela) and Europhor Instruments, Parc Technologique du Canal, 10 Avenue de l'Europe, 31520 Ramonville (France)

Narahari Joshi and Euro Murzi

Los Andes University, Apartado 109, Merida 5101A (Venezuela)

Philippe Verdeguer and Jean Christophe Mifsud

Europhor Instruments, Parc Technologique du Canal, 10 Avenue de l'Europe, 31520 Ramonville (France)

Norberto Guzman

Princeton Biochemicals Ind., Princeton, NJ (USA)

ABSTRACT

Experiments with capillary electrophoresis using a laser-induced fluorescence detector with a collinear optical arrangement demonstrated several important points. First, increasing the numerical aperture of the microscope objective that is used simultaneously for focusing the excitation laser light as well as collection of emitted fluorescence enhances the signal used for the measurement of the emitted fluorescence and at the same time decreases the noise of interfering light. Second, detection of fluorescein-labelled amphetamine was performed at high-picomolar (10^{-10} *M*) levels. Third, the signal-to-noise ratio of 280 found at the above-mentioned picomolar concentrations indicates that the measurement of low-picomolar concentrations (10^{-12} *M*) of this compound in biological samples should be possible. Fourth, narrow-bore capillaries (5–10 μm internal diameter) were used to detect the neurotransmitters glutamic acid and aspartic acid as their naphthalene-2,3-dicarboxaldehyde derivatives in brain dialysates obtained from a freely moving rat. A mathematical model was developed to explain the relationship between numerical aperture, working distance, magnification of the lens, noise due to laser scattering and signal due to fluorescence. The model correctly predicted the observed values of photomultiplier tube current due to both laser scattering and fluorescence. The potential of the application of capillary electrophoresis with laser-induced fluorescence detection in the neurosciences is discussed.

* Corresponding author. Address for correspondence: Los Andes University, Apartado 109, Merida 5101A, Venezuela.

☆ Presented at the *4th International Symposium on High Performance Capillary Electrophoresis, Amsterdam, February 9–13, 1992*. The majority of the papers presented at this symposium were published in *J. Chromatogr.*, Vol. 608 (1992).

0021-9673/93/$06.00

INTRODUCTION

Laser-induced fluorescence detection (LIF) is the most sensitive detection method for capillary electrophoresis (CE). The detection limits of CE–LIF are approaching the molecular counting level [1]. New denominations (zepto or 10^{-21} and yocto or 10^{-24}) had to be created to refer to the small amounts of substance that CE–LIF is capable of detecting [2]. Because of this extremely high sensitivity CE–LIF has great potential to become a standard analytical tool in areas of biomedical research requiring better sensitivity than that provided by other currently available analytical techniques.

The development of CE–LIF has been gradual but sustained. Since the seminal article by Gasman *et al.* [3] showing the feasibility of CE–LIF, improvements in this technique have evolved in several directions.

The main axes developed thus far have been: (1) The introduction of new laser lines for excitation to expand the range of detectable compounds. To date, the principal lines which have been used are: 257 nm [4], 325 nm [3,5], 442 nm [6], 476 nm [7], 488 nm [8] and 514 nm [2]. (2) The introduction of charge-coupled devices to perform quick spectral analysis of the sample to distinguish between scattered laser radiation (Raman and Rayleigh scatters) and the emitted fluroescence [2,9]. (3) Post-column detection rather than on-column detection to reduce laser scattering from the walls of the capillary and reach very high sensitivity [1,10,11]. (4) Indirect LIF for the detection of non-fluorescent compounds [12,13]. (5) New fluorescent tags to overcome the poor tagging at low concentrations of analytes [14]. (6) Introduction of collinear rather than orthogonal optical geometrical arrangement to take advantage of very high numerical aperture lenses to improve sensitivity in the on-column detection mode and facilitate the industrial production of CE–LIF instruments [15].

In addition, LIF, along with electrochemical detection, is one of the two methods that enables the experimenter to work with very narrow-bore capillaries [16,17]. These capillaries create advantageous conditions for CE. In very narrow-bore capillaries, less than 20 μm internal diameter (I.D.), the surface-to-volume ratio (S/V) is greater than in 50 μm or 75 μm I.D. capillaries. For instance, the S/V for 15 μm I.D. capillaries is 267 and for 75 μm I.D. capillaries, the S/V is 53, *i.e.*, five times smaller. As a consequence, the heat dissipation in very narrow-bore capillaries is superior. Moreover, the reduction in the cross-sectional area increases the electrical resistance. This in turn reduces the current flowing through them and less Joule heat is generated. This facilitates the use of short capillaries (30 cm or less) and the application of very high voltages (25–30 kV). The length reduction shortens the retention time of the analytes and the very high voltage increases the separation power and the resolution of the capillary. However, there are also disadvantages when very narrow-bore capillaries are used. Some loss of concentration sensitivity occurs. Typically, the minimum detectable concentration (MDC) increased by between two and four orders of magnitude.

In our previous work, we suggested that the loss in the MDC, in very narrow-bore capillaries, might be counteracted by raising the numerical aperture (NA) of the collecting lenses [15,18]. In the capillary diameter *vs.* fluorescence curve, the fluorescence collected shows a sharp rise between 5 μm diameter I.D. and 10 μm I.D. capillaries when a 0.75-NA objective is used. Therefore, we speculated that the high NA permitted by the collinear geometry could enhance the signal and raise the MDC while preserving the excellent resolution and the separation efficiency of very narrow-bore capillaries. We also found that increasing the laser power increases the signal due to the fluorescence and the background light due to laser scattering. However, when NA increases, the signal is enhanced at a higher rate than the background light, improving the signal-to-noise ratio (S/N). These advantageous but disparate changes of signal and noise were unexpected and intuitively contradictory. Therefore, we decided to investigate further the advantages of high-NA lenses and very narrow-bore capillaries.

Then, we decided to use CE–LIF in narrow-bore capillaries to solve a biologically relevant analytical problem. Currently, by using brain

microdialysis, it is possible to monitor changes in the chemical composition of the brain *in vivo* [19]. So far, the techniques that have been used for chemical analysis of the brain dialysates have a good concentration sensitivity and a poor mass sensitivity. Therefore, large amounts of sample (greater than 5 μl) have to be collected in order to obtain enough quantity of analytes. Typically, the sampling times of 5–30 min are required. However, certain amino acid neurotransmitters, such as glutamic acid and aspartic acid, are released and taken up in fractions of a second. An analytical technique to study the *in vivo* release of these neurotransmitters has to be fast and sensitive enough to allow the analysis of these very small volumes of sample. CE–LIF in very narrow-bore capillaries seems to fulfil these requirements. Volumes smaller than 1 nl, can be used and the analysis time is reduced to less than 2 min.

In the present article, we report experiments carried out to clarify why the S/N ratio improves as a function of NA in a collinear detection system. Then, we present data showing the efficiency of the detector to make fast measurements of excitatory amino acids in brain dialysates when 15 μm I.D. capillaries are used.

MATERIALS AND METHODS

Instrument

The general design of the instrument is described elsewhere [15]. Briefly, the detector was made of a 141-FD standard model epiillumination fluorescence microscope (Zeiss, Caracas, Venezuela). The lasers used for excitation were either air-cooled argon ion lasers (Ion Laser Technology, Salt Lake City, UT, USA; Model 5425) or an air-cooled helium–cadmium ion laser (He–Cd) from Liconix, Santa Clara, CA, USA; Model 4214). The work was done either with the 476-nm line of the argon ion laser at a power of 3 mW or with the 442-nm line of the He–Cd at a power of 12 mW. For all the experiments, the detector was equipped with a dichroic mirror. The objective used had one of the following numerical apertures: 0.20, 0.40, 0.75 or 0.85. All of the objectives were of non-immersion type and lenses were constructed of calcium fluoride (Zeiss, Caracas, Venezuela). The fluorescence was filtered through a long-pass filter and a notch filter to attenuate background radiation. Optical properties of the filters were varied according to the laser line being used and the emitted fluorescence. For the 476-nm line, the dichroic mirror reflected below 490 nm, no notch filter was used and the high-pass filter was centred at 490 nm with a bandwidth of 30 nm. For the 442-nm line, a band-pass filter centred at 440 nm, followed by a dichroic mirror centred at 470 nm, and a notch filter centred at 442 nm with a 20 nm bandwidth (Andover Corporation, Salem, NH, USA). No high-pass filter was used. The light was detected by a photomultiplier tube (PMT) from Hamamatsu (Bridgewater, NJ, USA; Model R928 Multialkali), operated a 700 V, and connected to a microammeter for current-to-voltage conversion (Keithley, Cleveland, OH, USA; Model 485). The picoammeter was connected to a Model L-6512 Linseis strip-chart recorder (Lanseis, Princeton Junction, USA).

The CE separations were performed in fused-silica capillaries obtained from Polymicro Technologies (Phoenix, AZ, USA). The length of the capillaries were 30 cm and 80 cm, and the I.D.s were 15 μm and 75 μm, respectively. The power supply was a Bertan Model 30R high-voltage power supply (Hicksville, NY, USA), and the injection electrodes were platinum–iridium wires. The capillary was set on the instrument as described elsewhere [15,18].

Reagents

Sodium borate, sodium cyanide, fluorescein isothiocyanate (FITC), amphetamine sulphate, glutamic acid, aspartic acid and methanol were obtained from Sigma (Saint Quentin Fallavier, France). Naphthalene-2,3-dicarboxaldehyde (NDA) was obtained from Molecular Probes (Eugene, OR, USA), and 18 MΩ water from a Millipore system.

Amphetamine sample was prepared by dissolving 1 mg in 1 ml of 0.05 *M* borate buffer at pH 9.5 to obtain a $2.7 \cdot 10^{-4}$ *M* solution, and FITC was prepared by dissolving 1 mg in 5 ml of acetone to obtain a $5 \cdot 10^{-4}$ *M* solution. Then 1 ml of each solution was mixed to obtain a $2.5 \cdot 10^{-4}$ *M* solution of fluorescein thiocarbamyl–

amphetamine (FTC–amphetamine), assuming full reaction and amphetamine as the limiting reagent. A blank solution was similarly prepared by mixing $5 \cdot 10^{-4}$ *M* FITC with 1 ml of borate buffer. These solutions were allowed to react for 4 h in the dark and afterwards they were diluted with borate buffer to obtain $2.5 \cdot 10^{-6}$ *M*, $2.5 \cdot 10^{-7}$ *M*, $2.5 \cdot 10^{-8}$ *M*, $2.5 \cdot 10^{-9}$ *M*, $2.5 \cdot 10^{-10}$ *M* and $2.5 \cdot 10^{-11}$ *M* solutions of FTC–amphetamine in one series and blank in another series.

In the first experiment, the effect of numerical aperture on fluorescence and background illumination was tested. Either the $2.5 \cdot 10^{-10}$ *M* solution of FTC–amphetamine or the buffer was continuously drawn through a 75 μm I.D. capillary by vacuum. The 476-nm line of the argon ion laser was used. The PMT current was measured for both solutions using different objectives. The PMT current due to FTC–amphetamine was obtained by subtracting the PMT current due to FTC–amphetamine minus the PMT current due to the buffer. The results were plotted on a NA *vs.* PMT current graph.

In the second experiment, FTC–amphetamine or the corresponding blank was injected by gravity (siphon effect) into a 75 μm I.D. capillary and electrophoresed at 25 kV. For the injection, the anodic end of the capillary was raised 5 cm above the grounded end for 5 s.

In the third experiment, glutamic acid and aspartic acid were measured in the brain dialysate of a rat. A brain microdialysis experiment was peformed as described elsewhere [19]. The microdialysis probe was inserted into the striatum of a rat and perfused with artificial cerebrospinal fluid (ASCF) at 0.1 μl/min. Samples were collected every 10 min and reacted with 5 μl of 0.1 m*M* NDA in methanol, 5 μl of 10 m*M* sodium cyanide, in water and 10 μl of 20 m*M* borate buffer at pH 9.5. A blank solution containing only 1 μl of ACSF was mixed with the reagents as described above. Standard solutions of glutamic acid and aspartic acid were prepared and derivatized to determine the migration time of these amino acids. After 30 min of reaction in the dark, the sample, blank and standards were electrokinetically injected (6 kV, 3 s) in a 30-cm-long 15 μm I.D. × 150 μm O.D. fused-silica capillary filled with buffer. Then, 30 kV were applied to separate the components of the mixture. The 442-nm line of the He–Cd laser was used for excitation.

RESULTS

The results of the first experiment are shown in Fig. 1. The upper curve corresponds to the measurement of the FTC–amphetamine solution. The middle curve corresponds to the PMT currents produced by the buffer. The lower curve is the difference between these two curves. It is clear that the amount of light generated by the buffer-filled capillary decreases as the NA of the lenses increases and reaches an asymptote at 0.75 NA (middle curve). However, the amount of light due to the fluorescence increases as a quadratic function of the NA. Therefore, for the 0.20-NA objective, the fluorescence of FTC–amphetamine represents less than 2% of the total amount of light that the objective is collecting and the buffer-filled capillary is producing 50 times more light than the fluorescence. For the 0.85-NA objective the situation changes. The fluorescence is 50% of the total amount of light collected by the objective and the buffer-filled

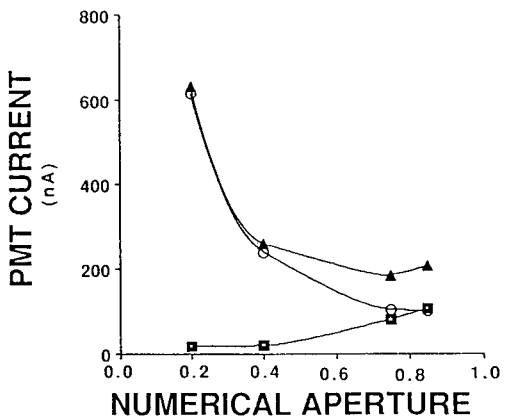

Fig. 1. The PMT current generated by a buffer-filled capillary (open circles) decreases as the NA of the lenses increases. The PMT current due to a capillary flushed with fluorescent material increases (black squares) as a function of NA. However, it increases between the 0.75-NA and 0.85-NA objectives. As a result, the PMT current due to fluorescence (black squares) increases as a function of NA. The final result is an enhancement of S/N ratio as a function of NA.

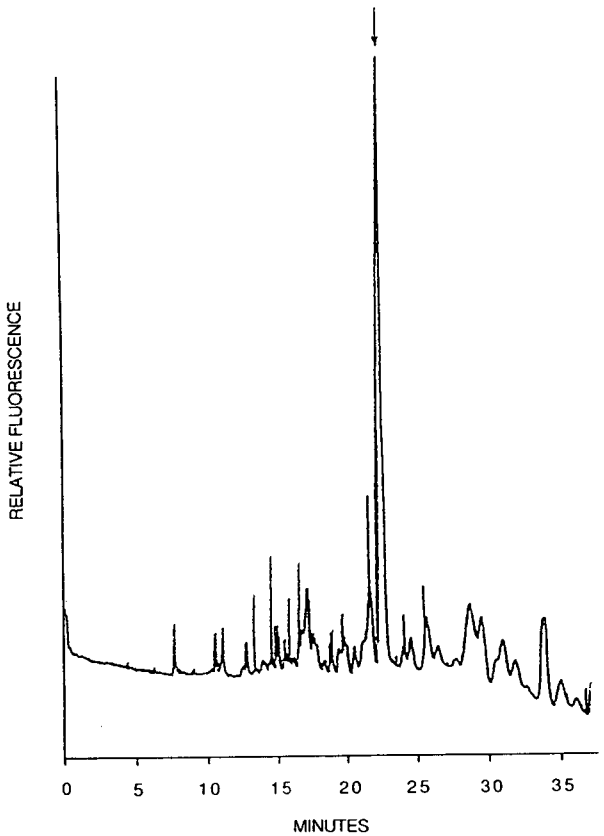

Fig. 2. FTC–amphetamine at 10^{-10} *M* concentration.

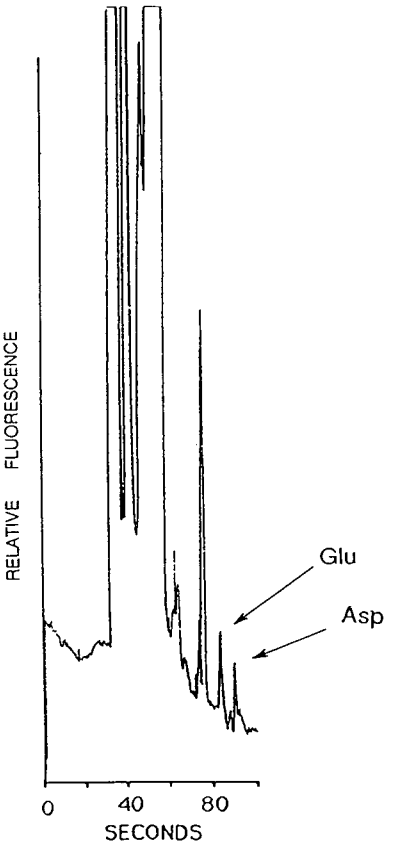

Fig. 3. Glutamic acid and aspartic acid are detected in 23 pl of brain dialysate from a freely moving rat.

capillary produces about the same amount of light as the fluorescent material.

The results of the second experiment are shown in Fig. 2. The $2.5 \cdot 10^{-10}$ *M* FTC–amphetamine solution produces a peak with a *S/N* of 280 and 21.6 min migration time.

The electropherogram of Fig. 3 shows the results of the third experiment. In less than 85 s the peaks corresponding to glutamic acid and aspartic acid were observed.

DISCUSSION

The results presented in Fig. 1 may seem contradictory at the first glance. The effects of increasing the NA on the PMT current are twofold. First, the collection efficiency of the photoluminescence radiation increases. This behaviour can be understood by examining the details of the geometry and the prominent scattering mechanism of the system.

Frequently, the increase in the collection efficiency with the increase in the NA is described by the equation:

$$\text{Collection efficiency} = \sin^2\left(\frac{\arcsin\left(\frac{NA}{\eta}\right)}{2}\right) \quad (1)$$

where NA is the numerical aperture and η is the refractive index of the lens material. The use of this formula in the present context is not adequate as it does not take into account the area of the illuminating surface, which in the present case is not a point source. In fact, the illuminating area varies inversely with the NA and this environment demands a different treatment.

The power, $\Delta\Phi$, incident on the objective is given by:

$$\Delta\Phi = \frac{L\Delta A_1 \Delta A_2}{D^2} \quad (2)$$

where ΔA_1 is the illuminating area, ΔA_2 is the area of the objective, L is the irradiance of the photoilluminating area and D is the distance between illuminating area and the objective.

Even though the illuminating area decreases with the increase in NA, the brightness or irradiance of the spot increases and the product $L\Delta A_1$ remains constant as long as the power of the exciting laser is unaltered. Thus, in the present analysis, the product $L\Delta A_1$ is considered constant in eqn. 2.

For objectives of higher NA, the working distance is smaller than those of lower NA and, therefore, higher collection efficiency is expected. In order to evaluate the experimental results numerically, the intensity of photoluminescence was plotted against distance, D. Pertinent data of the objectives needed in the present investigation, such as working distance and amplification factors, are given in Table I.

Curve-fitting procedures by using the program Mathematica [22] were carried out and indeed the best fit was obtained with the expected expression given by:

$$\text{PMT current} = K + \frac{14}{(D + 0.2)^2} \quad (3)$$

For the present detecting system, the value of K was found to be 15.7. This constant is related to the dark current of the PMT and hence depends upon the applied voltage, type of PMT, radiation leakage and details of the experiment set-up.

TABLE I

CHARACTERISTICS OF THE LENS USED IN EXPERIMENT 1

NA	Working distance (mm)	Magnification
0.2	10.8	6.3
0.4	0.9	16.0
0.75	0.33	40.0
0.85	0.18	50.0

It was found that the effective distance is slightly increased as compared with the working distance of the objective provided by the manufacturer. This is also understandable, since the design of the instrument (optical position of the PMT with respect to the eyepiece) always affects the working distance.

Fig. 1 also shows the PMT current induced by the scattering process. It can be seen that the scattered intensity decreases as the NA of the objectives increases. This observation is apparently contradictory as collection efficiency increases with NA. This behaviour can be explained on the basis of the area of the scattering region.

In the present experimental technique, major contributions to the scattering originate from the cylindrical surface of the capillary rather than the photoluminescent material. The area of the spot illuminated on the capillary decreases substantially as the magnification increases, which occurs as the NA of the lenses increases (see Table I). In other words, the spot area is inversely proportional to the magnification factor of the lens. We have, therefore, plotted PMT current against magnification of the objectives (not of the total system). Curve fitting was carried out with the above-mentioned program. In this case, the best fit was obtained, as expected, for an inverse relation. The analytical expression of PMT current due to scattering is given by:

$$\text{PMT current} = 14.7 + \frac{3744.5}{M} \quad (4)$$

where M is the magnification factor. Here also, 14.7 represents PMT dark current.

It is clear from the above discussion that objectives with higher NA provide two advantages. First, the light-gathering power of the system is enhanced and, second, scattering is reduced because of the smaller size of the focal spot on the capillary.

The values estimated with eqns. 3 and 4 for four different values of NA of the objectives are shown in Table II along with the experimental values. Note that the predicted values are in accordance with the experimental values. This

TABLE II

PREDICTED AND OBSERVED VALUES OF PMT CURRENT (nA) DUE TO SCATTERING AND FLUORESCENCE MECHANISMS

NA	Predicted fluorescence	Observed fluorescence	Predicted scattering	Observed scattering
0.2	15.8	16	613	630
0.4	27.0	19	248	240
0.75	66.0	80	104	108
0.85	112.0	106	100	90

strengthens our views about the importance of high NA in collinear detection systems.

The detection of FTC–amphetamine at 10^{-10} M concentration improves the MDC that we obtained for fluorescamine–amphetamine in our first collinear fluorescence detector [18]. Furthermore, it opens up the possibility of using CE–LIF for amphetamine detection in blood.

Glutamic acid and aspartic acid were measured in brain dialysates. According to the standard measurements, the concentration of glutamate was $0.6 \cdot 10^{-6}$ M, which fits with the concentrations reported by other authors using liquid chromatographic techniques [20]. Several characteristics of the present analysis make it interesting. The amount of sample injected into the capillary was estimated to be about 0.5 nl. Since the actual dialysate represented 4.7% of the whole injection, the volume of dialysate injected was 23 pl. The flow-rate of perfusion was 100 nl/min. The 23 pl injected correspond to the dialysate collected during 72 ms. Thus, at least in theory, it should be possible to follow the release of glutamic acid in the brain on the scale of milliseconds. In practice, several technical problems will have to be solved before reaching that point. For instance, extremely low volumes of dialysate have to be derivatized at the nanoliter level. The technology to manipulate nanoliter volumes already exists [21]. Moreover, the rapidity of the analysis itself can be increased to reach a few seconds. If that turns out to be achievable in practice, then CE–LIF will be a very attractive technique for the *in vivo* monitoring of substances in the brain, such as neurotransmitters.

ACKNOWLEDGEMENT

This work was supported by grants M-413-03-A and BID-CONICIT BTS-37.

REFERENCES

1 S. Wu and N.J. Dovichi, *J. Chromatogr.*, 480 (1989) 141.
2 J.V. Sweedler, J.B. Shear, M.A. Fishman, R.H. Scheller and R.N. Zare, *Anal. Chem.*, 63 (1991) 496.
3 E. Gasman, J.E. Kuo and R.N. Zare, *Science (Washington, D.C.)*, 230 (1985) 813.
4 D.F. Swaile and M.J. Sepaniak, *J. Liq. Chromatogr.*, 14 (1991) 869.
5 D. Burton, M.J. Sepaniak and M.P. Maskarenik, *J. Chromatogr. Sci.*, 24 (1986) 347.
6 B. Nickerson and J.A. Jorgenson, *J. High Resolut. Chromatogr. Chromatogr. Commun.*, 11 (1988) 878.
7 T.A.A.M. van der Goor, B.J. Wanders and F. Everaerts, presented at the *2nd International Symposium on High Performance Capillary Electrophoresis*, San Francisco, CA, 1990, poster MP-106.
8 Y.F. Cheng and N.J. Dovichi, *Science (Washington, D.C.)*, 242 (1988) 562.
9 Y.Y. Cheng, R.D. Piccard and T. VoDinh, *Appl. Spectrosc.*, 44 (1990) 755.
10 D.Y. Cheng, H.P. Swerdlow, H.R. Harke, J.Z. Shang and N.J. Dovichi, *J. Chromatogr.*, 559 (1991) 237.
11 W. Kuhr and E. Yeung, *Anal. Chem.*, 60 (1988) 2642.
12 E. Yeung, *LC · GC*, 7 (1989) 118.
13 B.L. Hogan and E. Yeung, *J. Chromatogr. Sci.*, 28 (1990) 15.
14 J. Liu, K.A. Cobb and M. Novotny, *J. Chromatogr.*, 519 (1990) 189.
15 L. Hernandez, J. Escalona, N. Joshi and N.A. Guzman, *J. Chromatogr.*, 559 (1991) 183.
16 B. Nickerson and J.W. Jorgenson, *J. High Resolut. Chromatogr. Chromatogr. Commun.*, 11 (1988) 533.
17 R.A. Wallingford and A. Ewing, *Anal. Chem.*, 61 (1989) 98.
18 L. Hernandez, J. Escalona, N. Joshi, N.A. Guzman, *J. Chromatogr.*, 502 (1990) 247.
19 L. Hernandez, B.G. Stanley and B.G. Hoebel, *Life Sci.*, 39 (1986) 2629.
20 S. Dijk, H.C. Klein, W. Krop, T.P. Obrenovitch and J. Korf, in H. Rollema, B. Westerink and W.J. Drijfthout (Editors), *In Vivo Monitoring Molecules in Neuroscience*, University Centre for Pharmacy, Groningen, 1991, p. 455.
21 R.T. Kennedy, M.D. Oates, B.R. Cooper, B. Nickerson and J.W. Jorgenson, *Science (Washington, D.C.)*, 246 (1989) 57.
22 S. Wolfram, *Mathematica Software*, Wolfram Research, Champaigne, IL, 1991.

Journal of Chromatography A, 652 (1993) 407–416
Elsevier Science Publishers B.V., Amsterdam

CHROM. 25 047

Assessment of automated capillary electrophoresis for therapeutic and diagnostic drug monitoring: determination of bupivacaine in drain fluid and antipyrine in plasma

Hanspeter Wolfisberg, André Schmutz, Regula Stotzer and Wolfgang Thormann*

Department of Clinical Pharmacology, University of Berne, Murtenstrasse 35, CH-3010 Berne (Switzerland)

ABSTRACT

In an effort to evaluate the use of electrokinetic capillary technology for therapeutic and diagnostic drug monitoring, samples were analysed batchwise with an automated, high-throughput capillary electrophoretic instrument coupled to an inexpensive PC data acquisition and evaluation system. Examples studied included the capillary electrophoretic (HPCE) determination of bupivacaine in drain fluid collected after pulmonary surgery and the micellar electrokinetic capillary chromatographic (MECC) determination of antipyrine in human plasma. Analyses for antipyrine could be accomplished without any sample pretreatment whereas bupivacaine required extraction prior to analysis. Antipyrine determination was effected through external calibration using either peak areas, relative peak areas or peak heights. The intraday and interday reproducibilities ($n = 15$) of the evaluated concentrations were 1.5–3% and 5–6%, respectively. For bupivacaine, determination based on internal and external calibration employing peak areas and peak heights was investigated. The intraday and interday reproducibilities ($n = 5$) of bupivacaine concentrations were about 1% and 2%, respectively, for internal calibration and both about 5% for external calibration. The electrokinetic capillary data compared well with data obtained by gas chromatography (bupivacaine) and high-performance liquid chromatography (antipyrine).

INTRODUCTION

With the more efficient therapeutic application of various drugs and the necessity for screening and confirmation of drugs in body fluids for diagnostic purposes, there has evolved a need for reliable analytical procedures. Currently used methods are based on the principles of spectrophotometry, immunoassays and chromatography [1–3]. All of these techniques have advantages and disadvantages. The reagents for many of the immunological assays are available in kit form, together with highly automated instrumentation. This permits such analyses to be performed easily and efficiently and with high sensitivity and precision. They provide the most rapid (high sample throughput) analytical procedures available to date. However, immunological techniques are prone to disturbances by molecules of similar structure (cross-reactivity) and the availability of antibodies is limited to the most frequently measured drugs. Owing to separation, the chromatographic assays provide specific results for multiple compounds but typically require extensive sample preparation and derivatization. The sample throughput is low because of sequential injection of the samples, and complete automation of chromatographic protocols is difficult.

Recently, instrumentation for electrokinetic separations in capillaries with very small I.D. (25–75 μm) has become available [4–8]. Both high-performance capillary electrophoresis

* Corresponding author.

0021-9673/93/$06.00

(HPCE) and micellar electrokinetic capillary chromatography (MECC) have not yet been adopted in routine applications for drug monitoring. However, their feasibility for therapeutic and diagnostic drug determinations has been tested in various laboratories [8–17]. Compared with chromatographic assays, the advantages of electrokinetic capillary analyses are high resolution, efficiency and speed, automation, small sample size, rapid method development and the use of small amounts of inexpensive and non-polluting chemicals. Although little work has been reported on the ability of HPCE and MECC to provide quantitative analyses for drugs in biological matrices [11,13,17,18], this emerging technology has already been promoted for therapeutic drug monitoring [19].

In an effort to evaluate the use of automated electrokinetic capillary technology for therapeutic and diagnostic drug monitoring, several hundred patients' samples were analysed batchwise with a high-throughput capillary electrophoresis instrument coupled to a PC data acquisition and evaluation system. Examples studied included the MECC determination of antipyrine in human plasma and the HPCE determination of bupivacaine in drain fluid collected after pulmonary surgery, drugs which are typically measured by chromatographic techniques. Antipyrine levels are employed to determine microsomal enzyme activity of the liver [20,21] and bupivacaine monitoring is essential for optimized administration of this drug [22,23]. The aims of this work were to demonstrate the high-quality data obtained by HPCE and MECC, to elucidate the potential of employing this technology in a routine laboratory and to compare the electrokinetic data for antipyrine and bupivacaine with those obtained by high-performance liquid chromatography (HPLC) and gas chromatography (GC), respectively.

EXPERIMENTAL

Drugs and chemicals

The local anaesthetics, purchased as hydrochlorides, antipyrine and phenacetin were of European Pharmacopoeia quality. Bupivacaine was obtained from Sintetica (Mendrisio, Switzerland) and antipyrine, phenacetin, mepivacaine and lidocaine [supplied in vials as 2% (w/v) solutions] were supplied by the university hospital pharmacy (Berne, Switzerland). Hexane, methanol, 2-propanol, methylene chloride and ethyl acetate (all of HPLC grade) were obtained from Rathburn Chemicals (Walkerburn, UK), NaH_2PO_4, $Na_2B_4O_7$ and H_3PO_4 (85%) from Merck (Darmstadt, Germany) and sodium dodecyl sulphate (SDS) was from Sigma (St. Louis, MO, USA). Our own plasma, employed as a calibration matrix, was prepared by centrifugation [1350 *g* (3600 rpm) for 10 min] and stored at −20°C in aliquots of about 200 μl.

Origin of samples

Pleural drain fluid samples containing bupivacaine were received from the Department of Thoracic and Cardiovascular Surgery, University of Berne, and stemmed from patients undergoing thoracotomy. Plasma samples containing antipyrine stemmed from subjects who had been dosed with 1 g of antipyrine and blood samples drawn over a period of 48 h after administration.

Sample preparation for analysis of local anaesthetics

Aqueous standard solutions of bupivacaine (500 μg/ml), mepivacaine (300 μg/ml) and lidocaine (200 μg/ml) were prepared and stored at 4°C. For calibration, aqueous (HPCE) or plasma (GC) samples containing 0.5, 1, 2.5, 5, 10, 15 and 20 μg/ml of bupivacaine, each with 12 μg/ml of mepivacaine (internal standard), were employed. Independently prepared calibration samples were used as controls. Patients' samples were spiked by addition of known aliquots of the standard solutions to the drain fluid prior to sample extraction. Liquid–liquid extraction of the three local anaesthetics was achieved under basic conditions employing either ethyl acetate or hexane (modification of the procedure reported in ref. 22). Typically, 1 ml of tenfold diluted drain fluid (or 1 ml of a calibration or control solution), spiked with mepivacaine (40 μl of standard solution), 1 ml of 0.5 *M* NaOH and 6 ml of the organic solvent (ethyl

acetate or hexane) were added to an 11-ml screw-capped Sovirel test-tube. After vortex mixing for 30 s (HPCE) or vigorous shaking for 5 min (GC) and centrifugation at 1500 *g* (4000 rpm) for 5 min, the upper (organic) phase was transferred into a glass centrifuge tube with a short conical bottom and evaporated to dryness at 40°C. The residue was dissolved in a mixture of 50 μl of running buffer and 50 μl of 0.1 *M* HCl (for HPCE) or 50 μl of methanol (for GC) and vortex mixed for about 30 s. Using HPCE, the recoveries for bupivacaine and mepivacaine were determined to be 68 and 54% (hexane extraction) and 67 and 91% (ethyl acetate extraction), respectively.

Sample preparation for determination of antipyrine

Methanolic standard solutions of antipyrine (200 μg/ml) were prepared and stored at 4°C. Blank plasma (preparation of calibrator and 20 μg/ml control samples) was spiked by addition of known aliquots of these solutions to a test-tube and evaporation to dryness, followed by reconstitution with plasma prior to sample application (MECC) or extraction (HPLC). For MECC, patients' samples were vortex mixed for 30 s and filtered using 0.45-μm Nalgene (25-mm diameter) disposable syringe filters (Nalge, Rochester, NY, USA). Blank, calibration and control sera were defrosted and vortex mixed prior to application to the capillary (no filtration). For HPLC, antipyrine was extracted prior to sample analysis (see below).

HPCE of local anaesthetics

A Model 270A-HT capillary electrophoresis system (Applied Biosystems, San Jose, CA, USA) was employed. This apparatus features automated capillary rinsing, sampling and execution of the electrophoretic run. For our experiments it was equipped with a 75 μm I.D. fused-silica capillary of effective separation length *ca.* 72 cm. A PC Integration Pack (PCIP, version 3.0, Kontron Instruments, Zurich, Switzerland) together with a Mandax AT 286 computer system were used for data acquisition, raw data storage, peak integration and peak-height determination of the signals. The pack features automatic range switching and a dynamic sampling rate allowing sampling every 10 ms for rapidly changing signals. Before each run the capillary was rinsed sequentially with 0.1 *M* NaOH (2 min), water (1 min) and buffer (4 min). The running buffer was composed of 35 m*M* $Na_2B_4O_7$ and 45 m*M* NaH_2PO_4 (adjusted to pH 8.1 with 0.1 *M* phosphoric acid). Samples were injected via vacuum suction (typically 1 s). If not stated otherwise, a constant voltage of 19 kV (current 96–98 μA) was applied, the temperature was set at 30°C and detection was effected at 200 nm.

MECC of antipyrine

The Model 270A-HT capillary electrophoresis system was employed as described above. It was equipped with 75 μm I.D. fused-silica capillaries of effective separation length 40–50 cm. Before each run the capillary was rinsed with 0.1 *M* NaOH (2 min) and with buffer (4 min). The running buffer, if not stated otherwise, was composed of 50 m*M* SDS, 9 m*M* NaB_4O_7 and 15 m*M* NaH_2PO_4 and contained 2% (v/v) of 2-propanol (pH *ca.* 8.1). Samples were injected via vacuum suction (typically 1 s). If not stated otherwise, a constant voltage of 20 kV (current 70–80 μA, depending on the column length) was applied, the temperature was set at 35°C and detection was effected at 240 nm.

GC of local anaesthetics after extraction with ethyl acetate

Aliquots of 5 μl were injected into a Model 3920 B gas chromatograph (Perkin-Elmer, Kuessnacht, Switzerland) equipped with a temperature programmer and a thermionic nitrogen–phosphorus-sensitive detector (Perkin-Elmer) operated in the nitrogen mode. A 1.8 m × 2 mm I.D. glass column packed with 3% SE-30 on Chromosorb W HP (80–100 mesh) (Supelco, Gland, Switzerland) was employed. The temperatures of the column, injector and interface were 200, 230 and 250°C, respectively. The carrier gas flow-rate and detector gas supply (nitrogen and hydrogen) were set at 45 ml/min and 0.8 kg/cm^2 respectively. Peak registration and integration were effected with an HP 3390A

sponding mean y-intercepts were 0.185, 0.055, 0.076 and −0.031 μg/ml. Not surprisingly, these data suggest that internal calibration, *i.e.*, the use of an internal standard, should provide more accurate data than external calibration.

Reproducibility data are summarized in Table I. First, a drain sample containing about 100 μg/ml of bupivacaine was extracted once and analysed with five consecutive injections (intraday data with one extraction). For that case, R.S.D.s of retention time, peak areas and signal ratios were all found to be smaller than 1%. For peak heights, R.S.D.s between 0.9 and 1.4% were obtained. The intraday data listed in the central columns of Table I were obtained with the same sample extracted separately and analysed on the same day, whereas the interday data represent those which were generated on five different days. While the R.S.D.s of peak areas and heights of these intraday and interday data are about the same (5–6%), the variations of the ratios and the detection times were smaller for the intraday runs. Hence concentration values determined with external calibration are of lower accuracy than those obtained with internal calibration. This is clearly seen with the concentration data given in Table I. Using internal calibration, the R.S.D.s for intraday and interday evaluations were found to be 1 and 2.3%, respectively, a result which is excellent in comparison with such data reported for immunoassays and chromatographic procedures [1,2].

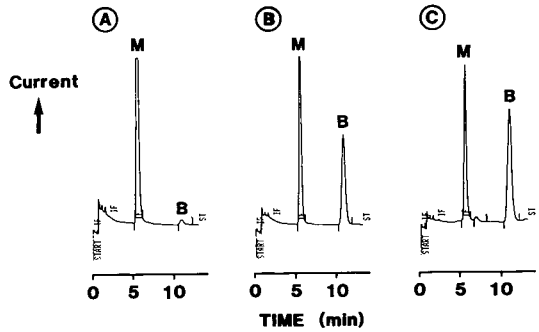

Fig. 2. GC of (A) a calibrator sample containing 0.5 μg/ml of bupivacaine, (B) a calibrator sample containing 10 μg/ml of bupivacaine and (C) a twentyfold diluted patient's sample containing 374 μg/ml of bupivacaine. B = bupivacaine; M = mepivacaine (internal standard).

Over 80 drain samples containing bupivacaine levels up to 500 μg/ml were analysed by HPCE

TABLE I

HPCE REPRODUCIBILITY DATA FOR BUPIVACAINE DETERMINATIONS (n = 5)

Intraday refers to evaluations which were made via five consecutive injections of the same extract, and with five extracts of the same sample analysed on the same day. Interday data were obtained through analysis of the same sample on five different days.

Property	Intraday (one extraction)		Intraday (five extractions)		Interday (five extractions)	
	Mean	R.S.D. (%)	Mean	R.S.D. (%)	Mean	R.S.D. (%)
Detection time (min)	10.58	0.09	10.34	0.30	10.44	2.53
Peak area (mV min)	1.868	0.66	2.160	5.55	1.895	5.18
Peak area I.S.[a] (mV min)	2.191	0.82	2.684	6.07	2.275	5.32
Peak-area ratio	85.15	0.54	80.83	0.98	83.39	1.91
Peak height (mV)	39.87	1.34	47.75	5.00	41.13	4.98
Peak height I.S.[a] (mV)	43.58	0.94	54.75	4.97	46.00	4.46
Peak-height ratio	91.50	0.47	87.29	0.98	89.43	2.08
Concentration (int-a) (μg/ml)	104.3	0.55	100.4	0.96	104.1	2.32
Concentration (int-h) (μg/ml)	105.5	0.48	103.6	0.98	105.9	2.31
Concentration (ext-a) (μg/ml)	101.7	0.67	102.5	5.36	101.7	4.46
Concentration (ext-h) (μg/ml)	103.6	1.33	106.8	4.87	104.9	4.70

[a] Internal standard.

sponding mean y-intercepts were 0.185, 0.055, 0.076 and −0.031 μg/ml. Not surprisingly, these data suggest that internal calibration, *i.e.*, the use of an internal standard, should provide more accurate data than external calibration.

Reproducibility data are summarized in Table I. First, a drain sample containing about 100 μg/ml of bupivacaine was extracted once and analysed with five consecutive injections (intraday data with one extraction). For that case, R.S.D.s of retention time, peak areas and signal ratios were all found to be smaller than 1%. For peak heights, R.S.D.s between 0.9 and 1.4% were obtained. The intraday data listed in the central columns of Table I were obtained with the same sample extracted separately and analysed on the same day, whereas the interday data represent those which were generated on five different days. While the R.S.D.s of peak areas and heights of these intraday and interday data are about the same (5–6%), the variations of the ratios and the detection times were smaller for the intraday runs. Hence concentration values determined with external calibration are of lower accuracy than those obtained with internal calibration. This is clearly seen with the concentration data given in Table I. Using internal calibration, the R.S.D.s for intraday and interday evaluations were found to be 1 and 2.3%, respectively, a result which is excellent in comparison with such data reported for immunoassays and chromatographic procedures [1,2].

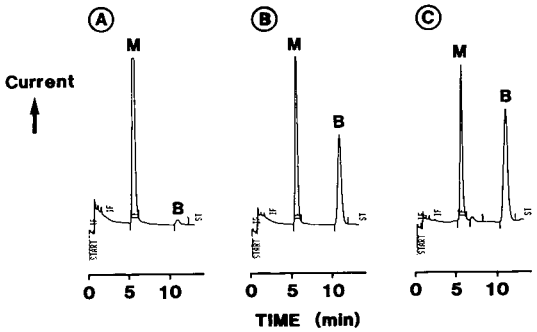

Fig. 2. GC of (A) a calibrator sample containing 0.5 μg/ml of bupivacaine, (B) a calibrator sample containing 10 μg/ml of bupivacaine and (C) a twentyfold diluted patient's sample containing 374 μg/ml of bupivacaine. B = bupivacaine; M = mepivacaine (internal standard).

Over 80 drain samples containing bupivacaine levels up to 500 μg/ml were analysed by HPCE

TABLE I

HPCE REPRODUCIBILITY DATA FOR BUPIVACAINE DETERMINATIONS ($n = 5$)

Intraday refers to evaluations which were made via five consecutive injections of the same extract, and with five extracts of the same sample analysed on the same day. Interday data were obtained through analysis of the same sample on five different days.

Property	Intraday (one extraction)		Intraday (five extractions)		Interday (five extractions)	
	Mean	R.S.D. (%)	Mean	R.S.D. (%)	Mean	R.S.D. (%)
Detection time (min)	10.58	0.09	10.34	0.30	10.44	2.53
Peak area (mV min)	1.868	0.66	2.160	5.55	1.895	5.18
Peak area I.S.[a] (mV min)	2.191	0.82	2.684	6.07	2.275	5.32
Peak-area ratio	85.15	0.54	80.83	0.98	83.39	1.91
Peak height (mV)	39.87	1.34	47.75	5.00	41.13	4.98
Peak height I.S.[a] (mV)	43.58	0.94	54.75	4.97	46.00	4.46
Peak-height ratio	91.50	0.47	87.29	0.98	89.43	2.08
Concentration (int-a) (μg/ml)	104.3	0.55	100.4	0.96	104.1	2.32
Concentration (int-h) (μg/ml)	105.5	0.48	103.6	0.98	105.9	2.31
Concentration (ext-a) (μg/ml)	101.7	0.67	102.5	5.36	101.7	4.46
Concentration (ext-h) (μg/ml)	103.6	1.33	106.8	4.87	104.9	4.70

[a] Internal standard.

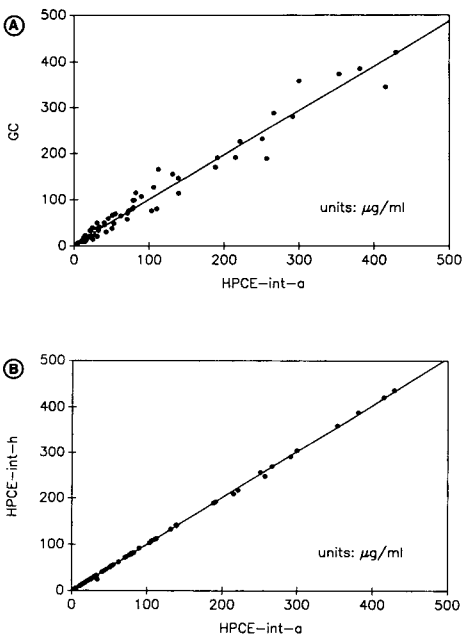

Fig. 3. Comparative analysis of bupivacaine levels in 82 patients' samples (A) monitored by GC and HPCE with internal calibration and using peak areas and (B) monitored by HPCE with internal calibration based on peak areas and peak heights. The data represent those given in sections 1 (line 1) and 2 (line 3), respectively, of Table II.

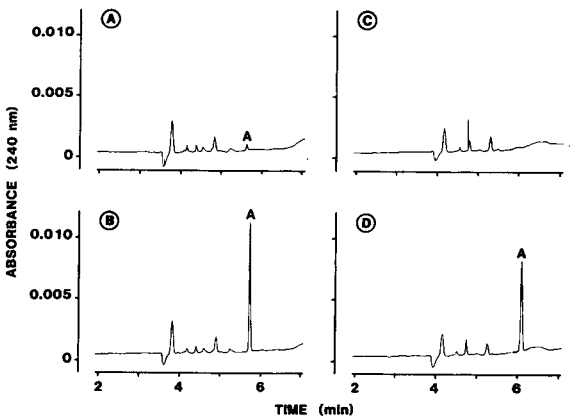

Fig. 4. MECC of (A) a calibrator plasma sample spiked with 1 μg/ml of antipyrine (A), (B) a calibrator plasma sample containing 20 μg/ml of antipyrine, (C) a patient's plasma sample drawn prior to drug intake and (D) a patient's plasma sample containing 16.9 μg/ml of antipyrine. Capillaries of effective length *ca.* 43 and 46 cm were used for the runs shown in (A) and (B), and in (C) and (D), respectively.

and GC (Fig. 2). The comparative results are shown in Fig. 3A and regression data are given in section 1 of Table II. When internal calibration was employed, good agreement between the data from these two methods was obtained, the calculated regression lines showing only small deviations from the line of equality. For HPCE with external calibration, the correlation was found to be in poorer agreement (correlation coefficients of about 0.976 compared to 0.984). It was interesting that according to these correlations HPCE peak areas and peak heights can be recommended for quantification. This is further demonstrated with the correlation data shown in Fig. 3B. Comparison of the data evaluated with the four different approaches (discussed above; for data see section 2 in Table 2) reveal the superiority of data obtained with internal calibration over those evaluated without the inclusion of the internal standard. The mean bupivacaine

TABLE II

LINEAR REGRESSION ANALYSIS DATA FOR COMPARATIVE BUPIVACAINE LEVELS

Section No.	Assay 1 (*x*-axis)	Assay 2 (*y*-axis)	*n*	Slope	*y*-Intercept (μg/ml)	*r*
1	HPCE-int-a	GC	82	0.967	4.02	0.984
	HPCE-ext-a	GC	82	0.899	7.09	0.976
	HPCE-int-h	GC	82	0.956	4.55	0.985
	HPCE-ext-h	GC	82	0.847	8.78	0.977
2	HPCE-int-a	HPCE-ext-a	82	1.060	−2.16	0.994
	HPCE-int-h	HPCE-ext-h	82	1.113	−3.73	0.995
	HPCE-int-a	HPCE-int-h	82	1.013	−0.624	1.000
	HPCE-ext-a	HPCE-ext-h	82	1.062	−2.07	1.000

levels ($n = 82$) obtained with GC, HPCE-ext-a, HPCE-ext-h, HPCE-int-a and HPCE-int-h were 81.2, 82.4, 85.4, 79.8 and 80.1 μg/ml, respectively. Together with the intraday and interday reproducibilities reported in Table I, these data suggest that bupivacaine can be reliably determined using HPCE with internal calibration based on peak areas or peak heights.

MECC determination of antipyrine using direct sample injection

Typical electropherograms obtained with direct injection of plasma blank spiked with 1 and 20 μg/ml of antipyrine are presented in Fig. 4A and B, respectively. Fig. 4C and D depict data obtained with plasma drawn from a patient prior to and after antipyrine administration, respectively. Antipyrine is shown to form a sharp peak that is well separated from endogenous compounds. Using HPLC (Fig. 5) the plasma sample was found to have an antipyrine level of 16.9 μg/ml. Hence MECC with direct injection appears to have the potential to determine this drug at clinically interesting concentration levels. Employing the external standard approach, calibration graphs between 1 and 40 μg/ml (five data points) were constructed and data evaluation was based on peak areas (referred to as MECC-ext-a), relative peak areas (MECC-ext-ra), which represent areas divided by detection times, and peak heights (MECC-ext-h). All graphs showed excellent linearity with R.S.D.s ranging from 1 to 3%. The y-intercepts for peak area, relative peak area and peak height calibrations were all considerably smaller than 1 μg/ml.

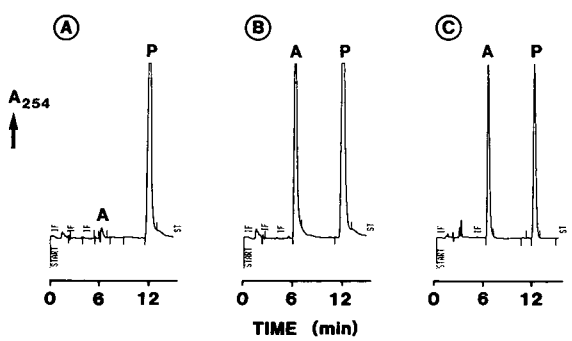

Fig. 5. HPLC of (A) a calibrator sample containing 0.5 μg/ml of antipyrine, (B) a calibrator sample containing 10 μg/ml of antipyrine and (C) a patient's sample containing 16.8 μg/ml of antipyrine. A = antipyrine; P = phenacetin (internal standard). Note that the attenuation for registration of the data in (C) was different to that in (A) and (B).

Not only the excellent calibration graphs but also the reproducibility data summarized in Table III suggest that external calibration should be sufficiently reliable for MECC with direct sample injection. For fifteen consecutive injections of the same sample, the R.S.D.s for retention times, peak areas, relative peak areas and peak heights were 0.20, 3.11 and 2.51 and 1.45%, respectively (first set of intraday data in Table III). With the exception of retention times, lower values were obtained with the implementation of buffer renewal in the anodic electrode compartment after every fifth run (second set of intraday data in Table III). The R.S.D.s of the intraday concentration levels were in the range 1.3–3.1%, with the lowest values being observed for quantification based on peak heights. The data further suggest that quantification based on relative peak areas should provide better accuracy than that based on peak areas. Peak areas, relative peak areas and peak heights were employed for the calculation of the MECC data discussed below. Interday reproducibilities were determined to be about 5.5% for all three quantitation schemes (third set of data in Table III). The determined mean levels were found to be very close to the expected spike values of 10 and 20 μg/ml for intraday and interday data, respectively.

The results of the MECC determination of antipyrine in 72 plasma samples in comparison with the values obtained by HPLC are depicted in Fig. 6A. Correlation data based on linear regression analysis are presented in Table IV. Irrespective of the basis for quantification in MECC, there was good agreement between the data obtained by these two methods, the calculated regression lines showing only small deviations from the line of equality.

The mean plasma levels evaluated with HPLC, MECC-ext-a, MECC-ext-ra and MECC-ext-h were 12.33, 12.37, 12.04 and 10.73 μg/ml, respectively. Although the MECC data based on peak-height calibration deviate the most from both the HPLC data and the MECC data ob-

TABLE III

MECC REPRODUCIBILITY DATA FOR ANTIPYRINE

Buffer change refers to a change of the buffer in the anodic electrode compartment after every fifth run. Intraday evaluations were made via fifteen consecutive injections of a sample and interday data were obtained through analysis of a control sample on fifteen different days. Relative peak areas are peak areas divided by the detection time. NA = not applicable.

Type	Property	Buffer change	n	Mean	R.S.D. (%)
Intraday	Detection time (min)	No	15	6.04	0.20
	Peak area (mV min)	No	15	0.219	3.11
	Relative peak area (mV)	No	15	0.0363	2.51
	Peak height (mV)	No	15	4.75	1.45
	Concentration (ext-a) (μg/ml)	No	15	9.51	3.12
	Concentration (ext-h) (μg/ml)	No	15	9.38	1.56
	Concentration (ext-ra) (μg/ml)	No	15	9.88	2.25
Intraday	Detection time (min)	Yes	15	6.42	1.77
	Peak area (mV min)	Yes	15	0.242	2.13
	Relative peak area (mV)	Yes	15	0.0376	1.86
	Peak height (mV)	Yes	15	5.07	1.24
	Concentration (ext-a) (μg/ml)	Yes	15	10.5	2.70
	Concentration (ext-h) (μg/ml)	Yes	15	10.1	1.32
	Concentration (ext-ra) (μg/ml)	Yes	15	10.2	1.67
Interday	Concentration (ext-a) (μg/ml)	NA	15	20.46	5.36
	Concentration (ext-h) (μg/ml)	NA	15	21.68	5.46
	Concentration (ext-ra) (μg/ml)	NA	15	20.40	5.71

tained with peak-area calibration (Fig. 6B), all three evaluation principles seem to provide MECC data of clinical relevance. The excellent agreement between the MECC-ext-a and MECC-ext-ra data (Fig. 6C) indicates that there is no need to use calibrations based on relative peak areas. Together with the intraday and interday reproducibilities reported in Table III, these data suggest that antipyrine can be reliably determined using MECC peak areas obtained with direct plasma injection.

CONCLUSIONS

It has been shown that high-quality HPCE and MECC data with clinical relevance can be generated using an automated capillary electrophoresis system equipped with untreated fused-silica capillaries and an inexpensive (*ca.* US$ 3500) chromatographic PCIP data station. Automated data evaluation can be based on peak areas or peak heights employing either external or internal calibration. For the two examples discussed, the determination of bupivacaine in drain fluid and antipyrine in plasma, series of up to 30 samples each could easily be run overnight. Based on linear regression analysis and considering the correlation coefficient r between two measurement methods, the HPCE and MECC data agree well with those obtained by conventional chromatographic methods (GC and HPLC; Figs. 3A and 6A, respectively). However, as was pointed out by Bland and Altman [24], such a comparison could be misleading. Therefore, comparative data were further evaluated graphically by plotting the difference against the average of the corresponding drug levels (Fig. 7). For antipyrine (Fig. 7A), the mean difference ± standard deviation ($n = 72$) between the HPLC and MECC-ext-a data was found to be -0.046 ± 1.981 μg/ml, indicating that the two methods provide very comparative levels. Sixty-eight of the 72 data points are within the region defined by the mean

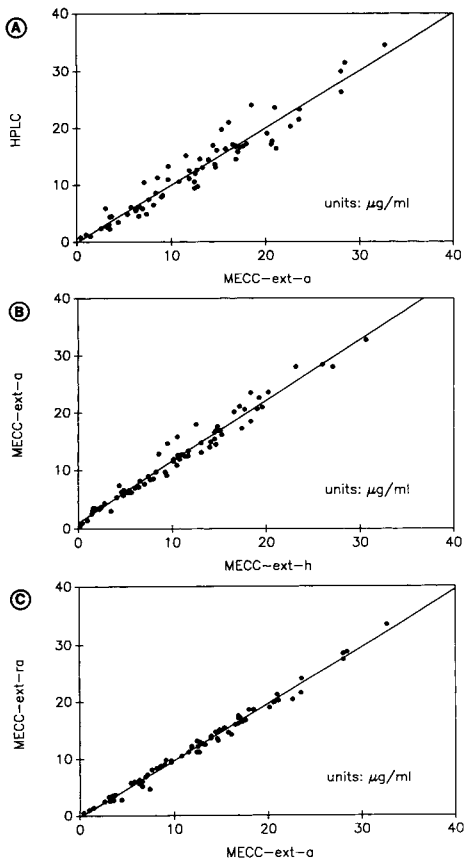

Fig. 6. Comparative analysis of antipyrine levels in 72 patients' samples monitored by (A) HPLC and MECC with external calibration and using peak areas, (B) MECC with external calibration based on peak areas and peak heights and (C) MECC with external calibration based on peak areas and relative peak areas. The data represent those given in lines 1, 4 and 5, respectively, in Table IV.

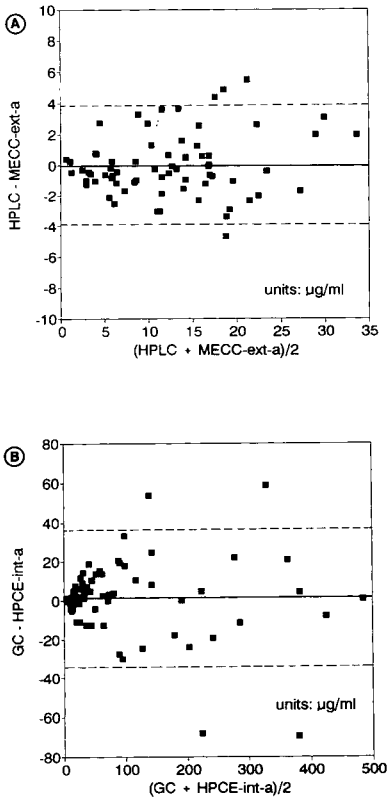

Fig. 7. Difference *versus* mean for comparative (A) antipyrine ($n = 72$) and (B) bupivacaine ($n = 82$) data. The solid line represents the mean of the differences and the broken lines this mean ± two standard deviations.

difference ± two standard deviations. The differences are clinically not important. Hence the two methods can be employed interchangeably. The mean difference ± standard deviation ($n = 72$) between the MECC-ext-a and MECC-ext-h data was calculated to be 1.582 ± 1.313 μg/ml, in-

TABLE IV

LINEAR REGRESSION ANALYSIS DATA FOR COMPARATIVE ANTIPYRINE LEVELS

Assay 1 (x-axis)	Assay 2 (y-axis)	n	Slope	y-Intercept (μg/ml)	r
MECC-ext-a	HPLC	72	1.009	−0.151	0.965
MECC-ext-h	HPLC	72	1.094	0.584	0.972
MECC-ext-ra	HPLC	72	1.013	0.124	0.968
MECC-ext-h	MECC-ext-a	72	1.059	1.008	0.983
MECC-ext-a	MECC-ext-ra	72	0.994	−0.249	0.995

dicating that data evaluation based on peak heights tends to give a lower antipyrine level. For bupivacaine, a different picture was obtained (Fig. 7B). The mean difference ± standard deviation ($n = 82$) between the GC and HPCE-int-a data was found to be 1.243 ± 17.84 μg/ml. Again, most of the differences fall within the limits of agreement (mean ± two standard deviations). The scatter of the differences increases with increasing bupivacaine level.

The data presented clearly suggest that automated capillary electrophoresis (HPCE and MECC) is well suited for therapeutic and diagnostic drug monitoring. Its superiority over chromatographic methods is based on several important facts, including the feasibility of directly injecting proteinaceous samples (such as plasma or serum, as is illustrated with the antipyrine example), the high degree of efficiency and automation, the intraday and interday reproducibility data being at the 1–3% and 5% levels, respectively, the small sample size, no requirement for large amounts of organic solvents and the rapidity of analysis. All data obtained so far are very encouraging and demonstrate the high potential of HPCE and MECC. However, instrumental problems associated with the reliability of autosampling and capillary fouling will have to be solved prior to the adoption of these techniques as routine methodologies in a drug assay laboratory. For example, when sampling plasma (or serum) for the MECC determination of antipyrine, the proportion of failures (drop outs, runs without a driving current and therefore no data) was observed to be 12% ($n = 457$) or even higher in other assays (data not shown). On dilution (threefold) of the antipyrine samples with saline this number was reduced to 5% ($n = 119$) and no such failures were obtained in either of the assays described when aqueous samples were applied. The exact origin of this sampling problem could not be identified, but employment of another instrument from the same manufacturer did provide significantly better data (failure rate *ca.* 2% with direct serum injection). Another problem associated with this kind of technology is occasional plugging of the capillary on the sampling side.

ACKNOWLEDGEMENTS

The authors acknowledge the excellent technical assistance of Mrs. B. Hurni. This work was partly sponsored by the Research Foundation of the University of Berne, the Liver Foundation in Berne and the Swiss National Science Foundation.

REFERENCES

1 W.J. Taylor and M.H. Diers Caviness, *A Textbook for the Clinical Application of TDM*, Abbott Laboratories, Irving, CA, 1986.
2 K. Aziz, *Am. Lab.*, April (1988) 78.
3 R. DeCresce, A. Mazura, M. Lifshitz and J. Tilson, *Drug Testing in the Workplace*, ASCP Press, Chicago, 1989.
4 J.W. Jorgenson and K.D. Lukacs, *Science*, 222 (1983) 266.
5 B.L. Karger, A.S. Cohen and A. Guttman, *J. Chromatogr.*, 492 (1989) 585.
6 N.A. Guzman, L. Hernandez and B.G. Hoebel, *BioPharm*, 2 (1989) 22.
7 Z. Deyl and R. Struzinsky, *J. Chromatogr.*, 569 (1991) 63.
8 S. Terabe, *Trends Anal. Chem.*, 8 (1989) 129.
9 T. Nakagawa, Y. Oda, A. Shibukawa, H. Fukuda and H. Tanaka, *Chem. Pharm. Bull.*, 37 (1989) 707.
10 H. Nishi, T. Fukuyama and M. Matsuo, *J. Chromatogr.*, 515 (1990) 245.
11 D.K. Lloyd, A.M. Cypess and I.W. Wainer, *J. Chromatogr.*, 568 (1991) 117.
12 W. Thormann, P. Meier, C. Marcolli and F. Binder, *J. Chromatogr.*, 545 (1991) 445.
13 W. Thormann, A. Minger, S. Molteni, J. Caslavska and P. Gebauer, *J. Chromatogr.*, 593 (1992) 275.
14 P. Wernly and W. Thormann, *Anal. Chem.*, 63 (1991) 2878.
15 D.K. Lloyd, K. Fried and I.W. Wainer, *J. Chromatogr.*, 578 (1992) 283.
16 H. Nishi and S. Terabe, *Electrophoresis*, 11 (1990) 691.
17 P. Meier and W. Thormann, *J. Chromatogr.*, 559 (1991) 505.
18 M. Miyake, A. Shibukawa and T. Nakagawa, *J. High Resolut. Chromatogr.*, 14 (1991) 181.
19 M.A. Evenson and J.E. Wiktorowicz, *Clin. Chem.*, 38 (1992) 1847.
20 M. Eichelbaum and N. Spannbruckner, *J. Chromatogr.*, 140 (1977) 288.
21 A. El-Yazigi, D.A. Raines, H. Ali, J. Sieck, P. Ernst and M. Dossing, *Pharm. Res.*, 8 (1991) 269.
22 M.E. Kruczek, *J. Pharmacol. Methods*, 5 (1981) 137.
23 B.J. Clark, A. Hamdi, R.G. Berrisford, S. Sabanathan and A.J. Mearns, *J. Chromatogr.*, 553 (1991) 383.
24 J.M. Bland and D.G. Altman, *Lancet*, 1 (1986) 307.

Journal of Chromatography A, 652 (1993) 417–426
Elsevier Science Publishers B.V., Amsterdam

CHROM. 25 101

Investigation of the metabolism of the neuroleptic drug haloperidol by capillary electrophoresis

Andy J. Tomlinson, Linda M. Benson, James P. Landers and Gale F. Scanlan

Department of Biochemistry and Molecular Biology, Guggenheim C061Z, Mayo Clinic, Rochester, MN 55905 (USA)

Jian Fang

Neuropsychiatric Research Unit, University of Saskatchewan, Saskatoon, Saskatchewan S7N 0W0 (Canada)

John W. Gorrod

Chelsea Department of Pharmacy, King's College, University of London, London SW3 6LX (UK)

Stephen Naylor*

Department of Pharmacology and Department of Biochemistry and Molecular Biology, Guggenheim C061Z, Mayo Clinic, Rochester, MN 55905 (USA)

ABSTRACT

Free solution capillary electrophoresis (FSCE) conditions were previously reported to be of limited use for the separation of pharmaceuticals, since many of these compounds are neutral. We show that by consideration of compound hydrophobicity and ionisable functional groups, FSCE conditions can be developed to effect the separation of a drug and its phase I metabolites. This is brought about by adding a suitable organic modifier to aid solubility, and modifying pH to effect a change in the mass to charge ratio of the metabolites present. Furthermore, we show that in this drug metabolism study, FSCE presents an advantage over both reversed-phase HPLC and micellar electrokinetic chromatography. We also demonstrate the use of FSCE for investigation of the phase I metabolites produced by the *in vitro* incubation of haloperidol (a neuroleptic agent) with both mouse and guinea pig hepatic microsomes and show that such an approach can be used to detect both qualitative and quantitative differences in species metabolism.

INTRODUCTION

Haloperidol (HAL) (see Fig. 1) is a clinically proven neuroleptic agent that belongs to the butyrophenone class of drugs used to treat psychotic disorders, such as schizophrenia [1]. It is used in the treatment of hyperexcitable children, as well as in the control of abnormal movements and verbal utterances associated with Tourette's syndrome [1]. However, it has been demonstrated in both humans and animals that the use of this drug can cause debilitating side-effects, such as acute dystonic reactions, akasthisia, tardive dyskinesia, and induction of Parkinsonian-like symptoms [1–3].

Despite widespread clinical use of HAL, little is known about factors that affect correct therapeutic dose and its metabolism. Recently, we and others have investigated the phase I metabolism of HAL using reversed-phase HPLC [4,5], tandem mass spectrometry (MS–MS) [6], and

* Corresponding author.

0021-9673/93/$06.00

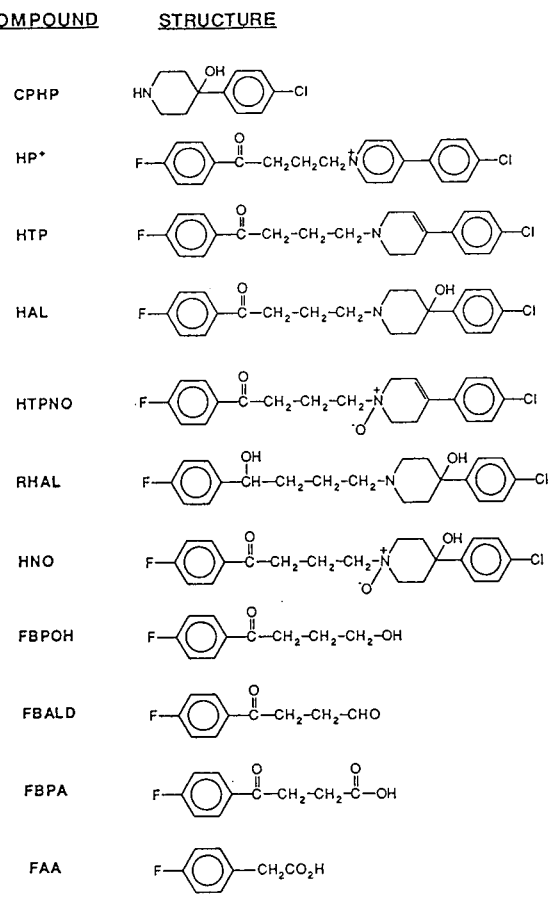

Fig. 1. Structures of the parent drug HAL and ten synthetic standards/putative metabolites.

on-line HPLC–MS–MS [7–11]. These studies have demonstrated that one pathway of HAL metabolism is similar to that involved in the bioactivation of the neurotoxin N-methyl-4-phenyl-1,2,3,6-tetrahydropyridine (MPTP), a known Parkinsonian-inducing agent [12–14]. This suggests that a similar mechanism for the induction of Parkinsonian-like symptoms is operating for both compounds [8,10,15].

We are in the process of developing methods to rapidly and efficiently separate such metabolites in order to investigate their pharmacokinetic and toxic properties. Conventional methods for separation of complex drug metabolite mixtures usually involve the use of reversed-phase HPLC. However, phase I metabolism of a drug often results in only minor structural modification of the parent compound, *e.g.*, oxidation, reduction, dehydration, or hydrolysis (see for example ref. 16). These minor structural changes make it particularly difficult to determine suitable chromatographic conditions to effect separation of metabolites due to the limited resolving capability of HPLC. To this end, the high-efficiency separations of capillary electrophoresis (CE) combined with the ease of rapid analysis present obvious advantages over the use of HPLC for the detection of new and possibly relatively short-lived reactive drug metabolites.

The explosive growth of CE in the analysis of biopolymers, such as peptides/proteins, oligosaccharides, and DNA/RNA, has continued unabated [17–19]. However, its use in the analysis of small organic molecules ($M_r < 500–600$), such as conventional pharamaceutical agents, natural products, and drug metabolite products, has received much less attention [18,19].

Most of the reported literature on the use of CE in the separation of small molecules predominantly involves micellar electrokinetic capillary chromatography (MECC). This technique was first introduced by Terabe *et al.* [20,21] and utilizes buffers that contain surfactants at concentrations above their critical micellar concentration (CMC) [22]. Analytes in solution are differentially partitioned between the micellar phase and the surrounding aqueous phase. Since each phase migrates at a different velocity, separation is affected through a variety of complex interactions [23–26]. A number of small molecules, including derivatised amino acids [27], substituted benzenes [28], purine-like bases [29], nucleotides and nucleosides [30], vitamins [25,31–33], and catechols [34–36], have been separated using this methodology. MECC has also been used in the analysis of pharmaceutical agents, such as antibiotics [25,37,38], anti-inflammatory agents [24,25], and antipyretic analgesic preparations [23,25]. Comparative studies that have been undertaken on MECC and free solution capillary electrophoresis (FSCE) in the separation of small molecules have reported that the former is superior in resolving such components [24,26].

The use of CE in drug metabolism studies remains virtually unexplored. Roach *et al.* [39]

used CE to monitor the metabolism of the antifolate methotrexate to its major metabolite, 7-hydroxymethotrexate in serum, and Fugiwara and Honda [40] analysed the levels of the drug γ-oryzanol and its metabolite ferulic acid in plasma. De Bruijn *et al.* [41] have described buffer conditions to separate the pyrimidine analogue 5-fluorouracil and its metabolites by CE. Recently, Johansson *et al.* [42] reported the use of CE coupled to a mass spectrometer (CE–MS) to analyse a mixture of sulfonamide drugs, as well as a series of benzodiazepine drugs.

In the present study, we have investigated the utility of CE in separating metabolites of the neuroleptic drug haloperidol. We have attempted to develop some simple guidelines for buffer selection in order to separate drug metabolites using FSCE. Furthermore, we compare the use of HPLC and MECC with FSCE to separate metabolites of haloperidol. Finally, we demonstrate the usefulness of FSCE in rapidly detecting differences in species metabolism (in this case, guinea pig and mouse) of haloperidol.

EXPERIMENTAL

Chemicals

Haloperidol HAL, 4-(4-chlorophenyl)-1-[4-(4-fluorophenyl)-4-oxobutyl]-4-piperidinol, potassium phosphate (monobasic), and zinc sulphate were obtained from Sigma (St. Louis, MO, USA). Gold grade ammonium acetate, glacial acetic acid, and magnesium chloride were obtained from Aldrich (Milwaukee, WI, USA). NADP, sodium dodecyl sulphate (SDS), glucose-6-phosphate, and glucose-6-phosphate dehydrogenase were supplied by Boehringer Mannheim Biochemicals (Indianapolis, IN, USA). HPLC-grade solvents methanol and methylene chloride were obtained from Baxter (Minneapolis, MN, USA). High-purity water was prepared in-house using a Sybron Barnstead PCS water purifier system (ex-Millipore) supplied by VWR (Minneapolis, MN, USA). 4-(4-Chlorophenyl)-4-hydroxypiperidine (CPHP), 4-(4-chlorophenyl)-1-[4-(4-fluorophenyl)-4-oxybutyl]-4-piperidinol N-oxide (HNO), 4-(4-chlorophenyl)-1-[4-(4-fluorophenyl)-4-oxobutyl]-1,2,3,6-tetrahydropyridine (HTP), 4-(4-chlorophenyl)-1-[4-(4-fluorophenyl)-4-oxobutyl]-1,2,3,6-tetrahydropyridine N-oxide (HTPNO), 4-(4-chlorophenyl)-1-[4-(4-fluorophenyl)-4-oxobutyl]-pyridinium (HP^+), 4-fluorobenzoyl propionic acid (FBPA), 4-fluorobenzoyl propanol (FBPOH), 4-fluorobenzoyl propanal (FBALD), and 4-fluorophenyl acetic acid (FAA) were synthesised as described previously [11].

High-performance liquid chromatography

The HPLC chromatographic system comprised a ConstaMetric 3000 solvent delivery system (Milton Roy, FL, USA), a Rheodyne 7125 injector with a 100-μl loop and a Rapiscan SA6508 detector set to measure at 220-nm and 245-nm wavelengths. A Tandon TM7002 computer was used to record, store, and analyse chromatograms. Separation was carried out on a 5-μm Hypersil CPS-5 column (250 × 4.6 mm) (Thames Chromatography, Berkshire, UK) coupled with an Upright C-130B guard column (30 × 2 mm) (Upchurch Scientific, WA, USA) packed with 5-μm Hypersil CPS column material. The mobile phase was a combination of acetonitrile (67%) and ammonium acetate buffer (10 m*M*) adjusted to pH 5.4 with acetic acid. The solvent was delivered isocratically at a flow-rate of 1 ml/min [5].

Capillary electrophoresis

Capillary electrophoresis separations were performed using a Beckman P/ACE 2100 Model (Fullerton, CA, USA), coupled to an IBM PS2/76 PC with control and data capture by System Gold software. An uncoated capillary (57 cm × 75 μm) as supplied by Beckman Instruments was used throughout; the effective length of this capillary was 50 cm. Prior to its use, the capillary was rinsed with 0.1 *M* sodium hydroxide (20 column volumes), water (20 column volumes), and buffer (10 column volumes). Between analyses, the capillary was washed with the same order of reagents (10 column volumes of each). The buffer used to afford optimum separation of metabolites was 50 m*M* ammonium acetate containing 10% methanol and 1% glacial acetic acid in water at pH of 4.1. For MECC experiments, a variety of buffers were used, including 50 m*M* phosphate (30 m*M* KH_2PO_4–20 m*M*

Na_2HPO_4), 50 m*M* NH_4OAc, and 100 m*M* borate (sodium borate–boric acid). All buffers contained the surfactant SDS at concentrations above its CMC.

Synthetic standards were individually dissolved in MeOH (1 mg/ml) and 5 μl was removed from each vial and mixed in a single, clean vial to give the mixture containing HAL plus CPHP, HP^+, HTP, RHAL, HNO, HTPNO, FBPOH, FBALD, FBPA, and FAA. The mixture was introduced by pressure injection (1 s), and all experiments were conducted with an applied voltage of 30 kV and a capillary temperature maintained at 25°C. Analyte detection was by UV at a wavelength of 214 nm.

Microsomal incubations

English short-hair male guinea pigs were obtained from the Charles River Co. (Montreal, Canada). Animals were fasted overnight before sacrifice. Hepatic microsomal preparations were prepared using the centrifugation method described previously [43].

Mouse hepatic microsomes were prepared by differential centrifugation of freshly prepared liver homogenates from male $CD2F_1$ mice obtained from the National Cancer Institute (Bethesda, MD, USA) [44]. Cytochrome P_{450} enzymes were induced by pretreatment with phenobarbitone (80 mg/(kg day) × 3 days) prior to sacrifice of the mice on the fourth day [45].

Incubation procedures were as follows: a nicotinamide adenine dinucleotide phosphate (NADPH) generating system consisting of the sodium salt of NADPH ($NADP^+$) (2 μmol), glucose-6-phosphate disodium salt (10 μmol), glucose-6-phosphate dehydrogenase (1 unit), and $MgCl_2$ (2 mg) all in 2 ml phosphate buffer (0.2 M, pH 7.4) was preincubated for 2 min. Enzymatic reactions were initiated by addition of HAL (2 μmol) and microsomal preparations equivalent to 0.5 g original tissue. In control incubates, heat inactivated microsomes were used instead of fresh microsomal preparations. Incubations were carried out for 30 min at 37°C.

Enzymic reactions were terminated by addition of $ZnSO_4$ (200 mg) to the incubation mixture. The precipitated proteins were removed by centrifuging (IEC Cru-5000) at 2300 rpm (*ca.* 1200 *g*) for 20 min. The supernatant was passed through a preconditioned [methanol (4 ml) followed by distilled water (4 ml)] Sep-Pak C_{18} cartridge. Excess $ZnSO_4$ was removed by washing with distilled water (4 ml). The retained compounds were eluted by methanol (4 ml), which was subsequently evaporated to dryness at 45°C under nitrogen [46]. The residues were reconstituted in methanol (200 μl) and subjected to FSCE separation.

RESULTS

High-performance liquid chromatography separation

A mixture consisting of the parent drug HAL and six synthetic standards, previously demonstrated to be metabolites [6], [CPHP, HP^+, HTP, HTPNO, RHAL, and HNO (see Fig. 1)] was used to determine optimal HPLC conditions. IS is the internal standard pirenzepine. In excess of fifty mobile phase solvent systems, as well as a number of different stationary phases, *e.g.*, reversed phase C_{18}, C_4, and phenyl, were also evaluated in order to try to resolve the eight component mixture [5]. Optimum separation conditions were obtained on a 5-μm Hypersil CPS-5 cyano column using an isocratic mobile phase of 67% CH_3CN with 10 m*M* NH_4OAc buffer adjusted to pH 5.4 with acetic acid. The flow-rate used was 1 ml/min [5], and the total run time was 20 min. It should be noted that even using these conditions, it was not possible to baseline resolve the two clusters of com-

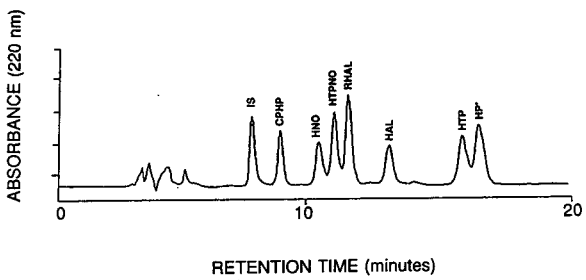

Fig. 2. Reversed-phase HPLC chromatogram (220 nm) of HAL and a mixture of six synthetic standards using a 5-μm Hypersil CPS-5 column, using an isocratic mobile phase of 67% CH_3CN with 10 m*M* NH_4OAc and AcOH (pH 5.4) at a flow-rate of 1 ml/min. IS is the internal standard.

pounds consisting of HNO, HTPNO, RHAL and HTP, HP^+, respectively (see Fig. 2). The detection limit for CPHP and RHAL (monitored at 220 nm) was *ca.* 400 pmol on-column, whereas for the remaining five components (245 nm), it was possible to detect *ca.* 150 pmol of each compound on-column.

Micellar electrokinetic chromatography separation

Previous studies have indicated that MECC is the method of choice for separation of mixtures of small molecules, such as pharmaceutical agents [24,26]. Most workers have reported the use of either phosphate buffer [23,34,35] or borate buffer [47], or a combination of the two [24,26,32,34] in conjunction with SDS to effect MECC separation. In this study, we investigated a variety of buffers containing SDS. We initially used 50 m*M* phosphate [Na_2HPO_4–KH_2PO_4 (1:1)] containing 10 m*M* SDS at pH *ca.* 7.0 in order to effect separtion of a mixture containing *ca.* equimolar amounts of the synthetic standards HNO, HTPNO, FBPOH, and FAA. Only three peaks were detected in the electropherogram (migration times 6.00–6.25 min), and they were not baseline resolved (results not shown). Furthermore, problems were encountered with the solubility of the phosphate buffer in the presence of SDS. Attempts at separating the mixture containing eleven synthetic standards CPHP, HP^+, HTP, HAL, RHAL, HNO, HTPNO, FBPOH, FBALD, FBPA, and FAA (see Fig. 1) using 50 m*M* NH_4OAc with 20 m*M* SDS were also unsuccessful. This in part was due to the high current (*ca.* 210 μA) produced (equivalent to 11 W/m) at 30 kV, leading to substantial Joule heating and arcing in the capillary (results not shown). Partial resolution of the eleven component mixture was achieved using 100 m*M* borate buffer (sodium tetraborate–boric acid) containing 20 m*M* SDS.

Free solution capillary electrophoresis separation

A variety of free solution buffer systems were investigated, including phosphate and borate at various ionic strengths and pH values. However, optimal separation of the eleven synthetic standards was effected in 50 m*M* NH_4OAc containing 1% AcOH and 10% MeOH (pH 4.1), and this is shown in Fig. 3. Electrokinetic separations were conducted using 30 kV across the capillary (57 cm × 75 μm), running a current of 140 μA. Nine of the eleven components were baseline resolved, with only FBPOH and FAA co-migrating as neutrals with the EOF. Under these pH conditions CPHP, HP^+, HTP, HAL, RHAL, HNO, and HTPNO, were of cationic character and migrated before the EOF, whereas FBPA and FAA possessed anionic character and were detected at longer migrations times than the EOF. In all cases, detection limits were *ca.* 100 fmol injected onto the capillary. Since the volume of injection was *ca.* 10 nl, sample concentrations of *ca.* 15 pmol/μl were required to enable component detection. The relatively high current of 140 μA led to some Joule heating which affected the reproducibility of migration times. However, with the exception of the two anionic species FBPA and FAA, relative migration times of the synthetic standards in repetitive analyses were very good. These results are detailed in Table I.

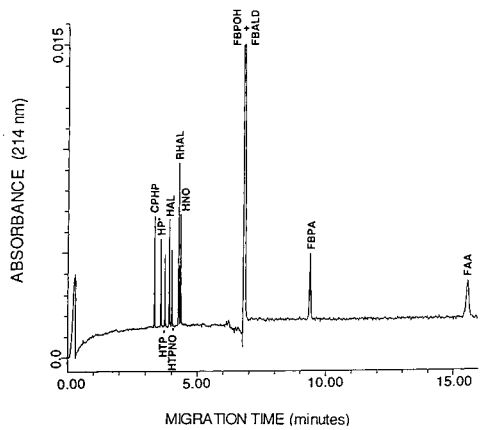

Fig. 3. Electropherogram of HAL and ten synthetic standards by FSCE monitored at a UV of 214 nm. Buffer consisted of 50 m*M* NH_4OAc containing 10% MeOH and 1% AcOH, on a capillary of 57 cm × 75 μm I.D. A voltage of 30 kV gave a current of *ca.* 140 μA.

The mixture of HAL plus the ten synthetic standards was also subjected to FSCE using only 50 m*M* NH_4OAc containing 0.1% AcOH (pH 4.1). Organic modifier (MeOH) was not used in the buffer; however, the sample mixture was

corrected 9 Sep. 94 (AP

TABLE I

MIGRATION TIMES OF SYNTHETIC STANDARDS RELATIVE TO HAL USING FSCE (50 m*M* NH_4OAc CONTAINING 10% MeOH AND 1% AcOH)

Synthetic standard	Mean migration time relative to haloperidol	R.S.D. (%) ($n = 5$)
CPHP	0.87	0.57
HP^+	0.93	0.43
HTP	0.96	0.00
HAL	1.00	–
RHAL	1.02	0.00
HNO	1.08	0.46
HTPNO	1.10	0.36
FBPOH + FBALD	1.65	1.94
FBPA	2.16	4.49
FAA	3.05	2.82

injected (*ca.* 10 nl) in 100% MeOH. Only five of the eleven components were baseline resolved, namely CPHP, HP^+, HNO, FBPA, and FAA (Fig. 4). Although HTPNO was resolved from the other components, it had very poor peak shape.

Microsomal incubations

Employing conditions developed for the separation of the synthetic standards mixture, both mouse and guinea pig hepatic microsomal incubates were subjected to FSCE. These results are shown in Figs. 5 and 6, respectively. Since microsomal incubates are a complex mixture of proteins and buffers, it was necessary to remove these matrices by precipitation of the microsomal proteins using $ZnSO_4$ and subsequent removal of the $ZnSO_4$ and other salts using a solid-phase C_{18} cartridge prior to analysis by CE.

Comparison of the relative migration times (metabolite to unmetabolised parent drug HAL) of samples with synthetic standards (see Table I) revealed the presence of CPHP, HP^+, HTP,

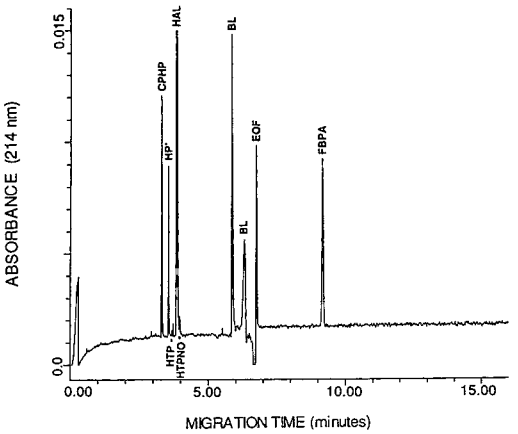

Fig. 5. Electropherogram of a mouse hepatic microsomal incubate. All conditions as described in Fig. 3. BL are observed in a control mouse hepatic microsomal incubate.

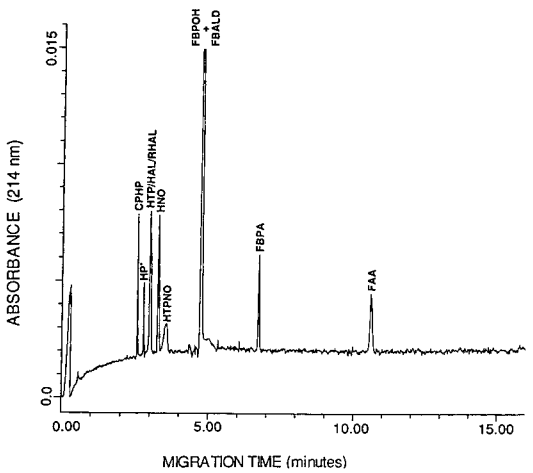

Fig. 4. Electropherogram of HAL and ten synthetic standards by FSCE. All conditions as for Fig. 3 except that the buffer did *not* contain any MeOH.

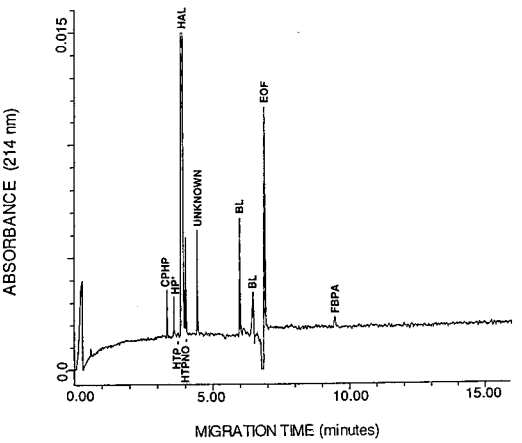

Fig. 6. Electropherogram of a guinea pig microsomal incubate. All conditions as described in Fig. 3. BL are observed in the control incubation. UNKNOWN is a metabolite of HAL yet to be fully characterised.

corrected 9 Sep. 94 / AP

RHAL, and FBRA in the mouse microsomal incubate (Fig. 5). Analysis of the guinea pig microsomal incubate confirmed the presence of the same metabolites as those found in the mouse incubate, as well as a major new component (marked as UNKNOWN in Fig. 6).

In control incubations, using heat inactivated microsomes, no metabolites of HAL were detected in the electropherograms (results not shown). However, unmetabolised HAL, as well as two unidentified components marked BL in Figs. 5 and 6, were detected.

DISCUSSION

The structural diversity of the multitude of modern drugs available for the treatment of disease is well documented (see for example ref. 48). Hence, the evolution of separation methods for complex mixtures of drug metabolites, derived from both *in vitro* and *in vivo* sources, has tended to be specific for a particular drug or class of drugs. Furthermore, due to the structural similarity of phase I drug metabolites, development of conventional separation techniques, such as HPLC, have tended to be time-consuming and, due to the relatively limited resolving capabilities, difficult to achieve. This is reflected in the HPLC separation of the six synthetic standards of HAL metabolites plus the parent drug shown in Fig. 2. It was not possible to effect baseline resolution of five of the six components even after investigating, in excess of, fifty different solvent systems [5]. In addition, polar molecules, such as FBALD, FBPA, and FAA are often co-eluted with the solvent front in reversed-phase HPLC runs and therefore are difficult to detect.

In the present study, we were interested in determining separation conditions that would be functional for a wide variety of drug types based upon consideration of simple structural features of the drug. Due to the rapid method development and high resolution of components achievable by CE, we have investigated the use of this technology to develop conditions that effect the separation of phase I metabolites derived from HAL. In our studies, both MECC and FSCE conditions were evaluated for this application.

The initial impetus for the development of MECC was to achieve the separation of neutral compounds [49–51], since such species have no electrophoretic mobility and will flow past the detector as a single band under the influence of only the EOF. Under MECC conditions, a variety of factors affect the migration times of analytes, including (a) ion pair formation between solute and micelle; (b) distribution of solutes between micelles and aqueous buffer; and (3) electrophoretic mobility of the solute [26,35]. Thus, while this technique was introduced to separate neutral compounds, it has recently been extended to aid the separation of mixtures of small cations [26,34,35] and anions [26,40]. However, acknowledging the success reported in the literature regarding the use of MECC to separate mixtures of small organic molecules, such as pharmaceuticals [23–25,37,38], *a priori* it is difficult to select suitable buffer conditions to effect separations and a variety of buffer and surfactant compositions have been empirically developed.

Using an empirical approach, we investigated a number of buffers containing SDS to effect the separation of HAL and ten synthetic standards previously determined as metabolites [6–11]. Our most successful results were obtained using a 100 m*M* sodium borate buffer with 20 m*M* SDS. However, under these conditions, still we were unable to baseline resolve all eleven synthetic standards, and co-migration of the majority of analyte species was evident (results not shown).

Due to the complexity of the separation factors affecting MECC, we have been unable to determine optimal buffer and surfactant conditions by consideration of the structures of the synthetic standards. Therefore, we considered the use of FSCE where the separation of component mixtures is dependent on both mass and charge of analytes. Furthermore, we have determined that two simple factors are important for prediction of buffer conditions to effect separation, namely hydrophobic character and ionisable functional groups of analyte molecules, and these factors are discussed below.

The hydrophobicity of a compound is frequently expressed as its partition ratio between

octanol and water [52]. However, a qualitative determination of the hydrophobic character of molecules is readily assignable from consideration of functional groups present. Hence, while aromaticity and aliphatic nature clearly determine the hydrophobic character of the molecule, the presence of quaternary amine nitrogens, polyhydroxyl groups, and carboxylic acid functionality add considerable hydrophilic character to the molecule.

In the consideration of a suitable buffer for FSCE separation of drug metabolites, the solubility of the drug and its metabolities in aqueous buffer systems are dependent upon their hydrophilic character. In the present study, the hydrophobic character of HAL and the synthetic standards of putative metabolites prevented their solubilisation in any of the conventional aqueous buffers used, such as phosphate, borate, or ammonium acetate. However, addition of 10% MeOH was enough to solubilise all eleven components in a 50 m*M* buffer solutions of phosphate, borate, or acetate.

Furthermore, it has been documented that addition of some organic modifiers can dramatically affect resolution of mixtures in both MECC [53] and FSCE [54–56]. It has been shown that addition of MeOH slows EOF due to increased buffer viscosity, leading to improved resolution of analytes [54,56]. This is demonstrated further in the separation of HAL and the ten synthetic standards with and without MeOH in the buffer system. In the absence of MeOH from the buffer (see later for discussion of buffer conditions), only five components of the mixture are baseline resolved (Fig. 4). However, addition of 10% MeOH to the buffer composition slows EOF by approximately 1.5 min and results in a marked improvement of resolution with nine compounds now baseline resolved, as shown in Fig. 3.

It should be noted, however, that addition of certain other modifiers, such as acetonitrile, can decrease EOF but increase electrophoretic mobility [54]. Therefore, selection of an organic modifier to aid in metabolite solubility in the buffer must also include consideration of the effects on EOF and migration times of components, since both will ultimately affect resolution.

A limitation of FSCE is that it cannot separate neutrals, since they possess no electrophoretic mobility. Indeed, some authors have questioned the limitations of FSCE in the analysis of pharamaceutical agents, since most species are neutral [32,57]. However, the majority of pharmaceuticals and their subsequent metabolites possess functional groups that are either acidic (–COOH, –SH) or basic ($-NR_2$). Hence, modifying the pH of the buffer solution affects the charge on the parent drug and its metabolites. In the case of HAL and its metabolites, at acidic pH (4.1) protonation of basic nitrogens led to cationic character for parent drug and several putative metabolites (CPHP, HP^+, HTP, RHAL, HNO and HTPNO). In addition, two reported metabolites, FBPA and FAA, were observed to be relatively strong acids, and hence were predominantly dissociated in buffer solution at pH 4.1 and detected as anions. Only two compounds, FBPOH and FBALD, co-migrated under these conditions, since the functional groups of these species were not ionised at pH 4.1. Hence, both were neutrals migrating with the EOF.

A third consideration for FSCE separations is buffer composition. This is usually developed by empirical investigations [58]. We also investigated empirically the effects of buffer composition on the separation of HAL and its phase I metabolites. The results of these experiments demonstrated that a 50 m*M* ammonium acetate buffer gave better resolution of components (particularly HAL/RHAL and HNO/HTPNO) than a phosphate buffer (1.5:1 mix of KH_2PO_4–Na_2HPO_4) of equal concentration. It is suggested that this is due to the slower EOF developed by the ammonium acetate buffer caused by a lower mobility of the ammonium ion in comparison to that of the smaller alkali metal ions. The mobility of analyte cations is determined by the sum of their electrokinetic mobility and the velocity of EOF [59]. Therefore, better resolution of such species will be achieved with slower EOF, since analytes are on the capillary longer as they migrate slower.

Development of FSCE conditions to separate HAL metabolites was prompted by our interest in the metabolism of this widely used clinical

drug. One area of particular interest is the difference in metabolism by humans and different animals species. Species dependent differences in metabolism can occur in both phase I and II metabolism and can be either qualitative and/or quantitative [60]. Such variations have been ascribed to differences in enzyme activity [16], and more recently, to molecular aspects of gene evolution [61]. Clearly, the problems raised by the variation in metabolism by different species for new and clinically used drugs is important in understanding the toxicological and pharmacological activity of metabolites.

We investigated the *in vitro* metabolism of HAL by both mouse and guinea pig hepatic microsomes using the developed FSCE conditions. The electropherograms resulting from the analysis of the microsomal incubates, after solid-phase clean-up, are shown in Fig. 5 (mouse) and Fig. 6 (guinea pig). Comparison of the relative migration times (metabolite:HAL) of metabolites to standards enable us to tentatively identify five metabolites (CPHP, HP^+, HTP, RHAL, and FBPA) from the mouse microsomal incubate (Fig. 5). The same five metabolites were also tentatively identified in the guinea pig microsomal incubate, as well as a further unknown metabolite (marked as UNKNOWN in Fig. 6). A clear difference in metabolism is exhibited by mouse and guinea pig in both a qualitative and quantitative manner. The induced mouse microsomes produce much more CPHP, HP^+, HTP, and FBPA than produced by the guinea pig microsomes. However, the guinea pig microsomal incubate contains much more of RHAL, as well as the UNKNOWN, as previously described by Fang and Gorrod [5]. Further structural studies are underway to characterise the unknown peak.

CONCLUSIONS

Our studies of haloperidol metabolism have demonstrated that FSCE offers major advantages for separation of this drug and its phase I metabolites over both HPLC and MECC techniques. Furthermore, method development was much faster by FSCE than either of the other techniques. This was also aided by the FSCE mass/charge ratio separation mechanism, since ionisable functional groups can play a role in component resolution at appropriate pH values. Consideration of molecule hydrophobicity and addition of MeOH to the FSCE buffer was also shown to improve component separation.

ACKNOWLEDGEMENTS

The authors wish to thank Mrs. Val Langworthy for her invaluable help in preparing this manuscript. One of us (J.P.L.) acknowledges funding by the Medical Research Council of Canada.

REFERENCES

1 R.J. Baldessarini, in A.G. Goodman, T.W. Rall, A.S. Nies and P. Taylor (Editors), *The Pharmacological Basis of Therapeutics*, Pergamon Press, New York, 1991, pp. 383–435.
2 R.E. See and G. Ellison, *Psychopharmacology*, 100 (1990) 404.
3 J.L. Waddington, *Psychopharmacology*, 101 (1990) 431.
4 K. Igarashi and N. Castagnoli Jr., *J. Chromatogr.*, 579 (1992) 277.
5 J. Fang and J.W. Gorrod, *J. Chromatogr.*, 614 (1993) 267.
6 J. Fang, J.W. Gorrod, M. Kajbaf, J.H. Lamb and S. Naylor, *Int. J. Mass Spectrom. Ion Proc.*, 122 (1992) 121.
7 B. Subramanyam, S.M. Pond, D.W. Eyles, H.A. Whiteford, H.G. Fouda and N. Castagnoli Jr., *Biochem. Biophys. Res. Commun.*, 181 (1991) 573.
8 J. Fang and J.W. Gorrod, *Toxicol. Lett.*, 59 (1991) 117.
9 B. Subramanyam, T. Woolf and N. Castagnoli Jr., *Chem. Res. Toxicol.*, 4 (1991) 123.
10 J. Fang and J.W. Gorrod, *Med. Sci. Res.*, 20 (1992) 175.
11 J.W. Gorrod and J. Fang, *Xenobiotica*, 23 (1993) 495.
12 R.H. Heikkila, L. Mazino, F.S. Cabbat and R.C. Duvoison, *Nature*, 311 (1984) 467.
13 J.W. Langston, I. Irwin, E.B. Langston and L.S. Forno, *Science*, 225 (1984) 1480.
14 I.J. Kopin and S.P. Markey, *Ann. Rev. Neurosci.*, 11 (1989) 81.
15 B. Subramanyam, H. Rollema, T. Woolf and N. Castagnoli Jr., *Biochem. Biophys. Res. Commun.*, 166 (1990) 238.
16 G.G. Gibson and P. Skett, *Introduction to Drug Metabolism*, Chapman & Hall, London, 1986.
17 W.G. Kuhr, *Anal. Chem.*, 62 (1990) 403R.
18 W.G. Kuhr and C.A. Monnig, *Anal. Chem.*, 64 (1992) 389R.
19 J.P. Landers, R.P. Oda, T.C. Spelsberg, J.A. Nolan and K.J. Ulfelder, *Biotechniques*, 14 (1993) 98.

20 S. Terabe, K. Otsuka, K. Ichikawa, A. Tsuchiya and T. Ando, *Anal. Chem.*, 56 (1984) 111.
21 S. Terabe, K. Otsuka and T. Ando, *Anal. Chem.*, 57 (1985) 834.
22 M.J. Rosen, *Surfactants and Interfacial Phenomena*, Wiley-Interscience, New York, 1978.
23 S. Fujiwara and S. Honda, *Anal. Chem.*, 59 (1987) 2773.
24 H. Nishi, T. Fukuyama, M. Matsuo and S. Terabe, *J. Chromatogr.*, 513 (1990) 279.
25 H. Nishi, S. Terabe and T. Seiyaku, *Electrophoresis*, 11 (1990) 691.
26 H. Nishi, T. Fukuyama, M. Matsuo and S. Terabe, *J. Pharm. Sci.*, 79 (1990) 519.
27 K. Otsuka, J. Kawahara and K. Tatekawa, *J. Chromatogr.*, 559 (1991) 209.
28 J. Snopek, H. Soini and M. Novotny, *J. Chromatogr.*, 559 (1991) 215.
29 D.E. Burton, M.J. Sepaniak and M.P. Maskarinec, *Chromatographia*, 21 (1987) 583.
30 A.S. Cohen, S. Terabe, J.A. Smith, and B.L. Karger, *Anal. Chem.*, 59 (1987) 1021.
31 D.E. Burton, M.J. Sepaniak and M.P. Maskarinec, *J. Chromatogr. Sci.*, 24 (1986) 347.
32 D.F. Swaile, D.E. Burton, A.T. Balchunas and M.J. Sepaniak, *J. Chromatogr. Sci.*, 26 (1988) 406.
33 H. Nishi, N. Tsumagari, T. Kakimoto and S. Terabe, *J. Chromatogr.*, 465 (1989) 331.
34 R.A. Wallingford and A.G. Ewing, *J. Chromatogr.*, 441 (1988) 299.
35 R.A. Wallingford and A.G. Ewing, *Anal. Chem.*, 60 (1988) 258.
36 C.P. Ong, S.F. Pang, S.P. Low, H.K. Lee and S.F.Y. Li, *J. Chromatogr.*, 559 (1991) 529.
37 H. Nishi, N. Tsumagari and S. Terabe, *Anal. Chem.*, 61 (1989) 2434.
38 H. Nishi, N. Tsumagari, T. Kakimoto and S. Terabe, *J. Chromatogr.*, 477 (1989) 259.
39 M.C. Roach, P. Gozel and R.N. Zare, *J. Chromatogr.*, 426 (1988) 129.
40 S. Fugiwara and S. Honda, *Anal. Chem.*, 58 (1986) 1811.
41 B.E.A. De Bruijn, G. Pattyn, F. David and P. Sandra, *J. High Resolut. Chromatogr.*, 14 (1991) 627.
42 I.M. Johansson, R. Pavelka and J.D. Henion, *J. Chromatogr.*, 559 (1991) 515.
43 J.W. Gorrod, D.J. Temple and A.H. Beckett, *Xenobiotica*, 5 (1975) 453.
44 L. Ernster, P. Sickevitz and G.E. Palade, *J. Cell Biol.*, 15 (1962) 541.
45 J.M. Reid, D.A. Mathiesen, L.M. Benson, M.J. Kuffel and M.M. Ames, *Cancer Res.*, 52 (1992) 2830.
46 M. Kajbaf, M. Jahanshahi, K. Pattichis, J.W. Gorrod and S. Nayor, *J. Chromatogr.*, 575 (1992) 75.
47 A. Wainwright, *J. Microcol. Sep.*, 2 (1990) 166.
48 A.G. Goodman, T.W. Rall, A.S. Nies and P. Taylor (Editors), *The Pharmacological Basis of Therapeutics*, Pergamon Press, New York, 1991.
49 K. Otsuka, S. Terabe and T. Ando, *J. Chromatogr.*, 332 (1985) 219.
50 K. Otsuka, S. Terabe and T. Ando, *J. Chromatogr.*, 348 (1985) 39.
51 K. Otsuka, S. Terabe and T. Ando, *Nippon Kagaku Kaishi* (1986) 950.
52 C. Hansch and A. Leo, *Substitutent Constants for Correlation Analysis in Chemistry and Biology*, Wiley-Interscience, New York, 1979, pp. 18–43.
53 A.T. Balchunas and M.J. Sepaniak, *Anal. Chem.*, 59 (1987) 1466.
54 S. Fugiwara and S. Honda, *Anal. Chem.*, 59 (1987) 487.
55 E. Kenndler and B. Gassner, *Anal. Chem.*, 62 (1990) 431.
56 C. Schwer and E. Kenndler, *Anal. Chem.*, 63 (1991) 1801.
57 W. Steuer, I. Grant and F. Erni, *J. Chromatogr.*, 507 (1990) 125.
58 A.J. Tomlinson, J.P. Landers, I.A.S. Lewis and S. Naylor, *J. Chromatogr. A*, 652 (1993) 171.
59 J.P. Landers, R.P. Oda and M.D. Schuchard, *Anal. Chem.*, 64 (1992) 2846.
60 R.T. Williams, *Biochem. Soc. Trans.*, 2 (1974) 359.
61 D.W. Nerbert and F.J. Gonzales, *Ann. Rev. Biochem.*, 56 (1987) 945.

Journal of Chromatography A, 652 (1993) 427–429
Elsevier Science Publishers B.V., Amsterdam

CHROM. 25 206

Short Communication

Separation of estrogens and rodenticides using capillary electrophoresis with aqueous–methanolic buffers

Karen J. Potter, Robert J.B. Allington and Joseph Algaier*

Isco, Inc., 4700 Superior Street, Lincoln, NE 68504 (USA)

ABSTRACT

Capillary electrophoresis (CE) has proven to be an efficient method for the separation of various charged and neutral analytes. For analytes having limited solubility in water, the CE mode of separation has been micellar electrokinetic capillary chromatography (MECC). However, another approach is the direct addition of an organic solvent to a non-MECC CE separation system. Walbroehl and Jorgenson and also Balchunas and Sepaniak have reported on the use of organics in CE but the focus of their work was using MECC to separate small organic compounds. This work examines the use of aqueous–methanolic buffers in non-MECC CE separations of estrogens and rodenticides.

INTRODUCTION

The fact that most capillary electrophoretic (CE) separations are performed using aqueous separation buffers restricts the range of analytes to those soluble or partially soluble in water. Walbroehl and Jorgenson [1] reported on the use of acetonitrile as a non-aqueous CE medium in the separation of small organic bases (quinoline and isoquinoline), and later used acetonitrile with tetraalkylammonium perchlorate [2]. They concluded that the improved resolution obtained in the separation of small non-polar organic compounds was due to the increased electrophoretic mobilities of the analytes and the decreased electroosmotic flow due to the presence of acetonitrile. Thus, there appeared to be a role for this single-phase non-aqueous CE separation system in resolving non-polar analytes. This conclusion was confirmed by Fujiwara and Honda [3] in the separation of positional isomers of benzoic acid using an acetonitrile-water mixture.

Another approach is the addition of solvents to a micellar electrokinetic capillary chromatography (MECC) system. Here, Balchunas and Sepaniak [4] reported using 2-propanol to extend the sample range and capacity factor of MECC, while Gorse *et al.* [5] and Bushey and Jorgenson [6] demonstrated the use of organics in MECC separations of small organic compounds. But the question still remains as to the role of organic solvents in non-MECC separations of larger molecules of limited water solubility. Thus, this work examines the role of methanol in aqueous non-MECC separation of analytes of biochemical interest, the estrogens and rodenticides.

* Corresponding author.

0021-9673/93/$06.00

EXPERIMENTAL

All capillary electrophoretic separations were performed at 20°C using Isco Model 3850 or Model 3140 variable-wavelength UV CE systems. The columns, 75 μm I.D. fused-silica capillaries (Polymicro Technologies, Phoenix, AZ, USA), were base treated (0.1 *M* NaOH) and rinsed with water prior to use. Samples were injected on column by vacuum. Acetone, methanol and acetonitrile (EM Science, Gibbstown, NJ, USA) were HPLC grade. Phosphoric acid (Midland Scientific, Omaha, NE, USA), acetic acid, boric acid and sodium hydroxide (Mallinckrodt, Paris, KY, USA), were all ACS-reagent grade. Cyclohexylamino-1-propanesulfonic acid (CAPS) was obtained from Research Organics (Cleveland, OH, USA). Warfarin and coumachlor were obtained from Aldrich (Milwaukee, WI, USA). Estriol, β-estradiol and estrone were obtained from Sigma (St. Louis, MO, USA).

RESULTS AND APPLICATIONS

Since Walbroehl and Jorgenson [1,2] reported a decreasing electroosmotic flow (EOF) with increasing concentration of acetonitrile, while Fujiwara and Honda [3] reported the opposite, we re-examined EOF as a function of percent acetonitrile or methanol. Fig. 1 confirms the effect of acetonitrile and likewise methanol on decreasing the EOF. Shown in Fig. 2 this effect is pH dependent, confirming a more complete study by Kenndler and co-workers [7,8]. Thus, the organic solvent component of the separation buffer serves a dual purpose by solvating the analyte and by lowering the EOF, which can aid the resolving power of the system.

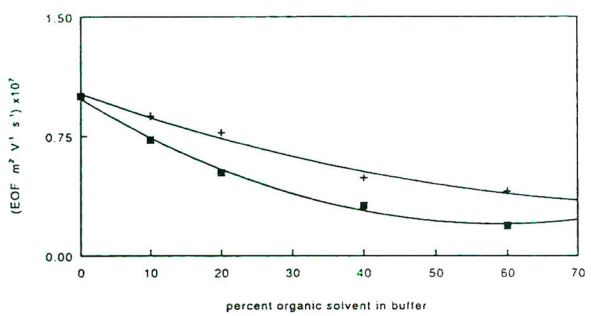

Fig. 1. The effect of methanol (■) and acetonitrile (+) on electroosmotic flow. Conditions: buffer, 50 m*M* sodium borate, pH 10; column, uncoated, 75 μm I.D., 65 cm total, 40 cm effective; 20°C; EOF marker, 0.01% mesityl oxide.

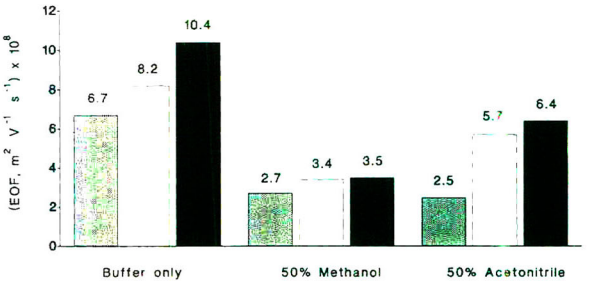

Fig. 2. Addition of methanol and acetonitrile to common capillary electrophoresis buffers: effect on electroosmotic flow. Conditions: final buffer concentration, 10 m*M*, not adjusted for ionic strength differences; column, uncoated, 75 μm I.D., 70 cm total, 45 cm effective; EOF marker, 0.01% mesityl oxide. Hatched bars = sodium acetate, pH 5; open bars = sodium phosphate, pH 7; solid bars = sodium borate, pH 9.

The first application of this work is the CE separation of the estrogens. These analytes have very limited solubility in water and are generally prepared in acetone. Fig. 3 demonstrates the effect of increasing methanol in the separation

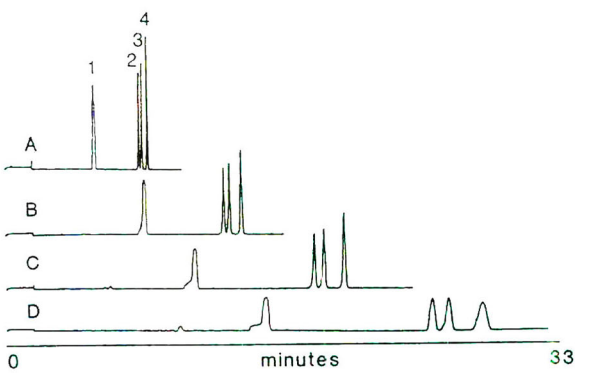

Fig. 3. Effect of increasing methanol concentration in buffer on the separation of steroids. (A) 0% methanol in buffer; (B) 10% methanol; (C) 20% methanol; (D) 30% methanol. Buffer: 100 m*M* CAPS, pH 11.5; 21 nl injection (4 ng). Peaks: 1 = acetone; 2 = estriol, 0.2 mg/ml; 3 = β-estradiol, 0.2 mg/ml; 4 = estrone, 0.2 mg/ml.

buffer on the resolution of the estrogens. Although 20% methanol is the practical limit of the organic solvent component because of the compromise between the loss of peak efficiency versus the limit of detection, this example does show promise should the sample contain interfering compounds.

The second application is the rodenticide, warfarin and its related compound coumachlor. Since compounds very similar to these are used clinically as anticoagulants, this separation is of biochemical interest. Fig. 4 shows the separation of these compounds as a function of increasing percent methanol in the separation buffer. As in the example of the steroids, there is a loss of peak efficiency at a gain of peak resolution, demonstrating a practical limit to the percent methanol.

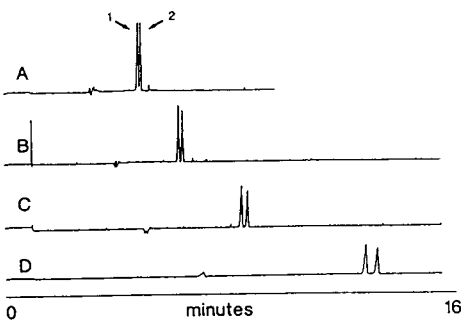

Fig. 4. Effect of increasing methanol concentration in buffer on the separation of rodenticides. (A) 0% methanol in buffer; (B) 10% methanol; (C) 20% methanol; (D) 40% methanol. Conditions: buffer, 20 m*M* sodium phosphate, pH 6.5; column, uncoated, 75 μm I.D., 70 cm total, 45 cm effective; 357 v/cm: 237 nm. Peaks: 1 = coumachlor, 100 μM; 2 = warfarin, 100 μM.

CONCLUSION

This work demonstrates that for the estrogens and rodenticides the addition of methanol to a non-MECC separation buffer improves resolution but at a loss of peak efficiency, and increased separation times. Thus, this approach may be limited to only specific applications of biomolecules.

ACKNOWLEDGEMENTS

We thank Ms. Tracy Doane-Weideman for her assistance in preparing the figures and Ms. Phylis Vosta for her work on the text.

REFERENCES

1 Y. Walbroehl and J.W. Jorgenson, *J. Chromatogr.*, 315 (1984) 135.
2 Y. Walbroehl and J.W. Jorgenson, *Anal. Chem.*, 58 (1986) 479.
3 S. Fujiwara and S. Honda, *Anal. Chem.*, 59 (1987) 487.
4 A.T. Balchunas and M.J. Sepaniak, *Anal. Chem.*, 59-1987 1470.
5 J. Gorse, A.T. Balchunas, D.F. Swaile and M.J. Sepaniak, *J. High Resolut. Chromatogr. Chromatogr. Commun.*, 11 (1988) 554.
6 M.M. Bushey and J.W. Jorgenson, *J. Microcolumn Sep.*, 1 (1989) 125.
7 E. Kenndler and B. Gassner, *Anal. Chem.*, 62 (1990) 431.
8 C. Schwer and E. Kenndler, *Anal. Chem.*, 63 (1991) 1801.

Journal of Chromatography A, 652 (1993) 431–439
Elsevier Science Publishers B.V., Amsterdam

CHROM. 25 205

Separation of gangliosides using cyclodextrin in capillary zone electrophoresis

Young Sook Yoo* and Young Sook Kim

Doping Control Centre, Korea Institute of Science and Technology, P.O. Box 131, Cheongryang, Seoul 130-650 (South Korea)

Gil-Ja Jhon

Department of Chemistry, Ewha Womens University, 11-1 Daehyun-Dong, Seodaemun-Ku, Seoul (South Korea)

Jongsei Park

Doping Control Centre, Korea Institute of Science and Technology, P.O. Box 131, Cheongryang, Seoul 130-650 (South Korea)

ABSTRACT

Gangliosides are glycosphingolipids containing sialic acid. These glycolipids have been suggested to play important roles in biological processes such as cell growth, differentiation and malignant transformation. Based on these proposed biological functions, gangliosides can be used as diagnostic tools and therapeutics for various human diseases. In this study, capillary zone electrophoresis (CZE) was used to determine the major gangliosides G_{M1}, G_{D1a}, G_{D1b} and G_{T1b} in mammalian brains, in addition to G_{M3} and Lac. Enhancement of selectivity and efficiency of separation was obtained by using 50 m*M* borate–phosphate buffer containing 16.5 m*M* α-cyclodextrin (α-CD). Under this condition, several forms of gangliosides were successfully separated from extracts of deer antler, apricot seed and rat brain. The results demonstrate that the CD-modified CZE is a useful method for detecting glycolipids from various biological matrices.

INTRODUCTION

Gangliosides are carbohydrate-rich sphingolipids that contain acidic sugars as shown in Fig. 1 [1]. The acidic sugar is N-acetylneuraminate or N-glycolylneuraminate, and is also known as sialic acid. Gangliosides are found in high concentrations in nervous systems, plasma membranes of virtually all vertebrate tissues and some plant nuts. Although the biological functions of these glycolipids are not clearly known, gangliosides have been suggested to play important roles in the regulation of biological processes such as cell growth and differentiation [2,3]. Some investigators have shown that the concentrations of the ganglioside G_{M1} on the cell surface of the differentiated neuron cell was also increased by neuraminidase activation. A recent study showed that G_{M1} has some therapeutic effect on Alzheimer's disease and dementia [4]. As other gangliosides are overexpressed as antigens in several cancer cells, gangliosides could also be used in immunotherapy. Recently, gangliosides G_{M1}, G_{D1a}, G_{D1b}, G_{T1b} and their sulphate derivatives have also been reported to show antiviral activity towards the human immunodeficiency virus 1 (HIV-1) [5]. Based on these biological functions, gangliosides can be used as diagnostic tools and therapeutics for various diseases in humans.

Determination of gangliosides in biological

* Corresponding author.

0021-9673/93/$06.00

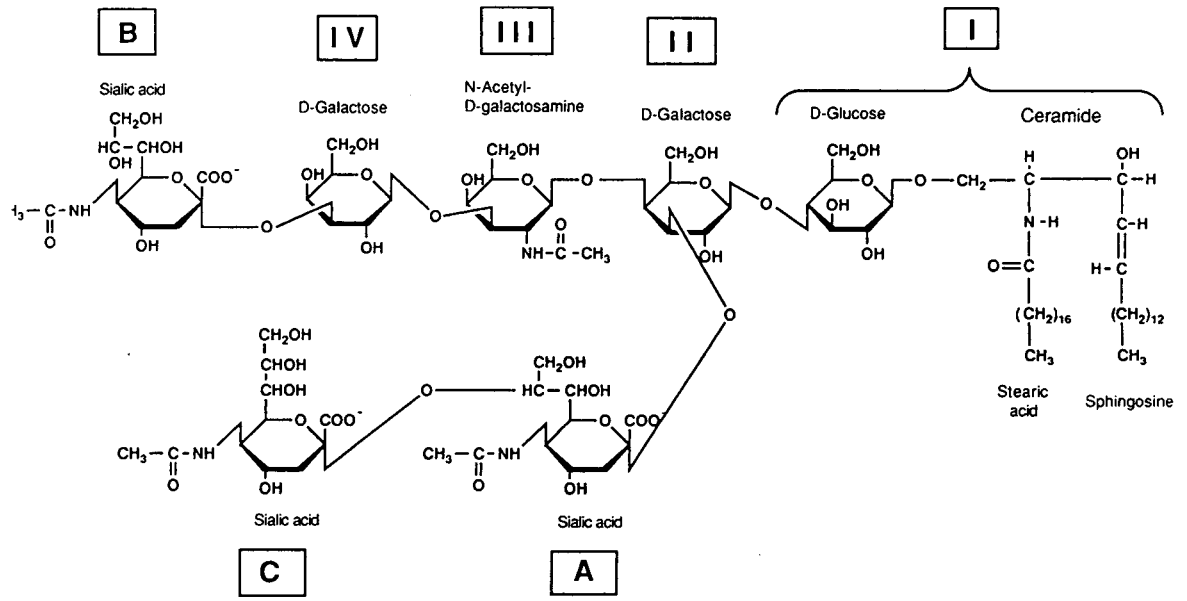

Fig. 1. Structures of some representative brain gangliosides. G_{M1}: I, II, III, IV, A. G_{D1a}: I, II, III, IV, A, B. G_{D1b}: I, II, III, IV, A, C. G_{T1b}: I, II, III, IV, A, B, C.

samples has frequently been carried out by high-performance liquid chromatography (HPLC) or thin-layer chromatography (TLC) [6]. The separation by HPLC usually employs aminosilica columns and a linear gradient of increasing salt concentration in the eluent. By using conventional UV techniques, the identification of gangliosides, which are characterized by a lack of chromophores in their structures, has been difficult owing to the low selectivity in addition to an unfavourable signal-to-noise ratio. In general, the identification of gangliosides after separation by HPLC is achieved using TLC with the UV peaks obtained and subsequent staining with resorcinol, which is specific for sialic acid [7]. Recently, the advent of photodiode-array UV detectors has improved the peak identification of gangliosides to some extent [8].

High-performance capillary electrophoresis is a recently developed and powerful technique with great potential for high-resolution separations and the determination of various molecules, from ions to biological macromolecules [9–18]. Separation by capillary electrophoresis is not limited to a single mode which is the case with liquid chromatography. Analytes can be determined by any of charge/mass ratio, hydrophobicity, size, affinity, absorption, etc. [19–22].

An elegant feature of capillary zone electrophoresis (CZE) is the ability to alter the electrophoretic performance by adding reagents such as surfactants, organic solvents, chelating agents and other additives to the mobile phase [23–26]. Cyclodextrins (CDs) are used as buffer additives to obtain better resolution. The most commonly occurring CDs contain six, seven and eight glucopyranose units, designated α-, β- and γ-CD, respectively [27]. These compounds are able to form inclusion complexes with many molecules. The formation of an inclusion complex is determined by the solute hydrophobicity and size [26,28–31].

In this study, we used CD-modified CZE to determine gangliosides. Parameters such as CD type and concentration and the pH of the mobile phase were varied to obtain the best resolution. The developed method was applied to the determination of gangliosides from various biological matrices including rat brain, deer antler and apricot seed. Gangliosides G_{M1}, G_{D1a} and G_{D1b} were found to exist in deer antler and G_{D1a} was detected in the electropherogram of apricot

seed. In rat brain, G_{M1} and G_{D1a} were the major components and G_{T1b} a minor component of the gangliosides.

EXPERIMENTAL

Instrumentation

The capillary electrophoresis instrument for this study was a Quanta 4000 capillary electrophoresis system (Millipore, Waters Chromatography Division, Milford, MA, USA), with detection using a fixed-wavelength UV detector equipped with a mercury lamp and a 185-nm filter. Some analyses were done with a zinc lamp and a 214-nm filter. The system was operated at a constant voltage of 20–30 kV. Fused-silica capillary tubes of 50 μm I.D. with a tube length ranging from 60 to 100 cm were used. All experiments were carried out at ambient temperature (*ca.* 25–28°C). Sample injections were made by raising the sample reservoir 10 cm higher than the collection reservoir for 10 s. The electropherograms were recorded on a Waters 746 data module.

Reagents

All chemicals were of analytical-reagent grade unless stated otherwise. Ganglioside standards, G_{M1}, G_{D1a}, G_{D1b}, G_{T1b}, G_{M3} and Lac, were purchased from Sigma (St. Louis, MO, USA). α-CD and β-CD were also obtained from Sigma and γ-CD from Merck (Darmstadt, Germany).

Deionized water was prepared with a Milli-Q system (Millipore, Bedford, MA, USA). Water of 18 MΩ was used for the preparation of all the solutions, electrolyte buffer and standards. All the solutions were passed through a 0.22-μm membrane filter unit (Green Cross Medical, Seoul, Korea) and carefully degassed before use.

Sample preparation

Standard ganglioside, *i.e.*, G_{M1}, G_{D1a}, G_{D1b}, G_{T1b}, G_{M3} and Lac, solutions were prepared by dissolution in deionized, 18-MΩ water. The final concentration of the standard samples was 0.5 mg/ml. For some experiments with the 214-nm wavelength filter unit 1 mg/ml sample solutions were used.

Extraction of gangliosides from biological matrices was performed by modified Folch–Suzuki methods [32,33]. The sample preparations from rat brain and apricot seed were homogenized with four volumes of water. Chloroform–methanol–water (4:8:3) was added to the homogenate and the mixture was centrifuged after shaking. Chloroform–methanol (2:1) was added to the supernatant. After partitioning the sample by the Folch method, the samples were vacuum distilled, dialysed, freeze-dried and dissolved in deionized, 18-MΩ water for CE analyses. Sample preparations from deer antler were subjected to further purification by Sephadex G-50 column chromatography and fractionation by the solvent method to collect the ganglioside fraction.

Procedure

To obtain good separation and reproducibility, the capillary tube was cleaned each time the buffer or sample solution was changed. All the cleaning procedures were done by vacuum purging at 12–15 p.s.i. (1 p.s.i. = 6894.76 Pa). The capillary tube was purged for 5 min with 0.5 *M* potassium hydroxide solution, flushed with water for 10 min and then purged with the new electrolyte solution for 10 min. The washed column was equilibrated with the working buffer for 30 min prior to use. After the analyses of biological matrices had been run 3–5 times, the capillary tube was washed as in the above procedure. In addition, the capillary tube was purged for 2 min automatically with the working electrolyte before each injection.

RESULTS AND DISCUSSION

CZE separation and inclusion pseudo-phase analyses using cyclodextrin

Initial studies were focused on investigating the separation of the standard gangliosides. Fig. 2 shows a comparison of electropherograms for plain CZE separation and inclusion pseudo-phase analyses using cyclodextrin of standard gangliosides G_{M1}, G_{D1a}, G_{D1b} and G_{T1b}. The electrolyte used for CZE was a 50 m*M* borate–phosphate buffer. In the CZE analysis for G_{M1}, G_{D1a}, G_{D1b} and G_{T1b}, only the monosialoganglioside G_{M1}, was separated at 8.3 min, with a broad peak. The di- and trisialogangliosides were

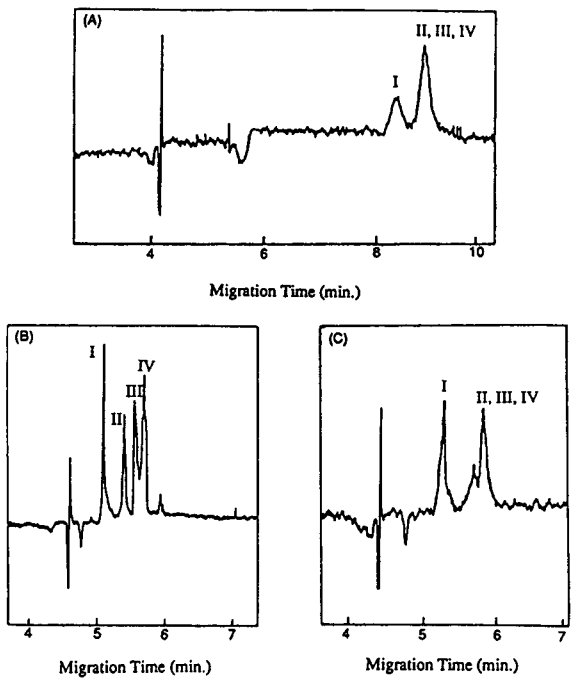

Fig. 2. Electropherograms of standard mixture of gangliosides with or without buffer additive. Conditions: 50 m*M* borate–phosphate buffer (pH 9.3); 20–30 kV; 10-s injection, hydrostatic; UV detection at 185 nm. Peaks: I = G_{M1}; II = G_{D1a}; III = G_{D1b}; IV = G_{T1b}. (A) No modifier; (B) with 11 m*M* α-CD; (C) with 11 m*M* β-CD.

not separated and co-migrated at 9.0 min (Fig. 2A).

As gangliosides contain not only hydrophilic sugar moieties but also hydrophobic lipid components in their structure, they have been known to form stable micelles. Sometimes, even mixed micelles were formed among mono-, di- and trisialogangliosides on prolonged incubation [34]. Although we did not attempt incubation to form mixed micelles in our CZE studies, Fig. 2A shows that mixed micelles were formed more easily between polysialogangliosides than poly- and monosialoganglioside at ambient temperature, *ca.* 25–28°C. However, when the gangliosides samples were pretreated by sonication or kept at room temperature for a long time, we noticed that the peak of G_{M1} merged with the peak of mixed micelles of polysialogangliosides (G_{D1a}, G_{D1b} and G_{T1b}). These observations are in agreement with the results of other investigators [34,35].

In order to separate di- and trisialogangliosides, micellar electrokinetic capillary chromatographic (MECC) methods using several surfactants such as sodium dodecyl sulphate (SDS), sodium cholate and sodium deoxycholate were attempted. Also, a number of buffer additives such as urea and some organic solvents were tried, but none of the above modifications improved the separations of the polysialogangliosides. The use of α-CD, however, improved the separation dramatically as shown in Fig. 2B. We also tried β- and γ-CD as buffer additives in CZE, but although some improvement in the resolution of the peaks was achieved, no separations of di- and trisialogangliosides were obtained, as shown for β-CD in Fig. 2C. When any of the CDs was added to the electrolyte buffer, the migration times of the gangliosides were slightly reduced.

CDs are neutral oligomers with different numbers of units of D-(+)-glucopyranose. In chromatographic analyses including separations of enantiomers, α-, β- and γ-CD with six, seven and eight glucose units, respectively, are most commonly used as modifiers. The structure of the CD forms a cavity that can contribute to partitioning of the solutes [27,36]. The inner diameters of the cavity for α-, β- and γ-CD are 0.47–0.52, 0.60–0.64 and 0.75–0.83 nm, respectively. Perhaps the size of the cavity of α-CD provides the best fit for the lipid moiety of gangliosides. Although we do not have any direct evidence through the measurement of light scattering, our results for the separations of gangliosides using CD in CZE suggest that the α-CD in the electrolyte buffer may also act as an inhibitor of ganglioside micelle formation.

Optimization of inclusion pseudo-phases with CD

Fig. 3 shows the separations of gangliosides with various concentrations of α-CD as a buffer additive. As the concentration of α-CD in the electrolyte increased, the migration speed of the peaks increased. As CDs are neutral, unlike SDS micelles, they are expected to have no electrophoretic velocity and to migrate faster than SDS.

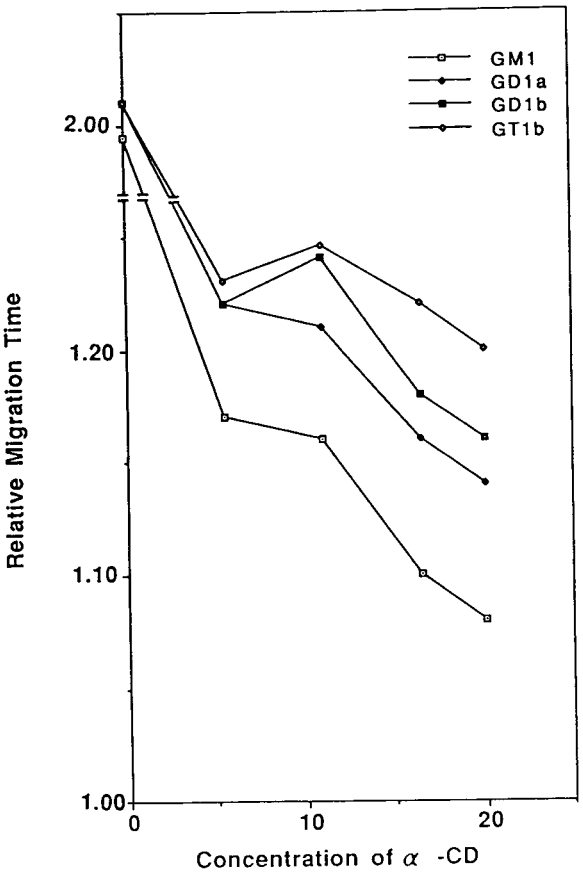

Fig. 3. Effect of concentration of α-CD in the electrolyte on relative migration times of gangliosides. Electrophoretic conditions as in Fig. 2A except for the concentration of α-CD. The relative migration time of the solutes were obtained with respect to the migration time of water, t_0.

Further, at higher concentrations of CD, the general tendency of solutes to be solubilized in the cavity would be increased. Therefore, as the concentration of α-CD increases, the inclusion complexation increases, and consequently the migration speeds of the solutes would be increased. Our results are in agreement with theoretical expectations and the findings of Yik *et al.* [36]. As the concentration of α-CD increases, the resolution of the peaks and the separations of the di- and trisialogangliosides were improved (Fig. 3). When the concentration of α-CD in the electrolyte was higher than 16.5 m*M*, the separation efficiency (number of theoretical plates, *N*) of the gangliosides appeared to be slightly impaired, as shown in Table I.

In order to optimize the α-CD concentration in the electrolyte for the determination of gangliosides, calculation of the separation efficiency was done in terms of *N*. As an indication of peak asymmetry due to tailing, the *B*/*A* ratio, *A* and *B* represent the distance from the centre of the peak to the left-hand side and right-hand side of the peak, respectively, at 10% of the peak maximum, was also measured. As a perfect Guassian peak has a *B*/*A* ratio of 1.0, any peak with a *B*/*A* ratio close to 1.0 would be preferable [37].

Table I shows the efficiency and *B*/*A* ratio for four individual peaks of gangliosides at three different concentrations of α-CD. The three higher concentrations of α-CD in Fig. 3 were

TABLE I

EFFICIENCY (THEORETICAL PLATES, *N*) AND *B*/*A* RATIO FOR GANGLIOSIDES WITH VARIOUS CONCENTRATIONS OF α-CD AS BUFFER ADDITIVE

The optimum experimental conditions (see text) were used, apart from the α-CD concentration. The number of theoretical plates was obtained based on the equation $N = 5.54\ (t_R/W_h)^2$, where t_R is the migration time of the peak and W_h the peak width at half-height. The asymmetry factor, *B*/*A*, was taken at 10% of the peak maximum [37] (a perfect Gaussian peak has *B*/*A* = 1.0).

Ganglioside	11 m*M* α-CD		16.5 m*M* α-CD		20 m*M* α-CD	
	N	*B*/*A*	*N*	*B*/*A*	*N*	*B*/*A*
G_{M1}	$6.2 \cdot 10^4$	1.4	$1.1 \cdot 10^5$	1.1	$8.9 \cdot 10^4$	1.2
G_{D1a}	$6.9 \cdot 10^4$	1.1	$1.1 \cdot 10^5$	1.0	$9.8 \cdot 10^4$	1.2
G_{D1b}	$4.6 \cdot 10^4$	0.6	$1.0 \cdot 10^5$	1.2	$1.0 \cdot 10^5$	0.7
G_{T1b}	$4.8 \cdot 10^4$	0.7	$1.1 \cdot 10^5$	1.1	$9.7 \cdot 10^4$	1.1

chosen to calculate N and the B/A ratio. When the concentration of α-CD was increased from 11 to 16.5 mM, N increased sharply by *ca.* 1.5–2.3 fold. A further increase in the α-CD concentration to 20 mM, however, caused N to decrease slightly. Although the B/A ratios were not affected significantly with variation in the α-CD concentration, the B/A ratios of the peaks at 16.5 mM showed the best result. Based on these observations, an α-CD concentration of 16.5 mM was chosen for subsequent work.

Attempts were made to perform separations in the pH range 4.5–9.3 (Fig. 4). In CZE analysis, ionic species are separated on the basis of the differential electrophoretic mobilities of the analytes. The resolution in CZE could, in principle, be improved by either increasing the difference in electrophoretic mobility of the separated zones or by reducing the electroosmotic flow of the running buffer [38]. At a higher pH, *i.e.*, above the pK_a of analytes, gangliosides exist as negative species and the interaction between the analytes and the capillary wall was minimized. Fig. 4 shows the changes in the relative migration time of each individual ganglioside on increasing the pH of the electrolyte. The migration time of water, t_0, in the electropherogram was used to obtain the relative migration times of the individual solutes. On increasing the pH from 4.5 to 5.5, the relative migration times of all the gangliosides were reduced significantly, although two of the disialogangliosides were not separated. The separation of gangliosides was improved at pH above 8.0. At pH 9.3, all four gangliosides were well separated, as shown in Fig. 4, and the peak shapes in the electropherogram showed the best result (data not shown).

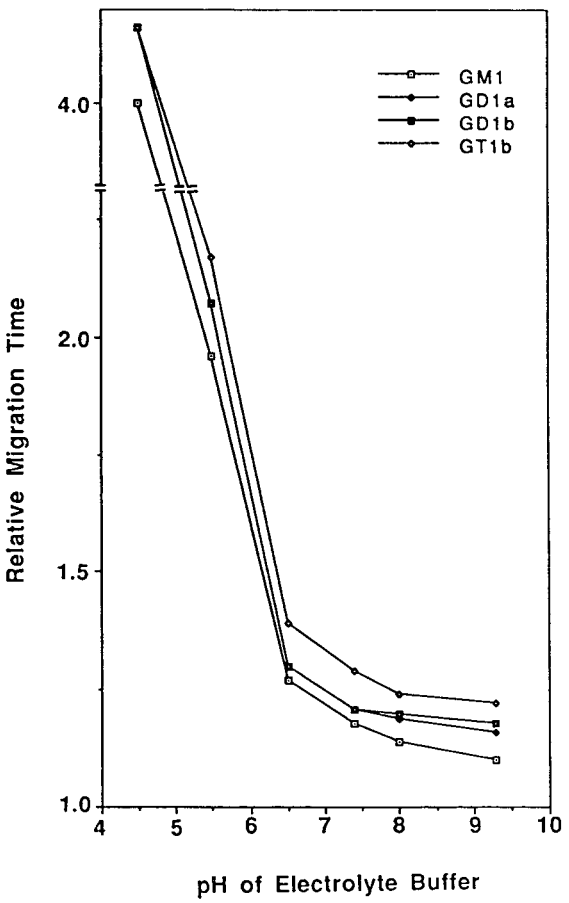

Fig. 4. Effect of pH of the electrolyte on relative migration times of gangliosides. Apart from the pH variation and the addition of 16.5 mM α-CD to the electrolyte buffer, the electrophoretic conditions were as in Fig. 2A.

Initial attempts to determine gangliosides were carried out by using a zinc lamp at 214 nm owing to the limited availability of commercial filter units at the time. When the 185-nm filter unit became available, the responses for gangliosides at 214 and 185 nm were compared. The molar absorptivity of many analytes increased with decreasing wavelength, sometimes significantly. Two drawbacks, *i.e.*, the low intensity of most of the light sources and the low transmission of most solvents in this range, have limited the use of sub-200-nm wavelengths in spectropho-

TABLE II

COMPARISON OF PEAK AREAS AT 185 AND 214 nm, AND SENSITIVITY RATIO

Experiments were performed under the optimum conditions with equal concentrations of sample.

Ganglioside	Peak area (arbitrary units)		Ratio
	214 nm	185 nm	
G_{M1}	1583	32 856	20.8
G_{D1a}	500	10 557	21.1
G_{D1b}	820	18 138	22.1
G_{T1b}	3960	82 242	20.8

tometry, HPLC and CZE. However, in CZE with a fixed-wavelength detection system, UV detection below 200 nm is feasible owing to the short path length of the light source and the separation medium being an isocratic aqueous solution. Table II gives the peak area (arbitrary units) of gangliosides obtained at 214 nm with a zinc lamp and at 185 nm with a mercury lamp. It can be seen that there is a dramatic increase in sensitivity of *ca.* twenty-fold for gangliosides when operating at 185 nm.

Separation of standard ganglioside mixture and reproducibility

Based on the above investigations, the optimum conditions for the determination of gangliosides were established. The electrolyte buffer was 50 m*M* borate–phosphate (pH 9.3) containing 16.5 m*M* of α-CD as buffer additive. The CE instrument was equipped with a 60 cm × 50 μm I.D fused-silica capillary column. The separation was performed at 30 kV. Fig. 5 shows the electropherogram for a standard mixture of gangliosides obtained using the optimum conditions.

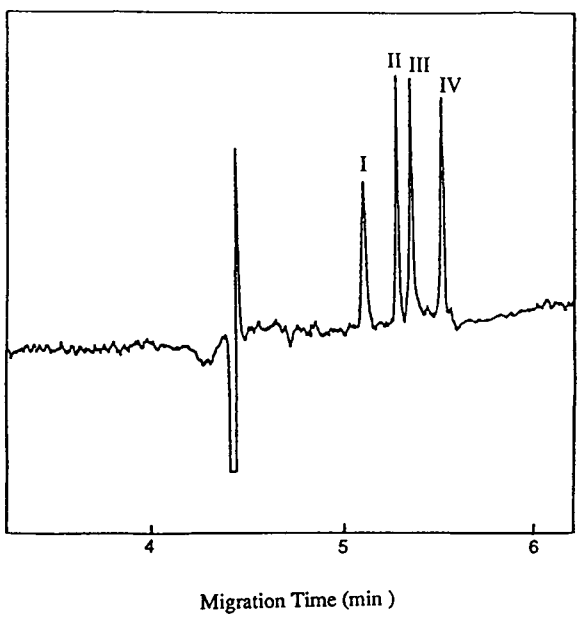

Fig. 5. Electropherogram of standard mixture of gangliosides under the optimum conditions (see text). Peaks: I = G_{M1}; II = G_{D1a}; III = G_{D1b}; IV = G_{T1b}.

To confirm the reproducibility of the migration time and peak area of the four standard gangliosides, G_{M1}, G_{D1a}, G_{D1b} and G_{T1b}, under the optimum conditions, the standard mixture was injected repeatedly, three times per day for three consecutive days. Almost no day-to-day variation observed, and the relative standard deviations ($n = 9$) for migration time and peak area were 0.12–0.24% and 2.0–2.7%, respectively.

Application to samples from biological matrices

The method was applied to the detection of gangliosides in the extracts of deer antler, apricot seed and rat brain. Other investigators have demonstrated that the sensitivity of CZE analysis for monosialoganglioside, *i.e.*, G_{M1}, was much greater (*ca.* 10^4–10^5 fold) than that of the resorcinol–hydrochloric acid method [34]. As the main purpose of this study was the improvement of the separation of gangliosides, especially from various biological matrices, we did not attempt to investigate quantitative aspects.

Fig. 6A depicts the detection of gangliosides in extracts of deer antler, which is commonly used in Chinese medicine as a tonic. To confirm the peaks of the individual components of gangliosides, the extracts were spiked with each standard ganglioside. In the extracts of deer antler, G_{D1a}, G_{D1b} and possibly G_{M1} were identified (Fig. 6A). Because the signal-to-noise ratio of peak I in Fig. 6A was low, not only was the standard G_{M1} added to the sample but also a comparison was made with the results of HPTLC. The standard G_{M1} co-migrated with peak I in the electropherogram and the HPTLC data also showed the possibility of the presence of G_{M1} in the extracts of deer antler. Although standard G_{M3} and Lac, which are thought to be the major ganglioside components in deer antler, were also added to the extracts, they appeared to co-migrate (*ca.* 4.7 min).

In the extracts of apricot seed, the migration time of standard G_{D1a} was matched with the peak at 5.4 min (Fig. 6B). As shown in Fig. 6C, G_{M1} and G_{D1a} were detected in rat brain, although a small peak at 5.5 min co-migrated with the added G_{T1b}. This observation is in good agreement with the results of other investigators [2]. Fig. 6 shows a distinct peak of an unknown

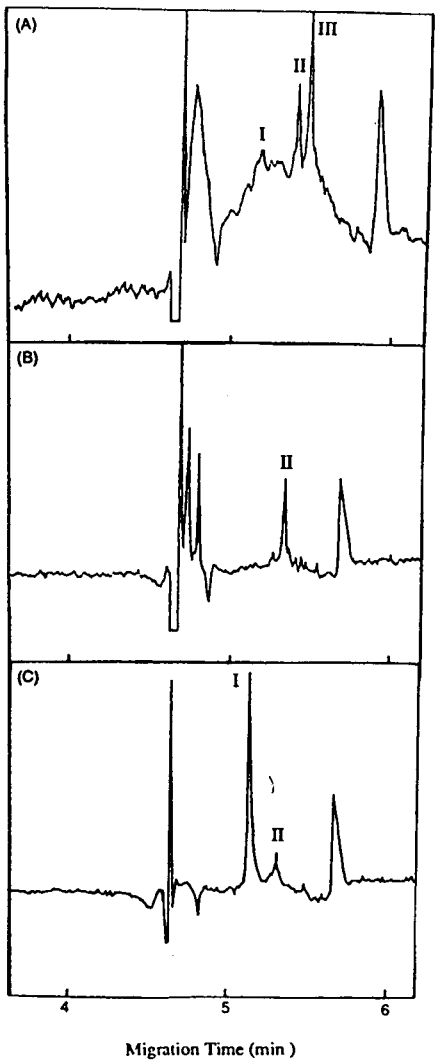

Fig. 6. Electropherogram of gangliosides in biological matrices: (A) deer antler; (B) apricot seed; (C) rat brain. Conditions as in Fig. 5. Peaks: I = G_{M1}; II = G_{D1a}; III = G_{D1b}.

compound around 5.7 min (Fig. 6B and C) or 5.9 min (Fig. 6A). Although this peak has not been identified, presumably the properties of the compound might be similar to those of glycosphingolipids.

CONCLUSIONS

We have investigated the separation conditions for the gangliosides G_{M1}, G_{D1a}, G_{D1b} and G_{T1b}, by using CD-modified CZE. The optimum conditions established were 50 m*M* borate–phosphate buffer (pH 9.3) electrolyte containing 16.5 m*M* α-CD, 60 cm × 50 μm I.D. column and applied voltage 30 kV.

The developed method was applied to the determination of gangliosides from various types of biological matrices, *i.e.*, extracts of deer antler, apricot seed and rat brain. G_{D1a}, G_{D1b} and possibly G_{M1} were shown to exist in deer antler and G_{D1a} was detected in the electropherogram of apricot seed. In rat brain, G_{M1} and G_{D1a} were major components and G_{T1b} was a minor component.

The results demonstrate that CZE using CD is a useful method for detecting glycosphingolipids, which have previously been difficult to detect especially in various biological matrices owing to the lack of chromophores and mixed micelle formation.

REFERENCES

1 L. Svennerholm, *J. Neurochem.*, 10 (1963) 613.
2 R.W. Ledeen, E.L. Hogan, G. Tettamanati, A.J. Yates and R.K. Yu (Editors), *New Trends in Ganglioside Research; Neurochemical and Neuroregenerative Aspects*, Liviana Press, Padova, 1988.
3 P.E. Spoerri, A.K. Dozier and F.J. Roisen, *Dev. Brain Res.*, 56 (1990) 177.
4 D.F. Emerich and T.J. Walsh, *Brain Res.*, 527 (1990) 299.
5 A. Handa, H. Hoshino, K. Nakajima, M. Adachi, K. Ikeda, K. Achiwa, T. Itoh and Y. Suyuki, *Biochem. Biophys. Res. Commun.*, 175 (1991) 1.
6 R. Kannagi, K. Watanabe and S. Hakomori, *Methods Enzymol.*, 138 (1987) 3.
7 G.W. Jourdian, L. Dean and S. Roseman, *J. Biol. Chem.*, 246 (1971) 430.
8 M. Previi, F. Dotta, G.M. Pontier, U.D. Mario and L. Lenti, *J. Chromatogr.*, 605 (1992) 221.
9 J.W. Jorenson and K.D. Lukacs, *Anal. Chem.*, 53 (1981) 1298.
10 J.W. Jorgenson and K.D. Lukacs, *Science*, 222 (1983) 266.
11 S. Terabe, K. Otsuka, K. Ichikawa, A. Tsuchiya and T. Ando, *Anal. Chem.*, 56 (1984) 113.
12 J.W. Jorgenson, *Anal. Chem.*, 58 (1986) 743A.
13 H.H. Lauer and D. McManigill, *Anal. Chem.*, 58 (1986) 166.
14 A.S. Cohen and B.L. Karger, *J. Chromatogr.*, 397 (1987) 409.
15 S. Hjertén, K. Elenbring, F. Kilar, J. Liao, A.J.C. Chem and M. Zhu, *J. Chromatogr.*, 403 (1987) 47.

16 S.W. Compton and R.G. Browniee, *BioTechniques*, 6 (1988) 432.
17 K.-F.J. Chan and W.H. Chen, *Electrophoresis*, 11 (1990) 15.
18 S.A. Swedberg, *Anal. Biochem.*, 185 (1990) 51.
19 A.G. Ewing, R.A. Wallingford and T.M. Olefirowicz, *Anal. Chem.*, 61 (1989) 292A.
20 B.L. Karger, A.S. Cohen and A. Guttman, *J. Chromatogr.*, 492 (1988) 585.
21 S. Terabe and T. Isemura, *Anal. Chem.*, 61 (1989) 2434.
22 J.D. Olechno, J.M.Y. Tso, J. Thayer and A. Wainright, *Am. Lab.*, (1990) 51.
23 S. Terabe, K. Otsuka and T. Ando, *Anal. Chem.*, 57 (1985) 834.
24 A. Guttman, A. Paulus, A. Cohen, N. Grinberg and B. Karger, *J. Chromatogr.*, 448 (1988) 41.
25 S. Terabe, M. Shibata and Y. Miyashita, *J. Chromatogr.*, 480 (1989) 403.
26 S.K. Yeo, C.P. Ong and S.F.Y. Li, *Anal. Chem.*, 63 (1991) 2222.
27 J. Snopek, I. Jelinek and E. Smolkova-Keulemansova, *J. Chromatogr.*, 452 (1988) 571.
28 M. Tazaki, T. Hayeshita, Y. Fujino and M. Takagi, *Bull. Chem. Soc. Jpn.*, 59 (1986) 3459.
29 I. Jelinek, J. Snopek and E. Smolkova-Keulemansova, *J. Chromatogr.*, 405 (1987) 379.
30 I. Jelinek, J. Snopek and E. Smolkova-Keulemansova, *J. Chromatogr.*, 411 (1987) 153.
31 I. Jelinek, J. Dohnal, J. Snopek and E. Smolkova-Keulemansova, *J. Chromatogr.*, 435 (1988) 496.
32 J. Folch, M. Lees and G.H. Sloane-Stanley, *J. Biol. Chem.*, 226 (1957) 497.
33 K. Suzuki, *J. Neurochem.*, 12 (1965) 629.
34 Y. Liu and K.-F.J. Chan, *Electrophoresis*, 12 (1991) 402.
35 E. Heuser, K. Lipp and H. Wiegandt, *Anal. Biochem.*, 60 (1974) 382.
36 Y.F. Yik, C.P. Ong, S.B. Khoo, H.K. Lee and S.F.Y. Li, *J. Chromatogr.*, 589 (1992) 333.
37 J.P. Foley and J.G. Dorsey, *Anal. Chem.*, 55 (1983) 730.
38 R.A. Wallingford and A.G. Ewing, *J. Chromatogr.*, 441 (1988) 299.

Journal of Chromatography A, 652 (1993) 441–450
Elsevier Science Publishers B.V., Amsterdam

CHROM. 25 209

Screening for diuretics in urine and blood serum by capillary zone electrophoresis

J. Jumppanen, H. Sirén and M.-L. Riekkola*

Analytical Chemistry Division, Department of Chemistry, University of Helsinki, P.O. Box 6, 00014 University of Helsinki, Helsinki (Finland)

ABSTRACT

Diuretics are therapeutic agents used to promote the excretion of bodily fluids and salts. They are also misused by some athletes to decrease body mass or to mask the use of anabolic steroids and other drugs. We have developed a method that screens for diuretics in urine and blood serum. Two successive runs were required because of the heterogeneity of this group of compounds. Screening for diuretics that contained sulphonamide and/or carboxylic groups was done at pH 10.6 with 3-(cyclohexylamino)-1-propanesulphonic acid (0.06 *M*) as buffer. Diuretics that contained primary, secondary or tertiary amine groups were investigated at pH 4.5 with an acetate (0.07 *M*)–betaine (0.5 *M*) buffer system. Hydrostatic injection mode for 5 s gave the best efficiency. Longer injection times were acceptable but efficiency was then somewhat reduced. Detection limits at the low femtomole level are achievable for most compounds with a UV–Vis detector operating at 220 and 215 nm. Temperature affected the separation, and 20°C proved best. All compounds were separated in less than 30 mins. A confirmation analysis of all compounds was done by GC–MS.

INTRODUCTION

Capillary zone electrophoresis (CZE) [1] is a powerful separation technique which is rapidly gaining popularity in a number of analytical fields, among them the determination of pharmaceuticals in biological fluids. The separation efficiency of CZE depends on the electrophoretic mobilities of the analytes, if there are no interactions between the analytes and the silanol groups of the capillary wall which may cause, *e.g.*, adsorption of the analytes on the wall. Silanols can work as cation exchangers [2]. All analytes are carried from the anode to the cathode by the electro-osmotic flow [3], whose magnitude is normally significantly greater than the electrophoretic mobilities of the analytes.

The adsorption of polyelectrolytes, such as proteins, can be prevented or diminished by several different methods, alone or in combination. For example, the pH can be adjusted so that the coulombic repulsion forces between the capillary wall and the adsorbing compound become strong enough to prevent adsorption [4]. The pH can be made so low that the negative charge of the capillary wall becomes weak [5], or so high that the polyelectrolytes become negatively charged [6]. The adsorption of polyelectrolytes can also be prevented by adding salt [7] or zwitterionic compounds [8] to the electrolyte solution. Yet a further method involves dynamic modification of the capillary wall by adding organic modifiers to the electrolyte solution [4,9–13]. An alternative approach is to add the modifier to the sample [14,15]. Adsorption can also be prevented by coating the capillary in a permanent fashion [16–22].

Diuretics are a heterogeneous group of compounds which promote excretion of bodily fluids and salts. They vary in mechanisms of operation and duration of their efficacy, and hence in their clinical use. Despite the total ban on them by the International Olympic Committee (IOC),

* Corresponding author.

0021-9673/93/$06.00

diuretics are also misused by some athletes to decrease body weight or to mask the use of anabolic steroids. A number of screening methods have been published for diuretics, based on urine samples and HPLC [23,24]. Sample preparation is usually done by liquid–liquid extraction, but solid phase extraction has also been successfully employed [24,25]. No methods have been published in which blood serum is screened for diuretics.

We have developed a method for detecting diuretics in both urine and blood serum. Two consecutive runs at different pH values are required to separate all compounds.

EXPERIMENTAL

Apparatus

CZE was performed in a fused-silica column with 50 μm I.D. and 360 μm O.D. (Polymicro Technologies, Phoenix, AZ, USA). A detection window was placed 60 cm from the injection end of the column. The instrument was a Beckman 2000 P/ACE System 2000 capillary electrophoresis system with UV–VIS detector (Beckman Instruments, Fullerton, CA, USA). The system is temperature controlled as it employs liquid cooling. The pH of the solutions was adjusted using a Jenway 3030 pH meter and electrode (Jenway, Felsted, UK).

The GC–MS studies were carried out with a Hewlett-Packard Model 5989A single-stage quadrupole mass spectrometer and electron impact mode (EI, 70 eV) (Avondale, PA, USA). A Hewlett-Packard Model 5890A gas chromatograph, an HP 98785A monitor, an HP 6000 330S digital data storage system, an HP 9000 345 data system and an HP Laserjet III printer were used for analysis, data storage and reporting. The carrier gas (helium) was purified with a Supelco high-capacity carrier gas purifier (Supelco, Bellefonte, PA, USA). The compounds were separated on an HP ULTRA-I high-performance GC column (12.5 m × 0.20 mm I.D., 0.33 μm film thickness).

TABLE I

RELATIVE RETENTION TIMES, MAIN FRAGMENTS AND DETERMINATION LIMITS FOR THE METHYLATED DIURETICS

Compound and its group, (A or B)	Relative retention times	Main fragments	Determination limits (ng)	
			Serum	Urine
Diphenylamine (I.S.)	1.00	169		
Amiloride (B)	1.35	229, 204, 202, 171, 144, 116	38	50
Caffeine	1.46	194, 165, 137, 109, 98, 82, 55	14	16
Metyrapone (B)	1.51	226, 135, 120, 106, 92, 78	68	74
Acetazolamide (A)	1.78	264, 249, 142, 108, 83	36	42
Probenecid (A)	2.03	299, 270, 228, 199, 135, 76	20	19
Ethacrynic acid (A)	2.10	316, 281, 261, 243, 203, 109	21	34
Dichlorphenamide (A)	2.53	362, 360, 316, 255, 253, 108	53	51
Chlorothiazide (A)	2.81	355, 248, 220, 168, 140, 108	28	26
Benzthiazide (A)	2.95	353, 351, 259, 244, 56	39	35
Clopamide (A)	2.98	429, 358, 281, 207, 127, 111	36	26
Furosemide (A)	3.03	372, 357, 339, 96, 81, 53	20	13
Chlorthalidone (A)	3.13	363, 351, 255, 176	31	27
Bumetanide (A)	3.21	406, 363, 318, 254, 167, 77	11	19
Hydrochlorothiazide (A)	3.29	357, 355, 248, 220, 168, 140	21	31
Trichlormethiazide (A)	3.36	355, 341, 281, 207, 147, 73	73	98
Triamterene (B)	3.41	337, 323, 308, 294, 280, 265	58	57
Bendroflumethiazide (A)	3.75	386, 278, 145, 91	30	30

Materials

3-(Cyclohexylamino)-1-propanesulphonic acid (CAPS) and all diuretics (Table I) were purchased from Sigma (Poole, UK). Potassium dihydrogenphosphate, dipotassium hydrogenphosphate, morpholine, methanol, potassium hydroxide, hydrochloric acid, sodium acetate, potassium carbonate, diphenylamine and methyl iodide were purchased from Merck (Darmstadt, Germany), and betaine (trimethyl glycine) from Fluka (Buchs, Switzerland). Acetonitrile was purchased from Rathburn (Walkerburn, UK) and was of glass-distilled grade. All chemicals were used as received. Blood and urine were donated by the staff. Samples were taken with sterilized equipment and were frozen until used. Distilled water was further purified with a Water-I system from Gelman Sciences (Ann Arbor, MI, USA). All water needed for buffer or sample solutions was filtered through 0.45-μm membrane filters (Millipore, Molsheim, France). Solid phase extractions of urine and blood serum were carried out with Supelclean LC-18 tubes (3 ml) (Supelco). The calibration of the pH meter was done with standard buffer solutions purchased from Radiometer (Copenhagen, Denmark).

Methods

Separation of compounds by CZE

All injections were made on hydrostatic injection mode by applied pressure. Detection for group A compounds was at 220 nm because this gave the best average signal with minimum background noise. For the same reason group B compounds were detected at 215 nm. The capillary was rinsed with running buffer for 2 min prior to each run. The capillary was regenerated, as required, by treatment with 0.1 *M* potassium hydroxide (10 min) and water (15 min). Spiked sample solutions (water, blood serum and urine) were prepared by combining 10% (v/v) 0.1 *M* potassium hydroxide and 10% (v/v) methanol with 100 ppm of each diuretic and 80% (v/v) sample matrix. This gave 10 ppm as the concentration of each diuretic. The urine was diluted 1:10 (v/v) with water prior to spiking in order to simulate the real density of urine after the abuse of diuretic agents. The elution order of the compounds was determined via spiking of the samples.

Endogenous and the possible exogenous compounds were almost totally removed from the urine by solid-phase extraction (SPE). SPE columns were regenerated with 3 ml of methanol and water, prior to operation. The matrix compounds were removed by washing with 3 ml of water, and diuretics were then extracted with 3 ml of methanol. After this the methanol was evaporated and water, potassium hydroxide and methanol with 100 ppm of each diuretic were added to the sample to give the initial sample volume. This step can, of course, also be used to concentrate the sample if it is large enough. Proteins in blood serum were precipitated with methanol prior to the SPE procedure.

The pH of CAPS buffer solutions was adjusted with potassium hydroxide (0.1 *M*), and the pH of acetate and glycine buffer solutions with hydrochloric acid (0.1 *M*). The pH of phosphate buffers was adjusted by calculating the amounts of potassium dihydrogenphosphate and dipotassium hydrogenphosphate needed to give a solution of desired pH and ionic strength.

Identification of compounds by GC–MS

Solid-phase extraction. SPE columns were regenerated with methanol (3 ml) and distilled, deionized water (3 ml). The blank urine and serum samples each contained 100 ppm of each diuretic, were adsorbed on the C_{18} phase, washed with 1 ml of water, dried in a vacuum and eluted with 2 ml of water–methanol (10:90, v/v).

Preparation of methyl derivatives

After the SPE treatment the methanol extract was evaporated to dryness in a heating block under nitrogen. A 1.5-g amount of potassium carbonate, 200 μl of acetonitrile and 50 μl of methyl iodide were added to the dry residue. The resulting solution was incubated at 60°C for 60 min before the acetonitrile was evaporated under nitrogen and the residue was dissolved in 100 μl of methanol–toluene (4:96, v/v) mixture.

GC–MC procedure

GC–MS was carried out by injecting 1 μl of the derivatized solution. The temperature was programmed from 120 to 280°C at 15°C/min and from 280 to 310°C at 10°C/min. The temperatures of the injector, transfer line, source and quadrupole were 290, 290, 200 and 120°C, respectively. The carrier gas was helium (1.0 ml/min at 150°C). Injection was done by the solvent flush method (2 μl with the solvent plug) with methanol–toluene (4:96, v/v) as solvent. The full-scan mass spectra of the diuretics were scanned from 60 to 650 u at a rate of 1.09 ms/u.

RESULTS AND DISCUSSION

Diuretics are such a heterogeneous group of compounds that there is no pH within the operational range at which all of them carry a charge. Because of this, two consecutive runs at different pH values were required to screen all compounds. Compounds containing carboxylic (–COOH) and/or sulphonamide ($-SO_2NH_2$) groups (group A) were separated under basic conditions, at which all of them are anionic. Molecules containing primary, secondary or tertiary amine groups (group B) were separated at acidic pH as cations. All compounds are listed in Table I.

To find conditions giving a satisfactionary separation in reasonable time, we studied the effects of pH, ionic strength, organic modifier, temperature, running voltage and injection time on the separation.

The effect of pH was studied from pH 3.5 to 5.5 with acetate buffer, from 6.0 to 8.5 with phosphate buffer and from 9.0 to 11.2 with CAPS buffer. The pH was increased in steps of 0.5 units or less. The concentration of the buffer constituent was always 0.03 *M*. Best separations were achieved at pH 10.6 for group A and at pH 4.5 for group B. Caffeine, which is nearly always present in human urine and serum, was separated from the other compounds of interest. However, its detection at 215 and 220 nm was found to be difficult, especially at pH 4.5, when its presence only broadened the system peak. Its location was confirmed with detection at 260 nm.

The effect of concentration of the buffer was then studied at both pH values, from 0.01 to 0.08 *M*. The best separation at pH 10.6 was achieved with 0.06 *M* CAPS. All compounds from group A were separated in less than 20 min. Probenecid and ethacrynic acid were better resolved with 0.08 *M* CAPS, but the separation of caffeine, metyrapone, triamterene and amiloride from the system peak was worse than with 0.06 *M* CAPS. This last separation had to be maintained in order to achieve preliminary information about whether or not compounds from group B existed in the sample. The best separation at pH 4.5 (group B) was achieved with 0.07 *M* acetate. All three components were adequately separated in less than 6.5 min.

Organic modifier was added to the system in the hope of inhibiting the possible adsorption of the endogenous and exogenous compounds in urine and the residue of proteins in blood serum on the capillary wall. Morpholine was tested because it had been found to improve the separation and repeatability at pH 7.0–8.5. The pK_a value of morpholine is 8.5 [26] and over 99% of it is neutral at pH 10.6 so it cannot work as a masking agent for the silanol groups at such a high pH. Nevertheless, experiments were carried out at pH 10.6 to see if it might have some other effect. Addition of morpholine (0.01, 0.02 and 0.03 *M*) to 0.06 *M* CAPS buffer increased the time of analysis and resulted in overlapping peaks of chlorthalidone, ethacrynic acid and probenecid. At the highest concentration of morpholine the three compounds co-eluted as a single peak. However, the resolution of the group B compounds from the system peak was improved. Morpholine was not tested at pH 4.5 because we did not want to increase the analysis time excessively. Instead, the experiments were made with betaine. This zwitterionic compound is reported to be good at preventing adsorption on the capillary wall [27]. Addition of betaine to acetate buffer both improved the separation and gave better repeatability. This also yielded in faster time of analysis because the addition of betaine increased the time of analysis only a little, while it resulted in sharper peaks. Because of this we did not have to increase the concentration of acetate further to achieve these sharper peaks. This behaviour was best seen with

metyrapone. Also, the addition of betaine resulted in the absence of a negative peak prior to the caffeine peak. A combination of 0.07 *M* acetate and 0.5 *M* betaine was found to give a good and fast separation for the group B compounds.

Temperature is always a very important parameter in capillary electrophoresis because the viscosity (η) of the liquid is exponentially proportional to the absolute temperature (T), as can be seen from the equation [28]:

$$\eta = A \exp(E_\eta / RT)$$

where R is the universal gas coefficient, A is a constant and E_η is an effective activation energy for molecular displacement. The effect of temperature was studied from 20 to 30°C. Although the separation time was increased, the peaks were sharper at lower temperature. At pH 10.6 the elution order of trichlormethiazide and benzthiazide was reversed when the temperature was raised from 20 to 30°C. Some unknown components, probably generated by the breakdown of sample constituents when the sample was maintained at room temperature for few days while exposed to light, displayed similar behaviour. We do not yet fully understand this effect of temperature on elution order. Trichlormethiazide and benzthiazide co-eluted as one peak when the temperature was 28°C. The best of the investigated temperatures was 20°C. Lowering the temperature further was not studied because the operational temperature range of the P/ACE 2000 is ambient temperature ±5°C.

The running voltage was selected to yield fast times of analysis without causing a deterioration in the resolution. The effect of running voltage on the separation was studied from 10 to 30 kV, and 25 kV was found to be suitable for both runs.

The effect of injection time (hydrostatic injection with pressure) on the final peak width was studied from 1 to 30 s, with 5 s found to give the best result at pH 10.6 and 4.5. However, through sample stacking, much longer injection times could be exploited with only a slight loss of separation efficiency [29]. Without any off-line preconcentration the detection limit for hydrochlorothiazide at 220 nm was 0.1 ppm ($S/N = 3$) when the injection time was 30 s [29]. Very probably most of the other compounds can also be detected at the low femtomole range.

To summarize, suitable running conditions for group A were pH 10.6; CAPS 0.06 *M*; $T = 20$°C; voltage = 25 kV; hydrostatic injection for 5 s. The electropherograms for spiked urine and serum are reproduced in Fig. 1a and b. The samples were spiked with the diuretics so as to yield a final concentration of 10 ppm each. For group B, suitable running conditions were pH 4.5; acetate 0.07 *M*–betaine 0.5 *M*; $T = 20$°C; voltage = 25 kV; hydrostatic injection for 5 s. The electropherograms for spiked urine and serum at pH 4.5 are presented in Fig. 2. These samples were spiked only with group B compounds and caffeine (10 ppm) since it had been confirmed earlier that none of the compounds of group A elute before caffeine.

GC–MS IDENTIFICATION

The poor response of diuretics was attributed to the high boiling temperatures and decomposition of the compounds. Derivatization was carried out to facilitate the GC analysis. Three of the diuretics —amiloride, caffeine and metyrapone— did not react with methyl iodide. In addition, diphenylamine, the internal standard used in GC–MS studies, was not derivatized.

Total ion chromatograms for blood serum and urine are reproduced in Figs. 3 and 4, respectively. The extracted endogenous and exogenous compounds did not interfere with the identification of the methylated diuretics in either serum or urine samples owing to the good resolution of the components under optimized conditions.

The GC retention times increased as follows: diphenylamine < amiloride < caffeine < metyrapone < acetazolamide < probenecid < ethacrynic acid < dichlorphenamide < chlorothiazide < benzthiazide < clopamide < furosemide < chlorthalidone < bumetanide < hydrochlorothiazide < trichlormethiazide < triamterene < bendroflumethiazide. With the help of full-scan mass spectra a library was created for the derivatized diuretics. The main peaks in the total ion chromatograms of blank urine and

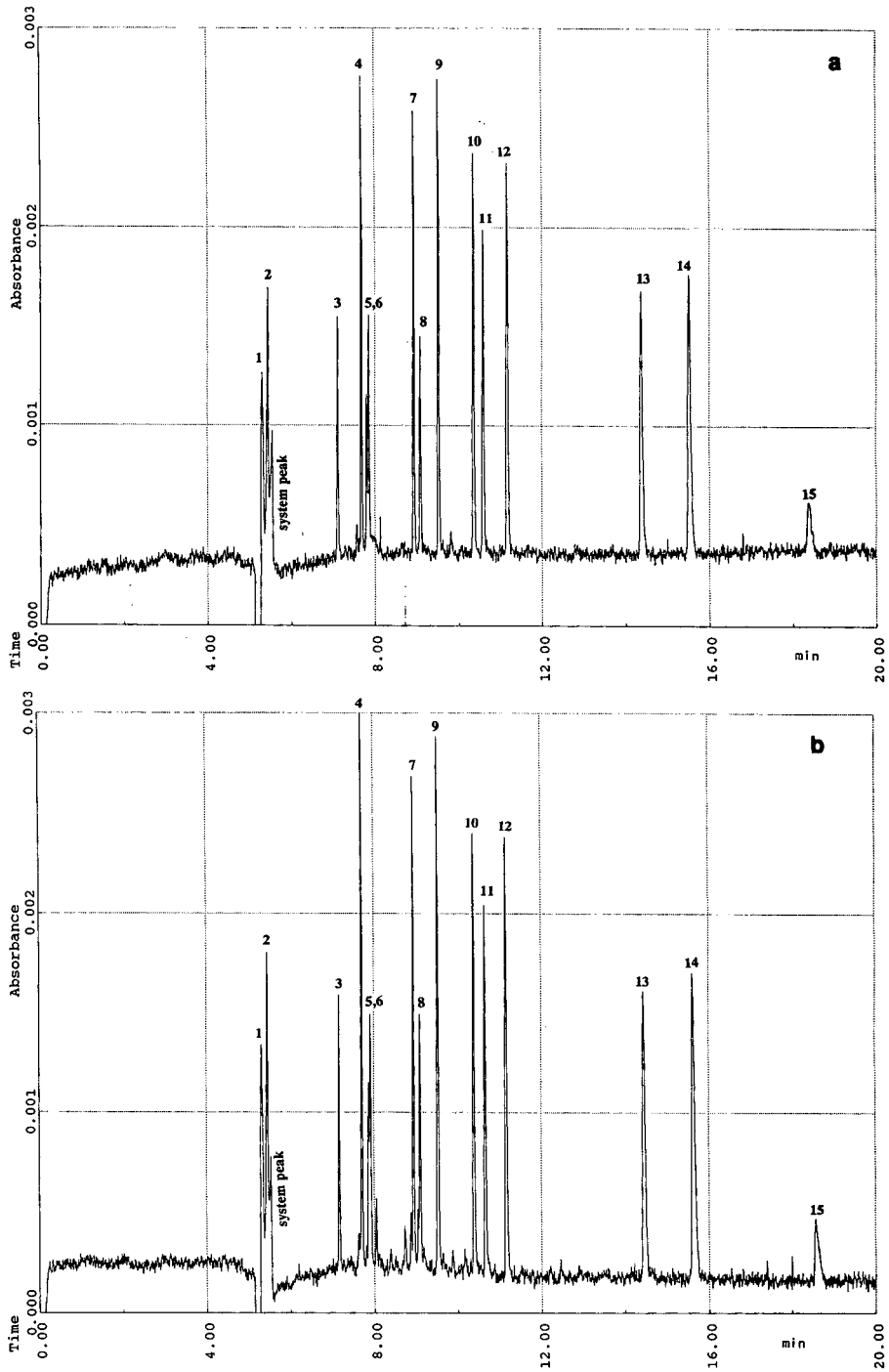

Fig. 1. Electropherograms of (a) spiked serum and (b) spiked urine. Running conditions were: uncoated silica capillary 67 cm (60 cm to the detector), 50 μm I.D., 360 μm O.D.; 220 nm; pH 10.6; CAPS 0.06 *M*; 20°C; 25 kV; hydrostatic injection by pressure 5 s. The spiked samples contained all of the diuretics (10 ppm each) (Table I). Elution order was: 1 = metyrapone and caffeine; 2 = triamterene and amiloride; 3 = clopamide; 4 = chlorthalidone; 5 = ethacrynic acid; 6 = probenecid; 7 = bumetadine; 8 = bendroflumethiazide; 9 = furosemide; 10 = trichlormethiazide; 11 = benzthiazide; 12 = hydrochlorothiazide; 13 = dichlorphenamide; 14 = chlorothiazide; and 15 = acetazolamide.

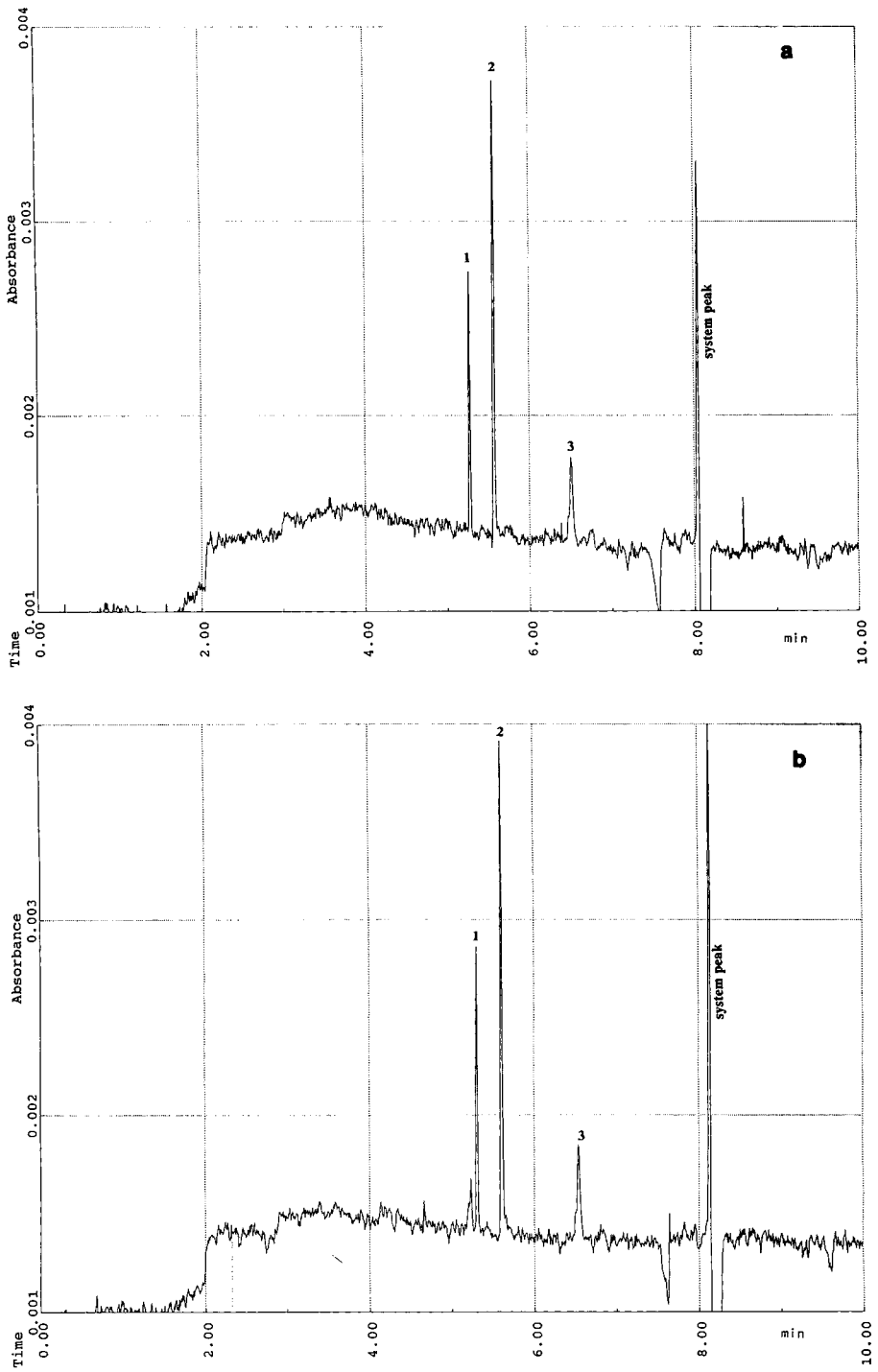

Fig. 2. Electropherograms of (a) spiked serum and (b) spiked urine. Running conditions were: uncoated silica capillary 67 cm (60 cm to the detector), 50 μm I.D., 360 μm O.D.; 215 nm; pH 4.5; acetate 0.07 *M*–betaine 0.5 *M*; 20°C; 25 kV; hydrostatic injection by pressure 5 s. The spiked samples contained the group B compounds and caffeine (10 ppm each) (Table I). The elution order was: 1 = amiloride; 2 = triamterene; 3 = metyrapone; and 4 = caffeine.

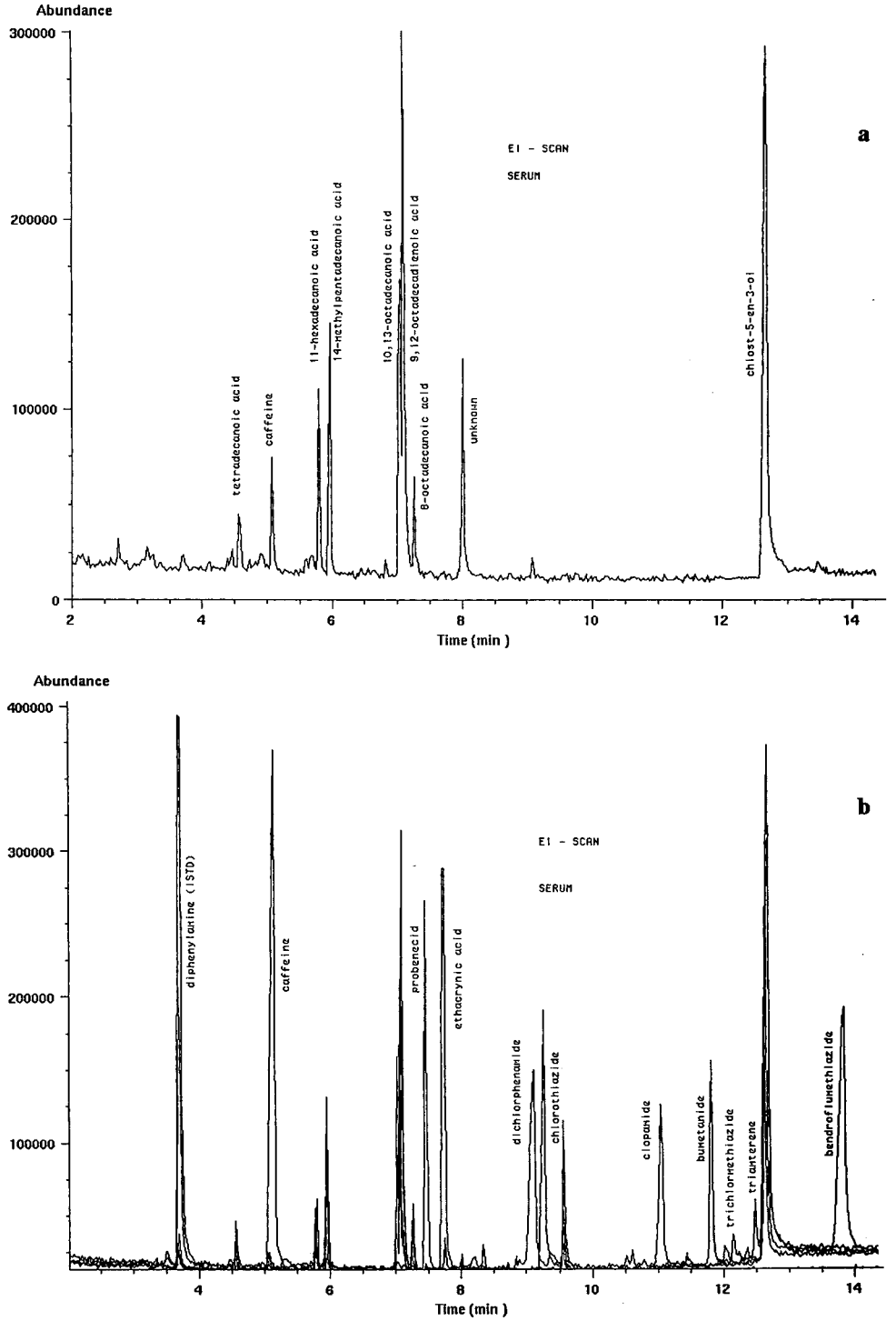

Fig. 3. Total ion chromatograms of (a) blank human serum and (b) spiked serum samples. Preparation by SPE. Running conditions are reported in the Experimental section.

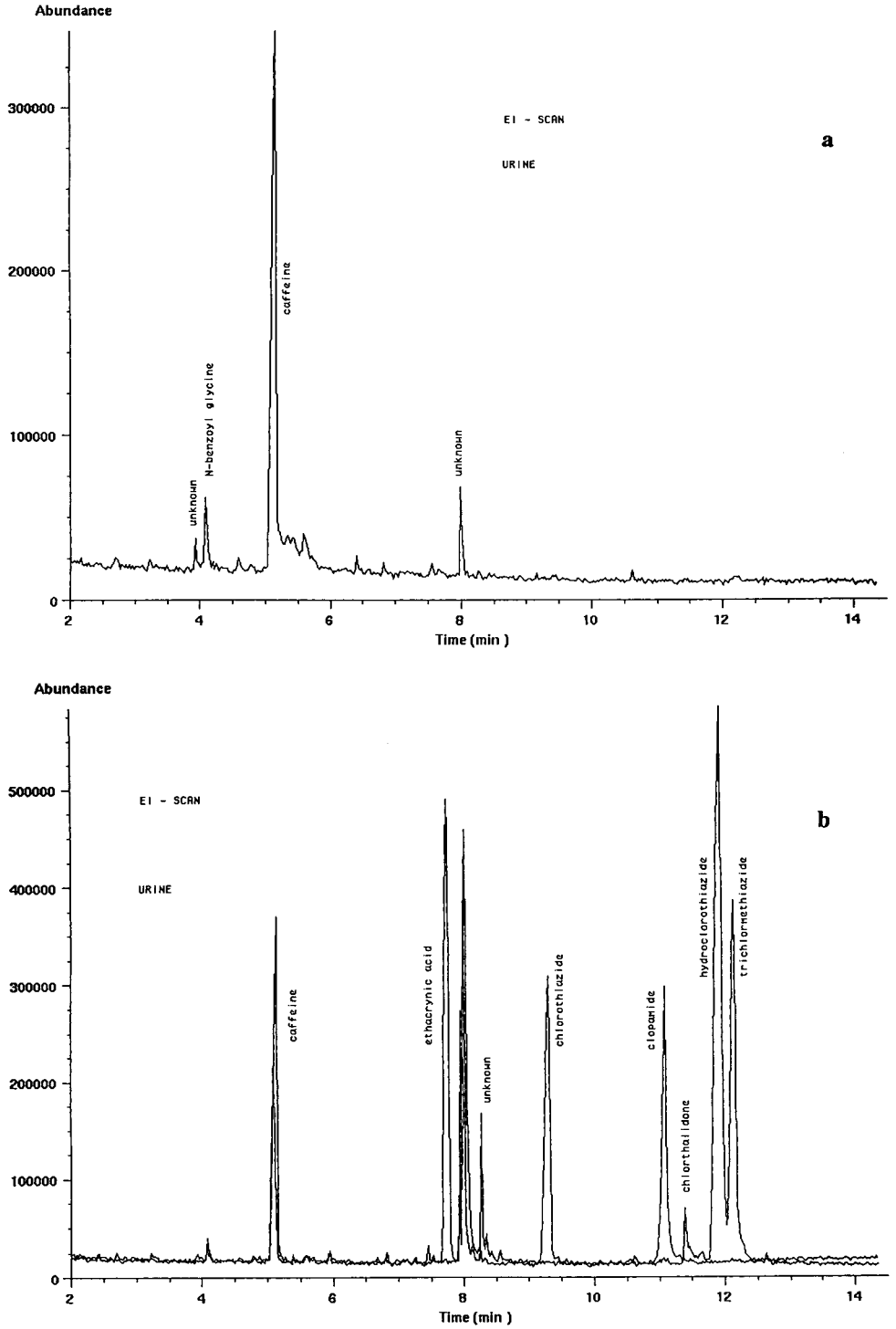

Fig. 4. Total ion chromatograms of (a) blank human urine containing caffeine and (b) spiked urine samples prepared by SPE. Running conditions are reported in the Experimental section.

serum were identified as methyl esters except cholest-5-en-3-ol, which was identified as the parent compound using the Wiley library. The relative retention times and determination limits are listed in Table I.

CONCLUSIONS

With our CZE method, urine and serum can be effectively screened for diuretics in less than 30 min. Although the heterogeneity of the diuretics made it impossible to separate them all in one run, all seventeen compounds that were investigated were well separated in two successive runs. CZE is a good alternative to HPLC since less sample is required and separation is as good or better and lower detection limits are achievable for most of the compounds.

Some problems may nevertheless arise when CZE is used to analyse biological fluids. If proteins are not completely removed from blood serum, they may destroy a good resolution of otherwise easily determined sample constituents by causing irregular electro-osmotic flow inside the capillary. Some of the endogenous compounds in urine behave in a similar way. In view of this it is advisable to design separation methods for pharmaceuticals that do not allow small amounts of disturbing compounds, such as proteins, left in the sample matrix to hinder the separation. Unfortunately, although the repeatability of the method may thus be improved, it may be at the cost of a slight decrease in separation efficiency. Matrix effects can be minimized by methods that have been reported for protein and peptide analyses. These methods can also be combined with each other, to solve even very difficult analytical problems.

Further research on the on-line concentration, electrolyte systems and the diffusion-related processes and their mathematical treatment is in progress.

REFERENCES

1 J.W. Jorgenson and K.D. Lukacs, *Anal. Chem.*, 53 (1981) 1298.
2 K.K. Unger, in *Porous Silica —Its Properties and Use as Support in Column Liquid Chromatography*, Elsevier, Amsterdam, 1977, p. 130.
3 V. Pretorius, B.J. Hopkins and J.D. Schinke, *J. Chromatogr.*, 99 (1974) 23.
4 H.H. Lauer and D. McManigill, *Anal. Chem.*, 58 (1986) 166.
5 P.D. Grossman, K.J. Wilson, G. Petrie and H.H. Lauer, *Anal. Biochem.*, 173 (1988) 265.
6 W. Kopaciewicz and F.E. Regnier, *Anal. Biochem.*, 126 (1982) 8.
7 J.S. Green and J.W. Jorgenson, *J. Chromatogr.*, 478 (1989) 63.
8 M.M. Bushey and J.W. Jorgenson, *J. Chromatogr.*, 480 (1989) 301.
9 R.S. Rush, A.S. Cohen and B.L. Karger, *Anal. Chem.*, 63 (1991) 1346.
10 F.S. Stover, B.L. Haymore and R.J. McBeath, *J. Chromatogr.*, 470 (1989) 241.
11 V. Rohlicek and Z. Deyl, *J. Chromatogr.*, 494 (1989) 87.
12 Å. Emmer, M. Jansson and J. Roeraade, *J. Chromatogr.*, 547 (1991) 544.
13 R.G. Nielsen and E.C. Rickard, *J. Chromatogr.*, 516 (1990) 99.
14 M. Zhu, D.L. Hansen, S. Burd and F. Gannon, *J. Chromatogr.*, 480 (1989) 311.
15 M.J. Gordon, K.-J. Lee, A.A. Arias and R.N. Zare, *Anal. Chem.*, 63 (1991) 69.
16 R.M. McCormick, *Anal. Chem.*, 60 (1988) 2322.
17 S.A. Svedberg, *Anal. Biochem.*, 185 (1990) 51.
18 G.J.M. Bruin, J.P. Chang, R.H. Kuhlman, K. Zegers, J.C. Kraak and H. Poppe, *J. Chromatogr.*, 471 (1989) 429.
19 G.J.M. Bruin, R. Huisden, J.C. Kraak and H. Poppe, *J. Chromatogr.*, 480 (1989) 339.
20 J.K. Towns and F.E. Regnier, *J. Chromatogr.*, 516 (1990) 69.
21 K.A. Cobb, V. Dolnik and M. Novotny, *Anal. Chem.*, 62 (1990) 2478.
22 S.A. Svedberg, *Eur. Pat. 0 354 984 A2* (1990).
23 S.F. Cooper, R. Massé and R. Dugal, *J. Chromatogr.*, 489 (1989) 65.
24 S.-J. Park, H.-S. Pyo, Y.-J. Kim, M.-S. Kim and J. Park, *J. Anal. Toxicol.*, 14 (1990) 84.
25 P. Campíns-Falco, R. Herraéz-Hernández and A. Sevillano-cabeza, *J. Liq. Chromatogr.*, 14 (1991) 3575.
26 M. Windholz (Editor), *The Merck Index*, Merck, Rahway, NJ, 10th ed., 1983.
27 M.M. Bushey and J.W. Jorgenson, *J. Chromatogr.*, 480 (1989) 301.
28 R.C. Reid, J.M. Prausnitz and T.K. Sherwood, *The Properties of Gases and Liquids*, McGraw-Hill, New York, 3rd ed., 1977.
29 J. Jumppanen, H. Sirén and M.-L. Riekkola, in preparation.

Journal of Chromatography A, 652 (1993) 451–457
Elsevier Science Publishers B.V., Amsterdam

Effect of buffer solution pH on the elution and separation of β-blockers by micellar electrokinetic capillary chromatography

Pekka Lukkari

Analytical Chemistry Division, Department of Chemistry, University of Helsinki, P.O. Box 6, 00014 University of Helsinki, Helsinki (Finland)

Heikki Vuorela

Pharmacognosy Division, Department of Pharmacy, University of Helsinki, P.O. Box 15, 00014 University of Helsinki, Helsinki (Finland)

Marja-Liisa Riekkola*

Analytical Chemistry Division, Department of Chemistry, University of Helsinki, P.O. Box 6, 00014 University of Helsinki, Helsinki (Finland)

ABSTRACT

Study was made of the effect of the pH of phosphate buffer (0.08 *M*) containing 15 m*M* cetyltrimethylammonium bromide as surfactant on the elution order of eleven widely used β-adrenergic blocking agents. In the pH range 6.0–7.8 the elution order of six of the β-blockers remained the same, while the order of five of them changed. Sotalol eluted as the sixth compound at pH 6.8 and migrated more quickly with increasing pH. Below pH 7.0 labetalol eluted before propranolol and above pH 7.0 afterwards. Likewise, the order of elution of atenolol and timolol was reversed at pH 7.0. The pH also affected the resolution; the best resolution values were achieved between pH 6.6 and 7.0 and between pH 7.4 and 7.8. The relationship between the structure of the β-blockers described by molecular and molecular connectivity indices and the elution order and separation of the β-blockers in micellar electrokinetic capillary chromatography at varying pH of the buffer solution is discussed.

INTRODUCTION

Adrenergic β-receptor blocking agents, commonly known as β-blockers, are a relatively new group of drugs. β-Blockers are widely used to treat angina pectoris, cardiac arrhythmias and hypertension [1]. They are also used as doping agents by athletes in order to reduce sympathetic activity in cases where high psychcological pressure may impair performance [2]. Propranolol, in 1965, was the first β-blocker to be formally approved for clinical use, and many more β-blockers have been introduced during the last 20 years. The structures of the studied β-blockers are shown in Fig. 1.

Micellar electrokinetic capillary chromatography (MECC) is a recently developed form of capillary zone electrophoresis (CZE) used for the analysis of electrically neutral species [3]. MECC utilizes as a pseudo-stationary phase a surfactant system at concentrations above the critical micelle concentration (CMC) of the surfactant. Separation of neutral particles is accomplished by partitioning of the solute between the pseudo and aqueous phases. Migration times of solutes in MECC systems are affected by the

* Corresponding author.

0021-9673/93/$06.00

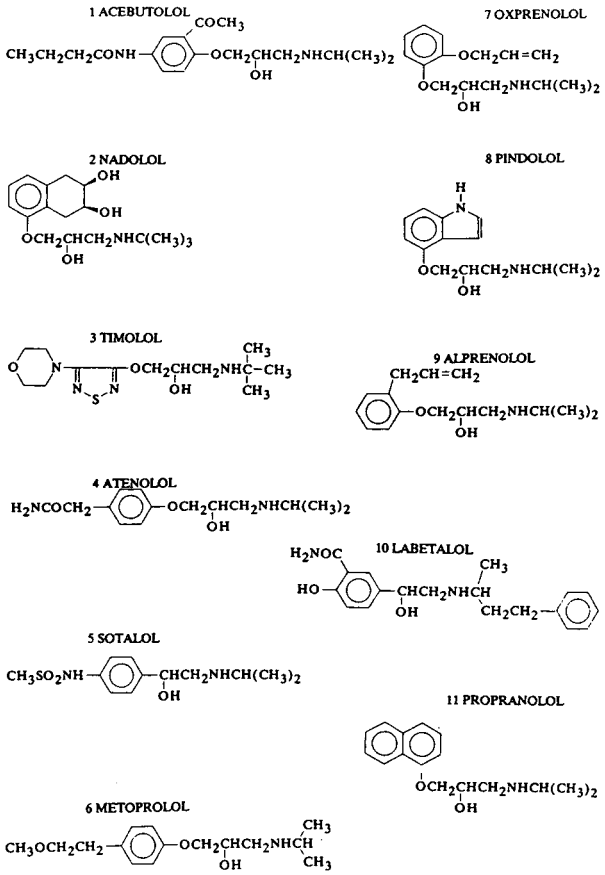

Fig. 1. Structures of the β-blockers.

electrophoretic mobility of the solute, the reactions between the solute molecules and the micelles and the magnitude of electro-osmotic flow (EOF) [4].

Proper selection of the pH of the buffer solution is often critical in MECC because the migration times of solutes, as well as the resolution and separation, tend to change rapidly with even small changes in the pH [5–7]. Moreover, EOF decreases inside the capillary at more acidic pH, owing to the decrease in the ζ-potential and the suppressed dissociation of SiOH groups of the capillary wall [8].

The addition of N-cetyl-N,N,N-trimethylammonium bromide (CTAB) to the buffer reverses the EOF towards the anodic end of the silica capillary by changing the negative charge of the wall to positive. With the decrease in the pH the molecular interactions between CTAB and the capillary wall increase. That is, the electroosmotic flow towards the anodic end of the capillary increases as the pH decreases, leading to changes in the migration times of solutes [9]. In addition, micellar partitioning of solutes around their pK_a values is very sensitive to the changes in pH [10].

In order to estimate quantitatively the relationship between the structure of analytes and their chromatographic behaviour, molecular connectivity indices, introduced by Randic [11] and developed further by Kier and Hall [12], have often been used [13]. These are numerical values that define and quantitatively describe the adjacency relationships in a molecular structure. When the nature of the atom is not taken into consideration, the index is referred to as the connectivity level index, χ, and when it is the index is described as the valence level, χ^v. Kier and Hall [12] extended the connectivity indices to a higher order, classifying the subgraphs into four types —path, cluster, path/cluster and chain— described by the subscripts p, c, pc and ch, respectively.

We studied the effect of the pH of phosphate buffer solution on the elution and separation of eleven β-blockers. The pH range was from 6.0 to 7.8. In addition, the effect of changing pH on the corrected migration times ($t'_r = t_r - t_0$) of the β-blockers and on the electroosmotic breakthrough time (t_0) was studied. Resolution (R) values for each peak pair were calculated by the half-width method. An aim of the study was also to explain the migration behaviour of the β-blockers with reference to the structure of solutes.

EXPERIMENTAL

MECC was performed in 580 × 0.050 mm I.D. fused-silica capillary tubes (Polymicro Technologies, White Associates, Pittsburgh, PA, USA); 500 mm was the effective length for separation. A Waters Quanta 4000 capillary electrophoresis system (Millipore Corporation, Waters Chromatography Division, Milford, MA, USA) was employed. Detection was at wavelength 214 nm. All experiments were carried out

at ambient temperature. Samples were injected hydrostatically for 15 s and the running voltage was −20 kV. The data (peak height) were collected with an HP 3392A integrator (Hewlett-Packard, Anondale, PA, USA).

The MolconnX 1.0 program (Lowell H. Hall, Hall Associates Consulting, Eastern Nazarene College, Quincy, MA, USA) was used to calculate the molecular and molecular connectivity indices of the β-blockers up to ten order indices. The Stat View II 1.03 (Abacus Concepts, Berkeley, CA, USA) and Systat 5.1 (Systat, Evanston, IL, USA) procedures were used as the statistics programs. All of these programs were run on a Macintosh IIsi computer.

The pH of the buffers was adjusted with a Jenway 3030 pH meter connected to a Jenway electrode (Jenway, Felsted, UK) containing 4 *M* potassium chloride in saturated silver chloride. Calibration of the electrode system was done with potassium hydrogenphthalate (0.05 *M*, pH 4.00) and sodium tetraborate (0.01 *M*, pH 9.81) solutions.

Materials

The reagents used in analysing the β-blockers were acebutolol hydrochloride, alprenolol hydrochloride, atenolol, labetalol hydrochloride, (±)-metoprolol (+)-tartrate, nadolol, oxprenolol hydrochloride, pindolol, (*S*)-(−)-propranolol hydrochloride, sotalol hydrochloride and timolol maleate, all from Sigma (St. Louis, MO, USA). Sodium dihydrogenphosphate monohydrate, disodium hydrogenphosphate dihydrate and CTAB were from Merck (Darmstadt, Germany). Other reagents used were of analytical grade. Distilled water was ion-exchanged through a Water-I system from Gelman Sciences (Ann Arbor, MI, USA). All the micellar buffer solutions were filtered through 0.45-μm membrane filters (Millipore, Molsheim, France).

The buffers were prepared from 0.08 *M* sodium dihydrogenphosphate and 0.08 *M* disodium hydrogenphosphate solutions. Both solutions contained 15 m*M* CTAB. The accurate pH of buffer solutions was increased from 6.0 to 7.8 in steps of 0.2 or 0.4 units, with degassing after each step.

MECC procedure

Between injections the capillary was purged for 2 min with the buffer solution before each injection.

RESULTS AND DISCUSSION

We confirmed the repeatability of migration of the β-blockers by measuring t'_r and t_0 values (measured with methanol) as six replicates at pH 6.2, 6.6, 7.0, 7.4 and 7.8. The relative standard derivations (R.S.D.) of t'_r of the β-blockers varied from 0.3% to 3.4% ($n = 6$), and the R.S.D.% of the t_0 values from 0% to 1.5% ($n = 6$). The R.S.D. of the R values varied from 0.6 to 10.1% ($n = 6$). The measurements can be regarded as quite reliable. However, day-to-day repeatability of t'_r values of β-blockers described as R.S.D.% varied from 33.4% to 42.6% ($n = 6$) and can be considered to be low. One of the reasons could be the lack of temperature control in our apparatus. Therefore the changes in migration of β-blockers caused by changes in pH were measured on the same day.

The effect of pH change on migration was studied by increasing pH from 6.0 to 7.8. The elution order of the eleven β-blockers changed with pH, as shown in Fig. 2 (for numbering of the compounds, see Fig. 1). At pH 6.0 sotalol (**5**) migrated as the sixth solute. With increasing pH it migrated more quickly until above pH 7.0 it migrated as the first compound. Propranolol (**11**) migrated after labetalol (**10**) below pH 7.0 and before it above pH 7.0. Likewise, the elution order of atenolol (**4**) and timolol (**3**) changed at pH 7.0. If the R value between two β-blockers was less than 0.45, the compounds were considered to elute together.

Increased pH caused some changes in the t'_r of the β-blockers (Fig. 3). The migration time of sotalol was significantly reduced, while the migration times of alprenolol, labetalol and propranolol were increased with the increase in pH. Sotalol migrated 1.6 times faster at the basic end of the pH range, and the other three compounds migrated 1.4, 1.9 and 1.6 times slower under basic conditions. The t_r' of the other β-blockers was affected only very little by the change in pH. The migration window (differ-

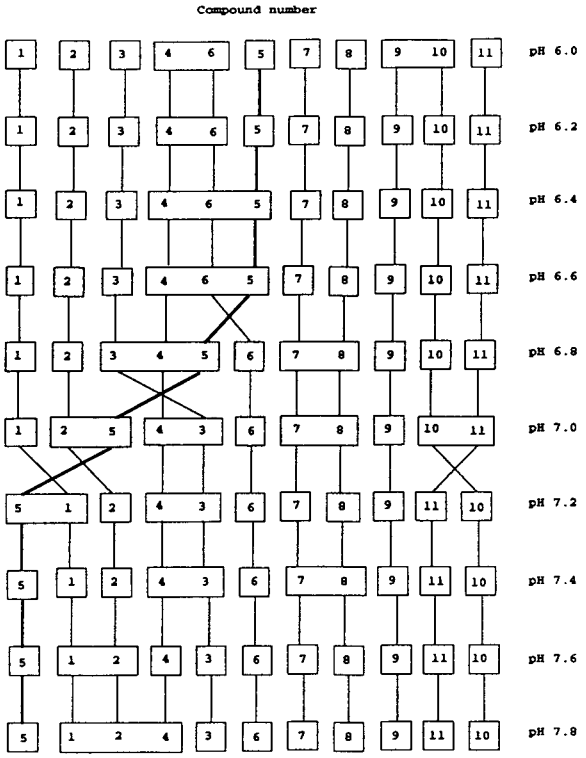

Fig. 2. Elution order of the β-blockers at ten different pH values of the phosphate buffer (0.08 *M*) solution containing 15 m*M* CTAB (for compound numbers, see Fig. 1).

ence between the first and last compound) was three times as wide at pH 7.8 as at pH 6.2 (Fig. 3). Even small variations in pH can cause unexpected changes in migration times of solutes and, especially in the analysis of complex mixtures, changes in migration order relative to other analytes.

The pH of the buffer solution also strongly affected the resolution of the β-blockers (Fig. 4). The major cause of the change in resolution was the change in migration behaviour of sotalol. As sotalol migrated more quickly it eluted, in turns, together with metoprolol, atenolol, timolol, nadolol and acebutolol. At pH 7.0 labetalol and propranolol eluted together, but otherwise separately. Oxprenolol and pindolol eluted together in the middle of the pH range. Likewise, atenolol and timolol eluted together at pH 7.0 and pH 7.4, and acebutolol and nadolol were not separated from each other at the highest pH values. The best resolution between the eleven β-blockers appeared to be between pH 6.6 and pH 7.0 as well as between pH 7.4 and pH 7.8. The migration window was wider at the basic end of the pH range but the total analysis time was much shorter at lower pH values. The t'_r for the last-migrating β-blocker was 10.4 min and 12.9 min at pH 7.4–7.8, whereas at pH 6.6 and pH 7.0 the times were 8.4 min and 8.9 min, respectively. Further optimization of analytical conditions is therefore more attractive at lower pH.

In order to explain the exceptional migration behaviour of some analytes, the structure was related to migration by the molecular and molecular connectivity indices. The effect of the pH of the buffer solution on the migration was also tested by factor analysis (Table I). Factor 1 can be related to pH, *i.e.* it is a pH-dependent factor, and factor 2 can be regarded as the non-pH-dependent factor. The results show that the effect of the pH of the buffer solution on the migration behaviour was significant only for sotalol, alprenolol, labetalol and propranolol.

To diminish the intercorrelations later in regressions, 183 molecular structure descriptors were calculated by the MolconnX program and the indices were divided into nine groups by cluster analysis using one Pearson-correlated coefficient single-linkage method (nearest neighbour). From nine groups, 1–3 best indices were selected for the multiple variable and stepwise regression model. The indices were tested against the migration changes of the studied β-blockers during the pH change. These migration changes were described as migration differences between pH 6.6 and pH 6.2 as well as between pH 7.8 and pH 6.2: $\Delta t'_{r(pH\ 6.6-6.2)}$ and $\Delta t'_{r(pH\ 7.8-6.2)}$, respectively. These regression analyses showed that three indices, SI3 (electrotopological atom state index for atom number 3), K^3 (the third-order kappa index) and KA^3 (the third-order kappa-alpha index), are related to substitution (SI^3) and shape of the molecule (K^3, KA^3). Fig. 5 shows the atom numbering of the skeleton common to all the studied β-blockers which were used in the calculation of SI indices. The indices can describe relatively well the migration changes due to pH (eqn. 1):

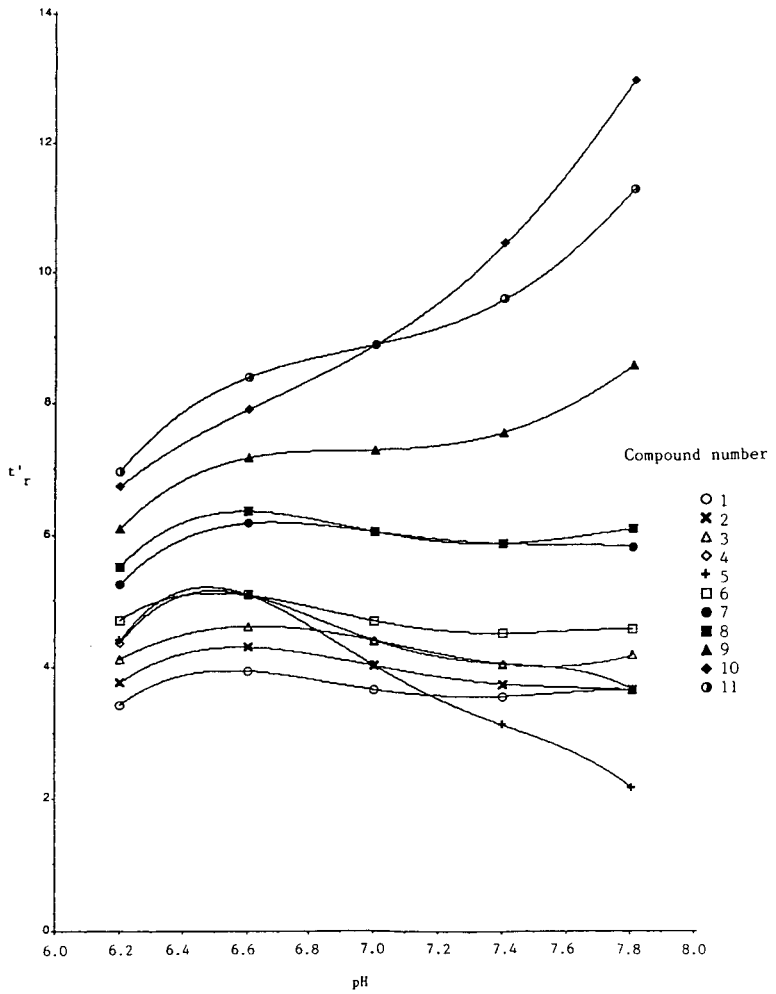

Fig. 3. Migration behaviour of eleven β-blockers at five different pH values of the buffer solution (buffer solutions and compound numbers as in Fig. 2).

$$\Delta t'_{r(pH\ 6.6-6.2)} = 2.62\ SI3 + 0.13\ K^3 - 0.21\ KA^3 - 7.44\ (r = 0.80, n = 11) \quad (1a)$$

$$\Delta t'_{r(pH\ 7.8-6.2)} = 7.75\ SI3 + 1.11\ K^3 - 1.26\ KA^3 - 26.35\ (r = 0.90, n = 11) \quad (1b)$$

As eqn. 1a shows, the data do not correlate very well, because the pH change from 6.2 to 6.6 was too small. However, with the larger change in pH (from 6.2 to 7.8) the correlation between the migration data and molecular structure of the β-blockers can be considered satisfactory (eqn. 1b). The SI3 index of the nitrogen atom (Fig. 5) as well as the K^3 and KA^3 indices, which describe the shape of molecule, were found to be significant when the effect of the pH of the buffer solution on the elution of β-blockers was studied. Also, the deductions made about the structures of β-blockers clearly support the conclusion based on these calculations.

The β-blockers can be divided into two groups according to their migration behaviour: I, acebutolol, atenolol, metoprolol, oxprenolol, alprenolol and propranolol; and II, nadolol, timolol, sotalol, pindolol and labetalol. The

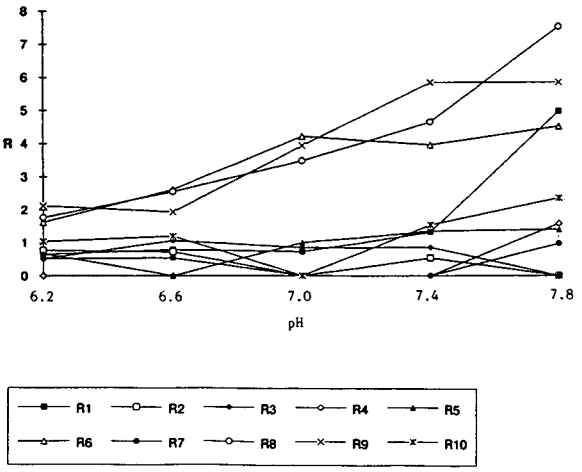

Fig. 4. Plotted resolution values for the β-blockers at different pH values. For the identification of R values, see the elution order (Fig. 2; for analysis conditions, see the Experimental section).

compounds always eluted in the same order within the groups in the studied pH range. In group I *p*-substituted β-blockers eluted before *o*-substituted compounds. Also, the molecules with smaller and less polar substituents eluted more slowly than the molecules with larger and more polar substituents because of their more

TABLE I

FACTOR ANALYSIS OF THE pH OF THE BUFFER SOLUTION ON THE MIGRATION BEHAVIOUR OF ELEVEN β-BLOCKERS

Factor 1 is the pH-dependent factor and factor 2 is the non-pH-dependent factor

Variable	Factor 1	Factor 2
pH	0.9942	−0.0162
Acebutolol	0.0717	0.9857
Nadolol	−0.4737	0.8731
Timolol	−0.2846	0.9323
Atenolol	−0.736	0.6656
Sotalol	−0.8981	0.435
Metoprolol	−0.5846	0.7615
Oxprenolol	0.3284	0.8813
Pindolol	0.3378	0.9402
Alprenolol	0.9689	0.2353
Labetalol	0.9939	−0.057
Propranolol	0.9928	0.1055

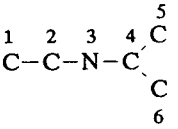

Fig. 5. The atom numbering of the skeleton common to all the studied β-blockers.

intense interactions with the micelles. In group II nadolol and timolol have the same propanol amine side chain and nadolol eluted before timolol because in timolol the ring structures probably interact more intensely with the micelles. For the same reason pindolol elutes before labetalol. The exceptional behaviour of sotalol is also due to its structure (Fig. 1): the sulphonamide group obtains a negative charge under neutral and basic conditions, causing sotalol to migrate more quickly towards the positive electrode (detector end of the capillary). Because the pK_a values of β-blockers are between 9.2 and 9.8 they are ionized at the studied pH range, and thus further ionization of β-blockers should cause only minor if any changes in their electrophoretic mobilities. The increased migration times of alprenolol, labetalol and propranolol are probably due to the lower EOF, which gives them more time to react with the slowly eluted micelles.

CONCLUSIONS

The pH of the buffer solution needs to be carefully controlled and optimized when ionic compounds are analysed by MECC because at different pH values the compounds elute in dissimilar order and at different rates. The migration window can be much wider at the basic end of the pH range. Likewise, pH greatly affects the resolution of the compounds. The migration behaviour of compounds can be related to the structure.

REFERENCES

1 R.G. Shanks, *Trends Pharm. Sci.*, 5 (1984) 451.
2 J. Park, S. Park, D. Lho, H.P. Choo, B. Chung, C. Yoon, H. Min and M.J. Choi, *J. Anal. Toxicol*, 14 (1990) 66.

3 S. Terabe, K. Otsuka, K. Ichikava, A. Tsuchiya and T. Ando, *Anal. Chem.*, 56 (1984) 111.
4 P. Lukkari, J. Jumppanen, K. Jinno, H. Elo and M.-L. Riekkola, *J. Pharm. Biomed. Anal.*, 10 (1992) 561.
5 E. Kenndler and W. Frield, *J. Chromatogr.*, 608 (1992) 161.
6 M.G. Khaledi, S.C. Smith and J.K. Strasters, *Anal. Chem.*, 63 (1991) 1820.
7 J. Vindevogel and P. Sandra, *J. High Resolut. Chromatogr.*, 14 (1991) 795.
8 K. Otsuka and S. Terabe, *J. Microcolumn Sep.*, 1 (1989) 150.
9 H.-T. Chang and E.S. Yeung, *J. Chromatogr.*, 608 (1992) 65.
10 K.-J. Lee, G.S. Heo, N.J. Kim and D.-C. Moon, *J. Chromatogr.*, 577 (1992) 135.
11 M. Randic, *J. Am. Chem. Soc.*, 97 (1975) 6609.
12 L.B. Kier and L.H. Hall, *Molecular Connectivity in Chemistry and Drug Research*, Academic Press, London, 1976, p. 40.
13 P. Lehtonen, *Academic Dissertation*, University of Helsinki, Helsinki, 1987.

Journal of Chromatography A, 652 (1993) 459–463
Elsevier Science Publishers B.V., Amsterdam

CHROM. 25 100

Validation of a capillary electrophoresis method for the determination of a quinolone antibiotic and its related impurities

K.D. Altria* and Y.L. Chanter

Pharmaceutical Analysis, Glaxo Group Research, Park Road, Ware, Herts. SG12 0DP (UK)

ABSTRACT

Free solution capillary electrophoresis (FSCE) has been employed for the novel determination of a quinolone antibiotic which has limited solubility between pH values of 2 and 11. This limited pH range gave problems with HPLC methods that were attempted for quantitative analysis. The fused-silica capillaries utilised in CE are able to withstand pH extremes, therefore CE was used in preference to HPLC for determining both drug content and levels of related impurities present in drug substance.

A CE method operating at pH 1.5 was shown to be suitable for this analysis. The sample was prepared at 0.5 mg/ml in 0.1 *M* NaOH and injected utilising pH mediated sample stacking. This represents the first report describing the analytical performance of this stacking procedure.

Although several reports have shown CE to be suitable for pharmaceutical analysis this report is the first to provide validation details for an impurity determination method. Acceptable levels of precision, linearity, limits of detection and quantitation were achieved. Capillary electrophoresis of basic drug compounds at low pH offers a useful alternative and complement to HPLC.

INTRODUCTION

Renewed interest in electrophoresis was generated by the work of Jorgenson and Lukacs [1] in the early 1980's concerning capillary electrophoresis. Subsequently CE has been shown to be of use for the separation of a range of drug classes including antibiotics [2–5], non-steroidal anti-inflammatories [6], steroids [7] and analgesics [8]. Specific applications have included the determination drug content in formulations [9], clinical analysis [10], determination of related impurities content [11,12], and chiral separations [13,14]. Performance details have been described for the quantitative determination of the drug content in pharmaceutical formulations [9].

When analysing basic compounds by HPLC problems can occur [15] regarding peak tailing and the limited pH operating range of many columns. CE is well suited to this analysis as methods can be operated at pH extremes.

New drug classes are currently being developed to supplement the "traditional" antibiotics as many organisms have now become resistant. Such a group are the quinolones [16] of which Ciprofloxacin [17] is the most active. The structure of Ciprofloxacin is given in Fig. 1. To date CE has not been applied to this class of compounds.

A quinolone antibiotic with limited solubility between pH 2–11 presented considerable problems when analysed by HPLC. It may have been possible, after extensive method development, to have developed a suitable HPLC method. However, in this instance, suitable CE operating conditions were quickly developed and then validated for the separation and quantitation of this compound and its related impurities. Method validation including measures of precision,

* Corresponding author.

0021-9673/93/$06.00

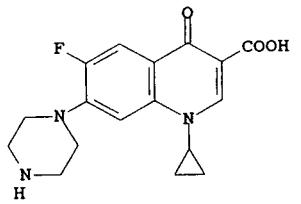

Fig. 1. Structure of Ciprofloxacin.

linearity, the determination of limits for both quantitation and detection. The results obtained are comparable to those expected from a standard HPLC method. Reliable HPLC data could not be obtained for comparison with that generated by CE.

EXPERIMENTAL

Chemicals were obtained from Aldrich (Poole, UK), and water was obtained from a Millipore Milli-Q system (Watford, UK).

The work was performed on an ABI 270HT CE instrument (San Jose, CA, USA) which was connected to a Hewlett-Packard (Bracknell, UK) data collection system. The fused-silica capillaries used in this study were purchased from Metal Composites (Hallow, UK).

The separation conditions employed are as follows: Pre-separation rinse 1:1 min with 0.1 *M* NaOH; pre-separation rinse 2:1 min with electrolyte; sampling: 10 s vacuum; separation: +20 kV applied for 20 min, UV at 272 nm, 30°C, 72 cm × 50 μm fused-silica capillary; electrolyte: 50 m*M* borax pH adjusted to 1.5 with concentrated H_3PO_4; sample concentration: (0.5 mg/ml) dissolved in 0.1 *M* NaOH.

RESULTS AND DISCUSSION

Method development

The principal method development options in CE [12,18] are variations in pH and the use of micellar based electrolytes. In this instance, given the pH solubility range of the solute, the choice was limited and the electrolyte ultimately chosen was 50 m*M* borax pH adjusted to 1.5 with concentrated orthophosphoric acid. The compound was soluble in this electrolyte. A typical separation achieved is given in Fig. 2. Minimum peak tailing was observed.

Low UV detection wavelengths (sub 220 nm) are often employed in CE [11,12] to compensate for the relative insensitivity of CE when directly compared to HPLC. However, in this example, the strong UV absorbance coefficient of the test solute at 272 nm enabled adequate response to be obtained at this wavelength.

Sample dissolving solvent. The choice of dissolving solvent in CE is critical as an incorrect choice can result in a severe loss of separation efficiency and resolution. Sample solutions containing either high ionic strength [19] or containing high percentage levels of organic solvents [20] cause particular problems. Given these limitations and the solubility problems encountered with this compound, the dissolving solvent options were either an acid or base. The latter option was selected for the reasons given below.

The ionic strength of the dissolving solvent is usually chosen to be lower than the electrolyte employed to achieve an on-column preconcentration [21] of sample within the capillary. This process has been termed "stacking" [21] and can improve method performance in terms of separation efficiency, resolution and sensitivity.

An alternative stacking procedure has been

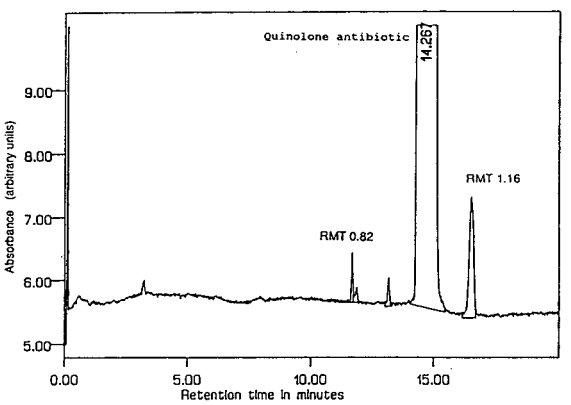

Fig. 2. Typical electropherogram. Separation conditions: 10 s vacuum sampling, +20 kV applied for 20 min, UV at 272 nm, 30°C, 72 cm × 50 μm fused-silica capillary, electrolyte: 50 m*M* borax pH adjusted to 1.5 with concentrated H_3PO_4, sample concentration: (0.5 mg/ml) dissolved in 0.1 *M* NaOH.

described which has been termed "pH-mediated sample introduction" [22]. In this procedure the pH of the dissolving solvent is selected such that the sample is present as an anion. A separation electrolyte is chosen in which the compound would be protonated. When a sample is introduced into the capillary and the separation voltage is applied the sample anions migrate to the back of the sample zone, become protonated, and are focussed at the boundary of the sample and electrolyte. The analytical performance of this procedure has not previously been studied.

It was appropriate in this instance to utilise pH-mediated stacking by employing a low-pH electrolyte for the separation, and by dissolving the sample in an alkaline solution.

METHOD VALIDATION

The validation undertaken for the CE method follows the general guidelines suggested for a HPLC method [23].

Linearity

It is usual practice to perform linearity determinations over a wide range of sample concentrations to fully assess the linear dynamic range of the detection system. For main peak assay purposes, linearity of the CE method was demonstrated (correlation coefficient = 0.9990) over the range 1–150% of the nominal target concentration (0.5 mg/ml). In a separate exercise the linearity of a narrower concentration range (20–150% of nominal) was assessed and a correlation coefficient of 0.9997 was obtained. Intercept values were less than 1% of the nominal concentration.

Precision of peak area and migration time

A single sample solution was injected 10 times and an acceptable R.S.D. of 0.6% was obtained for the main peak. The R.S.D. on the migration time of the main peak was 0.4%.

Reports [12,24,25] concerning the precision of peak area employing automated CE instruments indicate a precision level of 0.5–2% R.S.D. can be achieved. By employing an internal standard, variability can be reduced still further with typical R.S.D.s of below 1% being obtained [26].

Limit of quantitation (LOQ)

This figure can be defined [27] as the lowest concentration of sample that can be reproducibly quantified above the baseline signal. An R.S.D. of 4.9% was obtained for 10 injections of a solution equivalent to 0.3% of the nominal concentration. This is considered acceptable performance.

Limit of detection (LOD)

This figure may be defined as the lowest concentration of sample that can be clearly detected above the baseline signal. A solution equivalent to 0.1% of the nominal concentration gave a reproducible peak (Fig. 3) with a signal-to-noise ratio greater than 3. Swartz has reported [12] similar detection limits for salicylamide-related impurities by CE. This LOD represents a molar sensitivity of $1.6 \cdot 10^{-6}$ M which is comparable to that reported for other pharmaceuticals as determined by CE [5,9].

Levels as low as 0.02% (w/w) of selected dimeric impurities present in salbutamol drug substance have been reported using low UV wavelength detection and external standards of the impurities [11].

Consistency of impurity levels with sample concentration

A further part of method validation is to demonstrate that the impurity profile and con-

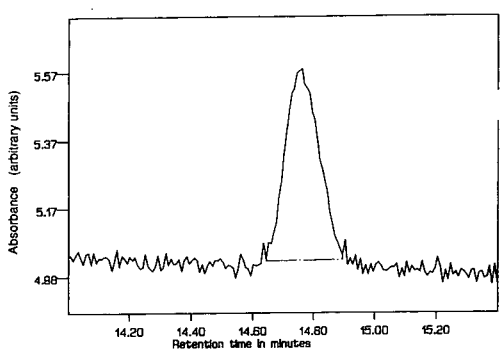

Fig. 3. Electropherogram of a solution equivalent to 0.1% (w/w) of the nominal sample concentration. Separation conditions: as given in Fig. 2.

TABLE I

CONSISTENCY OF IMPURITY PROFILE WITH SAMPLE DILUTION

	Concentration (% nominal)		
	100	75	50
Number of impurities	6	4	4
Total % impurities[a]	0.68	0.64	0.64
Greatest impurity (%)	0.45	0.47	0.46
RMT greatest impurity[b]	1.16	1.16	1.16
2nd greatest impurity (%)	0.11	0.10	0.11
RMT 2nd greatest impurity	0.82	0.82	0.82

[a] % = % total corrected area.
[b] RMT = Relative migration time.

tent do not vary with sample concentration. A single sample was diluted and aliquots of each solution were injected in duplicate and the impurity levels were determined (Table I). The peak area of each peak was divided by its migration time to compensate for the difference residence times of the peaks in the detector [28]. The corrected areas were used to calculate the impurity levels as %area/area. The need to normalise peak areas when quoted impurity levels has been reported [29]. Failure to normalise peak areas will result in incorrect %area/area data being reported [29].

The results (Table I) indicate that the impurity levels are consistent with dilution of the sample down to 50% of the nominal sample concentration. At the higher sample concentration two additional impurities, present at low levels (<0.05% area/area), could be detected.

Freedom from interference

A solution of the dissolving solvent (0.1 *M* NaOH) was injected onto the system, in duplicate, and no interfering peaks were observed.

CONCLUSIONS

A low-pH CE method has been validated for the determination of drug related impurities in a quinolone antibiotic drug substance. Analysis of this compound had presented a formidable challenge to HPLC due to the limited pH solubility range of the analyte. Therefore, in this instance, CE was used preferentially over HPLC due to the wide range of pH extremes that can be employed in CE.

To optimise method performance the sample dissolving solvent was selected to utilise pH mediated stacking of the sample. The performance of the method employing this sampling procedure indicates that this is a successful approach.

Method validation showed good levels of performance in terms of precision, linearity, LOD and LOQ. No interfering peaks were obtained from the dissolving solvent.

Capillary electrophoresis of basic drug compounds at low pH offers a useful alternative and complement to HPLC and has been demonstrated to give similar levels of method performance.

REFERENCES

1 J.W. Jorgenson and K.D. Lukacs, *Science*, 222 (1983) 266.
2 A.M. Hoyt and M.J. Sepaniak, *Anal. Lett.*, (1989) 861.
3 H. Nishi, N. Tsumagari, T. Kakimoto and S. Terabe, *J. Chromatogr.*, 477 (1989) 259.
4 H. Nishi, N. Tsumagari and S. Terabe, *Anal. Chem.*, 61 (1989) 2434.
5 K.D. Altria and M.M. Rogan, *J. Pharm. Biomed. Anal.*, 8 (1990) 1005.
6 H. Nishi, T. Fukuyama, M. Matsuo and S. Terabe, *J. Chromatogr.*, 498 (1990) 313.
7 H. Nishi, T. Fukuyama, M. Matsuo and S. Terabe, *J. Chromatogr.*, 513 (1990) 279.
8 S. Fujiwara and S. Honda, *Anal. Chem.*, 59 (1987) 2773.
9 M.T. Ackermans, J.L. Beckers, F.M. Everaerts and I.G.J.A. Seelen, *J. Chromatogr.*, 590 (1992) 341.
10 P. Meier and W. Thormann, *J. Chromatogr.*, 559 (1991) 505.
11 K.D. Altria, *J. Chromatogr.*, 634 (1993) 323.
12 M. Swartz, *J. Liq. Chromatogr.*, 14 (1991) 923.
13 M.J. Sepaniak, R.O. Cole and B.K. Clark, *J. Liq. Chromatogr.*, 15 (1992) 1023.
14 K.D. Altria, D.M. Goodall and M.M. Rogan, *Chromatographia*, 34 (1992) 19.
15 R.J.M. Vervoort, F.A. Maris and H. Hindriks, *J. Chromatogr.*, 623 (1992) 207.
16 K. Grohe, *Chem. Britain*, Jan. (1992) 34.
17 H.J. Zeiler and K. Grohe, *J. Clin. Microbiol.*, 2 (1984) 339.
18 G.M. McLaughlin, J.A. Nolan, J.L. Lindahl, J.A. Morrison and T.J. Bronzert, *J. Liq. Chromatogr.*, 15 (1992) 961.

19 F.E.P. Mikkers, F.M. Everaerts and Ph.P.E.M. Verheggen, *J. Chromatogr.*, 169 (1979) 11.
20 M.T. Ackermans, F.M. Everaerts and J.L. Beckers, *J. Chromatogr.*, 585 (1991) 123.
21 S.E. Moring, J.C. Colburn, P.D. Grossman and H.H. Lauer, *LC–GC Int.*, 3 (1990) 46.
22 R. Aebersold and H.D. Morrison, *J. Chromatogr.*, 516 (1990) 89.
23 E. Debresis, *Pharm. Tech.*, Sept. (1982) 120.
24 P.C. Rahn, *Am. Biotechnol. Lab.*, (1990) 22.
25 H.E. Schwartz, M. Melera and R.G. Brownlee, *J. Chromatogr.*, 480 (1989) 129.
26 E.V. Dose and G.A. Guiochon, *Anal. Chem.*, 63 (1991) 1154.
27 P.A.D. Edwardson, G. Bhaskar and J.E. Fairbrother, *J. Pharm. Biomed. Analysis*, 8 (1990) 929.
28 M.W.F. Nielen, *J. Chromatogr.*, 588 (1991) 321.
29 K.D. Altria, *Chromatographia*, 35 (1993) 177.

Journal of Chromatography A, 652 (1993) 465–469
Elsevier Science Publishers B.V., Amsterdam

CHROM. 25 084

Sample matrix effects in capillary electrophoresis

I. Basic considerations

L. Liliana Garcia and Z.K. Shihabi*

Department of Pathology, Bowman Gray School of Medicine, Wake Forest University, Winston-Salem, NC 27157 (USA)

ABSTRACT

Serum samples contain high concentrations of proteins and ions which interfere in the analysis of small molecules such as theophylline. These effects are minimized by employing an electrophoresis buffer with high ionic strength. Although such buffers slow the speed of the analysis, they minimize the effects of proteins and ions, improve the separation and enable a larger volume of sample to be introduced into the capillary leading to enhanced signals. Therefore, serum samples can be diluted in weak buffers and analyzed directly rendering capillary zone electrophoresis an attractive technique in the clinical laboratories.

INTRODUCTION

The sample represents a small portion of the total capillary volume, yet it plays an important role in the overall separation and plate number. This is due to the nature of current conductance and the tendency of proteins to adsorb to the capillary walls. In general, plate number and peak height can be improved by using lower conducting conditions in the sample. This technique is known as stacking [1,2].

Analysis of serum or urine samples for endogenous substances and drugs presents special problems because of the high and variable content of proteins and ions. Although solvent extraction eliminates such effects, it is not suited for routine analysis in the clinical laboratories. To overcome these problems in high-performance liquid chromatography (HPLC), direct injection of diluted serum and acetonitrile deproteinization are quite commonly used for sample preparation [3–5]. These same techniques have been applied to capillary zone electrophoresis (CZE). It has been shown previously that both acetonitrile deproteinization and direct serum introduction are feasible as demonstrated by the analysis of iohexol by CZE [6]. Using micellar electrokinetic capillary electrophoresis, Thormann and co-workers [7,8] have shown that drug analysis by direct serum injection is also possible. The effect of proteins and different ions on the analysis of endogenous compounds and drugs in serum by CZE have not been extensively examined, mainly because the technique is relatively new. In this study, theophylline, a drug commonly analyzed in the clinical laboratory, was used as a model compound to study the effect of various sample parameters such as the presence of serum, proteins and ions, and the effects of sample volume on analysis of small molecules by CZE.

MATERIALS AND METHODS

Instrument

An automated capillary electrophoresis instrument (Beckman Instruments, Palo Alto, CA, USA) was set at 9 kV, 24°C and 280 nm. The capillary was 25 cm × 50 μm I.D. The elec-

* Corresponding author.

0021-9673/93/$06.00

trophoresis buffer was in most experiments 100 m*M* borate adjusted to pH 8.8 with sodium carbonate. Samples were introduced by pressure injection for 5 s. The capillary was washed with NaOH (1 mmol/l, 0.7 min), phosphoric acid (50 mmol/l, 0.7 min) and electrophoresis buffer (1 min).

Standards

An aqueous solution containing 20 mg/l of theophylline and 20 mg/l of 8-chlorotheophylline (internal standard) (Sigma Chemicals, St. Louis, MO, USA) was used in these experiments. Peak height was used for quantitation. Serum and ions were added to this solution as described later on.

RESULTS AND DISCUSSION

The optimum conditions for separating theophylline from the internal standard 8-chlorotheophylline were investigated first. As expected, the separation was faster at higher voltages. A voltage of 9 kV was chosen for subsequent experiments. The ratio of theophylline to 8-chlorotheophylline seemed to be constant for peak height and migration time, indicating that the use of an internal standard can correct for changes in migration time and peak height. There was a good separation at pH 8.2 and 8.8, but the two compounds co-eluted at pH 10. Therefore, a pH of 8.8 was chosen for the following experiments. Changing the ionic concentration of the electrophoresis buffer between 50–200 mmol/l did not affect the peak height, but the high ionic strength increased the separation time. For the majority of the subsequent experiments a 100 mmol/l buffer concentration was used. Fig. 1A represents the separation of theophylline and 8-chlorotheophylline under these conditions.

After selecting the optimum conditions for separating theophylline and 8-chlorotheophylline, various factors present in the sample which might affect the separation by CZE such as the presence of proteins, ion concentration, and sample volume injected were studied.

The addition of moderate amounts of serum to aqueous standards of theophylline and 8-

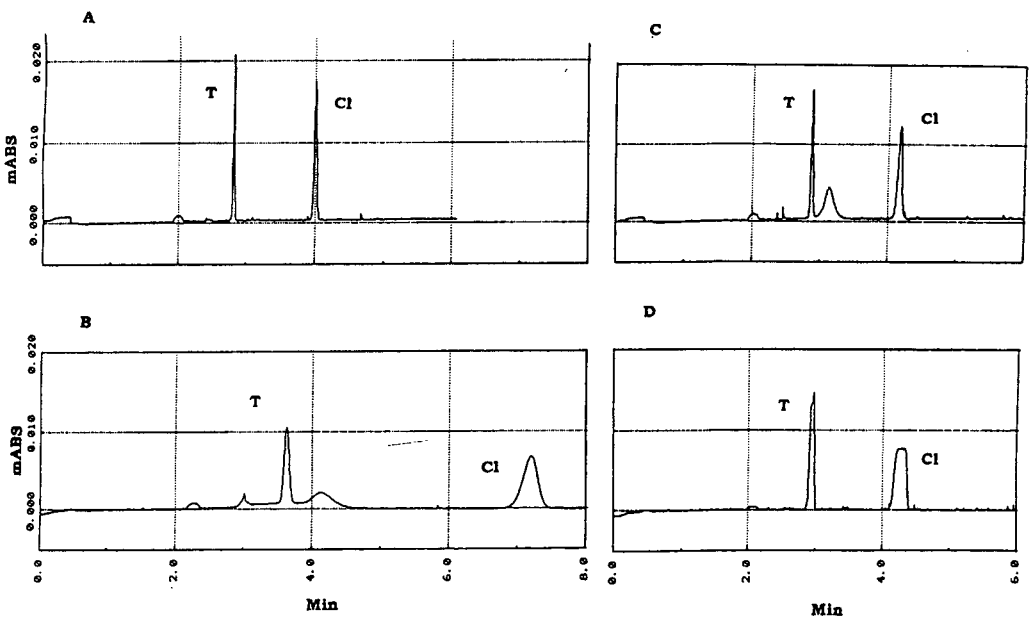

Fig. 1. Electropherogram for the separation of theophylline (T; 20 mg/l) and 8-chlorotheophylline (Cl; 20 mg/l) at 9 kV, 24°C, 280 nm, 100 m*M* borate buffer, pH 8.8 and 5 s pressure injection. (A) Sample dissolved in water; (B) as in A, but containing serum proteins at 3 g/l; (C) as in A, but containing albumin at 3 g/l; (D) sample dissolved in 100 m*M* borate buffer, pH 8.8 and introduced by pressure injection for 10 s.

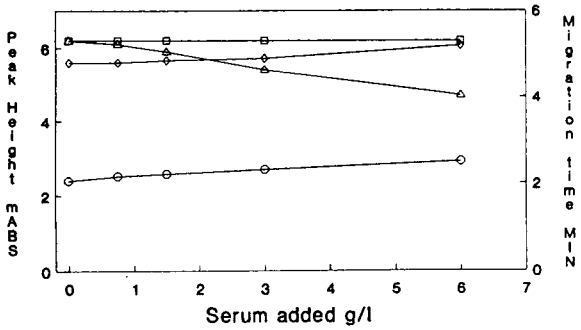

Fig. 2. Effect of different concentrations of serum added to aqueous solutions of theophylline with a 50 and 200 m*M* borate buffer, pH 8.8. Same separation conditions as in Fig. 1. □ = Peak height, 200 m*M*; △ = peak height, 50 m*M*; ◇ = migration time, 200 m*M*; ○ = migration time, 50 m*M*.

chlorotheophylline did not affect peak height or migration time appreciably; however, high concentrations (>3 g/l) affected peak height and increased the migration time (Fig. 1B). This effect is much more pronounced when an electrophoresis buffer of low ionic concentration is used (Fig. 2), and with high sample volumes. Albumin, the major serum protein, only caused a slight change in peak height at a high concentration (6 g/l) when using a low-ionic-strength buffer, and no effect was observed with a high-ionic-strength one (Figs. 3 and 1C). Addition of sodium chloride to the sample (Fig. 4), or borate ions decreased the peak height and increased the migration time as seen on the addition of serum.

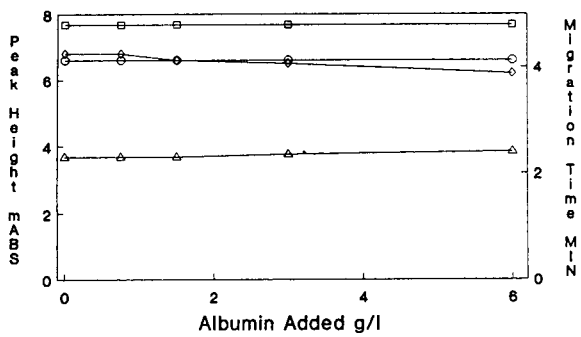

Fig. 3. Effect of different concentrations of albumin added to aqueous solutions of theophylline with a 50 and 200 m*M* borate buffer, pH 8.8. Same separation conditions as in Fig. 1. ◇ = Peak height, 50 m*M*; ○ = peak height, 200 m*M*; △ = migration time, 50 m*M*; □ = migration time, 200 m*M*.

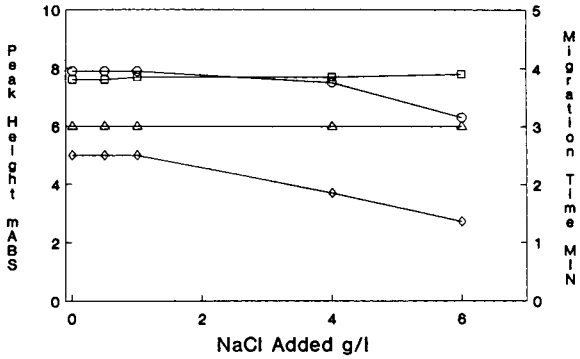

Fig. 4. Effect of different concentrations of NaCl added to aqueous solutions of theophylline and 8-chlorotheophylline. Same separation conditions as in Fig. 1. ○ = Theophylline peak height; △ = theophylline migration time; ◇ = 8-chlorotheophylline peak height; □ = 8-chlorotheophylline migration time.

At high concentrations of these ions, the peaks were wide (Fig. 1D) and sometimes split, especially when the sample volume was large (>10 s injection). Increasing the sample pH from 7.0 to 10.0 decreased the peak height, while the migration time remained constant.

Separations using electrophoresis buffers of low ionic strength are much more susceptible to various effects caused by high ionic concentrations of the sample (Fig. 5), especially when the sample volume is large (>5 s injection). On the other hand, separations with electrophoresis

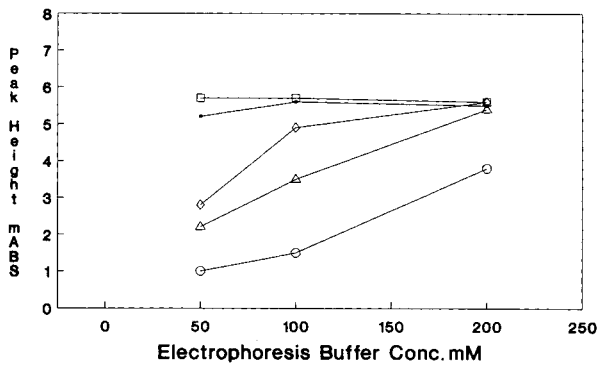

Fig. 5. Effect of different concentrations of borate ions added to aqueous solutions of theophylline. Electrophoresis buffers pH 8.8: 50, 100, 200 mM. Other separation conditions the same as in Fig. 1. Sample buffer concentration: □ = 0 m*M*; ● = 25 m*M*; ◇ = 50 m*M*; △ = 100 m*M*; ○ = 200 m*M*.

TABLE I

PRECISION OF THEOPHYLLINE PEAK HEIGHT AS A FUNCTION OF THE ELECTROPHORESIS BUFFER IONIC CONCENTRATION

Molarity (m*M*)	Relative standard deviation (%) ($n = 10$)	
	Theophylline	Theophylline/8-chlorotheophylline
25	2.2	1.3
100	1.9	1.3
200	0.9	0.9

buffers of high ionic strength are not as susceptible to these effects; however, the separations are slower. Even when assaying pure aqueous standards, the precision of the theophylline peak height tends to improve slightly by using high-ionic-strength buffers (Table I). Electrophoresis buffers of high ionic strength have the added advantages of giving better resolution and producing sharper peaks, *i.e.* higher plate numbers, especially for proteins [9,10]. These advantages are probably a consequence of the decrease in band diffusion.

Due to the small light path in CZE, the minimum detection level is limited; for this reason, the maximum amount of sample which can be introduced into the capillary in order to enhance the signal was investigated. Fig. 6 indicates that for serum samples, a high-ionic-strength buffer (300 m*M*) enabled a larger volume of sample to be introduced before the signal reached a plateau. The increased sample volume lead to an increase in sensitivity as reflected by the peak height (Fig. 6). Vinther and Soeberg [1], using a weak electrophoresis buffer (10 m*M* tricine), found that the plate number (N) decreased greatly with increasing sample size. In this work, using high-ionic-strength buffers, it was also observed that a larger sample volume decreased N, but to a lesser extent than that observed by Vinther and Soeberg. We have used this approach successfully for the determination of iohexol in serum [6].

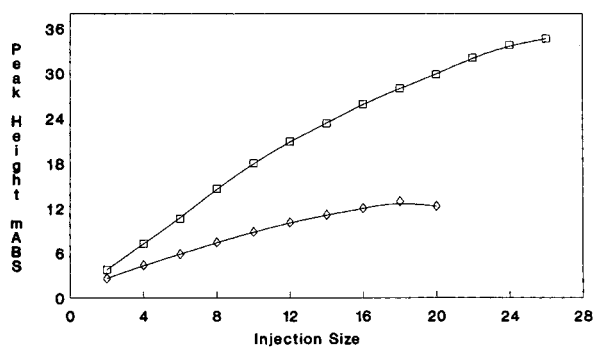

Fig. 6. Effect of the injection size (in seconds) of serum solutions of theophylline on peak height. Capillary: 25 cm × 50 μm. Electrophoresis buffers pH 8.8: 30 and 300 m*M*. Other separation conditions the same as in Fig. 1. □ = Buffer 300 m*M*; ◇ = buffer 30 m*M*.

CONCLUSIONS

Based on these results, it is evident that serum samples can be analyzed directly using a simple dilution in a low-ionic-strength buffer (10–20 times lower than that of the electrophoresis buffer). A 10–20-fold dilution of serum samples yields an acceptable peak shape, height and migration time, provided the molarity of the borate buffer is high enough (>200 mmol/l). Previously, it has been demonstrated using micellar electrokinetic capillary electrophoresis that serum can be directly injected without dilution [7,8]. This is possible because the micelles solubilize the serum proteins. Here we show that diluted serum samples can also be directly injected using CZE conditions.

Addition of standards directly into serum rather than into aqueous solutions will keep the migration time and peak height very close to the unknown samples [6,8]. It is, however, important to remove the small amounts of proteins

which adsorb to the capillary walls with thorough washings between samples. It is recommended to use high-ionic-strength buffers when analyzing samples derived from serum or urine even though these buffers slow the analysis time. The analysis time can be shortened by using a short capillary. The high strength buffers allow a larger sample volume to be introduced into the capillary without a significant sacrifice in plate number leading to an enhanced detector signal.

Since protein removal is not necessary, CZE becomes an attractive technique for analysis in clinical laboratories, provided the compound of interest produces an adequate detector signal. Traditional solvent extraction, of course, eliminates the problem of proteins and ions present in the sample with an enhancement of the detection due to sample concentration. However, it requires several additional steps increasing the analysis time.

REFERENCES

1 A. Vinther and H. Soeberg, *J. Chromatogr.*, 559 (1991) 3.
2 X, Huang, W.F. Coleman and R.N. Zare, *J. Chromatogr.*, 480 (1989) 95.
3 Z.K. Shihabi, *J. Liq. Chromatogr.*, 11 (1989) 1579.
4 D.J. Popovich, E.T. Butts and C.J. Lancester, *J. Liq. Chromatogr.*, 1 (1978) 469.
5 I.H. Hagestam and T.C. Pinkerton, *Anal. Chem.*, 57 (1985) 1757.
6 Z.K. Shihabi and M.S. Constantinescu, *Clin. Chem.*, 38 (1992) 2117.
7 W. Thormann, A. Minger, S. Molteni, J. Caslavska and P. Gebauer, *J. Chromatogr.*, 593 (1992) 275.
8 W. Thormann, P. Meier, C. Marcolli and F. Binder, *J. Chromatogr.*, 545 (1991) 445.
9 F.A. Chen, L. Kelly, R. Plamieri, R. Biehler and H. Schwartz, *J. Liq. Chromatogr.*, 15 (1992) 1143.
10 A. Vinther and H. Soeberg, *J. Chromatogr.*, 589 (1992) 315.

Journal of Chromatography A, 652 (1993) 471–475
Elsevier Science Publishers B.V., Amsterdam

CHROM. 25 085

Sample matrix effects in capillary electrophoresis

II. Acetonitrile deproteinization

Z.K. Shihabi

Department of Pathology, Bowman Gray School of Medicine, Wake Forest University, Winston-Salem, NC 27157 (USA)

ABSTRACT

Acetonitrile deproteinization [acetonitrile–serum (3:2, v/v)] was found to be a suitable method for removal of serum proteins for the analysis of drugs and small molecules by capillary electrophoresis. Many compounds exhibited higher plate numbers and peak heights in the presence of 60% acetonitrile. This effect is due to a special stacking brought along by the low resistivity of the acetonitrile in the sample. In addition to removing serum proteins, acetonitrile improves the solubility of some compounds and increases the sample volume which can be introduced into the capillary. Serum theophylline analysis was used here as an example for the analysis of drugs by capillary electrophoresis using acetonitrile deproteinization.

INTRODUCTION

The sample matrix plays an important role in capillary electrophoresis. Under proper conditions a stacking effect [1–4] can be obtained by preparing the sample in a buffer of ten times lower ionic strength than the running buffer leading to sharper peaks, higher plate number [1], and an increased detector signal [2]. In the previous work, it was shown that some drugs and metabolites can be determined in a complex biological matrix, such as serum, directly by dilution [5,6], especially if a high ionic strength running buffer is used. However, for analytes present in low concentrations, the ions and proteins present in serum interfere with their assay. The majority of drugs are present in very low concentrations in serum. Proteins may interfere by three means: by binding the drug, masking its absorption, and adsorbing to the capillary walls affecting reproducibility. In order to detect these compounds by capillary electrophoresis (CE) a clean-up step is necessary. Although liquid- and solid-phase extraction are excellent means for extraction and concentration of drugs and small molecules, these methods are time consuming and therefore they are not suitable for rapid assays such as demanded in clinical laboratories [7]. A simple alternative technique which has been used successfully in HPLC is acetonitrile deproteinization [5]. Here, we optimize this method for CE and show that this method has some advantages. In addition to removing proteins, it can increase the plate number and peak height for some compounds by a special stacking effect.

MATERIALS AND METHODS

Instrumental

An automated capillary electrophoresis instrument (Beckman, Palo Alto, CA, USA) was set at 13 kV, 24°C and 254 nm. The capillary was 25 cm × 50 μm (I.D.). The electrophoresis buffer was 300 m*M* boric acid adjusted to pH 8.5 with sodium hydroxide. Samples were introduced by pressure injection for 15 s. The capillary was washed for 1 min with the electrophoresis buffer after each sample.

0021-9673/93/$06.00

Samples

As a model compound, we used in most of the experiments iohexol {bis(2,3-dihydroxypropyl)-5-[N-(2,3 dihydroxypropyl)-acetamido]-2,4,6-tri-iodoisophthalamide} (Winthrop Pharmaceuticals, New York, NY, USA), a tri-iodinated, non-ionic radiographic contrast medium which is a highly water-soluble compound and does not bind to serum proteins.

Serum deproteinization

Serum (100 μl) was deproteinized by mixing with 150 μl acetonitrile for 15 s and the mixture was centrifuged for 1 min at 15 000 *g*.

Plate number (N)

Calculation [1] was based on the electrophoretic mobility of the compound (t_R) and width of the peak at half height ($W_{1/2}$) using the formula $N = 5.5(t_R/W_{1/2})^2$.

Serum theophylline analysis

The same method of serum deproteinization was used except the acetonitrile contained 25 mg/l of 3-isobutyl-1-methylxanthine (Aldrich, Milwaukee, WI, USA) as an internal standard. The supernatant was pressure injected for 6 s and electrophoresed at 11 kV with detection at 280 nm using a capillary of 25 cm × 75 μm.

RESULTS AND DISCUSSION

Acetonitrile is a very good deproteinization agent. However, in capillary electrophoresis, it does not conduct current. Mixtures of acetonitrile in aqueous solutions on the other hand, do conduct current. The effect of 60% acetonitrile compared to that of water on the separation of several compounds is illustrated in Fig. 1. The separation is improved; the peak height is higher and the retention time is increased. However, the extent of these effects differ from one compound to another. The increase in peak height for iohexol (about five fold) is much greater than that for the other compounds. This improvement in peak height and plate number was also present and further enhanced if these compounds were added to the supernatant of serum deproteinized with acetonitrile (final acetonitrile concentration 60%). Thus acetonitrile does not just remove serum proteins but also improves the peak height of some compounds.

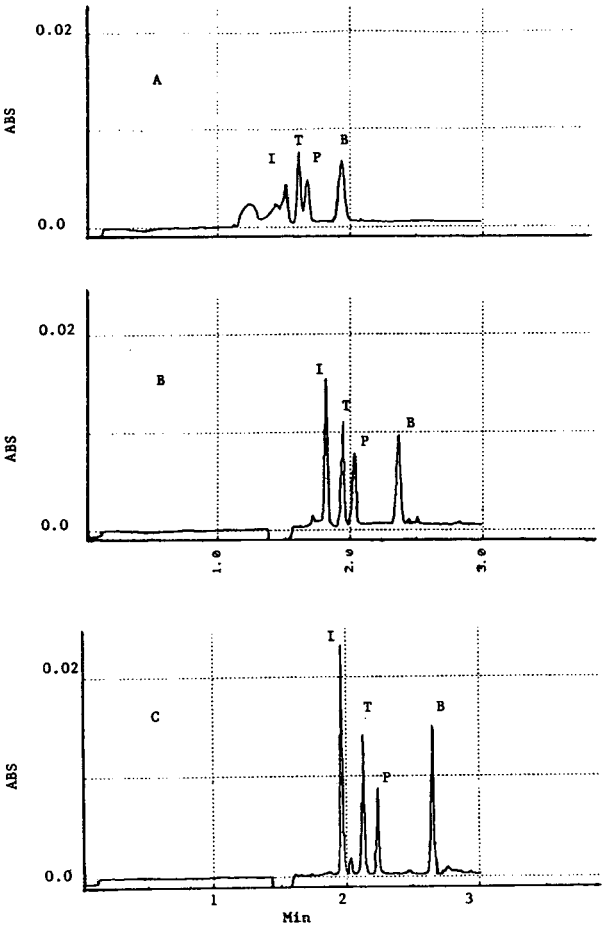

Fig. 1. Electropherogram of different compounds dissolved in: (A) water, (B) acetonitrile–water (60:40), and (C) supernatant of serum deproteinized by acetonitrile. I = iohexol, T = theophylline, P = phenytoin, B = phenobarbital. Capillary 25 cm × 50 μm, 15-s injections, 13 kV. ABS = absorbance in AU.

Since the major ions in serum are sodium and chloride at about 150 m*M* an equivalent amount of NaCl was added to the acetonitrile mixture. Further improvement in peak height and plate number occurred following NaCl addition (Table I). Different alcohols which occasionally are used for deproteinization also increased the plate number but not to the extent of that of acetonitrile (Table II) The acetonitrile effect on plate number and peak height occurs with large sam-

TABLE I

EFFECT OF DIFFERENT ACETONITRILE CONCENTRATIONS ON PEAK HEIGHT (mAU) AND PLATE NUMBER FOR IOHEXOL (200 mg/l)

Sample introduced by pressure injection for 15 s.

Sample diluent	$N \cdot 10^3$	Absorbance (mAU)
Serum deproteinized by acetonitrile (60%)	110	44
In absence of 60 mM NaCl in the sample		
30 m*M* borate	35	15
300 m*M* borate	10	6
% Acetonitrile in water		
0	21	11
10	27	13
20	32	14
40	37	18
60	59	26
In presence of 60 mM NaCl in the sample		
% Acetonitrile		
0	35	20
10	37	22
20	48	37
40	108	42
60	120	44

ple volume (Table III). The high sample volumes used here represent capillary overloading. Thus, it seems that acetonitrile increases the capacity of the capillary for a larger sample volume as it is common in stacking. The stacking effect increases at lower voltages approaching a plate number close to 400 000 for the 25-cm capillary (Table IV).

TABLE II

EFFECT OF DIFFERENT ALCOHOLS IN THE PRESENCE OF 60 m*M* NaCl ON IOHEXOL (200 mg/l) PEAK HEIGHT (mAU) AND PLATE NUMBER

Alcohols used for deproteinization	$N \cdot 10^3$	mAU
Water	35	19
60% Acetonitrile	120	42
60% Methanol	30	21
60% Ethanol	40	26
60% 1-Propanol	52	27

The stacking effect produced here by the acetonitrile shares some similarities, as well as some differences, with the traditional stacking produced in low concentration of aqueous buffers. In both cases, the stacking is produced by the difference in the resistivity of the sample and the running buffer and it allows a larger sample volume to be introduced into the capillary. However, the stacking in acetonitrile is different because the high resistivity of the sample results here from introduction of an organic solvent into the sample. In addition, to removing the proteins, acetonitrile improves the solubility of some compounds but not all. For example phenobarbital is more soluble in acetonitrile than in water. On the other hand iohexol which exhibits here a better stacking effect than phenobarbital is a

TABLE III

EFFECT OF SAMPLE VOLUME BY PRESSURE INJECTION (s) AND ACETONITRILE ON PEAK HEIGHT (mAU) AND PLATE NUMBER

Sample volume (s)	60% Acetonitrile				0% Acetonitrile			
	+NaCl		−NaCl		+NaCl		−NaCl	
	$N \cdot 10^3$	mAU	$N \cdot 10^3$	mAU	$N \cdot 10^3$	mAU	$N \cdot 10^3$	mAU
20	110	40	45	40	–	–	–	–
15	115	30	75	31	26	13	15	11
10	120	21	65	24	41	13	40	11
5	102	10	64	12	101	10	96	11
3	95	5	30	5	122	6	115	7
1	90	2	–	–	110	2	–	–

TABLE IV

EFFECT OF THE VOLTAGE (kV) ON PLATE NUMBER

Sample introduced for 10 s.

kV	$N \cdot 10^3$	
	60% Acetonitrile (+NaCl)	0% Acetonitrile (−NaCl)
16	96	37
14	140	48
10	172	58
6	314	138
3	395	159

highly water-soluble compound (>300 mg/ml). The stacking effect is also aided by the presence of relatively high ion concentrations in the sample (optimum about 100 m*M* for NaCl) which may improve the stacking by forming a transient isotachophoresis or interacting with the capillaries walls. The effect of acetonitrile on stacking is more pronounced in short-length capillaries (about 25 cm) compared to longer ones. Although we previously [6] used acetonitrile to deproteinize serum samples for CE, its stacking effect was not well appreciated.

The main purpose in using acetonitrile is to remove serum proteins. In HPLC, a 50% ratio of acetonitrile to serum has been used traditionally. Fig. 2 shows that this ratio is not adequate to remove serum proteins, especially albumin. In HPLC, albumin binds to the column packing and does not appear on the chromatogram. In CE, albumin migrates and can be seen on the electropherograms. Increasing the acetonitrile ratio to 60% was more effective in removing serum proteins.

To illustrate the suitability of this technique for analyzing drugs in serum, we measured serum theophylline by this technique. The regression analysis for serum theophylline assayed by this method compared to a fluorescence immunoassay is good (CE = 0.98immuno − 4, $n = 21$, $r = 0.98$). The test was linear between 3–40 mg/l. Fig. 3 shows an electropherogram from a patient on theophylline treatment. In order to avoid the variable effects of different ions on separation and drug recovery, the standards were prepared in serum matrix rather than in aqueous solutions.

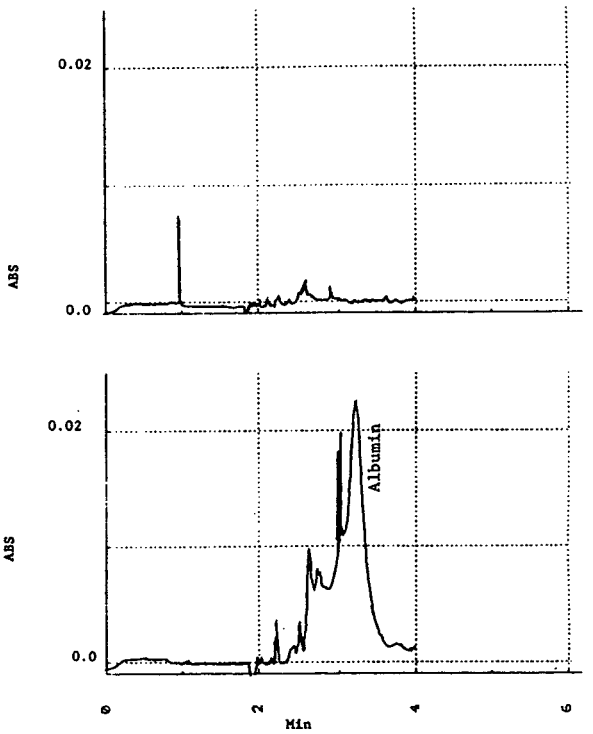

Fig. 2. Electropherogram of serum supernatant using: (top) 60% deproteinization and (bottom) 50% deproteinization. Capillary 25 cm × 50 μm, 10-s injections, 13 kV, 214 nm wavelength. ABS = absorbance in AU.

These data show that acetonitrile extraction is

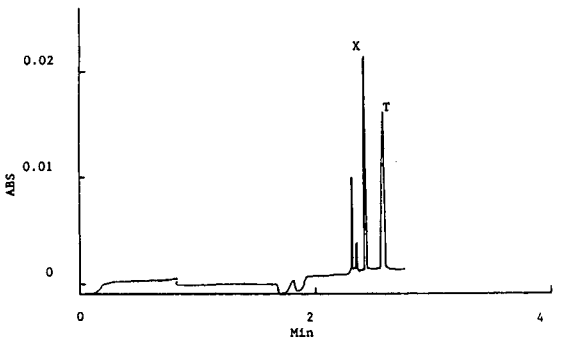

Fig. 3. Electropherogram of serum theophylline (10 mg/l) from a patient treated with the drug. T = theophylline, X = internal standard = 3-isobutyl-1-methylxanthine. Capillary 25 cm × 75 μm, injection 6 s, 11 kV. ABS = absorbance in AU.

a good method for preparing samples for CE. This method permits the introduction of larger volumes into the capillary with an increase in plate number for many compounds. Previously, we have shown that reproducibility of the assay is improved when acetonitrile is used compared to serum dilution [5] and furthermore, the capillary does not need extra washing with sodium hydroxide between samples leading to a faster analysis time. This work demonstrates that CE has a good potential for therapeutic drug monitoring especially for those compounds lacking a good immunoassay.

REFERENCES

1 A. Vinther and H. Soeberg, *J. Chromatogr.*, 559 (1991) 3.
2 R-L. Chen and D.S. Burgi, *J. Chromatogr.*, 559 (1991) 141.
3 F.E. Mikkers, F.M. Everaerts and T.P. Verheggen, *J. Chromatogr.*, 169 (1979) 1.
4 R. Abersold and H.D. Morrison, *J. Chromatogr.*, 516 (1990) 79.
5 L.L. Garcia and Z.K. Shihabi, *J. Chromatogr.*, in press.
6 Z.K. Shihabi and M.S. Constantinescu, *Clin. Chem.*, 38 (1992) 2117.
7 Z.K. Shihabi, *J. Liq. Chromatogr.*, 11 (1989) 1579.

Journal of Chromatography A, 652 (1993) 477–485
Elsevier Science Publishers B.V., Amsterdam

CHROM. 25 178

Determination of flavonoids by micellar electrokinetic capillary chromatography

Charlotte Bjergegaard, Søren Michaelsen[☆], Kirsten Mortensen and Hilmer Sørensen*

Chemistry Department, Royal Veterinary and Agricultural University, 40 Thorvaldsensvej, DK-1871 Frederiksberg C (Denmark)

ABSTRACT

HPCE based on cetyltrimethylammonium bromide (CTAB) or cholate micellar electrokinetic capillary chromatography (MECC) was found suitable for the separation of individual flavonoid glycosides following a rapid and simple technique of isolation, purification and group separation. Kaempferol and quercetin glycosides with varying degrees of glycosylation, and with or without additional esterification on the carbohydrate part, were included in the study. The influence of temperature and voltage as well as electrolyte, CTAB and organic modifier concentrations in the buffer on the migration order, migration times, and peak areas of the flavonoids was investigated. The method developed gives possibilities for the separation and specific determination of flavonoids isolated from vegetative parts of cruciferous plants.

INTRODUCTION

Flavonoids are plant constituents comprising one of the most numerous and widespread groups of natural products. Of the total of more than 4000 known flavonoids, about one quarter belong to the well defined group of flavone and flavonol glycosides [1]. These compounds accumulate especially in vegetative parts of plants, and often to appreciable concentrations [2]. Kaempferol, quercetin and isorhamnetin are the most common flavonol aglycones. They show great variation in the type of glycosylation and as reported during recent years with an increasing number of acyl-substituted compounds [1].

The flavonoids have attracted much attention, owing not only to their various colours and great number, but also to their biological activities, as they possess many different physiological properties [2–4]. These variations in properties are closely related to their structure, with special effects caused by the type of glycosylation [2]. Therefore, efficient methods for analysis, isolation and identification have a high priority [5,6], and major developments in recent years have been in the more general use of high-performance liquid chromatographic (HPLC) techniques [1]. However, high-performance capillary electrophoresis (HPCE) is a method that has additional possibilities and great potential as an efficient method of flavonoid analysis with the technique based on micellar electrokinetic capillary chromatography (MECC) [7,8].

This paper describes and compares the separations of flavonoids obtained with two different HPCE–MECC methods. In the first method, cetyltrimethylammonium bromide (CTAB) was used as a detergent, and in the second method,

* Corresponding author.
☆ Present address: Department of Research in Fur Animals, National Institute of Animal Science, Research Centre Foulum, P.O. Box 39, DK-8830 Tjele, Denmark.

0021-9673/93/$06.00

cholate was used as detergent in combination with taurine. The methods were compared and evaluated by studying the influences of different separation conditions on various separation parameters. The migration order of the various flavonoids is presented and discussed, and examples of analyses of flavonoids in samples of vegetative parts of cruciferous plants are presented.

EXPERIMENTAL

Apparatus

An ABI Model 270 A capillary electrophoresis instrument (Applied Biosystems, Foster City, CA, USA) was used with a 720 mm × 50 μm I.D. fused-silica capillary (J & W Scientific, Folsom, CA, USA). Detection was effected by measurement of UV absorption at 500 mm from the injection end of the capillary. Data processing was performed on a Shimadzu (Kyoto, Japan) Chromatopac C-R3A instrument.

Materials and reagents

The flavonoids (Fig. 1) were from the collection in this laboratory. The compounds were obtained from various cruciferous plants [2,9]. The methods applied were group separation

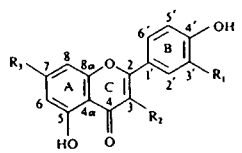

No.	Name	R_1	R_2	R_3
1	Kaempferol	H	OH	OH
2	Kaempferol-3-glucoside	H	Glucoside	OH
3	Kaempferol-3,7-diglucoside	H	Glucoside	Glucoside
4	Rustoside	H	Xylopyranosyl-(1,2)-galacto-pyranosyl	OH
5	Kaempferol-3-sophoroside-7-glucoside	H	Sophoroside	Glucoside
6	Kaempferol-3-sinapoylsophoroside-7-glucoside	H	Sinapoyl-sophoroside	Glucoside
7	Kaempferol-3-(6''-carboxyglucoside)	H	6''-carboxy-glucoside	OH
8	Quercetin	OH	OH	OH
9	Quercetin-3-glucoside	OH	Glucoside	OH
10	Rutin	OH	Rutinoside	OH
11	Quercetin-3-(6''-carboxyglucoside)	OH	6''-carboxy-glucoside	OH
12	Isorhamnetin-3-(6''-carboxyglucoside)	OMe	6''-carboxy-glucoside	OH

Fig. 1. Names, structures and numbering of flavonoids used.

[10,11], purification by column chromatography (CC) [2] and identification by paper chromatography (PC), thin-layer chromatography (TLC), high-voltage electrophoresis (HVE) and nuclear magnetic resonance (NMR) spectrometry [2,10].

Disodium tetraborate, disodium hydrogenphosphate, sodium cholate and taurine were from Sigma (St. Louis, MO, USA) and CTAB from BDH (Poole, UK). All chemicals were of analytical-reagent grade.

Procedure

Buffer preparations for the CTAB–MECC separations were performed according to Michaelsen *et al.* [12]. Samples were dissolved in water, except **1** and **8**, which were dissolved in water–dimethyl sulphoxide (1:1). Samples were introduced from the cathodic end of the capillary by 1-s vacuum injection in the CTAB system, and from the anodic end of the capillary by 1-s vacuum injection in the cholate–taurine system. Separations were performed under various separation conditions as specified in the text. On-column UV detection was at 350 nm (CTAB system) and at 250 nm (cholate–taurine system). Washings of the capillary were performed with 1.0 *M* NaOH for 5 min, water for 2 min and buffer for 5 min before each analysis. Calculations of normalized peak areas (*NA*), resolution (R_s) and the number of theoretical plates (*N*) were performed according to Michaelsen *et al.* [12].

Mixtures of flavonoids were obtained from plants homogenized and extracted in boiling methanol–water (70:30). The flavonoid extract was then purified by group separation through a weekly acidic cation exchanger, a strongly acidic cation exchanger and a weakly basic anion exchanger according to a previously described procedure [11].

RESULTS AND DISCUSSION

The names, structures and numbers of the flavonoids used in this study are shown in Fig. 1. The differences in structures between the investigated flavonoids are due to variation in the aglycones at C-3′ with R_1 as either hydrogen (kaempferol), hydroxy (quercetin) or methoxy

(isorhamnetin) groups or various glycosides attached to the 3- or 7-position of these aglycones.

The separation mechanisms which are most likely to give successful separations of these compounds in HPCE are based on differences in hydrophobic interactions for all of the compounds and differences in electrophoretic mobilities for the charged carboxy-substituted glucosides at pH values above 4.5. MECC separations of flavonoids were therefore tested with the previously described CTAB method [12–15], and the data obtained were compared with results obtained with MECC based on a cholate- and taurine-modified buffer [16].

The CTAB–MECC method results in hydrophobic interactions with flavonoid aglycones as well as ion-pairing interaction chromatography with the flavonoids containing carboxy groups and the positively charged CTAB monomers and micelles and the CTAB-coated capillary wall. This results in differential partitioning of flavonoids between the micellar and the aqueous buffer phases [13]. The neutral flavonoids migrate with the electroosmotic flow towards the anode, and they are retarded by CTAB migrating towards the cathode. The negatively charged flavonoids will migrate towards the anode owing to their electrophoretic mobility, and with electroosmotic flow increasing their velocity, whereas CTAB will decrease their velocities. In addition, complex formation of the carbohydrate parts of the flavonoids with borate in the buffer may occur [17]. This will increase the velocity of the flavonoids towards the anode.

The cholate–MECC separation is based on hydrophobic interaction with all flavonoids and ion repulsion of the flavonoids with carboxy groups and the negatively charged cholate monomers and micelles. This also results in differential partitioning of flavonoids between the micellar and the aqueous buffer phases. Compared with the likely spherical form of CTAB micelles with the charged groups situated on the surface of the micelle and a hydrophobic interior [18], cholate micelles have been suggested to form rod-like or cylindrical micelles with the hydrophobic part situated on the surface and the hydrophilic portions turned inward [19]. The effect of the zwitterion taurine in the system is less clear. Taurine may affect the degree of binding of the counter ions to the cholate micelles, and thereby affect the critical micelle concentration (CMC) [18]. The high ionic strength of the buffer due to taurine may also result in increased aggregation number of the micelles and decreased CMC values [18,20]. The association of taurine with either the capillary surface or the negatively charged flavonoids will probably not have a large influence on the separation, as both the capillary surface and the flavonoids will still be negatively charged. According to the theory, neutral flavonoids will migrate with the electroosmotic flow towards the cathode, and the cholate monomers and micelles migrating towards the anode will have a retarding effect on the flavonoids. The negatively charged flavonoids will migrate towards the anode owing to their electrophoretic mobility, and the cholate monomers and micelles migrating towards the anode will change their velocity depending on the effect of hydrophobic interaction compared with ion repulsion. Finally, the electroosmotic flow will decrease their velocity. Owing to the size of the electroosmotic flow compared with the influence of the other mechanisms involved, flavonoids will migrate towards the cathode end of the capillary.

Migration order

The separations of flavonoids in the CTAB and the cholate–taurine systems are shown in Fig. 2. The migration order of the compounds in the CTAB system was **5**, **6**, **4**, **3**, **10**, **2**, **9**, **7**, **8** and **1**. The migration order was apparently not affected by changes in 1-propanol, electrolyte or CTAB concentration as well as changes in temperature or voltage, whereas the separations and migration times were affected by changes in these parameters (see below). The migration order of the compounds in the cholate–taurine system was **5**, **6**, **10/11**, **12**, **4**, **8**, **1**, **2** and **9**. However, in this system the migration order of **8**, **1**, **2** and **9** was affected by changes in temperature, voltage and concentration of 1-propanol (see below). The best separations were generally obtained with the cholate–taurine system. The separation efficiency, expressed as the number of

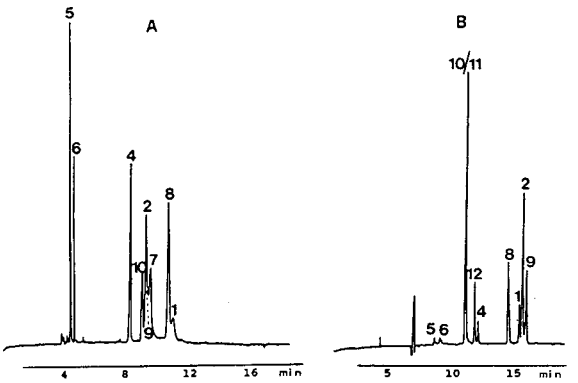

Fig. 2. (A) Electropherogram of flavonoids in the CTAB system. Separation conditions: temperature, 50°C; voltage, −26 kV; buffer composition, 12 m*M* borate–20 m*M* phosphate–40 m*M* CTAB adjusted to pH 7.0, 4% 1-propanol added; UV detection at 350 nm. (B) Electropherogram of flavonoids in the cholate–taurine system. Separation conditions: temperature, 40°C; voltage, 25 kV; buffer composition, 35 m*M* cholate–100 m*M* phosphate–500 m*M* taurine, 6% 1-propanol added; UV detection at 250 nm. Numbers as in Fig. 1.

theoretical plates per metre of capillary (N/m), and resolution (R_s) are given in Table I for the separation obtained with the cholate–taurine system under the conditions as described in Fig. 2B. The N/m values obtained were high, with values between 150 000 and 225 000, and the R_s values ranged from 1.21 for **1–2** to 12.91 for **4–8**.

Compounds **5** and **6** are the most hydrophilic compounds, and they migrate with the highest velocities in both systems. The 2″-sinapoylsophoroside group of **6** makes this compound more hydrophobic than **5** with the unsubstituted sophoroside group, and **5** therefore migrates faster than **6** in both the CTAB and the cholate–taurine systems (Fig. 2). The presence of a 3-glucoside in both kaempferol and quercetin (*i.e.*, **2** and **9**, respectively) compared with the unsubstituted kaempferol and quercetin (*i.e.*, **1** and **8**, respectively) resulted in decreases in migration times of 2 min in the CTAB system. In the cholate–taurine system the positions of kaempferol and quercetin compared with their glucosides depended on the applied voltage, temperature and 1-propanol concentration (see below).

Changing the 3-glucoside in **2** to the 3-diglycoside xylopyranosylgalactopyranosyl in **4** decreased the migration time in the CTAB system by 1 min, whereas in the cholate–taurine system the migration time decreased by 4.6 min (Fig. 2). Changing the 3-glucoside in **9** to the 3-diglycoside rutinoside in **10** also resulted in a minor change in the migration times in the CTAB system and a large change in the cholate–taurine system (Fig. 2). The change in hydrophobicity of these compounds apparently has a much larger effect in the cholate–taurine system than in the CTAB system.

Replacing hydrogen at C-3′ in **1** or **2** with the hydroxy group at C-3′ in **8** or **9** had little

TABLE I

NUMBER OF THEORETICAL PLATES PER METRE IN THOUSANDS (N/m) AND RESOLUTION (R_s) FOR FLAVONOIDS ANALYSED IN THE CHOLATE–TAURINE SYSTEM

Numbers as in Fig. 1 and separation conditions as in Fig. 2B.

Parameter	No.								
	5	**6**	**10/11**	**12**	**4**	**8**	**1**	**2**	**9**
N	139	77	151	185	181	150	170	227	210
	Pair								
	5–6	**6–10/11**	**10/11–12**	**12–4**	**4–8**	**8–1**	**1–2**	**2–9**	
R_s	2.82	11.75	4.87	1.84	12.91	4.41	1.21	1.69	

influence on migration times in both systems except for **1** and **8** in the cholate–taurine system. Replacing the hydroxy group at C-3′ in **11** with the methoxy group at C-3′ in **12** resulted in an increased migration time in the cholate–taurine system, probably owing to the increased hydrophobicity of **12** compared with **11**.

Finally, the presence of a carboxy group at the glucoside in **7** compared with **2** gave a small increase in migration time in the CTAB system. This is caused by the ion-pairing effect with CTAB, as reported for other compounds [12,15]. The presence of a carboxy group at the glucoside in **11** compared with **9** gave a very large decrease of 5 min in the migration time in the cholate–taurine system. Ion repulsion between the negatively charged cholate and the carboxy group of **7** and **11** can explain these results, as the influence of the hydrophobic interaction then decreases and the compounds migrate faster.

Separation conditions

Increasing voltages gave large non-linear decreases in migration times in both systems (Fig. 3). Further, the migration order of some of the flavonoids changed with increasing voltage in the cholate–taurine system. At a voltage of 15 kV **8** was in a position just after **9**, and at 20 kV **8** and **9** migrated together after **2** and in front of **1**, and finally, at 25 kV **8** had moved to a position in front of **2**, **9** and **1**. These results were obtained with separation conditions as described in Fig. 2B except for a buffer containing 4% 1-propanol. The general decrease in migration time with higher voltages is caused by an increase in electroosmotic flow, and the velocities of **7**, **11** and **12** are further affected owing to their negative charge. Increasing temperature in the capillary due to insufficient heat removal at high voltages may influence the interaction of analytes with micelles [15], and this can also cause the change in migration order seen for some of the compounds. The concave curves and the change in migration order may therefore be caused by a combination of the described effects. The *NA* values of **6** increased slightly, those of **1**, **4**, **5**, **9** and **12** were constant and those of **8** and **10/11** decreased with increasing voltage. Changes in *NA* values are probably caused by changes in the relative response factors of the flavonoids due to the changed interaction with cholate–taurine.

The migration times decreased markedly with increasing temperature in both systems. The decreases were linear for the CTAB system except for values obtained at 35°C, whereas in the cholate–taurine system the decreases were non-linear with a decreasing rate of reduction at higher temperatures (Fig. 4). The non-linear decrease in the cholate–taurine system indicates increased interaction of flavonoids with cholate–taurine at higher temperatures.

The flavonoids **1** and **8** moved from positions after **2** and **9** to positions in front of **2** and **9** when the temperature increased (Fig. 5). These

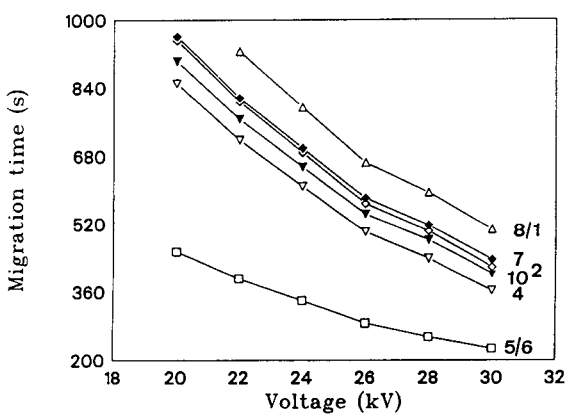

Fig. 3. Influence of applied voltage on migration times of flavonoids in the CTAB system. Numbers as in Fig. 1. Other separation conditions as in Fig. 2A.

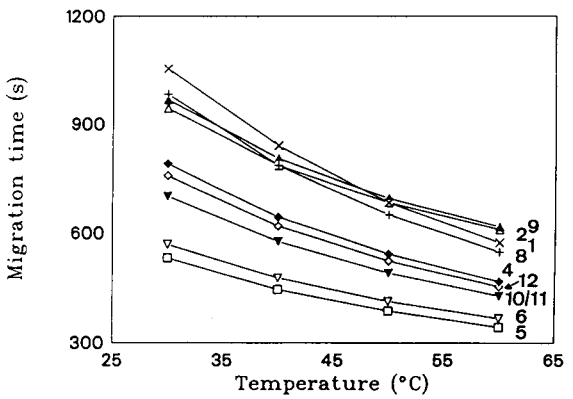

Fig. 4. Influence of temperature on migration times of flavonoids in the cholate–taurine system. Numbers as in Fig. 1. Other separation conditions as in Fig. 2B except 4% of 1-propanol in the buffer.

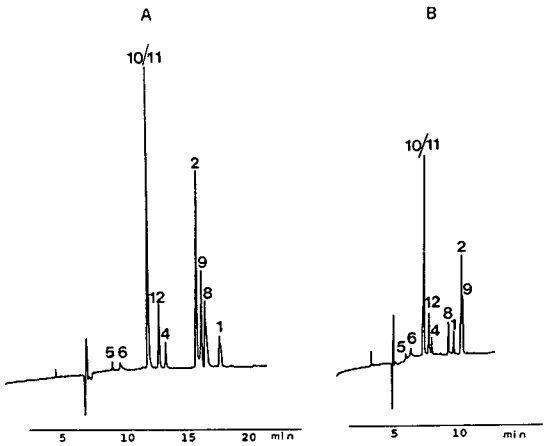

Fig. 5. Influence of temperature on migration order of flavonoids in the cholate–taurine system. (A) 30°C; (B) 60°C. Numbers as in Fig. 1. Other separation conditions as in Fig. 2B except 4% of 1-propanol in the buffer.

changes in migration order are probably also caused by changes in the interaction between analytes and cholate at high temperatures. The best separations with the CTAB system were obtained at 30 or 50°C and with the cholate–taurine system at 30 or 60°C.

The influence of the presence of 1-propanol in the buffer on the migration times of flavonoids depended strongly on the analyte (Fig. 6). Increasing the concentration resulted in decreasing migration times for most analytes when going from 0 to 2% 1-propanol in both systems, and from 2 to 8% of 1-propanol all migration times increased except for **1** in the cholate–taurine system. Finally, changing from 8 to 10% of 1-propanol resulted in increasing migration times in the CTAB system, whereas for **2**, **4**, **5**, **6**, **9**, **10**, **11** and **12** the migration times were constant in the cholate–taurine system but decreased for **1** and **8**.

The migration times generally increased less in the cholate–taurine system than in the CTAB system with increasing 1-propanol concentration. This may be explained by the likely ability of the cholate micelles to tolerate high concentrations of organic solvents [19]. The helical structure of the cholate micelles with a hydrophobic surface, compared with the normal spherical form of micelles [*e.g.*, sodium dodecyl sulphate (SDS)] with a hydrophobic interior, is believed to make

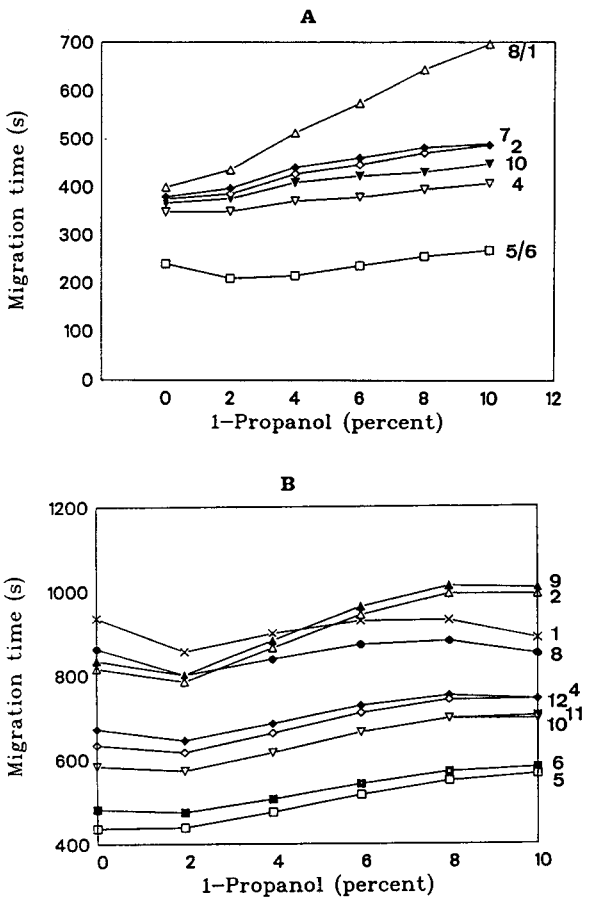

Fig. 6. Influence of 1-propanol concentration on migration times of flavonoids in (A) the CTAB system and (B) the cholate–taurine system. Numbers as in Fig. 1. Other separation conditions as in Fig. 2.

these cholate micelles less vulnerable to disassociation by the reduction of the polarity of the buffer solution, which occurs when the alcohol is added [19].

The migration order also changed for some of the compounds. Flavonoids **1** and **8** shifted from positions after **2** and **9** to positions in front of **2** and **9** when the concentration of 1-propanol increased (Fig. 7). Further, flavonoids **4** and **12** separated well at low concentrations of 1-propanol, whereas with 10% 1-propanol in the buffer they migrated as one peak (Fig. 7).

Increasing the amount of organic modifier in the buffer causes decreases in the electroosmotic flow [21], and the decreases become larger with

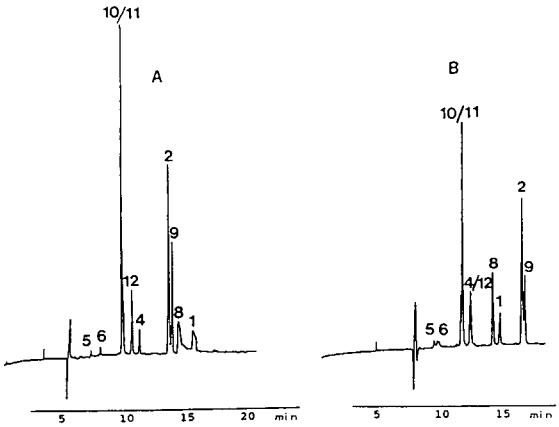

Fig. 7. Influence of 1-propanol concentration on the migration order of flavonoids in the cholate–taurine system. (A) 0 and (B) 10% 1-propanol. Numbers as in Fig. 1. Other separation conditions as in Fig. 2B.

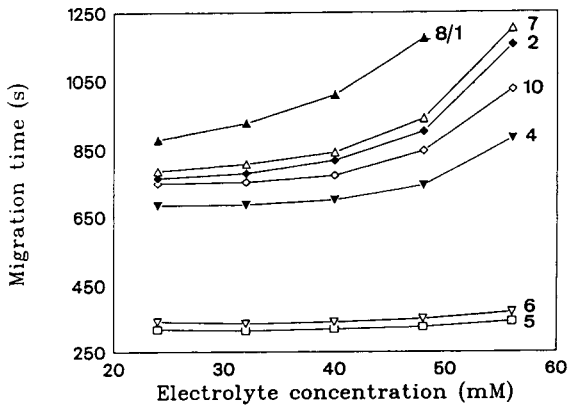

Fig. 8. Influence of electrolyte concentration on migration times of flavonoids in the CTAB system. Numbers as in Fig. 1. Other separation conditions as in Fig. 2A.

increasing length of the alcohol chain [22]. Further, the presence of an organic modifier also results in more of the analyte being present in the aqueous phase than in the micellar phase. Both effects are probably involved here as the migration times first decrease and then increase with higher amounts of organic modifier. The best separations were obtained with 4 or 6% 1-propanol in the buffer.

The *NA* values generally decreased for all compounds and the decrease was largest for **1**, **2**, **9** and **10/11**. The changes in *NA* values are probably caused by changes in the relative response factors of the flavonoids and changes in the viscosity of the buffer [15].

1-Propanol was chosen as a modifier because its boiling point is close to that of water. Other modifiers with lower boiling points were also tested, but the migration times from consecutive analyses of identical samples changed considerably owing to continuous changes in the buffer composition, as the modifier evaporated at a higher rate than water from the buffer.

The effects of increasing electrolyte concentration [borate–phosphate (3:5)] were investigated with the CTAB system. The migration times of **5** and **6** were unaffected, whereas the migration times showed non-linear increases for the other compounds (Fig. 8). The changes were greatest when going from 48 to 56 m*M*. A combination of decreasing electroosmotic flow with increasing electrolyte concentration [23,24] and changed interaction of flavonoids with CTAB [8] can explain the observed results. Also, a possible effect of the concentration and the equilibrium of the borate–glycoside complex formation [15,17] is a likely explanation of the observed results. An electrolyte concentration of 32 m*M* gave the best separation of the investigated flavonoids.

Finally, increasing CTAB concentration gave increased migration times for all of the flavonoids (Fig. 9). This result is expected owing to

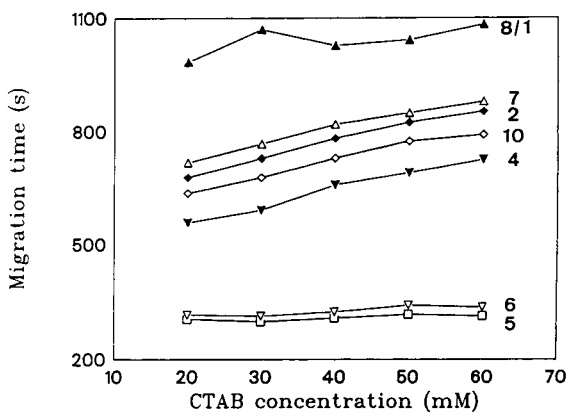

Fig. 9. Influence of CTAB concentration on migration times of flavonoids in the CTAB system. Numbers as in Fig. 1. Other separation conditions as in Fig. 2A.

an increase in the ratio of the micellar phase to that of the aqueous phase and possible changes in the electroosmotic flow [12]. The separation of the compounds studied was slightly improved for **5** and **6** and reduced for **2** and **7** and for **7** and **8/1** with increasing CTAB concentration. The best separation was obtained with 30 or 40 m*M* CTAB in the buffer.

The use of SDS–MECC for the separation of flavonoids has been reported [7]. However, compared with the separations reported here, the flavonoids migrated very close to each other and in the time interval from only 10 to 13 min. In our experiments flavonoids migrated with migration times between 4 and 11 min in the CTAB system and between 8 and 16 min in the cholate–taurine system. In both experiments not all flavonoids were separated with one set of separation conditions. Owing to the increased separation window the methods with CTAB or cholate–taurine may give better separations than the SDS method. Finally, isotachophoretic HPCE analyses of flavonoids have also been reported [4]. However, the separations obtained and the separation capacity of the isotachophoretic method make this method less promising than the CTAB and cholate–taurine methods.

Examples of analyses of flavonoids isolated and purified by group separation of plant extracts are shown in Fig. 10. The group separation procedure applied for the purification of flavonoids yields a sample of neutral compounds [11]. As seen in the electropherograms, the isolated compounds can be detected at either 350 or 250 nm, and it is therefore likely that most of the isolated compounds are flavonoid glycosides or other phenolics. The leaves of rapeseed (*Brassica napus*) and the vegetative parts of broccoli (*Brassica oleracea*) contained many possible flavonoids (Fig. 10A, C and D), whereas the vegetative parts of yellow mustard (*Sinapis alba*) contained only two possible flavonoids in large amounts (Fig. 10B). Good separations were obtained in both systems, although the separations were not identical. However, it is not possible to choose one system or the other from the separations obtained.

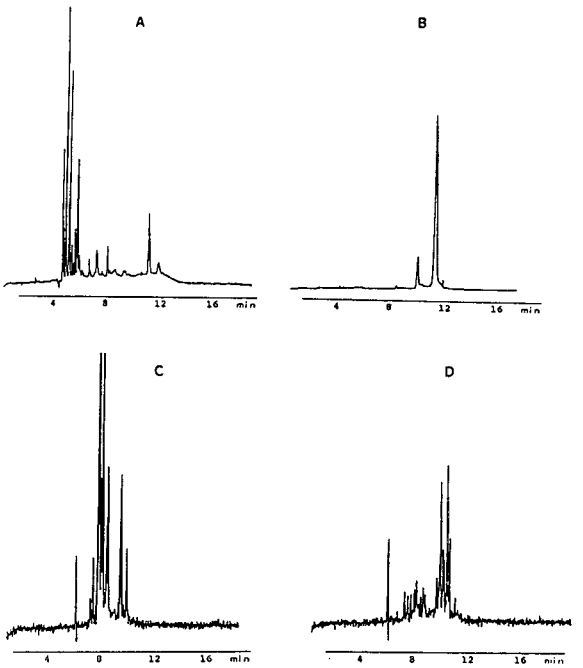

Fig. 10. Electropherograms of samples of neutral flavonoids from plants. (A) Leaves of rapeseed (*Brassica napus*) analysed in the CTAB system; (B) vegetative parts of yellow mustard (*Sinapis alba*) analysed in the CTAB system; (C) leaves of rapeseed (*Brassica napus*) analysed in the cholate–taurine system; (D) vegetative parts of broccoli (*Brassica oleracea*) analysed in the cholate–taurine system.

CONCLUSIONS

MECC–HPCE proved its value for analyses of flavonoids. Both the CTAB and the cholate–taurine systems can be applied to the separation of flavonoids, but the cholate–taurine system generally gave better separtions of the investigated flavonoids. The investigated separation systems resulted in different migration orders of some of the flavonoids. The migration order of flavonoids in both systems could be explained by the differences in the hydrophobicity and charge of the compounds. Further, the change in hydrophobicity of some of the flavonoids had a much larger effect on migration times in the cholate–taurine system than in the CTAB system. The separation parameters were much affected by the separation conditions in both systems, but the effects depended strongly on the system. Finally,

analyses of samples of flavonoids prepared from various plants showed the practical analytical use of both system for the analysis of flavonoids.

ACKNOWLEDGEMENTS

The authors gratefully acknowledge support from the Danish Agricultural Ministry, the Danish Natural Research Council and the Danish Agricultural and Veterinary Research Council.

REFERENCES

1 J.B. Harborne and C.A. Williams, in J.B. Harborne (Editor), *The Flavonoids*, Chapman and Hall, London, 1988, Ch. 8, p. 303.
2 L.M. Larsen, J.K. Nielsen and H. Sørensen, *Phytochemistry*, 21 (1982) 1029.
3 L.A. Griffiths, in J.B. Harborne and T.J. Mabry (Editors), *The Flavonoids: Advances in Research*, Chapman and Hall, London, New York, 1982, Ch. 12, p. 681.
4 U. Seitz, G. Bonn, P. Oefner and M. Popp, *J. Chromatogr.*, 559 (1991) 499.
5 K. Hostettmann and M. Hostettmann, in J.B. Harborne and T.J. Mabry (Editors), *The Flavonoids: Advances in Research*, Chapman and Hall, London, New York, 1982, Ch. 1, p. 1.
6 K.R. Markham and V.M. Chari, in J.B. Harborne and T.J. Mabry (Editors), *The Flavonoids: Advances in Research*, Chapman and Hall, London, New York, 1982, Ch. 2, p. 19.
7 P.G. Pietta, P.L. Mauri, A. Rava and G. Sabbatini, *J. Chromatogr.*, 549 (1991) 367.
8 C. Bjergegaard, S. Michaelsen and H. Sørensen, *J. Chromatogr.*, 608 (1992) 403.
9 J.K. Nielsen, L. Dalgaard, L.M. Larsen and H. Sørensen, *Entomol. Exp. Appl.*, 25 (1979) 227.
10 O. Olsen and H. Sørensen, *Phytochemistry*, 19 (1980) 1717.
11 B. Bjerg, O. Olsen, K.W. Rasmussen and H. Sørensen, *J. Liq. Chromatogr.*, 7 (1984) 691.
12 S. Michaelsen, P. Møller and H. Sørensen, *J. Chromatogr.*, 608 (1992) 363.
13 S. Michaelsen, P. Møller and H. Sørensen, *Bull. GCIRC*, 7 (1991) 97.
14 C. Bjergegaard, S. Michaelsen, P. Møller and H. Sørensen, in D.I. McGregor (Editor), *Proceedings of the Eighth International Rapeseed Congress, Saskatoon, July 9–11, 1991*, Vol. 3, Group Consultatif International de Recherche sur le Colza, Canola Council of Canada, Winnipeg, 1992, p. 822.
15 S. Michaelsen, M.-B. Schrøder and H. Sørensen, *J. Chromatogr. A*, 652 (1993) 503.
16 L. Ingwardsen, S. Michaelsen and H. Sørensen, in preparation.
17 S. Hoffstetter-Kuhn, A. Paulus, E. Gassmann and H.M. Widmer, *Anal. Chem.*, 16 (1991) 1541.
18 M.J. Rosen, *Surfactants and Interfacial Phenomena*, Wiley, New York, 1978, Ch. 3, p. 83.
19 R.O. Cole, M.J. Sepaniak, W.L. Hinze, J. Gorse and K. Oldiges, *J. Chromatogr.*, 557 (1991) 113.
20 J. Snopek, I. Jelinek and E. Smolková-Keulemansová, *J. Chromatogr.*, 452 (1988) 571.
21 C. Schwer and E. Kenndler, *Anal. Chem.*, 63 (1991) 1801.
22 B.B. Van Orman, G.G. Liversigde and G.L. McIntire, *J. Microcol. Sep.*, 2 (1991) 176.
23 T. Tsuda, K. Nomura and G. Nakagawa, *J. Chromatogr.*, 248 (1982) 241.
24 H.T. Rasmussen and H.M. McNair, *J. Chromatogr.*, 516 (1990) 223.

Journal of Chromatography A, 652 (1993) 487–493
Elsevier Science Publishers B.V., Amsterdam

CHROM. 25 159

Determination of theophylline in plasma using different capillary electrophoretic systems

I. Monika Johansson*, Maj-Britt Grön-Rydberg and Birgitta Schmekel

Medical Products Agency, Box 26, S-751 03 Uppsala (Sweden)

ABSTRACT

Theophylline was determined in human plasma by capillary electrophoresis (CE). The drug was used as a model substance to study a simple sample pretreatment often used in HPLC: to 200 μl of plasma were added 400 μl of acetonitrile to precipitate the plasma proteins and the supernatant was injected into the capillary after centrifugation. Three capillary electrophoretic systems were compared with respect to migration time and electrophoretic migration reproducibility. UV detection at 280 nm was applied. The separation was preferably made in an uncoated fused-silica capillary (57 cm × 75 μm I.D.) with 10 m*M* phosphate–borate buffer (pH 9.0) as the electrophoretic buffer. A linear calibration graph was obtained in the concentration range studied, 1.8–36 μg/ml (10–200 μM). The method permits the determination of theophylline in plasma at therapeutic concentrations of 4.5–20 μg/ml (25–110 μM) with acceptable precision.

INTRODUCTION

Capillary electrophoresis (CE) has in recent years become an important separation technique owing to improvements in sensitivity, reliability and speed [1]. Various methods for the determination of drugs in body fluids has been reported recently [2–15]. Detection has been effected by UV absorbance measurements [2–10,12–14], by laser-induced fluorescence [11,14,15] and in one application by a conventional LC fluorescence detector with a laboratory made micro-LC cell [13].

To obtain the required separation for relatively small molecules, micellar phases are often added to the electrophoretic buffer. The fundamental principles of micellar electrokinetic chromatography (MEKC) have been described by Terabe and co-workers [16,17]. Micellar systems have been demonstrated to increase the separation capability for neutral and positively charged compounds. The presence of surfactants such as sodium dodecyl sulphate (SDS) has also been useful to prevent adsorption of plasma proteins on the capillary walls and rinsing with buffer between injections led to reproducibility of migration times when plasma samples were injected directly into the capillary [4,5]. It is more common, however, to rinse the capillary with both sodium hydroxide and buffer between sample injections. Micellar systems with direct injection of plasma or serum samples have been used for the determination of cefiramide [3,4], aspoxicillin [5], barbiturates [6], β-adrenoceptor blocking agents [7], thiopental [8], cicletanine enantiomers [9] and cimetidine [10]. Other sample pretreatments have included liquid–liquid extraction [8,9] and solid-phase extraction [10,11] to concentrate the sample before injection into the capillary.

Several methods for determination of drugs have also been developed without micelles in the electrophoretic buffer. Ferulic acid was determined in dog plasma after liquid–liquid extraction using 25 m*M* phosphate buffer (pH 9.2) [2]. Cytosine-β-D-arabinoside was determined in

* Corresponding author.

0021-9673/93/$06.00

plasma after solid-phase extraction using citrate buffers [12]. Thiols were determined in human whole blood after pretreatment and derivatization using 0.1 *M* phosphate buffer (pH 2.5) [13]. Naproxen was determined in serum after extraction with hexane–diethyl ether. The residue was dissolved in water–ethanol (1:1) and about 10 nl were injected hydrodynamically into the capillary [14]. Anthracyclines in human plasma were determined after liquid–liquid extraction with chloroform and back-extraction into phosphoric acid. Analyte interaction with the capillary wall was prevented by using 70% acetonitrile in phosphate buffer as the electrophoretic buffer [15].

Methanol and acetonitrile have been added to the electrophoretic buffer to improve the separation [9,11] or to increase the detection response in atmospheric pressure ionization mass spectrometry [18]. Addition of acetonitrile, methanol and other organic solvents to the electrophoretic buffers reduces the electroosmotic flow in the capillary [19,20].

A simple plasma sample pretreatment in HPLC is to add methanol, acetonitrile or a strong acid to remove proteins from the plasma sample before injection on to the LC column [21]. The technique is used for compounds that are present in high concentrations where no preconcentration of the samples is needed and for hydrophilic compounds that have low recoveries in liquid–liquid extraction procedures. We were interested in exploring the technique for CE and to investigate whether it is possible to inject plasma extracts on to the capillary that contained high concentrations of acetonitrile. Theophylline was chosen as a model substance because the drug is often present in high concentrations in human plasma after therapeutic doses.

It was possible to detect theophylline in therapeutic concentrations of 4.5–20 μg/ml (25–110 μM) with acceptable precision. Three electrophoretic systems were compared with respect to migration time and electrophoretic mobility for theophylline when repeated injections of theophylline dissolved in dilute electrophoretic buffers and in plasma extract were made.

EXPERIMENTAL

Materials

Theophylline was kindly obtained from Kabi Biopharma (Stockholm, Sweden). Acetonitrile was of LiChrosolv quality (E. Merck, Darmstadt, Germany) and water was purified with a Milli-Q reagent water system (Millipore, Bedford, MA, USA). All other chemicals were of analytical-reagent grade and were used as received.

Capillary electrophoresis instrumentation and methods

A Beckman (Palo Alto, CA, USA) P/ACE System 2100 capillary electrophoresis system was used. The electrophoretic separation was performed either in a fused-silica capillary, eCAP (Beckman), or in a coated capillary, CElect H175 (Supelco, Bellefonte, PA, USA). The dimensions were 57 cm × 75 μm I.D. × 375 μm O.D. The electrophoretic buffers were prepared from an aqueous solution of sodium dihydrogenphosphate to which disodium tetraborate decahydrate solution was added to give pH 9.0. Sodium dodecyl sulphate (SDS), 25 m*M*, was added to the final solution in some of the experiments. The buffers were filtered through a 0.45-μm Miller-HV filter (Millipore) prior to use. Hydrodynamic injections were made by applying a 0.5 p.s.i. (3.45 kPa) pressure for 1–5 s using the "low-pressure" device in the instrument at the inlet end of the capillary. Detection was performed by on-column measurement of UV absorbance at 280 nm at a position 50 cm from the capillary inlet. All separations were performed at 12 kV. The current was continuously monitored during analysis using the second data collection channel in the P/ACE.

Reproducibility of migration times. Variations in migration times and electrophoretic mobilities after repeated injections of plasma samples were first studied using uncoated capillaries. Study 1 was performed with an electrophoretic buffer consisting of 25 m*M* SDS in 10 m*M* sodium phosphate–borate buffer (pH 9.0) and study 2 with 10 m*M* sodium phosphate–borate buffer (pH 9.0) as the electrophoretic buffer. To each

experiment a new uncoated fused-silica capillary (eCAP) was used. The new uncoated capillary was rinsed for 5 min with 1 *M* sodium hydroxide solution, 2 min with water, 2 min with 0.1 *M* hydrochloric acid and 2 min with water by pressurizing the inlet of the capillary at 138 kPa ("high pressure") using the standard pressure device of the CE instrument followed by 30 min with electrophoretic buffer using the "low-pressure" device. Thereafter nine determinations of acetone (10% solution in water) were made to monitor the electroosmotic flow in the capillary. Acetone was injected for 1 s (5 nl injected).

A 10 μg/ml standard solution of theophylline in the electrophoretic buffer diluted 1:10 with water and plasma extracts with theophylline (see *Sample preparation*) was then injected. One injection of theophylline standard solution was followed by five injections of plasma extract from the same vial. The cycle was repeated 7–9 times. The theophylline sample was injected for 5 s (26 nl injected). Acetone was also injected (1 s) with each theophylline sample to monitor the electroosmotic flow.

A standardized washing procedure, 1 min with 0.1 *M* sodium hydroxide solution and 3 min with electrophoretic buffer using "high pressure", was applied before each injection. Study 1 was repeated once and in the second experiment the capillary was rinsed for 4 min with electrophoretic buffer only before injections. The separation was made at 12 kV for 10 min.

Study 3 was performed with a coated capillary. The coated capillary (CElect) was treated according to the manufacturer's instructions, *i.e.*, no initial washing procedure was performed. The electrophoretic buffer was 20 m*M* sodium phosphate–borate (pH 9.0). The equilibration of the capillary with buffer was monitored by the injection of acetone as described above, performing a separation at 12 kV for 10 min. Then the same cycle, one injection of theophylline standard solution followed by five injections of plasma extracts with theophylline (3 s), was performed. With each injection acetone was also injected (1 s) to monitor the electroosmotic flow. The separation was made at 12 kV for 26 min. Before each injection, the capillary was rinsed for 1 min with 0.1 *M* sodium hydroxide solution and 3 min with electrophoretic buffer using "high pressure".

A capillary equilibrated with 25 m*M* SDS in 10 m*M* sodium phosphate–borate buffer (pH 9.0) was filled with buffer diluted 1:10 with water (study 4) and plasma extract (study 5) to simulate the injection situations. Acetone and standard theophylline solution were then injected and the migration times of the compounds were monitored when 12 kV was applied.

Calculations. The calculation of column efficiency was based on $N = 5.54\ (t_m/w_{0.5})^2$, where N is the number of theoretical plates, t_m is the migration time of the compound and $w_{0.5}$ is the peak width at half-height.

The electroosmotic flow, u_{eo}, was calculated by $u_{eo} = L_d L_t / V t_0$, where L_d is the capillary length to the detector, L_t the total length of the capillary, V the applied voltage and t_0 the time for a neutral marker (acetone) to reach the detector [1]. The observed electrophoretic mobility, $u_{ep,obs}$, was calculated in a similar way using t_m, the migration time for the substance. The mobility of the substance, u_{ep}, was then obtained from the relationship $u_{ep} = u_{ep,obs} - u_{eo}$.

The injection volume was calculated from the flow obtained in the capillary during injection. The flow was measured from the time, t_n, needed for a neutral compound to reach the detector applying the "low-pressure" device in the instrument and the volume of the capillary to the detector, $(\pi r^2 L_d)/t_n$.

Sample preparation

Stock solutions of theophyline were prepared in methanol and further dilutions were made with 0.05 *M* phosphate buffer (pH 7.4).

A calibration graph for theophylline in plasma was prepared from plasma samples containing 0.45, 0.9, 1.8, 2.7, 4.5, 9.0, 18, 27 and 36 μg/ml. Quality control plasma samples of theophylline contained 2.7, 9.0 and 18 μg/ml. The plasma samples were stored at −20°C until analysed.

In the work-up procedure, plasma samples were deproteinized with acetonitrile. To 200 μl plasma were added 400 μl of acetonitrile in an

Eppendorff tube. The tubes were capped, shaken for 2–3 min and centrifuged at 6890 *g* (6000 rpm) for 5 min. The supernatant was transferred into a 400-μl vial inserter and injected into the CE. The plasma extract for the reproducibility studies was prepared in the same way in a large batch and stored at −70°C until used. The concentration of theophylline in plasma was 10 μg/ml.

When plasma samples from patients were analysed the CE conditions used in study 2 described above were used. Daily the capillary was rinsed for 5 min with 1 *M* sodium hydroxide solution, 2 min with water, 2 min with 0.1 *M* hydrochloric acid and 2 min with water using "high pressure" and then equilibrated with electrophoretic buffer for 30 min using "low pressure".

RESULTS AND DISCUSSION

The described CE instrumentation offers the possibility of obtaining highly reproducible results owing to the standardized washing procedure that can be programmed and automation of injection. Three different CE systems were compared to obtain the best CE system for the determination of theophylline in plasma with little sample pretreatment.

Reproducibility of migration times

The results from study 1 are given in Fig. 1, where the obtained run-to-run variability for acetone, standard theophylline dissolved in buffer diluted 1:10 with water, theophylline in plasma extract and an endogenous plasma peak are shown. Fig. 1A gives the migration times found. The relative standard deviation (R.S.D.) of the migration time for theophylline in the plasma extract was 2.1% (36 injections) and 0.54% of the standard theophylline (8 injections). After a total of 55 injections some erroneous values were obtained with unexpectedly long migration times. When the capillary had been rinsed using the same procedure as for a new capillary, the migration times were restored.

When study 1 was repeated with a 4-min rinse with buffer only between sample injections, the theophylline peak in the plasma extract disappeared after ten injections whereas the endogenous plasma peak could still be recorded. It seems that theophylline was adsorbed on the capillary walls when the capillary was rinsed only with buffer between injections. Other systems, in which plasma was injected directly, have been reported to be stable when the capillary was rinsed with buffer between injections [4,5]. These separations were performed in 50 μm I.D. capillaries with 20 m*M* buffers. Theophylline standard solution injected dissolved in dilute buffer gave the same result as in Fig. 1A, *i.e.*, R.S.D. = 0.72% for the migration time (eight injections).

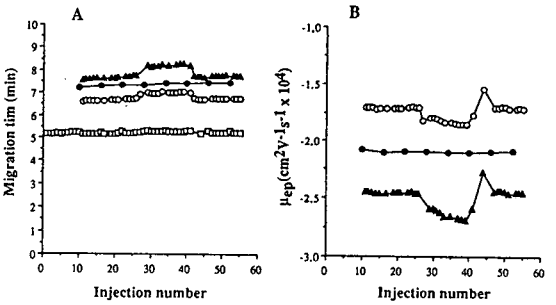

Fig. 1. Reproducibility in micellar capillary electrophoresis. Capillary, uncoated fused silica, 75 μm I.D. × 57 cm, 50 cm to the detector; temperature, 30°C; voltage, 12 kV; current, 31 μA; buffer, 25 m*M* SDS in 10 m*M* phosphate–borate buffer (pH 9.0); injection volume, 26 nl (5-s pressure injection). (A) Variation of migration times for repeated injections; (B) variation of electrophoretic mobility for repeated injections. □ = Acetone; ● = theophylline (standard); ○ = theophylline (plasma); ▲ = endogenous plasma peak.

The electrophoretic mobilities for the compounds were calculated and are given in Fig. 1B. The graph shows that fluctuations in the electroosmotic flow could not explain the larger variation in migration times for theophylline in the plasma extract compared with theophylline dissolved in dilute buffer. The variations in the electrophoretic mobility for theophylline in plasma extract and the endogenous plasma peak with time are the same. It can also be noticed that theophylline in the plasma extract has a shorter migration time than theophylline dissolved in dilute buffer. Theophylline is negatively charged to 70% at pH 9.0 and did not seem to be partitioned into the micelles as the electrophor-

etic mobility for the standard theophylline was roughly the same with and without SDS in the electrophoretic buffer (compare Figs. 1B and 2B).

For study 2, the migration times for 60 injections are shown in Fig. 2A. After 39 injection there was a break in power and the system was stopped for 10 h. The study was continued without any additional washing of the capillary. A small jump in migration times can be seen in Fig. 2A after 39 injections but they remained fairly constant. Inspection of the peak shape for the theophylline plasma peak showed, however, a tendency for fronting. The asymmetry factor was 0.62 for theophylline for the first injection of plasma extract after the stop. This fronting of the peaks increased thereafter and the last set of plasma samples had asymmetry factors of about 0.31. This can be compared with asymmetry factors in the range 0.94–1.04 before the stop. We concluded that some adsorption of plasma components on the capillary wall occurred during the run and that additional washing was needed after a certain number of injections. The R.S.D. for the migration time of theophylline in the plasma extract was 1.8% (40 injections).

The electrophoretic mobility was calculated for each run and is shown in Fig. 2B. There is also a tendency in this system for theophylline in plasma extracts to migrate faster than theophylline standard, but the differences between the electrophoretic mobility for theophylline standard and theophylline in plasma extracts are much smaller than in study 1.

In study 3, a coated capillary (CElect) was used. In this system the injection volumes had to be decreased from 26 to 16 nl (3-s injections). The design of the study was the same as for the earlier studies but the separation time was increased to 26 min owing to the longer migration times of the compounds in this system. The migration times for acetone, theophylline standard and plasma extract are given in Fig. 3A and the electrophoretic mobilities in Fig. 3B. The plasma peak was not recorded owing to the long migration time. The migration times for theophylline increase with time and the fluctuations in migration times are very pronounced for theophylline in the plasma extract, R.S.D. = 10% (fourteen injections). The electrophoretic mobility of theophylline in the plasma extract was surprisingly constant, R.S.D. = 0.65%. The observed variation in migration times seems to be due to changes in the electroosmotic flow during the study. Acetonitrile may interact with the capillary wall and the coating does not seem to be compatible with acetonitrile. Very stable migration times have been reported on this type of capillary when peptides and proteins were injected in a pure aqueous system [22].

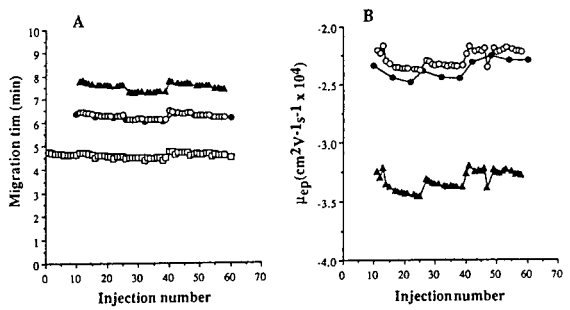

Fig. 2. Reproducibility in capillary electrophoresis. Capillary, uncoated fused silica, 75 μm I.D. × 57 cm, 50 cm to the detector; temperature, 30°C; voltage, 12 kV; current, 20 μA; buffer, 10 m*M* phosphate–borate buffer (pH 9.0); injection volume, 26 nl (5-s pressure injection). (A) Variation of migration times for repeated injections; (B) variation of electrophoretic mobility for repeated injections. Symbols as in Fig. 1.

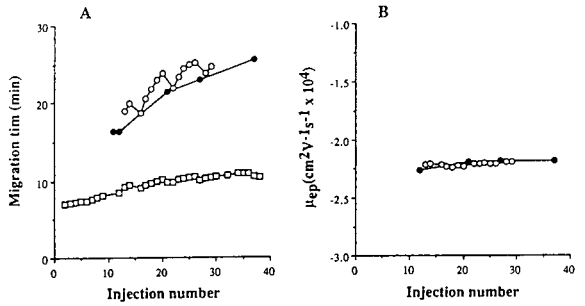

Fig. 3. Reproducibility in capillary electrophoresis. Capillary, coated, CElect, 75 μm I.D. × 57 cm, 50 cm to the detector; temperature, 30°C; voltage, 12 kV; current, 37 μA; buffer, 20 m*M* phosphate–borate buffer (pH 9.0); injection volume, 16 nl (3-s pressure injection). (A) Variation of migration times for repeated injections; (B) variation of electrophoretic mobility for repeated injections. Symbols as in Fig. 1.

Sample solvent and electroosmotic flow

It is preferable to inject the sample in a solvent where the conductivity of the sample is lower than in the surrounding buffer. The sample will then move very fast to the boundary between the injection plug and the buffer solution when the voltage is applied. A concentration of the sample at the boundary occurs and highly efficient peaks are obtained. A threefold improvement in detectability has been reported for peptides injected dissolved in water compared to the electrophoretic buffer [23].

In our studies, theophylline was negatively charged and was swept toward the cathode and the detector by the electroosmotic flow in the capillary. To obtain an idea of the velocities in the injection plug, studies 4 and 5 were performed. For a tenfold dilution of the electrophoretic buffer with water, $u_{ep,obs} = 8.0 \cdot 10^{-4}$ was calculated for theophylline. In the plasma extract, however, a much lower value, $u_{ep,obs} = 1.5 \cdot 10^{-4}$, was obtained. This was the lowest value of $u_{ep,obs}$ obtained in all the electrophoretic buffers used in studies 1–3 (Table I).

Addition of 50% of acetonitrile to the electrophoretic buffer has been shown to reduce the electroosmotic flow by *ca.* 40% [19,20]. We observed a small decease in u_{eo} in studies 2 and 3 when plasma extracts were injected. In contrast, in study 1, with SDS present a small increase in u_{eo} was observed for the plasma extracts.

A strong electroosmotic flow in the capillary seems desirable for our separation. The same high efficiency, $N = 210\,000$, was obtained for the theophylline peaks, injected dissolved in dilute buffer and in the plasma extract, in study 2 with the highest electroosmotic flow. Highly efficient peaks were obtained despite the long injection plug of 6 mm for a 26-nl injection.

The discontinuity of the solvent in the capillary caused a decrease in current over the capillary until the injection plug had migrated to the capillary end. This was most pronounced for the plasma extracts with SDS in the system. Electropherograms of theophylline are given in Fig. 4 together with the recorded current. Fig. 4A shows theophylline dissolved in dilute buffer

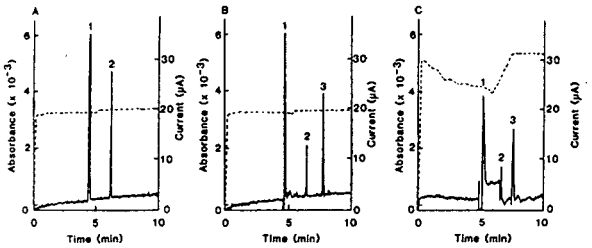

Fig. 4. Electropherograms of theophylline. (A) Standard theophylline, 10 μg/ml, dissolved in electrophoretic buffer diluted 1:10 with water; (B) plasma extract with theophylline, corresponding to 10 μg/ml plasma. Conditions in (A) and (B) as in Fig. 2. (C) Plasma extract with theophylline, corresponding to 10 μg/ml plasma. conditions as in Fig. 1. Peaks: 1 = acetone (neutral marker for the electroosmotic flow); 2 = theophylline; 3 = endogenous plasma peak.

TABLE I

ELECTROOSMOTIC FLOW AND OBSERVED ELECTROPHORETIC MOBILITY FOR THEOPHYLLINE IN DIFFERENT SYSTEMS

Conditions: 1 = 25 m*M* SDS in 10 m*M* phosphate–borate buffer (pH 9.0); 2 = 10 m*M* phosphate–borate buffer (pH 9.0); 3 = 20 m*M* phosphate–borate buffer (pH 9.0); 4 = buffer 1 diluted 1:10 with water; 5 = plasma extract (mainly acetonitrile); voltage, 12 kV; temperature, 30°C.

Samples: a = theophylline (10 μg/ml), dissolved in electrophoretic buffer diluted 1:10 with water; b = theophylline in plasma extract. Injection volume = 16 nl in system 3 and 26 nl in the other systems.

Parameter	1		2		3		4	5
	a	b	a	b	a	b	a	a
μ_{eo} (10^{-4} cm^2 V^{-1} s^{-1})	7.48	7.55	8.76	8.62	4.0	3.9	10	2.2
$\mu_{ep,obs}$ (10^{-4} cm^2 V^{-1} s^{-1})	5.38	5.81	6.40	6.35	1.8	1.7	8.0	1.5

from study 2. The same current profile was obtained for standard theophylline with SDS in the electrophoretic buffer. Fig. 4B shows theophylline in plasma extract from study 2 and Fig. 4C theophylline in plasma extract from study 1. To obtain reproducible results, standards and samples should be prepared in the same solvent.

Analysis of plasma samples

The electrophoretic conditions used in study 2 were chosen for the determination of theophylline in plasma from patients. The procedure was studied in the range 1.8–36 μg/ml. The correlation coefficient was 0.996 ($y = 0.024 + 0.162x$) for the calibration graph (peak-height measurements). Plasma samples from patients were analysed together with three quality control samples in each series. Two electropherograms are shown in Fig. 5A and B. The plasma sample in Fig. 5B contained theophylline (6.9 μg/ml). The reproducibility (between-series) was 8.0% at a level of 2.7 μg/ml, 4.4% at 9.0 μg/ml and 2.6% at 18 μg/ml. The limit of determination was 1.8 μg/ml (10 μM).

The reproducibility was of the same order as for our standard HPLC method [24]. The limit of determination for theophylline in plasma was lower with HPLC, however, 0.45 μg/ml (2.5 μM).

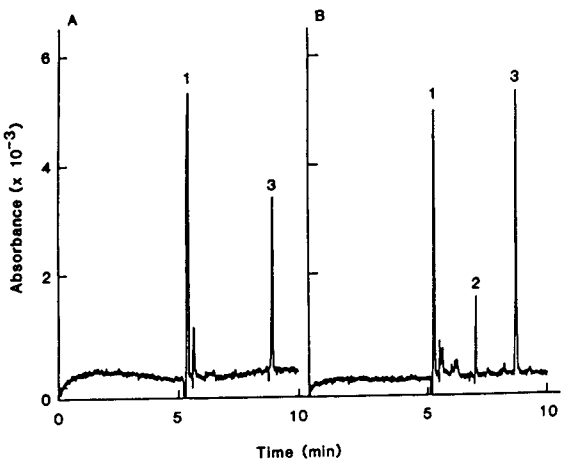

Fig. 5. Electropherograms of plasma samples. (A) Blank plasma; (B) plasma sample from a patient, containing theophylline (6.9 μg/ml). Conditions as in Fig. 2. Peaks as in Fig. 4.

This study has shown that it is possible to determine theophylline in plasma at therapeutic concentrations by CE with acceptable precision.

REFERENCES

1 S.F.Y. Li, *Capillary Electrophoresis*, Elsevier, Amsterdam, 1992.
2 S. Fujiwara and S. Honda, *Anal. Chem.*, 58 (1986) 1811.
3 T. Nakagawa, Y. Oda, A. Shibukawa and H. Tanaka, *Chem. Pharm. Bull.*, 36 (1988) 1622.
4 T. Nakagawa, Y. Oda, A. Shibukawa, H. Fukuda and H. Tanaka, *Chem. Pharm. Bull.*, 37 (1989) 707.
5 H. Nishi, T. Fukuyama and M. Matsuo, *J. Chromatogr.*, 515 (1990) 245.
6 W. Thormann, P. Meier, C. Marcolli and F. Binder, *J. Chromatogr.*, 545 (1991) 445.
7 P. Lukkari, H. Siren, M. Pantsar, A. Ennelin and M.L. Riekkola, presented at the *8th International Symposium on Capillary Electrophoresis and Isotachophoresis, Rome, October 1992*, poster 44.
8 P. Meier and W. Thormann, *J. Chromatogr.*, 559 (1991) 505.
9 J. Prunososa, R. Obach, A. Diez-Cascón and L. Gousesclou, *J. Chromatogr.*, 574 (1992) 127.
10 H. Soini, T. Tsuda and M.V. Novotny, *J. Chromatogr.*, 559 (1991) 547.
11 M.C. Roach, P. Gozel and R.N. Zare, *J. Chromatogr.*, 426 (1988) 129.
12 D.K. Lloyd, A.M. Cypress and I.W. Wainer, *J. Chromatogr.*, 568 (1991) 117.
13 B. Lin Ling, W.R.G. Baeyens and C. Dewaele, *Anal. Chim. Acta*, 255 (1991) 283.
14 H. Soini, M.V. Novotny and M.-L. Riekkola, *J. Microcol. Sep.*, 4 (1992) 313.
15 N.J. Reinhound, U.R. Tjaden, H. Irth and J. van der Greef, *J. Chromatogr.*, 574 (1992) 327.
16 S. Terabe, K. Otsuka, K. Ichikawa, A. Tsuchiya and T. Ando, *Anal. Chem.*, 56 (1984) 111.
17 S. Terabe, K. Otsuka and T. Ando, *Anal. Chem.*, 57 (1985) 834.
18 I.M. Johansson, R. Pavelka and J.D. Henion, *J. Chromatogr.*, 559 (1991) 515.
19 C. Schwer and E. Kenndler, *Anal. Chem.*, 63 (1991) 1801.
20 B.B. VanOrman, G.G. Liversidge and G.L. McIntire, *J. Microcol. Sep.*, 2 (1991) 176.
21 J. Blanchard, *J. Chromatogr.*, 226 (1981) 455.
22 G. Piccoli, B. Biagiarelli, F. Palma, L. Potenza, M. Fiorani, L. Vallorani, L. Cucchiarini and V. Stocchi, presented at the *8th International Symposium on Capillary Electrophoresis and Isotachophoresis, Rome, October 1992*, poster 68.
23 S.E. Moring, J.C. Colburn, P.D. Grossman and H.H. Lauer, *LC · GC*, 8 (1990) 34.
24 K.C. van Horne and T. Good, *International Clinical Products Review*, September (1983) 14.

Journal of Chromatography A, 652 (1993) 495–501
Elsevier Science Publishers B.V., Amsterdam

CHROM. 25 307

Separation of water-soluble vitamins via high-performance capillary electrophoresis

Ulrike Jegle

Hewlett-Packard GmbH, Waldbronn Analytical Division, Hewlett-Packard-Strasse 8, 76337 Waldbronn (Germany)

ABSTRACT

A standard sample and method for performance evaluation in capillary zone electrophoresis is defined. The sample, containing thiamine, nicotinamide and nicotinic acid, was analysed in a 20 m*M* sodium phosphate buffer pH 7. The impact of pH, buffer type and ionic strength on electroosmotic flow, electrophoretic mobility, and peak shape was investigated. The separation of several water-soluble vitamins in phosphate buffer pH 7 was developed in order to analyse an over-the-counter vitamin preparation. Spectral analysis and peak purity tests were applied on-line for peak identification.

INTRODUCTION

Capillary electrophoresis (CE) is a relatively new analytical method currently under investigation for routine use in industrial laboratories. There is still no complete understanding of parameters that influence the separation process for CE. The purpose of this investigation was to define a standard sample and method for performance evaluation and system suitability test in capillary zone electrophoresis (CZE). It is desirable for the standard sample and method to have the following features:

(1) The standard should contain substances of different charge types to demonstrate the separation principle of the zonal technique.

(2) To provide good signal-to-noise ratios, the substances should have high molecular extinction coefficients in the UV–Vis range.

(3) The standard separation should provide good peak area and time reproducibility.

The vitamins thiamine, nicotinamide and nicotinic acid satisfy these requirements.

These well-defined standards allow the study of fundamental parameters in CZE. In this context the impact of different analysis conditions, such as buffer type, ionic strength and pH, on the performance of the standard separation were investigated. In addition, a separation method for several water-soluble vitamins was developed in order to analyse an over-the-counter vitamin tablet preparation. This study demonstrates the impact of matrix effects in CZE.

Previously, separations of vitamins have been reported using high-performance liquid chromatography (HPLC) [1–5]. This technique requires gradient elution and suffers from poor efficiency and peak tailing [4,5]. In CE, vitamins have been separated using micellar electrokinetic capillary chromatography (MECC) [6–9]. The application of micelles leads to complex equilibrium states before separation occurs. This complexity and diversity makes understanding and optimization difficult. In this study, a simplified approach using CZE was taken.

EXPERIMENTAL

Apparatus

A Hewlett-Packard (Waldbronn, Germany) three-dimensional capillary electrophoresis system was used in all measurements. The fused-

0021-9673/93/$06.00

silica capillaries (50 μm I.D., straight and with extended path length detection cell) are available from Hewlett-Packard.

Chemicals

Thiamine hydrochloride (vitamin B_1 hydrochloride), nicotinamide (vitamin PP), nicotinic acid (vitamin B_3), pyridoxine hydrochloride (vitamin B_6 hydrochloride), cyanocobalamin (vitamin B_{12}), folic acid calcium salt pentahydrate (vitamin B_8), all BioChemika grade, and orotic acid (vitamin B_{13}) of analytical grade were obtained from Fluka (Buchs, Switzerland). L-Ascorbic acid (vitamin C) and calcium D (+) pantothenate, both biochemistry grade, were obtained from Merck (Darmstadt, Germany). HPCE-grade sodium phosphate buffer pH 7, sodium tetraborate buffer pH 8 and sodium citrate buffer pH 5, all 20 m*M*, were provided by Fluka.

Sample preparation

The standard vitamins, thiamine, nicotinamide and nicotinic acid, were dissolved in water (each 0.001 *M*). The resulting pH of the solution was 3.5. The samples including all vitamin compounds (each 0.001 *M*, except calcium folinate and ascorbic acid, each 0.015 *M*) were dissolved in citrate buffer pH 5 since folinate is not stable at lower pH values. The over-the-counter vitamin preparation was ground, dissolved in pH 5 buffer, filtered through a 0.2-μm syringe filter and injected immediately.

Analysis conditions

For optimal performance, the capillaries were preconditioned for 10 min with 1.0 *M* NaOH, for 2 min with 0.1 *M* NaOH and finally for 3 min with run buffer before the first use. Between runs, capillaries were flushed for 2 min with 0.1 *M* NaOH and 3 min with run buffer. In order to ensure area reproducibility, subsequent injection of a buffer plug was necessary.

RESULTS AND DISCUSSION

Standard separation method

The vitamins thiamine, nicotinamide and nicotinic acid selected as standards were separated in a fused-silica capillary. Sodium phosphate buffer pH 7, 20 m*M*, was used as electrolyte. Several electropherograms of a sequence of 42 runs are shown in Fig. 1.

Through the relationship of mobility vectors:

$$\mu_{total} = \mu_{EOF} + \mu_{mobility} \quad (1)$$

it is anticipated that, given a constant electroosmotic flow (EOF), components will separate reproducibly according to their electrophoretic mobility. In this example the first-eluting compound is expected to be thiamine, which carries a permanent positive charge. Since nicotinamide is neutral at pH 7, it is transported with the velocity of the EOF and can therefore be used as an EOF marker. Nicotinic acid, which is negatively charged at the chosen pH, eluted last.

The average migration times and areas as well as the values for the relative standard deviation (R.S.D.) are given in Table I. The R.S.D. values of all compounds were about 0.5% for migration time and 1.7% for the peak area over 42 injections. Theoretical plate numbers of 179 809,

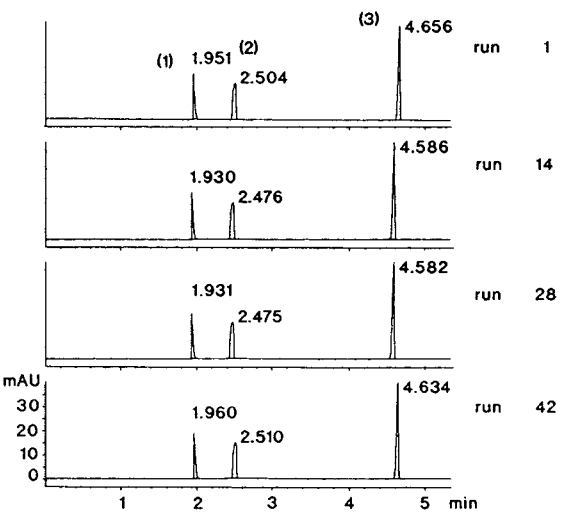

Fig. 1. Reproducibility of the standard separation method. Capillary: fused-silica, I.D. 50 μm, straight, length to detector 400 mm, total length 485 mm. Sample and peak identification: 1 = thiamine hydrochloride; 2 = nicotinamide; 3 = nicotinic acid dissolved in water. Injection pressure: 4.6 s at 40 mbar. Post-injection pressure: 4 s at 40 mbar. Run buffer: 20 m*M* sodium phosphate pH 7, run buffer replenishment every third run. Separation: polarity positive, voltage 20 kV, capillary temperature 25°C. Detection: 215 nm.

TABLE I

REPRODUCIBILITY OF STANDARD VITAMIN SEPARATION

Capillary: fused-silica, I.D. 50 μm, straight, length to detector 400 mm, total length 485 mm. Sample: 0.001 *M* each thiamine hydrochloride, nicotinamide, nicotinic acid (in water). Injection pressure: 4.6 s at 40 mbar. Post-injection pressure (run buffer): 4 s at 40 mbar. Run buffer: 20 m*M* sodium phosphate buffer pH 7, run buffer replenishment every third run. Separation: polarity positive, voltage 20 kV, capillary temperature 25°C.

	Migration time (min)	Peak width	Peak area (not time corrected)
Thiamine			
Average (42 runs)	1.937	0.017	25.38
R.S.D. (%)	0.52	1.58	1.68
Nicotinamide			
Average	2.485	0.048	43.40
R.S.D. (%)	0.49	8.36	1.67
Nicotinic acid			
Average	4.600	0.025	69.04
R.S.D. (%)	0.48	0.61	1.71

371 121 and 468 906 per metre were calculated for the peaks of thiamine, nicotinamide and nicotinic acid, respectively.

Influencing parameters

The impact of pH, buffer type and ionic strength on EOF and electrophoretic mobility of the solutes as well as on the peak shape was examined.

Four different buffers —sodium phosphate buffer pH 7 and 8, sodium tetraborate buffer pH 8 and sodium citrate buffer pH 6— were used to test the influence of the described parameters. The concentration of each buffering ion was 20 m*M*. The ionic strength of these buffers was increased from tetraborate pH 8 to phosphate pH 7 and pH 8 and to citrate pH 6 using sodium as the counter ion. The data for ionic strength of the buffers, the EOF and the electrophoretic mobilities of the solutes are summarized in Table II. Increasing the pH of buffers used in unmodified fused-silica capillaries is known to in-

TABLE II

IONIC STRENGTH, ELECTROOSMOTIC FLOW AND ELECTROPHORETIC MOBILITIES CALCULATED FOR DIFFERENT BUFFERS

Capillary: fused-silica, I.D. 50 μm, length to detector 608 mm. Sample: 0.001 *M* each thiamine hydrochloride, nicotinamide, nictonic acid (in water). Injection pressure: 4.6 s at 40 mbar. Post-injection pressure: 4 s at 40 mbar. Run buffer 1: 20 m*M* sodium phosphate buffer pH 7. Run buffer 2: 20 m*M* sodium phosphate buffer pH 8. Run buffer 3: 20 m*M* sodium tetraborate buffer pH 8. Separation: polarity positive, voltage 25 kV, capillary temperature 25°C.

Buffer	Ionic strength	Thiamine mobility (10^{-4} cm^2 V^{-1} s^{-1})	EOF (10^{-4} cm^2 V^{-1} s^{-1})	Nicotinic acid mobility (10^{-4} cm^2 V^{-1} s^{-1})
Sodium tetraborate pH 8	0.0235	0.93	5.63	−1.94
Sodium phosphate pH 7	0.0352	1.04	3.91	−1.77
Sodium phosphate pH 8	0.0548	1.03	3.77	−1.78
Sodium citrate pH 6	0.0772	1.45	5.54	−2.90

crease the EOF. In contrast, increasing the ionic strength has the opposite effect: the EOF is decreased. In the series of tetraborate buffer to phosphate buffers of pH 7 and 8 listed in Table II the EOF decreased as expected. The electrophoretic mobilities of thiamine and nicotinic acid changed only little in this series. Although in the case of citrate buffer both the pH and the ionic strength led to the expectation that the EOF should decrease further, the opposite occurred. The electrophoretic mobilities of the solutes in citrate buffer differed significantly compared with those observed in the other three buffers. This effect is not yet understood. Further investigations are under way. Comparison of the EOF measured for the different buffers and the electrophoretic mobilities of the vitamin compounds in these buffers (Table II) indicated that, besides the ionic strength and the pH, the buffer type is a third important parameter determining the EOF and the zeta potential. Depending on the buffer type, different kinds of interactions of buffering ions with the silica surface occur. Phosphate is known to chemically modify the fused-silica surface [10,11], whereas other anions dynamically interact with the surface. Thus buffer ion type may have an influence not only on the surface zeta potential and on the counter-ion shielding of the solute, but also on the nature of solute–surface interactions. Systematic measurements with more buffer systems are necessary to clarify these assumptions.

The ionic strength of a run buffer has an important impact on the peak shape and therefore on the efficiency of the separation. Fig. 2 shows a series of standard vitamin separations in 20 m*M* tetraborate buffer solution pH 8, in which the ionic strength has been increased by adding the neutral salt sodium chloride to the run buffer. The amounts of added salt are summarized in Table III. This table also shows the number of theoretical plates calculated for the three standard vitamins depending on the ionic strength of the buffer system. With increasing sodium concentration the plate numbers of the thiamine peaks increased strongly and the tailing peak developed to an almost Gaussian peak. This behaviour can be explained by competitive ion-exchange properties of sodium ions

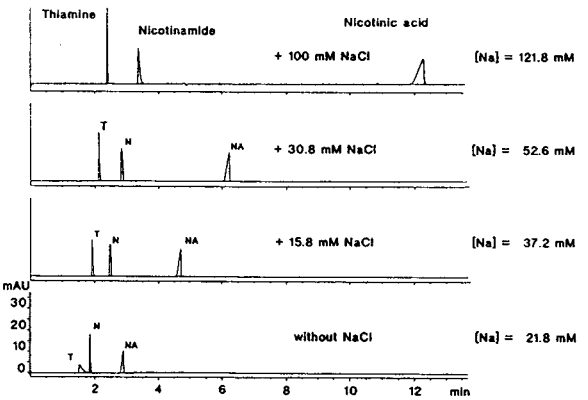

Fig. 2. Peak shape dependence on ionic strength. The ionic strength of a 20 m*M* sodium tetraborate buffer pH 8 was increased by adding different amounts of the neutral salt sodium chloride to the solution. For conditions, see Fig. 1.

versus the positively charged thiamine. In contrast, the peak shape of nicotinic acid is determined by isotachophoretic effects. The fronting effect of the peak increased with increasing conductivity of the anions in the buffer (Fig. 2). It has to be considered that within the test set-up not only the conductivity of the buffer was changed but also the electrolyte type from mainly tetraborate to mainly chloride. It is known from the theory of isotachophoretic separations that electrolyte type has an impact on solute mobility.

Separation of water-soluble vitamins

The separation of the eight water-soluble vitamins was performed under the sample conditions as previously stated except that a longer capillary with an extended path length detection cell was used. The capillary was selected to improve separation and detection properties. Fig. 3 shows the separation of the vitamins at different wavelengths optimized for the different analytes. Peak identification was performed by single analyte injection and on-line spectral comparison. Peak purity was tested by measurements of spectral differences at several points of the peak considered. These tests indicated no impurities in the obtained peaks.

Using buffer without micellar additives for the analysis an electrophoretic separation of neutral vitamins is not possible. Nevertheless, a quantitative determination of these compounds is

TABLE III

NUMBER OF THEORETICAL PLATES DEPENDING ON IONIC STRENGTH

Capillary: fused-silica, I.D. 50 μm, straight, length to detector 400 mm, total length 485 mm. Sample: 0.001 *M* each thiaminehydrochloride, nicotinamide, nicotinic acid (in water). Injection pressure: 4.6 s at 40 mbar. Post-injection pressure (run buffer): 4 s at 40 mbar. Run buffer: 20 m*M* sodium tetraborate pH 8 plus various amounts of sodium chloride, run buffer replenishment. Separation: polarity positive, voltage 20 kV, capillary temperature 25°C. *N* = Number of theoretical plates.

	N/m			
	Tetraborate without NaCl	Tetraborate +15.4 m*M* NaCl	Tetraborate +30.8 m*M* NaCl	Tetraborate +100 m*M* NaCl
Thiamine	5120	74 900	135 993	273 975
Nicotinamide	15 111	36 823	36 123	62 843
Nicotinic acid	66 762	101 139	109 301	85 515

possible by using spectral suppression. This is shown for nicotinamide and cyanocobalamin in the electropherograms of Fig. 4, in which both vitamins are separated from other vitamins. The determination of nicotinamide was performed at 260 nm, at which wavelength the spectral absorbance of cyanocobalamin could be suppressed by its reference absorbance at 285 nm. Cyanocobalamin has an absorption maximum at 360 nm and a lower one at 550 nm. As nicotinamide showed no absorption at these wavelengths, a quantitative determination of cyanocobalamin can be carried out without any interference.

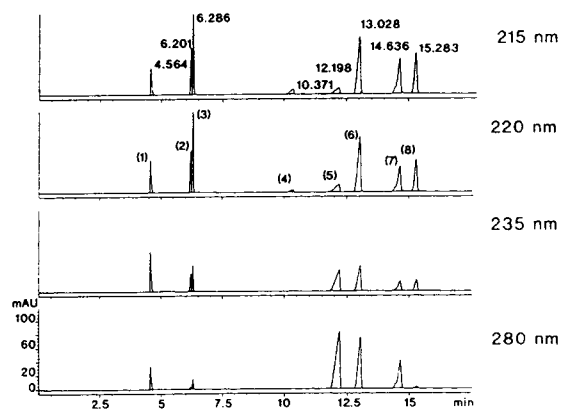

Fig. 3. Separation of eight water-soluble vitamins. Capillary: fused-silica, I.D. 50 μm, extended path length detection cell, length to detector 560 mm, total length 645 mm. Sample and peak identification: 1 = thiamine hydrochloride; 2 = nicotinamide; 3 = pyridoxine; 4 = pantothenate; 5 = ascorbic acid; 6 = folinate; 7 = orotic acid; 8 = nicotinic acid dissolved in citrate buffer pH 5. For conditions, see Fig. 1.

Analysis of an over-the-counter vitamin preparation

The above-described separation of eight water-soluble vitamins was taken as reference for determining the ingredients of an over-the-counter vitamin preparation (tablet). Fig. 5 shows the analysis of the vitamin tablet in comparison with the reference separation of the vitamins in phosphate buffer pH 7. Thiamine, nicotinamide, pyridoxine, pantethonate and ascorbic acid were identified. The identification was only possible

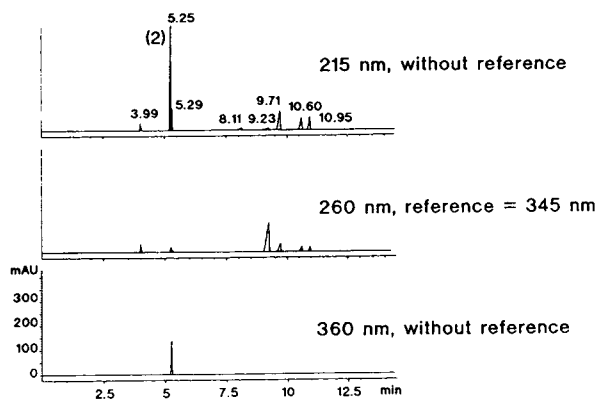

Fig. 4. Analysis of nine water-soluble vitamins using spectral suppression. For sample and peak identification, see Fig. 3, except that here peak 2 = cyanocobalamin. For conditions, see Fig. 3.

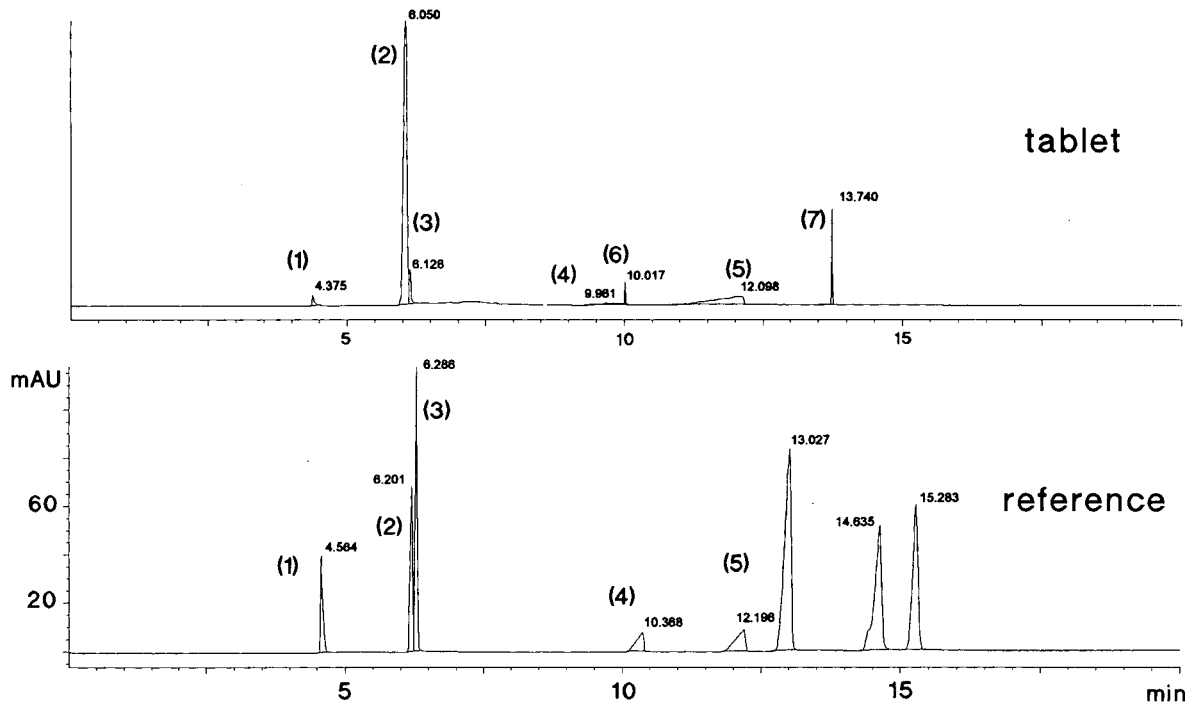

Fig. 5. Comparison of tablet analysis with the reference sample containing eight vitamins. Peak identification: 1 = thiamine; 2 = nicotinamide; 3 = pyridoxide; 4 = pantothenate; 5 = ascorbic acid; 6 and 7 = matrix peaks. For conditions, see Fig. 3.

by measuring and comparing spectra because the interfering matrix influenced migration times and peak shapes. The spectra of peaks 6 and 7 (Fig. 5, tablet) were unlike any vitamin spectra measured before and thus these peaks were classified as matrix peaks.

CONCLUSIONS

The vitamins thiamine, nicotinamide and nicotinic acid turned out to be well suited for a standard sample set in CZE. Excellent repeatability and performance of the standard method could be shown.

Of the tested parameters, pH had a minor impact on the standard separation procedure over the range studied. Parameters such as ionic strength and buffer type strongly influenced the EOF, electrophoretic mobility of the solutes and peak shapes. When analysing an over-the-counter vitamin preparation, shifts in migration times and peak shapes were observed. This led to the conclusion that complex matrices influence these parameters.

The determination of nine compounds and the analysis of a commercially available vitamin preparation showed that vitamin analysis is possible with a simple buffer system, avoiding difficult micellar techniques. Spectral analysis and peak purity tests proved to be useful for peak identification.

ACKNOWLEDGEMENTS

The author wishes to thank Sally Swedberg for helpful discussions, Petra Seitz and Gerard Rozing for comments on the manuscript and the Capillary Electrophoresis Group for support in daily work.

REFERENCES

1 B. Glatz, *Application Note No. 12-5954-6266*, Hewlett-Packard, Waldbronn, 1986.

2 A. Gratzfeld-Huesgen, R. Schuster and W. Haecker, *Application Note No. 12-5091-3194E*, Hewlett-Packard, Waldbronn, 1992.
3 M.C. Gennaro, *J. Chromatogr. Sci.*, 29 (1991) 410.
4 P. Jandera and J. Churacek, *J. Chromatogr.*, 197 (1980) 181.
5 R.M. Kothari and M.W. Taylor, *J. Chromatogr.*, 247 (1982) 187.
6 S. Fujiwara, S. Iwase and S. Honda, *J. Chromatogr.*, 447 (1988) 133.
7 S. Kobayashi, T. Ueda and M. Kikumoto, *J. Chromatogr.*, 480 (1989) 179.
8 C.P. Ong, C.L. Ng, H.K. Lee and S.F.Y. Li, *J. Chromatogr.*, 547 (1991) 419.
9 Y.F. Yik, H.K. Lee, S.F.Y. Li and S.B. Khoo, *J. Chromatogr.*, 585 (1991) 139.
10 R.M. McCormick, *Anal. Chem.*, 60 (1988) 2322.
11 A.N. Tran, S. Park and P.J. Lisi, *J. Chromatogr.*, 542 (1991) 459.

Journal of Chromatography A, 652 (1993) 503–515
Elsevier Science Publishers B.V., Amsterdam

CHROM. 25 102

Separation and determination of glycosaminoglycan disaccharides by micellar electrokinetic capillary chromatography for studies of pelt glycosaminoglycans

Søren Michaelsen*

Department of Research in Fur Animals, National Institute of Animal Science, Research Centre Foulum, P.O. Box 39, DK-8830 Tjele (Denmark)

Mai-Britt Schrøder and Hilmer Sørensen

Chemistry Department, Royal Veterinary and Agricultural University, 40 Thorvaldsensvej, DK-1871 Frederiksberg C (Denmark)

ABSTRACT

Capillary electrophoresis based on cetyltrimethylammonium bromide micellar electrokinetic capillary chromatography (MECC) was developed for the separation and determination of glycosaminoglycan (GAG) disaccharide units without derivatization. The influence of changes in several separation conditions was studied, and the separation mechanisms are discussed. Tests of repeatability and linearity were performed for qualitative and quantitative evaluation of the method. The described procedure gives a rapid and efficient determination of GAG disaccharides. Samples of chondroitin sulphates and mink skin were treated with proteases, and the extent of protein cleavage was followed by free zone capillary electrophoresis. The result of the chondroitinase ABC treatment following the protease treatment was evaluated by the MECC method.

INTRODUCTION

Proteoglycans, which are highly glycosylated glycoproteins with distinctive features of the carbohydrate parts, are found in animal connective tissues. The carbohydrate part consists of oligosaccharides and polysaccharides or glycosaminoglycans (GAGs) covalently attached to the polypeptide core of the proteoglycan through a trisaccharide unit. Structural studies of intact proteoglycan molecules indicate that different types of GAG chains can be attached to a single polypeptide, and that large numbers of oligosaccharide units may also be attached to the same core protein [1]. The GAGs contain repeating disaccharide subunits generally consisting of a uronic acid linked to a hexosamine and with various numbers of sulphate groups attached to either the uronic acid or the hexosamine [1,2]. Classification of proteoglycans is based on the structure of the peptide core and the GAG side-chains [3]. The hyaluronate and chondroitin sulphate species have fairly simple structures whereas others, such as dermatan sulphate, heparin sulphate and other heparin species, may contain a large number of different disaccharide units, arranged either in block structures or in less well ordered complex sequences [2].

The GAGs are essential for maintaining the structural integrity of many connective tissues. In addition, their ability to bind water and micro-ions and steric exclusion of some macromolecules may also be of importance [2]. Although

* Corresponding author.

0021-9673/93/$06.00

no detailed structure–function relationships have been found, the presence of sulphate GAGs has been related to normal collagen fibrillogenesis with some influence on the diameter and size of the collagen fibres [4,5]. When the unsulphated hyaluronic acid is the only GAG present in the dermis, thinning of the hair occurs [6], and when the amount of sulphate GAGs increases in the skin, *e.g.*, after testosterone treatment, thickening of the hair occurs [7].

Studies of the cyclic hair growth of various species of animals have revealed that in connection with anagen there is an increase in the amount of sulphated GAGs in skin [8], whereas in telogen there is an increase in the amount of non-sulphated GAGs [9]. Further, the ratio of 4- and 6-sulphated isomers of chondroitin varies with age and in various pathological states [10]. The properties and functions of GAGs make these compounds interesting in connection with the properties and quality of fur animal pelts. Exact structural information on GAGs in skin is therefore needed.

Determinations of individual GAG disaccharides have been based on techniques such as paper chromatography, TLC, paper or cellulose acetate membrane electrophoresis, LC and HPLC [1,11–16]. HPLC methods are usually superior to the other techniques. However, the disadvantages of HPLC include large sample volumes, large solvent volumes, usually long-term analyses, expensive columns, long equilibration and regeneration times of columns and an inability to resolve some of the isomers.

Recently, high-performance capillary electrophoresis (HPCE) as free zone or micellar electrokinetic capillary chromatography (MECC) with sodium dodecyl sulphate (SDS) has been introduced to separate monosaccharides, disaccharides and oligosaccharides with or without derivatization [10,17–21]. However, the published methods using free zone or MECC with SDS do not separate all GAG disaccharides well enough. MECC based on ion pairing and hydrophobic interaction with positively charged cetyltrimethylammonium bromide (CTAB) was very likely to improve the separation of the negatively charged GAG disaccharides, as has been shown for other negatively charged hydrophilic compounds in HPCE [22]. Further, it is preferable to avoid derivatization, because it is a further complication of the method and a time-consuming step. Underivatized and unsaturated GAG disaccharides are well suited for direct UV detection with a characteristic absorbance at 232 nm. Generally, HPCE techniques are rapid and inexpensive, have the potential for high resolution of analytes, require only small amounts of sample and inexpensive fused-silica capillaries are used [10,22,23].

This paper describes an efficient HPCE method based on MECC with CTAB, developed for the determination of individual GAG disaccharide isomers. The parameters studied include the evaluation of the effects of temperature, voltage and pH and CTAB, electrolyte and modifier concentration. Tests of linearity and repeatability were performed. Finally, results from enzymatic cleavages of GAGs from various chondroitins and mink skin and peptides from mink skin and the separation of the mixtures of GAG disaccharides obtained are described. The procedure developed gives a rapid and efficient determination of GAG disaccharides.

EXPERIMENTAL

Apparatus

An ABI Model 270 A and 270 A-HT capillary electrophoresis system (Applied Biosystems, Foster City, CA, USA) was used with a 750 mm × 50 μm I.D. Fused-silica capillary (J & W Scientific, Folsom, CA, USA). The detection point was 522 mm from the injection end of the capillary. Data processing was performed on a Shimadzu (Kyoto, Japan) Chromatopac C-R3A instrument.

Materials and reagents

Chondroitin disaccharides (sodium salts) Δ^4-GlcUA→GalNAc (ΔDi-OS; **1**), Δ^4GlcUA→4-O-sulpho-GalNAc (ΔDi-4S; **2**), Δ^4GlcUA→6-O-sulpho-GalNAc (ΔDi-6S; **3**), $\Delta^4$2-O-sulpho-GlcUA→4-sulpho-GalNAc (ΔDi-diS_B; **4**) (Fig. 1), chondroitin sulphate A from bovine trachea (*ca.* 70% and 30% C), chondroitin sulphate B from bovine mucosa (dermatan sulphate, *ca.* 85% and 15% A + C) and chondroitin sulphate

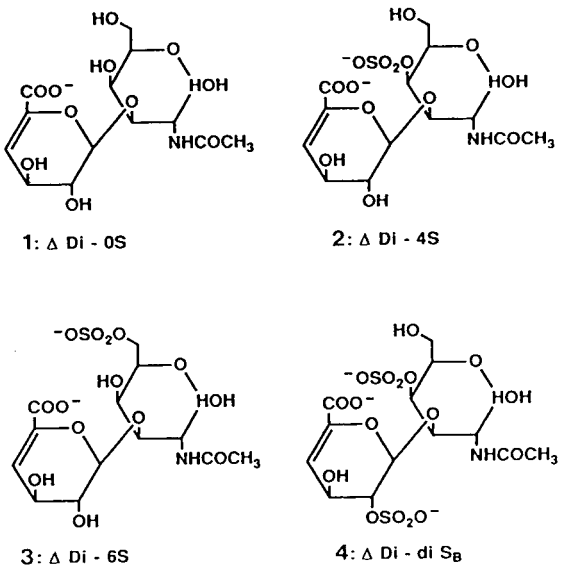

Fig. 1. Structures of the individual GAG disaccharides used in the HPCE analyses.

C from shark cartilage (*ca.* 90% and 10% A), and also chondroitinase ABC (chondroitin ABC lyase; EC 4.2.2.4) and trypsin were obtained from Sigma (St. Louis, MO, USA). Pepsin and pancreatin were purchased from Merck (Darmstadt, Germany). Skin samples were from the back of standard mink pelts, and the samples were obtained from the National Institute of Animal Science, Department of Research in Fur Animals, Foulum, Denmark. The samples were stored at −20°C until used.

Sodium tetraborate and sodium phosphate were obtained from Sigma and CTAB from BDH (Poole, UK). All chemicals were of analytical-reagent grade.

Procedure

Buffer preparations for the HPCE separations were performed according to Michaelsen *et al.* [22]. Samples were introduced from the cathodic end of the capillary by 1-s vacuum injection. Separations were performed at 30–60°C and 10–30 kV. On-column UV detection was at 232 nm unless indicated otherwise. Washing with buffer was done between each analysis for 5 min. After a number of analyses had been carried out, the capillary was washed for 5 min with 1.0 *M* NaOH and for 2 min with water.

Calculations of relative migration times with respect to **2** (*RMT*), normalized peak areas (*NA*), relative normalized peak areas with respect to **2** (*RNA*), resolution (R_s) and the number of theoretical plates (N) were performed according to Michaelsen *et al.* [22].

Enzyme treatments

Chondroitin sulphate A, B and C (1 mg of each) were treated with 0.30 mg of chondroitinase ABC in 100 μl of water plus 900 μl of 50 m*M* Tris–HCl (pH 8.0) buffer. The reaction mixtures were incubated at 37°C for 18 h and the reactions were stopped by transfering the mixtures into 100-μl Dowex 50W-X8 (H^+) columns and collecting the unretained solutes. Samples were then filtered through 0.2-μm filters, which were washed twice with 0.5 ml of water. The filtrates were either analysed directly by HPCE or evaporated to dryness and the residues dissolved in 100 μl water and analysed by HPCE.

Skin samples to be treated with chondroitinase were homogenized with an Ultra Turrax in 50 m*M* Tris–HCl (pH 8.0), enzyme was added and the mixture incubated at 37°C for 18 h. The reaction was stopped and the mixture filtered as described for chondroitin sulphate samples. Pepsin- and pancreatin-treated samples were prepared from skin samples homogenized with an Ultra Turrax in water (*ca.* 50 mg of skin per 2 ml), the pH of the solution was adjusted to 1.5 with HCl, pepsin (5.0 mg) was added and the mixture was incubated at 40°C for 60 min. Tris–HCl (50 m*M*, pH 8.0) was added to adjust the pH to 6.8, followed by pancreatin (5.0 mg) and the mixture (4 ml) was incubated at 40°C for 60 min. A 1-ml volume of this reaction mixture was mixed with 3.0 mg of chondroitinase and incubated at 37°C for 18 h. The reaction was stopped and the mixture filtered as described above for chondroitin sulphate samples. The samples were evaporated and the residues dissolved in one tenth the volume of water.

Fat extraction prior to protease and chondroitinase treatments was performed with either butanol, hexane or diethyl ether, and followed by either pepsin–pancreatin or trypsin treat-

ment. The extraction and homogenization of samples (*ca.* 20 mg) were performed with an Ultra Turrax for 2 min. Butanol (1.0 ml) or hexane (1.0 ml) was added to water (2.0 ml) before the pepsin (2.5 mg) and the pancreatin (2.5 mg) treatments (see above) and to 50 m*M* Tris–HCl (pH 8.0) (2.0 ml) before the trypsin (2.0 mg) treatment. Diethyl ether extractions (2 × 5 ml) of skin samples (*ca.* 20 mg) were performed with a glass spatula, and the samples were dried and homogenized in water or Tris–HCl as above. The aqueous phase was used for protease and chondroitinase treatments (see above). The hexane extraction in Tris–HCl of skin samples resulted in a hexane phase, a gel-like intermediate phase and the Tris–HCl aqueous phase. The gel-like phase and the Tris–HCl phase were treated separately with trypsin.

The protease treatments were followed by HPCE analyses of released peptides. The separation conditions were 20 m*M* citrate buffer (pH 2.5), temperature 30°C, voltage 25 kV, on-column UV detection at 200 nm, and sample introduction from the anodic end of the capillary by 1-s vacuum injection.

RESULTS AND DISCUSSION

The unsaturated uronic acid of the GAG disaccharide unit exhibits an absorbance maximum at 232 nm with a molar absorptivity of 5000–6000 l mol^{-1} cm^{-1} [19]. Various GAGs are found in different animal tissues such as skin, cartilage, bone, arterial walls and intestinal mucosa [2, 24]. The location of and the number of sulphate residues vary both between the GAGs and within the actual group of GAGs [2,24].

A systematic investigation of the influence of changes in the separation conditions on the migration times (*MT*), *RMT*, *NA*, *RNA*, R_s and *N* values were carried out. Chondroitin disaccharide standards **1–4** (Fig. 1) were dissolved in water and analysed under the initially applied separation conditions with an 18 m*M* borate and 30 m*M* phosphate buffer with 50 m*M* CTAB added and adjusted to pH 7.0, a temperature of 30 or 40°C and a voltage set at 20 kV. A complete separation of the disaccharides was obtained (Fig. 2).

The separation principles have been described by Michaelsen *et al.* [22] and Bjergegaard *et al.* [23]. Briefly, the CTAB–MECC separation is based on hydrophobic and ion-pairing interaction of the negatively charged disaccharides, the positively charged CTAB micelles and the CTAB-covered capillary wall. Further, complexation of some of the disaccharides may occur with the borate ions. Compared with published HPCE disaccharide methods, this CTAB system results in a reversal of the electroosmotic flow in the capillary.

Voltage

Increasing the applied voltage from 10 to 30 kV resulted in non-linear reductions in migration times of a factor of 4.5 (Fig. 3). The *MT* values of the compounds decreased with decreasing rate as the applied voltage was increased from 10 to 30 kV. An increase in the field strength is

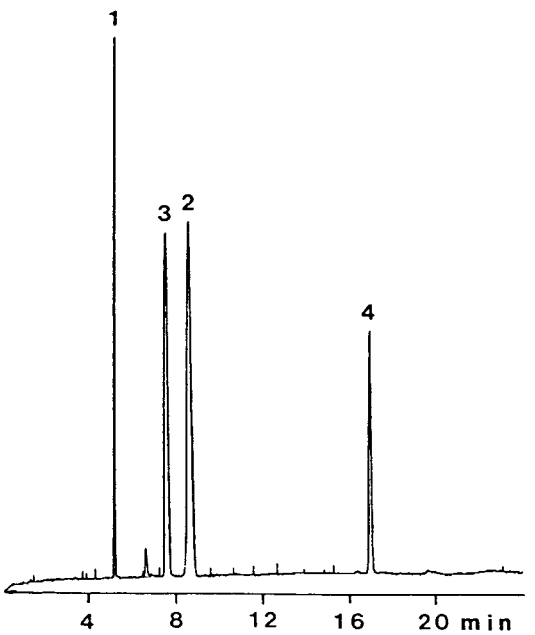

Fig. 2. Electropherogram of the mixture of GAG disaccharides dissolved in water and used in the optimization studies. Peak numbers represent compounds in Fig. 1. Concentrations: **1** = 1.13 m*M*; **2** = 1.60 m*M*; **3** = 3.19 m*M*; **4** = 0.63 m*M*. Conditions: 18 m*M* borate–30 m*M* phosphate–50 m*M* CTAB buffer, adjusted to pH 7.0; temperature, 30°C; voltage, −20 kV; detection wavelength, 232 nm, vacuum injection for 1 s.

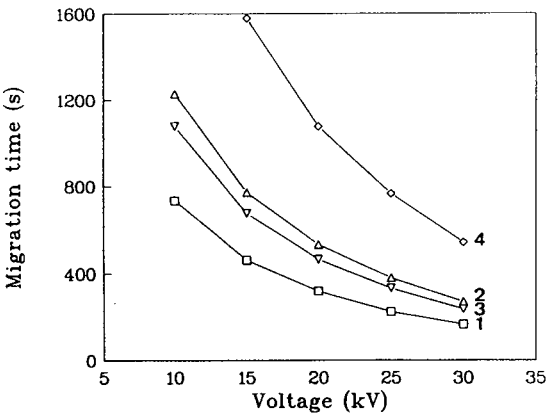

Fig. 3. Influence of applied voltage on migration times of GAG disaccharides. Numbers represent compounds in Fig. 1. Other separation conditions as in Fig. 2.

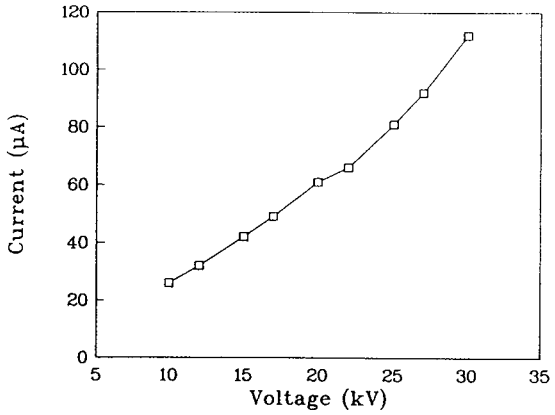

Fig. 4. Current as function of applied voltage. Other separation conditions as in Fig. 2.

expected to give a linear decrease in *MT* due to increasing velocity of the analytes. This was not seen. However, if the temperature increases in the capillary as the voltage is increased, a lower viscosity will result in a further decrease in migration times. Further, increasing temperatures may change the ratio between the micellar phase and the aqueous phase, the shape and size of micelles and the interaction of analytes with CTAB [23,25,26]. Evidence of increasing temperature within the capillary was seen from a plot of voltage *versus* current. Plotting the resulting current against voltages of 10–30 kV showed a linear relationship up to 22 kV, but the current increased relatively more than expected from a linear relationship above 22 kV (Fig. 4). This indicates that the temperature increases in the capillary due to insufficient heat removal at voltages above 22 kV. The concave curves may therefore represent a combination of increasing analyte velocity and temperature effects.

The *RMT*, *NA* and *RNA* values remained nearly constant with increasing voltage, whereas the R_s values decreased from 10 to 20 kV and were constant at higher voltages. The *N* values for **2** and **3** were low and nearly constant, whereas those for **1** had a maximum at 25 kV and the lowest value at 30 kV and **4** had a minimum at 25 kV and a maximum at 15 kV. The expected increase in R_s and *N* with increasing voltage according to the HPCE theory was not observed, which is probably due to the mentioned temperature effects [22,23]. From the results a voltage of 20 kV was chosen.

Temperature

The migration times decreased by a factor of 1.4–1.8 when the temperature was increased from 25 to 60°C. The decrease was linear except for **4**, which indicates a possible change in the interaction of CTAB and **4** and a general decrease in the viscosity of the solvent. The *RMT* values were also constant except for **4**, for which they increased by *ca.* 8%, indicating an increased interaction with CTAB. If borate complexation occurs, only **1–3** are likely to form complexes with borate ions owing to their vicinal hydroxyl groups. Changes in borate complexation therefore cannot explain the changes in the *MT* and *RMT* values for **4**. The *NA* values increased for all disaccharides (Fig. 5) and the *RNA* values were constant. The increasing *NA* values are therefore most likely to be caused by increasing injection volumes as the viscosity of the buffer decreases with increasing temperature. However, the increased injection volume may not alone explain the changes in the *NA* values. Changes in the actual response factors of disaccharides with increased temperature due to changes in borate complexation may be involved, as proposed for other compounds [22].

The R_s values were nearly constant except for a higher value at 25°C for **2–4**. The *N* values

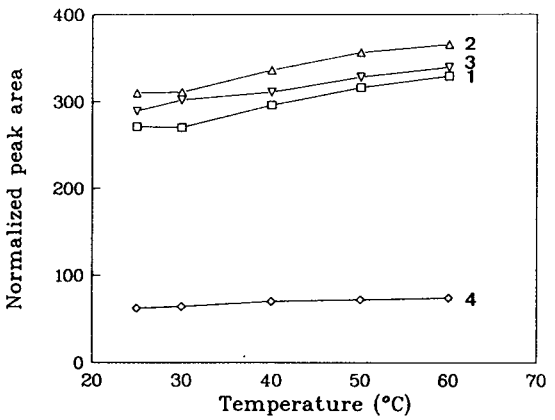

Fig. 5. Influence of temperature on normalized peak areas of GAG disaccharides. Numbers represent compounds in Fig. 1. Other separation conditions as in Fig. 2.

were highest for **1** and **4** at 30°C, whereas for **2** and **3** the *N* values were highest at high temperatures. A temperature of 30 or 40°C was chosen.

Electrolyte concentration

Increasing the electrolyte concentration [borate–phosphate (3:5)] from 16 to 48 m*M* gave interesting results for *MT* and *RMT* values (Fig. 6). The *MT* values increased by a factor of 1.3 for **1** and 1.45 for **4**, and decreased by a factor of 1.3 for **2** and 1.4 for **3**. The *RMT* values increased for **1** and **4** and were constant for **3**. No single mechanism can explain these results.

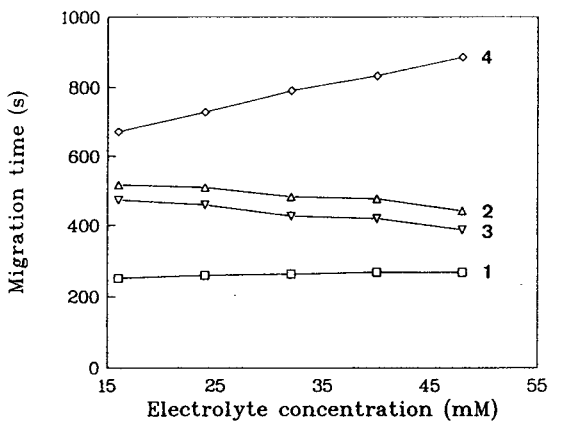

Fig. 6. Influence of electrolyte concentration [borate–phosphate (3:5)] on migration times of GAG disaccharides. Numbers represent compounds in Fig. 1. Other separation conditions as in Fig. 2, except temperature (40°C).

The electroosmotic flow decreases with increasing electrolyte concentration [23,27]. This could explain the increasing *MT* values of **1** and **4**. The higher electrolyte concentration may also lead to temperature increases, resulting in lower *MT* values. However, this was only seen for **2** and **3**. Further, a change in the critical micelle concentration (CMC) of CTAB or changes in the hydrophobic and ion-pairing interaction of GAG disaccharides with CTAB may also be involved [23]. Finally, the effect of the borate concentration on the borate–disaccharide complex concentration and equilibrium may explain some of the observed changes [28]. The observed *MT* values of the compounds are probably a result of a combination of these effects, especially the effects of electroosmotic flow and CTAB interaction.

The *NA* and *RNA* values were constant. The R_s values were constant for **2** and **3**, decreased by a factor of 1.5 for **1** and **3** and increased by a factor of 3.8 for **2** and **4**. This was a result of the large changes in *MT* values. The *N* values varied with the electrolyte concentration, and were generally highest at high electrolyte concentrations. From these results, an electrolyte concentration of 48 m*M* was chosen.

CTAB concentration

Increasing the CTAB concentration from 10 to 60 m*M* resulted in large changes in some of the parameters. Disaccharides **2** and **3** moved from positions in front of the peak normally seen between **1** and **2** at 10 m*M* to positions after this peak at 30 m*M* and higher concentrations of CTAB (Fig. 7). The *MT* values increased for **2**–**4** and were constant for **1** with increasing CTAB concentration (Fig. 8). The *RMT* values decreased for **1** and **4** and were constant for **3**. Increasing *MT* values are expected due to the increase in the ratio of the micellar phase to that of the aqueous phase and possible changes in the electroosmotic flow [22]. The constant value for **1** compared with the other diaccharides may be explained by a stronger ion-pairing effect with CTAB compared with hydrophobic interaction for the more charged disaccharides **2**–**4**. The fact that the more negatively charged disacharides

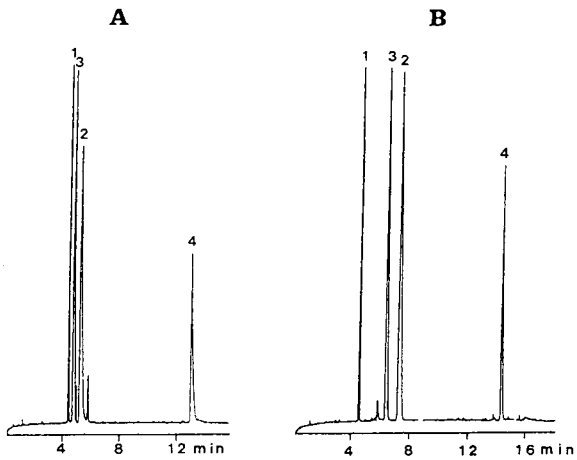

Fig. 7. Electropherograms of the GAG disaccharides at (A) 10 m*M* and (B) 40 m*M* CTAB. Peak numbers represent compounds in Fig. 1. Other separation conditions as in Fig. 2, except temperature (40°C).

migrate at a lower velocity than **1** in spite of positive polarity at the detection end also shows the great importance of ion pairing. This observation is also in agreement with results obtained for other negatively charged analytes in the CTAB system [22].

The *NA* values decreased and the *RNA* values were constant for all analytes with increasing CTAB concentration. A lower injection volume due to the higher viscosity of the buffer can probably explain these results. The R_s values increased with increasing CTAB concentration and the *N* values were highest at 50 m*M* CTAB. A CTAB concentration of 50 m*M* was chosen.

pH

Changing the pH from 6.0 to 8.0 slightly increased the migration times for all the disaccharides. The *RMT* values were nearly constant. The *NA* and *RNA* values were constant except at the low pH of 6.0 (Fig. 9). The changes observed are probably caused by changes in the actual response factors of disaccharides. The possible effects of complexation with borate ions at high pH values [28] are illustrated in Fig. 10. At pH 7.0 four disaccharide peaks are seen, at pH 7.5 peaks **1**, **2** and **3** are each followed by a minor peak and at pH 8.0 only four disaccharide peaks are seen again. Disaccharide **4** is less likely to yield complexes with borate owing to the lack of vicinal hydroxyl groups [28], whereas disaccharides **1**, **2** and **3** can form complexes with borate in the tetrahydroxyborate form at high pH values. Hoffstetter-Kuhn *et al.* [28] mentioned pH values above 8.0. Although equilibria between disaccharides and borate ions are expected to be dynamic [28], changing the pH from 7.0 to 8.0 might result in the two forms of the disaccharides **1**, **2** and **3** seen.

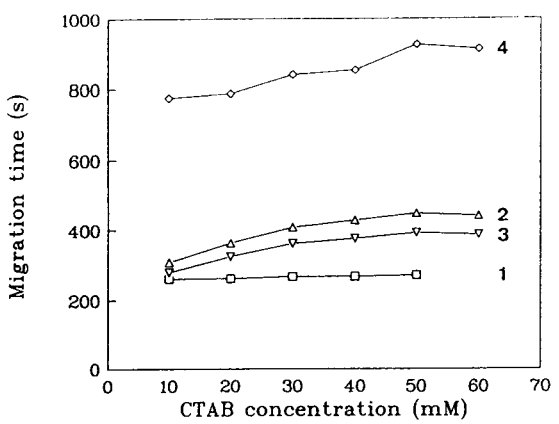

Fig. 8. Influence of CTAB concentration on migration times of GAG disaccharides. Numbers represent compounds in Fig. 1. Other separation conditions as in Fig. 2, except temperature (40°C).

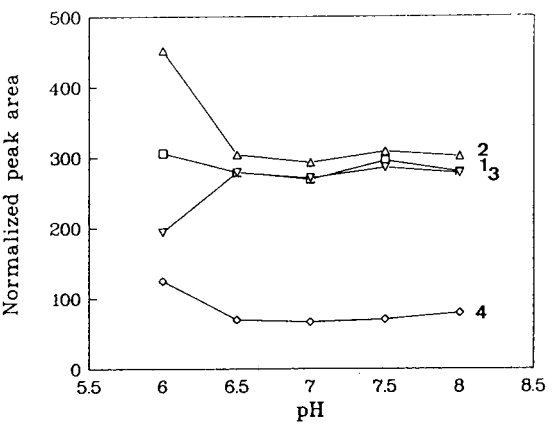

Fig. 9. Influence of pH on normalized peak areas of GAG disaccharides. Numbers represent compounds in Fig. 1. Other separation conditions as in Fig. 2, except temperature (40°C).

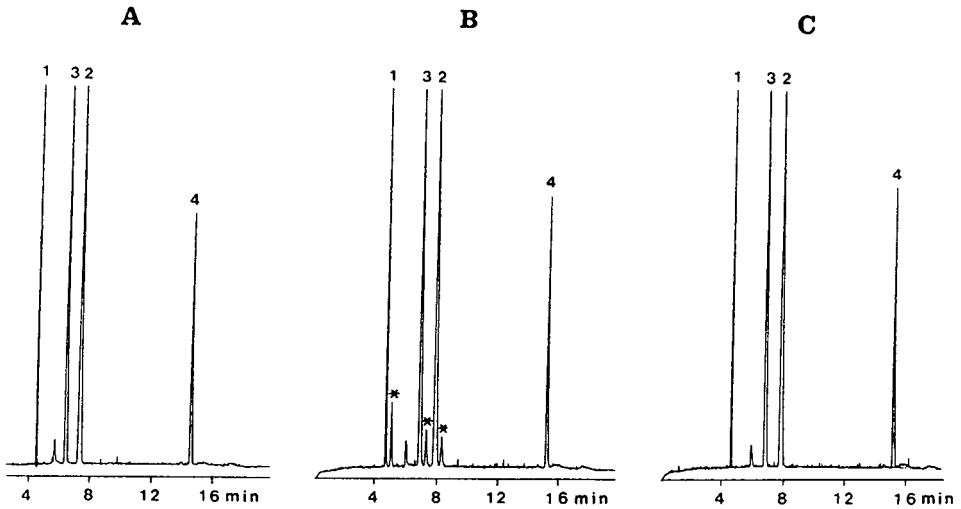

Fig. 10. Electropherograms of the GAG diaccharides at (A) pH 7.0, (B) pH 7.5 and (C) pH 8.0. Peak numbers represent compounds in Fig. 1. The minor peaks following each of the major disaccharides **1**, **2** and **3** are marked with asterisks. Other separation conditions as in Fig. 2, except temperature (40°C).

Modifier

Increasing the concentration of 1-propanol in the buffer from 1 to 10% resulted in increased *MT* values for **1** and **4**, whereas the *MT* values for **2** and **3** remained constant. Increasing amounts of organic modifiers except acetonitrile cause reductions in the electroosmotic flow [22] and less interaction of analytes with detergent. The former will increase and the latter will decrease the migration times. Both effects are probably responsible for the observed results, as the migration times of **1** and **4** increased and those of **2** and **3** remained constant. The influence on migration times therefore varies with different types of compounds, which further supports the mechanism of hydrophobic interaction with detergent. The *NA* values decreased and the *RNA* values were constant with increasing modifier concentration. The changes in *NA* values are probably a result of changes in the relative response factors of the compounds [22,23] in combination with changes in the viscosity of the buffer.

Repeatability

The repeatabilities of the *MT*, *RMT*, *NA* and *RNA* values were determined from fifteen analyses of the four GAG disaccharides. The buffer was changed between each five analyses at the injection end, and the separation conditions were as in Fig. 2. The repeatabilities of the *MT* values were very good, with relative standard deviations below 0.44% (Table I). However, transforming *MT* values to *RMT* values slightly improved the repeatabilities. The repeatabilities of the *NA* values were good with relative standard deviations below 2.05% (Table I). Trans-

TABLE I

RELATIVE STANDARD DEVIATIONS OF MIGRATION TIMES (*MT*), RELATIVE MIGRATION TIMES (*RMT*), NORMALIZED PEAK AREAS (*NA*) AND RELATIVE NORMALIZED PEAK AREAS (*RNA*) FOR GAG DISACCAHRIDES

Compound numbers as in Fig. 1 and separation conditions as in Fig. 2.

Parameter	Relative standard deviation (%) ($n = 15$)			
	1	**2**	**3**	**4**
MT	0.33	0.24	0.23	0.44
RMT[a]	0.29	0.07	–	0.36
NA	1.48	1.85	1.96	2.05
RNA[a]	0.93	1.19	–	1.26

[a] Relative to **2**.

forming *NA* values to relative values (*RNA*) also improved these repeatabilities. The *RMT* and *RNA* values correspond to the use of internal standards in analyses, which is generally recommended [22]. The results show that the repeatabilities are good and at an acceptable level for qualitative and quantitative analyses.

Linearity

The linearity of the method was determined from five repetitions at five concentrations of each of the four GAG disaccharides. The concentration ranges were 0.6–3.0 m*M* for **1**, 0.4–2.1 m*M* for **2**, 1.5–7.6 m*M* for **3** and 0.5–2.7 m*M* for **4**. The buffer was changed between each five analyses at the injection end, and the separation conditions were as in Fig. 2. The correlation between increasing concentration and the corresponding peak areas was calculated form linear regression analyses by the least-squares method for peak areas. The correlation coefficients obtained were 0.9975 for **1**, 0.9987 for **2**, 0.9982 for **3** and 0.9976 for **4**. These results show that this CTAB method gives a linear increase in peak area with increasing concentration of GAG disaccharides in the samples.

Mesityl oxide was included in the analyses in order to establish whether the small peak between **1** and **3** was a peak of neutral compounds following the electroosmotic flow. The peak of mesityl oxide, however, appeared between **3** and **2**. This indicates that **1** and **3** migrate faster than and **2** and **4** more slowly than the electroosmotic flow.

In conclusion, the separation conditions have large effects on the separation parameters, and no single effect can explain the changes observed. However, complete separations can be obtained and determinations can be performed from *NA* or *RNA* values. The use of *RNA* values corresponds to the use of internal standards in analyses, which is always recommended in order to obtain more accurate and reproducible results.

This CTAB method gives shorter times of analysis than the method described by Al-Hakim and Linhardt [19], as the separation of the four compounds is complete in less than 18 min, compared with 30 min under the optimum separation conditions in the method described by Al-Hakim and Linhardt [19]. Further, the resolution of **2** and **3** is higher in this method than that described by Al-Hakim and Linhardt [19]. Carney and Osborne [10] obtained very high peak efficiencies with a phosphate–borate–SDS buffer, but the resolution of **2** and **3** was higher in the present study and the peaks were baseline separated. However, when Carney and Osborne [10] used an orthophosphoric acid buffer, they also obtained a high resolution of **2** and **3**. Finally, Honda *et al.* [20] obtained high peak efficiencies and relatively good separations of phenylmethylpyrazolone-derivatized GAG disaccharides in a borate buffer. However, the derivatization step is time consuming and the increased sensitivity obtained by derivatization is offset by the increase in analysis time.

Chondroitin sulphates

Chondroitin sulphate A, B and C were treated with chondroitinase ABC under conditions described by Yamagata and co-workers [29,30]. The analyses performed with the sample filtrates (see Experimental) gave well separated peaks, as seen in Fig. 11. The identities of the peaks are based on spiking with reference standards (**1–4**) and on data in refs. 10, 16, and 19. The compounds found in the three chondroitin sulphates are also in agreement with information of purity according to the manufacturer.

In chondroitin sulphate B, α-L-iduronic acid dominates. However, it is not possible to distinguish between β-O-glucuronic acid, β-O-galaturonic acid and α-L-iduronic acid originally present in GAGs from disaccharides formed after chondroitinase cleavage, because of the identical structures of these compounds in disaccharides after enzymatic cleavage.

The redissolved samples, which were concentrated by a factor of ten compared with the sample filtrates, had too high concentrations of solutes to give proper HPCE separations. A 5–10-fold dilution of the redissolved samples resulted in well separated peaks. However, after the evaporation, dissolution of the residue and dilution, at least two new peaks appeared between **1** and **3** (Fig. 11). Further, the normalized peak areas of the redissolved disaccharides were

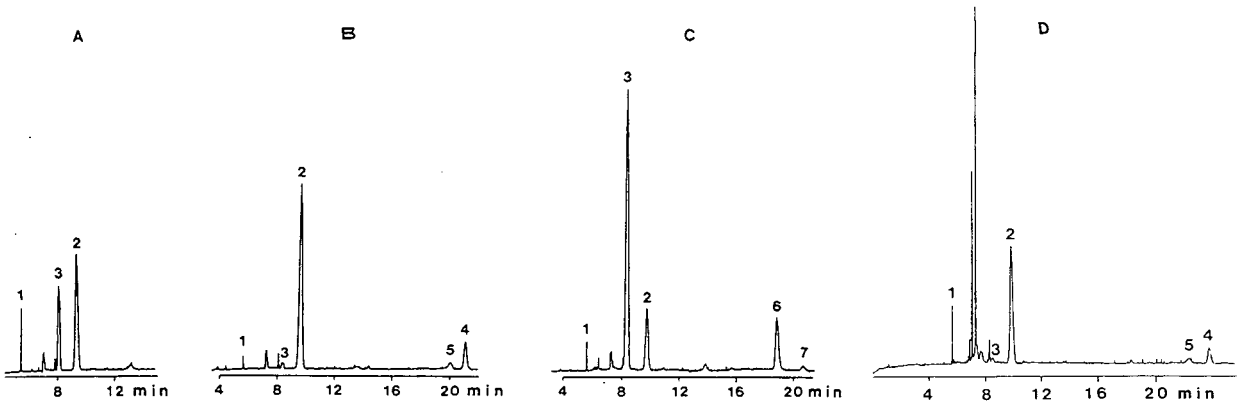

Fig. 11. Electropherograms of disaccharides obtained after chondroitinase ABC treatment of (A) chondroitin sulphate A (0.5 mg/ml), (B) chondroitin sulphate B (0.6 mg/ml) and (C) chondroitin sulphate C (0.9 mg/ml); (D) as (B) but sample evaporated and residue dissolved in an equal volume. Peak numbers **1–4** represent compounds in Fig. 1, **5** = ΔDi-diS; **6** = Δ^4-2-O-sulpho-GlcUA→6-O-sulpho-GalNAc (ΔDi-diS_D); **7** = Δ_4-GlcUA→4,6-bis-O-sulpho-GalNAc (ΔDi-diS_E). Separation conditions as in Fig. 2.

lower than expected. Instability of the GAG disaccharides during evaporation of the solvent is the probable reason for the additional peaks and the lower *NA* values.

Skin samples

Five experiments were performed with skin samples from mink. In the first two experiments only chondroitinase treatment was applied, whereas in the other experiments protease treatments with either pepsin and pancreatin or trypsin were applied prior to chondroitinase treatment. The first chondroitinase treatment (0.3 mg) of skin samples (12.9 mg) showed too small amounts of GAGs to be positively identified. A phosphate buffer was tested for the protease treatments. However, very poor HPCE separations were obtained after the chondroitinase treatment, possibly owing to the high ionic strength in the sample. HPCE analyses of samples in 50 m*M* Tris–HCl buffer (pH 8.0) gave good separations, hence this buffer was chosen for the pancreatin, trypsin and chondroitinase treatments of skin samples.

Increasing the chondroitinase and sample amounts to 3.2 and 53.6 mg, respectively, and treating the samples with pepsin and pancreatin prior to chondroitinase treatment improved the peak sizes (Fig. 12A). Peaks appearing at the same positions as those for the disaccharides in Fig. 2 are marked with the corresponding numbers. However, owing to instability of GAGs during the applied evaporation and redissolution of samples (see above) and the possible presence of other anions after the Dowex cation exchanger, other peaks were also seen. Comparing the electrophrograms of samples analysed at 232, 260, 280 and 320 nm with those for chondroitinase-treated chondroitin sulphate B analysed at the same wavelengths did, however, indicate that **3** and **2** were peaks 1 and 2, respectively, after the large peak at 6.1 min. Further work on peak identification is needed to obtain a precise peak identification. Several peaks were seen in the skin sample at 260 and 280 nm, but none at 320 nm. The analyses of chondroitin sulphate B showed a very small peak of **2** at 260 nm and no peak at 280 nm. The observed peaks at 260 and 280 nm from the skin sample are therefore not GAG disaccharides. The peaks could represent nucleic acids and nucleotides or peptides with aromatic amino acids and negatively charged at pH 7.0.

HPCE analyses of released peptides were made in order to evaluate whether the pepsin and pancreatin treatments had been performed for a long enough period. The electropherograms of pepsin (1 h)-and pepsin and pancreatin (1 h + 1 h)-treated skin sample were nearly identical, whereas the pepsin (24 h)-treated

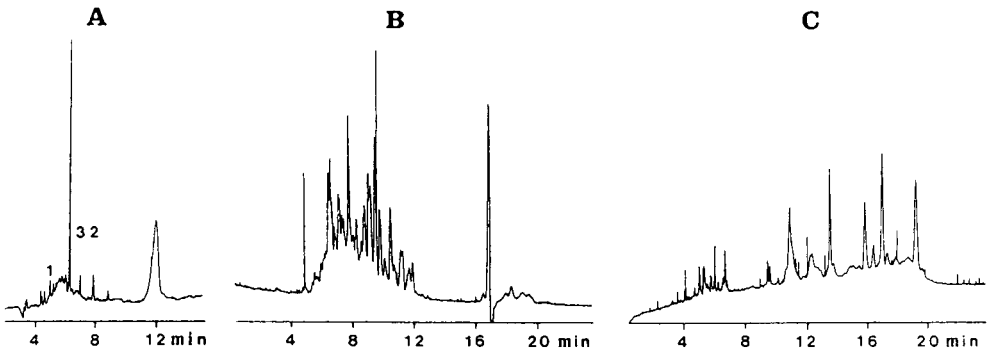

Fig. 12. (A) Electropherogram from GAG analysis of a sample of mink skin (53.6 mg) after pepsin and pancreatin treatment, followed by chondroitinase (3.2 mg) treatment in 50 m*M* Tris–HCl buffer (pH 6.8). Peak numbers represent compounds in Fig. 1. Separation conditions as in Fig. 2, except temperature (40°C). (B) Electropherogram of peptides of a mink skin sample (23.4 mg) after butanol extraction (1 ml) in 50 m*M* Tris–HCl buffer (pH 8.0) (2.0 ml) followed by trypsin treatment (2 mg) at 37°C for 18 h. Separation conditions as under Experimental. (C) Electropherogram from GAG analysis of a butanol-extracted, trypsin-treated skin sample [see (B)] after chondroitinase treatment. Separation conditions as in Fig. 2.

sample showed a large increase in low-molecular-mass peptides. This indicated that the 1-h incubation periods were too short for skin samples, although these time periods are used in protease treatments to cleave proteins in feed samples prior to gravimetric analysis of dietary fibres [23].

Trypsin treatment with and without removal of fat compared with pepsin and pancreatin treatment also with and without removal of fat were tested to improve the GAG analyses. Three different solvents were used for fat extraction: butanol, hexane and diethyl ether. The HPCE analyses of peptides after the trypsin treatment showed large amounts of low-molecular-mass compared with high-molecular-mass peptides (Fig. 12B), except for the diethyl ether-extracted sample. No marked changes were seen between 18 and 23 h of protease treatment, and therefore it can be concluded that the longest time of treatment does not improve the cleavage of proteins in the skin sample.

The protease-treated skin sample after the hexane extraction seemed to yield larger amounts of peptide when the amounts in the aqueous and the gel-like phases were added than the results obtained after the other fat extraction methods. However, the additional gel-like intermediate phase is inconvenient for routine analyses. Further, the amount of peptide obtained after the diethyl ether extraction was very small. Therefore, the butanol treatment seems to be the best choice for fat extraction of skin samples prior to trypsin treatment, and the trypsin treatment improved the amount of peptides released compared with the pepsin–pancreatin treatment.

HPCE analyses by the GAG disaccharide method performed before chondroitinase treatment and Dowex purification showed some peaks in the electropherograms. HPCE analyses of GAG disaccharides after chondroitinase treatment showed new peaks in addition to the peaks seen before the enzyme treatment (Fig. 12C). Repeated Dowex purification (100-μl column) resulted in fewer and smaller peaks in the electropherograms, but large differences in the electropherograms were seen between the various treatments. However, some of the peaks seen are probably a result of the evaporation and redissolution of the samples after the chondroitinase treatment and the repeated column purification, as discussed before. The peaks that disappeared were probably not GAG disaccharides, as the GAGs were not removed by the Dowex purification of the chondroitinase-treated chondroitin sulphates. The effect of the repeated Dowex purification is probably due to overloading of the columns in the first purification.

It can be concluded that the column purification method can probably be used to remove impurities in samples prior to GAG disaccharide analysis. At present the exact identification of GAG disaccharides in the skin samples is not clean-up procedures do not have to be as extensive as in HPLC and the peak efficiency and resolution are superior in HPCE.

CONCLUSIONS

Generally, HPCE methods of analyses have many advantages over HPLC methods. HPCE methods are inexpensive and small amounts of reagents and sample are needed. The sample clean-up procedures do not have to be as extensive as in HPLC and the peak efficiency and resolution are superior in HPCE.

The HPCE method based on CTAB–MECC with reversal of the electroosmotic flow can be applied to GAG disaccharide analyses. Compared with the HPCE methods described previously, this CTAB–MECC method might allow other compounds to be detected simultaneously with the GAG disaccharides or omitted from the analysis, depending on which material is being analysed. The possibility of rapid and easy changes in the separation conditions makes it easy to adjust the conditions for actual samples. Analysing GAG disaccharides in skin samples might need pre-isolation of GAG-containing proteoglycans or derivatization of the GAGs to obtain reasonable detection limits without interfering compounds.

This study demonstrates the possibilities of using HPCE for method development for protease and chondroitinase treatments of skin samples. Crude samples after protease treatments can be analysed directly in order to evaluate the extent of protein cleavage. This results in rapid answers as to whether prolonged treatment will result in further cleavage of proteins. The applied procedure with butanol fat extraction of skin samples and trypsin treatment followed by chondroitinase treatment seems to give the most promising results. However, further work including tests with other proteases and establishment of the identities of peaks appearing after evaporation and redissolution of samples is necessary in order to obtain a complete procedure for the analysis of GAG disaccharides in skin samples.

ACKNOWLEDGEMENTS

The authors gratefully acknowledge support from the Danish Natural Research Council, The Danish Agricultural and Veterinary Research Council and the Danish Fur Breeders Association.

REFERENCES

1 J.G. Beeley, *Glycoprotein and Proteoglycan Techniques*, Elsevier, Amsterdam, 1985, Ch. 2, pp. 5–28.
2 U. Lindahl and M. Höök, *Annu. Rev. Biochem.*, 47 (1978) 385.
3 A.R. Poole, *Biochem. J.*, 236 (1986) 1.
4 M.B. Mathews and L. Decker, *Biochem. J.*, 109 (1968) 517.
5 B.P. Toole and D.A. Lowther, *Biochem. J.*, 109 (1968) 857.
6 S. Schiller, G.A. Slover and A. Dorfman, *Biochim. Biophys. Acta*, 58 (1962) 27.
7 D.A. Allalouf and A. Bev, *Endocrinology*, 69 (1961) 210.
8 A. Savill and C. Warren, in A. Savill (Editor), *The Hair and Scalp. A Clinical Study*, Arnold, London, Ch. 1, pp. 1–26.
9 G. Moretti, C. Cipriani, A. Rebora, E. Rampini and F. Crovato, *J. Invest. Dermatol.*, 48 (1967) 498.
10 S.L. Carney and D.J. Osborne, *Anal. Biochem.*, 195 (1991) 132.
11 N. Seno, F. Akiyama and K. Anno, *Biochim. Biophys. Acta*, 264 (1972) 229.
12 N. Seno and K. Murakami, *Carbohydr. Res.*, 103 (1982) 190.
13 D.C. Seldin, N. Seno, K.F. Austen and R.L. Stevens, *Anal. Biochem.*, 141 (1984) 291.
15 A.-M. Säämänen and M. Tammi, *Anal. Biochem.*, 140 (1984) 354.
14 T. Gherezghier, M.C. Koss, R.E. Nordquist and C.P. Wilkinson, *J. Chromatogr.*, 413 (1987) 9.
16 Y. Nomura, H. Tade, K. Takahashi and K. Wada, *Agric. Biol. Chem.*, 53 (1989) 3313.
17 W. Nashabeh and Z. El Rassi, *J. Chromatogr.*, 514 (1990) 57.
18 J. Liu, O. Shirota and M. Novotny, *Anal. Chem.*, 63 (1991) 413.
19 A. Al-Hakim and R.J. Linhardt, *Anal. Biochem.*, 195 (1991) 68.
20 S. Honda, T. Ueno and K. Kahehi, *J. Chromatogr.*, 608 (1992) 289.
21 S. Michaelsen, M.-B. Schrøder and H. Sørensen, *Norw. J. Agric. Sci., Suppl.*, No. 9 (1992) 604.

22 S. Michaelsen, P. Møller and H. Sørensen, *J. Chromatogr.*, 608 (1992) 363.
23 C. Bjergegaard, S. Michaelsen and H. Sørensen, *J. Chromatogr.*, 608 (1992) 403.
24 J.E. Silbert, in L.A. Goldsmith and J.H. Sterner (Editors), *Biochemistry and Physiology of the Skin*, Oxford University Press, New York, Oxford, 1983, Ch. 20.
25 M.J. Rosen, in M.J. Rosen (Editor), *Surfactants and Interfacial Phenomena*, Wiley, New York, 1978. Ch. 3.
26 M.J. Sepaniak and P.O. Cole, *Anal. Chem.*, 59 (1987) 472.
27 T. Tsuda, K. Nomura and G. Nakagawa, *J. Chromatogr.*, 248 (1982) 241.
28 S. Hoffstetter-Kuhn, A. Paulus, E. Gassmann and H.M. Widmer, *Anal. Chem.*, 16 (1991) 1541.
29 T. Yamagata, H. Saito, O. Habuchi and S. Suzuki, *J. Biol. Chem.*, 243 (1968) 1523.
30 H. Saito, T. Yamagata and S. Suzuki, *J. Biol. Chem.*, 243 (1968) 1536.

Journal of Chromatography A, 652 (1993) 517–524
Elsevier Science Publishers B.V., Amsterdam

CHROM. 25 153

Determination of oligosaccharides by capillary zone electrophoresis

Anne Marie Arentoft, Søren Michaelsen and Hilmer Sørensen*

Chemistry Department, Royal Veterinary and Agricultural University, 40 Thorvaldsensvej, DK-1871 Frederiksberg C (Denmark)

ABSTRACT

Oligosaccharides occur in various biological materials, and the α-galactosides raffinose, stachyose, verbascose and ajugose are important in relation to the quality or nutritive value of legume seeds. A simple technique for the isolation and group separation of oligosaccharides was developed as an appropriate purification step prior to determination of the individual oligosaccharides by high-performance capillary electrophoresis (HPCE). The HPCE technique adapted to the separation of α-galactosides was based on capillary zone electrophoresis (CZE) in borate buffers with UV detection at 195 nm. The influence of various separation conditions, including voltage, pH, temperature and buffer composition, on the resolution, migration times, number of theoretical plates and peak areas was studied by the use of galactinol and the mono-, di-, tri- and tetra-α-galactosides of sucrose. Up to about 375 000 plates/m were obtained with the described CZE method. Tests of repeatability and linearity and the use of internal standards and relative response factors were used for evaluations of the qualitative and quantitative aspects of the method. With the combined technique of group separation, purification and CZE, a rapid and efficient method for the determination of naturally occurring oligosaccharides is now available for even complex mixtures of these carbohydrates.

INTRODUCTION

Oligosaccharides of the raffinose family are α-(1→6)-galactosides linked to C-6 of the glucose moiety of sucrose [1,2]. Raffinose is the template of this homologous series with only one galactoside unit attached. By successive binding of one, two and three additional α-galactoside units to C-6 of the terminating galactose unit of the lower homologue, the compounds stachyose, verbascose and ajugose are formed. These carbohydrates are synthesized in various plants, and appreciable amounts accumulate in legume seeds [2–4], where they seem to serve as storage compounds as found for other plants [5]. When present in too high concentrations in diets fed to animals, they may behave as anti-nutritional compounds owing to the problems they obviously can create in monogastric animals [6–9].

Methods of analysis for determination of carbohydrates require special attention as the compounds are important in many connections. In recent years, high-performance liquid chromatography (HPLC) has been the method of choice for the determination of individual oligosaccharides [2,10]. HPLC techniques for this purpose have some drawbacks, however, as they are not sufficiently rapid, cheap or efficient. The disadvantages have initiated searches for other techniques. The possibilities of using high-performance capillary electrophoresis (HPCE) for carbohydrate analysis seem promising [11–14], and for non-reducing oligosaccharides separations of borate-complexed compounds seem especially advantageous [15].

Capillary zone electrophoresis (CZE) of borate–oligosaccharide complexes was the subject for this work, with investigations of various

* Corresponding author.

0021-9673/93/$06.00

important parameters affecting the separation, including buffer composition and pH, temperature and voltage. The effects of these parameters on migration time, peak shape and area, number of theoretical plates, resolution and repeatability were evaluated. A procedure for an efficient and simple sample preparation involving group separation was developed, as this was found to be a critical step in relation to the success of the CZE method for the determination of oligosaccharides occurring in plants, feed and food.

EXPERIMENTAL

Chemicals and solvents

All chemicals and solvents were of analytical-reagent grade and the water was purified using a Milli-Q system (Millipore, Bedford, MA, USA).

Raffinose and stachyose were obtained from Aldrich Chemie (Steiheim, Germany), melibiose, methyl-α-galactopyranoside and fucose from Sigma (St. Louis, MO, USA) and sucrose, lactose, maltose, pentoses, hexoses, rhamnose and *myo*-inositol from the laboratory collection of reference carbohydrates. Galactinol isolated from sugar beet was avaliable and verbascose (purity 78%) and ajugose were preparatively isolated from peas using paper chromatography and preparative HPLC [10].

Sample preparation

Mature seeds of selected pea lines were ground in a coffee mill. Subsequent grinding in a mortar was occasionally necessary to obtain a uniform powder. Lactose (200 μl, 60 mg/ml) and melibiose (200 μl, 60 mg/ml) were added to 0.5 g of pea flour as internal standards prior to extraction with 3 × 5 ml of methanol–water (7:3). The pea flour was homogenized by means of an Ultra Turrax T 25 (Janke & Kunkel, Staufen, Germany) for 3 × 1.5 min. After each extraction cycle the homogenate was centrifuged in a table centrifuge (Labofuge, Heraeus Sepatech, Osterode, Germany) at 2000 *g* for 1 min. The extract was evaporated to dryness in an evaporator (Rotavapor-R; Büchi, Flawil, Switzerland) and the residue was dissolved in 1 ml of water.

The crude extract was centrifuged and subjected to group separation according to the principles described by Bjerg *et al.* [16]. Aqueous suspensions (1:1) of (A) Dowex 50W-X8, 200–400 mesh (H^+) and (B) Dowex 1-X8, 200–400 mesh (OH^-), (Sigma) were prepared. Portions of 1 ml of A or B were packed into 1-ml syringes (columns) supplied with discs of silica material as the bottom. Column A was placed above column B in a vacuum manifold (Supelco, Bellefonte, PA, USA), and 1 ml of crude extract was transferred to column A. The sample was allowed to pass into the column material, which subsequently was washed with 3 × 3 ml of water. The aqueous effluent was concentrated to an appropriate volume, kept at −20°C until use and analysed by CZE. Volumes of *ca.* 50 μl were transferred into vials (0.5 ml, Model 1298; Kartell, Milan, Italy), which were supplied with rubber caps (Model 4E1634; Applied Biosystems, Foster City, CA, USA) supplied with a slit to diminish evaporation.

Apparatus

The capillary electrophoresis instrument used was an ABI Model 270 A-HT (Applied Biosystems). The fused-silica capillary had the dimensions 720 mm × 50 μm I.D. × 360 μm O.D., including coating material. The detector window was placed 500 mm from the injection end (anode). On-column UV detection was performed at 195 nm and data processing was effected on a Shimadzu (Kyoto, Japan) Chromatopac C-R3A.

Separation conditions

The influence of separation parameters, including concentration of borate electrolyte (20–100 m*M* $Na_2B_4O_7$; Merck, Darmstadt, Germany), pH (9.2–10.3), temperature (30–60°C), voltage (10–20 kV) and concentration of 2-propanol modifier (0–15%, v/v), were investigated. Fresh solutions of borate were prepared every day and stored at room temperature. Unless specified otherwise, the injection time was 2.0 s, the detector rise time was 0.5 s and the range was 0.01. Between each run the capillary was flushed with 1 *M* NaOH for 3 min and with borate buffer for 5 min. The buffer at the

injection end (anodic) was changed each ten runs.

The influence of the running conditions on the separation was described for individual compounds by the migration time (MT, min), the normalized area (NA = absolute peak area/MT) and the number of theoretical plates per metre of capillary (plates/m), and for pairs of compounds by the resolution (R_s) [17].

Concentrations of individual sugars were calculated primarily based on lactose as internal standard. In situations where lactose co-eluted with ajugose, or where the peak was followed by a trough, the melibiose peak was used for correction. Calibration graphs were made by determining increasing concentrations (20, 40, 60, 80 and 100%) of a standard solution consisting of sucrose, raffinose, stachyose, verbascose, lactose and melibiose. Suitable detector signals were obtained for a stock solution (100%) with a concentration of each carbohydrate of about 6 μmol/ml.

RESULTS AND DISCUSSION

The overall method for the determination of sucrose and oligosaccharides in mature peas and other plant products consists of extraction, sample preparation by group separation and analysis by CZE.

Efficient extraction of low-molecular-mass carbohydrates from dietary fibres and other high-molecular-mass compounds in mature peas was achieved by repeated homogenizations in boiling methanol–water (7:3). This extraction medium was preferred to other methanol–water proportions, to cold methanol–water and to ethanol–water (7:3). Extraction with hot water was avoided because of the gelling properties of the pectin fraction, which can trap extractable compounds. Gel formation was disrupted in the presence of methanol. Moreover, effective inactivation of glycosidases was obtained, and no products of oligosaccharide or starch hydrolysis were observed such as melibiose, galactose and maltotriose or larger glucose oligomers. The enzyme inactivation during the initial extraction is important as products of enzymatic hydrolysis have been observed with extraction in water at temperatures below 60°C [18,19].

The group separation procedure developed for sample preparation appeared to be essential for the attainment of high-quality electropherograms (Fig. 1). The samples were passed directly from a strongly acidic cation exchanger to a strongly basic anion exchanger in order to remove compounds that had a positive or negative net charge under the conditions specified. The neutral carbohydrates were recovered in the aqueous effluent. The method is a modification of the procedure used for the preparation of oligosaccharide samples for HPLC [2,10]. The major improvement was the substitution of weakly basic anion-exchange material with strongly basic material. Substances interfering with the separation and with detection at 195 nm, which is within the absorbance range of a wide group of compounds, was efficiently avoided with the modified method.

A simple and inexpensive CZE method was adapted from Hoffstetter-Kuhn *et al.* [15] for the determination of oligosaccharides in extracts of

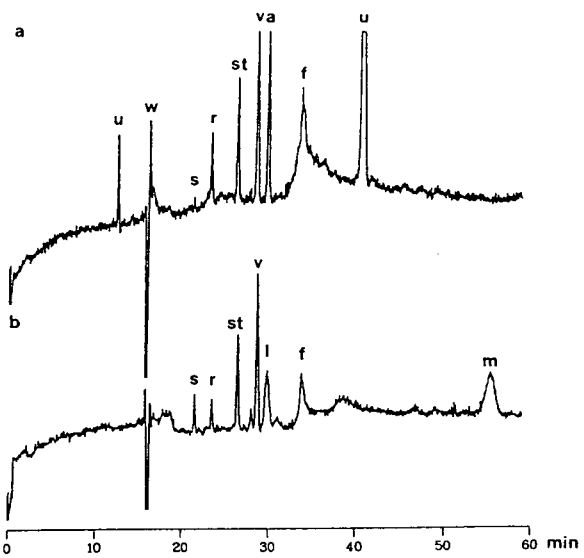

Fig. 1. (a) Electropherogram of a mixture of oligosaccharides. Peaks labelled u are impurities from the ajugose preparation. (b) Electropherogram of a pea extract purified by group separation. Separation conditions: 100 mM $Na_2B_4O_7$, pH 9.9, 50°C, 10 kV. s = Sucrose; r = raffinose; st = stachyose; v = verbascose; a = ajugose; l = lactose; w = water front; m = melibiose; u = unknown; f = "false peak".

mature peas. Separation and UV detection of carbohydrates by this method were based on the formation of borate–polyol complexes. The separation parameters borate concentration, pH, temperature and voltage were varied in order to find the best compromise that complied with the demands for high separation efficiency (plates/m and R_s), short durations of analyses (MT) and sufficiently high detector responses (NA). With the described system, the MT of oligosaccharides increased as a function of the molecular mass, whereas reducing sugars and especially monosaccharides migrated more slowly compared with their molecular mass (Fig. 1).

The formation of borate–polyol complexes was favoured with increasing concentrations of sodium tetraborate, which positively affected the electrophoretic mobility of the carbohydrates. As a consequence, the MT increased by a factor of 2 for raffinose, 2.2 for stachyose and 2.3 for verbascose when the borate concentration was increased from 20 to 100 mM. Simultaneously the number of plates/m increased by a factor of 1.7–2.0, while the R_s of raffinose and stachyose rose 3.9 times and that of stachyose and verbascose 3.3 times. The carbohydrate signals were hardly detectable at 10 mM borate and the absolute peak areas increased considerably with increasing borate concentrations. The NA values were also positively affected by increasing borate concentration, and increased by a factor of about 1.5 over the whole concentration range (20–100 mM). Hence borate complexation is important for both separation and detection [15]. At concentrations ≤60 mM verbascose co-eluted with a false peak that appeared in every electropherogram. Therefore, either 80 or 100 mM sodium tetraborate was used. At higher concentrations the analyses proceeded too slowly.

Electropherograms of sufficiently high quality were only obtained within the pH range 9.2–10.3. This pH was required for sufficient complex formation, and at lower and higher pH the noise of the baseline increased unacceptably. Two series of measurements were performed, where the pH was increased within the ranges 9.2–9.9 and 9.7–10.3. MT (Fig. 2a), NA and R_s (Fig. 2b) increased when the pH of the electrolyte was increased. The number of theoretical

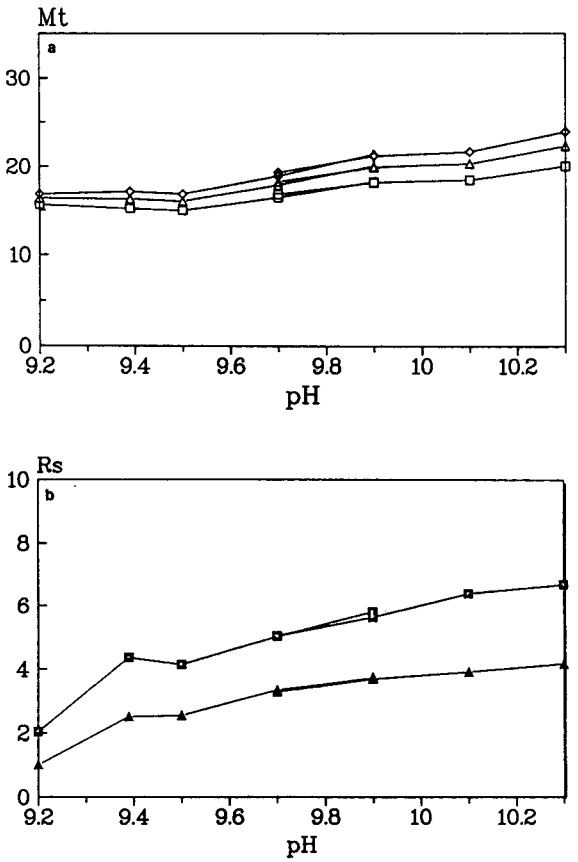

Fig. 2. (a) Migration times (MT, min) for (□) raffinose, (△) stachyose and (◇) verbascose and (b) resolution (R_s) of (■) raffinose and stachyose and (▲) stachyose and verbascose as a function of pH of the borate electrolyte (80 mM $Na_2B_4O_7$, 10 kV, 60°C).

plates/m also rose with increase in pH, but only small effects were observed within the pH range 9.4–10.1, and at pH 10.3 there was a tendency for a decline. The electropherogram at pH 9.2 was of poor quality because of noise. At pH 9.4, which was the pH of the dissolved $Na_4B_4O_7$, the baseline was planar. The baseline started to slant with increase in pH, especially when the voltage was also increased. A convenient compromise between the utilization of the advantageous effect of higher pH on separation and detection on the one hand and acceptable migration times and slope of the baseline on the other was found to be pH 9.9.

The migration times decreased by a factor of

about 1.5 when the temperature was increased from 30 to 60°C (Fig. 3a). Within the same temperature range *NA* increased by a factor of 1.4–2.0 owing to the injection of larger sample volumes because of the reduced viscosity of the electrolyte (Fig. 3b). The number of theoretical plates/m and the resolution between the oligosaccharides decreased with increasing temperature (Fig. 3c and d). In contrast, an increase in the resolution of borate–monosaccharide complexes as a function of the temperature was reported in another study [15]. Usually band broadening becomes more pronounced at higher temperatures owing to diffusion, but it was argued that the enhanced rates of complex formation made the compounds move in narrower zones, which compensated for the diffusion effect. This observation could not be verified in this study. The formation of hemiacetals seemed to be strongly involved in the formation of borate–monosaccharide complexes [15]. For non-reducing sugars such as sucrose and oligosaccharides of the raffinose family, however, this reaction can be excluded. The rate of ring opening may depend more on the temperature than the reaction rate for borate–polyol complex formation. Hence the optimum temperature for the CZE analysis of reducing sugars seems to be higher than for non-reducing sugars.

An increased voltage resulted in decreased *MT* and higher *NA* (especially for verbascose), whereas almost constant plate numbers were observed within the range 10–15 kV, with a decline at 18–20 kV (Fig. 4). The resolution was relatively constant, with a declining tendency, when the voltage was increased from 10 to 20 kV.

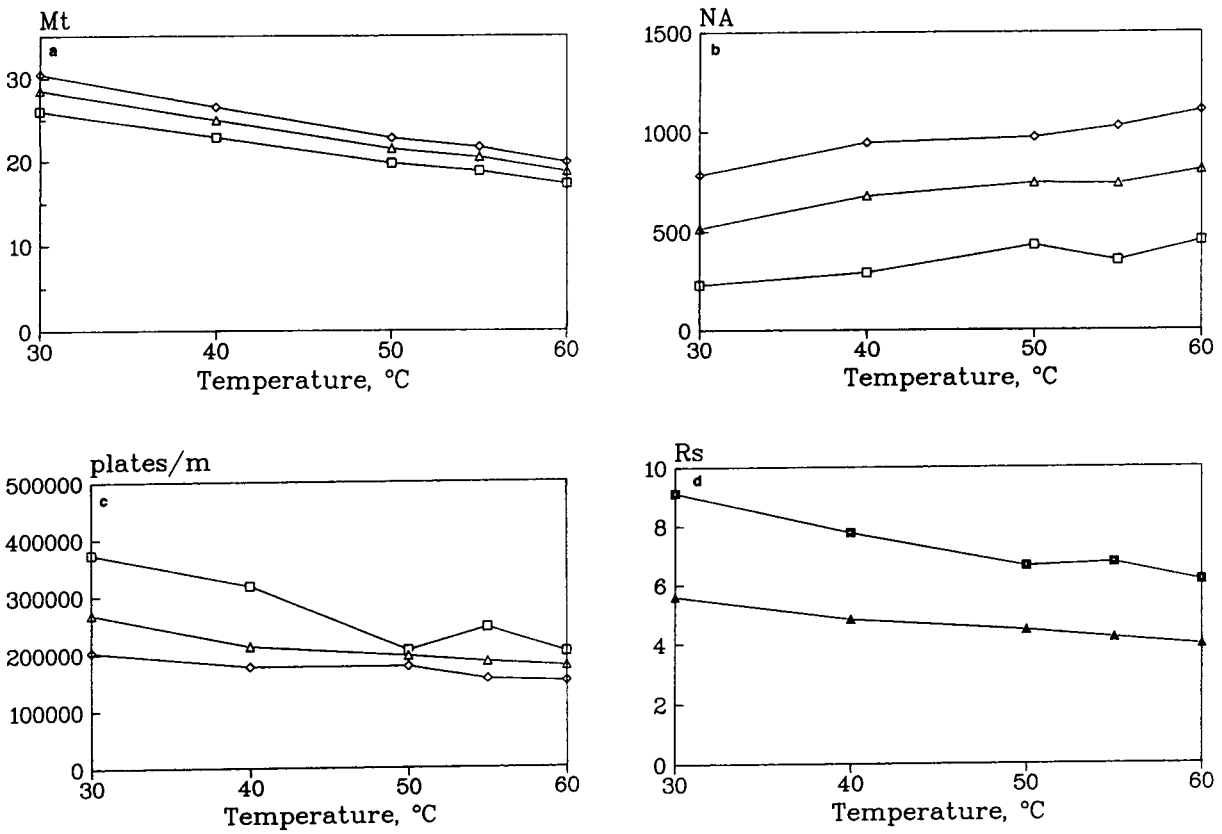

Fig. 3. (a) Migration times (*MT*, min), (b) normalized areas (*NA*) and (c) number of theoretical plates per metre (plates/m) for (□) raffinose, (△) stachyose and (◇) verbascose and (d) resolution (R_s) of (■) raffinose and stachyose and (▲) stachyose and verbascose as a function of temperature (100 m*M* $Na_2B_4O_7$, pH 9.4, 10 kV).

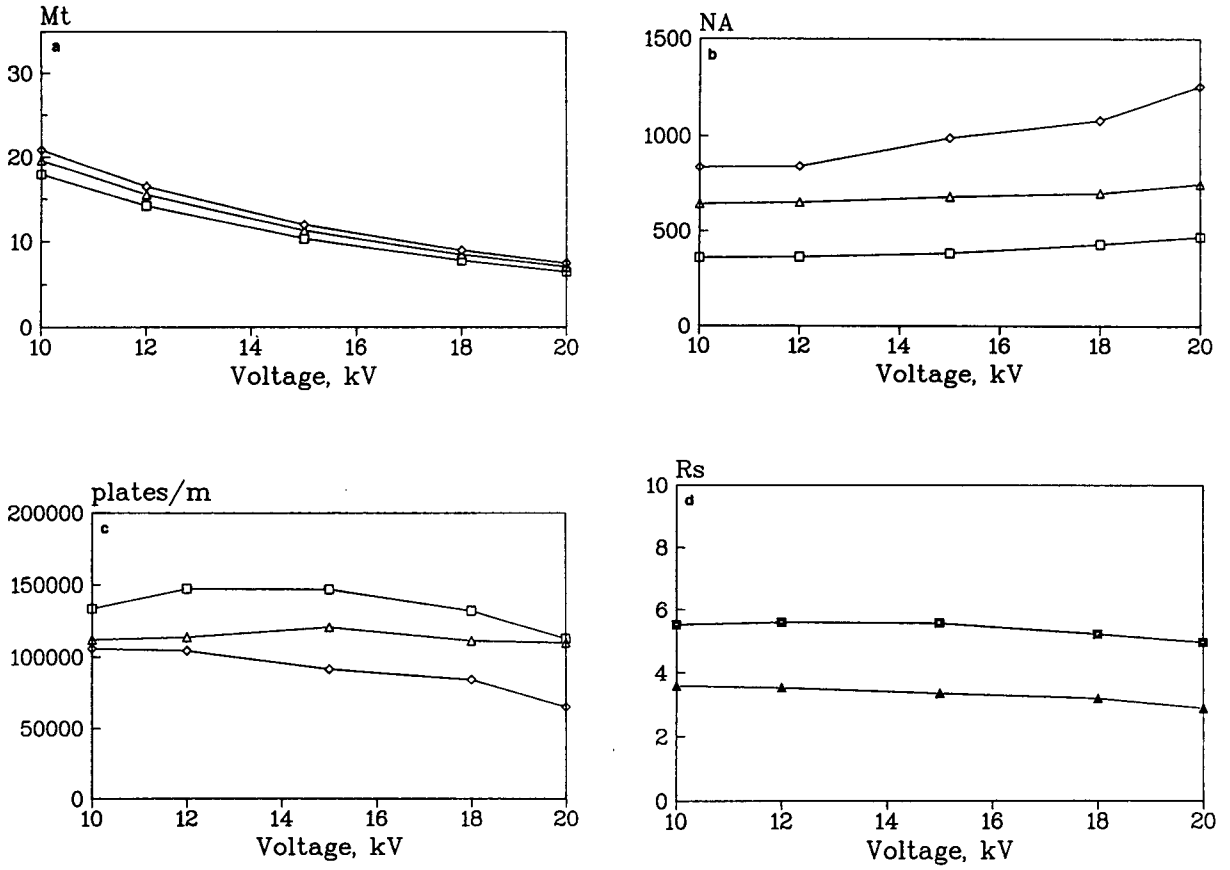

Fig. 4. (a) Migration times (*MT*, min), (b) normalized areas (*NA*), (c) number of theoretical plates per metre (plates/m) for (□) raffinose, (△) stachyose and (◇) verbascose and (d) resolution (R_s) of (■) raffinose and stachyose and (▲) stachyose and verbascose as a function of voltage (80 m*M* $Na_2B_4O_7$, pH 9.9, 60°C).

The baseline became inclined and more noise was observed when the voltage was increased. The most appropriate voltage was found to be 10 kV.

2-Propanol (0–15%) was added to the electrolyte as a modifier. Improved resolution was obtained, but at the same time *NA* and the number of plates/m decreased and MT increased. The reduced number of theoretical plates was a result of asymmetric peaks (fronting) with a broad base. The modifier could be used at concentrations up to about 8% without affecting the peak shape seriously.

Linear calibration graphs were obtained for sucrose and individual oligosaccharides with correlation coefficients (r) between 0.99 and 1.00. Lactose was eluted as a broader peak than sucrose and oligosaccharides of the raffinose family, and the correlation coefficients were generally lower for this compound (0.97–1.00).

Lactose and melibiose, which were both absent from the plant material studied, were chosen as internal standards. For samples containing considerable amounts of ajugose the choice of lactose is not ideal, as the compounds migrated with almost identical velocities through the capillary (Fig. 1). However, the ajugose content in peas is usually negligible, and the inclusion of the second internal standard melibiose in the samples allowed correction in those few instances where a contribution to the peak area from ajugose could not be excluded. Disadvantages of the use of melibiose are its higher migration time compared with the

oligosaccharides, prolonging the time of analysis, and its relatively broad peak shape. The peak is well defined, however, and does not co-elute with sample carbohydrates or any of the reference compounds tested. Suitable alternatives to the chosen internal standards with good absorbance properties at 195 nm and with *MT*s lower than that of sucrose are required.

Relative response factors (*RRF*) were calculated by dividing the slope of the calibration graph for lactose by the corresponding slope for individual analytes. Mean *RRF* values calculated on the basis of thirteen calibration graphs are given in Table I. Decreasing *RRF* values were observed when the number of galactose units per molecule increased, *i.e.*, higher detector signals were recorded per molecule as a function of the length of the α-galactoside chain in a non-linear manner. Thus, a *ca.* fourfold decrease was observed on going from sucrose to raffinose. The second and third galactose units caused smaller decreases in the *RRF*.

The relative standard deviation (R.S.D.) of the relative response factors describes the accuracy of determinations of individual compounds (Table I). The highest R.S.D. was found for sucrose (7.5%), which also has the lowest UV absorption and electrophoretic mobility, because the structure of sucrose does not favour complex formation with borate. The R.S.D.s for raffinose, stachyose and verbascose ranged from 3.5 to 5.4%.

TABLE I

MEANS AND VARIATION OF RELATIVE RESPONSE FACTORS (*RRF*) FOR SUCROSE AND OLIGOSACCHARIDES USING CAPILLARY ZONE ELECTROPHORESIS

The slopes of calibration graphs ($n = 13$) were used for the calculation of *RRF* [=slope of graph for the internal standard (lactose)/slope for the analyte]. Separation conditions: 100 m*M* $Na_2B_4O_7$, pH 9.9, 50°C, 10 kV. S.D. = standard deviation; R.S.D. = relative standard deviation = S.D./mean *RRF*.

Analyte	*RRF*	S.D.	R.S.D. (%)
Sucrose	5.15	0.39	7.5
Raffinose	1.23	0.05	4.1
Stachyose	0.76	0.03	3.5
Verbascose	0.60	0.03	5.5

CONCLUSIONS

Repeated homogenizations in boiling methanol–water (7:3) ensured efficient extraction of oligosaccharides and other low-molecular-mass sugars from mature peas. Moreover, no artifact formation was observed with the procedure owing to immediate inactivation of glycosidases. The introduction of the internal standards lactose and melibiose prior to extraction allowed corrections for differences among samples in injection volume.

Compounds with positive or negative net charges at relatively extreme pH values were removed by group separation, as the seed extracts were purified using a strongly acidic cation exchanger, which was connected with a strongly basic anion exchanger. This procedure was essential to obtain high-quality electropherograms by CZE analysis.

The determination of oligosaccharides by CZE was based on the formation of borate–carbohydrate complexes. Increasing borate concentration (20–100 m*M* $Na_2B_4O_7$) and pH favoured the complex formation, which improved the UV absorption at 195 nm and increased the electrophoretic mobility of the compounds, leading to improved separation and longer *MT*s. The running conditions that were found to provide the best compromise between acceptable separation and detection efficiency and duration of analysis were 100 m*M* $Na_2B_4O_7$, pH 9.9, 50°C, 10 kV and omission of 2-propanol modifier. Under these conditions about 144 000, 105 000, 84 000 and 74 000 plate/m for sucrose, raffinose, stachyose and verbascose, respectively, were obtained. With other combinations of running conditions up to about 375 000 plates/m were obtained for raffinose. The number of theoretical plates/m that can be obtained by HPLC using amino-bonded silica was at least one order of magnitude lower for sucrose and raffinose compared with the CZE method. Other advantages of the CZE procedure over the widely used HPLC methods based on refractive index detection are

the use of on-column UV detection, low cost per analysis, ease of operation and the use of non-toxic chemicals. Moreover, rapid analyses are possible because of the relatively short migration times of the non-reducing oligosaccharides. Hence the CZE method presented provides a good alternative to existing methods for the determination of oligosaccharides of the raffinose family, and it can be adapted for the determination of other low-molecular-mass carbohydrates.

ACKNOWLEDGEMENTS

The authors gratefully acknowledge support form the Danish Agricultural and Veterinary Research Council, the Danish Natural Research Council and the EEC–ECLAIR Programme. E. Smed, manager of the laboratory at Maribo Seeds, generously supplied the reference compound galactinol.

REFERENCES

1 A.M. Arentoft, C. Bjergegaard and H. Sørensen, *Växtodling*, 23 (1990) 182.
2 A.M. Arentoft and H. Sørensen, in P. Plancquaert (Editor), *Proceedings of the 1st European Conference on Grain Legumes, Anger, June 1992*, Edition Soft Publicité, Reims, 1992, p. 457.
3 P.M. Dey, in P.M. Dey and R.A. Dixon (Editors), *Biochemistry of Storage Carbohydrates in Green Plants*, Academic Press, New York, 1985, p. 53.
4 O. Kandler and H. Hopf, in F.A. Loewus and W. Tanner (Editors), *Encyclopedia of Plant Physiology, New Series, Volume 13A: Plant Carbohydrates I, Intracellular Carbohydrates*, Springer, Berlin, Heidelberg, New York, 1982, p. 348.
5 U. Holthaus and K. Schmitz, *Planta*, 185 (1991) 479.
6 E. Cristofaro, F. Mottu and J.J. Wuhrmann, in H.L. Sipple and K.W. McNutt (Editors), *Nutrition Foundation Monograph Series. Sugar in Nutrition. International Conference. Nashville, Tenn., USA*, Academic Press, New York, London, 1974, p. 313.
7 D. Marthinsen and S.E. Fleming, *J. Nutr.*, 112 (1982) 1133.
8 K.R. Price, J. Lewis, G.M. Wyatt and G.R. Fenwick, *Nährung*, 32 (1988) 609.
9 G.R. Fenwick, *J. Food Sci.*, 46 (1981) 784.
10 A.M. Arentoft, *Pea Quality, Ph.D. Thesis*, The Royal Veterinary and Agricultural University, Copenhagen, 1992, p. 124.
11 T.W. Garner and E.S. Yeung, *J. Chromatogr.*, 515 (1990) 639.
12 J. Liu, O. Shirota and M. Novotny, *J. Chromatogr.*, 559 (1991) 223.
13 W. Nashabeh and Z.E. Rassi, *J. Chromatogr.*, 600 (1992) 279.
14 S. Suzuki, K. Kakehi and S. Honda, *Anal. Biochem.*, 205 (1992) 227.
15 S. Hoffstetter-Kuhn, A. Paulus, E. Gassmann and H.M. Widmer, *Anal. Chem.*, 63 (1991) 1541.
16 B. Bjerg, O. Olsen, K.W. Rasmussen and H. Sørensen, *J. Liq. Chromatogr.*, 7 (1984) 691.
17 S. Michaelsen, P. Møller and H. Sørensen, *J. Chromatogr.*, 608 (1992) 363.
18 I.M. Knudsen, *J. Sci. Food Agric.*, 37 (1986) 560.
19 A.W. Wight and J.M. Datel, *Food Chem.*, 21 (1986) 167.

Journal of Chromatography A, 652 (1993) 525–533
Elsevier Science Publishers B.V., Amsterdam

CHROM. 25 139

Micellar electrokinetic capillary chromatography analysis of the behavior of bilirubin in micellar solutions

Andrew D. Harman, Richard G. Kibbey, Marjorie A. Sablik, Yolanda Fintschenko, William E. Kurtin and Michelle M. Bushey*

Department of Chemistry, Trinity University, San Antonio, TX 78212 (USA)

ABSTRACT

The capacity factor of bilirubin is determined by micellar electrokinetic capillary chromatography (MECC) techniques in three different surfactant systems. The capacity factor of bilirubin in cholic acid, taurocholic acid, and taurochenodeoxycholic acid solutions are compared to each other as a function of pH. The pH range studied is 6.5 to 9.5 which includes the pH range of bile, and includes the most likely pK_a values of bilirubin carboxyl groups. MECC techniques are used to estimate these apparent pK_a values for bilirubin as well as to determine the capacity factors for the separate ionization states of bilirubin in the three different surfactants. Due to the complexity of the bilirubin–bile salt system, it appears as though it is not possible to use MECC to accurately determine the bilirubin apparent pK_a values. Separations are performed in 75 μm capillaries, typically 36 to 52 cm in length. UV detection, electrokinetic injection, and run voltages of 7 kV are typical. Solutions of 25 m*M* of each bile salt are prepared in a 20 m*M* phosphate–borate buffer system.

INTRODUCTION

Micellar electrokinetic capillary chromatography (MECC) was originally introduced in the middle 1980s as a way to utilize capillary electrophoresis (CE) systems for separations of neutral compounds [1,2]. It was soon realized, however, that MECC techniques could also offer enhancement of separations of charged compounds [3,4]. Indeed, since many samples contain components that are neutral as well as charged, it is important to study MECC separations of charged analytes. While some studies of charged analyte MECC separations have been performed, most studies of MECC systems have been separations of neutral analytes. What both types of studies have in common is that the vast majority of all MECC studies make use of sodium dodecyl sulfate (SDS) as the micelle phase [5]. This is to be expected as SDS is an extremely well behaved and well characterized surfactant.

There are other surfactants that can be used successfully in MECC applications. Some of the other pseudo-stationary phases that have been utilized include cyclodextrins [6,7], dodecyltrimethylammonium bromide (DTAB) [7] or cetyltrimethylammonium chloride (CTAB) [8], sodium decyl sulfate (STS) [8] and bile salts [9–13]. Most of the applications utilizing bile salts are separations of chiral compounds. Bile salts are synthesized in the liver from cholesterol and are concentrated in the gall bladder. They have a steroid backbone with various points of substitution. The positions marked R_1, R_2, and R_3 in Fig. 1 determine the general class of bile salts. Cholic acid, deoxycholic acid and chenodeoxycholic acid varieties are shown. In addition, bile salts can be unconjugated or conjugated with compounds such as taurine or glycine in the

* Corresponding author.

0021-9673/93/$06.00

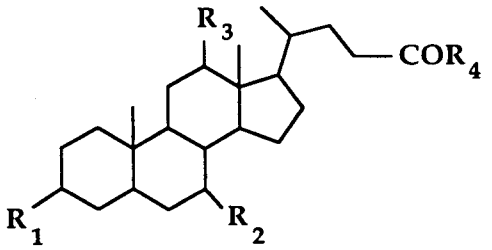

R1	R2	R3	BILE SALT CLASSIFICATION
-OH	-OH	-OH	Cholic Acid
-OH	-OH	-H	Chenodeoxycholic Acid
-OH	-H	-OH	Deoxycholic Acid

R4	CONJUGATES
-OH	Unconjugated
$-NHCH_2CH_2SO_3H$	Tauro-
$-NHCH_2CO_2H$	Glyco-

Fig. 1. Generalized bile salt structure, showing substitution positions for different classifications of bile salts as well as conjugated structures.

position marked R_4. Bile salts will form micelles, although the structure of these micelles is poorly characterized in comparison with more familiar surfactants such as SDS. In fact, all bile salts do not form the same type of micelle, the structure of the micelle can change as a function of bile salt concentration, and the critical micelle concentration (CMC) of various bile salts can change as a function of pH [14]. Nevertheless, bile salt micelles can be successfully used in MECC applications.

The primary biological function of bile salts and bile salt micelles is to solubilize dietary lipids and thereby aid in their elimination from the body. Perhaps the most important compound to be eliminated in this manner is bilirubin. Bilirubin is the breakdown product of haem. Normal human secretions of bile pigment are mainly composed of 65–85% bilirubin diconjugates with the remainder being monoconjugates and unconjugated bilirubin (UCB) [15]. UCB accounts for only 1–3% of the bilirubin forms found in

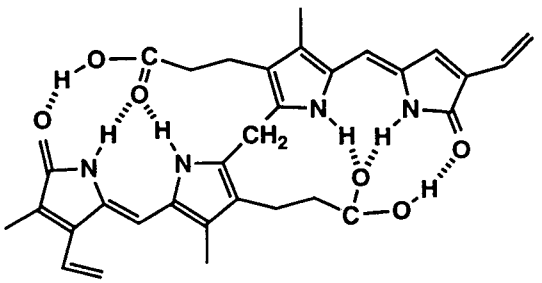

Fig. 2. Structure of fully protonated, unconjugated bilirubin, showing intramolecular hydrogen bonding.

bile [16]. The structure of UCB is shown in Fig. 2. While conjugates of bilirubin are water soluble, unconjugated bilirubin is relatively insoluble in aqueous solutions at pH 7.0 [17]. Yet, the concentrations of UCB in hepatic and gall bladder biles are 10 and 35 μM [18]. These high concentrations of UCB are stabilized in bile solutions through interactions with bile salt micelles and monomers. Bilirubin will begin to precipitate in bile fluids if the UCB concentration rises above the saturation level, if there is a decrease in the binding of UCB by biliary components, or through a combination of these two phenomena [19]. The precipitation of unconjugated bilirubin is thought to be an important step in pigment gallstone formation. Pigment gallstones contain precipitated UCB either in the form of calcium salts or polymers of pigment.

Any change in the bile fluid environment which influences either the concentration or solubility of UCB, or changes the binding of UCB to bile salt micelles, can thus be a precursor to pigment gallstone formation. For instance, the concentration or relative proportion of UCB in bile can change as a result of hemolysis, phototherapy, or hydrolysis of bilirubin conjugates [16]. There are numerous factors which are believed to be important in influencing the binding of UCB to bile salt micelles. Certainly a change in the total concentration of micelles present will affect how much bilirubin is solubilized. Also, if the various bile salts present in bile solutions can solubilize UCB to different degrees, then a change in the bile salt profile can influence the amount of solubilized bilirubin.

Changes in the concentration of calcium ion can change the CMC of bile salts [20]; a change in the CMC of a micelle can then in turn affect binding of solutes. Changes in the levels of lecithin and cholesterol may also affect the binding of bilirubin to bile salt micelles [21,22]. While these numerous factors are believed to influence the bile chemistry of bilrubin, analysis of these solutions is hampered in part by the extremely low solubility of bilirubin at physiological pH values as well as poor understanding of the bile salt micelle structures; thus, the interaction between the bile salt micelles and bilirubin remains incompletely understood.

The pK_a values for the two propionic groups on bilirubin have been the subject of controversy in the literature. Because of bilirubin's low solubility, these values can not be measured directly. Determination of these two pK_a values has been attempted in solvents other than water. Studies of bilirubin in solvents such as dimethyl sulfoxide (DMSO) probably yield inaccurate information as to bilirubin's behavior in aqueous solution. Reported values fall typically in the range of 5 to 9 [17,18]. This is considerably more basic than the pK_a value of typical carboxyl groups. This can be explained in part by the fact that these bilirubin carboxyl groups are known to be involved in intramolecular hydrogen bonding as depicted in Fig. 2. There is also some disagreement in the literature as to whether or not the two pK_a values are identical to each other. One study reported that the pK_a values were quite different from each other, with values of 6.5 and 9.0 [21]. This conclusion was later modified, and the pK_a values are reported to be 8.1 and 8.4 [23]. It is very interesting, and somewhat surprising, that this former work is the only work in the literature to date which attempts to determine the apparent pK_a values of bilirubin in the presence of bile salts.

MECC should be a very convenient method with which to probe the bilirubin–bile salt system. We have examined the behavior of bilirubin in a variety of bile salt solutions as a function of pH. The primary purposes of this study are to: first, determine if MECC systems can be used effectively in these studies; second, to determine the pK_a values of bilirubin; third, to determine the effects of pH on bilirubin's ability to associate with bile salts; fourth, to determine if bilirubin behaves differently in different bile salt solutions. We began these investigations by determining the capacity factor of bilirubin in cholic acid, taurocholic acid, and taurochenodeoxycholic acid solutions as a function of pH. The pH range chosen for study was pH 6.5 to 9.5. This includes the pH range of bile, which varies from pH 6.8 to 7.6, and thus represents the region of most interest in terms of physiological conditions. Our pH range also covers the pK_a range most often reported for bilirubin carboxyl groups. Lower pH values are difficult to study due to the insolubility of bilirubin and the instability of the micelle system. Higher pH values are of little interest physiologically and would slowly etch the fused silica surface of the capillaries.

EXPERIMENTAL

Apparatus and reagents

Separations were performed on fused-silica capillaries purchased from Polymicro Technologies (Phoenix, AZ, USA) with an inner diameter of 75 μm. The capillaries varied in length from 36 cm to 52 cm. A Linear Instruments UVIS 200 detector (Reno, NV, USA) fitted with a deuterium lamp was used for detection (225 nm) of peaks. The detector was placed 26 to 28 cm from the grounded end of the capillary. High voltage was supplied by a Spellman high-voltage d.c. unit (Plainview, NY, USA) with an output range of $+/-30$ kV. A Dell 316SX computer (Austin, TX, USA) was used for data acquisition. The computer was fitted with a multi-function data acquisition board from National Instruments (Austin, TX, USA). Software was developed in house with Microsoft QuickBasic (Redmond, WA, USA) and National Instrument's Lab Windows software. Distilled water was provided by a Barnstead NANO pure system purchased through Fisher Scientific (Austin, TX, USA). All reagents were purchased from Sigma (St. Louis, MO, USA) except for DMSO which was obtained from Fisher.

Separations performed with SDS systems were detected with a Jasco 2550 UV detector with a

100 μm slit in a microcell holder. Data were recorded directly on a chart recorder. The capillary lengths on this system were 62 cm for the entire capillary length and 33 cm to the detection window.

Bilirubin recrystallization

Bilirubin was purified according to the method of McDonagh and Assisi [24]. Approximately 400 mg of bilirubin IXα was stirred and heated in 460 ml of chloroform (analytical-reagent grade containing ethanol stabilizer) until the solution boiled. The mixture was cooled to room temperature and washed in a separatory funnel with 0.1 *M* $NaHCO_3$ (3 × 100 ml or until the washings were colorless). The solution was dried over 10 g of anhydrous Na_2SO_4 and filtered. The filtrate was heated until boiling and approximately one third of the chloroform was distilled off. Methanol was added to the boiling solution until the solution became perceptibly turbid. The mixture was cooled to room temperature, and after two hours the crystalline precipitate was collected by filtration. The precipitate was washed with chloroform–methanol (1:1) and dried under high vacuum for at least 12 h. The entire procedure was carried out under reduced lighting in order to prevent the isomerization of bilirubin. Typical yields were in the range of 60–70%. Bilirubin prepared in this manner was stored in the dark in a freezer.

Buffer preparation and sample preparation

Solutions of 20 m*M* monobasic sodium phosphate and 20 m*M* sodium tetraborate were prepared. The pH of the monobasic sodium phosphate was adjusted to 6.00 using phosphoric acid, and the pH of the sodium tetraborate was adjusted to 9.60 using sodium hydroxide. For the studies where pH was varied, these two solutions were mixed until the desired pH was obtained. For the SDS studies, equal volumes of the two buffers were mixed and the pH adjusted to 8.5 with phosphoric acid.

A 25-m*M* solution of the desired bile salt was prepared using the above buffer solution. The pH of this solution was recorded as the operating pH. This solution was then filtered using a 45-μm syringe filter (Gelman Sciences, Ann Arbor, MI, USA).

Bilirubin and Sudan III were dissolved separately in DMSO. The sample was then prepared by adding 20 μl of the bilirubin solution and 10 μl of the Sudan III to 1000 μl of the bile salt solution. This mixture was then filtered using a 45-μm syringe filter.

Capillary preparation and run conditions

A detection window was prepared on the capillary by holding a drop of hot sulfuric acid on the capillary surface. The length of the entire capillary and the length from the injection end of the capillary to the center of the window was then recorded for future calculations. The window was then washed with deionized water and then methanol and allowed to dry.

The capillary was rinsed every morning with 1 *M* KOH for 10 min and then with deionized water for 5 min. The rinsing was accomplished by aspirating the solution through the capillary using a Nalgene hand pump (Fisher Scientific) equipped with a solution trap. The bile salt solution was then aspirated into the capillary for 10 min and then the voltage was applied for 5 min. At this point the capillary was ready for a sample injection. If the bilirubin precipitated in the capillary, the capillary was treated again to remove the bilirubin. At the end of the day the capillary was rinsed with 1 *M* KOH for 5 min then deionized water for 5 min and stored in water overnight.

Run voltage was typically 7 kV. The sample was injected onto the capillary by placing the capillary tip and the electrode into sample vial and applying a voltage of 5 kV for 3 to 10 s. The capillary and the electrode were then placed back into the running buffer and the run was started.

RESULTS AND DISCUSSION

While MECC studies of neutral analytes are relatively straight forward, studies of ionizable compounds can be more involved. In a recent article, Khaledi *et al.* [25] developed mathematical models to deal with the behavior of anionic analytes in the presence of anionic micelles. In

that article, it was shown that the capacity factor of such a compound can be determined by the compound's mobility with (μ) and without micelles (μ_0) and the mobility of the micelle itself (μ_{mc}) as shown in eqn. 1.

$$k' = \frac{\mu - \mu_0}{\mu_{mc} - \mu} \quad (1)$$

The problem with analyses of bilirubin is that in the absence of micelles the insolubility of the compound makes determination of μ_0 impossible. In the same article, it was shown that the free solution mobility of an anionic analyte is related to the free solution mobility of the fully ionized species (μ_{A^-}), the ionization constant, and the hydrogen ion concentration as shown in eqn. 2.

$$\mu_0 = \frac{\mu_{A^-}(K_a/[H^+])}{1 + K_a/[H^+]} \quad (2)$$

But again the problem arises of applying this equation to an analysis of the bilirubin system in that the K_a is unknown. But we can make use of another equation found in this article that shows that the observed capacity factor of an anionic analyte is determined by the capacity factor of the protonated species (k'_{HA}), the capacity factor of the ionized species (k'_{A^-}), the ionization constant and the hydrogen ion concentration as shown in eqn. 3.

$$k' = \frac{k'_{HA} + k'_{A^-}(K_a/[H^+])}{1 + K_a/[H^+]} \quad (3)$$

If it is assumed that the capacity factor of the ionized species is significantly less than the capacity factor of the protonated species, then eqn. 3 can be simplified and rearranged to yield eqn. 4.

$$1/k' = 1/k'_{HA} + (K_a/k'_{HA})(1/[H^+]) \quad (4)$$

This equation shows that if the inverse of the observed capacity factor is plotted *versus* the inverse of the hydrogen ion concentration, then the slope and intercept of the resulting line will yield the capacity factor of the protonated species and the ionization constant of the anionic species under investigation.

In order to correct the apparent capacity factor of bilirubin for its mobility when ionized, an iteration process was used. The first step was to determine the mobility of the bilirubin anion in the absence of micelles. As this species is fairly soluble this number can be easily obtained. The next step was to calculate the capacity factor of bilirubin as if it were a neutral compound using the well known equations [1,25]. Using eqn. 4, a rough approximation of the ionization constant and fully protonated capacity factor were determined. The ionization constant and deprotonated, free solution mobility were used in eqn. 2 in order to calculate the mobility of bilirubin at the lower pH values. Finally, this mobility could be used in eqn. 1 to calculate the capacity factor of bilirubin taking into account it's ionization. This calculated capacity factor was then reintroduced into eqn. 4, and the entire process was repeated until the ionization constant and capacity factor each converged.

An example separation is shown in Fig. 3. Run conditions are provided in the figure caption. The resulting plots of calculated capacity factor *versus* pH for each of the three bile salt systems investigated are shown in Fig. 4. There

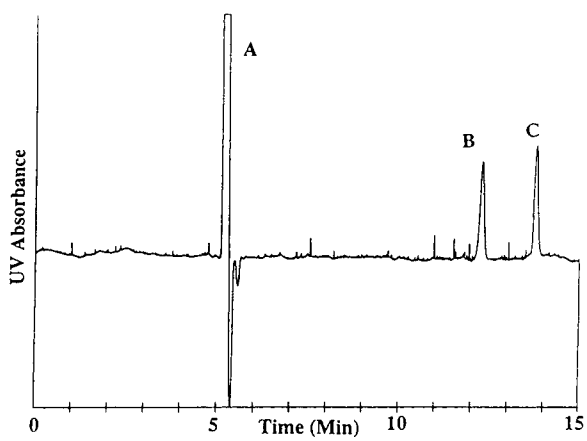

Fig. 3. Example separation. Peaks: A = DMSO; B = bilirubin; C = Sudan III. Run conditions were as follows: 20 m*M* phosphate–borate buffer with 25 m*M* taurochenodeoxycholic acid at pH 8.15; injection, 5 kV for 10 s; run voltage, 7 kV; capillary length 45 cm total, 27 cm from point of injection to detection window; UV detection at 225 nm; capillary inner diameter, 75 μm.

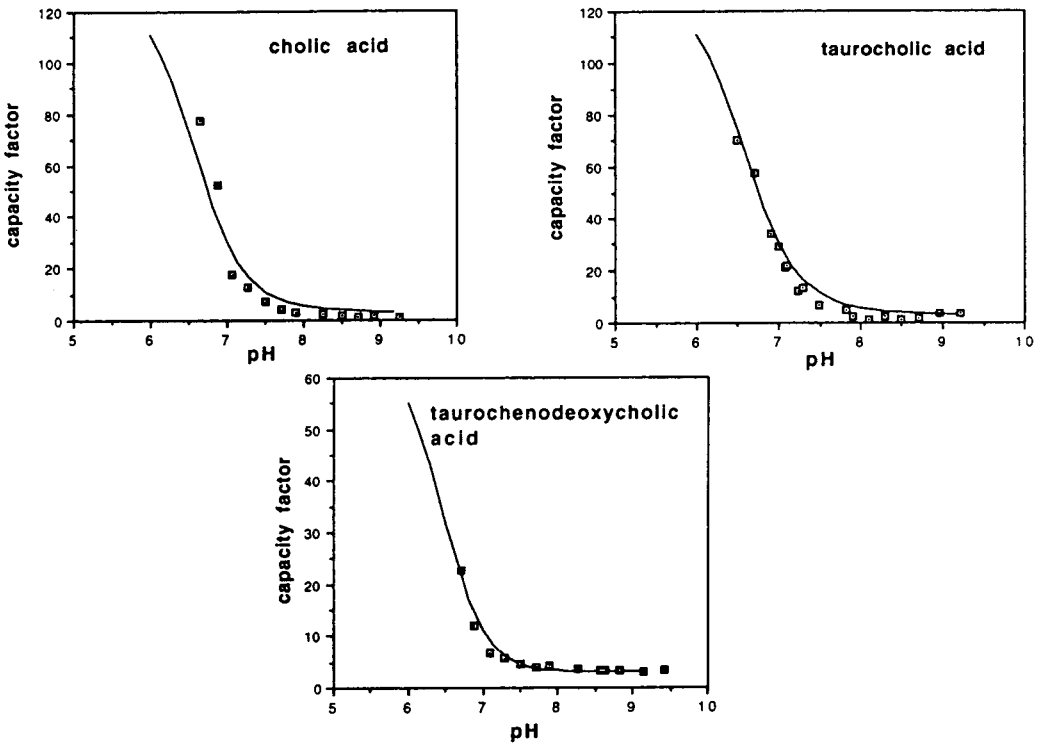

Fig. 4. Plots of capacity factor of bilirubin in cholic, taurocholic and taurochenodeoxycholic acid solutions as a function of pH. Symbols represent actual data, solid lines represent fitted equation five. See text for fitting parameters.

are several key features to these plots. First, the sharp decline in capacity factor occurring in the pH range of 6.5 to 7.5 is evidence of an ionization. It should be noted that this closely corresponds to the pH range of the biliary tract. This means that as bilirubin is transported in bile, it's state of ionization will vary. Therefore, at different points in the bile system, bilirubin should exhibit different capacities to interact with the bile salts, depending on the pH at these points. Second, there is no evidence for a second, distinct ionization of bilirubin. The two ionizations must both occur either at the same pH value or at pH values very close to each other. This assumes both ionizations occur over the pH range investigated which seems likely. Finally there are some apparent differences in the bilirubin capacity factor among the three different bile salts.

In order to visualize these differences more clearly, the solid line on each of the three graphs was generated using eqn. 5.

$$k' = \frac{k'_{H_2A} + k'_{HA^-}(K_{a1}/[H^+]) + k'_{A^{2-}}(K_{a1}K_{a2}/[H^+]^2)}{1 + K_{a1}/[H^+] + K_{a1}K_{a2}/[H^+]^2} \quad (5)$$

We are proposing eqn. 5 as an extension of eqn. 3 which was introduced by Khaledi *et al.* [25]. The difference is that where eqn. 3 applies to analytes which can undergo a single ionization, eqn. 5 applies to analytes which can undergo two ionizations in the pH range of study. Eqn. 5 shows that the observed capacity factor is related to the capacity factor of the fully protonated (k'_{H_2A}), intermediate (k'_{HA^-}), fully deprotonated species ($k'_{A^{2-}}$), the first (K_{a1}) and second (K_{a2}) ionization constants, and the hydrogen ion concentration. In order to determine the best fit,

values were chosen for eqn. 5 as follows: the three capacity factors were chosen initially according to values which seemed to fit visually with the three plots. Ionization constant values were then arbitrarily chosen, and eventually it was determined that the best fits were obtained if the ionization constants were chosen to be equal to each other, with pK_a values equal to 6.6. Since the pK_a values determined by this method are the pK_a values for the analyte in the buffer solution and not in the micelle [25], the same pK_a values were used for each of the three fits. The capacity factor values were then varied until a reasonable fit was achieved. For the cholic acid data capacity factors of 130, 30 and 1 were arrived at for the fully protonated, intermediate and fully deprotonated species respectively. For taurocholic acid the capacity factors were 130, 45 and 1, and for taurochenodeoxycholic acid the values were 80, 5 and 3. It should be noted that since the fitting was accomplished manually, these values must be viewed with caution.

It should also be noted that a slightly different data treatment would provide the ionization constants of bilirubin in the micelles themselves [25]. However, this data treatment requires that the mobility instead of capacity factor of bilirubin be plotted as a function of pH. It appears as though the electroosmotic flow value in a bile salt system is not as stable as an SDS system. This variation in electroosmotic flow imparts sufficient variation in mobility plots as to make this type of data analysis tenuous at best. These variations seem to be canceled out when capacity factors are used. Another explanation of our inability to determine intramicellar pK_a values is offered in the conclusions section.

While the apparent differences in capacity factor value for the fully deprotonated species in the different bile salts systems are probably within experimental error, there does appear to be a significant difference for the fully protonated species. It appears that protonated bilirubin does not interact as effectively with taurochenodeoxycholic acid as it does with cholic acid or taurocholic acid. This is important as the protonated species of bilirubin is quite prevalent at the pH range of bile if our apparent pK_a values are correct. If this is a real difference in the capacity factor, and not an artifact of the data treatment, it means that bilirubin interacts differently with different bile salts in the biliary tract. Should a patient show a change in his or her bile salt profile, that patient may be more or less susceptible to bilirubin precipitation. We are currently examining the behavior of bilirubin in other bile salt solutions to see if other differences in the capacity factor can be observed.

In order to determine if these differences in capacity factor among the different bile salts are real, we are currently conducting experiments to determine the capacity factor of bilirubin as a function of bile salt concentration at pH values of interest. Plots of capacity factor *versus* concentration will yield the partition coefficient of bilirubin once the plots have been corrected for the differing micelle volumes [2]. We have completed similar work in a buffer system containing 25 m*M* SDS at pH 8.5. The result is shown in Fig. 5. This plot shows that in comparison to some other test compounds, bilirubin interacts significantly with the SDS micelles at this pH. This is somewhat surprising since bilirubin is a dianion at this pH. On the same plot, the behavior of bilirubin is compared to two neutral compounds, caffeine and theobromine, as well as a monoanion, uric acid, and a partially charged compound, theophylline. The anions show little interaction with the micelles while the neutrals show limited interaction as compared to bilirubin. This might be explained by the fact that

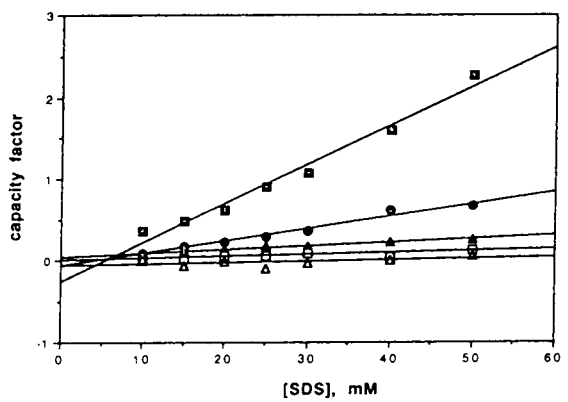

Fig. 5. Plot of capacity factor of test compounds in SDS solutions at pH 8.5. ■ = Bilirubin; ● = caffeine; ▲ = theobromine; □ = theophylline; △ = uric acid.

bilirubin is not a flat compound but rather has approximately a 90° bend across the center of the molecule. This structure may allow a significant portion of the molecule to interact with the SDS micelle while the charged groups, which are fairly well protected as compared to the comparison compounds shown in Fig. 5, are able to be held at some distance from the micelle surface.

CONCLUSIONS

There are several pieces of information to keep in mind when interpreting these results. Although it appears as though there are reasonable differences between the bilirubin capacity factor in the different bile salt solutions, these differences must be viewed with caution. Our procedures require an extensive data work up and these differences in capacity factor may be a result of data treatment procedures. The bile salt concentration studies currently underway in our laboratory will help to sort this out. Through MECC techniques, the apparent pK_a values for the bilirubin carboxyl groups appear to be similar, if not identical, to each other and fall within the range of 6.2 and 6.6. The value of 6.2 comes from the iteration procedure used to generate the corrected capacity factors, and the value of 6.6 comes from the fitted equation results. The value of 6.2 corresponds well to other data obtained at Trinity University by spectroscopic techniques [26]. Unfortunately, it appears as though MECC does not provide sufficiently conclusive data for the accurate determination of apparent pK_a values in this particular system. Perhaps the most important considerations to keep in mind when viewing this data is that the bilirubin–bile salt system is a very complicated system. The equations and theories we are using in our interpretation have been tested primarily on SDS based systems. SDS systems seem to fit these theories fairly well but several important assumptions were made in the development of these equations and theories which do not apply to the bilirubin–bile salt system. First is the assumption that the presence of an analyte does not appreciably change the structure or migration time of the micelle. While true for SDS, it is quite possible that this is not true for bilirubin and bile salts. Second is the assumption that the analyte does not interact appreciably with the surfactant monomer. Again, this is most likely true for bilirubin in SDS systems but probably is not true for bilirubin in bile salt systems [27]. Finally, we must also assume that the operating conditions chosen are those that will provide for a stable bile salt micelle. It is known that bile salt micelle structures, unlike SDS micelles, are a function of surfactant concentration. What is true at one concentration may not necessarily be true at another. Our inability to determine the intramicellar ionization constants may be an indication that this system does not comply with the criteria for interpretation of MECC systems as it it now developed. Exactly how much these considerations impact our results is unknown at this time. It appears as though we can apply these equations and theories to interpret our data but these interpretations must then be viewed with caution. However, it does seem clear that MECC techniques can yield valuable and interesting information about complicated systems such as the bilirubin–bile salt system.

ACKNOWLEDGEMENTS

Acknowledgement is made to the Donors of The Petroleum Research Fund, administered by the American Chemical Society, for the partial support of this research. Additional support was received from a William and Flora Hewlett Foundation Grant of Research Corporation, Trinity University, a Biomedical Research Support Grant, and the National Science Foundation, Grant No. CHE-9200033. The Jasco 2550 UV detector was generously provided by Varian Associates, Palo Alto, CA, USA. M.M.B. wishes to thank M.G. Khaledi for an informative discussion on the behavior of anionic species in anionic micelle systems.

REFERENCES

1 S. Terabe, K. Otsuka, K. Ichikawa, A. Tsuchiya and T. Ando, *Anal. Chem.*, 56 (1984) 111.
2 S. Terabe, K. Otsuka and T. Ando, *Anal. Chem.*, 57 (1985) 834.

3 K. Osuka, S. Terabe and T. Ando, *J. Chromatogr.*, 332 (1985) 219.
4 T. Kaneta, S. Tanaka, M. Taga and H. Yoshida, *Anal. Chem.*, 64 (1992) 798.
5 W.G. Kuhr, *Anal. Chem.*, 62 (1990) 403R.
6 K. Nishi and M. Matsuo, *J. Liq. Chromatogr.*, 14 (1991) 973.
7 J. Liu, K.A. Cobb and M. Novotny, *J. Chromatogr.*, 519 (1990) 189.
8 D.E. Burton, M.J. Sepaniak and M.P. Maskarinec, *J. Chromatogr. Sci.*, 24 (1986) 514.
9 S. Terabe, M. Shibata and Y. Miyashita, *J. Chromatogr.*, 480 (1989) 403.
10 R.O. Cole, M.J. Sepaniak and W.L. Hinze, *J. High Resolut. Chromatogr.*, 13 (1990) 579.
11 H. Nishi, T. Fukuyama, M. Matsuo and S. Terabe, *J. Chromatogr.*, 513 (1990) 279.
12 R.O. Cole, M.J. Sepaniak, W.L. Hinze, J. Gorse and K. Oldiges, *J. Chromatogr.*, 557 (1991) 113.
13 H. Nishi, T. Fukuyama, M. Matsuo and S. Terabe, *J. Chromatogr.*, 498 (1990) 313.
14 M.C. Carey and D.M. Small, *Arch. Intern. Med.*, 130 (1972) 506.
15 W. Spivak and W. Yuey, *Biochem. J.*, 234 (1986) 101.
16 R.V. Rege, C.C. Webster and J.D. Ostrow, *J. Lipid Res.*, 28 (1987) 673.
17 M.C. Carey and W. Spivak, in J.D. Ostrow (Editor), *Bile Pigments and Jaundice: Molecular, Metabolic and Medicinal Aspects*, Marcel Dekker, New York, 1986, p. 81.
18 H. Masuda and F. Nakayama, *J. Lab. Clin. Med.*, 93 (1979) 353.
19 R.V. Rege, C.C. Webster and J.D. Ostrow, *J. Lipid Res.*, 29 (1988) 1289.
20 E.W. Moore, L. Celic and J.D. Ostrow, *Gastroenterology*, 83 (1982) 1079.
21 J.D. Ostrow and L. Celic, *Hepatology*, 4 (1984) 38S.
22 U. Wosiewitz and S. Schroebler, *Experimentia*, 35 (1979) 717.
23 H.S. Halm, J.D. Ostrow, P. Mukerjee and L. Celic, *J. Lipid Res.*, 33 (1992) 1123.
24 A.F. McDonagh and F. Assisi, *Biochem. J.*, 129 (1972) 797.
25 M.G. Khaledi, S.C. Smith and J.K. Strasters, *Anal. Chem.*, 63 (1991) 1820.
26 W.E. Kurtin, unpublished results.
27 M.C. Carey and A.P. Koretsky, *Biochem. J.*, 179 (1979) 675.

Journal of Chromatography A, 652 (1993) 535–538
Elsevier Science Publishers B.V., Amsterdam

CHROM. 25 258

Isolation and quantification of ergovaline from *Festuca arundinacea* (tall fescue) infected with the fungus *Acremonium coenophialum* by high-performance capillary electrophoresis

Yinfa Ma*, Kevin G. Meyer and Dawood Afzal

Division of Science, Northeast Missouri State University, Kirksville, MO 63501 (USA)

Elizabeth A. Agena

Department of Chemistry, Simpson College, Indianola, IA 50125 (USA)

ABSTRACT

We developed an easy and sensitive high-performance capillary zone electrophoresis method for the determination of ergovaline in the seeds of *Festuca arundinacea* (tall fescue) infected with the endophytic, ascomycetous fungus *Acremonium coenophialum*. The seeds were extracted with chloroform, and the chloroform extract was filtered and evaporated with a Rotavapor. The concentrated extract was passed through a SM2 Bio-Beads and the alkaloids on the Bio-Beads were redissolved by methanol. A 60 cm × 75 μm I.D. fused-silica capillary was used for separation by capillary electrophoresis. A UV detector was used for detection, which was set at 250 nm. A 0.1 *M* sodium dihydrogenphosphate in 50% (v/v) methanol, pH 3.5, was used as a buffer. With this method, the ergovaline at low μg per kg seeds can be detected and quantified.

INTRODUCTION

Many grasses, including several agronomically important forage species, harbor endophytic, ascomycetous fungi. These fungal endosymbionts markedly modify the attributes of infected grass individuals, influencing the physiology, morphology, reproductive biology and palatability of grass hosts [1]. These effects are due to the ergopeptine alkaloids, especially ergovaline, produced by the endophytic fungus. The presence of high levels of ergovaline in endophyte-infected (*Acremonium coenophialum* Morgan-Jones and Gams) tall fescue is of interest because of its potential physiological activities [2–4], which typically exert central nervous system effects upon vertebrate consumers. Pharmacological studies [5] have shown that ergopeptine alkaloids, principally ergovaline, can interact with a variety of receptors and alter dopaminergic pathways [6]. Affected cattle gained mass poorly or lost mass, salivated profusely, had reduced milk production, and exhibited increased respiration rate [7,8] and body temperature [9]. Siegel *et al.* [9] has reported that approximately US$

* Corresponding author.

0021-9673/93/$06.00

$50 \cdot 10^6$ to $200 \cdot 10^6$ were lost to the cattle producers annually due to presence of higher level of ergovaline in the infected tall fescue. Therefore, developing a simple and fast method for analysis of ergopeptine alkaloids, especially ergovaline, will be very useful for agricultural development of the USA.

Tandem mass spectrometry (MS–MS) has been used for identifying the level of ergopeptine alkaloids in crude extracts of tall fescue [10]. However, the lack of MS–MS in many fescue research laboratories has hampered the analysis of ergopeptine alkaloids. Recently, high-performance liquid chromatographic (HPLC) methods for the analysis of ergovaline in fescue seed have been reported by several researchers [11,12]. Even though these methods can be used for quantitating ergovaline in endophyte-infected tall fescue, it was inadequate for fresh plant tissue analysis [11], and the complicated HPLC procedure limited the number of samples that could be analyzed conveniently per day.

High-performance capillary zone electrophoresis (HPCZE) has been proven to be a powerful technique in the separation of charged biomolecules with very high resolution [13,14]. The separation of standard ergot alkaloids by using cyclodextrins as a background electrolyte modifier in HPCE has been demonstrated by Fanali *et al.* [15]. However, the isolation and quantification of ergovaline in tall fescue, which is highly interested by American farmers, have not been studied by HPCE. In this paper, we developed an easy and sensitive HPCZE method for the quantitation of ergovaline in the endophyte-infected fescue seed. With this method, the ergovaline at low micrograms per kilogram of seed can be detected and quantified.

EXPERIMENTAL

Equipment

The HPCZE system (Model 3580) with a UV detector was purchased from ISCO (Lincoln, NE, USA). A positive high voltage was applied to the capillary by maintaining the injection end at a positive high potential while the cathodic end was held at ground potential. Data were collected with a Datajet computing integrator (Spectra-Physics, Mountain View, CA, USA). The capillary columns (Polymicro Techniques, Phoenix, AZ, USA) were 60 cm (35 cm to the detection system) × 150 μm O.D. × 75 μm I.D. The polymer coating was burned off 25 cm from the cathodic end of the capillary to form the detection window. The Rotavapor (Model RE111) was bought from Fisher Scientific (Fairlawn, NJ, USA).

Reagents and seed samples

All chemicals were of analytical-reagent grade unless stated otherwise. Deionized water was prepared with a Milli-Q system (Millipore, Bedford, MA, USA). Ergovaline standard was a gift from Dr. George E. Rottinghaus, University of Missouri at Columbia. Ergonovine and ergotamine tartrate were purchased from Sigma (St. Louis, MO, USA).

HPLC-grade chloroform and methanol were purchased from Aldrich (Milwaukee, WI, USA). Sodium phosphate and hydrochloric acid were obtained from Fisher Scientific. SM-2 Bio-Beads were purchased from Bio-Rad (Richmond, CA, USA).

1991 Missouri endophyte-infected tall fescue seeds were obtained from Missouri Southern Seed Company (Rolla, MO, USA).

Pretreatment of the capillary column

All new capillary columns were filled with 0.01 *M* sodium hydroxide solution for about 30 min to clean the column. The column was then washed with deionized water and buffer solution. The capillary was ready for use thereafter.

Extraction and cleanup

A 1-kg amount of ground 1991 Missouri endophyte-infected tall fescue seed was mixed with 5 l of chloroform and stirred for 30 min. The liquid extract was separated from seed residue by filtering through cheesecloth, and the extract was roto-evaporated to 280 ml at a 30°C setting. The 280 ml of the extract were passed through Whatman 1 filter paper by vacuum filtration to remove any fine seed precipitant. A 56-g amount of SM-2 Bio-Beads was added to the extract and stirred for 1 h, so that the alkaloids would bind to the Bio-Beads. The liquid was removed by

vacuum filtration through Whatman 1 filter paper, and the beads were collected and washed 4 times with methanol (100 ml each time). The methanol eluent, which was concentrated to 25 ml by roto-evaporation, was ready to be analyzed by HPCZE.

HPCZE analysis

About 10 nl of methanol extract were injected for analysis. 0.1 *M* sodium dihydrogenphosphate in 50% (v/v) aqueous methanol, pH 3.5, was used as a buffer (the pH was adjusted by 1 *M* hydrochloric acid). HPCZE was operated at 30 kV for separation and 250 nm wavelength was used for UV detection.

RESULTS AND DISCUSSION

Fig. 1 shows the separation of three standard alkaloids. Here it needs to be pointed out that peak B, ergovalinine, is the isomer of peak C, ergovaline, and they co-exist in the same standard solution. Ergovaline is very sensitive to light and heat. So, as time goes on, some ergovaline will be gradually isomerized to ergovalinine until the equilibrium is reached. Fig. 1 also demonstrate that femtomoles of alkaloids can be easily separated and detected. The calibration curve for ergovaline was linear over the range 100–1200 μg/kg, with a correlation coefficient 0.975. The detection limit was 90 μg/kg seed.

Fig. 2 shows the separation and detection of ergovaline in endophyte-infected tall fescue seeds. There was no interference from sample matrix. The unidentified peaks are due to the other compounds extracted from tall fescue seeds; the small peak eluting at 10 min was ergovalinine, the isomer of ergovaline, which was proven by the standard addition method in Fig. 3. From Fig. 2, we also can see that the ergotamine produced by the endophyte is too low to be detected, as was also found by the HPLC method developed by Rottinghaus *et al.* [11], in which they used ergotamine as an internal standard to analyze ergovaline. Based on the ergovaline peak areas of the sample seeds, the ergovaline contents in the 1991 Missouri endophyte-infected seeds were calculated to be 290 μg/kg seeds with a standard deviation of 16 for 5 analysis, which is compatible with the results analyzed by HPLC method [11]. This level is sufficient to induce symptoms of toxicity in heat-stressed cattle. The recovery of the ergovaline

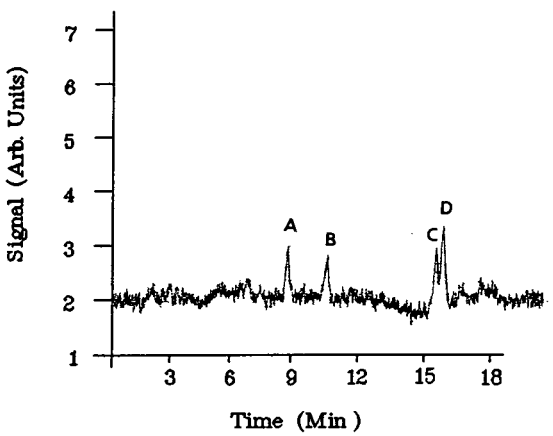

Fig. 1. The separation of three alkaloid standards which are commonly present in endophyte-infected tall fescue by HPCZE with a UV absorption detector. Sodium dihydrogenphosphate (1 *M*) in 5% (v/v) aqueous methanol, pH 3.5, was used as a buffer. Injection was made by a manual injector with a splitter. The injection volume was 10 nl. The concentration of the standards was 100 μM each. The electrophoresis was carried out at 30 kV on a 60 cm × 75 μm I.D. pretreated column. Detection wavelength was set at 250 nm. Peaks: A = ergonovine; B = ergovalinine (the isomer of ergovaline which co-exists in the ergovaline standard we obtained); C = ergovaline; D = ergotamine.

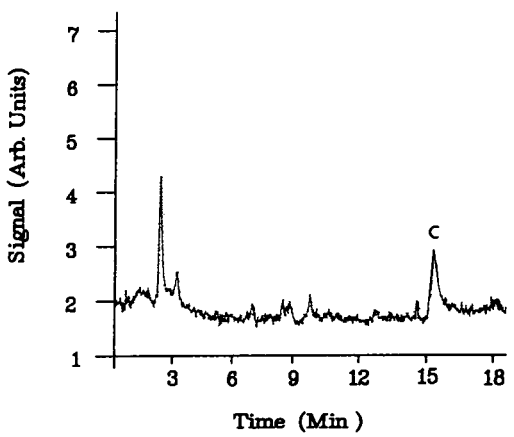

Fig. 2. The separation of ergovaline from endophyte-infected tall fescue seeds by HPCZE. Peak C = ergovaline. The electrophoresis conditions were the same as those of Fig. 1.

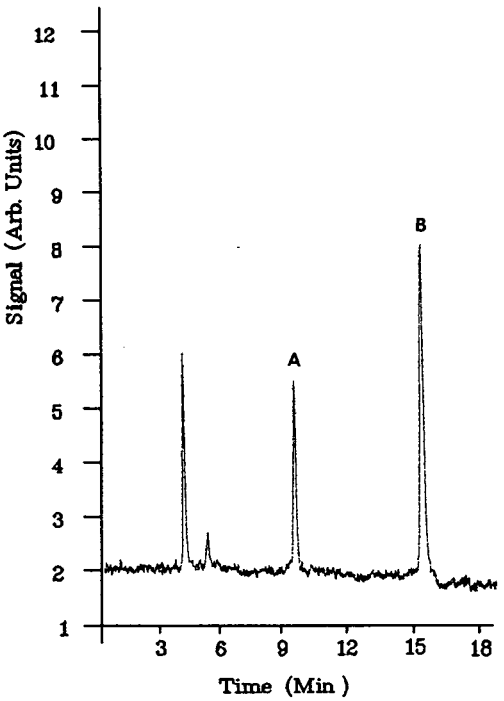

Fig. 3. The verification of ergovaline peak in Fig. 2 by standard addition method. Peaks: A = ergovalinine; B = ergovaline. The electrophoresis conditions were the same as those of Fig. 1.

has also been studied, and the average percent recovery is 95.1% for 5 extractions.

In order to verify the ergovaline peak in the sample electropherogram (Fig. 2), we also did a standard addition experiment, in which standard ergovaline was added to the methanol extract of the sample seeds. To 10 μl of methanol extract, 20 μl of 200 μl ergovaline standard were added and electrophoresis was carried out at the same conditions as those of Fig. 2. The electropherogram is shown in Fig. 3. From Fig. 3, we can see that the standard ergovaline peak exactly matches the ergovaline peak of the sample seed extract. This also proves that the small peak at 10 min was the ergovalinine peak.

CONCLUSIONS

We have developed an HPCZE method to analyze ergovaline in the endophyte-infected tall fescue seed. The method is easy, fast and sensitive, through which femtomoles of ergovaline can be detected. The method should be highly suitable for separation and determination of ergovaline in the endophyte-infected tall fescue seeds.

ACKNOWLEDGEMENTS

The authors sincerely thank Professor George E. Rottinghaus of the University of Missouri at Columbia for the ergovaline analytical standard and Dr. Ali S. Moubarak at the Department of Animal and Poultry Science, University of Arkansas, for the technical assistance on the extraction of ergovaline.

The work was supported by Faculty Research Grants awarded to Y.M. and D.A. from Northeast Missouri State University and NSF-REU grant BIO-9200423.

Y.M. and D.A. would like to thank the other participants of the NSF-REU grant at Northeast Missouri State University, especially Dr. Thomas Bultman, for the helpful discussions.

REFERENCES

1 K. Clay, *Ann. Rev. Ecol. Syst.*, 21 (1990) 275.
2 J.C. Read and B.J. Camp, *Agron. J.*, 78 (1986) 848.
3 K. Clay, *Ecology*, 69 (1988) 10.
4 C.P. West, E. Izekor, D.M. Oosterhuis and R.T. Robbins, *Plant Soil*, 112 (1988) 3.
5 B. Berde and E. Sturmer, in B. Berde and H.O. Schild (Editors), *Ergot Alkaloids and Related Compounds*, Springer, Berlin, 1978, pp. 1–28.
6 M.C. Henson, E.L. Piper and L.B. Daniels, *Domest. Animal Endocrinol.*, 4 (1987) 7.
7 R.J. Crawford, Jr., J.R. Forwood, R.L. Belyea and G.B. Garner, *J. Prod. Agric.*, 2 (1989) 147.
8 J.C. Read, C. Davis, B.J. Camp and E. Giroir, in *Proceedings, Forage and Grasslands Conference, Houston, TX*, American Forage and Grassland Council, Lexington, KY, 1984, pp. 240–243.
9 M.R. Siegel, M.C. Johnson, D.R. Varney, W.C. Nesmith, R.C. Buckner, L.P. Bush, P.B. Burrus, T.A. Jones and J.A. Boling. *Phytopathology*, 74 (1984) 932.
10 S.G. Yates, R.D. Plattner and G.B. Garner, *J. Agric. Food Chem.*, 33 (1985) 719.
11 G.E. Rottinghaus, G.B. Garner, C.N. Cornell and J.L Ellis, *J. Agric. Food Chem.*, 39 (1991) 112.
12 S.G. Yates and R.G. Powell, *J. Agric. Food Chem.*, 36 (1988) 337.
13 J.E. Wiktovowicz and J.C. Colburn, *Electrophoresis*, 11 (1990) 769.
14 M.V. Novotny, K.A. Cobb and J. Liu, *Electrophoresis*, 11 (1990) 735.
15 S. Fanali, M. Flieger, N. Steinerova and A. Nardi, *Electrophoresis*, 13 (1992) 39.

Journal of Chromatography A, 652 (1993) 539–546
Elsevier Science Publishers B.V., Amsterdam

CHROM. 25 259

Ion-association capillary electrophoresis

New separation mode for equally and highly charged metal chelates

Nobuhiko Iki*, Hitoshi Hoshino and Takao Yotsuyanagi

Department of Molecular Chemistry and Engineering, Tohoku University, Aoba, Aramaki, Aoba-ku, Sendai 980 (Japan)

ABSTRACT

A new separation method for highly charged metal chelates based on ion association in capillary zone electrophoresis (CZE) has been developed. Metal chelates of Al(III), Co(III), Cr(III) and Fe(III) ions with 2,2′-dihydroxyazobenzene-5,5′-disulphonate could not be separated by a conventional CZE system (electrophoretic buffer: $[NaH_2PO_4]_T = 0.02$ *M*, pH 7.0, $V = 21.7$ kV, $i = 20$ μA, $l = 50$ cm), because they have fixed and identical (−5) charges. However, when 25 m*M* tetrabutylammonium bromide was added to the same electrophoretic buffer, each of the four chelates was well resolved and migrated in the order Fe(III), Co(III), Cr(III) and Al(III) with theoretical plate numbers of 210 000–250 000 per 50 cm within 11 min ($V = 21.3$ kV, $I = 40$ μA). The detection limits ($S/N = 3$) as determined by spectrophotometric detection ($\lambda = 494$ nm, I.D. = 50 μm) were 1.00, 1.89 and 3.11 fmol for Al, Co and Fe, respectively, in $6.0 \cdot 10^{-9}$ dm^3 of sample solution injected. The effect on the separation of the sizes, types and the concentrations of quaternary ammonium ions added to the electrophoretic buffer was also investigated. As a result, some evidence was obtained that the ion-association reaction between the chelates and ammonium ions probably took the major role in the separation mechanism.

INTRODUCTION

High-performance capillary electrophoresis (HPCE), which is a general term for capillary electrophoresis (CE) or capillary zone electrophoresis (CZE) and related methods such as micellar electrokinetic chromatography (MEKC), capillary gel electrophoresis and so on, has been intensively applied to bioorganic molecules in recent years [1]. By contrast, the application of HPCE to the separation of inorganic species such as metal chelates is still quite rare. In 1989 the first report on the separation of 4-(2-pyridylazo)resorcinolato (PAR) chelates by MEKC was published [2]. Also, in 1991, we reported MEKC of $\alpha,\beta,\gamma,\delta$-tetrakis(4-carboxyphenyl)porphinato chelates [3]. Since then CZE separation of metal chelates with 8-hydroxyquinoline-5-sulphonic acid (HQS) [4], ethylenediamine-N,N,N′,N′-tetraacetic acid (EDTA) [5] and 1,2-cyclohexanediamine-N,N,N′,N′-tetraacetic acid (CyDTA) [6] has been performed. It should be noted that the separation principle of these CZE systems always lies in the complexation equilibria between the injected metal ions and the ligands in the electrophoretic buffer. In other words, a difference in the degree of complexation of each metal ion in the capillary produces individual electrophoretic mobilities, μ_{ep}. This separation principle is exactly the same one that has been widely employed in conventional electrophoretic separation of metal complexes such as paper electrophoresis [7] and isotachophoresis [8]. Although the migration behaviour is easily explained by

* Corresponding author.

0021-9673/93/$06.00

corrected 9 Sep. 94/AP.

the formation constants and intrinsic μ_{ep} values of the aqueous ion and the complex(es), as shown by the HQS–Ca(II) and Mg(II) system [4], this separation strategy has two restrictions or problems. First, it can only be applied to kinetically labile chelates, *i.e.* unless the complexation reaction is faster than the electrophoretic process, peak broadening or splitting corresponding to each composition occurs. Second, the reagent stream always causes a background signal, which often damages the sensitivity of the system even when a highly sensitive detection method such as laser-induced fluorescence detection is used [4].

Compared with a reversed-phase high-performance liquid chromatography (RP-HPLC) system using a reagent stream, an RP-HPLC system that uses mobile phase without a chelating reagent is free from the background signal caused by the reagent. Therefore higher amplification of signal intensity by the detector is readily achievable and thus detection at the sub-ppb level is always feasible. In addition, since kinetically labile chelates are decomposed on-column and not detected, detection using this method is highly selective for inert metal chelates. In a sense, the separation column behaves as if it could differentiate the kinetic stability of the chelates [kinetic differentiation (KD) mode] [9].

When this mode is transferred to CZE, the system requires a distinct design strategy for pre-column derivatizing ligands and separation systems. Recently, we reported the CZE separation of five kinds of PAR chelates in the KD mode [10]. Only pH control was required in order to manipulate the migration and resolution of the chelates. It was advantageous that the acid dissociation constants of the 1-hydroxy groups of each PAR chelate as well as free PAR are different so that they migrated with different electrophoretic mobilities. This fact provides crucial information on the ligand design, *i.e.* the ligand should have at least one functional group to express the characteristics of the central metal ion by means of the magnitude of the acid dissociation constant.

For this reason it is impossible to separate the complexes of Al(III), Co(III), Cr(III) and Fe(III) with 2,2′-dihydroxyazobenzene-4,4′-disulphoate (DHABS, H_2L^{2-}) by CZE (KD mode) because they have no such functional groups. Therefore, various approaches to the resolution of these chelates by system design have been attempted. For instance, MEKC and ion-exchange EKC [11] systems were examined but did not afford resolution either. In this paper, a new effective separation method for DHABS chelates by CZE coupled and the ion-association reaction is reported. In addition, the effects of the sizes and types of ion-associating agents are discussed.

EXPERIMENTAL

The ligand for pre-column derivatization was the disodium salt of DHABS, Na_2H_2L, synthesized by the method of Süs [12], which was used as a 10 m*M* aqueous solution. Standard metal ion solutions were made by dissolving metal salts of chloride or nitrate, except for V(V) and Mo(VI), ammonium metavanadate and ammonium molybdate, in diluted hydrochloric acid. The buffer for complex formation was 1 *M* tris(hydroxymethyl)aminomethane (Tris)–HCl buffer (pH 8.0). Phosphate buffer was not used, as it interfered with the chelate formation of Al(III) and Fe(III). The electrophoretic buffer was 20 m*M* NaH_2PO_4 solution, which was adjusted to pH 7.0 by NaOH solution. The buffer modifiers used were tetramethylammonium bromide (TMABr) (Kanto Chemical, Japan), tetraethylammonium bromide (TEABr), tetrapropylammonium bromide (TPABr), tetrabutylammonium bromide (TBABr) tetraamylammonium bromide (TAABr) (Tokyo Kasei Kogyo, Japan) and tetraphenylphosphonium chloride (TPPCl) (Dojindo Lab., Japan). All other chemicals used were of analytical reagent grade. Triply distilled water was used throughout this study.

The capillary electrophoresis equipment, photometric detector and data processor were the same as described elsewhere [2]. Fused-silica capillary tubing (650–720 mm × 0.05 mm I.D.) was purchased from Scientific Glass Engineering (Australia). On-column detection at 490 or 494 nm was performed 150 mm from the negative

end. The temperature of the system was kept at 30 ± 1°C in a thermostated safety box with an interlocking system.

A typical procedure is as follows: sample solution containing eleven kinds of metal ions [Al(III), Cd(II), Co(II), Cr(III), Cu(II), Fe(III), Ni(II), Mn(II), Mo(VI), V(V) and Zn(II)] was added to 5 cm^3 of DHABS solution and 0.5 cm^3 of Tris–HCl buffer, then made up to 50 cm^3, and heated at 60°C for 15 min. After cooling to room temperature, $6.0 \cdot 10^{-9}$ dm^3 was injected into the positive end of the capillary by siphonic action. Electrophoresis was accomplished by applying about 20 kV by constant-current supply mode.

RESULTS AND DISCUSSION

buffer of pH 7.0–9.0, which consisted of 0.02 *M* NaH_2PO_4 or a mixture of 0.01 *M* NaH_2PO_4 and 0.01 *M* $Na_2B_4O_7$ solutions. Although free DHABS, M(III), Cu(II), and V(V) chelates were separated, as typically shown in Fig. 1a, mutual separation of M(III)–DHABS chelates was impossible, where M(III) denotes Al(III), Co(III), Cr(III) and Fe(III) ions. The compositions of all M(III) chelates except Cr(III) chelate was confirmed to be 1:2 by the molar ratio method. Therefore these chelates are expressed as $[M(III)L_2]^{5-}$, have the identical charge of −5, and thus migrated at the same mobility. In addition, the chelates of Cd(II), Ni(II), Mn(II) and Zn(II) were not detected. This was probably due to the lack of kinetic stability of these chelates, which might result in their dissociation in the capillary and the absence of the peaks,

Erratum

Ion-association capillary electrophoresis. New separation mode for equally and highly charged metal chelates [*Journal of Chromatography A*, 652 (1993) 539–546]

Nobuhiko Iki, Hitoshi Hoshino, Takao Yotsuyanagi

p. 540, right column, first line, "2,2′-dihydroxyazobenzene-4,4′-disulphoate" should read "2,2′-dihydroxyazobenzene-5,5′-disulphonate".

p. 541, caption to Fig. 1, "(b) $[NaH_2PO_4]_T = 0.02$ *M*, pH 7.0, [TBABr] = 25 m*M*, *V* = 21.7 kV, *I* = 20 μA." should read "(b) $[NaH_2PO_4]_T = 0.02$ *M*, pH 7.0, [TBABr] = 25 m*M*, *V* = 21.3 kV, *I* = 40 μA."

p. 543, left column, first line, "10^{-7} m" should read "10^{-7} *M*".

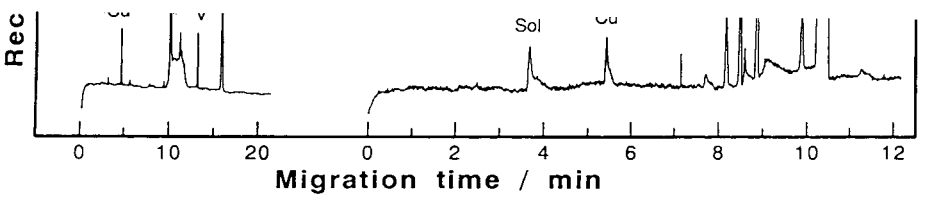

Fig. 1. Typical electropherograms for DHABS chelates. (a) $[NaH_2PO_4]_T = 0.02$ *M*, pH 7.0, *V* = 21.7 kV, *I* = 20 μA. (b) $[NaH_2PO_4]_T = 0.02$ *M*, pH 7.0, [TBABr] = 25 mM, *V* = 21.7 kV, *I* = 20 μA. Total capillary length, *L* = 65 cm, effective capillary length, *l* = 50 cm.

corrected 9 Sep. 94/AP

electrostatic attraction between these modifiers and the solutes was too strong.

Interestingly, when the modifier was changed to TBABr, a rather smaller quaternary ammonium salt than DTMABr and HDBr, M(III) chelates were easily resolved. A typical electropherogram is shown in Fig. 1b. Separations were performed within 12 min with theoretical plate numbers, N, described by eqn. 1, of Al, 253 000; Co, 243 000; and Fe, 214 000 per 50 cm:

$$N = 5.54\left(\frac{t_m}{W_{1/2}}\right)^2 \quad (1)$$

where t_m and $W_{1/2}$ are migration time and full-width at half-height for each solute, respectively. The effect of TBA concentration in the electrophoretic buffer on the electrophoretic mobility, μ_{ep}, given by eqn. 2, is shown in Fig. 2:

$$\mu_{ep} = \mu_{obs} - \mu_{eo} = -\left(\frac{1}{t_m} - \frac{1}{t_0}\right)\left(\frac{L \cdot l}{V}\right) \quad (2)$$

where μ_{obs} is apparent electrophoretic mobility, $-(1/t_m)(L \cdot l/V)$, and μ_{eo} is electroosmotic mobility, $-(1/t_0)(L \cdot l/V)$; t_m and t_0 are the migration times of solute and solvent peak; l is the effective capillary length; L is the total capillary length; and V is the applied voltage. When the direction of electrophoretic velocity and electroosmotic flow is toward positive end, the value of μ_{ep} and μ_{eo} are defined as positive.

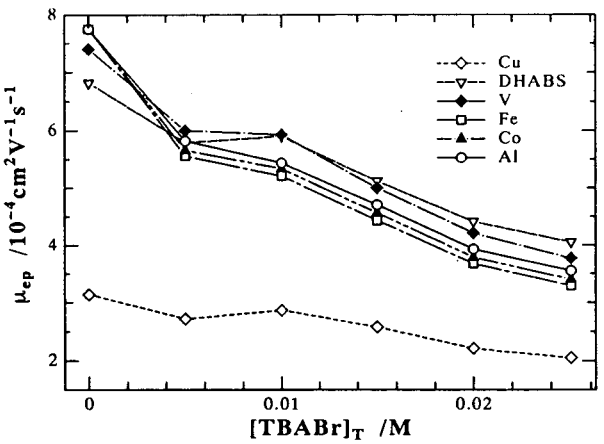

Fig. 2. The effect of TBA ion on the migration of DHABS chelates. Buffer: $[NaH_2PO_4]_T = 0.02$ M, [TBABr] = 0–25 mM, pH 7.0. $L = 72$ cm, $l = 57$ cm.

When the concentration of TBA ion increased from 0 to 25 mM, the direction of electroosmotic flow was unchanged but the value of μ_{eo} simply varied from $-9.99 \cdot 10^{-4}$ to $-7.68 \cdot 10^{-4}$ cm^2 V^{-1} s^{-1}. This indicates that there was specific adsorption of the TBA ion onto the capillary wall to decrease the ζ potential. Although the resolution was not good enough, addition of only 5 mM TBA ion made the μ_{ep} values of the three M(III)–DHABS chelates different, as shown in Fig. 2. Optimum separation was obtained at $[TBA]_T = 25$ mM, as shown in Figs. 1b and 2. The decrease in μ_{ep} might originate from the formation of ion associates of higher degree between each solute and TBA ion to reduce the total charge of the associate. Therefore, the sequence of the peaks of M(III) chelates indicates the capacity for ion association to be Fe(III) > Co(III) > [Cr(III)] > Al(III) chelates.

The detectability of Al(III), Co(III) and Fe(III) ions of the CZE system using 25 mM TBA ion was investigated by decreasing the concentration of each M(III) ion from $2 \cdot 10^{-5}$ to $1 \cdot 10^{-7}$ M in samples. Calibration curves in the log–log scale, obtained by the least squares method, are given by eqns. 3–5, where PHA, r and n are peak-height absorbance at 494 nm, correlation coefficient and number of experimental points, respectively:

$$\log(\text{PHA} - 7.01 \cdot 10^{-5}) = 0.940 \log [Al]_T + 2.03$$
$$r = 0.9984, \; n = 10 \quad (3)$$

$$\log(\text{PHA}) = 0.996 \log [Co]_T + 2.16$$
$$r = 0.9984, \; n = 9 \quad (4)$$

$$\log(\text{PHA}) = 0.953 \log [Fe]_T + 1.68$$
$$r = 0.9982, \; n = 7 \quad (5)$$

Linear correlations between the concentrations of Co(III) and Fe(III) ions and peak-height absorbance were obtained. However, the calibration curve of Al(III) ion deviated upwards and finally reached its blank peak height ($7.01 \cdot 10^{-5}$ AU) as the concentration decreased. This is because of the contamination from the reagents and/or environment. The detection limits (D.L.), defined by $S/N = 3$, were for Al $1.67 \cdot 10^{-7}$ M, Co for $3.16 \cdot 10^{-7}$ M and for Fe $5.19 \cdot$

10^{-7} m, where noise levels were $\sigma_{baseline} = 1.62 \cdot 10^{-5}$ AU and $\sigma_{Al\ blank} = 1.52 \cdot 10^{-5}$ AU ($n = 8$). The absolute values of D.L. in a $6.0 \cdot 10^{-9}$ dm^3 injected sample solution were for Al 1.00 fmol, for Co 1.89 fmol and for Fe 3.11 fmol. These values are the smallest absolute detection limits by HPLC or CZE with spectrophotometric detection ever reported.

The effect of the sizes or types and concentrations (5–25 m*M*) of the ion-association agents in the electrophoretic buffer of 0.02 *M* NaH_2PO_4 (pH 7.0) were examined. Representative electropherograms for 5 m*M* and 25 m*M* are shown in Figs. 3–7. Separation of M(III) chelates by using TMA ion, the smallest ion, was impossible (Fig. 3). The significant peak broadening of M(III) chelates at 25 m*M* might be the results of adsorption of the ion associate onto the capillary wall. Separation was just beginning in the case of the 5 m*M* TEA system (Fig. 4a), but baseline resolution was not achieved. When using 25 m*M* TEA, each M(III) peak was separated but the peaks were slightly broad and on the tail of DHABS peak (Fig. 4b), while the TPA system exhibited sharper peaks of M(III) chelates (Fig. 5). However, peak overlap between V(V) and

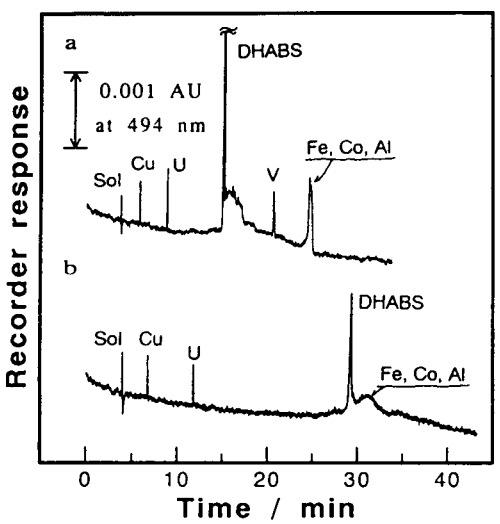

Fig. 3. Electropherograms for DHABS chelates in the TMA system. Buffer: $[NaH_2PO_4]_T = 0.02$ *M*, pH 7.0, [TMABr] = 5 and 25 m*M* for (a) and (b), respectively. $L = 72$ cm, $l = 57$ cm. (a) $I = 25$ μA, $V = 23.2$ kV. (b) $I = 50$ μA, $V = 22.7$ kV. Sol = solvent peak; U = unknown peak.

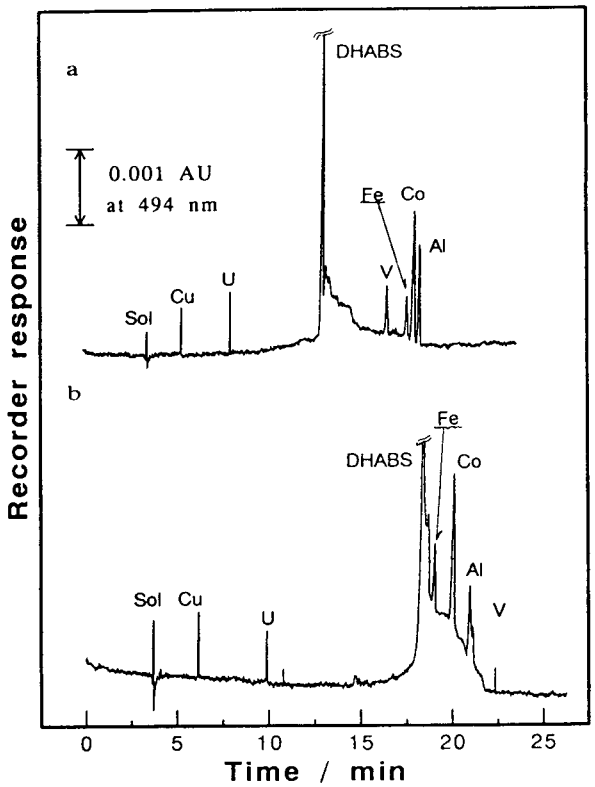

Fig. 4. Electropherograms for DHABS chelates in the TEA system. (a) [TEABr] = 5 m*M*, $I = 25$ μA, $V = 21.2$ kV. (b) [TEABr] = 25 m*M*, $I = 40$ μA, $V = 22.8$ kV. Other conditions are the same as in Fig. 3.

Co(III) chelates or DHABS and Al(III) chelate was observed. The addition of 25 m*M* TBA resulted in excellent electropherograms, as already shown in Fig. 1b. It is noteworthy that only 5 m*M* TAA ion, which is larger than TBA ion, could give quite good electropherograms (Fig. 6a). When the concentration exceeded the optimum TAA concentration at 15 m*M*, the separation of M(III) chelates became poorer (Fig. 6b). The system of 5 m*M* TPP, which is the bulkiest and has π-electron systems, behaved like the 25 m*M* TBA system except for V(V) peak (Fig. 7a). About 5–10 m*M* was optimum in the TPP system, while at 25 m*M*, the electroosmotic flow became extremely slow ($\mu_{eo} = -2.26 \cdot 10^{-4}$ cm^2 V^{-1} s^{-1}), and thus a longer migration time was required (Fig. 7b). For instance, the DHABS peak, which was the last one, appeared at 65 min. Peak broadening of

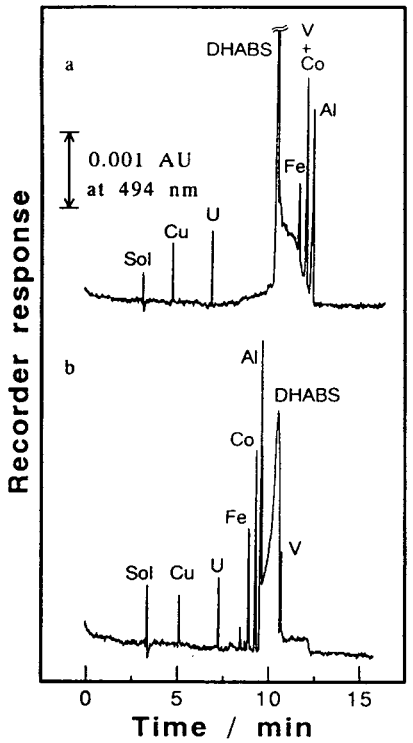

Fig. 5. Electropherograms for DHABS chelates in the TPA system. (a) [TPABr] = 5 mM, I = 25 μA, V = 21.1 kV. (b) [TPABr] = 25 mM, I = 40 μA, V = 22.3 kV. Other conditions are the same as in Fig. 3.

M(III) chelates was also observed, which led to loss of sensitivity.

The above results for 5 mM and 25 mM counter-ions are summarized in terms of the electrophoretic mobility in Figs. 8 and 9. As the added counter-ions become bulkier, the μ_{ep} value of each solute decreased in both cases, except for 5 mM TMA. (The reason for the dip in μ_{ep} at 5 mM TMA is not clear.) This implies that the hydrophobic interaction between solute anion and counter-cation significantly contributes to the formation of ion associates as well as electrostatic attraction. Also, the fact that each μ_{ep} value was positive and non-zero is a strong evidence of the presence of a negative charge on the ion associate. The resolution between M(III) chelates became better when bulkier counter-cations were used, as shown in Fig. 8. On the other hand (Fig. 9) the optimum resolution was obtained by the TBA ion but the larger counter-cations gave poorer resolution. Counter-ions such as TAA and TPP, which have larger hydrophobic interaction with M(III) chelates, should be used at lower concentrations.

In the area of separation science, ion-association or ion-pairing techniques are employed in various methodologies, such as ion-association

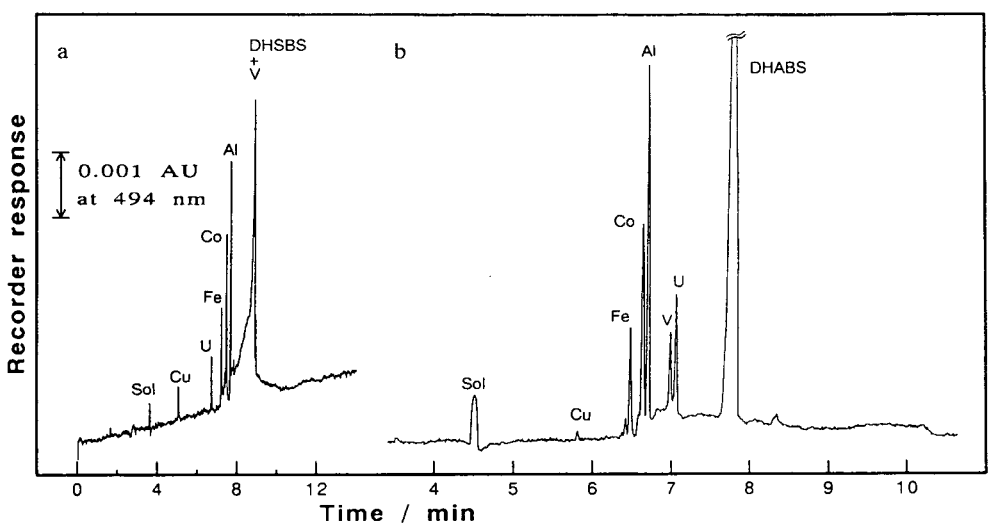

Fig. 6. Electropherograms for DHABS chelates in the TAA system. (a) [TAABr] = 5 mM, I = 20 μA, V = 20.8 kV. (b) [TAABr] = 25 mM, I = 25 μA, V = 20.1 kV. Other conditions are the same as in Fig. 3.

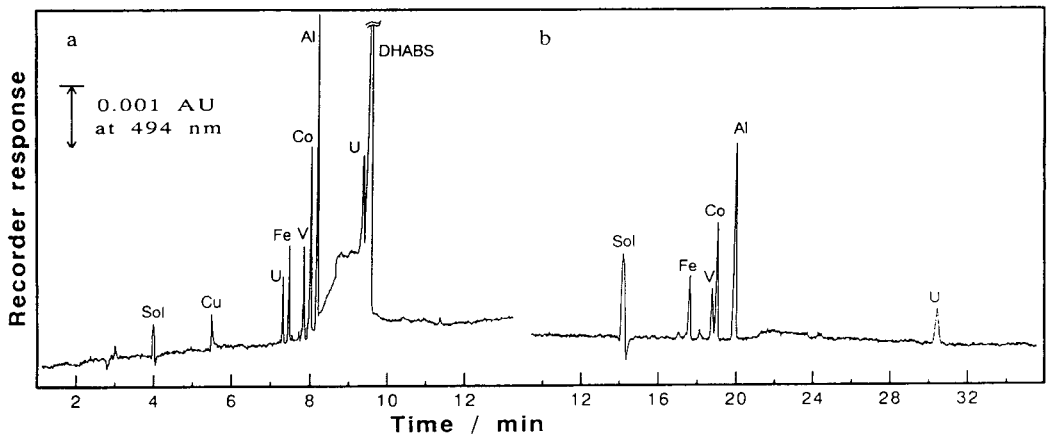

Fig. 7. Electropherograms for DHABS chelates in the TPP system. (a) [TPPCl] = 5 mM, I = 20 μA, V = 20.5 kV. (b) [TPPCl] = 25 mM, I = 30 μA, V = 21.3 kV. Other conditions are the same as in Fig. 3.

extraction [13] and ion-pair RP-HPLC [14]. Importantly in each case, it is essential for the analyte ion to form an ion associate with a suitable counter-ion in the polar phase and to be desolvated before it is partitioned into or adsorbed onto non-polar secondary phase. Also, in the area of HPCE, some attempts to utilize ion association in MEKC [15] and electrochromatography [16] have been made, in which case the ion-association agent serves as a modifier to enhance the phase transfer of analyte onto the pseudo-micellar phase and bonded hydrophobic phase, respectively. From the viewpoint of the separation principle, the CZE system studied in this paper is very peculiar because the separation process depends only on the ion association in the homogeneous phase and is not involved in the secondary phase at all. In conclusion, this separation method is one of a new HPCE mode and should be termed ion association CZE (IA-CZE) or ion association CE (IA-CE). The concept of IA-CE separation can be widely applied to highly charged organic species as well as inorganic molecules.

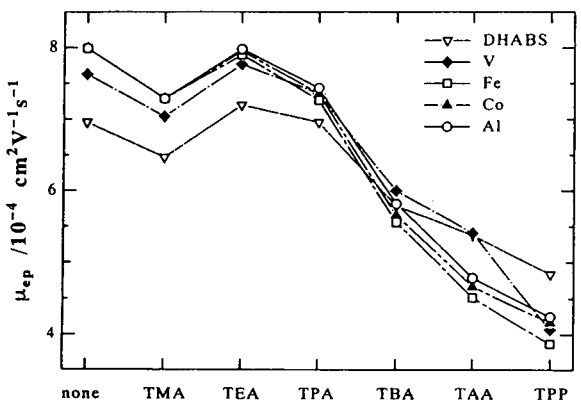

Fig. 8. The effect of counter-cation on the migration of DHABS chelates. Buffer: $[NaH_2PO_4]_T$ = 0.02 M, pH 7.0, [counter-cation] = 5 mM except "none". L = 72 cm, l = 57 cm.

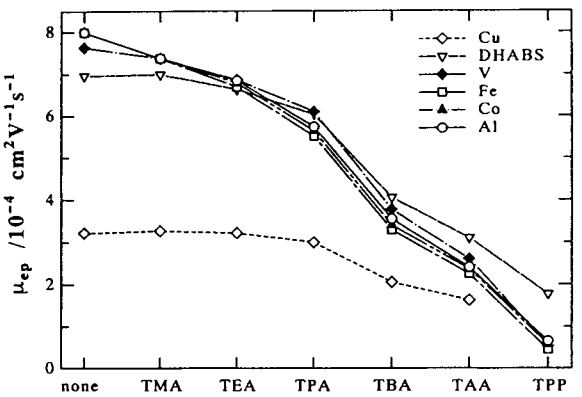

Fig. 9. The effect of counter-cation on the migration of DHABS chelates. Buffer: $[NaH_2PO_4]_T$ = 0.02 M, pH 7.0, [counter-cation] = 25 mM except "none". L = 72 cm, l = 57 cm.

REFERENCES

1 W.G. Kuhr and C.A. Monnig, *Anal. Chem.*, 64 (1992) 389R.
2 T. Saitoh, H. Hoshino and T. Yotsuyanagi, *J. Chromatogr.*, 469 (1989) 175.
3 T. Saitoh, H. Hoshino and T. Yotsuyanagi, *Anal. Sci.*, 7 (1991) 495.
4 D.F. Swaile and M.J. Sepaniak, *Anal. Chem.*, 63 (1991) 179.
5 S. Motomidzu, M. Oshima, S. Matsuda, Y. Obata and H. Tanaka, *Anal. Sci.*, 8 (1992) 619.
6 S. Motomidzu, S. Nishimura, Y. Obata and H. Tanaka, *Anal. Chem.*, 7 (supplement) (1991) 253.
7 Y. Kiso, I. Yamagata, Y. Yamamoto and M. Shinagawa, *Bull. Chem. Soc. Jpn.*, 38 (1965) 695.
8 Y. Nakabayashi, K. Nagaoka, Y. Masuda and R. Shinke, *Talanta*, 36 (1989) 639.
9 H. Hoshino, K. Nakano and T. Yotsuyanagi, *Analyst (London)*, 115 (1990) 133.
10 N. Iki, H. Hoshino and T. Yotsuyanagi, *Chem. Lett.*, (1993) 701.
11 S. Terabe and T. Isemura, *Anal. Chem.*, 62 (1990) 652.
12 O. Süs, *Liebig's Ann. Chem.*, 556 (1944) 65.
13 K. Tôei, *Anal. Sci.* 3 (1987) 479.
14 P.R. Haddad and P.E. Jackson, *Ion Chromatography (J. Chromatogr. Library*, Vol. 46), Elsevier, Amsterdam, 1990, Ch. 6.
15 H. Nishi, N. Tsumagari and S. Terabe, *Anal. Chem.*, 61 (1989) 2434.
16. W.D. Pfeffer and E.S. Yeung, *J. Chromatogr.*, 557 (1991) 125.

Journal of Chromatography A, 652 (1993) 547–553
Elsevier Science Publishers B.V., Amsterdam

CHROM. 25 304

Determination of organolead and organoselenium compounds by micellar electrokinetic chromatography

C.L. Ng, H.K. Lee and S.F.Y. Li*

Department of Chemistry, National University of Singapore, Kent Ridge, Singapore 0511 (Singapore)

ABSTRACT

The separation of selected organolead and organoselenium compounds by high-performance capillary electrophoresis was investigated. Satisfactory separation was achieved using β-cyclodextrin-modified micellar electrokinetic chromatography with on-column UV detection at 210 nm. This method was applied to the analysis of trialkyllead chlorides and organoselenium compounds in spiked distilled water and environmental samples. In addition, the effect of pH, sodium dodecyl sulphate and β-cyclodextrin concentrations on the migration behaviour of these compounds was examined.

INTRODUCTION

There has been a tremendous growth in the use of capillary electrophoresis (CE) in recent years [1–10]. The popularity of the technique can be partly attributed to its potential to achieve high efficiencies and its ease of operation. Many applications have been developed for biomedical [1–4] and pharmaceutical analysis [5–7]. However, only a few papers on the analysis of environmental pollutants using CE have appeared to date [8–10]. In view of the need for low detection limits, small sample volumes and rapid monitoring in environmental trace analysis, CE is a viable alternative for such applications.

Organic compounds of heavy metals such as lead and selenium have been shown to be carcinogenic [11]. These compounds are disseminated into the environment via mining, refining, paints and, in the case of tetraalkylleads, as antiknock additives in gasoline. Tetraalkyllead compounds undergo photochemical and metabolic dealkylation to form the trialkyllead compounds, which are chemically active and thermally sensitive. The most common technique used for the detection and determination of these trace elements is gas chromatography (GC) [12,13] with atomic absorption spectrometry because of their high element specificity and sensitivity. A major disadvantage of this technique is the need for highly sophisticated detectors (graphite furnace atomic absorption or microwave-excited helium plasma detector). Further purification steps are also needed to remove interferences from other forms of organic and inorganic compounds. More recently, high-performance liquid chromatography (HPLC) has been used for the determination of these compounds. For the determination of trialkyllead compounds, HPLC with on-line extraction does not yield better sensitivity than GC [14].

Since the first description of micellar electrokinetic chromatography (MEKC) by Terabe *et al.* [15], a large number of applications based on this technique have been reported [16–19]. In MEKC, a buffer solution containing a surfactant [*e.g.*, sodium dodecyl sulphate (SDS)] is used as the electrophoretic medium. The main advantage of MEKC is that both neutral and charged compounds can be separated by it. Further, by

* Corresponding author.

0021-9673/93/$06.00

introducing suitable additives (*e.g.*, cyclodextrins and complexing agents) into the buffer, unique separation mechanisms can be exploited [20]. In this work, the separation of a mixture of two organolead and two organoselenium compounds using MEKC with β-cyclodextrin was examined. The method was applied to the determination of these compounds in spiked distilled water and environmental samples. In addition, the effects of pH and SDS and β-cyclodextrin concentrations on the migration behaviour of these compounds were investigated.

EXPERIMENTAL

Experiments were conducted on a laboratory-built CE system. A Spellman (Plainview, NY, USA) Model RM15P10KD power supply, which is capable of delivering up to 15 kV, was used. Fused-silica capillary tubing of 44 cm × 50 μm I.D. was obtained from Polymicro Technologies (Phoenix, AZ, USA). An ISCO (Lincoln, NE, USA) CV^4 variable-wavelength UV detector with the wavelength set at 210 nm was used for the detection of peaks. Chromatographic data were collected and analysed using a Hewlett-Packard (Avondale, PA, USA) Model HP3394A integrator.

The pH of the buffer solutions used in the CE system was adjusted by mixing 25 m*M* sodium tetraborate and 25 m*M* sodium dihydrogenphosphate solutions. β-Cyclodextrin and sodium dodecyl sulphate (SDS) were purchased from Fluka (Buchs, Switzerland). Trimethyllead chloride (TML), triethyllead chloride (TEL), diphenyl selenide (Ph_2Se) and phenyl selenyl chloride (PhSeCl) were obtained from Johnson Matthey (Ward Hill, MA, USA). Standard solutions in methanol having a concentration of 666 ppm for TML, 400 ppm for TEL, 466 ppm for diphenyl selenide and 600 ppm for phenylselenyl chloride were used. Sample solutions were injected hydrodynamically at a height of 2 cm and over an injection time of 4 s. Each injection was calculated [21] to be *ca.* 0.3 nl.

Extraction from spiked distilled water

Trimethyllead and triethyllead chloride. A known amount of TML and TEL was added to 500 ml of distilled water and shaken for 5 min. The sample was evaporated under vacuum at 55°C until a residual volume of about 10 ml remained. The sample was quantitatively transferred into a 100-ml separating funnel and the volume was adjusted to 25 ml with distilled water. About 8–9 g of sodium chloride were added and the pH was brought to below 10, if necessary. The sample was then extracted twice with 25-ml portions of chloroform. The extracts were combined and dried with magnesium sulphate. The chloroform extract was filtered and evaporated to dryness under vacuum at 40°C. The TEL and TML thus obtained were dissolved in methanol and the solution was analysed by CE.

Diphenyl selenide and phenyl selenyl chloride. A known amount of the organoselenium compounds was dissolved in 30 ml of methanol and was then added to distilled water, giving a total volume of 200 ml in a 250-ml separating funnel. The sample was extracted three times with 30 ml of chloroform. The extracts were combined, dried with magnesium sulphate, filtered and evaporated under vacuum at 40°C until a residual volume of 2 ml of extract was left. The sample was then air dried at room temperature (25°C), after which the sample was dissolved in methanol and introduced into the CE system for analysis.

Analysis of environmental samples

Water samples (1.5 l) were collected from drains next to a car park. The samples were filtered and then extracted using procedures similar to those for TML and TEL.

RESULTS AND DISCUSSION

As the organometallic compounds are heat and light sensitive, the ionic strength of the electrophoretic medium (the concentrations of the phosphate and borate buffer solutions) used was kept low, *i.e.*, at 25 m*M* each for the phosphate and borate buffer solutions. This was to prevent excessive joule heating, which is likely to occur when high ionic strength buffer solutions are used. Thus, degradation of compounds

inside the capillary during the run was prevented or at least minimized.

Preliminary experiments were conducted to separate the organolead and selenium compounds using CZE conditions, *i.e.*, at pH 6.0, 7.0 and 8.0. The results obtained for the migration times at different pH values are shown in Fig. 1. It can be seen that with an increase in pH, there is an increase in the electroosmotic flow velocity. This is indicated by the decrease in migration times of the neutral diphenyl selenide, which co-eluted with the solvent, the unretained solute (methanol). This could be due to the increase in ionization of the surface functional groups with pH at the inside of the wall, which subsequently resulted in an increase in the zeta potential. The effect of the increased electroosmotic flow velocity could be seen from the decrease in migration times for neutral organoselenium compounds, Ph_2Se and PhSeCl. On the other hand, an opposite trend was observed for trimethyllead chloride (TML) while the migration times for triethyllead chloride (TEL) were fairly constant with changes in pH.

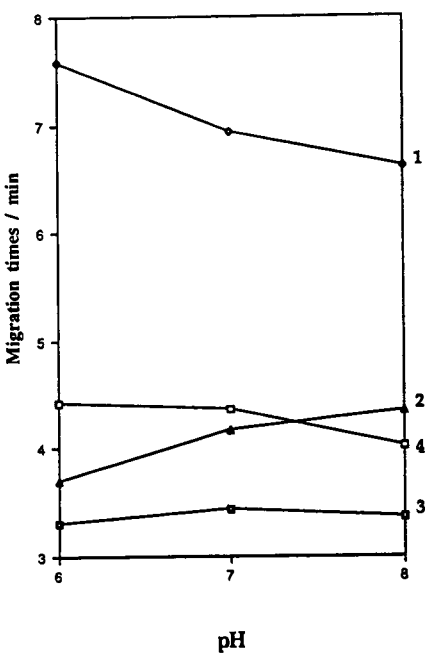

Fig. 1. Variation of migration time with pH. 1 = Phenyl selenyl chloride; 2 = trimethyllead chloride; 3 = triethyllead chloride; 4 = diphenyl selenide.

TEL and TML are known to be partially dissociated [22] in aqueous medium, forming PbR_3^+, as shown in the equation

$$PbR_3Cl \overset{k}{\rightleftharpoons} PbR_3^+ + Cl^-$$

where k = dissociation constant. Thus, these compounds carry a partial positive charge under these conditions. Consequently, they are attracted to the cathode, with the result that their migration times are shorter than that of the solvent (shown by the plot for Ph_2Se) at pH 6 and 7 in Fig. 1. With an increase in pH, there was an increase in the migration time for TML, and at pH 8 the TML peak was observed to elute after the solvent peak (compare the lines at pH 8 for Ph_2Se and TML). The increase in migration time of TML with pH (*i.e.*, a decrease in the apparent velocity) in spite of an increase in electroosmotic flow velocity could be attributed to an increase in the borate concentration in the electrophoretic medium at higher pH. The borate ions would tend to envelop the positively charged TML, resulting in partial neutralization of the positive charge on TML. Subsequently, the electrophoretic velocity towards the cathode was reduced. At high pH (pH > 8), TML was completely neutralized by the borate ions, and thus eluted after the solvent. The borate ions, on the other hand, had no significant effect on the migration times of TEL. This could be due to steric hindrance caused by the three bulky ethyl substituent groups attached to lead. Subsequently, the borate ions were prevented from approaching the central lead atom. Hence the partially positive charged TEL was the first to be eluted and it always migrated before the solvent peak at the pH values investigated.

Another interesting observation is the migration order of TML and TEL. It was noted that TEL always migrated earlier than TML under CZE conditions. This was surprising as TML, being smaller and thus possessing a higher charge-to-radius ratio, would be expected to have a higher electrophoretic velocity than TEL towards the cathode. Hence it would be expected to migrate faster than TEL. However, it is conceivable that a higher degree of ion pairing exists between borate and TML (because of the

smaller size compared with that of TEL), which reduces the effective charge on the TML. Consequently, the latter possesses a lower net velocity towards the cathode.

For organoselenium compounds, no unusual trends were observed. As they are neutral or dissociate only slightly, they either co-migrated with the solvent (*e.g.*, Ph_2Se) or migrated after the solvent peak (*e.g.*, PhSeCl).

In order to improve the separation of the neutral compounds, MEKC was performed. The effect of SDS concentration on the separation of this group of compounds is illustrated in Fig. 2. SDS concentrations of 25 and 50 m*M* were considered. The migration order followed the expected trend in MEKC, *i.e.*, the more hydrophobic solutes were retained longer than the less hydrophobic species. Hence, in this instance, TEL migrated after TML, followed by Ph_2Se and PhSeCl.

Although separation of peaks could be achieved for the four solutes in MEKC, peak tailing was observed for TEL and PhSeCl. In view of this problem, β-CD was added to the electrophoretic medium to improve the peak shape. The results obtained for different β-CD concentrations on the separation are illustrated in Fig. 3. It can be seen that the migration times of all the solutes decreased with increase in β-CD concentration. This could be due to the competitive interaction between the solutes with β-CD and SDS. As β-CD is neutral, it would migrate faster than SDS towards the cathode. Hence solutes forming host–guest complexes with β-CD would be brought to the cathode at a faster rate. It is noteworthy that at 15 m*M* β-CD, crossover of peaks for TEL and Ph_2Se is observed. At lower β-CD concentration, TEL migrated faster than Ph_2Se. At higher β-CD concentrations, because interaction with β-CD depends on the compatibility of the molecular

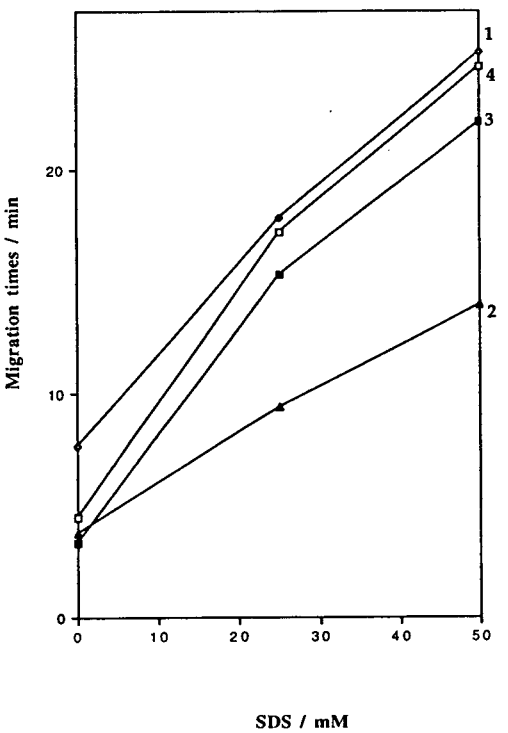

Fig. 2. Variation of migration time with SDS concentration. Compounds as in Fig. 1. Electrophoretic conditions: Micellar solution in 25 m*M* phosphate–borate buffer (pH 6.0); applied voltage, 15 kV.

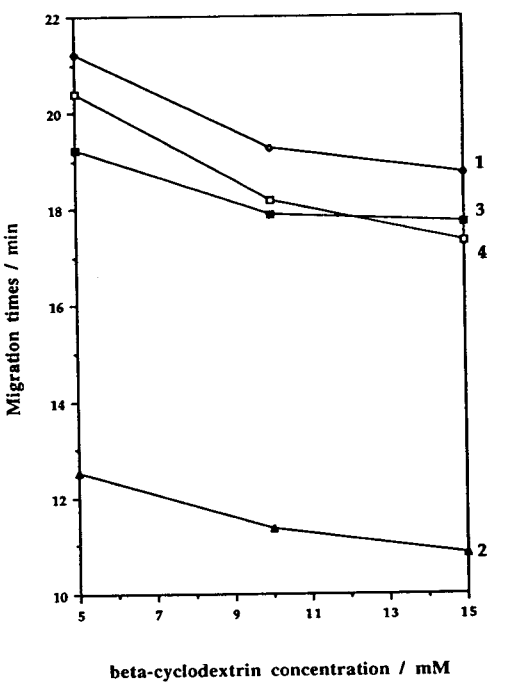

Fig. 3. Variation of migration time with β-CD concentration. Compounds as in Fig. 1. Electrophoretic conditions: 50 m*M* SDS in 25 m*M* phosphate–borate buffer (pH 6.0); applied voltage, 15 kV.

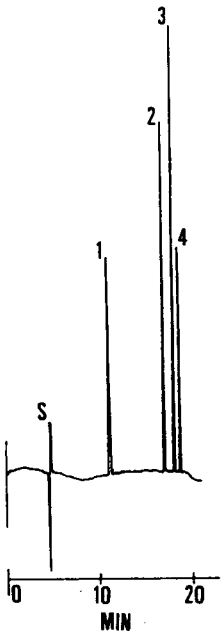

Fig. 4. Typical electropherogram obtained for organolead and organoselenium compounds. Peaks: S = solvent (methanol); 1 = trimethyllead chloride; 2 = triethyllead chloride; 3 = diphenyl selenide; 4 = phenylselenyl chloride. Electrophoretic conditions: 50 m*M* SDS and 5 m*M* β-cyclodextrin in 25 m*M* phosphate–borate buffer (pH 6.0); separation tube, 44 cm × 50 μm I.D. fused silica; applied voltage, 15 kV; wavelength, 210 nm.

size of the solutes with the cavity of β-CD and Ph_2Se tends to be incorporated more readily into the cavity of β-CD, it migrated earlier than TEL. It was also observed that at high β-CD concentrations, the resolution between TEL and Ph_2Se was unsatisfactory, and irreproducible migration times were obtained after every injection unless flushing of the column with 0.1 *M* NaOH was carried out for at least 15 min between runs. This problem was not observed at lower β-CD concentrations. Of the three concentrations of β-CD investigated, it was found that 5 m*M* β-CD offered sharp peaks and the best resolution. Hence the conditions of pH 6.0, 50 m*M* SDS and 5 m*M* β-CD were used for subsequent investigations. A typical electropherogram for this group of compounds is shown in Fig. 4. Typically, plate numbers greater than 200 000 were obtained for the separations.

Analysis of spiked distilled water

Linear calibration graphs in the range 80–600 ppm were obtained for the four solutes. The detection limits (signal-to-noise ratio = 3), correlation coefficients and recoveries are given in Table I. Typical electropherograms of the extracted samples for the two groups of compounds are illustrated in Fig. 5a and b. Water samples (1.5 l) from drains at a heavily used car park were collected for analysis. The organic compounds under investigation were not detected. The reason could either be that the compounds were present at levels below the detection limits, or they could have undergone photochemical degradation [13]. A typical electropherogram for the analysis of the water samples is shown in Fig. 6a. To confirm that the absence of these compounds was not attributable to the analytical procedure, known amounts of TML and TEL were added to 500 ml of the water sample before

TABLE I

ABSOLUTE DETECTION LIMITS, CORRELATION COEFFICIENTS AND RECOVERIES OF ORGANOLEAD AND ORGANOSELENIUM COMPOUNDS

Compound	Detection limit (pg)	Correlation coefficient	Recovery (%)
Trimethyllead chloride	20	0.998	90
Triethyllead chloride	8	0.999	80
Diphenyl selenide	9	0.998	104
Phenylselenyl chloride	18	0.999	83

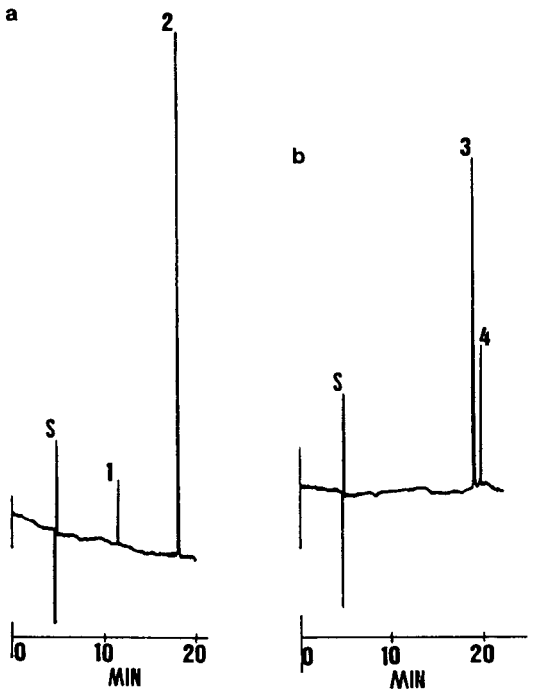

Fig. 5. Electropherograms obtained after extraction of (a) TML and TEL from spiked distilled water and (b) Ph_2Se and PhSeCl from spiked distilled water. Peaks as in Fig. 4. Electrophoretic conditions: 50 m*M* SDS and 5 m*M* β-cyclodextrin in 25 m*M* phosphate–borate buffer (pH 6.0); separation tube, 44 cm × 50 μm I.D. fused silica; applied voltage, 15 kV; wavelength, 210 nm.

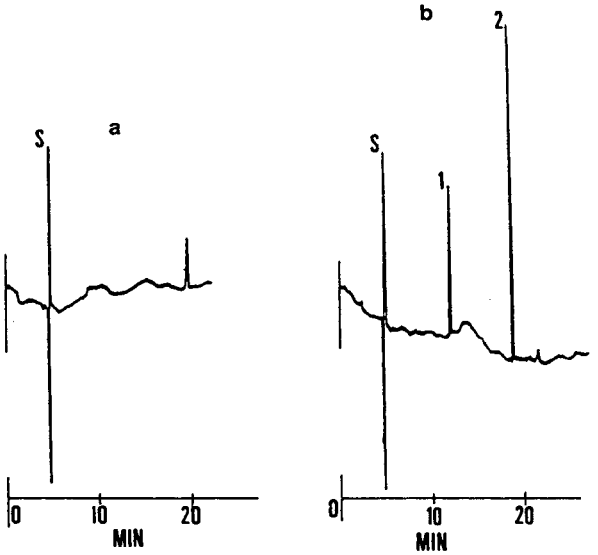

Fig. 6. Electropherograms obtained for (a) a water sample collected at a heavily used car park and (b) a water sample spiked with TML and TEL. Peak identification as in Fig. 4.

extraction. Both components were detected at the expected migration times. A typical electropherogram for the spiked water sample is shown in Fig. 6b.

CONCLUSIONS

The feasibility of using MEKC for the separation of a mixture of organolead and organoselenium compounds has been demonstrated. By the addition of β-cyclodextrin to the electrophoretic medium, improvements in the peak shapes were observed. To the best of our knowledge, this is the first reported analysis of these groups of compounds by MEKC. High separation efficiencies and detection limits comparable to those obtained by GC were achieved. However, the primary advantage of MEKC over GC is that the former is performed at temperatures that prevent potential thermal degradation of the compounds of interest. Given this advantage, the method may be used in analyses for other environmental pollutants with little modification of the fundamental conditions used in this work. Further, the technique offers rapid analyses, and low running costs and is aqueous rather than organic solvent based, all these being advantageous over traditional chromatographic procedures. An additional advantage is the potential incorporation into the MEKC method of enrichment procedures currently being exploited in CE such as isotachophoresis [23–25], field amplification injection [26–28] and in-capillary solid-phase extraction techniques [29,30]. None of these are available to GC for improving its detection limits.

ACKNOWLEDGEMENT

The authors thank the National University of Singapore for financial support.

REFERENCES

1 H. Soini, T. Tsuda and M.V. Novotny, *J. Chromatogr.*, 559 (1991) 547.
2 T.A.A.M. Van De Goor, P.S.L. Janssen, Jan W. Van Nispen, M.J. Van Zeeland and F.M. Everaerts, *J. Chromatogr.*, 545 (1991) 379.
3 E. Jellum, A.K. Thorsrud and E. Time, *J. Chromatogr.*, 559 (1991) 455.
4 J.S. Stamler and J. Loscalzo, *Anal. Chem.*, 64 (1992) 779.
5 A. Wainright, *J. Microcol. Sep.*, 2 (1990) 166.
6 K.D. Altria and N.W. Smith, *J. Chromatogr.*, 538 (1991) 506.
7 A. Pluym, W. Van Ael and M. De Smet, *Trends Anal. Chem.*, 11 (1992) 27.
8 H. Nishi, T. Fukuyama and S. Terabe, *J. Chromatogr.*, 553 (1991) 503.
9 C.P. Ong, H.K. Lee and S.F.Y. Li, *J. Chromatogr.*, 542 (1991) 473.
10 C.P. Ong, C.L. Ng, N.C. Chong, H.K. Lee and S.F.Y. Li, *J. Chromatogr.*, 516 (1990) 263.
11 L. Fishbein, *Chromatography of Environmental Hazards, Vol. II: Metals, Gaseous and Industrial Pollutants, Elsevier, Amsterdam*, 1973, Chs. 4 and 6.
12 S.A. Estes, P.C. Uden and R.M. Barnes, *Anal. Chem.*, 53 (1981) 1336.
13 W.R.A. De Jonghe, W.E. Van Mol and F.C. Adams, *Anal. Chem.*, 55 (1983) 1050.
14 D.S. Bushee and I.S. Krull, *Anal. Chim. Acta*, 194 (1987) 235.
15 S. Terabe, K. Otsuka, K. Ichikawa, A. Tsuchiya and T. Ando, *Anal. Chem.*, 56 (1984) 111.
16 K. Otsuka, J. Kawahara, K. Tatekawa and S. Terabe, *J. Chromatogr.*, 559 (1991) 209.
17 K. Otsuka, S. Terabe and T. Ando, *J. Chromatogr.*, 332 (1985) 219.
18 L.N. Amankwa and W.G. Kuhr, *Anal. Chem.*, 63 (1991) 1733.
19 T. Lee, E.S. Yeung and M. Sharma, *J. Chromatogr.*, 565 (1991) 197.
20 S.F.Y. Li, *Capillary Electrophoresis: Principles, Practice and Applications (Journal of Chromatography Library*, Vol. 52), Elsevier, Amsterdam, 1992, Ch. 5.
21 R.A. Wallingford and A.G. Ewing, *Adv. Chromatogr.*, 29 (1990) 1.
22 V. Lucchini and P.R. Wells, *J. Organomet. Chem.*, 199 (1980) 217.
23 F. Foret, V. Sustacek and P. Bocek, *J. Microcol. Sep.*, 2 (1990) 229.
24 D. Kaniansky and J. Marak, *J. Chromatogr.*, 498 (1990) 191.
25 D.S. Stegehuis, U.R. Tjaden and J. van der Greef, *J. Chromatogr.*, 591 (1992) 341.
26 D.S. Burgi and R.L. Chien, *Anal. Chem.*, 63 (1991) 2042.
27 R.L. Chien and D.S. Burgi, *Anal. Chem.*, 64 (1992) 489A.
28 R.L. Chien and D.S. Burgi, *Anal. Chem.*, 64 (1992) 1046.
29 M.E. Swartz and M. Merion, *J. Chromatogr.*, 632 (1993) 209.
30 C.L. Ng, C.P. Ong, H.K. Lee and S.F.Y. Li, *J. Chromatogr. Sci.*, in press.

Journal of Chromatography A, 652 (1993) 555–561
Elsevier Science Publishers B.V., Amsterdam

CHROM. 25 106

Use of capillary electrophoresis for monitoring citrus juice composition

Paul F. Cancalon* and Charles R. Bryan

Florida Department Citrus, 700 Experiment Station Road, Lake Alfred, FL 33850 (USA)

ABSTRACT

New trends in adulteration monitoring, favor the development of methods analyzing simultaneously as many compounds as possible. Capillary electrophoresis has been applied to the examination of a broad spectrum of citrus juice molecules that absorb in the UV and in the visible light. Depending on the conditions up to thirty compounds could be separated. The identified molecules included phenolic amines, amino acids, flavonoids, polyphenols and vitamin C. Samples can be analyzed without specific preparation and the best separations were obtained with diluted solutions due to a stacking effect. This method has been applied to the comparison of pure orange juice and pulpwash, a major adulterant of orange juice. Several significant quantitative differences were seen and it is hoped that this procedure will provide a more precise way of estimating pulpwash in orange juice.

INTRODUCTION

High-performance capillary electrophoresis (HPCE) has become a major separation tool for the rapid analysis of a large variety of molecules [1,2], including amino acids [3], peptides and proteins [2,4], nucleotides [3] and oligonucleodides [5], saccharides [6], oligosaccharides [7], flavonoids [8] or catechols and catecholamines [9]. The ability to separate molecules of a different nature is particularly important when analyzing a natural biological product which may contain hundreds of chemicals. Recently HPCE has been used to investigate biological samples ranging from hepatoma membrane proteins [10] to Maillard reaction products [11].

A large spectrum of compounds with widely different chemical properties have been identified in citrus products [12]. In the past, Petrus and Attaway [13] have estimated various classes of molecules in citrus juices, using UV and visible spectrophotometry and fluorometry. Individual constituents could not be examined since these techniques do not involve a separation process. The analysis of individual citrus components has been achieved by HPLC, a method which requires successive analyses associated with each chemical species [14–17]. Recently, a multiple detector linked with an HPLC system, has been developed by ESA to analyze numerous citrus compounds [18]. HPCE may allow many of these chemicals to be quantitated in a single run. In this study, an HPCE method has been developed that allows the monitoring of citrus products. Compounds present in orange juice, grapefruit juice and pulpwash showed significant quantitative differences.

EXPERIMENTAL

Apparatus

Analyses were performed with a Spectra-Physics 1000 electrophoresis apparatus (Spectra-Physics, San Jose, CA, USA) equipped with high-speed scanning detection in the UV and in the visible for spectral analysis. Separations were performed with uncoated fused silica tubings 70

* Corresponding author.

0021-9673/93/$06.00

cm × 75 μm (J & W Scientific, Folsom, CA, USA) or 70 cm × 50 μm (Polymicro Technologies, Phoenix, AZ, USA).

Sample and buffer preparation

Juice samples were centrifuged for 5 min on a Sorvall RC-5B (DuPont, Newton, CT, USA) centrifuge at 500 *g* to remove any particulate material. Centrifugation was followed by filtration on a polysulfone membrane, dual Acrodisc PF filter (Gelma, Ann Harbor, MI, USA): 0.8-μm prefilter and 0.2-μm filter. In some cases, sodium dodecyl sulfate (SDS) was added to the juice (10 m*M* final concentration) before centrifugation, to enhance the solubilization of the compounds absorbing in the visible. The stacking effect was induced by diluting the juices fourfold with HPLC grade distilled water and injecting the sample for 10 s.

A 50 m*M* solution of phosphate buffer was used as acidic electrolyte (pH 6.8). A 50 m*M* solution of boric acid–borax provided the buffer between pH 7.6 and 9.2. A 50 m*M* solution of borax–NaOH provided the pH 10 electrolyte. Sample were also ran with concentrations of borax (pH 9.3) ranging from 10 to 50 m*M*.

Running conditions

A 100-ppm (w/w) amount of each standard was injected hydrodynamically for 2 s and ran at 18 kV at 30°C, with a solution of 20 m*M* borax pH 9.3 as electrolyte. Originally, single strength juices were injected for 10 s and ran under the same conditions. Amino acids were separated with this buffer using a potential gradient rising from 21 to 25 kV during the first 16 min of the run.

A good separation was obtained with a 10-s injection of diluted juice into a 75 μm column, ran at 30°C with a 35 m*M* solution of borax pH 9.3, under which conditions, the voltage was maintained at 21 kV for the initial 12 min and raised to 25 kV in 30 s for the remainder of the analysis. The optimal conditions were met with a

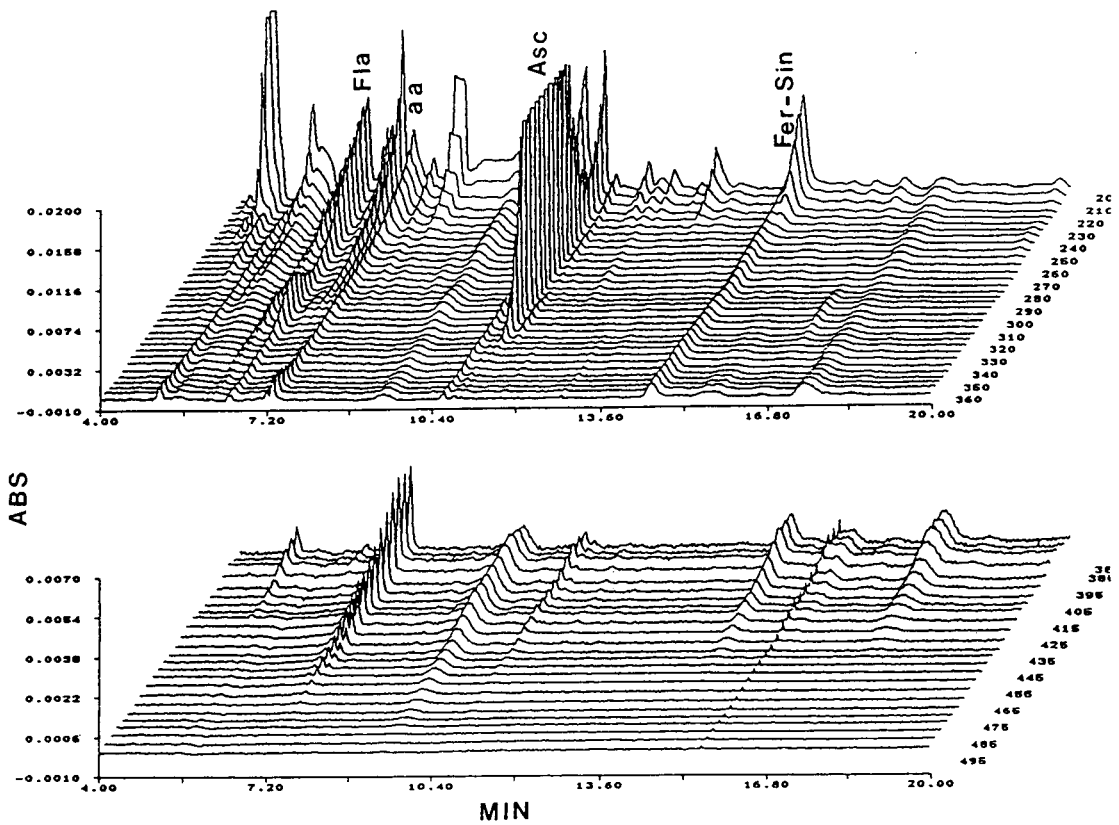

Fig. 1. UV and visible electropherogram of single strength orange juice under the original conditions. Fla = Flavonoids; aa = amino acids; Asc = ascorbic acid; Fer-Sin = feruloyl and sinapyl glucose.

15 s injection into a 50 μm column, at 21 kV and 25°C using the same borax buffer.

RESULTS AND DISCUSSION

The Spectra-Physics system allowed results to be expressed as (1) two-dimensional electropherograms for any given wavelength, (2) three-dimensional graphs containing multiple UV (200–360 nm) or visible (370–500 nm) wavelengths, or (3) spectra of single peaks. The nature of the detectors limited the observable molecules to those absorbing in the UV or the visible light. Therefore, some molecules such as most amino acids, could not be detected with this system. Because of a lack of solubility in aqueous solvents, neutral, hydrophobic compounds such as carotenoids gave little or no

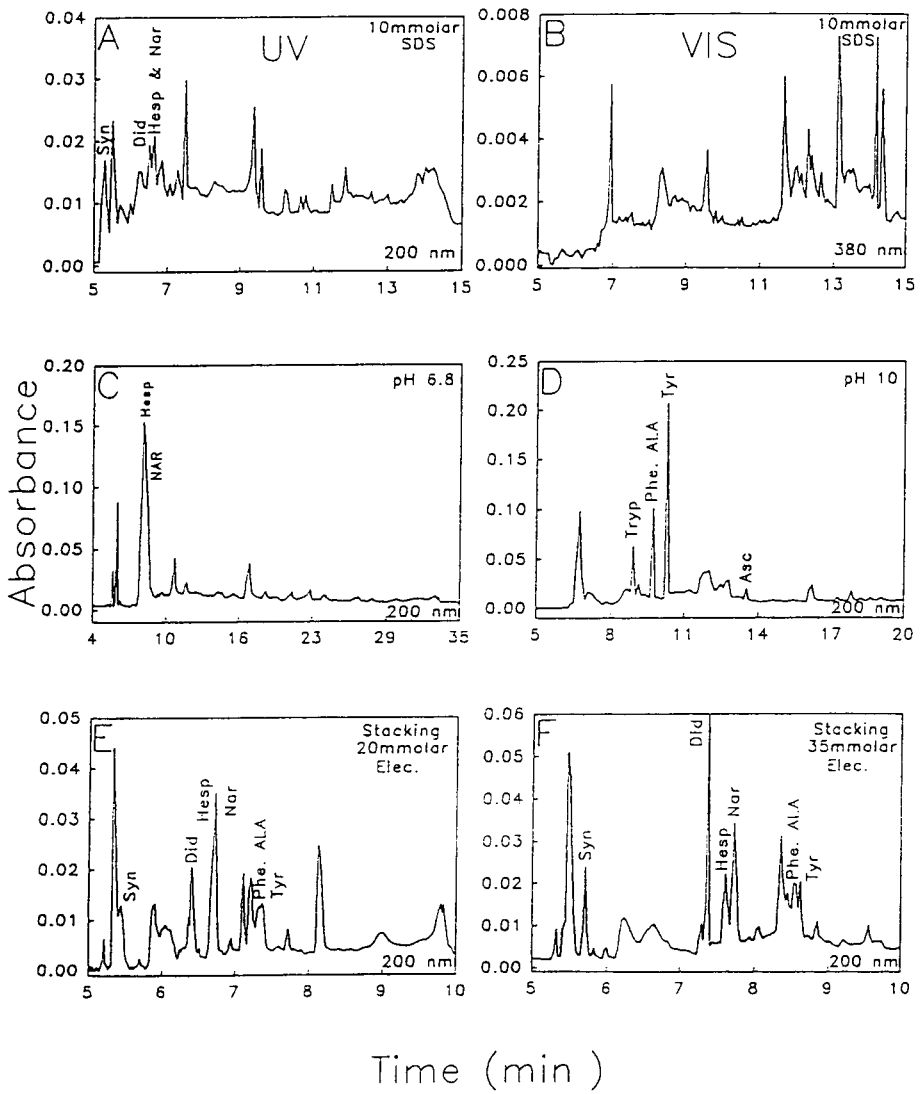

Fig. 2. Effect of the various modifications of the running conditions on the separation of orange juice components. (A) UV and (B) visible electropherograms of orange juice containing 10 m*M* SDS. Electropherogams of juice at (C) pH 6.8 and (D) pH 10 in this case, the juice was spiked with 35 ppm of tryptophan, phenylalanine and tyrosine. (E) Stacking effect at buffer concentration of 20 m*M*, only the first 10 min of a 25-min run are shown, the only major peak not shown is the feruloyl and synapyl glucose peak (see Fig. 5). (F) Electropherogram at the optimal buffer concentration (35 m*M*), also limited to the first 10 min.

response under the present conditions. When concentrated, neutral compounds were seen to move as a single peak displaced by the electroosmotic flow. Since in orange juice, most of the color is provided by carotenoids, the visible electropherogram of citrus juice products did not show any visible specific peak (Fig. 1). The observed peaks were the continuation in the visible of the spectra absorbing mainly in the UV.

Original conditions

Standards of various molecules present in orange juice were examined under the original conditions. Positive responses were obtained with ascorbic acid, coumarins, phenolic acids, flavonoids, polyphenols, tyrosine, phenylalanine, tryptophan and phenolic amines. The migration time and the spectrum of each standard were used to assess the presence of these molecules in citrus juice electropherograms. Under the original conditions (Fig. 1), amino acids were poorly resolved, hesperidin and narirutin as well as feruloyl and sinapyl glucose were not separated at all. Various modifications of the running conditions were tried in order to improve separation and increase responses.

Optimization of the running conditions

The addition of SDS to the juice sample and to the electrolyte, enhanced significantly the response in the visible portion of the electropherogram but it inhibited the UV response of some molecules, particularly the flavonoids (Fig. 2A and B).

Changes in peak resolution were induced by modifying the pH of the electrolyte. Low pH values (6.8–8.7) resulted in a doubling of the migration time and a major reduction in the response of the slow moving components (Fig. 2C). Above the pK_a of the amine group (pH 10), the amino acids behave as cations and were more easily separated. A very good separation of tryptophan, tyrosine and phenylalanine was obtained at pH 10 with a borate–NaOH buffer using a potential gradient to speed up the analysis (Fig. 2D). However, the procedure provided a somewhat poorer separation of other molecules. The best overall separation for most juice components was obtained at pH 9.3 (Fig. 2E).

Recently, the gel electrophoresis concept of stacking has been applied to CE [19]. In this technique, the sample is prepared in a diluted buffer that has the same composition as the support buffer. This results in the formation of an enhanced electric field at the injection point

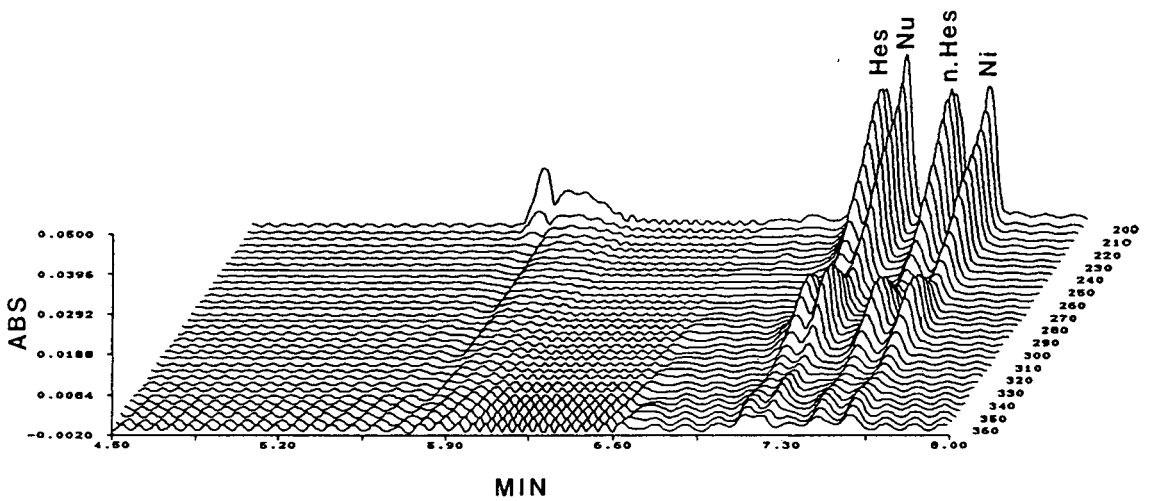

Fig. 3. Electropherogram of the four main flavonoids found in citrus products. Hes = Hesperidin; Nu = narirutin; n-Hes = neohesperidin; Ni = naringin.

and a sharp rise in the number of ions injected into the column. This process is particularly efficient with small ions [19], but since juices contain numerous large molecules, the phenomenon could only be partially reproduced. A significant improvement of the response and of the sharpness of the peaks was, nevertheless, obtained by diluting the juice four-fold in water. The dilution effect was largely compensated by a twelve-fold increase in peak sizes and a much better separation of adjacent peaks (Fig. 2E).

The effect of buffer concentration on separation was also examined. Borax solutions ranging in concentration from 10 to 50 m*M* were used as electrolyte. At low concentration most flavonoids appear as a single peak. Solutions of 50 m*M* provided a relatively good separation of most compounds with a short migration time but highly charged molecules migrated very slowly and therefore gave broad peaks. The best separation of citrus juices was obtained at a borax concentration of 35 m*M* (Fig. 2F). These conditions provided a very good separation for most compounds except feruloyl and sinapyl glucose. Finally, these two chemicals were separated without affecting the results achieved previously

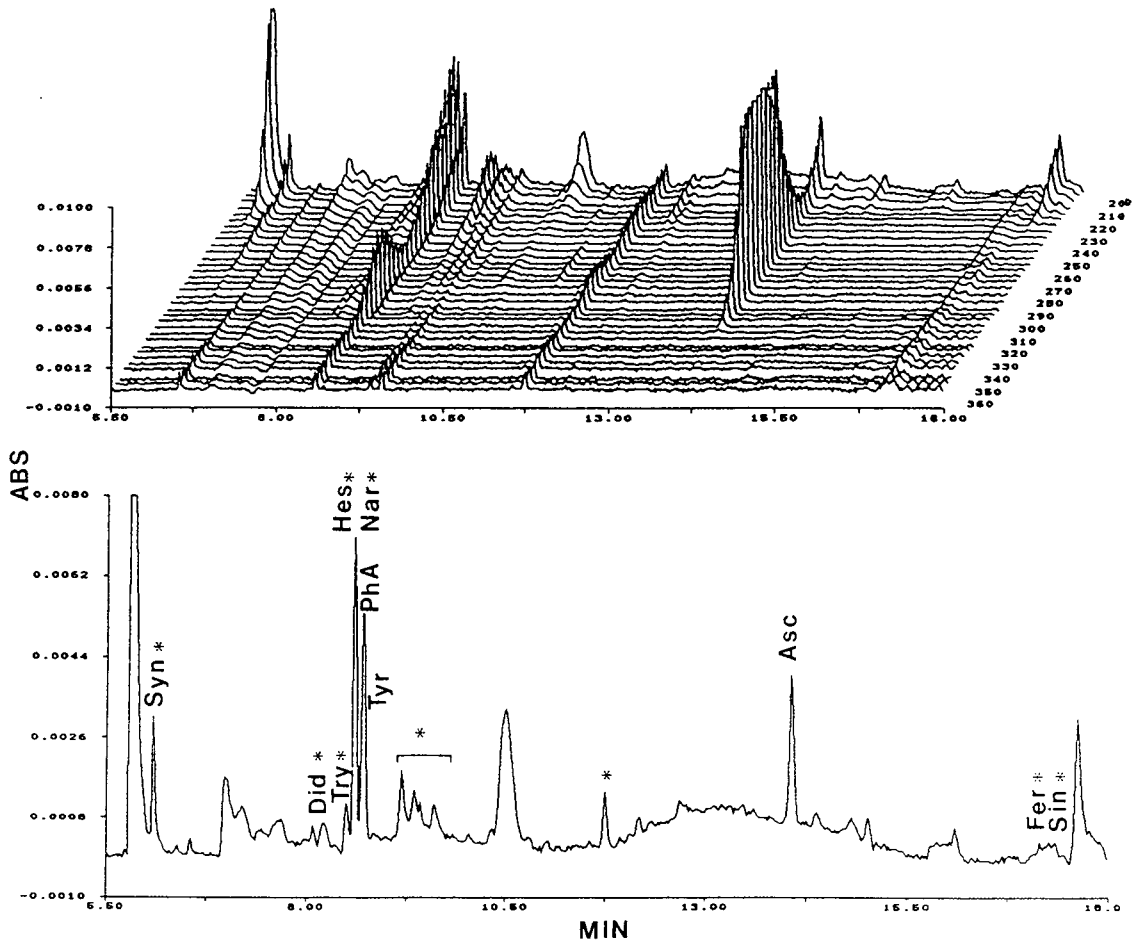

Fig. 4. Multiple and single (200 nm) wavelength electropherograms of orange juice under the optimal conditions. Syn = synephrine; Did = didymin; Try = tryptophan; Hes = hesperidin; Nar = narirutin; PhA = phenylalanine; Tyr = tyrosine; Asc = ascorbic acid; Fer = feruloyl glucose; Sin = sinapyl glucose. The asterisks indicate compounds whose concentrations were always significantly larger in pulpwash.

by using a 50 μm column at 25°C. The identified chemicals separated included: amines (tyramine, synephrine, octopamine), amino acids (tryptophan, tyrosine, phenylalanine), flavonoids (didymin, hesperidin, narirutin, neohesperidin, naringin) (Fig. 3), feruloyl and sinapyl glucose. These latest conditions were adopted for further analyses (Figs. 4 and 5). A very good reproducibility of the migration times was obtained with a relative standard deviation of 0.7% determined for synephrine, benzoic acid and ascorbic acid. Significant changes in retention times were produced only when the column was washed with NaOH.

Juice analysis

This method has been applied to the comparison of citrus products. In grapefruit juices (not shown) the presence of naringin and neohesperidin absent from orange juice could be detected. Analysis of pulpwash, a lower-quality juice product, did not reveal any peaks not already found in orange juice but showed that several components were present in much larger amounts (Figs. 4 and 5). They include synephrine, didymin, tryptophan, narirutin, hesperidin, feruloyl and sinapyl glucose, as well as at least four unidentified molecules, many having coumarin related spectra. These differences are

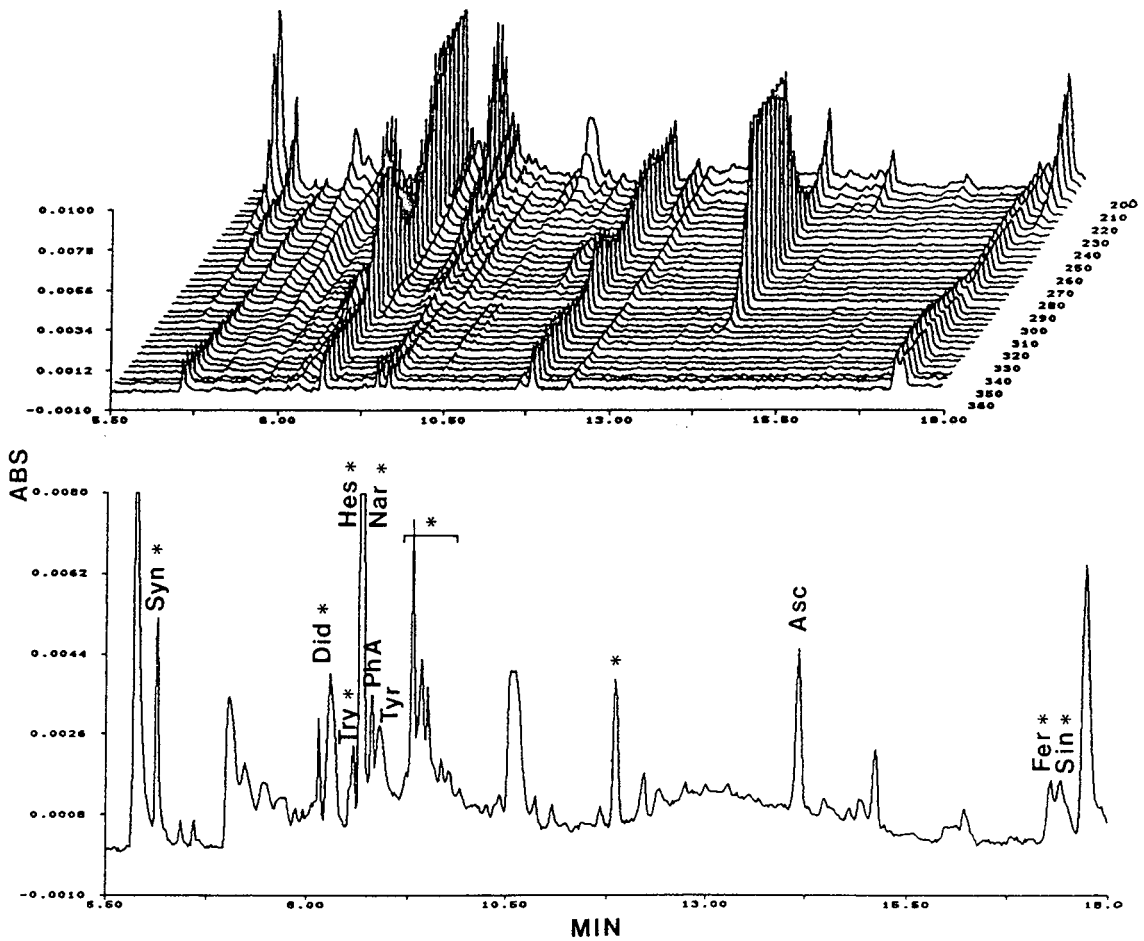

Fig. 5. Multiple and single (200 nm) wavelength electropherograms of pulpwash under optimal conditions.

being used to develop a method for detection and quantitation of pulpwash added to orange juice.

REFERENCES

1 J.W. Jorgenson and K.D. Lukacs, *Anal. Chem.*, 53 (1981) 1298–1302.
2 J.P. Landers, R.P. Oda, T.C. Spelberg, J.A. Nolan and K.J. Ulfelder, *Biotechniques*, 14 (1993) 98–111.
3 L.N. Amankwa and W.G. Kuhr, *Anal. Chem.*, 64 (1992) 1610–1613.
4 T. Higashijima, T. Fuchigami, T. Imasaka and N. Ishibsashi. *Anal. Chem.*, 64 (1992) 711–714.
5 A.S. Cohen, D. Najarian, J.A. Smith and B.L. Karger, *J. Chromatogr.*, 458 (1988) 323–333.
6 S. Honda, S. Iwase, A. Makino and S. Fujiwara, *Anal. Biochem.*, 176 (1989) 72–77.
7 S. Honda, A. Makino, S. Suzuki and K. Kakehi, *Anal. Biochem.*, 191 (1990) 228–234.
8 A. Seitz and G. Bonn, *J. Chromatogr.*, 559 (1991) 499–504.
9 C.P. Ong, S.F. Pand, S.P. Low, H.K. Lee and S.F.Y. Li, *J. Chromatogr.*, 559 (1991) 529–536.
10 D. Josic, K. Zeilinger and W. Reutter, *J. Chromatogr.*, 516 (1990) 89–98.
11 Z. Deyl, I. Miksik and R. Struzinsky, *J. Chromatogr.*, 516 (1990) 287–298.
12 R. Hegnauer, in P.G. Waterman and M.F. Grundon (Editors), *Chemistry and Chemical Taxonomy of the Rutales*, Academic Press, London, 1983, pp. 401–440.
13 D.R. Petrus and J.A. Attaway, *J. Assoc. Off. Anal. Chem.*, 63 (1980) 1317–1331.
14 S.M. Nolan and P.G. Koski, *Institute of Food Technologists Annual Meeting, New Orleans, LA, June 20–24, 1992*, Abstract No. 511.
15 S.T. Kirksey, J.O. Schwartz and R.L. Wade, *Institute of Food Technologists Annual Meeting, New Orleans, LA, June 20–24, 1992*, Abstract No. 509.
16 G.A. Perfetti, F.L. Joe, T. Fazio and S.W. Page, *J. Assoc. Off. Anal. Chem.*, 71 (1988) 469–473.
17 S.W. Page, F.L. Joe and L.R. Dusold, in S. Nagy, J.A. Attaway and M.A. Rhodes (Editors), *Adulteration of Fruit Juice Beverages*, Marcel Dekker, New York, 1988, pp. 269–278.
18 P.H. Gamache, *ESA Application Notes 10/1244*, ESA, Bedford, MA, 1989.
19 R.-L. Chien and D.S. Burgi, *Anal. Chem.*, 64 (1992) 489A–496A.

Journal of Chromatography A, 652 (1993) 563–569
Elsevier Science Publishers B.V., Amsterdam

CHROM. 25 176

Quantitation of organic acids in sugar refinery juices with capillary zone electrophoresis and indirect UV detection

Sam P.D. Lalljie, Johan Vindevogel* and Pat Sandra

Department of Organic Chemistry, University of Ghent, Krijgslaan 281 S4, B-9000 Ghent (Belgium)

ABSTRACT

During sugar refinement, monitoring of organic acids such as formate, tartrate, succinate, malate, glycolate and acetate in the process "juices" is important for process control. Matrix effects can lead to problems in conventional chromatographic ion analysis of these solutions. Capillary zone electrophoresis, with indirect UV detection, has been shown to be a good alternative, requiring almost no sample preparation, other than dilution, and with fast analysis time (less than 7 min). A co-elution problem for the formate–tartrate pair could be solved by adding small amounts of bivalent metal ions to the electrophoresis buffer. Quantitative analyses of the organic acids in the juices from beet sugar production and from the processing of a hydrolysed chicory root extract (*Cichorium intybus*) are reported.

INTRODUCTION

Organic acids can be determined with ion-exchange HPLC and refractive index detection. However, in the case of oligosaccharide- and polysaccharide-containing solutions, quantitation becomes difficult, if not impossible, because the small organic acid signals are partly or even totally obscured by the response of the accompanying sugars. Many attempts have been made [1] to work out alternative GC procedures, but the necessary isolation and derivatization steps, although performing well with standard mixtures, invariably fail to achieve reliable quantitation in the case of real-life matrices, especially with the more hydrophilic species such as formate and acetate.

Another alternative is electrokinetic analysis. The well-documented acid–base properties have made the carboxylic acids well suited as substrates for capillary isotachophoresis (ITP) [2,3] and also for capillary zone electrophoresis (CZE). The lack of chromophores, however, requires the use of a potential gradient [4] or a conductivity [5–7] detector. As this type of detection is not available on the instrumentation that has become commercially available, much attention is now being focused on CZE analysis with indirect UV detection [8–13]. This detection technique [14] relies on the presence of a UV-active buffer component with the same charge as the analytes. In the case of anions, an electroosmotic flow modifier [4], together with reversed polarity (cathode at the injection side), is applied to ensure movement of all anions towards the detector.

Samples from two different processes were analysed. Formate was determined in sugar beet juices and related samples (Fig. 1). Formate, tartrate, malate, succinate and glycolate were determined in chicory root extract juices.

* Corresponding author.

0021-9673/93/$06.00

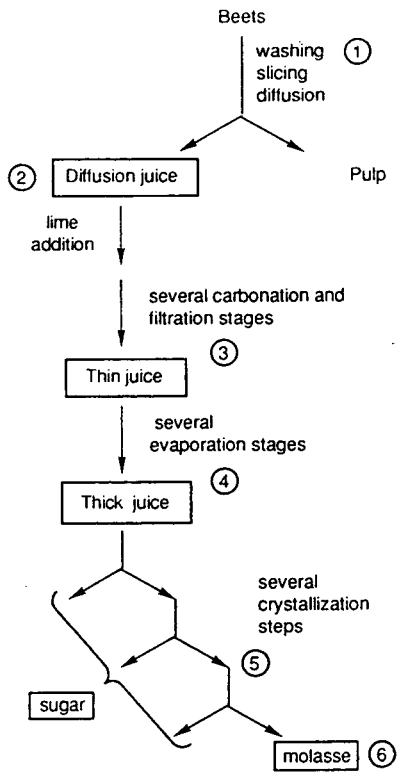

Fig. 1. Simplified scheme of beet sugar refinement. For fructose and oligofructose syrups from the chicory root juice, additional enzymatic hydrolysis steps (between first and second evaporation) are included for breakdown of the inulin to fructose. Raftilose results from complete hydrolysis, while Raftisweet is obtained by controlled partial hydrolysis.

EXPERIMENTAL

CZE was performed on a Quanta 4000 (Millipore, Bedford, MA, USA). Fused-silica capillaries were 75 μm internal diameter, 375 μm external diameter, 60 cm long, with the detection window at 53 cm.

Electropherograms were obtained with a phthalate buffer, prepared with deionized water (Milli-Q, Millipore) and adjusted to the appropriate pH with sodium hydroxide. Also, varying amounts of an electroosmotic flow modifier (OFM Anion-BT, Millipore) were added, resulting in a reversed electroosmotic flow and necessitating the use of a reversed-polarity source (high negative voltage at the column inlet). The indicated volume percentages of OFM refer to the volume of the commercial solution used for preparing the buffer (5%, v/v, is equivalent to 1 m*M* active substance [11]). The required calcium ion concentration was obtained by adding the appropriate amount of calcium chloride.

Standard samples were obtained by dissolving the acids, or their salts, in deionized water. Beet sugar juices, wash water samples and chicory root extract juices were obtained from a Belgian sugar refinement company (Tiense Suikerraffinaderij, Belgium). Highly viscous syrups, from the evaporation stage on, were stored in a refrigerator, while the less viscous samples from earlier stages were received frozen and kept in a deep freezer. The only treatment of the samples consisted of thawing where necessary and dilution with deionized water. Because of the high density of some of the samples, all organic acid concentrations are expressed as a w/w ratio (ppm).

Samples were introduced hydrodynamically (elevation, 10 cm; injection time, 20 s), analysed with an applied voltage of −20 kV (330 V/cm) and indirectly detected at 254 nm. Selection of the injection time was based on relative standard deviation data for peak area, which were found to decrease with injection time (for 10 ppm formate: 13.8%, 8.6%, 4.5% and 3.4% at, respectively, 5, 10, 15 and 20 s injection time). In between runs of standard mixtures, the column was rinsed with separation buffer for 2 min. For the actual samples, however, it was found necessary to use a more thorough rinsing procedure consisting of 0.1 *M* sodium hydroxide (1 min), deionized water (1 min) and separation buffer (2 min). The column was exclusively used for the analyses described here. Before storage, it was purged with water and then dried in an air stream. After remounting, it was flushed with buffer for at least 5 min.

RESULTS AND DISCUSSION

Separation optimization

The objective of this work was the separation and determination of formate, (DL-)tartrate, malate, succinate and glycolate. The initial selection of the background electrolyte (5 m*M* phthalate at pH 5.6) was based on literature data [11]. The osmotic flow modifier (OFM) concentration could be regulated to optimize the separation of most anions, except for the formate–tartrate pair

(Fig. 2a and b). Changing the pH in the range 5–7 did not improve resolution (Fig. 2c). It is significant that, in a recently published analysis of dental plaque [9] using these conditions, formate was identified in the electropherogram, but not tartrate (the hardened form of dental plaque is, just like wine deposits, also known as *tartar*).

The relative mobility of ions can be influenced by changing their charge state through selective complexation. This principle is commonly used in the analysis of cations with hydroxyisobutyric acid (HIBA) or citrate [15]. However, the complementary principle, cationic complexation to optimize the separation of anions, has not been much applied. Only recently, the separation of Pb^{2+}-complexed sulphate from organic anions has been reported [16,17]. The addition of alkaline earth cations to the buffer has been found effective for the separation of formate and tartrate (Fig. 3). With 0.2–0.6 m*M* Ca^{2+} added to the buffer, effective separation was obtained by selective retardation of the tartrate. Unfortunately, oxalate was also retarded, and although it was not a target compound overlap with the formate peak would result in poor quantitation of the latter (Fig. 4). Therefore, the following

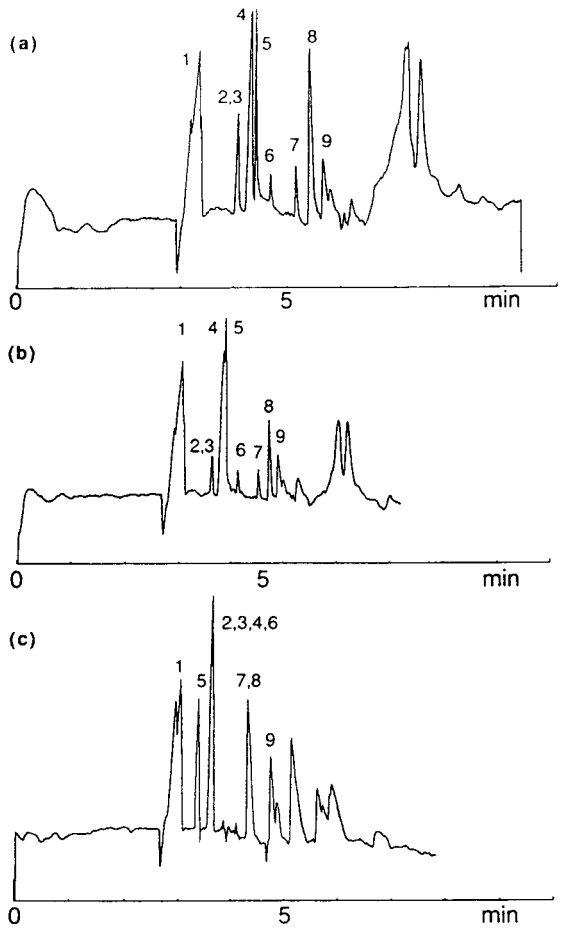

Fig. 2. Separation of organic acids in a chicory root thick juice (Raftisweet): (a) pH 5.6, 2.0% (v/v) OFM; (b) pH 5.6, 2.5% (v/v) OFM; (c) pH 7.0, 2.0% (v/v) OFM. Other conditions: see Experimental section. Peaks: 1 = inorganic anions; 2 = formate; 3 = tartrate (spiked); 4 = malate; 5 = citrate; 6 = succinate; 7 = glycolate; 8 = acetate; 9 = lactate.

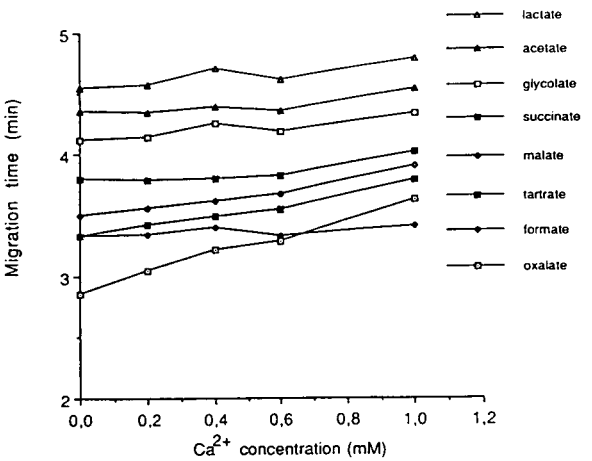

Fig. 3. Effect of Ca^{2+} concentration on the separation of organic acids. Same conditions as in Fig. 2a, except for the addition of Ca^{2+}.

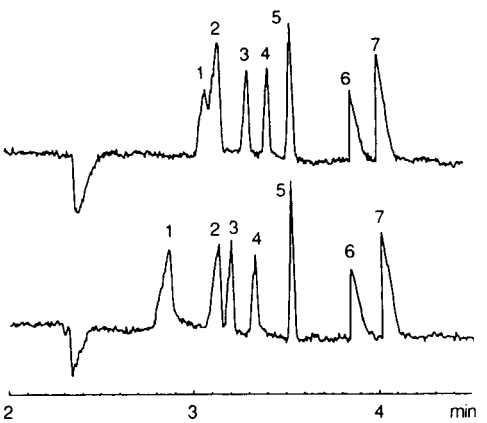

Fig. 4. Effect of Ca^{2+} concentration on the separation of organic acids (standards, 30 ppm each). Same conditions as in Fig. 2a, except for the addition of Ca^{2+}: 0.6 m*M* (top) or 0.2 m*M* (bottom). Peaks: 1 = oxalate; 2 = formate; 3 = tartrate; 4 = malate; 5 = succinate; 6 = glycolate; 7 = acetate.

approach was used: analysis was generally performed with 0.6 m*M* Ca^{2+} added to the buffer, which gave optimal separation between tartrate and formate. For diffusion juices, which still contain oxalate, a buffer containing 0.2 m*M* of Ca^{2+} was preferred. It must also be pointed out that, with the Ca^{2+} present, citrate is strongly retarded.

Good linearity was observed in the calibration graphs for the five acids of interest. In all cases the correlation coefficient was better than 0.999.

Quantitation applied to sugar refinery juices

For analysis, the native samples were diluted so that the actual concentration of the acids is in the 10–50 ppm range. Initially, extreme variability was observed. Triplicate, successive analyses gave reasonable standard deviations on the observed area (typically 1–5%), but the standard deviation for sets obtained by repetition of these triplicate analyses could be as high as 20%. Sample inhomogeneity was apparently not the cause of this effect, as this was equally well observed with new dilutions or repetitions on the same diluted sample. All efforts to correlate this with variations in analytical conditions such as temperature variation or small variations in buffer composition failed and forced us to conclude that the variability was inherent in the samples themselves. Indeed, some of the soil microorganisms, or their associated enzymatic activity, can survive the heat treatment during the diffusion process and result in further breakdown of some or build-up of other components in the mixture. The key step in achieving good performance was to give up automated analysis. Inevitably, extensive use of an autosampler requires that samples are prepared a relatively long time before analysis, and, consequently, have ample time to develop enzymatic activity.

This approach worked well, especially for the very viscous samples, which are relatively stable but start degrading after dilution. However, as will be indicated later, problems remain with some of the less viscous, inherently unstable samples. We would like to remark that addition of 0.1% sodium azide is not a good approach in this case as the large amount of azide ions interferes with the determination of the earlier-eluting organic carboxylates, especially formate.

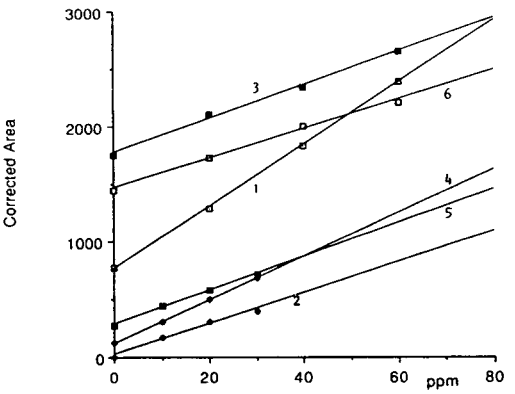

Fig. 5. Analysis of a chicory root evaporation juice by standard addition. Conditions as in Fig. 2a, except for the addition of 0.6 m*M* Ca^{2+} to the buffer. (See Discussion section for details on sample handling.) 1 = Formate; 2 = tartrate; 3 = malate; 4 = succinate; 5 = glycolate; 6 = acetate.

When care was taken to prepare the dilutions immediately before analysis, reliable results were obtained. This is further indicated by the response linearity, as verified by standard addition. The curves in Fig. 5 were obtained by preparing a dilution which was immediately stored at 0°C. For the successive points in the graph, aliquots were taken from the stored dilution, spiked with the appropriate amount of standard and analysed three times immediately.

For actual analyses, the system was calibrated

TABLE I

RUN-TO-RUN AND DAY-TO-DAY VARIABILITY FOR THE MIGRATION TIMES IN REAL SAMPLES (POOLED FROM DIFFERENT CHICORY ROOT JUICES)

Compound[a]	Run-to-run		Day-to-day	
	Mean (min)	R.S.D. (%) ($n = 10$)	Mean (min)	R.S.D. (%) ($n = 3$)[b]
Formate	3.26	1.0	3.51	13.7
Malate	3.63	1.0	3.91	14.1
Succinate	3.71	1.1	4.00	14.3
Glycolate	4.07	1.2	4.41	15.3

[a] Tartrate is not included as it occurred only rarely in these samples.

[b] Based on observations for 3 days covering a 3-month period (November 1992 to January 1993).

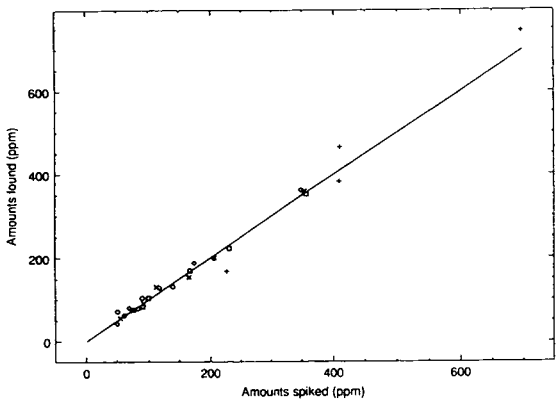

Fig. 6. Agreement between spiked amounts and observed differences between spiked and unspiked samples for the analyses from Table II (malate in diffusion juice not included, see Discussion section). The line represents the one-to-one correspondence.

daily. Although the run-to-run variability of the migration times was very good, considerable day-to-day variation occurs (Table I). As the capillary is cooled with ambient air, and the apparatus was situated in a non-thermostatted room, we believe that this variability is related to temperature variations in the surroundings.

Table II summarizes some typical results that were obtained for the analysis of five anions in chicory root juices (Raftilose). For a blind test, nine unidentified samples were obtained, consisting of three original and six spiked samples. With the exception of malate in the diffusion juices, good agreement was found between the amounts spiked and the amounts calculated after analysis of spiked and unspiked samples (Fig. 6).

The unreliability of the malate determinations in diffusion juices was related to sample instability, not to the analytical method. With capillary zone electrophoresis, it could further be demonstrated that the disappearance of malate was correlated with an increase in the acetate and lactate content (Fig. 7). Also, an unidentified compound was formed. Even when the sample was stored at low temperature (2–4°C) degradation of malate occurred. Apparently, degradation of malate in the unspiked sample led to an overestimation of the spiked amounts. Of course, in such a complex mixture, to conclude from Fig. 7 that the malate is effectively converted to lactate would require a more detailed study.

Table III summarizes typical results for the formate determinations in beet sugar-related samples (Fig. 8). Here again, the relatively large standard deviations for the diffusion juices reflect the stability problems of this type of sample.

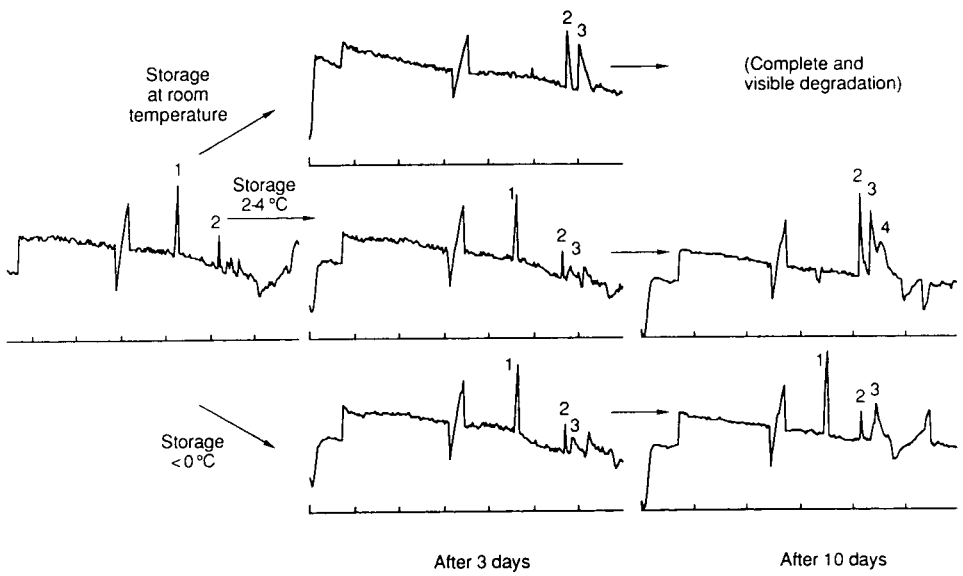

Fig. 7. The degradation of malate in a chicory root diffusion juice as monitored by CZE. The fresh sample (leftmost electropherogram) was received frozen. Conditions as in Fig. 5. Peaks: 1 = malate; 2 = acetate; 3 = lactate; 4 = unknown.

TABLE II

DETERMINATION OF ORGANIC ACIDS IN CHICORY ROOT JUICES. BLIND TEST WITH SPIKED SAMPLES

Juice analysed[a]	Formate				Tartrate				Malate				Succinate				Glycolate			
	b	*c*	*d*	*e*	*b*	*c*	*d*	*e*	*b*	*c*	*d*	*e*	*b*	*c*	*d*	*e*	*b*	*c*	*d*	*e*
R	n.d.[f]	–	0	–	n.d.	–	0	–	567	1.6	0	–	28	3.3	0	–	n.d.	–	0	–
M	76	1.7	76	76	73	3.8	51	73	1751	1.7	237	1184[g]	83	1.3	56	57	44	1.0	51	44
P	84	2.2	91	84	105	3.4	90	105	1921	3.1	444	1354[g]	120	2.6	92	92	81	0.7	89	81
K	274	2.4	0	–	n.d.	–	0	–	2631	0.8	0	–	93	1.5	0	–	150	3.1	0	–
H	379	2.5	100	105	63	9.7	62	63	2800	1.4	227	169	225	3.7	113	132	235	0.6	91	85
I	498	1.2	231	224	80	5.3	83	80	3015	0.6	409	384	294	3.3	207	201	349	3.2	206	199
F	474	3.3	0	–	n.d.	–	0	–	5557	2.2	0	–	214	1.2	0	–	252	1.3	0	–
B	644	2.9	168	170	130	6.2	118	130	6023	1.1	410	466	369	3.0	166	155	441	1.8	174	189
C	827	1.7	357	353	746	10.3	140	191	6303	0.2	697	746	575	1.6	354	261	615	4.1	348	363

[a] R, M, P = diffusion juices; K, H, I = evaporation juices (first stage); F, B, C = evaporation juices (second stage).
[b] Amounts found [ppm (w/w), average of three determinations].
[c] R.S.D. (%) on *b*.
[d] Amounts spiked [ppm (w/w)].
[e] Difference between amounts found and amounts found in the unspiked sample, to be compared with *d*.
[f] No detectable amounts.
[g] See text for a discussion of these values.

TABLE III

DETERMINATION OF FORMATE IN BEET SUGAR-RELATED SAMPLES

	Sample	ppm[a]	R.S.D. (%)	Method[b]
1[c]	Wash water (before washing)	n.d.[d]	–	A
1	Wash water (after washing)	6.9	0.9	A
2	Diffusion juice	6.2	9.6	B
2	Diffusion juice	4.2	5.9	B
2	Diffusion juice	6.3	3.4	B
3	Thin juice	58.3	0.4	A
3	Thin juice	64.5	0.9	A
5	Mother liquor II	1479	1.2	A
5	Mother liquor II	1589	1.5	A
6	Molasses	2333	2.0	A

[a] Average of three measurements (w/w).
[b] Refers to Ca^{2+} content of the separation buffer (A = 0.6 m*M*, B = 0.2 m*M*), all other conditions as in Fig. 2a.
[c] The number refers to the production stages in Fig. 1.
[d] No detectable amounts.

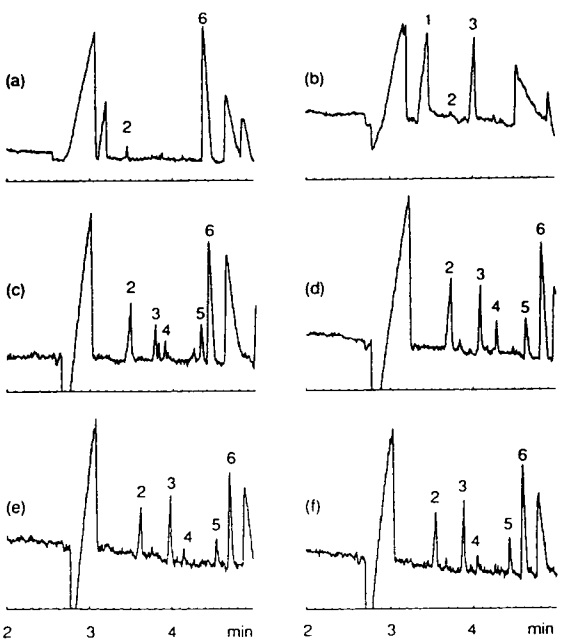

Fig. 8. Some typical beet sugar-related samples analysed in this work. Conditions as in Fig. 5, except for (b): 0.2 m*M* Ca^{2+}. (a) Wash water; (b) diffusion juice; (c) thin juice; (d) thick juice, (e) mother liquor II; (f) molasses. Peaks: 1 = oxalate; 2 = formate; 3 = malate; 4 = succinate; 5 = glycolate; 6 = acetate.

CONCLUSIONS

Determinations, similar to those mentioned in Tables II and III, have now been routinely used for several months and have provided process control parameters that were previously difficult to obtain. The minimal required sample preparation and short analysis time makes this type of analysis very attractive.

ACKNOWLEDGEMENTS

We thank the Belgian National Fund for Scientific Research and the National Lottery for financial support to our laboratory. We thank Hubert Hoebregs from the Tiense Suikerraffinaderij N.V., Belgium for providing spiked and unspiked samples and for discussing technicalities of the sugar refinery process.

REFERENCES

1 F. David and P. Sandra, unpublished results.
2 P.J. Oefner, R. Häfele, G. Bartsch and G. Bonn, *J. Chromatogr.*, 516 (1990) 251.
3 L. Křivánková and P. Boček, *J. Microcol. Sep.*, 2 (1990) 80.
4 T. Tsuda, *J. High Resolut. Chromatogr. Chromatogr. Commun.*, 10 (1987) 622.
5 X. Huang, J.A. Luckey, M.J. Gordon and R.N. Zare, *Anal. Chem.*, 61 (1989) 766.
6 X. Huang, M.J. Gordon and R.N. Zare, *J. Chromatogr.*, 480 (1989) 285.
7 X. Huang, R.N. Zare, S. Sloss and A.G. Ewing, *Anal. Chem.*, 63 (1991) 189.
8 F. Foret, S. Fanali, L. Ossicini and P. Boček, *J. Chromatogr.*, 470 (1989) 299.
9 J. Romano, P. Jandik, W.R. Jones and P.E. Jackson, *J. Chromatogr.*, 546 (1991) 411.
10 B.F. Kenney, *J. Chromatogr.*, 546 (1991) 423.
11 W.R. Jones and P. Jandik, *J. Chromatogr.*, 546 (1991) 445.
12 P. Jandik and W.R. Jones, *J. Chromatogr.*, 546 (1991) 431.
13 B.J. Wildman, P.E. Jackson, W.R. Jones and P.G. Alden, *J. Chromatogr.*, 546 (1991) 459.
14 E.S. Yeung and W.G. Kuhr, *Anal. Chem.*, 63 (1991) 275A.
15 A. Weston, P.R. Brown, P. Jandik, W.R. Jones and A.L. Heckenberg, *J. Chromatogr.*, 593 (1992) 289.
16 T. Groh and K. Bächmann, *Electrophoresis (Weinheim)*, 13 (1992) 458.
17 K. Bächmann, H. Steeg, T. Groh, I. Haumann, J. Boden and H. Holthues, *J. Microcol. Sep.*, 4 (1992) 431.

Author Index

PUBLICATION SCHEDULE FOR THE 1994 SUBSCRIPTION

Journal of Chromatography A and *Journal of Chromatography B: Biomedical Applications*

MONTH	O 1993	N 1993	D 1993	
Journal of Chromatography A	652/1 652/2 653/1	653/2 654/1 654/2 655/1	655/2 656/1 + 2 657/1 657/2	The publication schedule for further issues will be published later.
Bibliography Section				
Journal of Chromatography B: Biomedical Applications				

INFORMATION FOR AUTHORS

(Detailed *Instructions to Authors* were published in Vol. 609, pp. 437–443. A free reprint can be obtained by application to the publisher, Elsevier Science Publishers B.V., P.O. Box 330, 1000 AH Amsterdam, Netherlands.)

Types of Contributions. The following types of papers are published: Regular research papers (Full-length papers), Review articles, Short Communications and Discussions. Short Communications are usually descriptions of short investigations, or they can report minor technical improvements of previously published procedures; they reflect the same quality of research as Full-length papers, but should preferably not exceed five printed pages. Discussions (one or two pages) should explain, amplify, correct or otherwise comment substantively upon an article recently published in the journal. For Review articles, see inside front cover under Submission of Papers.

Submission. Every paper must be accompanied by a letter from the senior author, stating that he/she is submitting the paper for publication in the *Journal of Chromatography A* or *B*.

Manuscripts. Manuscripts should be typed in **double spacing** on consecutively numbered pages of uniform size. The manuscript should be preceded by a sheet of manuscript paper carrying the title of the paper and the name and full postal address of the person to whom the proofs are to be sent. As a rule, papers should be divided into sections, headed by a caption (*e.g.*, Abstract, Introduction, Experimental, Results, Discussion, etc.) All illustrations, photographs, tables, etc., should be on separate sheets.

Abstract. All articles should have an abstract of 50–100 words which clearly and briefly indicates what is new, different and significant. No references should be given.

Introduction. Every paper must have a concise introduction mentioning what has been done before on the topic described, and stating clearly what is new in the paper now submitted.

Experimental conditions should preferably be given on a *separate* sheet, headed "Conditions". These conditions will, if appropriate, be printed in a block, directly following the heading "Experimental".

Illustrations. The figures should be submitted in a form suitable for reproduction, drawn in Indian ink on drawing or tracing paper. Each illustration should have a legend, all the *legends* being typed (with double spacing) together on a *separate sheet*. If structures are given in the text, the original drawings should be supplied. Coloured illustrations are reproduced at the author's expense, the cost being determined by the number of pages and by the number of colours needed. The written permission of the author and publisher must be obtained for the use of any figure already published. Its source must be indicated in the legend.

References. References should be numbered in the order in which they are cited in the text, and listed in numerical sequence on a separate sheet at the end of the article. Please check a recent issue for the layout of the reference list. Abbreviations for the titles of journals should follow the system used by *Chemical Abstracts*. Articles not yet published should be given as "in press" (journal should be specified), "submitted for publication" (journal should be specified), "in preparation" or "personal communication".

Vols. 1–651 of the *Journal of Chromatography*; *Journal of Chromatography, Biomedical Applications* and *Journal of Chromatography, Symposium Volumes* should be cited as *J. Chromatogr.* From Vol. 652 on, *Journal of Chromatography A* (incl. Symposium Volumes) should be cited as *J. Chromatogr. A* and *Journal of Chromatography B: Biomedical Applications* as *J. Chromatogr. B.*

Dispatch. Before sending the manuscript to the Editor please check that the envelope contains four copies of the paper complete with references, legends and figures. One of the sets of figures must be the originals suitable for direct reproduction. Please also ensure that permission to publish has been obtained from your institute.

Proofs. One set of proofs will be sent to the author to be carefully checked for printer's errors. Corrections must be restricted to instances in which the proof is at variance with the manuscript. "Extra corrections" will be inserted at the author's expense.

Reprints. Fifty reprints will be supplied free of charge. Additional reprints can be ordered by the authors. An order form containing price quotations will be sent to the authors together with the proofs of their article.

0021-9673(19931022)652:2;1-Z